GEOLOGICAL SURVEY OF CANADA
MEMOIR 440

GEOLOGY OF THE CLYDE-COCKBURN LAND MAP AREA, NORTH-CENTRAL BAFFIN ISLAND, NUNAVUT

G.D. Jackson

2000

Natural Resources Canada Ressources naturelles Canada

Canada

GEOLOGICAL SURVEY OF CANADA

MEMOIR 440

GEOLOGY OF THE CLYDE-COCKBURN LAND MAP AREA, NORTH-CENTRAL BAFFIN ISLAND, NUNAVUT

G.D. Jackson

2000

©Her Majesty the Queen in Right of Canada, 2000
Catalogue No. M46-440E
ISBN 0-660-17902-4

Available in Canada from
Geological Survey of Canada offices:

601 Booth Street
Ottawa, Ontario K1A 0E8

3303-33rd Street N.W.
Calgary, Alberta T2L 2A7

101-605 Robson Street
Vancouver, B.C. V6B 5J3

A deposit copy of this publication is also available for reference
in selected public libraries across Canada

Price subject to change without notice

Cover illustration

View northwest at Mary River number 1 iron deposit, which rises about 500 m above low ground to the southwest and dips easterly. The deposit, in Mary River Group iron-formation (Mif, Amif), is 2.5 km long with calculated reserves of about 133 million tonnes of lump ore averaging 68.2% iron as hematite and/or magnetite, and 1% impurities, chiefly silica. The mottled area on the lower left slope is a megabreccia in map unit Agn (*see* text and Fig. 18). The inset photo shows folded magnetite bands invaded and partially assimilated by migmatitic pink granite (map unit Ag) east of number 4 iron deposit, 27 km northwest of number 1 deposit (*see* Fig. 39a). Large photograph courtesy of R. Von Guttenberg, Strathcona Mineral Services; inset photograph by G.D. Jackson; GSC 204194-X

Critical reviewers

J.B. Henderson
T. Frisch

Author's address

G.D. Jackson
Geological Survey of Canada
615 Booth Street
Ottawa, Ontario
K1A 0E9

Original manuscript submitted: 1992-07
Final version approved for publication: 1993-01

CONTENTS

- 1 Abstract
- 2 Résumé
- 3 Summary/Sommaire
- 15 Introduction
  - 15 Location, access, and habitation
  - 17 Wildlife and vegetation
  - 17 Climate
  - 17 Physiography
  - 21 Quaternary geology
  - 24 Previous bedrock studies
    - 24 Early explorations
    - 25 Recent studies
    - 27 Mineral explorations
  - 29 Present investigations
  - 32 General geology
  - 33 Acknowledgments
- 36 Archean
  - 36 Foliated monzogranite and granodiorite, nebulitic migmatite (Agn)
  - 42 Nebulitic granitic migmatite (Amn)
  - 48 Foliated monzogranite-granodiorite (gr-Agr)
  - 52 Mafic dykes and sills (b)
  - 55 Mary River Group (M, AM)
    - 55 General description
    - 56 Correlations
    - 57 Aeromagnetic pattern
    - 57 Contact relations
    - 59 Stratigraphy
    - 59 Metapelite-amphibolite unit
    - 66 Quartz-rich unit (Mq: 0 to >590 m)
    - 70 Felsic metavolcanics (Ma)
    - 72 Iron-formation (Mif, AMif)
    - 86 Classification and origin of the iron-formation
    - 92 Metasediments (Ms)
    - 96 Mafic metavolcanics (Mb, AMb)
    - 100 Metamorphosed ultramafic rocks (Mu, Amu)
    - 106 Metagabbro (Mg, AMb)
    - 108 Meta-anorthosite (Mn)
    - 109 Origin of igneous rocks (Ma, Mb, Mg, Mu, Mn)
    - 110 Age of the Mary River Group (M, AM)
    - 111 Origin of the Mary River Group
  - 111 Porphyritic monzogranite-granodiorite (Agp)
- 115 Aphebian and/or Archean
  - 115 Homogeneous quartz-biotite-feldspar gneiss (bg)
  - 116 Paragneiss, lit-par-lit gneiss (sv)
  - 116 Undifferentiated gneisses, mixed rocks (mu)
- 116 Aphebian
  - 116 Piling Group
    - 116 Regional description
    - 117 Occurrence in map area
    - 118 Stratigraphy
    - 118 Dewar Lakes Formation (ADL, APq)
    - 119 Flint Lake Formation (AFL, APs)
    - 121 Astarte River Formation (APif, APs)

122 Amphibolite, mafic gneiss (APs)
122 Longstaff Bluff Formation (APs)
123 Contact relations
124 Chemistry
124 Age
125 Correlations
125 Origin
126 Banded migmatite (Amg)
133 Porphyroblastic migmatite (Amp)
135 Late granitic intrusions (Ag, Ack)
137 Massive monzogranite (Ag)
139 Charnockites (Ack)
142 Chemistry of Ag, Ack
142 Ages of late massive granitic intrusions (Ag, Ack)
151 Origin of late massive granitic intrusions (Ag, Ack)
151 Neohelikian
151 Bylot Supergroup
151 Introduction
153 Eqalulik Group (NAS, NAB-L, NAB-U)
153 Adams Sound Formation (NAS)
157 Arctic Bay Formation (NAB, NAB-L, NAB-U)
166 Uluksan Group
166 Society Cliffs Formation (NSC)
168 History of Milne Inlet Trough
169 Mackenzie dykes
170 Hadrynian
170 Borden and Franklin diabase dykes (Hg)
175 Early Paleozoic strata
175 Introduction
175 Admiralty Group
175 Gallery Formation (COGA)
178 Turner Cliffs Formation (COTC)
178 Ship Point Formation (OSP)
179 Brodeur Group
179 Baillarge Formation (OBA)
180 Paleogeological setting
180 Cretaceous-Recent (T, KT_4)
180 Rimrock Bed (T)
181 Scott Inlet area (KT_4)
181 Regional geochemistry
181 Major and minor elements
189 Oxygen isotopes
191 Regional geochronology
192 U-Pb zircon and monazite ages
193 Sm-Nd ages
195 Rb-Sr ages
196 K-Ar ages
200 Metamorphism
200 Regional metamorphism
202 Subgreenschist facies
202 Greenschist facies
202 Lower amphibolite facies
202 Upper amphibolite facies
203 Granulite facies (Chiefly Dexterity Granulite Belt)
204 Some P-T considerations

100-03203/

212 Contact metamorphism
213 Summary and conclusions
214 Economic geology
214 Iron
215 Lead-zinc
216 Copper, molybdenum
216 Ultramafic rocks
216 Miscellaneous minerals
217 Gold
217 Carving stone
218 Oil, natural gas
218 Structural geology
218 Archean-Aphebian recumbent folds, nappes
220 Late open folds
221 Archean-Aphebian thrusts, shears
227 Post-Aphebian faults
228 Lineations
229 Tectonic domains
229 Domain 1
229 Domain 2
231 Domain 3: Foxe Fold Belt
234 Domain 4: Dorset Fold Belt
234 Domain 5: Nagssugtoqidian Mobile Belt
234 Domain 6: Cumberland Batholith
234 Domain 7: Northeast Baffin Thrust Belt
235 Domain 8: Borden Basin
235 Regional synthesis
236 Committee Orogen
237 Isortoq Fault Zone, Dexterity Granulite Belt
238 Baffin Orogen
241 Origin of late Aphebian granites
241 Northeast Baffin Thrust Belt
242 Milne Inlet Trough
242 Uplift episodes, crustal thickness
243 Summary
243 References

Appendices

257 1. Weather observations, north-central Baffin Island
259 2. Spectrographic analyses and locations for individual samples from map units
280 3. Some statistical data for spectrographic analyses in Appendix 2 arranged by element
290 4. Mean and median values of spectrographic analyses for map units
296 5. Additional chemistry for Mary River Group and Piling Group iron-formations
300 6. Additional chemistry for Mary River metapelites
301 7. Structural formulae and ratios for selected minerals in iron-formations and metapelites

Tables

34 Table of Formations
26 1. Recent geological studies in and adjacent to the Clyde-Cockburn Land map area
31 2. Layering classification used in the field
31 3. Grain sizes of igneous and metamorphic rocks

31 4. Comparison between classification of rock terms used in maps for the area and terminology used in this memoir
37 5. Stained slab modal analyses for map units with fewer than five analyses
38 6. Statistical summary of stained slab modal analyses
58 7. Generalized stratigraphy of Mary River Group
63 8. Some common prograde mineral assemblages in Mary River Group metapelites
64 9. Analyses of Archean and Proterozoic shales and metapelites
65 10. Average of spectrographic analyses for Mary River Group metapelites and metagreywackes
78 11. Stratigraphy of iron-formation and associated rocks in Mary River iron deposits area
79 12. Some common prograde mineral assemblages in Mary River Group silicate- and silicate-oxide-facies iron-formation
80 13. Some common prograde mineral assemblages in Mary River Group aluminous facies iron-formation
82 14. Analyses of Mary River Group iron "ore" and iron-formation
84 15. Analyses of mineral concentrates from Mary River iron-formation and iron "ore"
86 16. Summary of chemical differences between major iron-formation facies
88 17. Averages and standard deviations for Mary River Group and Piling Group iron-formation and derived mineral concentrates
94 18. Some common prograde mineral assemblages in metasiltstone-metagreywacke, and minor meta-arkose of the Mary River Group
97 19. Some common metamorphic mineral assemblages in Mary River Group mafic metavolcanics
98 20. Analyses of Mary River Group metabasalt and some other mafic rocks
103 21. Regression line constants (y=Mx+b) and statistics for some TiO_2 versus Fe/(Fe+Mg) plots
105 22. Some lower grade metamorphic mineral assemblages in Mary River Group metaultramafics
106 23. Spectrographic analyses of Mary River Group ultramafics compared with other ultramafics
108 24. Some metamorphic mineral assemblages in Mary River Group metagabbro and meta-anorthosite
118 25. Partial sections of lower Piling Group
121 26. Some prograde metamorphic mineral assemblages in the Flint Lake Formation of the Piling Group
123 27. Some prograde metamorphic mineral assemblages in the Longstaff Bluff Formation of the Piling Group
131 28. Most common mineral assemblages for granitic rocks and amphibolites in banded migmatite
139 29. Common mineral assemblages in massive granites and charnockites
143 30. Analyses, CIPW norms, and modal analyses for selected charnockites and granites
145 31. Comparison of average compositions of various granite types with charnockite in map area
148 32. Selected ratios calculated from analyses in Table 30
155 33. Adams Sound Formation element concentrations
157 34. Major lithologies in the Arctic Bay Formation
159 35. Thicknesses for the Arctic Bay Formation
160 36. Sedimentary structures in the Arctic Bay Formation
160 37. Arctic Bay Formation element concentrations
161 38. Major assemblages in Arctic Bay Formation cycles
161 39. Most common Arctic Bay Formation cycles
162 40. Composition of Arctic Bay Formation by units in cycles
162 41. Summary of cycle compositions for Arctic Bay Formation
164 42. Some sedimentation rates for the Bylot Supergroup, and deposition intervals for the Arctic Bay Formation and its average cycle
171 43. Modal analyses of Hadrynian diabases according to swarm
173 44. Mean chemical analyses of Franklin and Borden dykes
176 45. Ordovician faunas identified by T.E. Bolton and G.W. Sinclair
177 46. Paleozoic faunas identified in the field
182 47. Summary of chemical data for Clyde-Cockburn Land map area
184 48. Summary of spectrographic analyses for Clyde-Cockburn Land map units
189 49. Similarity of histograms for eight elements in the indicated map units
189 50. Baffin Island $\delta^{18}O$ determinations
192 51. Zircon U-Pb isotopic ages, Baffin Island
195 52. Rb-Sr isochron age determinations, Baffin Island
199 53. Whole rock and mineral K-Ar ages for the Clyde-Cockburn Land map area
199 54. K-Ar mineral ages for Aphebian rocks exclusive of study area on Baffin Island and on Melville Peninsula
210 55. Summary of P-T estimates, calculations
214 56. Physical characteristics, Mary River high grade iron deposits
215 57. Average analyses in weight per cent for high grade iron deposits, Mary River area
215 58. Analyses of Davis Tube separations for selected samples of iron ore from Mary River Group iron-formation
216 59. Semiquantitative analyses of gypsum and gypsiferous shale, Society Cliffs Formation
217 60. Analyses for base and precious metals

Figures

16 1. Location of map area, geological map coverage, and physiography
17 2. Old Inuit dwelling sites, west side of Adams Island
18 3. NAPL Landsat mosaic of north-central Baffin Island
19 4. Scenic view of Davis Highlands showing thrusts in granitic gneisses in foreground
20 5. Views of nebulitic granitoid gneiss and layered migmatites in 27F and 37E
21 6. The western Baffin Coastal Lowland north of Clyde
21 7. Looking west across Rowley River, Steensby Inlet, and Foxe Plain
22 8. Contrasting views of eastern and western Baffin Upland
22 9. The southeastern Lancaster Plateau and Central Borden Fault Zone
23 10. View southwest across "Sheardown Lake" at Mary River, and Lancaster Plateau from the edge of Baffin Upland
24 11. Selected Quaternary glacial features
25 12. Location and nature of recent geological studies
28 13. Revised geology for the northwest corner of the Clyde-Cockburn Land map area
30 14. Approximate locations of airborne traverse lines
31 15. General classification of some plutonic rocks
36 16. Quartz-alkali feldspar-plagioclase diagram for map unit Agn
in pocket 17. Mineral composition histograms for various rock types
40 18. Views of Mary River No. 1 iron deposit and nearby megabreccia
42 19. Quartz-alkali feldspar-plagioclase and quartz-feldspar-mafics plots for map unit Amn
in pocket 20. Triangular mineral plots for map units in individual map sheets
44 21. Nebulitic granitic gneiss and related rocks illustrating field relationships and local structural features
46 22. Sr versus Ba for map unit Amn
47 23. Rb/Sr errorchron diagram for map units Amn and gr-Agr in the Ayr Lake region
48 24. Quartz-alkali feldspar-plagioclase and quartz-feldspar-mafics plots for unit gr-Agr
49 25. Foliated monzogranite containing an amphibolite inclusion and quartz vein
51 26. Geochemical plots for map unit gr-Agr
52 27. Concordia diagram and U-Pb isotopic ratios for zircons from a foliated tonalite in map unit gr-Agr
53 28. Structural features of deformed amphibolite dykes in gneissic tonalitic rock, banded migmatite, and nebulitic granitoid gneiss

in pocket 29. Mineral composition histograms for the Mary River, Piling, and Eqalulik groups, and for map units b, bg, and **Hg**
60 30. Metaconglomerates in the lower member of the basal metapelite-amphibolite unit of the Mary River Group
61 31. Metamorphosed felsic pyroclastic and volcanic breccia-conglomerate in the basal metapelite-amphibolite unit of the Mary River Group, south of No. 1 iron deposit
61 32. Coarse cordierite in a biotite-rich matrix from the metapelite-amphibolite unit south of No. 1 iron deposit
64 33. Massive, jointed, white to pale pink granite intruding biotite schist and amphibolite, south of No. 1 iron deposit
68 34. Granite-pebble conglomerate in feldspar-mica-quartz schist from the quartz-rich unit southeast of No. 4 iron deposit
71 35. Photomicrographs of metarhyodacite (Ma) of the Mary River Group
73 36. Field relations between iron-formation and associated rocks east of No. 3A iron deposit
74 37. Oxide facies (magnetite) iron-formation, south-central 37G map area
75 38. Triangular plots for modal analyses of iron-formation
76 39. Magnetite ore at No. 4 iron deposit, and hematite ore at No. 2 iron deposit
77 40. Looking northwest at L-shaped Mary River No. 1 iron deposit
79 41. Folded and sheared aluminous iron-formation
92 42. Migmatitic biotite-hornblende paragneiss with minor arkosic paragneiss (SW37H), and amphibolite and paragneiss in an isoclinal fold with a detached granitic block in its core (NE 37E)
95 43. Metamorphosed conglomerate-breccia southeast of No. 1 iron deposit
95 44. Quartz-rich calc-silicate rock (NE 37F) and epidote-hornblende-plagioclase rock (37G)
96 45. Pillowed mafic metavolcanics, and Mary River Group amphibolite with minor paragneiss overlying massive, fractured pink granite along a fault, in the Mary River area (37G), No. 4 iron deposit area
99 46. Jensen cation plots of various felsic, intermediate, mafic, and ultramafic rocks
99 47. Log Ti versus Cr for mafic and ultramafic rocks of the Mary River Group
101 48. TiO_2 versus Zr and Ti/100-Zr-Sr/2 diagrams for various intermediate, mafic, and ultramafic rocks
102 49. TiO_2 versus Zr diagrams for various intermediate to mafic rocks
102 50. TiO_2 versus Fe/(Fe+Mg) diagrams for various intermediate to mafic rocks
103 51. Triangular modal analysis plots for ultramafic rocks
104 52. Dehydration fractures in serpentinite, serpentinite dyke, pyroxenite (enstatite) dyke in serpentinite, and thinly banded ultramafic intrusion in metabasalt
107 53. Leucogabbro and gabbroic anorthosite in the Mary River area (37G)
110 54. Concordia diagram and U-Pb isotopic ratios for zircons from a rhyodacite quartz porphyry (Ma) in the Mary River Group
112 55. Quartz-alkali feldspar-plagioclase and quartz-feldspar-mafic plots for map unit **Agp**
112 56. Foliated, locally deformed porphyritic monzogranite intruded by thin pegmatites (37G)
113 57. Concordia diagram and U-Pb isotopic ratios for zircons from porphyritic foliated monzogranite (37G)
114 58. Geochemical plots for map units **Agp** and **Ack**
120 59. Cave (SE 37E) and isocline (SW 27F) in Flint Lake Formation marble
127 60. Banded migmatite outcropping in "The Mitres", Buchan Gulf (37H)
128 61. Field relationships and structures of migmatite, agmatite, and migmatitic gneiss in map areas 37E and 37H
130 62. Quartz-alkali feldspar-plagioclase and quartz-feldspar-mafic plots for unit **Amg** and leucosome in **Amg**
132 63. Geochemical plots for some granitoid components in migmatites
133 64. Concordia diagram and U-Pb isotopic ratios for zircons from amphibolite and granite in unit **Amg**
134 65. Anatectic Mary River Group biotite paragneiss with potash feldspar porphyroblasts (SE 37F), and porphyroblastic migmatite west of the head of Cambridge Fiord (37H)
135 66. Quartz-alkali feldspar-plagioclase and quartz-feldspar-mafic plots for unit **Amp**
136 67. Field relationships of massive pink granite and pegmatite in the Mary River area (37G), and on Dexterity Island, and at The Bastions, Buchan Gulf (37H)
138 68. Quartz-alkali feldspar-plagioclase, and quartz-feldspar-mafic plots for map unit **Ag**
140 69. Various triangular plots for selected analyses of charnockites and granites
141 70. Quartz-alkali feldspar-plagioclase and quartz-feldspar-mafic plots for map unit **Ack**
141 71. Charnockite (**Ack**) with an inclusion of Mary River Group pyribolite (Mb?) and overlain by banded migmatite (**Amg**)
146 72. Geochemistry of unit **Ag**
146 73. Granite and charnockite analyses shown in selected classification plots
149 74. Plots of selected oxides and elements versus differentiation indices for granite and charnockite analyses
150 75. Plots of selected oxides and elements for some granite and charnockite analyses
152 76. Evolution of the stratigraphic nomenclature of the Bylot Supergroup
in pocket 77. Stratigraphic sections and coarsening-up cycles for Eqalulik and lower Uluksan groups (N 37G)
153 78. Adams Sound Formation resting nonconformably on banded migmatite and the Mary River Group (N 37G)
154 79. Crossbed measurements for the Eqalulik Group (N 37G)
156 80. Arctic Bay strata overlying banded migmatite and the Mary River Group, Paquet Bay area (37G)
157 81. Interlayered shale, siltstone, and quartz arenite of the lower Arctic Bay member
157 82. Lower Arctic Bay strata, interlayered
158 83. Coarsening- and thickening-upward cycles in the AB_2 submember of the lower Arctic Bay member
163 84. Shallowing-up cycle in the upper Arctic Bay member
170 85. Vertical diabase dykes in horizontally banded gneisses
171 86. Branching and en echelon diabase dykes intruding gently folded and downfaulted Arctic Bay strata
172 87. Triangular modal plots for Hadrynian diabases
172 88. TiO_2 versus Fe/(Fe+Mg) for Hadrynian diabase
174 89. Triangular modal plots for selected Hadrynian diabases according to swarm
in pocket 90. Stratigraphic correlations, paleocurrents, and fossil locations for early Paleozoic strata in the Mary River area (W 37G)
177 91. Brownish-pink to white crossbedded quartz arenite of the Gallery Formation (W 37G)
178 92. Thin- to medium-bedded siliciclastic dolostone interbedded with dolomitic quartz sandstone, Turner Cliffs and Ship Point strata (W 37G)
179 93. Nodular, very thin bedded, microcrystalline, grey weathering limestone of the Baillarge Formation (W 37G)
179 94. Receptaculites from the middle of member B of the Baillarge Formation (W 37G)
186 95. Line graphs for various map units showing mean abundances and standard deviations for 11 elements
190 96. Examples of element histograms used to compare map units
197 97. Locations of samples from the map area that have been dated isotopically
198 98. Comparison of isotopic age determinations
201 99. Distribution of metamorphic facies and granitic plutons in the map area
204 100. P-T petrogenetic grid for part of the model system K_2O-Na_2O-FeO-MgO-Al_2O_3-SiO_2-H_2O (KNFMASH)
206 101. Preliminary metamorphic pressures and temperatures for northern Baffin Island
208 102. P-T estimates for the map area and Eqe Bay and Generator Lake areas
219 103. Large-scale folds in banded migmatite (37E-G)
220 104. Large-scale folds and nappes in banded migmatite (37H)
222 105. Large-scale recumbent folds and ductile thrusts and shears in migmatitic rocks (NE 37G, SE 37H, 27F)
224 106. Geology of the No. 4 iron deposit area, Mary River region

225 107. Geology of the Mary River No. 1-3A deposits area
226 108. Stacked nappes, ductile thrusts, and other structural features in migmatitic and nebulitic rocks (27F, 27G, 37G)
228 109. Small-scale shears and plastic deformation in Amn and Amg (37E, 37H)
229 110. Typical thinly banded gneiss with linear fabric in Amg
in pocket 111. Colour shaded relief aeromagnetic anomaly map of the map area
230 112. Tectonic domains, major structural features, and granitic plutons
232 113. Relationship of the features noted in Figure 112 to those in the rest of Baffin Island
in pocket 114. Major lithological and tectonic terranes and fault and shear zones, vicinity of Baffin Island

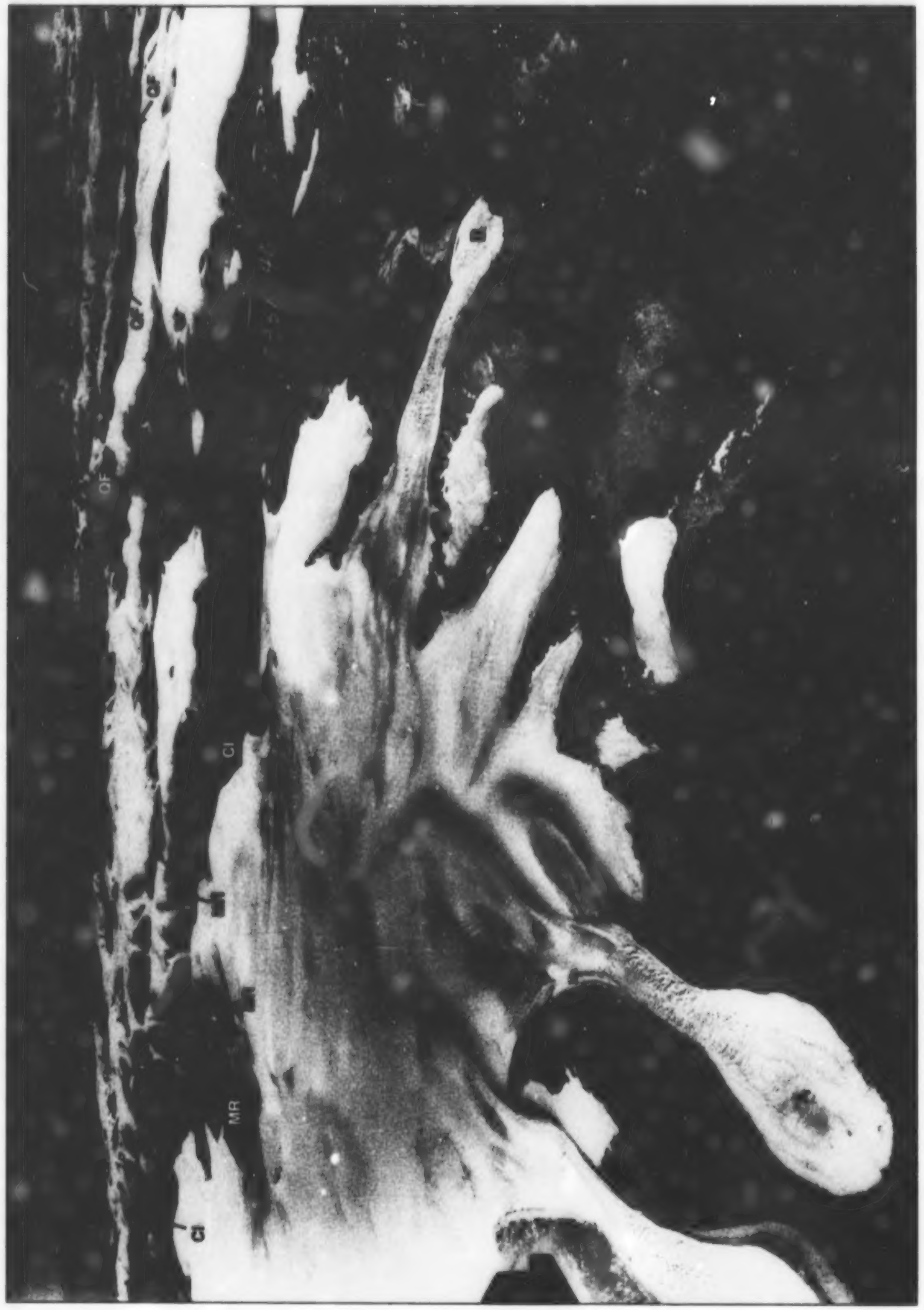

Frontispiece: *View east toward Baffin Bay across the high, incised plateau region of Davis Highlands (NTS 37H) from just south of the head of North Arm in the northeast corner of map area NTS 37G. Elevations to 1370 m above sea level at the mouth of Quernbiter Fiord. Note the damming of valleys by valley glaciers fed from plateau glaciers. The valley glaciers A and B are each about 1.5 km across and they are about 12 km apart. It is 100 km from A to Paterson Inlet (PI). BB – Baffin Bay, BG – Buchan Gulf, BM – Bruce Mountains, CF – Cambridge Fiord, CI – Coutts Inlet, IA – Icy Arm, MR – Mary River Group, PI – Paterson Inlet, QF – Quernbiter Fiord, RS – Royal Society Fiord, TB – The Bastions, TM – The Mitres. National Air Photo Library oblique air photo T235R-40.*

GEOLOGY OF THE CLYDE-COCKBURN LAND MAP AREA, NORTH-CENTRAL BAFFIN ISLAND, NUNAVUT

Abstract

Remnants of a dissected peneplain, tilted up to the northeast, cap low, hummocky to mountainous ice-capped terrane. At least 90% of the map area is an Archean-Aphebian crystalline complex in which at least three episodes of granitic intrusion, each probably accompanied by anatexis, are represented. The oldest recognized major unit is nebulitic granitic migmatite (ca. 3.7-2.85 Ga). The migmatite, foliated granitic intrusions (ca. 2.85 Ga), and deformed amphibolite dykes are overlain unconformably by the Archean Mary River Group (2.74-2.72 Ga), a bimodal greenstone sequence containing komatiite and mafic and ultramafic intrusions. Slightly younger (2.71 Ga) massive monzogranite and late Aphebian granite and charnockite, and the older foliated granitic intrusions represent melts formed from older crust. Most of the granitic intrusions, including the 1.9-1.8 Ga Cumberland Batholith to the south, and the Mary River Group and associated igneous rocks, were emplaced in volcanic arc environments of active continental margins. The charnockites may include both metamorphosed Archean plutons and late synorogenic dry-melt, late Aphebian plutons.

The late Aphebian Piling Group (1.9 Ga) contains a thin lower quartzite-dolostone shelf sequence, and a thick upper greywacke-shale turbidite sequence (with a basal mafic-ultramafic unit) deposited in a foredeep or back arc basin. The Neohelikian Bylot Supergroup (1.27-1.23 Ga) is chiefly fluvial quartz arenite, basinal shale, and shelf dolostone deposited in coarsening- and shallowing-up cycles. Northwest-trending Franklin (723 Ma) diabase dykes have slight chemical differences which may have resulted in selective magnetic overprinting of specific (Borden) dykes. Thin Cambro-Ordovician shelf carbonate and quartz arenite blanket the western margin of the area.

Metamorphic grade ranges from subgreenschist to granulite (about 0.8 GPa, 775°C – 1.1 GPa, 900°C in the Archean-Aphebian complex), but is mostly upper amphibolite facies (0.5-0.6 GPa, 600°-700°C). Two major Archean and one complex major late Aphebian orogenic events are recorded, and most of the mineral assemblages and P-T conditions probably relate to the late Aphebian.

Most of the map area lies across the 2000 km long northeast-trending Archean Committee greenstone-komatiite orogen (2.9-2.7 Ga), which is overprinted by late Aphebian orogenic events centred to the northwest and southeast. The Dexterity Granulite Belt (about 1.82 Ga) and the Isortoq Fault Zone originated in a compressive regime followed by extension and uplift of the Committee Orogen along its southeast margin in the Late Aphebian. The fault zone separates the Committee Orogen from the Foxe Fold Belt to the south. The latter is one of the three coeval fold belts within the Baffin Orogen that rim its core, the 1.9-1.84 Ga Cumberland Batholith. Formation of the Baffin Orogen is related to penecontemporaneous collision of three major crustal blocks to the south. Subsequent collision of a fourth block to the north formed the southeast-trending Northeast Baffin Thrust Belt (ca.1.81 Ga).

Seven of the eight major structural domains recognized in the Committee and Baffin orogens on Baffin Island are represented in the map area. Both orogens extend into Melville Peninsula and western and northwestern Greenland; the Baffin Orogen also extends into northern Quebec-Labrador. Related major shear zones probably include some sutures. The Milne Inlet Trough (domain 8) is the southeast extension of the Neohelikian Borden Rift Basin, which developed as an aulacogen along the western boundary of domain 7 during the opening of the Poseidon Ocean to the northwest.

Large high grade iron deposits occur at Mary River, and smaller ones are present chiefly in the western part of the map area. Lead-zinc mineralization occurs in the Bylot Supergroup along the north edge of the map area and in the Piling Group just south of the map area. Traces of lead-zinc-copper, molybdenum, nickel, silver, and gold occur locally.

Résumé

Des vestiges d'une pénéplaine disséquée, inclinée vers le haut en direction du nord-est, chapeautent un terrain bas, bosselé à montagneux et englacé. Au moins 90 % de la région cartographique est située dans un complexe cristallin archéen-aphébien dans lequel sont représentés au moins trois épisodes d'intrusion granitique, vraisemblablement tous accompagnés d'une anatexie. La plus ancienne unité majeure reconnue est une migmatite granitique nébulitique (3,7-2,85 Ga ?). La migmatite, des intrusions granitiques foliées (2,85 Ga ?) et des dykes d'amphibolite déformés sont recouverts en discordance par le Groupe archéen de Mary River (2,74-2,72 Ga), séquence de roches vertes bimodale renfermant des komatiites et des intrusions mafiques et ultramafiques. Des monzogranites massifs légèrement plus jeunes (2,71 Ga) et des granites et des charnockites de l'Aphébien tardif, ainsi que les intrusions granitiques foliées plus anciennes dérivent de liquides issus d'une croûte plus ancienne. La plupart des intrusions granitiques, y compris le batholite de Cumberland au sud, âgé de 1,9-1,8 Ga, de même que le Groupe de Mary River et les roches ignées associées, ont été mis en place dans des arcs volcaniques de marges continentales actives. Les charnockites dérivent de plutons archéens métamorphisés et/ou de plutons synorogéniques tardifs de fusion sèche datant de l'Aphébien tardif.

Le Groupe de l'Aphébien tardif de Piling (1,9 Ga) contient une mince séquence inférieure de quartzites-dolomies de plate-forme et une épaisse séquence supérieure de turbidites à grauwackes-shales (renfermant à la base une unité mafique-ultramafique) qui ont été déposées dans un bassin d'avant-fosse ou un bassin marginal. Le Supergroupe néohélikien de Bylot (1,27-1,23 Ga) se compose essentiellement d'arénites quartziques fluviales, de shales de bassin et de dolomies de plate-forme déposées au cours de cycles à granocroissance et à exhaussement ascendants. Des dykes de diabase Franklin de direction nord-ouest (723 Ma) présentent de légères différences chimiques qui ont peut-être engendré une surimpression magnétique sélective de dykes spécifiques (Borden). De minces couches cambro-ordoviciennes de carbonates et d'arénites quartziques de plate-forme recouvrent la marge occidentale de la région.

Le degré de métamorphisme varie de faciès inférieurs au faciès des schistes verts au faciès des granulites (env. 0,8 GPa, 775°C-1,1 GPa, 900°C dans le complexe archéen-aphébien), le sous-faciès supérieur des amphibolites (0,5-0,6 GPa, 600°-700°C) étant dominant. Deux épisodes orogéniques archéens majeurs et un événement orogénique complexe majeur de l'Aphébien tardif ont été observés; la plupart des assemblages minéraux et des conditions de P-T sont vraisemblablement liés à l'Aphébien tardif.

La plus grande partie de la région cartographique recouvre l'orogène archéen de 2 000 km de longueur, de direction nord-est et à roches vertes-komatiites de Comité (2,9-2,7 Ga), lequel est surimprimé par des épisodes orogéniques de l'Aphébien tardif centrés au nord-ouest et au sud-est. La ceinture granulitique de Dexterity (env. 1,82 Ga) et la zone de failles d'Isortok résultent d'un régime compressif suivi d'une extension et du soulèvement à l'Aphébien tardif de l'orogène de Comité le long de sa marge sud-est. La zone de failles sépare l'orogène de Comité de la zone de plissement de Foxe au sud. Cette dernière constitue une de trois ceintures de plissement contemporaines situées au sein de l'orogène de Baffin et qui bordent son noyau, le batholite de Cumberland, âgé de 1,9 à 1,84 Ga. La formation de l'orogène de Baffin est liée à la collision pénécontemporaine au sud de trois importants blocs crustaux. La collision ultérieure d'un quatrième bloc au nord s'est traduite par la formation de la zone de chevauchement de direction sud-est du Nord-est de Baffin (env. 1,81 Ga ?).

Les orogènes de Comité et de Baffin contiennent sept des huit domaines structuraux reconnus dans l'île de Baffin et se prolongent tous deux dans la presqu'île de Melville et l'ouest et le nord-ouest du Groenland. L'orogène de Baffin se prolonge aussi dans le nord du Québec-Labrador. D'importantes zones de cisaillement apparentées comprennent probablement des sutures. La fosse de l'inlet Milne (domaine 8) est l'extension sud-est du bassin d'effondrement néohélikien de Borden, qui est apparu sous forme d'aulacogène le long de la limite ouest du domaine 7 pendant l'ouverture de l'océan Poséidon.

On trouve de vastes gisements de fer à haute teneur à Mary River, ainsi que des gisements plus petits surtout dans la partie occidentale de la région cartographique. Des minéralisations de plomb-zinc sont présentes dans le Supergroupe de Bylot, le long de la bordure nord de la région cartographique, et dans le Groupe de Piling juste au sud de la région cartographique. Des traces de plomb-zinc-cuivre, de molybdène, de nickel, d'argent et d'or apparaissent localement.

SUMMARY

The Clyde-Cockburn Land map area covers 82 000 km^2 of north-central Baffin Island. The settlement of Clyde River lies near the mouth of Clyde Inlet on the east side. The map area lies in the largest of three large Mesozoic-Cenozoic fault blocks which make up Baffin Island. The three blocks are each uplifted toward the northeast, their surfaces being remnants of a dissected peneplain. Physiography ranges from the rugged beauty of the eastern fiords and mountains to monotonous coastal lowlands. Quaternary glacial events have been traced from about two million years ago to the Little Ice Age 450-100 years ago.

At least 90% of the map area is underlain by an Archean-Aphebian crystalline complex composed of granitic to intermediate gneisses, granitic and charnockitic plutons, early mafic dykes, and metamorphosed supracrustal sequences with associated felsic, mafic, and ultramafic rocks. Metamorphic grade in the complex ranges from subgreenschist to granulite (low to medium pressure), but is mostly upper amphibolite. Primary layering and foliations are variable, although individual structural domains are each characterized by a predominant trend.

Neohelikian strata, partially in subgreenschist facies, are restricted to the northwest corner of the map area. Northwest-trending Hadrynian diabase dykes occur throughout, and may include a few Neohelikian dykes. Unmetamorphosed early Paleozoic strata cover the western edge of the map area and Paleogene strata outcrop locally northwest of the Barnes Ice Cap.

Major units in the crystalline complex are nebulitic granitic migmatite or nebulite (25% – most abundant in the southeast), foliated monzogranite-granodiorite (18% – most abundant in the northwest), and banded migmatite (40% – most abundant in the southeast, south, and north-central). Contacts between all three major units range from sharply discordant to gradational.

Nebulite and foliated granite-granodiorite are similar overall but differ in detail. Both are mostly feldsparphyric granite-granodiorite although the former is bimodal, containing considerable tonalitic gneiss. Both units generally contain less than 15% mafic minerals, chiefly biotite. Nebulite is faintly banded and is characterized by a wispy to streaky appearance, abundant nebulitic schlieren and other remnants of various lithologies, and by extremely complex small-scale folding called "wildfolding" by other researchers. Banding, nebulitic schlieren, and remnants are minor and more diffuse in the uniformly foliated granite-granodiorite.

SOMMAIRE

La région cartographique de Clyde-Cockburn couvre 82 000 km² de la partie centre-nord de l'île de Baffin. La localité de Clyde River est sise à proximité de l'embouchure de l'inlet Clyde, sur la rive est. La région cartographique est située dans le plus étendu des trois vastes blocs faillés mésozoïques-cénozoïques qui constituent l'île de Baffin. Ces trois blocs sont tous relevés vers le nord-est, leurs surfaces constituant les vestiges d'une pénéplaine disséquée. La topographie varie de la beauté accidentée des fjords et des montagnes de l'est à la monotonie des basses terres côtières. Les événements glaciaires quaternaires ont été retracés à partir d'il y a environ deux millions d'années jusqu'au Petit âge glaciaire d'il y a 450-100 années.

Au moins 90 % de la région cartographique recouvrent un complexe cristallin archéen-aphébien composé de gneiss granitiques à intermédiaires, de plutons granitiques et charnockitiques, de dykes mafiques précoces et de séquences supracrustales métamorphisées accompagnées de roches felsiques, mafiques et ultramafiques. Le degré de métamorphisme du complexe varie des faciès inférieurs au faciès des schistes verts aux granulites (pression faible à moyenne), le sous-faciès supérieur des amphibolites étant dominant. La stratification et les foliations primaires sont variées; cependant, les domaines structuraux individuels sont tous caractérisés par une direction dominante.

Les strates néohélikiennes, qui appartiennent en partie à des faciès inférieurs au faciès des schistes verts, ne sont présentes que dans le coin nord-ouest de la région cartographique. Des dykes de diabase hadryniens de direction nord-ouest apparaissent dans l'ensemble de la région, dont quelques-uns sont peut-être néohélikiens. Des strates non métamorphisées du Paléozoïque précoce couvrent la bordure ouest de la région cartographique et des strates paléogènes affleurent localement au nord-ouest de la calotte glaciaire de Barnes.

Les principales unités du complexe cristallin sont des migmatites granitiques nébulitiques ou des nébulites (25 % – concentrées au sud-est), des monzogranites-granodiorites foliés (18 % – concentrés au nord-ouest) et des migmatites rubanées (40 % – concentrées au sud-est, au sud et au centre-nord). Les contacts entre ces trois grandes unités varient de nettement discordants à progressifs.

Les nébulites et les granites-granodiorites foliés sont dans l'ensemble semblables mais diffèrent dans le détail. Les deux unités sont composées essentiellement de granites-granodiorites à phénocristaux de feldspath, mais les premières sont bimodales car elles contiennent une proportion considérable de gneiss tonalitiques. Les deux renferment en général moins de 15 % de minéraux mafiques, essentiellement de la biotite. Les nébulites sont faiblement rubanées et se caractérisent par leur aspect vaporeux à rayé, par une abondance de schlierens nébulitiques et d'autres vestiges de lithologies diverses et par des plissements à petite échelle extrêmement complexes nommés «*wildfolding*» [«plissotement débridé»] par Kranck (1955) et d'autres. Le rubanement, les schlierens nébulitiques et les reliquats sont peu abondants et plus diffus dans les granites-granodiorites, qui sont uniformément foliés.

Nebulite and foliated granite-granodiorite are chemically more similar to one another, to the leucosome in banded migmatite, and to the charnockitic rocks than to other granitic rocks, but also have significant differences. Chemically, nebulites most resemble S-type and volcanic arc granitic rocks. They contain small, late, massive hornblende granite intrusions that may represent fused nebulite. Chemically, foliated granite-granodiorite most closely resembles arc granites from active continental margins and peraluminous I-type granites with relatively high differentiation indices. One U-Pb zircon age of 2851 +20/-27 Ma and several Nd T_{DM} model ages of 3.10-2.85 Ga have been obtained for the foliated granite-granodiorite unit. Nd T_{DM} model ages of 3.7-2.98 Ga have been obtained for nebulite; and Rb-Sr isochron data indicate old inheritance (>2.9 Ga).

The nebulite in general may be older than the foliated and massive granitic rocks, some of which intrude nebulite and may have formed during an early anatexis prior to deposition of the Archean Mary River Group. Although the nebulite locally includes highly deformed intrusions, it contains significantly more felsic metavolcanics and quartzofeldspathic metasediments than does the foliated granitic unit. The paucity of aluminosilicate minerals and garnet in both units suggests that the metasediments were deposited with a minimum of chemical decomposition. Most of the foliated granitic unit consists of thoroughly recrystallized and deformed intrusions emplaced in a calc-alkaline volcanic arc of an active continental margin, probably at about 2.85 Ga. Much of the nebulite may also have been formed then.

Banded migmatites form the most ubiquitous unit in the map area, comprising a complex of variously interlayered and intermixed rocks representing remnants of all the map units in the Archean-Aphebian complex. Concordant and crosscutting granitic rocks of several ages form the bulk of the unit. The older granitic rocks in the banded migmatite unit are mostly tonalite whereas the younger granitic components are mostly syenogranite-granodiorite. Modal plots illustrate the bimodal distribution of the tonalites and granites. Chemically, the banded migmatites most closely resemble the nebulite. The younger granitic rocks are most similar to volcanic arc I-type granites. Most components probably range in age from 2.9-1.8 Ga. Older components were overprinted by 2.1-1.8 Ga deformation, metamorphism, and granitic emplacement.

Chemically, remnants of mafic igneous rocks in nebulite and banded migmatite, and similar rocks in the Mary River Group, differ only in part. TiO_2 versus Fe/(Fe+Mg) diagrams show a different field and differentiation trend for mafic rocks in the nebulite than for mafic rocks in banded migmatite and in the Mary River Group. A cation plot for mafic rocks in nebulite and banded

Les nébulites et les granites-granodiorites foliés sont chimiquement plus semblables les uns aux autres, au leucosome des migmatites rubanées et aux roches charnockitiques qu'aux autres roches granitiques, mais elles présentent également d'importantes différences. Chimiquement, les nébulites ressemblent surtout aux roches granitiques du type S et d'arc volcanique. Elles contiennent de petites intrusions massives et tardives de granite à hornblende issues peut-être de nébulites fondues. En revanche, les granites-granodiorites foliés ressemblent surtout sur le plan chimique aux granites d'arc des marges continentales actives et aux granites hyperalumineux du type I présentant des indices de différenciation relativement élevés. Une datation par la méthode de l'U-Pb du zircon (2 851 +20/-27 Ma) et plusieurs datations modélisées par la méthode du Nd T_{DM} (3,10-2,85 Ga) ont été obtenues pour l'unité foliée de granites-granodiorites. Des datations modélisées par la méthode du Nd T_{DM} (3,7-2,98 Ga) ont été obtenues pour les nébulites; des données d'isochrones Rb-Sr indiquent en outre la présence de matériaux plus anciens (>2,9 Ga).

Les nébulites sont peut-être plus anciennes en général que les roches granitiques foliées et massives, dont certaines sont injectées dans les nébulites et ont peut-être été formées au cours d'une anatexie précoce avant le dépôt du Groupe archéen de Mary River. Bien que les nébulites renferment localement des intrusions très déformées, elles contiennent beaucoup plus de métavolcanites felsiques et de métasédiments quartzofeldspathiques que l'unité granitique foliée. La pauvreté des deux unités en minéraux aluminosilicatés et en grenat donne à penser que les métasédiments ont été déposés avec une décomposition chimique minimale. La plus grande partie de l'unité granitique foliée se compose d'intrusions largement recristallisées et déformées mises en place dans un arc volcanique calco-alcalin de marge continentale active, probablement à environ 2,85 Ga. Une bonne partie des nébulites a peut-être également été formée à cette époque.

Les migmatites rubanées constituent l'unité la plus étendue de la région cartographique; elles se composent d'un complexe de roches diversement interstratifiées et mélangées comportant des vestiges de toutes les unités cartographiques du complexe archéen-aphébien. Des roches granitiques concordantes et transverses d'âges divers constituent l'essentiel de l'unité. Les roches granitiques les plus anciennes de l'unité de migmatites rubanées sont constituées surtout de tonalites, les composantes granitiques plus jeunes étant composées pour l'essentiel de syénogranites-granodiorites. Les tracés modaux illustrent la distribution bimodale des tonalites et des granites. Chimiquement, les migmatites rubanées ressemblent surtout aux nébulites; les roches granitiques plus jeunes ressemblent surtout aux granites du type I d'arc volcanique. L'âge de la plupart des composantes varie probablement de 2,9 à 1,8 Ga. Les composantes plus anciennes ont été surimprimées par des déformations, un métamorphisme et la mise en place de granites à 2,1-1,8 Ga.

En termes chimiques, les vestiges de roches ignées mafiques dans les nébulites et les migmatites rubanées et des roches semblables dans le Groupe de Mary River ne diffèrent que partiellement. Les diagrammes du TiO_2 en fonction de Fe/Fe+Mg présentent des tendances de champ et de différenciation différentes dans les roches mafiques des nébulites et dans celles des migmatites rubanées et du Groupe de

migmatite, and felsic metavolcanics in nebulite yields a continuous pattern in the calc-alkaline-tholeiitic field. Mary River Group metamorphosed mafic and felsic volcanics, however, plot in separate fields, suggesting that they may represent different magma sources. Therefore, the mafic rocks in nebulite may be different and older than those in the Mary River Group.

Swarms of early, variously deformed and metamorphosed amphibolite-pyribolite dykes and sills are most abundant in nebulite, occur locally in banded migmatite, and are not known to intrude the late Archean Mary River Group and younger rocks. The distribution suggests that although they are concentrated in three northwest-trending belts, individual dykes trend predominantly east to east-northeast, and may represent three east-northeast-trending swarms.

The Mary River Group forms 5% of the bedrock, occurs in lenticular bodies throughout the map area, and is concentrated in a large arc, concave to the west, that passes through the Dexterity Granulite Belt in the western part of the map area. Only two isolated occurrences are known in the southeast (NTS 27E, F). Mary River strata nonconformably overlie nebulite, foliated granite-granodiorite, and early mafic dykes, and locally may be separated from them by a metamorphosed regolith and a megabreccia (clasts to 275 m). The group is composed chiefly of metamorphosed mafic and felsic volcanics, pelites, and greywackes. Quartzite, iron-formation, ultramafic rocks, and anorthositic and gabbroic intrusions are common. Conglomerate, breccia lenses, and disconformities occur locally; marble is rare. Primary features include bedding, crossbeds, graded beds, channels, conglomerates and breccias, slumps, pillows, and spinifex texture. Estimated preserved thicknesses are as much as 4000 m. The variability of the stratigraphy is due mostly to volcanism, and to folding and faulting. Metasedimentary units commonly occur in the following ascending order: metapelites with mafic metavolcanics and boulder conglomerate lenses (0 to >167 m); quartz-rich unit (0 to >590 m); iron-formation (0 to >195 m); and metapelite-metagreywacke (about 150 to 840 m).

Metasiltstone and metagreywacke occur mostly above the iron-formation and are probably the most abundant metasediments in the Mary River Group. Metapelites and minor meta-arkose are generally interbedded with them, and metapelites are also abundantly intercalated with other lithologies. Metaconglomerate, metabreccia, metatuff, and calcite-diopside beds occur locally. The most common mafic minerals in the metapelite-metagreywacke strata are: biotite, chlorite, muscovite, and garnet. Cordierite, andalusite, sillimanite, and staurolite

Mary River. Un tracé cationique de Jensen (1976) des roches mafiques des nébulites et des migmatites rubanées et des métavolcanites felsiques des nébulites met en évidence un motif continu dans le champ calco-alcalin-tholéiitique. Toutefois, les volcanites mafiques et felsiques métamorphisées du Groupe de Mary River apparaissent dans des champs différents, ce qui laisse supposer qu'elles sont peut-être issues de sources magmatiques différentes. Il est donc possible que les roches mafiques des nébulites diffèrent de celles du Groupe de Mary River et qu'elles soient plus anciennes que ces dernières.

Des essaims de dykes et de sills précoces d'amphibolite-pyribolite inégalement déformés et métamorphisés sont présents préférentiellement dans les nébulites et apparaissent localement dans les migmatites rubanées; ils n'ont pas été observés dans le Groupe de l'Archéen tardif de Mary River et dans les roches plus jeunes. Leur répartition indique que malgré qu'ils soient concentrés dans trois ceintures de direction nord-ouest, les dykes individuels sont orientés en général vers l'est-nord-est et appartiennent peut-être à trois essaims de direction est-nord-est.

Le Groupe de Mary River constitue 5 % du substratum rocheux, se présente en corps lenticulaires dans l'ensemble de la région cartographique et est concentré dans un vaste arc concave vers l'ouest passant à travers la ceinture granulitique de Dexterity dans la partie occidentale de la région cartographique. Seules deux occurrences isolées sont connues dans le sud-est (NTS 27E, F). Les strates de Mary River reposent en discordance sur des nébulites, des granites-granodiorites foliés et des dykes mafiques précoces; elles sont localement séparées de ces roches par un régolithe métamorphisé et une mégabrèche (clastes atteignant 275 m). Le Groupe comprend essentiellement des volcanites mafiques et felsiques, des pélites et des grauwackes métamorphisés. On trouve couramment des quartzites, des formations ferrifères, des roches ultramafiques et des intrusions anorthositiques et gabbroïques. Des conglomérats, des lentilles bréchiques et des discordances érosionelles apparaissent localement ainsi que, rarement, des marbres. Parmi les figures primaires on compte des stratifications, des stratifications obliques, des couches granoclassées, des chenaux, des conglomérats et des brèches, des glissements synsédimentaires, des coussins et des textures spinifex. On estime que les épaisseurs conservées atteignent 4 000 m. La diversité de la stratigraphie est due surtout au volcanisme et à l'action des plissements et des mouvements de cassure. Les unités métasédimentaires se présentent en général selon l'ordre ascendant suivant : des métapélites comprenant des métavolcanites mafiques et des lentilles de conglomérats de blocs (0 à >167 m); une unité riche en quartz (0 à >590 m); une formation ferrifère (0 à >195 m); et des métapélites-métagrauwackes (environ 150 à 840 m).

Les métasiltstones et métagrauwackes apparaissent surtout au-dessus de la formation ferrifère et constituent vraisemblablement les métasédiments les plus abondants du Groupe de Mary River. Les métapélites et une quantité mineure de métaarkoses sont généralement interstratifiées avec eux; les métapélites s'intercalent fréquemment dans d'autres unités lithologiques. On trouve localement des métaconglomérats, des métabrèches, des métatufs et des lits de calcite-diopside. Les minéraux mafiques les plus communs des strates de métapélite-métagrauwacke sont la biotite, la chlorite, la

are also abundant in the metapelites. Most of the metasiltstone-metagreywacke strata are turbidites, and associated metaconglomerate-metabreccia lenses were developed locally in response to rifting, erosion of basement rocks, and explosive volcanism.

Comparison of the metapelite chemistry with that of metapelites in the late Aphebian Piling Group, Neohelikian Arctic Bay Formation, and elsewhere agrees with the conclusions of others that ferrous oxide exceeds ferric oxide in the Archean compared to the reverse for younger rocks. This may be related to differences in oxygen content of the atmosphere. Most pelites show a slight decrease in total Fe and Na with decreasing age; whereas Na in metapelites within the map area conform with this trend, the Fe does not. Concentrations of CaO, CO_2, and Sr in the metapelites are low compared with some other Archean pelites. Many chemical differences probably represent factors other than secular changes. The metapelites were deposited in a variety of environments in interconnected marine depressions formed by volcanism.

The quartz-rich unit is commonly the lowermost unit of the Mary River Group, but is absent in several areas. The lower feldspar-mica-quartz paraschist member includes minor quartz- and granite-clast conglomerate lenses and locally may include a regolith and sheared basement gneisses. The upper member is mostly fuchsite-bearing metaorthoquartzite with considerable arkosic strata, and some metachert in its upper part. The change upward from conglomeratic schist to clastic metaorthoquartzite and metachert suggests marine transgression and deepening water during sedimentation.

Conformable, thin bedded iron-formation (maximum ca. 195 m) occurs in most areas underlain by the Mary River Group at one or two horizons below the middle of the group. Five main intergradational facies are dominated by oxide facies strata which predominate in the lower part of the iron-formation. Rare red jasper and granule-like shapes are restricted to siliceous beds in this facies. The oxide facies contains several generations of high grade magnetite and/or hematite zones that occur mostly in oxide facies strata and in the Mary River area, are mostly postsedimentation and premetamorphic. The No. 1-3A deposits at Mary River are postmetamorphic. Silicate, silicate-oxide, and aluminous facies are interbedded with oxide facies in the upper part of the iron-formation. Thin carbonate iron-formation occurs locally. Most of the iron-formation consists of quartz beds rhythmically interbedded with magnetite- and/or hematite-rich beds in oxide facies; cummingtonite-rich or hypersthene-rich (granulite grade) beds in silicate facies; alternating oxide- and Mg-Fe-silicate-rich beds in silicate-oxide facies; and cordierite, cordierite-quartz, and anthophyllite, garnet, biotite, and magnetite beds in aluminous facies with cummingtonite-sillimanite occurring instead of hypersthene in the granulite grade rocks. Carbonate facies iron-formation is mostly parankerite with variable calcite, and silicates. Rare sulphide facies is associated mostly with oxide facies.

The chemistry of minor elements in high grade iron deposits is similar to that of the oxide facies. Trace elements (Ti, S, V, Y, Zr, Cr, Ba) are most abundant in the aluminous facies. Of the coexisting minerals analyzed, magnetite and cummingtonite probably have the most similar trace element patterns. With increasing metamorphic grade, the proportion of Fe_2O_3 increases from anthophyllite schist to grunerite schist to ferrohypersthene gneiss. Also, sheared high grade iron deposits are invariably specularite, which suggests that the degree of oxidation may have increased during metamorphism. Positive Eu anomalies have been obtained for the Mary River iron-formation. Mary River Group iron-formation is typical of the Algoma-type. The oxide, silicate, and carbonate facies are mostly chemical strata whereas the aluminous facies is a mixture of chemical and clastic sediments. Chemical facies were probably derived from both weathering and hydrothermal-exhalative processes related to volcanism. There were probably no large-scale compositional changes in the iron-formation during diagenesis and metamorphism other than the loss of H_2O and CO_2, with concomitant modification of minor and trace elements.

Metarhyolites-metarhyodacites of the Mary River Group contain less Al, La, Ni, and Sr than older felsic metavolcanics. Both Archean felsic volcanics and intrusions contain more Ti, Fe, Cu, V, and Zr than Aphebian felsic intrusions.

Various chemical plots indicate that Mary River Group mafic metavolcanics range from high iron tholeiites to basaltic and probably ultramafic komatiites. Most of the ultramafic rocks in the map area, however, are intrusions and are chemically similar to alpine ultramafics and Al-depleted komatiites. Mary River Group metabasalts and metagabbros plot in the calc-alkaline and rift basalt field on a previously published TiO_2 versus Zr diagram. Metamorphosed basalts, gabbros, ultramafics, and anorthosite in the map area plot as part of a continuous series, and are chemically different from equivalent rocks in the nebulites. Mary River felsic and mafic metavolcanics, however, are bimodal.

The Mary River Group was probably deposited in a rift-related unstable environment in a calc-alkaline to tholeiitic volcanic arc on a continental margin. Generally, basalts were extruded first, followed by ultramafic intrusions and extrusions, and then gabbros and cumulate

muscovite et le grenat. Les métapélites contiennent fréquemment de la cordiérite, de l'andalousite, de la sillimanite et de la staurotide. La plupart des strates de métasiltstone-métagrauwacke sont des turbidites; les lentilles associées de métaconglomérat-métabrèche ont été formées localement à la suite de mouvements de distension, de l'érosion des roches du socle et d'un volcanisme explosif.

La comparaison de la chimie des métapélites avec celle des métapélites du Groupe de l'Aphébien tardif de Piling, de la Formation néohélikienne d'Arctic Bay et d'ailleurs va dans le sens de la conclusion d'autres auteurs (p. ex., Pettijohn, 1975) selon laquelle l'oxyde ferreux était plus abondant pendant l'Archéen que l'oxyde ferrique, l'inverse étant vrai pour les roches plus récentes. Cela peut tenir à des différences de concentration d'oxygène dans l'atmosphère. La plupart des pélites présentent une légère diminution du Fe et du Na total parallèlement à la diminution de l'âge; si le Na des métapélites de la région cartographique se conforme à cette tendance, il n'en va pas ainsi du Fe. Les concentrations de CaO, de CO_2 et de Sr des métapélites sont faibles comparées à celles de certaines autres pélites archéennes. De nombreuses différences chimiques traduisent probablement des facteurs autres que des changements séculaires. Les métapélites ont été déposées dans des milieux divers de dépressions marines communicantes d'origine volcanique.

L'unité riche en quartz constitue généralement l'unité inférieure du Groupe de Mary River, mais dans de nombreuses régions elle est absente. Le membre inférieur de paraschistes à feldspath-mica-quartz comprend, en quantités mineures, des lentilles de conglomérats à clastes de quartz et de granite et, par endroits, un régolithe et des gneiss de socle cisaillés. Le membre supérieur est composé essentiellement de métaorthoquartzite à fuchsite comprenant une quantité considérable de strates arkosiques et, dans sa partie supérieure, des métacherts. La transition ascendante des schistes conglomératiques aux métaorthoquartzites clastiques et aux métacherts évoque une transgression marine et l'approfondissement de l'eau au cours de la sédimentation.

Dans la plupart des régions où affleure le Groupe de Mary River, une formation ferrifère concordante en lits minces (maximum env. 195 m) est présente un ou deux horizons au-dessous du milieu du groupe. Cinq des principaux faciès interstratifiés sont dominés par des strates à faciès oxyde qui prédominent dans la partie inférieure de la formation ferrifère. Du jaspe rouge et des configurations granulaires n'apparaissent que rarement, et uniquement dans les lits siliceux de ce dernier faciès. Celui-ci renferme plusieurs générations de zones de magnétite et/ou d'hématite à haute teneur apparaissant surtout dans les strates à faciès oxyde et dans la région de Mary River; ces zones sont pour l'essentiel post-sédimentaires et prémétamorphiques. Les gisements No 1-3A à Mary River sont post-métamorphiques. Dans la partie supérieure de la formation ferrifère, des faciès silicatés, à silicates-oxydes et alumineux sont interstratifiés avec des faciès oxyde. Une mince formation carbonatée est présente localement. L'essentiel de la formation ferrifère est constitué de couches quartzeuses interstratifiées rythmiquement avec des couches riches en magnétite et/ou hématite dans le faciès oxyde; de couches riches en cummingtonite ou en hypersthène (faciès granulitique) dans le faciès silicaté; de couches alternativement riches en oxydes et en silicates à Mg et Fe dans le faciès silicate-oxyde; et de couches à cordiérite, à cordiérite-quartz et à anthophyllite, grenat, biotite et magnétite dans le faciès alumineux, la cummingtonite-sillimanite remplaçant l'hypersthène dans les roches de faciès granulitique. La formation ferrifère à faciès carbonaté est composée essentiellement de parankérite et de quantités variables de calcite, ainsi que de silicates. Un faciès sulfuré, qui n'apparaît que rarement, est associé surtout au faciès oxyde.

La chimie des éléments mineurs des gisements de fer à haute teneur est semblable à celle du faciès oxyde. Les éléments-traces (Ti, S, V, Y, Zr, Cr, Ba) abondent en particulier dans le faciès alumineux. Parmi les minéraux coexistants analysés, la magnétite et la cummingtonite présentent vraisemblablement les motifs d'éléments-traces les plus semblables. Corrélativement à l'accroissement du degré de métamorphisme, la proportion de Fe_2O_3 s'accroît en passant du schiste à anthophyllite au schiste à grunérite et au gneiss à ferrohypersthène. Les gisements cisaillés à haute teneur en fer contiennent dans tous les cas de l'hématite spéculaire, ce qui laisse supposer que le degré d'oxydation s'est accru au cours du métamorphisme. Des anomalies positives en Eu ont été relevées dans la formation ferrifère de Mary River. La formation ferrifère du Groupe de Mary River est représentative du type Algoma. Les faciès oxyde, silicate et carbonate sont essentiellement des strates chimiques, alors que le faciès alumineux est un mélange de sédiments chimiques et clastiques. Les faciès chimiques sont vraisemblablement issus de l'altération et de processus hydrothermaux-exhalatifs liés au volcanisme. Il n'y a probablement pas eu de changements de composition à grande échelle dans la formation ferrifère au cours de la diagénèse et du métamorphisme, exception faite de la perte de H_2O et de CO_2 et des modifications parallèles de concentration d'éléments mineurs et traces.

Les métarhyolites-métarhyodacites du Groupe de Mary River contiennent moins de Al, La, Ni et Sr que les autres métavolcanites felsiques. Les volcanites et intrusions felsiques archéennes contiennent plus de Ti, Fe, Cu, V et Zr que les intrusions felsiques aphébiennes.

Divers tracés chimiques (p. ex. Jensen, 1976) indiquent que les métavolcanites mafiques du Groupe de Mary River varient de tholéiites très ferrifères à des komatiites basaltiques et probablement ultramafiques. Cependant, la plupart des roches ultramafiques de la région cartographique sont intrusives et sont chimiquement semblables à des ultramafites alpines et à des komatiites appauvries en Al. Les métabasaltes et métagabbros du Groupe de Mary River s'inscrivent dans le champ calco-alcalin et des basaltes de rift sur le diagramme TiO_2-Zr de Condie (1985). Les basaltes, gabbros, ultramafites et anorthosites métamorphisés de la région cartographique décrivent une série continue partielle et diffèrente chimiquement des roches équivalentes dans les nébulites. Les métavolcanites felsiques et mafiques de Mary River sont toutefois bimodales.

Le Groupe de Mary River a vraisemblablement été déposé dans un environnement instable lié à un rift dans un arc volcanique calco-alcalin à tholéiitique sur une bordure continentale. En général, les basaltes ont été émis en premier, suivis d'intrusions et d'extrusions ultramafiques, de gabbros et

porphyritic anorthosites. Deposition of the iron-formation was in deep water, probably during an interval of relatively widespread stability, in several extensive, coeval basins with and without connections, and with a shoreline somewhere to the south. The U-Pb zircon and Nd T_{DM} model ages indicate that the group is 2.76-2.72 Ga with some inheritance from 2.89-2.86 Ga rocks. Correlative or penecontemporaneous strata extend throughout the 2000 km long Committee Orogen. The U-Pb zircon and Rb-Sr ages indicate some granitic emplacement and/or metamorphism occurred within the 2.72-2.50 Ga range.

Several hundred metres of late Aphebian Piling Group intergradational strata occur in complex swirly structures, napes, thrust sheets, and domal structures along the southern edge of the map area. The basal Dewar Lakes Formation (0 to >40 m) contains, in ascending order, quartzofeldspathic biotite paragneiss, muscovite-quartz schist, and quartzite. The overlying Flint Lake Formation (0 to >60 m) contains a variety of marbles and calc-silicate rocks in which calcite is about twice as abundant as dolomite.

The Astarte River Iron-formation (0-35 m) caps the relatively thin shelf sequence and forms the thin, discontinuous, basal unit of the overlying basinal sequence. Sulphide facies iron-formation (mica-graphite schist containing chert, pyrrhotite, pyrite, and chalcopyrite) predominates and grades locally into oxide facies and lesser silicate and aluminous facies.

Thin amphibolite, mafic gneiss bands, and rare ultramafics occur above the Astarte River Iron-formation in the basal Longstaff Bluff Formation. Most bands are probably metamorphosed sills and flows that are the northern extension of the more voluminous sequence to the south of the map area. The Longstaff Bluff Formation, as much as several hundred metres in thickness, comprises a thick sequence of turbidites, mostly greywacke, siltstone, and minor shale metamorphosed to quartz-feldspar-muscovite-biotite paragneiss.

Most contacts between Piling Group strata and underlying rocks are tectonic. Piling Group strata generally contain more Cr, U, Ni, Al, Na, and Co than their Archean Mary River counterparts. The U-Pb zircon ages and Nd T_{DM} model ages indicate that the Piling Group is younger than 2160 Ma, that the metasediments are a mixture of old Archean and late Proterozoic juvenile crust, and that the mafic igneous rocks are about 1.9 Ga. The shelf sequence was deposited in an encroaching sea and deepening marine basin on sialic crust during rifting. The Astarte River Iron-formation, deposited below wave base, marks a change to deposition in an environment partially restricted by increased rifting and mafic volcanism represented by

d'anorthosites porphyriques cumulitiques. Le dépôt de la formation ferrifère a eu lieu en eau profonde, probablement au cours d'un épisode de stabilité relativement généralisée dans de nombreux bassins étendus contemporains, communicants ou non communicants, le rivage étant situé quelque part au sud. Les datations par la méthode de l'U-Pb du zircon et les datations modélisées par la méthode du Nd T_{DM} indiquent que le Groupe date de 2,76-2,72 Ga, des éléments plus anciens remontant à 2,89-2,86 Ga. Des strates corrélatives ou pénécontemporaines affleurent dans l'ensemble de l'orogène long de 2 000 km de Comité (Fig. 113, 114). Les datations par la méthode de l'U-Pb du zircon et par celle du Rb-Sr indiquent qu'il y a eu dans une certaine mesure mise en place et/ou métamorphisme granitique pendant l'intervalle 2,72-2,50 Ga.

Plusieurs centaines de mètres de strates interstratifiées du Groupe de l'Aphébien tardif de Piling se présentent dans des structures tourbillonnaires complexes, des nappes, des nappes de chevauchement et des structures en forme de dôme le long de la bordure méridionale de la région cartographique. La Formation de base de Dewar Lakes (0 à >40 m) contient de bas en haut, des paragneiss à biotite quartzofeldspathiques, des schistes à muscovite-quartz et des quartzites. La Formation sus-jacente de Flint Lake (0 à >60 m) renferme divers marbres et roches silicatées dans lesquels la calcite est environ deux fois plus abondante que la dolomie.

La Formation ferrifère d'Astarte River (0-35 m) couronne la séquence de plate-forme continentale relativement mince et constitue la mince unité basale discontinue de la séquence de bassin sus-jacente. Une formation ferrifère à faciès sulfuré (schistes à mica-graphite renfermant du chert, de la pyrrhotine, de la pyrite et de la chalcopyrite) prédomine et passe localement à un faciès oxyde et, en quantités moindres, à des faciès silicaté et alumineux.

De minces couches d'amphibolite, des bandes de gneiss mafique et de rares ultramafites apparaissent au-dessus de la formation ferrifère d'Astarte River, dans la formation de base de Longstaff Bluff. La plupart des bandes sont probablement constituées de filons-couches et de coulées métamorphisées qui constituent l'extension nord de la séquence plus volumineuse au sud de la région cartographique. La Formation de Longstaff Bluff, qui atteint plusieurs centaines de mètres d'épaisseur, comprend une épaisse séquence de turbidites composée essentiellement de grauwackes, de siltstones et, en quantitiés mineures, de shales métamorphisés en paragneiss à quartz-feldspath- muscovite- biotite.

La plupart des contacts entre les strates du Groupe de Piling et les roches sous-jacentes sont tectoniques. Les strates du Groupe de Piling renferment généralement plus de Cr, U, Ni, Al, Na et Co que les roches archéennes de Mary River. Les datations par la méthode de l'U-Pb du zircon et les datations modélisées par la méthode du Nd T_{DM} indiquent que le Groupe de Piling est plus jeune que 2 160 Ma, que les métasédiments sont constitués d'un mélange d'ancienne croûte archéenne et de croûte juvénile protérozoïque tardive et que les roches ignées mafiques sont âgées d'environ 1,9 Ga. La séquence de plate-forme continentale a été déposée au cours d'un stade de distension sur une mer transgressive et dans un bassin en voie d'approfondissement sur une croûte sialique. La Formation ferrifère d'Astarte River,

the overlying amphibolites. The thick Longstaff Bluff turbidite flysch sequence was deposited in a rapidly subsiding area, probably a foreland or back-arc basin. Correlative strata occur throughout the Baffin Orogen and extend at least 1400 km from south of Committee Bay to West Greenland and at least 800 km from Steensby Inlet to south of Baffin Island. A major north-dipping suture may lie to the south.

Late Archean massive porphyritic monzogranite-granodiorite intrusions, and late Aphebian massive monzogranite-granodiorite and monzocharnockite-granoenderbite intrusions together underlie about 7% of the map area. The first two are most common in the northwestern part of the map area while the charnockites occur mostly in the Dexterity Granulite Belt. One U-Pb zircon age of 2709 ± 3 Ma for the late Archean porphyritic granites indicates emplacement only 33-9 Ma after deposition of the Mary River Group (at 2759-2718 Ma). Two U-Pb zircon ages for late Aphebian granites and other data indicate formation of Aphebian melt from Archean protolith and emplacement after deposition of the Piling Group. The Nd T_{DM} model ages for all three felsic intrusive units are 2.9-2.7 Ga. Locally, the charnockites are gradational with the other two units and with Archean foliated granites. Inclusions are rare in the late Aphebian granites but are more common in the charnockites. A U-Pb zircon age of ca. 2.55 Ga has been obtained recently for the charnockitic Bylot Batholith.

The older Archean foliated granite-granodiorite, the late Archean porphyritic granite, and the late Aphebian granites all plot in the middle of the quartz-potassium feldspar-plagioclase (Q-A-P) field in the position of minimal granitic melts. The charnockite plot is more dispersed. Chemically, late Aphebian monzogranites show relatively little similarity with other felsic map units other than late intrusions in banded migmatite. The charnockitic rocks, however, are especially similar to Archean foliated granites, late Archean porphyritic granites, and the concordant leucosome in banded migmatite. The charnockites in the map area are mostly metaluminous I-type granites that probably range from metamorphosed Archean to deep seated, synmetamorphic, late tectonic, late Aphebian plutons. Archean foliated granites, late Archean massive porphyritic granites, and late Aphebian granites in the map area, and, for comparison, the granites and charnockites of the Cumberland Batholith south of the map area, are all calc-alkaline to alkaline, metaluminous to peraluminous, I-and S-type granites. In general the potassium content and

déposée sous le niveau de base des vagues, marque la transition à un dépôt dans un milieu partiellement contraint par un stade de distension accrue et par un volcanisme mafique matérialisé par les amphibolites sus-jacentes. L'épaisse séquence de flysch turbiditiques de Longstaff Bluff a été déposée dans une région en voie d'affaissement rapide, probablement un bassin d'avant-pays ou d'arrière-arc. Des strates corrélatives sont présentes dans l'ensemble de l'orogène de Baffin; elles s'étendent sur une distance d'au moins 1 400 km à partir du sud de la baie Comité jusqu'à l'ouest du Groenland et d'au moins 800 km de l'inlet Steensby jusqu'au sud de l'île de Baffin. Une importante suture à pendage vers le nord est peut-être présente vers le sud.

Des intrusions porphyriques massives de monzogranite-granodiorite de l'Archéen tardif ainsi que des intrusions massives de monzogranite-granodiorite et de monzocharnockite-granoenderbite de l'Aphébien tardif recouvrent au total quelque 7 % de la région cartographique. Les deux premiers types d'intrusions sont concentrés dans la partie nord-ouest de la région, alors que les charnockites se manifestent surtout dans la ceinture granulitique de Dexterity. Une datation par la méthode de l'U-Pb du zircon des granites porphyriques de l'Archéen tardif (2 709 ± 3 Ma) indique qu'il y a eu mise en place seulement 33-9 Ma après le dépôt du Groupe de Mary River (2 759-2 718 Ma). Deux datations par la méthode de l'U-Pb des zircons de granites de l'Aphébien tardif ainsi que d'autres données indiquent que les produits fondus aphébiens ont été formés à partir d'un protolithe archéen et mis en place après le dépôt du Groupe de Piling. Les datations modélisés du Nd T_{DM} des trois unités intrusives felsiques s'inscrivent dans l'intervalle 2,9-2,7 Ga. Localement, les charnockites sont en contact progressif avec les deux autres unités et avec des granites foliés archéens. Les inclusions sont rares dans les granites de l'Aphébien tardif mais sont plus communes dans les charnockites. Une datation par la méthode de l'U-Pb du zircon obtenue récemment indique que la mise en place du batholite charnockitique de Bylot a eu lieu il y a environ 2,55 Ga.

Les granites-granodiorites foliés archéens plus anciens, les granites porphyriques de l'Archéen tardif et les granites de l'Aphébien tardif s'inscrivent tous au centre du champ quartz-feldspath potassique-plagioclase (Q-A-P) à la position des liquides granitiques minimaux. Le tracé des charnockites est plus dispersé. Sur le plan chimique, les monzogranites de l'Aphébien tardif présentent relativement peu de similarités avec les autres unités cartographiques felsiques, à l'exception des intrusions tardives dans les migmatites foliées. Par contre, les roches charnockitiques ressemblent tout particulièrement aux granites foliés archéens, aux granites porphyriques de l'Archéen tardif et au leucosome concordant dans les migmatites rubanées. Les charnockites de la région cartographique sont pour l'essentiel des granites métalumineux du type I variant vraisemblablement de plutons archéens métamorphisés à des plutons tarditectoniques et synmétamorphiques d'origine profonde de l'Aphébien tardif. Les granites archéens foliés, les granites porphyriques massifs de l'Archéen tardif et les granites de l'Aphébien tardif de la région cartographique, ainsi que, à titre de comparaison, les granites et charnockites du batholite de Cumberland au sud de la région cartographique sont tous des granites des types I et S calco-alcalins à alcalins et métalumineux à hyperalumineux. En général, la teneur en potassium et l'index de differentiation index increase from middle Archean to late Aphebian. Chemically all these units most closely resemble volcanic arc granites of active continental margins.

About 1900 m of Neohelikian (ca. 1.27-1.24 Ga) Bylot Supergroup strata in Milne Inlet Trough comprise three intergradational formations which contain microfossils and a large variety of sedimentary structures. These strata overlie older gneisses nonconformably and are separated from them by a thin discontinuous regolith. The basal Adams Sound Formation (2-122 m) contains three members that are mostly quartz-arenite with minor conglomerate, and are interpreted to be mostly braided fluvial strata deposited by a northwest-flowing stream. The uppermost strata are intertidal to subtidal sandstones.

Most of the Bylot Supergroup strata in the map area belong to the Arctic Bay Formation (837-1460 m), which locally overlaps the underlying Adams Sound Formation onto the older gneisses. The strata are mostly carbonaceous shales, with lesser quartz arenites, siltstones, and carbonates in the ratio of about 7:2:1:1. Four members have been differentiated of which the uppermost constitutes most of the formation. Synaeresis cracks, desiccation cracks, and ripple marks are especially common. Nickel and manganese are more abundant in upper Arctic Bay than in lower Arctic Bay strata. Deposition was mostly in stacked coarsening-, thickening-, and shallowing-up cycles, representing eight cycle types with up to three units each and an average thickness of 9-11.5 m. The basal unit is commonly shale and is the thickest unit in the cycles. The middle unit is commonly interbedded shale, siltstone, and sandstone, and the upper unit is quartz arenite. It may have taken 8.6-11.1 Ma to deposit the Arctic Bay Formation and 57 000-100 000 years to deposit an average cycle.

The two lower Arctic Bay members were deposited in subtidal to clastic shoreline and deltaic environments, whereas the third member represents subtidal environments with a deepening basin westward. The uppermost member was deposited in mixed clastic shoreline, shallow carbonate basin, deltaic, and intertidal to shallow subtidal environments.

The stromatolitic dolostones of the Society Cliffs Formation (308 m) conformably overlie Arctic Bay strata in the map area although a disconformity is present locally to the north. The lower Society Cliffs member is composed of shallowing-up cycles containing shale-siltstone units capped by dolostone. The cycles were deposited in response to repeated abrupt basin deepening followed by prograde filling in intertidal to supratidal environments. Upper member strata, almost entirely stromatolitic dolostone, were deposited in shallow subtidal to intertidal environments.

différenciation s'accroissent de l'Archéen moyen à l'Aphébien tardif. Chimiquement, toutes ces unités ressemblent surtout aux granites d'arc volcanique des marges continentales actives.

Environ 1 900 m de strates néohélikiennes du Supergroupe de Bylot (env. 1,27-1,24 Ga) à l'inlet Milne comprennent trois formations interstratifiées contenant des microfossiles et une grande diversité de structures sédimentaires. Ces strates recouvrent des gneiss plus anciens de manière discordante et sont séparés de ces derniers par un mince régolithe discontinu. La Formation basale d'Adams Sound (2-122 m) contient trois membres composés surtout de quartz-arénite et de quantités mineures de conglomérat; ils sont interprétés comme étant essentiellement des strates fluviales anastomosées déposées par un cours d'eau coulant vers le nord-ouest. Les strates supérieures sont des grès intertidaux à subtidaux.

La plupart des strates du Supergroupe de Bylot de la région cartographique appartiennent à la Formation d'Arctic Bay (837-1 460 m), qui chevauche localement la Formation sous-jacente d'Adams Sound sur les gneiss plus anciens. Les strates sont composées surtout de shales carbonacés et, en quantitiés moindres, d'arénites quartziques, de siltstones et de carbonates dans les rapports 7:2:1:1. Quatre membres ont été identifiés, le membre supérieur constituant la plus grande partie de la formation. Les craquelures de synérèse, les fentes de dessication et les rides sont courantes. Le nickel et le manganèse sont plus abondants dans les strates supérieures d'Arctic Bay que dans les strates inférieures. Le dépôt a eu lieu surtout au cours de cycles empilés à granocroissance ascendante, d'épaisseur croissante et de profondeur décroissante représentant huit types de cycles contenant jusqu'à trois unités chacun et d'une épaisseur moyenne de 9-11,5 m. L'unité de base se compose en général de shales constituant l'unité la plus épaisse des cycles. L'unité médiane se compose généralement de shales, de siltstones et de grès interstratifiés, et l'unité supérieure d'arénites quartziques. Le dépôt de la Formation d'Arctic Bay a peut-être nécessité de 8,6 à 11,1 Ma et le dépôt d'un cycle moyen de 57 000 à 100 000 ans.

Les deux membres inférieurs d'Arctic Bay ont été déposés dans des milieux littoraux et deltaïques subtidaux à clastiques, le troisième membre étant issu d'environnements subtidaux à bassin allant s'approfondissant vers l'ouest. Le membre supérieur a été déposé alternativement dans des milieux littoraux clastiques, à bassin carbonaté peu profond, deltaïques et intertidaux à subtidaux peu profonds.

Les dolomies stromatolithiques de la Formation de Society Cliffs (308 m) reposent en concordance sur les strates d'Arctic Bay dans la région cartographique, bien qu'une discordance érosionelle soit présente localement vers le nord. Le membre inférieur de Society Cliffs se compose de cycles de profondeur décroissante contenant des unités de shale-siltstone couronnées par des dolomies. Les cycles ont été déposés consécutivement à des approfondissements de bassin subits et répétés suivis d'un remplissage prograde dans des environnements intertidaux à supratidaux. Les strates du membre supérieur, composées presque exclusivement de dolomies stromatolithiques, ont été déposées dans des environnements subtidaux à intertidaux peu profonds.

Deposition of the Adams Sound Formation in Borden Basin was restricted to a fault-controlled channel in eastern Milne Inlet Trough that merged northwest into a shallow marine shelf. Syndepositional faulting was relatively active during deposition of Arctic Bay and lower Society Cliffs formations. An abrupt regional change led to relatively quiet, deeper water deposition of upper Society Cliffs dolostones. The major faults are listric and movement was mostly dip-slip. Some movement between Greenland and Baffin Island probably occurred in the Neohelikian, and the Borden and Thule basins and the Somerset Island area are probably parts of a single larger basin.

Franklin (723 Ma, includes Borden dykes), and probably a few Mackenzie (1270 Ma) unmetamorphosed tholeiitic diabase dykes are concentrated in seven northwest-trending swarms on Baffin Island, five of which pass through the map area. New data (Pehrsson and Buchan, 1999) indicate the Borden dykes belong to the Franklin swarm. Compared with other Franklin dykes, Borden dykes are slightly more differentiated; probably have less Mg and more Na, K, and Al; and also have some mineralogical differences. The Neohelikian and Hadrynian dykes have more Ti and Zr than the older metamorphosed mafic rocks.

As much as 400 m of fossiliferous Early Cambrian to Late Ordovician strata outcrop along the western edge of the map area above a thin local regolith. The basal Gallery Formation (0-70 m) is mostly fluvial to intertidal quartz-rich sandstone with minor conglomerate that grade upward into intertidal dolostones of the Turner Cliffs Formation (0-90 m). The Ship Point Formation (70-165 m) is mostly intertidal dolomite-cemented quartz sandstone, and dolostone. It is bounded by unconformities and is overlain by dolostones and limestones of the subtidal Baillarge Formation (100 m+). The lower formations were deposited largely in a shelf environment between the contemporary Admiralty Basin to the northwest and the ancestral Foxe Basin to the southwest. The two upper formations were each deposited during a marine transgression that followed a retreat of the sea. The strata are preserved in several southeast-trending grabens.

Some Archean rocks have probably undergone three episodes of anatexis, including two in the Archean at ca. 2.9-2.8 Ga and ca. 2.72-2.5 Ga. The latest was in the late Aphebian (1.9-1.8 Ga), and most prograde mineral assemblages are considered to represent this event. Rare subgreenschist, local greenschist, and minor lower amphibolite facies rocks are confined to the Mary River Group and may include some Archean metamorphic assemblages. Locally steep metamorphic gradients, and restriction of the lower amphibolite facies to core areas rimmed by higher grade rocks suggest steep thermal gradients, deformation after metamorphism, or both. Most of the map area is in prograde upper amphibolite facies. Most

Le dépôt de la Formation d'Adams Sound dans le bassin de Borden se limite à un chenal contrôlé par des failles dans la partie orientale de l'inlet Milne et passant vers le nord-ouest à une plate-forme marine peu profonde. Les mouvements de cassure contemporains du dépôt ont été relativement actifs au cours du dépôt de la formation d'Arctic Bay et de la partie inférieure de la formation de Society Cliffs. Un changement régional subit s'est traduit par le dépôt en eaux plus profondes relativement tranquilles des dolomies de la partie supérieure de la formation de Society Cliffs. Les principales failles sont listriques, et les mouvements étaient surtout à rejet transversal. Il y a probablement eu mouvement relatif entre le Groenland et l'île de Baffin au Néohélikien, aussi les bassins de Borden et de Thulé et l'île Somerset font-ils probablement partie d'un bassin unique plus étendu.

Les dykes de diabase tholéiitiques non métamorphisés de Franklin (723 Ma, y compris des dykes Borden) et, vraisemblablement, quelques dykes Mackenzie (1 270 Ma) sont concentrés sur l'île de Baffin dans sept essaims de direction nord-ouest, dont cinq traversent la région cartographique. De nouvelles données (Pehrsson et Buchan, 1999) indiquent que les dykes Borden appartiennent à l'essaim Franklin. Comparés aux autres dykes Franklin, les dykes Borden sont légèrement plus différenciés, contiennent probablement moins de Mg et plus de Na, K et Al et présentent en outre des différences minéralogiques. Les dykes néohélikiens et hadryniens contiennent plus de Ti et de Zr que les roches mafiques métamorphisées plus anciennes.

Jusqu'à 400 m de strates fossilifères du Cambrien précoce à l'Ordovicien tardif affleurent le long de la bordure occidentale de la région cartographique au-dessus d'un mince régolithe local. La Formation de base de Gallery (0-70 m) est composée essentiellement de grès riches en quartz fluviaux à intertidaux et de quantités mineures de conglomérats passant vers le haut aux dolomies intertidales de la Formation de Turner Cliffs (0-90 m). La Formation de Ship Point (70-165 m) est composée surtout de grès quartzeux intertidaux cimentés par de la dolomite ainsi que de dolomies. Elle est limitée par des discordances et recouverte de dolomies et de calcaires de la Formation subtidale de Baillarge (100 m+). Les formations inférieures ont été déposées pour l'essentiel dans un environnement de plate-forme entre le bassin contemporain d'Admiralty au nord-ouest et le bassin ancestral de Foxe au sud-ouest. Les deux formations supérieures ont été déposées au cours d'une transgression marine consécutive au retrait de la mer. Les strates sont conservées dans plusieurs grabens de direction sud-est.

Certaines roches archéennes ont probablement subi trois épisodes d'anatexie, y compris deux à l'Archéen à env. 2,9-2,8 Ga et env. 2,72-2,5 Ga. Le plus tardif date de l'Aphébien tardif (1,9-1,8 Ga), aussi considère-t-on que la plupart des assemblages minéraux prograde reflètent ce dernier événement. Des roches rares des faciès inférieurs au faciès des schistes verts, des roches apparaissant localement du faciès des schistes verts et des roches peu abondantes du sous-faciès inférieur des amphibolites sont restreintes au Groupe de Mary River; elles comprennent peut-être des assemblages métamorphiques archéens. La présence de gradients métamorphiques localement abrupts et la limitation du sous-faciès inférieur des amphibolites à des régions centrales bordées de roches de grade métamorphique

granulites are restricted to the northeast-trending Dexterity Granulite Belt, and upper amphibolite and granulite facies prograde assemblages are intergradational where faulting is absent. Minor retrograde minerals developed mostly during waning metamorphism. Granulties in the belt are post-Piling, and syn- to post-granitic plutons, and have been considered to be Late Aphebian. Metamorphism in the southwest end of the belt has recently been dated at ca. 1825 Ma.

Pressure-temperature calculations from mineral analyses and estimates using a petrogenetic grid have yielded comparable results, and indicate values of 0.35-0.40 GPa and 500°-570°C for most of the Mary River area. Pressures and temperatures increase southward toward the Dexterity Granulite Belt; values of 0.5-0.6 GPa and 600°-725°C are common for rocks adjacent to the north side of the belt (Rowley River, Buchan Gulf) and in the southeast part of the map area well south of the granulite belt (Sam Ford Fiord-Generator Lake). Determinations for the western part of the granulite belt indicate pressures of 0.8-0.87 GPa with temperatures up to 850°C in the south. Pressures and temperatures are higher in the northeast part of the Dexterity Granulite Belt, but the highest values obtained (1.3 GPa, 995°C) may be anomalous. A low grade belt (0.45 GPa, 584°C) parallels the granulite belt along its southeast side. High pressures and temperatures are also common in the southwest-directed, Northeast Baffin Thrust Belt and exceed 1 GPa and 800°C north of the granulite belt, which is transected by the thrust belt. High P-T values in both belts were obtained for charnockites and pyribolite inclusions in charnockite. By comparison, Cumberland Batholith charnockite gave mostly lower pressures.

Eight tectonic domains and several subdomains, bounded by major fault and shear zones, have been differentiated in the Precambrian of Baffin Island. Five of the domains are represented in the map area; two of the domains extending into the southern block (*see* below). Seven of the domains are dominated by late Aphebian deformation superimposed on Archean structures where present (e.g. northernmost and southernmost Baffin Island). Domain 1 includes the Mary River area and has the best likelihood of containing well preserved Archean structures in the map area. Domains 2 and 3 (Foxe Fold Belt) are separated by the northeast-trending southeast-dipping Isortoq Fault Zone. The fault zone separates the charnockite-bearing Dexterity Granulite Belt (subdomains 2a, 2b, 2c, 7b) to the north from chiefly amphibolite grade rocks of subdomain 3a to the southeast.

plus élevé témoignent de gradients thermiques élevés, de déformations post-métamorphiques ou des deux. La plus grande partie de la région cartographique appartient au sous-faciès supérieur prograde des amphibolites. La plupart des granulites ne sont présentes que dans la ceinture granulitique de direction nord-est de Dexterity; les assemblages progrades du sous-faciès supérieur des amphibolites et du faciès des granulites sont interdigités en l'absence de mouvements de cassure. Des minéraux rétrogrades en quantité mineure ont été formés surtout au cours d'un métamorphisme faiblissant. Les granulites de la ceinture sont post-Piling et contemporaines des plutons granitiques et postérieures à ces derniers; elles sont considérées comme datant de l'Aphébien tardif. Le métamorphisme à l'extrémité sud-ouest de la ceinture a récemment été daté à environ 1 825 Ma.

Des calculs de pression-température à partir d'analyses minérales et des estimations au moyen d'un schéma pétrogénétique (Fig. 101) ont fourni des résultats comparables; ils indiquent des valeurs de 0,35-0,40 GPa et de 500°-570°C pour la plus grande partie de la région de Mary River. Les pressions et températures s'accroissent vers le sud en direction de la ceinture granulitique de Dexterity; des valeurs de 0,5-0,6 GPa et 600°-725°C sont courantes parmi les roches adjacentes au côté nord de la ceinture (Rowley River, Buchan Gulf) et dans la partie sud-est de la région cartographique, largement au sud de la ceinture granulitique (Fjord de Sam Ford-lac Generator). Les déterminations pour la partie occidentale de la ceinture granulitique indiquent des pressions de 0,8-0,87 GPa, avec des températures atteignant 850°C au sud. Les pressions et les températures sont plus élevées dans la partie nord-est de la ceinture granulitique de Dexterity, mais les valeurs obtenues les plus élevées (1,3 GPa, 995°C) sont peut-être anormales. Une ceinture faiblement métamorphisée (0,45 GPa, 584°C) est parallèle à la ceinture granulitique le long de son côté sud-est. Des pressions et températures élevées sont également courantes dans la ceinture de chevauchement du Nord-est de Baffin, de direction sud-ouest, et dépassent 1 GPa et 800°C au nord de la ceinture granulitique, qui est recoupée par la ceinture de chevauchement. Dans ces deux ceintures, des valeurs élevées de P-T ont été obtenues pour les charnockites et pour les inclusions de pyribolite dans la charnockite. À titre de comparaison, les charnockites du batholite de Cumberland ont fourni dans la plupart des cas des pressions inférieures.

Huit domaines tectoniques et plusieurs sous-domaines, limités par d'importantes failles et zones de cisaillement, ont été identifiés dans le Précambrien de l'île de Baffin (Fig. 112-114). Cinq de ces domaines figurent sur la région cartographique et deux se prolongent dans le bloc méridional (*voir* plus bas). Sept des domaines sont dominés par une déformation de l'Aphébien tardif superposée à des structures archéennes lorsque celles-ci sont présentes (p. ex., à l'extrême nord et l'extrême sud de l'île de Baffin). Le Domaine 1 comprend la région de Mary River et présente la probabilité la plus élevée de contenir des structures archéennes bien conservées dans la région cartographique. Les domaines 2 et 3 (ceinture de plissement de Foxe) sont séparés par la zone de faille d'Isortok, de direction nord-est et à pendage sud-est. Cette zone de failles sépare la zone granulitique de Dexterity au nord, laquelle comprend des charnockites (sous-domaines 2a, 2b, 2c et 7b) de roches présentant surtout le

The fault zone is interpreted as the effective northern limit of late Aphebian northwest-directed overthrusting in the Foxe Fold Belt and the boundary between that belt to the south and the Committee Orogen to the north. Both the fault zone and the Dexterity Granulite Belt probably originated in a compressive regime during the overthrusting from the southeast, although the fault zone may represent a suture related to north-directed subduction and collision of northern Baffin (Committee Orogen) with the Baffin Orogen (domains 3-6) to the south. Subsequent rebound began with sinistral extensional movement obliquely upward on the north side of the fault during relatively low grade metamorphism. The Dexterity Granulite Belt was tilted upward toward the northwest and uplifted about 8 km adjacent to the western part of the Isortoq Fault Zone. Steep brittle faults developed along the Isortoq Fault Zone as rebound continued and are still active.

Late Aphebian southeast structural and lithological trends are overprinted over earlier late Aphebian east and northeast structural and lithological trends in domain 7 (Northeast Baffin Thrust and Belt) along the northeast coast of Baffin Island. The Isortoq Fault Zone is deformed in subdomain 7a, which contains thick cliff sections of stacked ductile nappes and thrust sheets that have been formed by southwesterly directed overthrusting.

Using regional structural, chemical, and geochronological data, the Precambrian of Baffin Island has also been separated along the Piling Fault, into northern and southern blocks that encompass the eight structural domains. Major accretion of sialic crust occurred throughout the north block, and locally in the south block at about 2.85 Ga, and the age data for the older rocks northwest from Cumberland Peninsula most closely resembles that for the Nain Province.

The smaller north Baffin Island block (domains and subdomains 1, 2, 3a, 7a, 7b, 8) extends across the northeast-trending, 2000 km long late Archean Committee Orogen, and includes most of the map area. The orogen was probably formed in the interval 2.75-2.70 Ga when deposition of greenstone-ultramafic (komatiitic) sequences was followed closely (43-9 Ma?) by metamorphism, deformation, and emplacement of granitic plutons. Extensive reworking of older crust accompanied the addition of new crust. North Baffin Island was overprinted by late Aphebian metamorphism and deformation when the subparallel Thelon Tectonic Zone (2.0-1.9 Ga) was emplaced to the northwest and the Baffin Orogen (1.9-1.8 Ga), part of the larger Trans Hudson Orogen, was emplaced to the south. These events, especially the Baffin Orogen, had a profound effect on the Committee Orogen,

faciès des amphibolites dans le domaine 3a au sud-est. La zone de failles est interprétée comme étant la limite septentrionale effective du chevauchement de direction nord-ouest de l'Aphébien tardif dans la ceinture de plissement de Foxe et la limite entre cette ceinture au sud et l'orogène de Comité au nord. La zone de failles et la ceinture granulitique de Dexterity ont vraisemblablement été formées en régime compressif au cours d'un épisode de chevauchement à partir du sud-est, bien que la zone de failles puisse constituer une suture liée à la subduction et à la collision dirigées vers le nord de la partie septentrionale de Baffin (orogène de Comité) avec l'orogène de Baffin (domaines 3-6) au sud. Un rebondissement ultérieur s'est amorcé avec un mouvement d'extension senestre dirigé obliquement vers le haut du côté nord de la faille au cours d'un épisode de métamorphisme relativement peu intense. La ceinture granulitique de Dexterity a été inclinée vers le haut en direction du nord-ouest et soulevée sur environ 8 km à proximité de la bordure occidentale de la zone de failles d'Isortok. Des failles cassantes abruptes ont été formées le long de la zone de failles d'Isortok à mesure que se poursuivait le rebondissement et sont encore actives.

Dans le domaine 7, les motifs structuraux et lithologiques de direction sud-est de l'Aphébien tardif sont surimprimés sur des motifs structuraux et lithologiques antérieurs de directions est et nord-est de l'Aphébien tardif (chevauchement et ceinture du nord-est de Baffin) le long de la côte nord-est de l'île de Baffin. La zone de failles d'Isortok est déformée dans le sous-domaine 7a, qui contient d'épaisses coupes de falaise de nappes et de nappes de charriage ductiles empilées et formées par des chevauchements dirigés vers le sud-ouest.

Sur la base de données structurales, chimiques et géochronologiques régionales, le Précambrien de l'île de Baffin a également été divisé le long de la faille de Piling en blocs septentrional et méridional englobant les huit domaines structuraux. À environ 2,85 Ga un épisode majeur d'accrétion de croûte sialique a eu lieu dans l'ensemble du bloc nord et, localement, dans le bloc sud; les données chronologiques sur les roches plus anciennes situées au nord-ouest à partir de la péninsule de Cumberland ressemblent surtout à celles sur la province de Nain.

Le bloc plus petit du Nord de l'île de Baffin (domaines et sous-domaines 1, 2, 3a, 7a, 7b, 8) s'étend transversalement à l'orogène de l'Archéen tardif de Comité, de direction nord-est et de 2 000 km de longueur, et recouvre la plus grande partie de la région cartographique. L'orogène a probablement été formé au cours de l'intervalle 2,75-2,70 Ga, pendant lequel le dépôt de séquences de roches vertes-ultramafites (komatiites) a été suivi de peu (43-9 Ma) par des épisodes de métamorphisme, de déformation et de mise en place de plutons granitiques. L'addition de croûte nouvelle s'est accompagnée d'un remaniement intensif de la croûte plus ancienne. Le nord de l'île de Baffin a été surimprimé à l'Aphébien tardif par un métamorphisme et une déformation lorsque la zone tectonique subparallèle de Thelon (2,0-1,9 Ga) a été mise en place au nord-ouest et que l'orogène de Baffin (1,9-1,8 Ga), qui fait partie de l'orogène transhudsonien, plus vaste, a été mis en place au sud. Ces événements, en particulier l'orogène de Baffin, se sont répercutés profondément sur l'orogène de Comité, aussi le and subdomain 3a, although chiefly Archean rocks, is sufficiently reworked to be considered as the northern end of the Baffin Orogen.

The south Baffin Island block (domains and subdomains 3b, 3c, 4, 5, 6, 7c) lies within the late Aphebian Baffin Orogen, which extends into Melville Peninsula, western and northwestern Greenland, and northern Quebec-Labrador. The core of the orogen is the 1.90-1.84 Ga monzogranite-monzocharnockite Cumberland Batholith. The equidimensional batholith may represent segments of a plutonic belt juxtaposed by strike-slip shearing. Three bordering thrust and fold belts (Foxe and Dorset fold belts, Nagssugtoqidian Mobile Belt) contain correlative late Aphebian (1.9 Ga) supracrustal sequences and variable amounts of polydeformed Archean rocks that are intruded by the batholith along fold belt margins. About forty to fifty million years may have elapsed between mafic volcanism and deformation and final pluton emplacement. Granulite metamorphism may have continued for another twenty to thirty million years. The Baffin Orogen was probably forged during the late Aphebian collision of at least three major continental masses, and some of the shear zones that separate domains and subdomains are likely candidates for sutures. The Northeast Baffin Thrust Belt (domain 7) along Baffin Island's northeast coast formed late in this event in response to southwest compression that may have been caused by collision of a fourth major crustal block to the northeast.

The charnockitic-granitic plutons of the anastomosing 1.9-1.8 Ga Cumberland Batholith represent magma ranging from ca. 1.9 Ga juvenile melt to anatectic melt from Archean crust. Most of the batholith, however, probably represents a mixing together of the Late Aphebian juvenile and older crusts by erosion and sedimentation prior to melting, and/or mixing in a magma chamber or chambers. Most other late Aphebian granitic plutons throughout Baffin Island were probably formed from fused Archean sialic crust during the late Aphebian (2.0-1.8 Ga) high temperature, low- to moderate-pressure metamorphism. Late Archean massive porphyritic granites and some charnockites in the map area probably formed during a similar event at about 2.71 Ga. The chemical signatures of late Archean and Aphebian granitic plutons are at least partially inherited from older sialic crust.

Borden Rift Basin (ca. 1.27-1.19 Ga; domain 8) developed as a Neohelikian aulacogen during the opening and closing of the Poseidon Ocean to the northwest. A rift stage followed by a downwarp stage are represented in the map area. The Milne Inlet Trough, within the basin, evolved along the boundary between domains 1 and

sous-domaine 3a, bien que composé essentiellement de roches archéennes, est-il suffisamment remanié pour être considéré comme constituant l'extrémité nord de l'orogène de Baffin.

Le bloc du sud de l'île de Baffin (domaines et sous-domaines 3b, 3c, 4, 5, 6, 7c) est situé au sein de l'orogène de l'Aphébien tardif de Baffin (Fig. 114), qui s'étend jusqu'à la presqu'île Melville, aux parties ouest et nord-ouest du Groenland et à la partie nord du Québec-Labrador. Le coeur de l'orogène est occupé par le batholite de Cumberland, constitué de monzogranites-monzocharnockites et âgé de 1,90-1,84 Ga. Ce batholite équidimensionnel représente peut-être un segment d'une ceinture plutonique disloquée par des mouvements cisaillants. Trois ceintures limitrophes de chevauchement et de plissement (ceintures de plissement de Foxe et de Dorset, ceinture mobile de Nagssugtoqidian) renferment des séquences supracrustales corrélatives de l'Aphébien tardif (1,9 Ga) et des quantités variables de roches archéennes polydéformées qui ont été injectées par le batholite le long des marges de la ceinture de plissement. Environ quarante à cinquante millions d'années se sont peut-être écoulés entre le volcanisme mafique et la déformation et la mise en place définitive des plutons. Le métamorphisme plutonique s'est peut-être poursuivi pendant quelque vingt à trente millions d'années. L'orogène de Baffin a vraisemblablement été formé au cours de la collision de l'Aphébien tardif entre au moins trois masses continentales majeures; certaines des zones de cisaillement séparant les domaines et sous-domaines constituent probablement des sutures. La ceinture de chevauchement du Nord-est de Baffin (domaine 7), le long de la côte nord-est de l'île de Baffin, a été formée à la fin de ces événements des suites d'une compression de direction sud-ouest qui est peut-être la conséquence d'une collision avec un quatrième bloc crustal majeur vers le nord-est.

Les plutons charnockitiques-granitiques du batholite anastomosé de Cumberland, âgé de 1,9-1,8 Ga, sont constitués de magmas variant de produits de fusion juvéniles de 1,9 Ga à des liquides d'anatexie de croûte archéenne. Cependant, l'essentiel du batholite est probablement issu du mélange de croûte juvénile de l'Aphében tardif et de morceaux de croûte plus anciens par érosion et sédimentation avant la fusion et/ou du mélange dans une ou plusieurs chambres magmatiques. La plupart des autres plutons granitiques de l'Aphébien tardif dans l'ensemble de l'île de Baffin ont vraisemblablement été formés à partir de croûte sialique archéenne fondue au cours du métamorphisme de haute température et de pression faible à modérée de l'Aphébien tardif (2,0-1,8 Ga). Les granites porphyriques massifs de l'Archéen tardif et certaines charnockites de la région cartographique ont probablement été formés au cours d'un événement semblable à environ 2,71 Ga. Les signatures chimiques des plutons granitiques de l'Archéen tardif et de l'Aphébien sont au moins partiellement héritées d'une croûte sialique plus ancienne.

Le bassin d'effondrement de Borden (env. 1,27-1,19 Ga; domaine 8 - Fig. 113) est le vestige d'un aulacogène néohélikien formé pendant l'ouverture et la fermeture de l'océan Poséidon au nord-ouest. La région cartographique porte les traces d'un stade de distension suivi d'un stade de gauchissement vers le bas. La fosse de l'inlet Milne (Fig. 13, 113), située au sein du bassin, a été formée le long de la limite entre les domaines 1 et

7. Helikian to Recent open folds and steep northwest-trending faults are superimposed on the gneisses throughout Baffin Island.

Six episodes of denudation followed by sedimentation, volcanism, or both occurred throughout Baffin Island at 400-800 Ma intervals. Locally as much as 50 km of crust has probably been denuded and the total crustal thickness may have been as great as 75 km. Such a thickness may be explained partially by continental subduction or by subsequent underplating.

At Mary River, the No. 1 iron deposit alone contains over 130 million tonnes averaging more than 68% soluble iron. Minor lead, zinc, copper, molybdenum, and asbestos, and local traces of silver and gold occur in supracrustals at various places.

7. Dans l'ensemble de l'île de Baffin, des plis ouverts hélikiens à récents et des failles à fort pendage de direction nord-ouest sont superposés aux gneiss.

Six épisodes de dénudation suivis de sédimentation, de volcanisme ou des deux ont eu lieu dans l'ensemble de l'île de Baffin à des intervalles de 400-800 Ma. Localement, une épaisseur maximale de 50 km de croûte a probablement été dénudée, l'épaisseur crustale totale ayant pu atteindre 75 km. Une telle épaisseur peut s'expliquer partiellement par une subduction continentale ou par une subduction ultérieure.

À Mary River, le gisement de fer numéro 1 renferme à lui seul plus de 130 millions de tonnes titrant en moyenne plus de 68 % de fer soluble. Des quantités mineures de plomb, de zinc, de cuivre, de molybdène et d'amiante ainsi que des traces locales d'argent et d'or sont présentes par endroits dans les roches supracrustales.

INTRODUCTION

Location, access, and habitation

The Clyde-Cockburn Land map area comprises that part of north-central Baffin Island east of longitude 80° and between 70° and 72° north latitude, about 82 000 km^2, covered by NTS sheets 27E-G and 37E-H (Fig. 1). This map area is part of the 137 300 km^2 examined on Operation Bylot, a helicopter-supported reconnaissance project, headed by the author, that was carried out in 1968 after an advance reconnaissance in August 1967 (Jackson, 1968, 1969). The project area included Bylot Island and that part of Baffin Island north of latitude 69° and east of longitude 80°. The geology of the Clyde-Cockburn Land map area is shown on five published maps, each with expanded legends (Fig. 1):

Geology, Icebound Lake, Map 1451A, NTS 37G (Jackson et al., 1978b);

Geology, Buchan Gulf-Scott Inlet, Map 1449A, NTS 37H and 27G (Jackson et al., 1978c);

Geology, Steensby Inlet, Map 1450A, NTS 37F (Jackson et al., 1978d);

Geology, Conn Lake, Map 1458A, NTS 37E (Jackson and Morgan, 1978b); and

Geology, Clyde River, Map 1582A, NTS 27E and 27F (Jackson, 1984).

Clyde River (Fig. 1), the only permanent settlement in this area, is situated at the head of Patricia Bay on the north side of Clyde Inlet near its mouth (map areas NTS 27E and 27F). A United States Coast Guard Loran station was formerly operated 14.5 km northeast of Clyde River at Cape Christian on the east coast of Baffin Island. Both localities possess airstrips, and a commercial air service connects Clyde River with Hall Beach (525 km west by south), Iqaluit (725 km south), and Nanisivik (625 km northwest). These three localities are serviced by major airlines several times a week. An airstrip is also present near Baffinland Iron Mines Ltd.'s No. 1 deposit at Mary River (map area 37G) in the northwestern part of the area. Other airstrips are present along the DEW Line about 160 km south of the area and west and north of the area at Hall Beach, Arctic Bay, and Pond Inlet. Northern Stores (formerly Hudson's Bay Company) maintains a store and trading post at Clyde River where an Atmospheric Environment Service (AES) weather station is also located. Satellite telecommunications link the Arctic communities with one another and with the rest of Canada.

Landings may be made on unprepared ground, by suitably equipped aircraft, at several localities including campsites 1, 2, and 4 (Fig. 1). Heavy cargo may be shipped via annual sealift and unloaded at any suitable locality along the coast.

Remains of former Inuit campsites and Inuit culture are scattered throughout Baffin Island. Sites within the Pond Inlet-Nova Zembla Island and Bylot Island map areas (Jackson and Davidson, 1975; Jackson et al., 1975), mapped during Operation Bylot, have been known for some time (Mathiassen, 1927). G. Mary-Rousselière, O.M.I. (unpub. manuscript, 1968, 1989), better known as Father Mary, studied archeological sites in this region from 1962 until his death in 1994.

Old Inuit sites were seen at several localities within the Clyde-Cockburn Land map area. A few square stone foundations occur 15 km southeast of the head of Coutts Inlet at estimated elevations of 90 to 180 m (Icebound Lake map area, NTS 37G). They may have been occupied when water once extended inland from the present heads of North Arm and Coutts Inlet.

Another site on the Keel River, 23 km west of the head of Cambridge Fiord, lies at an elevation of less than 150 m (map area NTS 37H-27G). The site contains several mainly circular stone rings, a large number of stone mounds, and one or two stone fish dams. Square stone foundations were also sited at Cape Hunter east of Dexterity Island (map area NTS 37H-27G) and on the west side of Adams Island, 32 km southwest of those at Cape Hunter. Both these sites are near sea level.

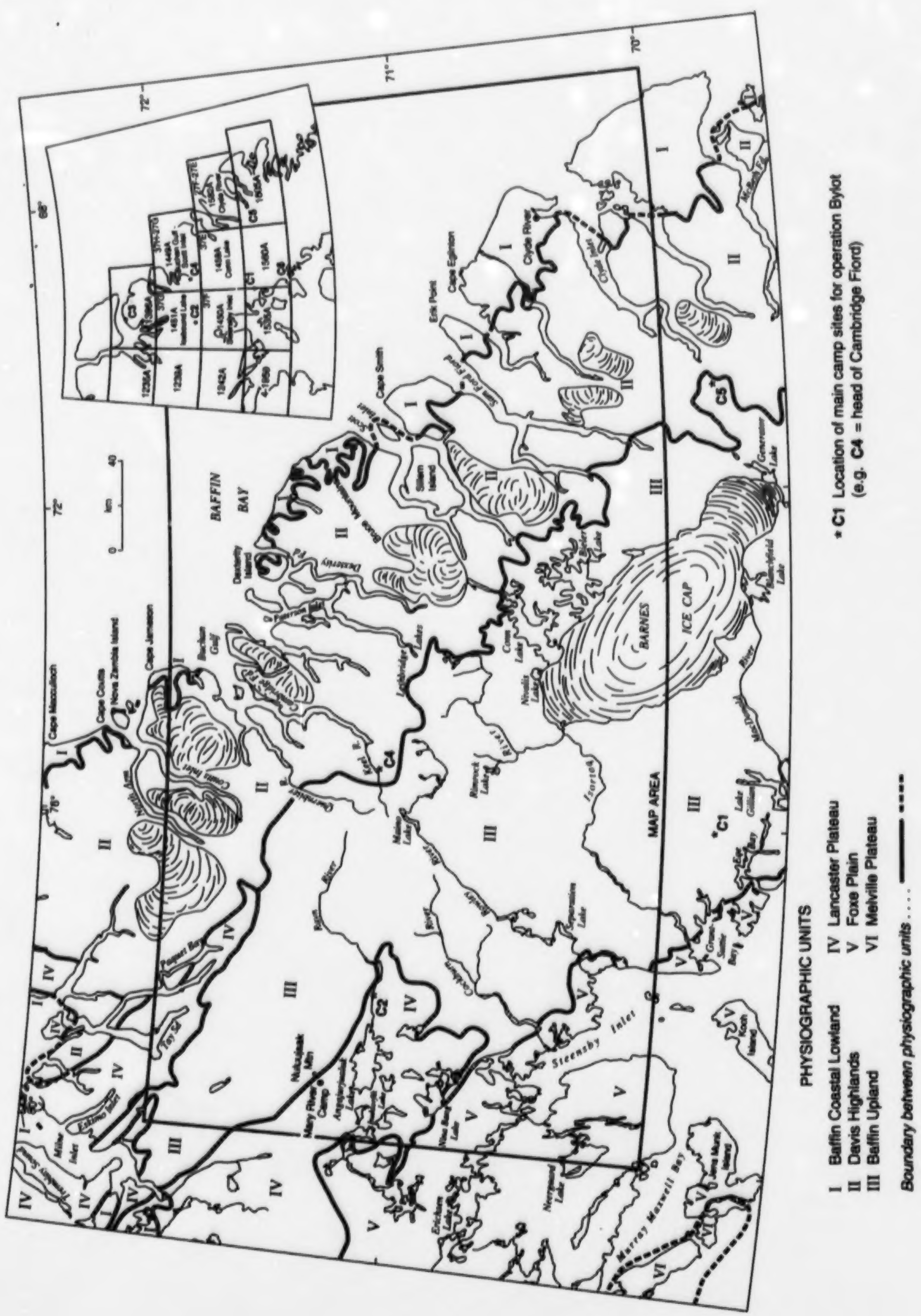
BAFFIN BAY
BARNES ICE CAP
MAP AREA
Steensby Inlet
Cape Macculloch
Cape Coutts
Nova Zembla Island
Cape Jameson
Buchan Gulf
Cape Smith
Erik Point
Cape Eglinton
Clyde River
Generator Lake
Bieler Lake
Conn Lake
Rimrock Lake
Isortoq
Nudlung Lake
Eqe Bay
Longstaff Bluff
Koch Island
Jens Munk Island
Murray Maxwell Bay
Mary River Camp
Nuluujaak Mtn
Milne Inlet
Eclipse Sound
Tay Sd
Dexterity Island
Sillem Island
Dexterity Fd
Cambridge Fd
Gibbs Fd
Scott Inlet
Hewett Inlet
Clyde Inlet
McBeth Fd
Koch River
Rowley River
Isortoq R
Cockburn R
Erichsen Lake
Neergaard Lake
Nina Bang Lake
Angajurjualuk Lake
Tupirvik Lake
Ravn River
I
II
III
IV
V
VI
C1
C2
C3
C4
C5
C6
C7
C8
72°
71°
70°
76°
68°
km
0
40
PHYSIOGRAPHIC UNITS
I Baffin Coastal Lowland
II Davis Highlands
III Baffin Upland
IV Lancaster Plateau
V Foxe Plain
VI Melville Plateau
Boundary between physiographic units . . . .
* C1 Location of main camp sites for operation Bylot
(e.g. C4 = head of Cambridge Fiord)

Figure 1. Index map showing the location of the Clyde-Cockburn Land map area, its regional geological map coverage, and the physiographic subdivisions within it (after Bostock, 1970a, b). Campsite locations are indicated by C1, C2, etc.

Figure 2. *Old Inuit dwelling sites on the west side of Adams Island (NTS 37H). Photograph by G.D. Jackson. GSC 186934*

At the Adams Island site (Fig. 2) whale bones, stones, and driftwood have been used in constructing the walls, which now are as much as one metre high. Some of the dwellings appear to have more than one floor and to have been used by different generations. Presence of boat remains and whale bones suggest habitation when the whaling industry was in operation, while some of the articles seen were clearly marked as having come from the DEW Line operation.

Wildlife and vegetation

An increasing number of Arctic wildlife studies are being carried out annually, and many of them provide data for the map area (e.g. Blomquist and Elander, 1981; McLaren and McLaren, 1982; Schweinsburg et al., 1982; Reeves et al., 1983; Stirling and Calvert, 1983). A useful summary of the wildlife, vegetation, and other features of part of the map area is contained in a regional analysis by Beardmore (1978).

Wildlife seen on Operation Bylot seemed less abundant within the present map area than in areas to the north and south. Ground squirrels and lemming were common and several small groups of caribou were seen. Foxes, wolves, and Arctic hares were encountered occasionally, and few polar bears were seen. Seals were the most common sea mammals seen, and were encountered mostly along the eastern coast. Narwhal and white whales were common, and walrus were also reported. A large variety of birds were encountered, chiefly in the coastal areas, and include Canada geese and snow geese, ducks, jaegers, gulls, Arctic terns, ptarmigan, plovers, owls, and sandpipers. Arctic char are common.

Baffin Island lies well north of the treeline and vegetation becomes increasingly sparse northward. The cold windy climate, abundant soil creep and mudflows, poor drainage due to permafrost, and formation of patterned ground by repeated freezing and thawing, all result in a sparse dwarfed vegetation. Dwarf willows, birch, and blueberry bushes hug the ground locally in protected areas. Heather, moss, grass, and several varieties of flowering and berry-producing plants are also present.

Climate

Five climatic regions have been outlined in the Canadian Arctic Islands by Maxwell (1981), who also provides an extensive list of selected references. Mean January temperatures for the map area are in the -20° to -32°C range and those for July are in the 4° to 8°C range. Annual precipitation is in the 200-250 mm range for most of the map area, but may be as much as 600 mm in the mountains and eastern coastal areas. Rain accounts for 40-50% of the moisture falling west of the mountains, as compared to 20-25% for the rest of the map area. Temperature inversions are most common in winter months. Detailed data for the Clyde weather station are provided annually in the Canada Year Book, published by Statistics Canada and available in most libraries (e.g. Statistics Canada, 1991).

The main breakup on Baffin Island, opening of streams, and disappearance of lake ice, usually occurs over several weeks from mid-June to late July. Occasionally, lakes at higher elevations, the large lakes Bieler and Conn (map area 37E), the lower reaches of some northern fiords, and some north-central areas, do not open up. This was so in 1967 and 1968.

In general, Baffin Island appears divisible into three rate of snow cover disappearance zones. Snow cover disappears earliest south of a line that trends northwest several kilometres north of Frobisher Bay, and remains longest north of the DEW Line and the Foxe Fold Belt, and in the Davis Highlands.

Temperature and humidity are fairly uniform for most of the summer (Appendix 1), but are more variable in the interior than along the coast. Wind, cloud cover, and amount of precipitation are quite variable, particularly after the sea ice breaks up. The east coast is particularly susceptible to fog. Although precipitation is low, rainy days, snow flurries, and, to a lesser extent, hail are common, particularly in the vicinity of the plateau glaciers which spawn gusting winds and their own individual weather conditions. There was still 80% snow cover the last week of June 1968 in the region around camp 1 (Fig. 1; *see* Fig. 8b). At least one snowfall of several centimetres occurs on low ground between mid-July and mid-August. Calm days are uncommon (10-12% in 1965, 1968).

Physiography

The surface of Baffin Island is an undulating, peneplained erosion surface broken by faults, tilted upward toward the northeast chiefly during Cretaceous-Tertiary time, and dissected to varying degrees by glacial and stream action (Fig. 3). A combination of dendritic and parallel streams were entrenched on the old peneplain surface and the drainage divide migrated westward to its present position a little west of the heads of the east coast fiords. Along the watershed the headwaters of short easterly flowing streams such as Quernbiter, Keel, Tay, and Erik rivers, intertwine with the uppermost reaches of the larger, longer southwesterly flowing streams such as Isortoq, Rowley, Cockburn, and Ravn rivers (Fig. 1). Only a few streams of any size flow easterly between the fiords. One, the Kogulu River, drains Ayr Lake (map area 27E and 27F), while a larger river flows easterly through the Bruce Mountains north of Clark Fiord (map area 37H and 27G).

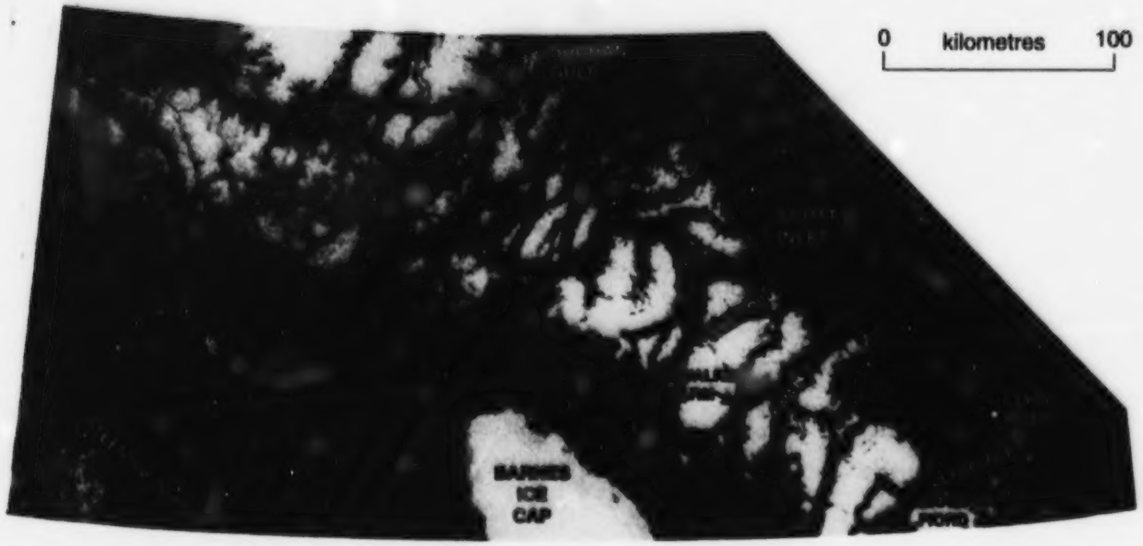

Figure 3. National Air Photo Library Landsat mosaic of north-central Baffin Island, showing submergence of uptilted northeast coast. Barely discernible ribbed topography in the Tay Sound area reflects the Neohelikian Bylot Supergroup and Hadrynian Franklin dykes. Note also the Paleozoic strata west of Steensby Inlet. LANDSAT mosaic EMG-1789.

The streams are poor transportation routes in the summer because they dry up rapidly, and contain numerous rapids and shallows. Also, water flow commonly changes markedly during the day because the streams are fed chiefly by melting snow and glaciers. The Rowley and Isortoq rivers are probably the most easily navigable.

The Baffin Bay coast is typical of coasts that have been extensively uplifted, dissected, and then submerged (Fig. 3). The Foxe Basin shoreline, also submerged, is relatively low, and has numerous shoals.

Five of the major physiographic divisions shown by Bostock (1970a, b) for the region are represented in the map area (Fig. 1). Three of them (Davis Highlands, Baffin Coastal Lowland, Baffin Upland) are underlain almost entirely by Archean and Aphebian metamorphic and igneous rocks. The Lancaster Plateau is underlain mainly by Neohelikian and Paleozoic strata and locally by older gneisses. The Foxe Plain is underlain mainly by Paleozoic strata.

The most scenic part of the map area is the mountainous fiord region of the Davis Highlands (frontispiece; Fig. 3, 4, and 5). Here the peneplained surface has been deeply dissected, and high, near-vertical cliffs up to more than 1000 m high are common along fiords that are up to 115 km long. Most of the terrain above 900 m in elevation is ice-covered and the higher peaks, which rise to 1900 m near Stewart Valley (Fig. 1; map area NTS 27E and 27F), tend to be concordant and flat-topped. Myriad hanging glaciers and valley glaciers with a complete representation of attendant moraines flow outward from plateau glaciers of all shapes and sizes (frontispiece; Fig. 3, 4, and 5). U-shaped valleys are common, and sandurs are well developed mainly along the lower reaches of streams flowing into the heads of fiords (*see* Church, 1972). Water depths of 900 m have been reported from Sam Ford Fiord (NTS 27F) and 474 m from the main basin of Clyde Inlet. Greatest depths generally occur below the highest mountains (Løken, 1967). Depths of 750 m occur in submarine troughs at the mouths of Scott Inlet (map area NTS 37H and 27G) and Buchan Gulf (Løken and Hodgson, 1971; MacLean, 1978; MacLean and Falconer, 1979).

Elevations drop off sharply along the eastern edge of the Davis Highlands to a low, flat, narrow, discontinuous stretch of terrain, called the Baffin Coastal Lowland. Segments of this plain occur throughout the coastal regions of Bylot and northern Baffin islands and extend from Cape Macculloch (north of Nova Zembla Island in map area NTS 48A) for about 675 km southeast to the vicinity of Broughton Island (Fig. 1, 6; *see* Fig. 113). It is best developed east of Inugsuin Fiord (immediately south of Clyde Inlet) where it is about 100 km wide (Fig. 1, 3). The Baffin Coastal Lowland may be divided into an eastern coastal area in which most elevations are 150 m or less, and a western, more hilly area, with elevations up to 460 m. The western hills occur mainly adjacent to the Davis Highlands and many rise abruptly from the lowland. These steep slopes probably represent modified wave-cut cliffs and the eastern part of the lowland an elevated wave-cut bench.

Elevations also drop off sharply west of the Davis Highlands to about 760-915 m in the watershed zone along the heads of the fiords where the highlands merge with the Baffin Upland to the west. The peneplain is prominent in the upland and is flat to rolling with a gentle slope southwest to elevations of about 30-155 m in the vicinity of Steensby Inlet and along the east coast of Foxe Basin where the upland surface

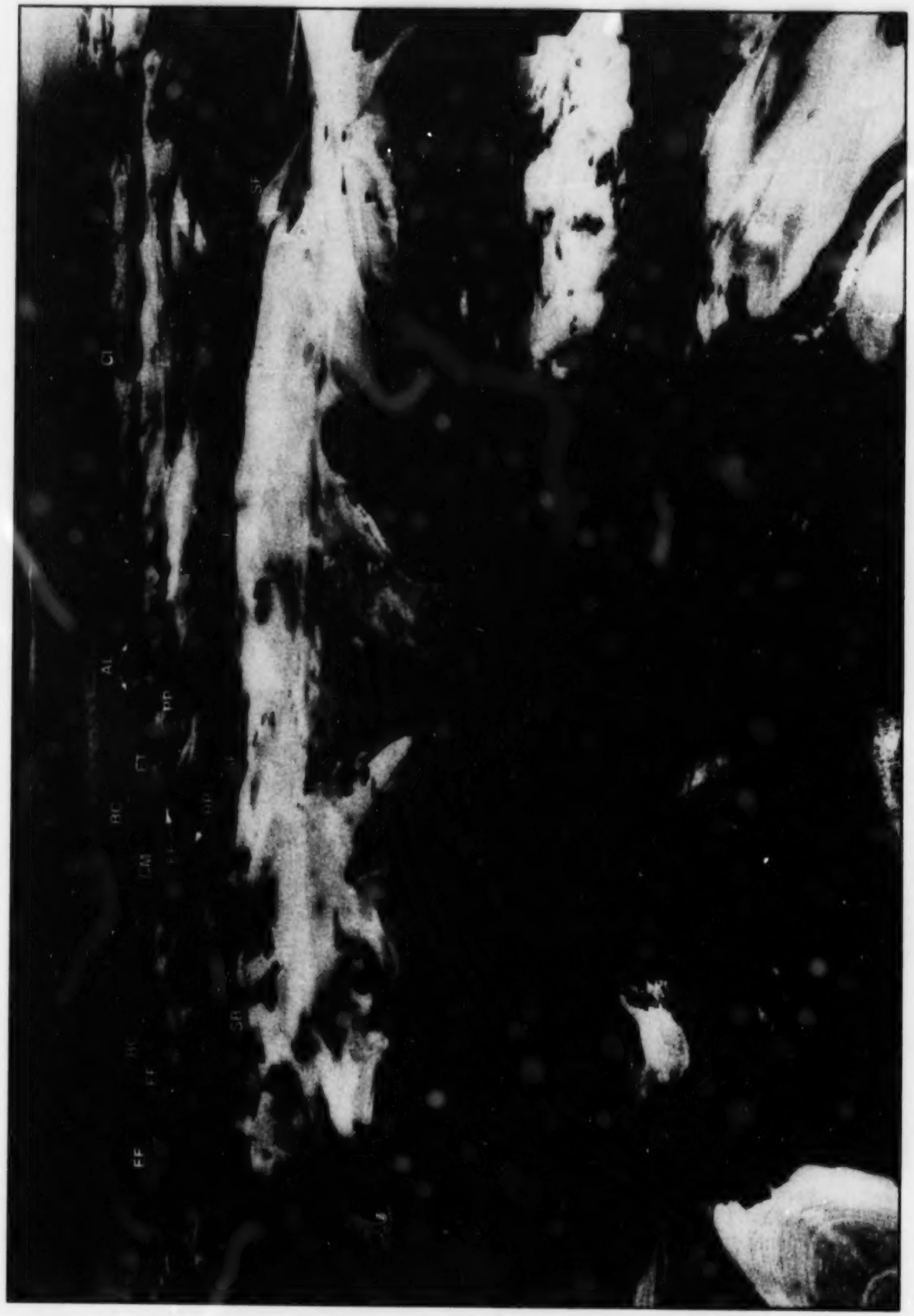

***Figure 4.** View est across Walker Arm and Davis Highlands toward Clyde Inlet (NTS 27 E, F). Subhorizontal planar features adjacent to Walker Arm include thrusts and nappes. Most gneisses are granitoid nebulites (Amn Jackson, 1984). NAPL oblique airphoto T219L-141. Al–Ayr Lake, BC – Baffin Coastal Lowland, CI – Clyde Inlet, CM – Cockscomb Mountain, EF – Eglington Fiord, ET – Eglington Tower, IF – Inugsuin Fiord, RP – Revoir Pass, PP – Pioneer Peak, SF – Sam Ford Fiord, SB – Swiss Bay.*

dips below the Foxe Plain. Streams commonly show evidence of rejuvenation and both streams and lakes occupy broad to narrow steep-sloped valleys, the floors of which are as much as 550 m below the upland surface (Fig. 1, 7, 8). The Barnes Ice Cap has a maximum elevation of about 1130 m and lies in the centre of the Baffin Upland.

The Lancaster Plateau is represented along the western edge of the map area in the Tay Sound-Paquet Bay area and between Mary River and Steensby Inlet (Fig. 1, 9, 10). The well dissected Lancaster Plateau has an elevation of approximately 460 m in the northern part of the map area and in the adjacent map area to the north (Jackson et al., 1975). The surface slopes southward to 30-155 m at Steensby Inlet where it meets the Foxe Plain. The surface of the Lancaster Plateau is consistently 155-305 m lower than the adjacent Baffin Upland from which it is separated by Nina Bang, Central Borden, Tikerakdjuak, and other fault zones (map areas NTS 37F and 37G). Thus, within the map area the Lancaster Plateau is present in graben structures that extend southeast into the map area from the main plateau area to the west (Blackadar, 1970).

Figure 5. ***a)*** *View west across central Ayr Lake (NTS 27F) at nebulitic granitoid gneiss* (Amn). *Peaks to 1500 m. Photograph by W.C. Morgan; GSC 186627-8.* ***b)*** *View south along the east side of Sam Ford Fiord from near Swiss Bay (NTS 27F). Banded migmatite* (Amg) *is overlain by nebulitic granitoid gneisses* (Amn)*. Peaks to 1200 m. Photograph by W.J. Crawford. GSC 186429.* ***c)*** *View north in Bruce Mountains at layered migmatites* (Amg) *in northeast corner of NTS 37E. Elevations to 1400 m. Photograph by S.L. Blusson. GSC 185543*

Figure 6. View southerly across the western Baffin Coastal Lowland north of Clyde. The ground rises toward the Sledge Pointers (snow-covered hills in the foreground), and the Davis Highlands beyond. Photograph by W.C. Morgan. GSC 186636

A low, flat to slightly hilly area west and north of Steensby Inlet (map area NTS 37F) is part of the Foxe Plain (Fig. 1). Elevations are commonly 30-155 m above sea level.

Quaternary geology

Evidence of glaciation is ubiquitous on Baffin Island (Fig. 4, 11), and there have been many studies of the Pleistocene-Recent (Holocene) record. Only those glacial features observed on Operation Bylot are shown on the five bedrock geological maps for the map area. Most of the raised beaches and moraines shown were plotted from airphotos without being checked on the ground, and locally may be misidentified for one another. For example, features interpreted as raised beaches north of lower Eglinton Fiord (map areas NTS 27F and 27E) are at a higher elevation than raised beaches reported from elsewhere along the east Baffin coast (e.g. Ives and Buckley, 1969). Information for the following brief Pleistocene-Recent summary is contained in reports by Falconer (1962), Andrews (1963, 1970, 1982), Ives and Andrews (1963), Ives (1964), Sim (1964), Prest et al. (1968), Prest (1970), Dyke (1974), Hodgson and Haselton (1974), Andrews and Barnett (1979), Dyke et al. (1982), and others referred to below.

Figure 7. *View west across Rowley River (RR) and Steensby Inlet (SI), and the Foxe Plain from near the boundary of NTS maps 37E and 37H. NAPL oblique airphoto T238L-115. AL – Angajurjualuk Lake, F – Fault, MR – Mary River Group, NB – Nina Bang Lake, SL – Separation Lake, VR – Ravn River.*

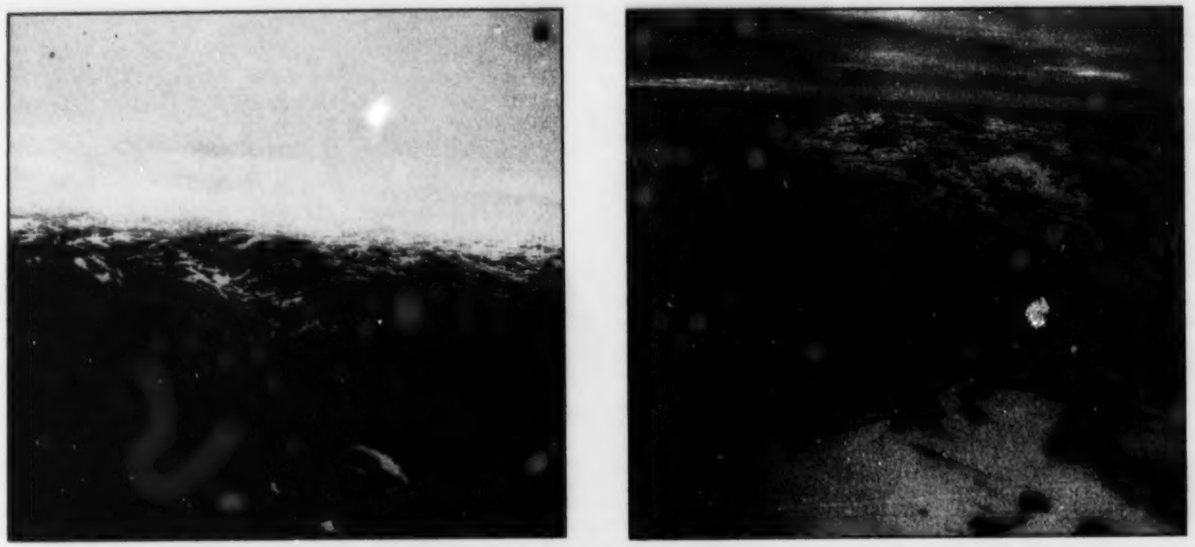

Figure 8. a) *View southwest across the dissected eastern Baffin Upland from the southwest edge of Davis Highlands and Lethbridge Lakes (NTS 37H). Note the general evenness of the skyline, and the small misfit, meandering stream in the valley. Local relief is about 600 m. Banded migmatites* (Amg) *are in the foreground. A faulted west limb of a synform lies on the left and mafic dykes can be seen on the right. Photograph by S.L. Blusson. GSC 185533.* ***b)*** *View northeast across the relatively muted topography of western Baffin Upland. The area around the unnamed lake is underlain chiefly by nebulitic granitic gneiss* (Amn; = Amg *in Morgan, 1982, 1983). Camp 1 is in the foreground, just south of the map area in the northwest corner of map area NTS 37D. Photograph shows snow cover at end of June. Photograph by S.L. Blusson. GSC 185476*

Figure 9.

View west across southeastern Lancaster Plateau from the southwest corner of NTS map area 37G. The Central Borden Fault Zone follows the line of lakes along the right edge of the airphoto. Light coloured areas in the centre of the airphoto and in the distance are underlain by Paleozoic strata. The ribbed bedrock pattern along the left side of the airphoto lies west of Angajurjualuk Lake (Fig. 1), and is underlain by layered migmatite (Amg) *containing layers of the Mary River Group (NTS 37G). A kettle plain and patterned ground occur in the foreground. NAPL oblique airphoto T222R-101.*

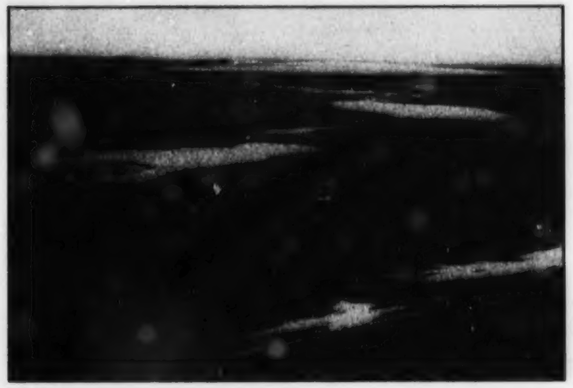

Figure 10. *View southwest across "Sheardown Lake" at Mary River (Fig. 1, NTS 37G), and Lancaster Plateau from the edge of Baffin Upland. The Central Borden Fault Zone, which separates the two surfaces, occurs in the gully running diagonally across the photograph. Round Lake at centre right lies along the right edge of Figure 9. Photograph by S.L. Blusson. GSC 185501*

Prest (1970) suggested the gross Pleistocene physiography of Baffin Island was similar to present physiography, and ascribed the island's complex glacial history to its physiography, latitude, and climate. Wisconsin Glaciation in the Canadian Arctic is taken as starting at least 100 ka ago (Prest, 1970; Andrews et al., 1975), and the Quaternary record may go back as much as two million years (Andrews and Miller, 1984). Relationships of glacial and interglacial deposits that predate the last or Wisconsin Glaciation (locally referred to as the Foxe Glaciation, ca. 120-5 ka) on Baffin Island have not yet been accurately determined. Old organic deposits in and adjacent to Clyde Inlet (map areas NTS 27F and 27E), Bruce Mountains (map areas NTS 27F and 27E, 37H and 27G), Isortoq River (map areas NTS 37E and 37F), and western Baffin Island (map areas NTS 37F and 37G) have yielded radiocarbon and U-series ages of 130-28 ka (Prest, 1970; Andrews et al., 1975, 1984; Feyling-Hanssen, 1976; Miller et al., 1977; Miller, 1979; Andrews and Miller, 1984). Andrews et al. (1975) suggested a significant continental ice sheet covered most of Baffin Island by 115 ka ago, and correlations based on several ice advances and recessions, with associated sea level changes, have been outlined for the interval 120-8 ka. There is great uncertainty in correlations for sediments that predate this interval (Andrews et al., 1984). Along the eastern coastal forelands of Baffin Island a common sequence consists of lower sediments (Kogalu Member) that are probably 120-70 ka old. These are overlain by 10-8 ka old distal glacial marine and beach sediments (Eglinton Member of the Clyde Foreland Formation), which in turn are overlain by aeolian sediments that are younger than 5 ka (Andrews and Miller, 1984). The lowermost unconsolidated sediments at Clyde Cliffs, along the coast north and south of Clyde River, may be of earliest Quaternary or Pliocene age. Burden and Holloway (1985) concurred with D.C. Umpleby (pers. comm., 1981) that two and probably all six of the small areas shown in the Scott Inlet region as Cretaceous-Paleogene(?) (KT4) by Jackson et al. (1978c) are Quaternary. Miller et al. (1977) have shown that one of these areas is probably part of the Quaternary Clyde Foreland Formation.

Initially, early Wisconsin ice probably accumulated rapidly on the high country of the Baffin Upland and expanded chiefly westward. Relatively little ice accumulated in the mountains or flowed eastward into the fiords. An ice dome, the "Foxe Dome" (the Foxe Glaciation) then developed in Foxe Basin and was a dispersal centre for much of Wisconsinan time (Ives and Andrews, 1963; Prest, 1970; Andrews et al., 1975, 1984; Miller et al., 1977; Andrews and Miller, 1979; Dyke et al., 1982). Some parts of eastern Baffin Island may have remained unglaciated during the glacial maximum, while other parts appear not to have been glaciated since the maximum (Løken, 1966; Ives and Buckley, 1969).

Periods of ice thinning accompanied by ice-marginal recessions and interspersed with ice readvances followed this maximum from about 60-9 ka ago (Prest, 1970; Andrews et al., 1975, 1984). One of the more recent ice readvances formed the Cockburn Moraine System (map areas NTS 27E, F, G and 37G, H) about 9-8 ka ago (Ives and Andrews, 1963; Falconer et al., 1965; Hodgson and Haselton, 1974; Andrews et al., 1975). This is a major system of moraines (Fig. 11d) that within the map area extends from Tay Sound (map area NTS 37G) southeast to the head of Sam Ford Fiord (map areas NTS 27E, F). From Cumberland Sound (*see* Fig. 114) northward these moraines probably represent the maximum Late Wisconsinan ice margin (Andrews and Miller, 1984).

The Foxe Dome deteriorated rapidly following the Cockburn advance and Foxe Basin was invaded by the sea 7.0-6.8 ka ago. However, a minor ice readvance, the "Isortoq phase", extended into the lower Isortoq River area 6.7 ka ago (Ives and Andrews, 1963; Andrews, 1966; Prest, 1970). The centre of ice dispersal shifted northeast onto Baffin Island as the Foxe Dome disintegrated. Glacial lakes formed around the northern part of the proto-Barnes Ice Cap about 5 ka ago and exist today as Conn and Bieler lakes (map area NTS 37E). Lakes once occupied the drift-covered areas north, northwest, and northeast of Barnes Ice Cap (map area NTS 37E). Cross-valley frontal moraines, marginal moraines, kames, beaches, and other features were formed during the same time period (Fig. 11). The cross-valley moraines (Fig. 11c) were probably deposited underwater (Andrews, 1963; Ives and Andrews, 1963; Prest et al., 1968; Andrews and Barnett, 1979).

Much of Baffin Upland was covered by thin ice and perennial snow fields during a period from 450-100 years ago (the Little Ice Age), but is now almost free of ice and deglaciation is still in progress (Ives and Andrews, 1963; Falconer, 1966; Miller, 1976; Andrews, 1982; Gilbert et al., 1985). Photographs taken more than a few years apart of the same glacier commonly show glaciers to be retreating. Some local mountain glaciers, insignificant in the overall glaciation of Baffin Island, have, according to Miller (1976), only recently (during the Little Ice Age) reached their maximum extents since mid-Wisconsinan time or earlier.

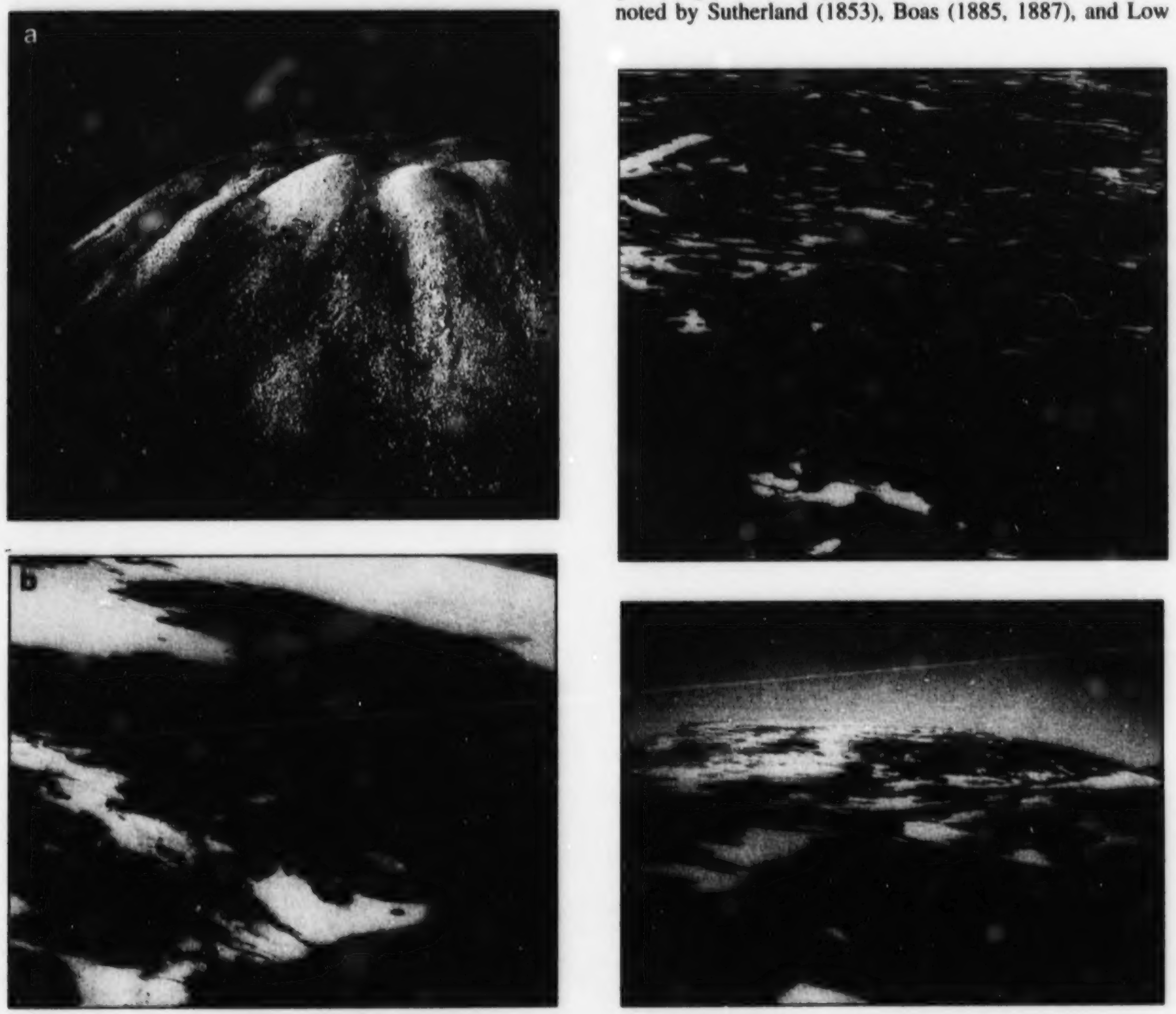

Figure 11. a) *Pingo on a sandur southwest of the head of Gibbs Fiord (NTS 37E). Photograph by S.L. Blusson. GSC 1997-54W.* **b)** *Kames adjacent to the east side of Barnes Ice Cap, just south of map area NTS 37E. Photograph by W.C. Morgan. GSC 186671.* **c)** *Cross-valley frontal moraines northeast of Barnes Ice Cap in map area NTS 37E, possibly formed underwater. Photograph by A. Davidson. GSC 204194-R.* **d)** *Cockburn Moraine System in the southwestern part of map areas NTS 27E and NTS 27F. Photograph by W.J. Crawford. GSC 186437*

Previous bedrock studies

Early explorations

Reports of Arctic explorations commonly refer at least briefly to some aspects of bedrock geology, and some contain sizeable sections devoted to this branch of "natural history". Bylot and Baffin sailed along the east coast of the map area in 1616 (Markham, 1881), as did Ross in 1818 (Ross, 1819). Parry (1821) noted the occurrence of granite, gneiss, limestone, and quartzite on the east coast of Baffin Island north of Scott Inlet. Parry (1824) also noted the presence of limestone around northern Foxe Basin and the widespread occurrence of granitic rocks northeast of Fury and Hecla Strait. The prevalence of granitic gneisses along the east coast of Baffin Island was noted by Sutherland (1853), Boas (1885, 1887), and Low (1906). The geology of the Black Bluff area south of Clyde River was described in a report by Bernier (1910) in which it was concluded that Clyde Inlet was formed by downfaulting. Tremblay (1921) referred to copper-bearing rocks having been found on the beach at Clyde River.

The Fifth Thule Expedition of 1921-1924 added considerably to the geographic and geological knowledge of the interior of northwestern Baffin Island. Mathiassen (1927, 1933) noted several aspects of geology along the west edge of the Clyde-Cockburn Land map area, and identified a fault along what is now called the Central Borden Fault Zone. Teichert (1937) discussed the late Precambrian rocks of the Bylot Supergroup, and identified Paleozoic fossils collected from this area.

Several localities in southern and northern Baffin Island were visited by Weeks (1927, 1928) from 1925 to 1927. He commented on the coal deposits in the Cretaceous-Eocene strata, on the Bylot Supergroup, and on the underlying gneiss-granite complex.

Recent studies

Bedrock, chemical, and geophysical studies carried out in and adjacent to the map area since 1950 are summarized in Figure 12 and Table 1. Some additional comments are provided below.

The systematic study of the geology of Baffin Island began in 1950 when Kranck (1951, 1953, 1955) and Eade (1953) outlined metasedimentary belts and discussed the

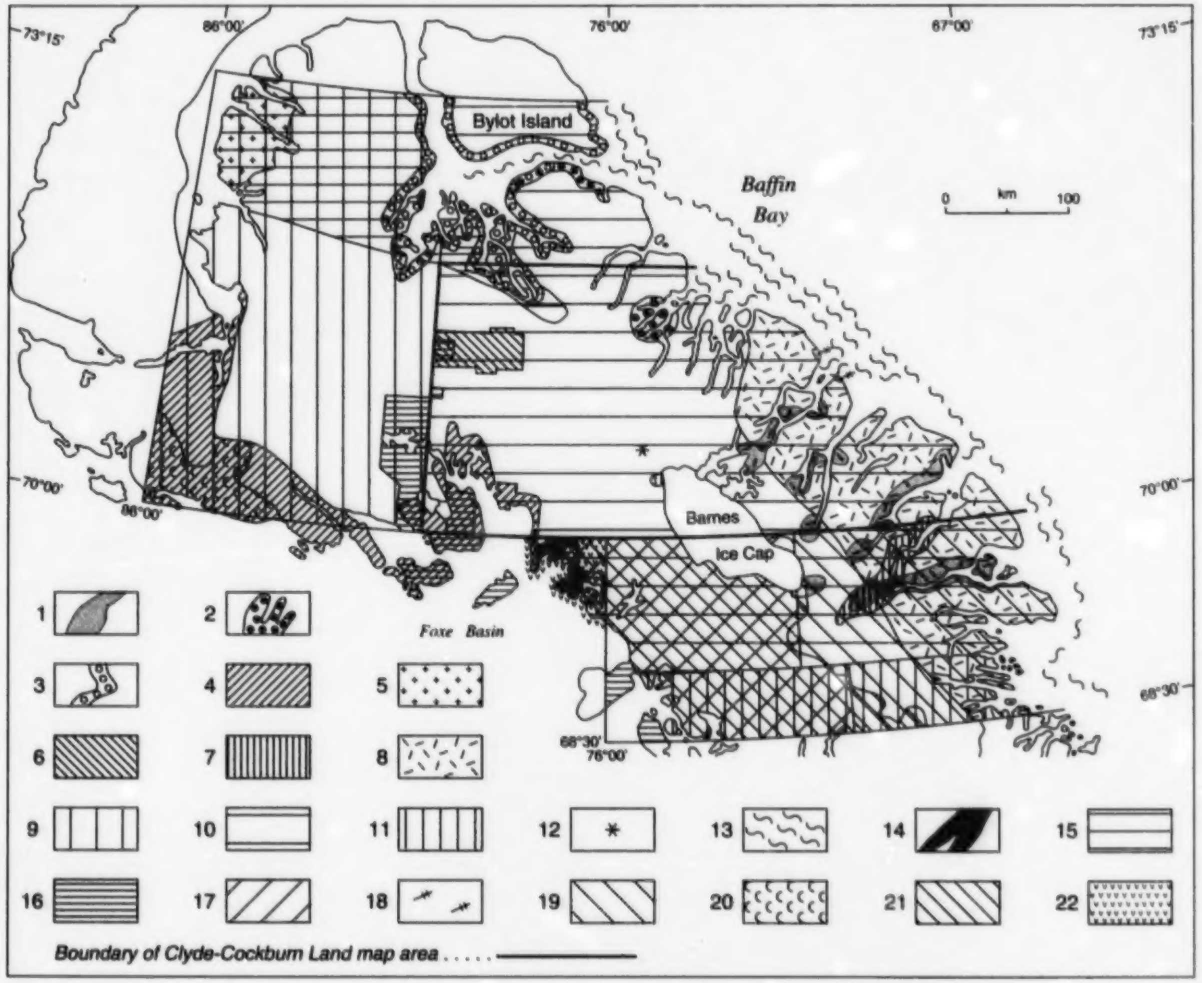

Figure 12. *Location and nature of geological studies done in and adjacent to the Clyde-Cockburn Land map area since 1950. The legend is keyed to Table 1, which indicates the authorship, type of study, and map scale of the various study areas.*

Table 1. Recent geological studies in and adjacent to the Clyde-Cockburn Land map area.

No.[1]	Area	References	Type of study, map scale
1	McBeth to Gibbs fiords	Kranck (1951, 1953, 1955), Eade (1953)	Reconnaissance, metamorphic petrology, structure, Aphebian stratigraphy
2	Pond Inlet, Buchan Gulf	Daniels (1956)	Metamorphic petrology, chemistry
3	Milne to Navy Board and Pond inlets	W.L. Davison (unpublished field data, and pers. comm., 1980)	Reconnaissance, Archean to Eocene
4	Fury and Hecla Strait to Steensby and Admiralty inlets	Blackadar (1958a, b, 1963)	Reconnaissance; 1:506 880 scale
5	Western Borden Basin	Lemon and Blackadar (1963)	Reconnaissance, Neohelikian and Paleozoic stratigraphy; 1:506 880 scale
6	Mary River	Baffinland Iron Mines Limited (1964, 1966), Gross (1966), Jackson (1966a, b, 1978b)	Metamorphism, structure, Archean and Paleozoic stratigraphy, geochronology, iron-formation and high grade iron deposits
7	Inugsuin Fiord	Gray (1966), Forester and Gray (1967)	Metamorphic petrology, structure, Aphebian sedimentology
8	Northeast Baffin Island	Shaw et al. (1967), McCulloch and Wasserburg (1978), Shieh and Schwarcz (1978)	Regional chemistry, model Sm-Nd and Rb-Sr ages, $\delta^{18}O$ isotope values
9	Northwest Baffin Island	Blackadar (1968a, b, c, 1970), Trettin (1969)	Reconnaissance, Neohelikian and Paleozoic stratigraphy; 1:253 440 scale
10	North-central Baffin Island	Jackson (1969, 1978a, 1984), Fahrig et al. (1971, 1973), Jackson and Taylor (1972), Bridgwater et al. (1973), Jackson and Davidson (1975), Jackson and Morgan (1978a, b), Jackson et al. (1975, 1978b, c, d, 1990a, b), Berman et al. (1993)	Reconnaissance, metamorphic and tectonic syntheses, Archean to Eocene stratigraphy, geochronology; 1:250 000 scale
11	South-central Baffin Island	Jackson (1971), Jackson and Taylor (1972), Bridgwater et al. (1973), Fahrig and Schwarcz (1973), Jackson and Morgan (1978a), Jackson et al. (1990a, b), Berman et al. (1993)	Reconnaissance, metamorphic and tectonic syntheses, Aphebian stratigraphy, geochronology
12	Northwest of Barnes Ice Cap	Andrews et al. (1972)	Paleogene sedimentology and palynology
13	Offshore, northeast Baffin Island	Keen et al. (1972, 1974), Jackson et al. (1977), Levy (1978, 1979), Loncarevic and Falconer (1977), MacLean (1978, 1982), MacLean and Falconer (1979), Levy and MacLean (1981), Reid and Falconer (1982), MacLean and Williams (1983), Loring (1984), Grant et al. (1986)	Seismic, gravity, and magnetic studies; bottom sampling and trace metal studies. In the Buchan Gulf to Scott Inlet area the sialic crust is 32-40 km thick and Cretaceous strata contain natural oil seepages
14	Eqe and Grant-Suttie bays	Crawford (1973)	Iron-formation and high grade iron deposits, Archean stratigraphy, metamorphism, chemistry; 1:6000 scale
15	Borden Rift Basin	Blackadar (1968a, b, 1970), Geldsetzer (1973a, b), Jackson and Davidson (1975), Jackson et al. (1975, 1978b, 1980, 1985), Olson (1977, 1984), Jackson and Iannelli (1981, 1989), Jackson (1986), Jackson and Sangster (1987), Knight and Jackson (1994), Hofmann and Jackson (1994), Iannelli (1992)	Neohelikian sedimentology and stratigraphy, tectonics; 1:253 440, 1:250 000 scales
16	Northern Foxe Basin to Mary River area	Trettin (1975)	Early Paleozoic stratigraphy and sedimentology; 1:250 000, 1:500 000 scales
17	West-central Baffin Island	Morgan et al. (1975, 1976), Tippett (1980), Morgan (1982, 1983), Henderson et al. (1988, 1989), Henderson and Henderson (1994)	Metamorphic petrology, structure, Aphebian stratigraphy, geochronology; 1:250 000 scale
18	Mouth of Scott Inlet	Miller et al. (1977), Burden and Holloway (1985)	Quaternary stratigraphy, palynology
19	East-central Baffin Island	Henderson et al. (1979), Henderson and Tippett (1980), Henderson and Loveridge (1981), Henderson (1985a, b)	Metamorphic petrology, structure, Aphebian stratigraphy, geochronology; 1:250 000 scale
20	Fury and Hecla Strait	North side: Chandler et al. (1980), Ciesielski (1983), Maurice and Charbonneau (1983), Chandler (1988); South side: Schau and Heywood (1984)	North side: Neohelikian stratigraphy and sedimentology, geochronology; 1:250 000 scale; metamorphic and igneous petrology, uranium mineralization. South side: Neohelikian stratigraphy and sedimentology, metamorphic and igneous petrology; 1:500 000 scale.
21	Southwest of Barnes Ice Cap	Cameron (1986)	Lake sediment and water regional geochemical survey, shows, arsenic and base metal anomalies; ca. 1:2 000 000 scale.
22	Eqe Bay-Grant-Suttie Bay	Bethune and Scammell (1993,1997), Scammell and Bethune (1995a), Bethune et al. (1996)	Igneous and metamorphic petrology, structure, Archean and Aphebian stratigraphy, geochronology; 1:100 000, 1:50 000 scale.

[1] Numbers keyed to areas on Figure 12.

metamorphic petrology and structure of several areas from McBeth Fiord northwest to Gibbs Fiord. A geological reconnaissance of the Admiralty Inlet area in 1954 by Lemon and Blackadar (1963) established Neohelikian and Paleozoic stratigraphy for northern Baffin Island. Subsequently Blackadar (1958a, b, 1963, 1968a, b, c, 1970) and Trettin (1969) completed the reconnaissance mapping of northwestern Baffin Island which included local observations in the western part of the Clyde-Cockburn Land map area.

In 1965, Gross (1966) examined the Mary River iron deposits (map area NTS 37G) in detail, while Jackson (1966a, b, 1978b) carried out studies in an area of about 1950 km^2 that includes the deposits. W.J. Crawford assisted Jackson in 1965 and 1968, and incorporated some of the data into a Ph.D. thesis on the metamorphosed iron-formations and high grade iron deposits of the Mary River Group (Crawford, 1973). The thesis deals mainly with the Eqe Bay area and is based largely on fieldwork carried out for Patino Mining Corporation in 1969. Data from the above studies were used in interpreting the Steensby Inlet (NTS 37F) and Icebound Lake (NTS 37G) map areas, and in this memoir.

Also in the mid-1960s a suite of 116 bedrock samples, from the eastern coastal region of Baffin Island, was used in a chemical study of the Canadian Shield by Shaw et al. (1967). The Baffin samples were divided into four lithological types, but could not at that time be differentiated as to age and map unit. The samples were obtained from Archean and early Proterozoic orthogneisses, paragneisses (clastic and chemical origins), and migmatites, and early Proterozoic granite-charnockite, and may include a few Cretaceous-Eocene samples.

McCulloch and Wasserburg (1978) obtained model Sm-Nd and Rb-Sr ages of 2.74 ± 0.05 Ga and 2.56 ± 0.03 Ga respectively for composites of the Baffin Island samples used by Shaw et al. (1967). The oxygen isotopes of these samples were studied by Shieh and Schwarcz (1978), who noted a bimodal distribution of their $\delta^{18}O$ values for quartzofeldspathic rocks.

In 1970, a large region south of 69°N (and Operation Bylot) was mapped during Operation Penny Highlands, a helicopter reconnaissance survey headed by the author (Jackson, 1971; Jackson and Taylor, 1972; Bridgwater et al., 1973; Jackson and Morgan, 1978a). W.F. Fahrig visited both Operation Bylot and Operation Penny Highlands in the field to collect samples for paleomagnetic studies of late Proterozoic diabases on Baffin Island (Fahrig et al., 1971, 1973; Fahrig and Schwarz, 1973).

Atlantic Geoscience Centre began offshore geophysical and geological bedrock studies along the east coast of Baffin Island in about 1972 (no. 13 of Fig. 12, Table 1).

In 1974, W.C. Morgan began regular 1:250 000 mapping of central Baffin Island, immediately south of the map area, between 68° and 70°N. This area contains the southernmost and northernmost areas covered by Operation Bylot and Operation Penny Highlands, respectively (Morgan et al., 1975, 1976; Morgan, 1982, 1983). Chernis (1976) and Tippett (1978, 1979, 1980) completed B.Sc. and Ph.D. theses respectively on parts of the area mapped by Morgan.

The eastern half of Morgan's project area was taken over by Henderson and mapped during 1978 and 1979 (Henderson, 1982, 1985a, b; Henderson and Tippett, 1980; Henderson et al., 1979). Brisbin (1979) completed a B.Sc. thesis on the geology of an island in the eastern part of Henderson's area (27A). Henderson and co-workers have carried out more detailed studies in central Baffin recently (Henderson et al., 1988, 1989; J.R. Henderson and R.R. Parrish, poster presented at Forum 92, Ottawa, Ontario, January 1992; Henderson and Henderson, 1994).

The Neohelikian Bylot Supergroup and underlying gneisses in and adjacent to the northwestern part of the map area, have been studied in recent years by several workers (Jackson et al., 1980; Jackson and Iannelli, 1981; Hofmann and Jackson, 1994; Fig. 12, Table 1). Jackson and Davidson (1975) and Jackson et al. (1975) first recognized the depositional environment as a rift basin.

A Sm-Nd study of certain Archean and Aphebian map units throughout Baffin Island and in northernmost Quebec-Labrador, and based on about 120 samples, has been carried out by E. Hegner and the author (Hegner and Jackson, 1990; Jackson et al., 1990a; Jackson and Hegner, 1991). Twelve of the samples come from the map area.

Aeromagnetic maps covering the map area east of the Davis Highlands have been published by the Geological Survey of Canada on a scale of 1:63 360 and 1:253 440.

Local base metal and strong arsenic anomalies were identified by a regional geochemical survey southwest of Barnes Ice Cap (Cameron, 1986).

A co-operative MDA scientific project between the Geological Survey of Canada and the Government of the Northwest Territories from 1991 to 1996 studied the geology and economic potential of the Eqe Bay area (NTS 27C/9, 10, 15, 16) in more detail. The project was carried out by K. Bethune and R. Scammell, with the author as scientific advisor. Fieldwork in 1992 and 1994 for map publication at 1:50 000 formed the basis for geochronological, petrological, and chemical studies (Bethune and Scammell, 1993, 1995, 1997; Scammell and Bethune, 1995a, b; Bethune et al., 1996). Bedrock and surficial geology and mineral occurrences on northwestern Baffin Island, including most of the map area, have recently been recompiled at scales of 1:500 000 and 1:1 000 000 as part of the North Baffin Project (deKemp and Scott, 1998; Dredge et al., 1998; Sangster, 1998; Scott and deKemp, 1998; Richardson, 1999. These are not shown on Fig. 12 or Table 1).

Mineral explorations

Serious mineral prospecting in northern Baffin Island began in the early 1900s (*see* Bernier, 1911; Blackadar, 1970), and has been concentrated in the Milne Inlet Trough of Borden Rift Basin and the North Baffin Rift Zone (Jackson et al., 1975; Jackson and Iannelli, 1981). The Milne Inlet Trough extends northwest from the Tay Sound-Paquet Bay area in the northwest part of the map area (map area NTS 37G; Fig. 1, 13). Numerous assessment reports, filed with the Department of Indian Affairs and Northern Development, are

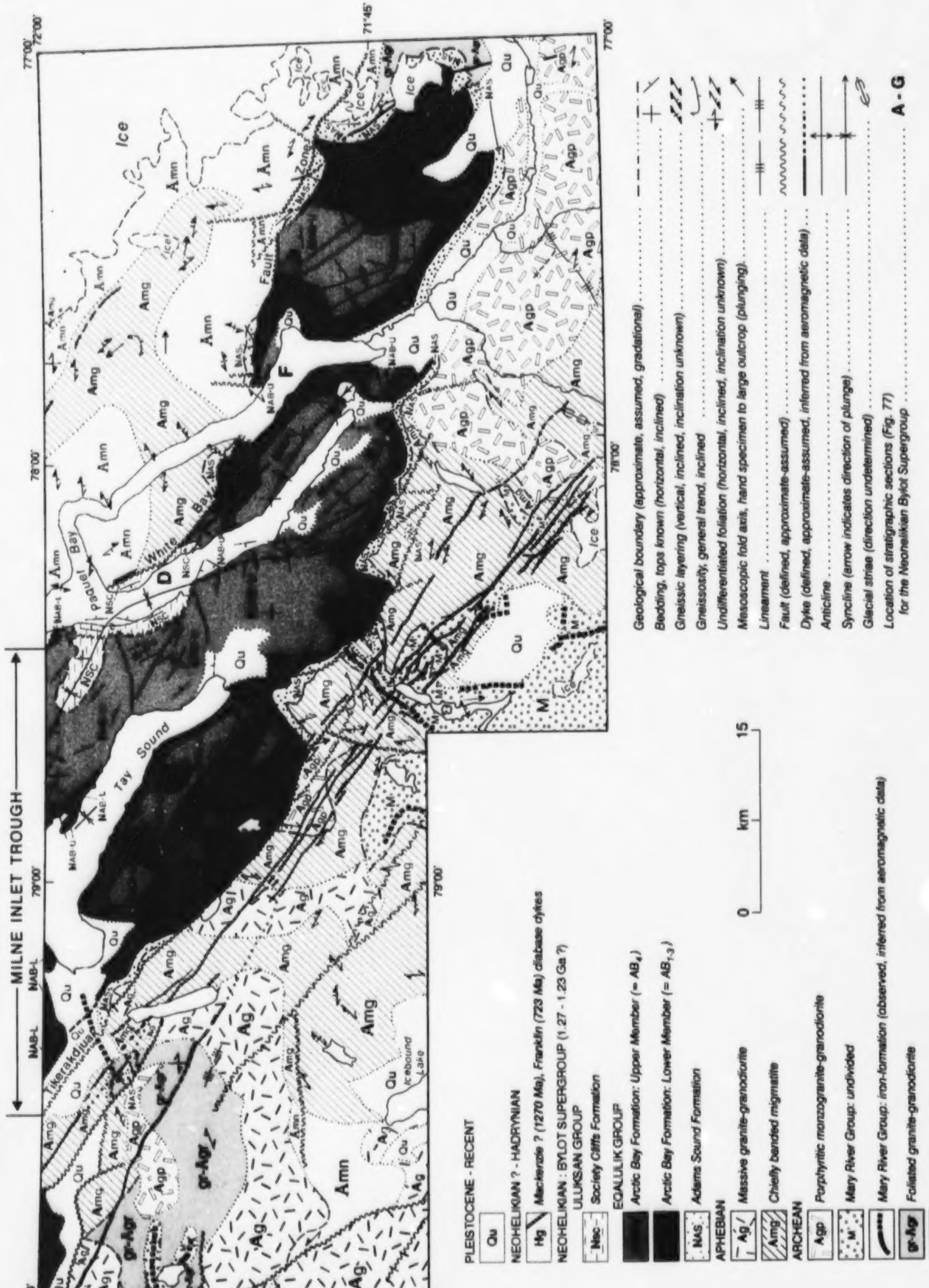
MILNE INLET TROUGH
NAB-L
Tay Sound
Paquet Bay
White Bay
Icebound Lake
Ice
0 km 15
PLEISTOCENE - RECENT
Qu
NEOHELIKIAN ? - HADRYNIAN
Hg Mackenzie ? (1270 Ma), Franklin (723 Ma) diabase dykes
NEOHELIKIAN : BYLOT SUPERGROUP (1.27 - 1.23 Ga ?)
ULUKSAN GROUP
NSc Society Cliffs Formation
EQALULIK GROUP
Arctic Bay Formation: Upper Member (= AB4)
Arctic Bay Formation: Lower Member (= AB1-3)
NAS Adams Sound Formation
APHEBIAN
Ag Massive granite-granodiorite
Amg Chiefly banded migmatite
ARCHEAN
Agp Porphyritic monzogranite-granodiorite
M Mary River Group: undivided
Mary River Group: iron-formation (observed, inferred from aeromagnetic data)
gr-Agr Foliated granite-granodiorite
Amn Nebulitic granodiorite migmatite
Geological boundary (approximate, assumed, gradational)
Bedding, tops known (horizontal, inclined)
Gneissic layering (vertical, inclined, inclination unknown)
Gneissosity, general trend, inclined
Undifferentiated foliation (horizontal, inclined, inclination unknown)
Mesoscopic fold axis, hand specimen to large outcrop (plunging)
Lineament
Fault (defined, approximate-assumed)
Dyke (defined, approximate-assumed, inferred from aeromagnetic data)
Anticline
Syncline (arrow indicates direction of plunge)
Glacial striae (direction undetermined)
Location of stratigraphic sections (Fig. 77) for the Neohelikian Bylot Supergroup
A - G
80°00'
79°00'
78°00'
77°00'
72°00'
71°45'

***Figure 13.** Revised geology for the northwest corner of Map 1451A (Icebound Lake, NTS 37G; Jackson et al., 1978b), northwest Clyde-Cockburn Land map area.*

listed in Jackson and Sangster (1987). The work resulted in a zinc-lead-silver mine being brought into production by Nanisivik Mines Limited in 1976 at the newly built town of Nanisivik, 27 km east of Arctic Bay and about 150 km northwest of Milne Inlet (Fig. 1; Agar and Farquharson, 1980; Clayton and Thorpe, 1982). Nanisivik Mines has an ongoing exploration program in the Nanisivik region. King Resources Co. carried out an extensive study of the Neohelikian strata in the Milne Inlet Trough in 1969, 1970, and 1971 (Fig. 13). Studies included mapping and facies studies, geophysical and geochemical surveys, and diamond drilling. Several sulphide showings were found, chiefly galena-sphalerite, and occurrences of several copper minerals were reported. The 1970 fieldwork by King Resources Co. included mapping the Neohelikian strata in the northwest corner of the Clyde-Cockburn Land map area (Fig. 13) where a few mineral showings were found (northwest Icebound Lake, map area NTS 37G) (Olson, 1970, 1977, 1984; Trigg, Woollett and Associates Ltd. and Geowest Services Ltd., 1970; Geldsetzer, 1973a, b).

Global Arctic Islands Limited investigated some Pb-Zn showings in the region in 1973. Uranerz Exploration and Mining Ltd. examined the Milne Inlet Trough and adjacent basement gneisses in 1977 for uranium and Pb-Zn mineralization. In 1981 an extensive mineral exploration program was carried out in the Milne Inlet Trough by Petro-Canada, who continued working there as recently as 1985.

Murray Watts discovered high grade iron deposits in the northwest corner of the map area (map area NTS 37G; Fig. 1) at Mary River in 1962 (Guimond, 1963). Extensive development work was carried out on these deposits by Baffinland Iron Mines Limited (1964, 1966) who also prospected the Neohelikian strata in the Tay Sound-Paquet Bay segment of the Milne Inlet Trough (Fig. 13), mostly for sulphides. Nanisivik Mines Limited prospected for gold and mapped much of the Mary River Group in the western part of the map area in 1987 and 1989.

Parts of the map area were included in a broad reconnaissance survey carried out by Inco Limited several years prior (approximately 1962-1963) to Operation Bylot in 1968 (H. Vuori, pers. comm., 1981). Further studies were made by Inco Limited in 1971 which included geochemical work as well as an examination of ultramafic bodies and copper staining reported from map area NTS 37H-27G (Jackson, 1969). Aquitaine Company of Canada Limited also examined parts of the map area in the early 1970s.

The Patino Mining Corporation carried out detailed mapping and diamond drilling of iron-formations at Eqe Bay (south of map area NTS 37F), and examined iron-formations south of Isortoq Fiord and near the head of Rowley River (Steensby Inlet map area NTS 37F) in 1969 (Boyd, 1970; Crawford, 1973). The Rowley River high grade occurrence was found on Operation Bylot, but the other two occurrences had been reported earlier by Blackadar (1958b). All three occurrences are prominent on the aeromagnetic maps.

Cominco Limited (1977, 1981) mapped and sampled selected areas in the Foxe Fold Belt in 1976 and 1981, and in later years, including an area around the head of Sam Ford Fiord (map area NTS 37E; Fig. 1). Exploratory work was carried out in the belt by Petro-Canada in 1985 and by various companies in the late 1980s and early 1990s. Strathcona Mineral Services Limited carried out an extensive program in 1989 to study the Mary River Group and assess its mineral potential, partly with respect to gold, lead, zinc, and copper, and particularly in map areas NTS 37F and 37G. Additional work was performed in NTS 37G and 37C in 1991 when a small amount of gold was found locally at Eqe Bay. Several companies have continued exploratory work in northern Baffin Island up to 1996, most concentrating on base metals and gold associated with supracrustal sequences, but some looking for diamonds and other gem-quality minerals.

Present investigations

Fieldwork reported on here was carried out between mid-June and early September in 1965 and 1968, and in August 1967. During the main part of the work in 1968 six major campsites (Fig. 1) were occupied during Operation Bylot, which in order were: C1-about 19 km northeast from the head of Eqe Bay (Fig. 8b), C2-about 32 km southeast from Mary River, C3-at Pond Inlet, C4-about 11 km southwest from the head of Cambridge Fiord, C5-on the Clyde River about 13 km southwest from the head of Clyde Inlet, and C6-at the Longstaff Bluff (Fox 2 DEW Line Site) airstrip, about 100 km south by east from the first camp (Fig. 113). The first five sites all offered reasonable unprepared STOL landing sites for aircraft up to Twin Otter size equipped with low pressure oversized tires. The party entered and left the field area via Hall Beach on Melville Peninsula.

One Bell 47G4 and one Bell 47G4A helicopter were chartered from Niagara Helicopters Limited. A single-engined Otter was chartered from Bradley Air Services Limited, Carp, Ontario. It was equipped with ski wheels and oversized, low pressure tires. Bradley Air Services Limited also supplied the Cessna 180, also equipped with oversized, low pressure tires, that was used for the advance reconnaissance in August 1967. The helicopters were used almost solely for traversing, and the work was so arranged that the traversing was carried out uninterrupted by camp moves. The Otter was used for moving camp, gas caching, initial reconnaissances, moving personnel and supplies to and from the field, and supply runs. About 315 hours were flown with each aircraft, including ferrying. Several hours were also flown in a Piper Super Cub on oversized, low pressure tires, that was on contract to H. Trettin.

Geological studies were carried out mainly on low level helicopter traverses flown in a rectangular pattern along lines spaced about 9 km apart (Fig. 14). For the most part, landings were made at about 8 km intervals along the traverse lines. Individual traverses ranged from 200 to 580 km in length. In general, the work carried out on supracrustal sequences was more detailed than that on other rocks. In addition to the helicopter and a few fixed wing traverses, two fly camps were put out to examine gneiss domes. Several stratigraphic sections of Neohelikian strata were examined, and several ground traverses were carried out adjacent to campsites. An airphoto interpretation, provided in advance of the operation, was most useful in the field.

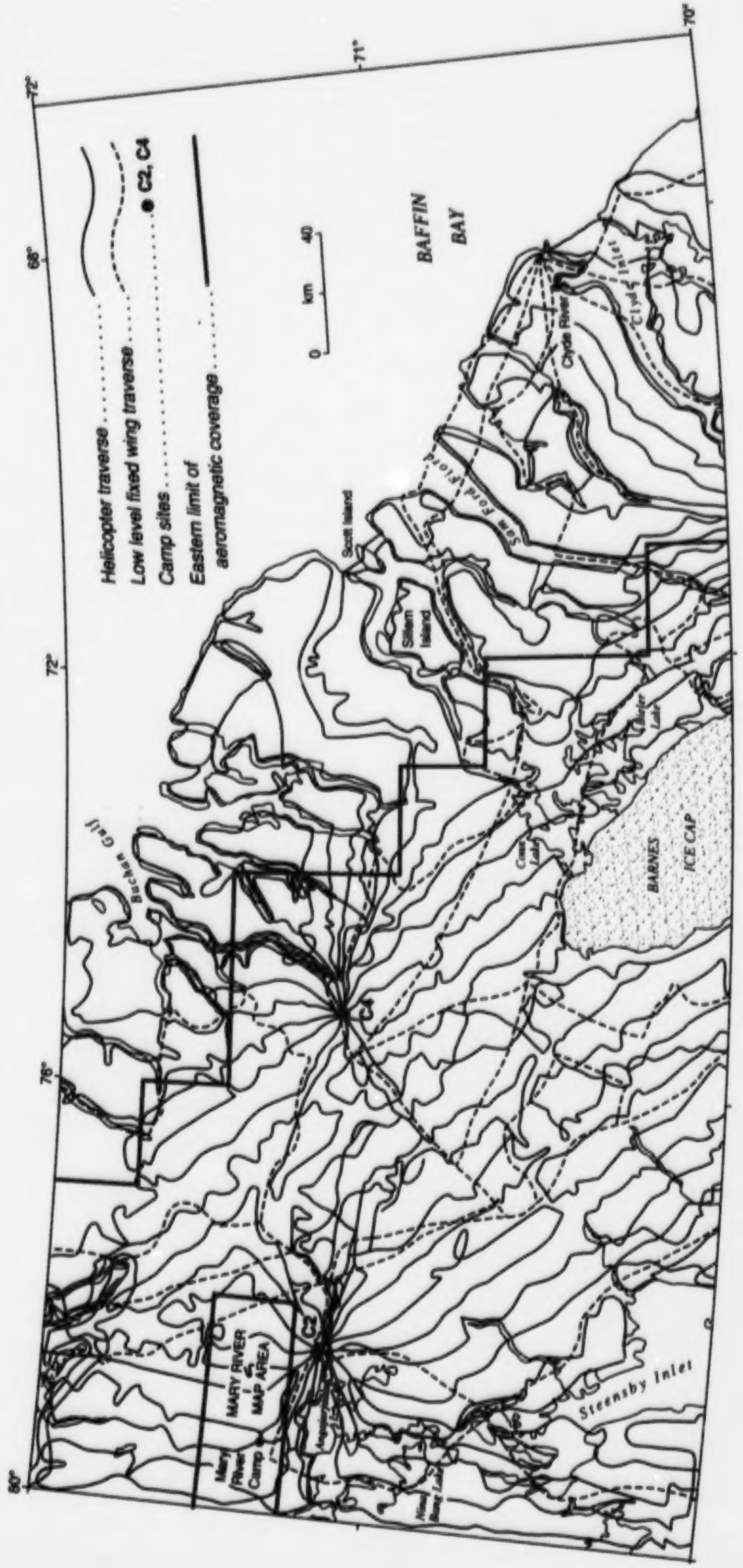

Figure 14. Approximate locations of airborne traverse lines.

A computer-oriented data form, conceived with some suggestions provided by E.W. Reinhardt, was utilized on Operation Bylot. The codes and classifications used are recorded in Reinhardt and Jackson (1973), and most need not be repeated here. A few comments are noted here for classifications that, for convenience, were modified from others that are commonly used. The classification for layering is given in Table 2. Wentworth's scale was used for grain sizes of sedimentary rocks whereas grain sizes of igneous and metamorphic rocks are shown in Table 3.

Sedimentary rocks have been classified according to Grabau (1904) and Pettijohn (1975). In this memoir, igneous rocks have been classified according to Streckeisen (1974, 1976, 1979), and there are a few minor differences compared with the terms used for the published maps, for which Brown's (1952) classification was used. The major differences involved granitoid and related rocks are listed in Table 4.

Table 2. Layering classification used in the field.

Sedimentary	Thickness	Igneous, metamorphic
thin laminated	<0.2 cm	finely foliated
thick laminated	0.2-<1 cm	foliated
very thin bedded	1-<5 cm	very thin banded
thin bedded	5-<10 cm	thin banded
medium bedded	10-<50 cm	medium banded
thick bedded	50-<100 cm	thick banded
very thick bedded	100-<1000 cm	very thick banded
massive	>1000 cm	massive
variable	variable	variable

Table 3. Grain sizes of igneous and metamorphic rocks.

glassy, aphanitic	microscopic
very fine grained	<0.1 mm
fine grained	0.1-1 mm
medium grained	1-5 mm
coarse grained	5-20 mm
very coarse grained, pegmatitic	>20 mm

Table 4. Comparison between classification of rock terms used in maps for the area and terminology used in this memoir.

Maps	This memoir (Fig. 15)
granite	syenogranite
quartz monzonite	monzogranite, minor quartz monzonite
granodiorite	granodiorite plus some tonalite, trondhjemite, quartz monzonite
syenite	syenite, some quartz monzodiorite
syenodiorite	monzodiorite, some quartz monzodiorite
monzonite	monzonite, some quartz monzonite
quartz latite	dacite-quartz latite, minor rhyolite-rhyodacite

In addition, some of Streckeisen's (1974, 1976) terms for charnockitic rocks have been modified here to be more compatible with his classification of granitic rocks and easier to remember (e.g. the charnockitic equivalent of monzogranite is named here monzocharnockite rather than farsundite – Fig. 15).

The main objective of the fieldwork was to study the Precambrian geology of the map area, but the early Paleozoic and Cretaceous-Eocene strata were also examined. About 550 thin sections (180 from Mary River area), 800 slabs stained for feldspars, and 510 spectrochemical analyses for 22 elements have been examined. These data are presented in this memoir in order to make them available, to provide background values for the map units, and to help in differentiating similar rocks of different ages.

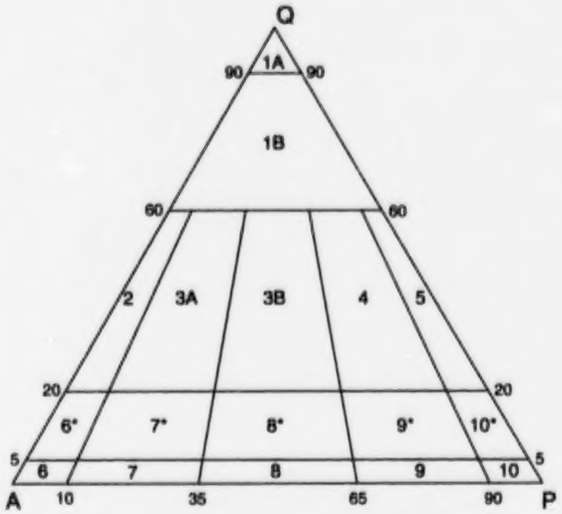

***Figure 15**. General classification of some plutonic rocks (volume per cent) after Streckeisen (1976). Q – quartz, A – alkali feldspars (orthoclase, microcline, perthite, anorthoclase, albite $An_{0.0\text{-}0.5}$), P – plagioclase $An_{0.5\text{-}100}$, scapolite. Charnockitic equivalents are shown in parentheses, some modified from Streckeisen (1976). 1A – quartzolite; 1B – quartz-rich granitoids; 2 – alkali-feldspar granite (alkali-feldspar charnockite); 3A – syenogranite (syenocharnockite); 3B – monzogranite (monzocharnockite); 4 – granodiorite (granoenderbite); 5 – tonalite (enderbite); 6* – quartz alkali-feldspar syenite (hypersthene quartz alkali-feldspar syenite); 7* – quartz syenite (hypersthene quartz syenite); 8* – quartz monzonite (quartz mangerite); 9* – quartz monzodiorite/quartz monzogabbro (quartz jotunite or quartz monzonorite); 10* – quartz diorite/quartz gabbro/quartz anorthosite (quartz norite); 6 – alkali-feldspar syenite (hypersthene alkali-feldspar syenite; 7 – syenite (hypersthene syenite); 8 – monzonite (mangerite); 9 – monzodiorite/monzogabbro (jotunite or monzonorite); 10 – diorite/gabbro/anorthosite (norite/anorthosite).*

In addition, about 105 rock and mineral samples were analyzed by both wet chemical and spectrochemical methods by the Analytical Chemistry Unit of the Geological Survey of Canada. More than half of these analyses were done for Crawford's (1973) Ph.D. thesis. An additional 12 samples were analyzed by Bondar and Clegg, Ottawa, for Crawford. Another suite of 35 samples, chiefly of possible economic interest, were analyzed spectrochemically for various elements by the Analytical Chemistry Unit of the Geological Survey of Canada. Davis Tube separations for seven iron ore samples and gold analyses for two quartz vein samples were carried out by CANMET Mineral Sciences Laboratories.

A large number of grain mounts were examined and an equally large number of X-ray mineral identifications were completed by the Mineralogy Section of the Geological Survey of Canada. Three Rb-Sr isochron studies, five Pb-U zircon ages, and a large number of K-Ar ages were carried out by the Geochronology Section of the Geological Survey of Canada. These have been incorporated into a recent paper on reconnaissance geochronology of Baffin Island (Jackson et al., 1990b).

Aquitaine Company of Canada Limited (internal report, 1971) made a study of the organic content of Cretaceous-Eocene Eclipse Group samples collected on Operation Bylot. W.S. Hopkins, Jr. and D.C. McGregor studied the contained microfossils. These studies are reproduced in Jackson and Davidson (1975) and Jackson et al. (1975). Paleozoic fossils collected by Jackson in the Mary River area prior to Operation Bylot have been reported on by T.E. Bolton and G.W. Sinclair (Bolton and Sinclair, 1967; Bolton et al., 1977).

Aeromagnetic maps were not available for most of the map area until shortly after the fieldwork was completed. They, together with airphotos and field photos, were used extensively to interpret and extrapolate from the gathered data.

Field and laboratory data for Operation Bylot have been included in several regional syntheses (Fahrig et al., 1971, 1973; Jackson and Taylor, 1972; Bridgwater et al., 1973; Jackson and Morgan 1978a; Jackson and Iannelli, 1981; Jackson and Sangster, 1987; Berman et al., 1993) and in a large number of maps and reports (Jackson, 1968, 1969, 1978a, 1984; Reinhardt and Jackson, 1973; Jackson and Davidson, 1975; Jackson et al., 1975, 1978b, c, d, 1985; Jackson and Cumming, 1981; Morgan, 1982, 1983; Henderson, 1985a). Data obtained for the northern part of the Icebound Lake map area (NTS 37G) during Operation Borden (e.g. Jackson and Iannelli, 1981) have been incorporated into this memoir (Fig. 13). A section across the Dexterity Granulite Belt, from Isortoq Fiord north to northwestern map area NTS 37E and northeastern map area NTS 37F (Fig. 1), was studied on a reconnaissance scale during two weeks in July, 1992, by R. Berman and the author. Some of the field and laboratory results of this study (e.g. Berman et al., 1993) are included in appropriate sections of this memoir. About two dozen previously unmapped remnants of the Mary River Group were noted by the author during a helicopter flight southeast across central map area NTS 37F in July 1994.

The area covered by this memoir adjoins the Pond Inlet map area (Jackson et al., 1975) on the north, Phillips Creek and Erichsen Lake map areas (Blackadar, 1968b, c) on the west, Koch Island and Lake Gillian map areas (Morgan, 1982, 1983) on the southwest, and McBeth Fiord-Cape Henry Kater map area (Henderson, 1985a) on the southeast.

General geology

The geology of the map area is shown on published Geological Survey of Canada 1:250 000 maps 1449A, 1450A, 1451A, 1458A, and 1582A (Fig. 1; Jackson et al., 1978b, c, d; Jackson and Morgan, 1978b; Jackson, 1984). Revisions for the northwest corner of Map 1451A (Icebound Lake, 37G), based on Operation Borden data (Jackson and Iannelli, 1981), are provided in Figure 13.

The map area lies within the northeastern Churchill Structural Province, which is also the northeastern part of Hoffman's (1989) Rae Province. Several episodes of deformation and metamorphism ranging in age from Archean to late Aphebian have affected the map area.

Consolidated rocks in the map area range from Archean to Cenozoic (Table of Formations), but most are complexly intermixed Archean rocks of various origins. All three Proterozoic eras are represented. Aphebian rocks are the most abundant and include a supracrustal sequence in the south and locally abundant granite-charnockite intrusions. Neohelikian strata are restricted to the northwest corner of the map area while Hadrynian diabase dykes are common throughout. Early Paleozoic strata outcrop in the western part of the map area and a lone Paleogene outcrop lies northwest of the Barnes Ice Cap.

Archean rocks are chiefly feldsparphyric and foliated to massive granitic plutons, nebulitic granitic migmatite, and banded migmatite. The plutons are most abundant in map areas NTS 37G and northern 37F, are common in western map area NTS 37E, and occur in a belt trending diagonally northeast from the southeast corner of map area NTS 37E to Cape Eglinton in map area NTS 27F (Fig. 1). Schlieren of granitic rocks, paragneisses, amphibolites, and pyroxene gneisses are common in the nebulitic migmatites. Metamorphosed felsic volcanics and amphibolite and felsic dykes are abundant locally. Amphibolite dykes are most common in the southeastern fiord region. The Mary River Group, an Archean metamorphosed greenstone sequence, occurs in variously shaped remnants up to 65 km long and contains sediments, mafic and felsic volcanics, gabbros, anorthosites, and ultramafics, including komatiite. These remnants unconformably overlie granitic rocks in the Mary River area and are rare in the southeastern part of the map area.

The Aphebian Piling Group is composed chiefly of metasediments, includes minor amphibolite, and occurs in the southern part of the map area where it is complexly deformed with the Archean rocks and with Aphebian migmatites. The group unconformably overlies Archean granitic gneisses south of the map area.

Banded migmatites are the most abundant rock types in the map area and probably include both Archean and Aphebian migmatites. Many of these rocks contain several ages of granite and pegmatite dykes and sills. Mary River type remnants are rare in the southeastern part of the map area while Piling remnants have only been recognized in the south.

Numerous late Aphebian granitic, possibly intermediate- to low-level intrusions are most abundant in an arcuate belt that extends from the northwest corner of the map area southeast to Lake Gillian (south of the map area) and then northeast past the north end of the Barnes Ice Cap to Cape Hunter (Fig. 1). Time of emplacement of these intrusions probably ranges from before, to penecontemporaneously with, the latest Aphebian major regional migmatization and metamorphism that affected the map area. Charnockitic rocks predominate in the southern, northeast-trending belt and *seem* to include both Archean and Aphebian intrusions that have undergone late Aphebian granulite facies metamorphism. Charnockitic nomenclature (Fig. 15) is used for granitic plutons that contain primary and/or metamorphic orthopyroxene.

Strata of the Neohelikian Bylot Supergroup, deposited in Borden Rift Basin (Fig. 13; *see* Fig. 112, 114), lie unconformably on the Archean-Aphebian gneiss complex in the northwest corner of the map area. The Milne Inlet Trough graben, located within the basin, extends southeast through the map area.

Swarms of Hadrynian Franklin diabase dykes and possibly a few Neohelikian Mackenzie diabase dykes occur throughout Baffin Island. They were emplaced along and parallel to northwest-trending extensional faults that have been active at least from Neohelikian to Recent time.

Cambro-Ordovician strata of the Admiralty and Brodeur groups and the Ship Point Formation outcrop in the western part of the map area, and are chiefly of shallow marine origin. A few early Paleozoic boulders in drift near the head of Cambridge Fiord may have been transported from the west, but may also have been derived locally from the upper plateau surface.

Mesozoic strata, complete with an oil *seep*, occur off the east coast in Buchan Gulf, but are not known to outcrop onshore in the map area. A small outcrop of lacustrine Paleogene limestone occurs a few kilometres northwest of the Barnes Ice Cap.

Although variable in detail, different structural trends predominate in different regions. Bedrock observations and aeromagnetic data enable the map area to be subdivided into several domains, some of which are probably separated by major structural breaks or shear zones (*see* Fig. 111, 112, 113, 114). Structures, especially recumbent folds and thrust faults, are best displayed in the fiord region.

Archean and Aphebian rocks are mostly in the upper amphibolite facies but range from greenschist to granulite. Neohelikian strata have at least in part undergone subgreenschist facies metamorphism. Younger rocks are unmetamorphosed.

Various chemical data are available for bedrock map units in and adjacent to the map area. The reader is referred to the introduction, to individual map units, to numerous tables and appendixes, and to the sections on "Regional geochemistry" and "Regional geochronology".

Acknowledgments

The author was most ably assisted in the field by S.L. Blusson, A. Davidson, and W.C. Morgan of the Geological Survey of Canada and by W.J. Crawford of Tacoma Community College. All shared in the preparatory and/or camp duties, as well as the mapping. R. Bain and H. Laplante were junior assistants, D. Connelly was general handyman and cook's helper, M. Lajoie the radio operator, and R. Senneville the cook. All performed their jobs in excellent fashion.

The helicopter crew consisted of pilots C. Dietrich and B. Small, and pilot-engineer F. Grover. The Otter pilot, R. Thom, also piloted the Cessna 180 in 1967. J. Dunn was the Otter engineer. The work of the air crews was frequently carried out under adverse conditions and they did much to make the summer a success.

Hospitality and assistance were received in 1967 and 1968 from personnel of the Department of Indian and Northern Affairs, the DEW Line stations from Fox Main to Fox 3, the Hudson's Bay Company, the Royal Canadian Mounted Police, the United States Coast Guard at Cape Christian (now closed), Nordair, and the Atmospheric Environment Service weather station at Clyde. In particular D. Nygaard, R. Pilot, H. Poyntz, R. Leclerc, C.E. Garnett, P. Peterson, and M. Ralston greatly facilitated the work of the project. The support received from the above is gratefully acknowledged.

Most of the thin sections were examined initially by M.B. Lambert and S. Tella whereas R. Batstone and G. Delaney examined most of the stained slabs. H. Bielenstein provided an advance airphoto interpretation.

The author is indebted to J. Maley who spent considerable time processing the chemical data into computer-drawn triangular and x-y plots. D. Stone was also consulted concerning the application of statistics. S. Marincak, K. Ross, and S. Sparks helped to enter data into the computer, make corrections, finalize diagrams and P-T results, and compile bar diagrams, etc. Ross prepared a university term paper on the granitic rocks of the map area in 1986, and Sparks did likewise for some metamorphic pressure and temperature estimates in 1987.

A 16 page preliminary summary of Neohelikian, Paleozoic, and Cretaceous-Eocene geology was prepared by A. Davidson, and a 26 page preliminary summary was prepared by W.C. Morgan for the intrusions and granitoid gneisses and migmatites. Data from these summaries as well as from several of the publications noted in the previous section, have been incorporated into this memoir. W.R.A. Baragar critically read an early version of the 'Regional chemistry' section. W.D. Loveridge and J.C. Roddick did the same for the 'Regional geochronology' section, and A.S. Dyke for the section on 'Quaternary geology'. G.A. Gross, who critically read the 'Mary River Iron-formation' section, also discussed several

Table of Formations

Age (Ma)	Group (Thickness)	Formation/Member (Thickness)	Map Symbol	Lithology
Pleistocene-Recent		Clyde Foreland Formation (0- ca. 15 m?)	Qu KT$_4$	Unconsolidated deposits, partially reworked; sandurs, bog deposits, etc. Poorly consolidated to unconsolidated sand, silt, clay, peat; may contain reworked Cretaceous strata
		Unconformity?		
Paleogene	Eclipse	Rimrock Bed (0.1 m)	T	Impure limestone
		Unconformity?		
Middle-Late Ordovician	Brodeur (100+ m)	Baillarge (100+ m) Formation	OBA	Member B (85+ m): dolostone, limestone; in part silty Member A (~15 m): grey shaly-silty carbonates
		Disconformity		
Early-Middle Ordovician		Ship Point (70-165 m) Formation	OSP	Member B (59-135 m): dolostone, chiefly silty Member A (10-30 m): dolostone, commonly siliciclastic
		Disconformity?		
Early Cambrian-Early Ordovician	Admiralty (0-110 m)	Turner Cliffs (0-90 m) Fm Gallery (0-70 m) Fm	COTC COGA	Dolostone, commonly siliciclastic; quartz arenite, chip conglomerate Arkose-orthoquartzite, conglomerate
		Unconformity		
Hadrynian[1] (723 Ma)		Franklin, Borden intrusions	Hg	Tholeiitic diabase
		Intrusive contact		
Neohelikian (1270-1230 Ma)	Bylot Supergroup (~1150-1910 m) Uluksan Group (308+ m)	Society Cliffs (308+ m) Formation	NSC	Upper member (SC$_2$:75+ m): dolostone, stromatolitic dolostone Lower member (SC$_1$:233 m): dolostone, shale, siltstone, quartz arenite
		Conformable to locally disconformable		
	Eqalulik Group (~840-1600 m)	Arctic Bay (837-1460 m) Formation	NAB	NAB-U (AB$_4$:670-790 m): shale, siltstone, quartz arenite, dolostone NAB-L (143-700 m) (AB$_3$:49-113+ m): shale; minor siltstone, dolostone (AB$_2$:58-183+ m): shale; siltstone, quartz arenite (AB$_1$:8-28+ m): quartz arenite, siltstone, shale
		Adams Sound (2-122 m) Formation	NAS	Upper member (AS$_3$:15-82 m) : quartz arenite, minor conglomerate Middle member (AS$_2$:9-20+ m): quartz arenite, minor conglomerate Lower member (AS$_1$:8-20 m): quartz arenite, minor conglomerate
		Nonconformity		
Aphebian (1825 Ma?)	Charnockite[2]		Ack	Hypersthene monzogranite-granodiorite, minor late dykes
		Contact gradational where seen		
	Massive granite[2]		Ag	Chiefly massive monzogranite, minor late dykes
		Intrusive contact		
	Porphyroblastic migmatite[2]		Amp	K-feldsparphyric banded migmatite
	Banded migmatite[2]		Amg	Variously interlayered and intermixed rocks
(ca. 1900 Ma)	Piling (AP) (several 100 m)	Longstaff Bluff (few 100 m?) Formation	APs in 37F APs (upper) in 37E and 27F	Paragneiss: metamorphosed greywacke, siltstone, and minor shale (sandy turbidite flysch), local amphibolite
		Astarte River (0-35 m?) Formation	APs (lower) in 37E, 27F APif in 37F	Rusty micaceous graphite-sulphide-quartz schist, sulphide facies iron-formation; minor oxide, silicate, and aluminous facies iron-formation; local amphibolite
		Flint Lake (Upper Formation) (0-60+ m) Dewar Lakes (0-40+ m) Formation	APm (37E-F) AFL (27F) ADL (27F) APq (37E-F) (=undifferentiated ADL)	Calcite and dolomite marble; calc-silicates; minor quartzite, metachert, amphibolite, sulphide schist, metapelite ADL-upper member (0-10+ m): quartzite, minor marble ADL-lower member (0-30+ m): muscovite-quartz schist underlain by meta-arkose
		? contacts uncertain ?		
Aphebian and/or Archean			mu sv bg	Undifferentiated gneisses, mixed rocks Paragneiss, lit-par-lit gneiss Homogeneous quartz-biotite-feldspar gneiss
		? contacts uncertain ?		
Archean (2709 Ma)	Porphyritic granite[2]		Agp	K-feldsparphyric monzogranite-granodiorite, minor late dykes
		Intrusive contact locally		
(2759-2718 Ma)	Mary River (M, AM) (1000-2600+ m)	Meta-anorthosite Metagabbro Metaultramafite	Mn Mg, AMb Mu, Amu	Metamorphosed massive to glomeroporphyritic anorthosite, gabbroic anorthosite Fine- to coarse-grained amphibolite Metamorphosed peridotite, komatiite; serpentinite, actinolite-, cummingtonite-, and hypersthene-rich rocks
	(1000-2600+ m)	Mafic metavolcanics (150-610+ m)	Mb, AMb	Massive to pillowed amphibolite, minor metatuff, and meta-agglomerate
		Metasediments (150-610+ m)	Ms	Metasiltstone, metagreywacke, metapelite; meta-arkose, lit-par-lit gneiss, metaconglomerate
		Metamorphosed iron-formation (0-195 m)	Mif, AMif	Facies: oxide, silicate, and silicate-oxide, aluminous, carbonate, sulphide
		Felsic metavolcanics (0-650 +m)	Ma	Metamorphosed rhyolite-dacite, tuff, agglomerate
		Quartz-rich unit (0-580+ m)	Mq	Upper member (0-122 m) : metaorthoquartzite, metachert; minor iron oxides, garnet, mica (includes fuchsite) Lower member (0-460+ m): feldspar-mica-quartz schist and paragneiss, aluminosilicate paragneiss, metaconglomerate lenses
		Metapelite-amphibolite (0-167+ m)		Upper member (0-122+ m): metapelites, minor amphibolite; local volcanic metaconglomerate Lower member (0-45 m) : lensitic metaconglomerate, metapelite, mafic and felsic metavolcanics
		Nonconformity?		
	Metagabbro[2]		b	Amphibolite, pyribolite sills, dykes, pods
		Intrusive contact		
(2851 Ma)	Foliated granite-granodiorite[2]		gr-Agr	Monzogranite-granodiorite; minor syenogranite, trondhjemite; local tonalite, syenodiorite
(3.7? Ga-2.8 Ga)	Nebulite, granite[2]		Amn	Nebulitic migmatite, and intrusions of monzogranite-granodiorite composition, felsic metavolcanics
	Granite, nebulite		Agn	Foliated monzogranite-granodiorite, granitic nebulitic migmatite, felsic metavolcanics

[1] May include some Mackenzie dykes. The + sign indicates that the thickness is considered to be greater than the value given.

[2] Probably includes rocks both older and younger than the Mary River Group. Indicated relative age believed to be the most common.

aspects of iron-formation sedimentology and formation of high grade iron deposits with the author, and provided several iron-formation analyses.

R. Berman and K. Venance provided pressure and temperature calculations, using Berman's TWQ program (Berman, 1988, 1990, 1991), for most of the author's probe data reported on in this memoir. The author is also grateful to them for advice and extensive discussions of the results. J. Stirling, assisted by the author, did most of the probe analyses, while G. Pringle tutored the author on the use of his Mineral Formula Utility program. Five of the analyses used were done or duplicated by V. Kitsul and S. Bushmin of the Russian Academy of Sciences.

I.F. Ermanovics, T. Frisch, S.K. Hanmer, J.B. Henderson, J.F. Henderson, P.F. Hoffman, T.R. Iannelli, O. Ijewliw, S.L. Jackson, J.A. Percival, M. Schau, and F.C. Taylor discussed various aspects of the geology with the author. Baffinland Iron Mines Limited provided copies of company reports and maps, including aeromagnetic data, for areas NTS 37G/5 and 37G/6. They also provided locations and samples of iron-formation and high grade iron for northeastern NTS 47H (Phillips Creek).

Gravity and extensive aeromagnetic data were obtained from the Geophysical Data Centre of the Geological Survey of Canada. M.D. Thomas, D.D. Abbinett, and especially P.H. McGrath were consulted concerning use and interpretation of these parameters. On several occasions E.E. Ready and D.A. Reveler made accessible and discussed unpublished aeromagnetic data.

An early version of much of the manuscript was critically read by K.E. Eade and the submitted manuscript was critically read by T. Frisch and J.B. Henderson. Frisch reviewed everything except the Phanerozoic geology whereas Henderson concentrated on the Archean, Proterozoic, and Phanerozoic supracrustal sequences, but also reviewed the introductory sections and the 'Regional synthesis'. The author is most grateful to all three reviewers, for their many thoughtful suggestions and improvements, and is fully appreciative of the large amount of time they expended.

The typing and retyping of text and tables by Beverly Cox and Nancy Devine is most appreciated. The latter also checked references and organized the table of contents. The author is also indebted to Sally Elliot-Meadows and Evelyn Inglis whose comments and excellent editing greatly improved the memoir. Figure layout and suggestions by Debby Busby and final typing by Janet Gilliland and Krista Lamer are also greatly appreciated.

ARCHEAN

Foliated monzogranite and granodiorite, nebulitic migmatite (Agn)

Description

Rocks of this map unit comprise a complex of metamorphosed granitic rocks that occupy irregularly shaped areas up to 30 km long for about 80 km along the northeast side of the Central Borden Fault Zone in the west-central part of the Icebound Lake map area (NTS 37G). Most of these areas are elongated southeast parallel to the regional trend. On aeromagnetic maps these areas have a subdued or gently undulating magnetic expression with trends roughly parallel to the regional trend and nanotesla values at about background.

Monzogranite (rhyolite) is the most abundant composition (Fig. 16), and commonly grades into granodiorite (dacite). Minor compositions include syenogranite, quartz-rich granitoid, and trondhjemite. Most of the map unit may be nebulitic migmatite or nebulite (Mehnert, 1968), and deformed and metamorphosed plutons; but metamorphosed felsic volcanics, including welded tuffs, are abundant locally. Some representative modal analyses are shown in Figure 17 (in pocket).

The rocks are chiefly light grey to pinkish grey, white, variegated pink and grey, and more rarely, pink. The pink rocks are more common in the southeastern part of the belt than in the northwest. The rocks are fine- to coarse-grained, and most of them have been recrystallized during metamorphism. Primary igneous textures and structures are preserved in some of the massive granitic rocks and felsic volcanics, and include phenocrysts, augen, and locally, shards and bombs. The rocks are commonly feldspar-phyric. Quartz, potassium feldspar, and plagioclase occur as relict phenocrysts (blastophenocrysts) in the massive blastoporphyritic granitic intrusions and metarhyolites, and as porphyroblasts (and blastophenocrysts?) in the other rock types. The blastophenocrysts are up to 1.5 cm long, but most are 0.6 cm or less, stretched, show some resorption, and form up to 25% of the rock. The quartz eyes are fairly coarse mosaics. The microcline appears relatively fresh, but many of the feldspar megacrysts have been recrystallized and contain abundant mica inclusions; some have a skeletal, relict-like appearance and a faint euhedral partial crystal outline. Locally, adjacent to younger granitic intrusions, the potassium feldspar content seems to have been augmented by potassium metasomatism. Quartz, oligoclase-andesine (An$_{16-35}$), and microcline are the major minerals (Fig. 17; Tables 5, 6). Retrograde albite (An$_{4-6}$) occurs in two thin sections, one of which is from monzogranite in a complex west of, and structurally below, Mary River No. 1 iron deposit. Mafic minerals commonly constitute less than 10% of the rocks. Biotite is the major mafic mineral and is chiefly brown but locally green. Blue-green hornblende, rare brown-green hornblende, and muscovite are minor minerals. Prehnite is rare and occurs in the cores of some biotite, probably as a later mineral.

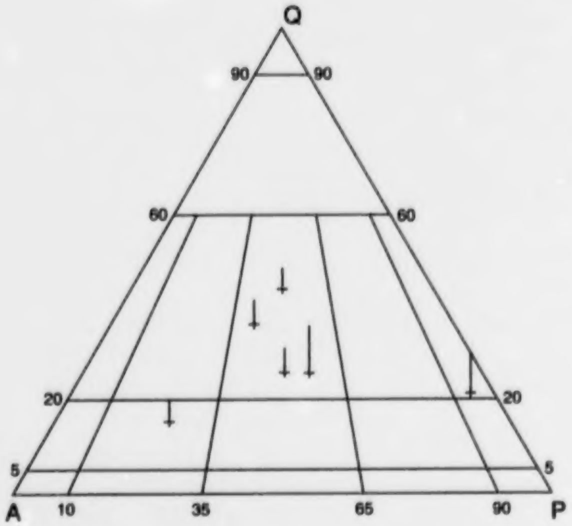

Figure 16. Quartz-alkali feldspar-plagioclase diagram showing some representative plots for unit Agn. *The vertical lines show the percentage of mafic minerals present as a proportion of the vertical distance between the AP line and a parallel line drawn through the apex Q.*

The most abundant accessory minerals are sphene, muscovite, apatite, magnetite, pyrite, allanite, and zircon. Muscovite, chlorite, epidote, and carbonate are common, and in most thin sections are *seen* to be late retrograde metamorphic products. Some muscovite, however, *seems* to be prograde. Common mineral assemblages are:

quartz+microcline+plagioclase+biotite±hornblende,

and

quartz+microcline+plagioclase+biotite+muscovite

Most of the rocks forming this unit are well foliated granitic rocks that contain nebulitic schlieren, and grade into indistinctly banded and massive varieties. Locally the rocks are thin- to medium-banded. Distinct bands and angular to subrounded inclusions of paragneiss and amphibolite are rare. Massive granitic intrusions within the map unit have sharp to crosscutting contacts with adjacent rocks. Some nebulitic granitic migmatites locally grade into the foliated rocks *seemingly* in the direction of increasing compositional homogenization related to greater plastic deformation and metamorphic recrystallization. The foliation and mineral lineations are displayed by elongated and flattened quartz and elongated crushed feldspar concentrations that contain augen, and by parallel orientation of mafic minerals in lenses and planes. An intense mineral rodding has been developed in the vicinity of No. 1 and No. 4 iron deposits in the Mary River area, and the rocks have been crushed in several places.

Table 5. Stained slab modal analyses for map units represented by fewer than five analyses (volume per cent; *see* Table 6).

Area	Unit	Sample	Quartz	K-feldspar	Plagioclase	Feldspar	Mafics[f]
37G	Agn	C71/1	23.7	28.7	37.6	66.3	10.0
37G	Amn[a]	J232/1	4.7	28.6	15.7	44.3	51.0
37E	Amn[a]	J64/2	27.7	1.0	40.0	41.0	31.3
27F	Amn[a]	J284/2	7.7	32.7	17.0	49.7	42.6
37G	b	J151/2	6.3	6.0	60.0	66.0	27.7
37G	Mb	J125/3	2.0	4.7	39.7	44.4	53.6
37H	Mb	C134/1	9.3	0.0	43.0	43.0	47.7
37H	Mn	C149/1	9.7	3.0	61.6	64.6	25.7
37H	Mn	B261/1	2.0	0.0	94.3	94.3	3.7
37E	Mn	J69/2	7.0	1.4	89.6	91.0	2.0
37H	Ma	D227/1	25.0	9.0	59.7	68.7	6.4
37G	Amg[b]	B110/12	37.3	14.7	38.7	53.4	9.3
37F	Amg[b]	B106/1	45.2	14.3	36.7	51.0	3.8
37H	bg	D237	16.3	1.7	59.3	61.0	22.8
27G	bg	J265/2	14.3	22.3	49.3	71.6	14.2
27G	bg	J265/3	33.0	12.0	36.3	48.3	18.7
37H	bg	J266	23.5	19.0	46.7	65.7	10.8
27F	sv	D258	41.0	25.3	19.6	44.9	14.0
37H	Amn[c]	D216/3	20.3	0.0	54.7	54.7	25.0
37H	M	D244/2	15.7	12.0	37.6	49.6	34.7
37E	M	B278/2	56.4	0.0	35.4	35.4	8.3
37G	Mq	J75A2	45.0	0.0	1.0	1.0	54.0
37G	M[d]	C56/1	9.7	26.0	25.3	51.3	12.0
37G	M[d]	C56/1	26.0	12.0	46.3	58.3	15.7
37F	M[d]	D87/2	28.7	0.3	64.0	64.3	7.0
37F	M[d]	D87/2	25.7	0.7	71.6	72.3	2.0
37F	APs	D8/5	50.0	2.0	44.3	46.3	3.8
37F	Agp[e]	J114/2	25.4	30.0	37.6	67.6	7.1

a - Intermediate to mafic inclusion in Amn
b - Felsic metavolcanics in Amg
c - Metasediments in Amn
d - Migmatized Mary River Group
e - Late granitic rock intrusive into Agp
f - Biotite is present in nearly all of the samples; magnetite, amphibole, and garnet each occur in nearly half the samples; chlorite and sulphides were noted in a few samples. No muscovite was observed.

A highly complex zone in unit Agn immediately southwest and west of the Mary River No. 1 iron deposit has been traced for at least 8 km to the northwest (Baffinland Iron Mines Limited, 1964; Jackson, 1966b) and is considered to be overlain unconformably by the Mary River Group (*see* Fig. 106). The complex is composed of metamorphosed, shallow, fine- to medium-grained, feldsparphyric, variously foliated monzogranite-granodiorite intrusions, porphyritic and very fine- to fine-grained metarhyolite-dacite (quartz, plagioclase phenocrysts) and associated pyroclastic rocks, quartzofeldspathic metasedimentary rocks, amphibolite-metagabbro, minor metaultramafite, minor amphibolite and pelitic schists (andalusite, sillimanite, kyanite, staurolite, garnet), and very minor quartzite. At least two ages of granitic and amphibolite intrusions are present.

The granitic intrusions contain more blastophenocrysts than do the felsic metavolcanics, the latter being less mafic than felsic metavolcanics in the overlying Mary River Group. The felsic metavolcanics commonly contain thin wispy fragments, up to 10-15 cm long, that are only slightly more mafic than the matrix, and which are probably chiefly flattened shards. Felsic metavolcanic blocks up to 150 m long occur in a matrix of felsic metavolcanics of similar composition.

Locally, south of the elbow in the Mary River No. 1 iron deposit (*see* Fig. 106), the complex includes a megabreccia composed chiefly of angular blocks, up to 275 m long, of metamorphosed felsic volcanics and associated porphyritic granitic intrusions in a matrix composed chiefly of amphibolite-metagabbro. The amphibolite is interpreted to be intrusive (Fig. 18). However, metasedimentary rocks occur with the amphibolite and some contacts suggest the amphibolite intrudes the granitic rocks, while others suggest the

Table 6. Statistical summary of stained slab modal analyses (volume per cent).

	Map unit	Amn	Amn	Amn[a]	gr-Agr[b]	gr-Agr[b]	gr-Agr[c]	gr-Agr[d]	Amp	Amg	Amg	Amg[e]	Amn[f]	Amg[g]	Ag[h]	Ag[k]	Ag[l]	Agp	Ack[m]	Ms, AMs	Amg[n]	Amg[o]
	Map areas	37E-H 27G	27E, F	37E, H 27E-G	37E-H 27G	27E, F	37F, G	37E, G, H 27G	37E-H 27G	37E-H 27G	27E, F	37E-H 27E-G	37E-H 27E-G	37E-G 27E, F	37E-H 27E-G	37G	37E, G, H 27G	37E-H 27G	37E, F, H 27G	37E- G	37E-H 27G	37E-H 27E-G
	No. of samples	158	63	6	40	11	7	10	15	123	14	133	20	17	29	5	11	44	24	13	7	13
QUARTZ	Maximum	70.0	47.0	36.6	52.0	43.0	51.8	44.0	38.0	53.0	42.0	60.2	46.0	34.4	48.2	39.0	37.6	45.0	47.0	36.3	49.7	34.0
	75 Percentile	32.3	32.7	36.0	32.0	35.1	37.0	34.3	27.0	29.8	29.6	34.0	33.0	32.3	33.7	39.0	33.0	31.6	31.0	30.4	43.0	20.0
	Median	28.0	26.3	33.3	28.3	27.2	33.7	30.2	22.3	24.3	24.6	27.0	29.0	29.3	29.7	28.5	31.0	25.0	26.3	19.5	38.3	12.3
	25 Percentile	23.3	22.4	30.0	23.0	25.0	29.3	27.4	14.3	18.0	21.3	23.0	23.3	26.8	25.3	21.2	24.6	23.2	23.7	17.3	25.3	6.4
	Minimum	12.3	14.7	15.6	4.7	19.7	21.3	17.0	2.0	0.7	17.3	3.0	8.3	15.7	7.6	11.8	15.0	5.4	6.0	2.7	13.4	0.1
	Mean	28.6	27.3	30.5	27.2	29.3	33.2	29.8	21.0	24.3	26.3	28.1	27.2	28.3	29.1	25.8	28.5	25.0	26.4	20.5	32.6	13.4
	Standard Deviation	8.48	6.43	7.73	8.91	6.77	10.06	7.80	10.30	9.65	7.20	9.56	8.16	4.85	8.47	10.07	6.69	8.41	8.08	9.72	14.10	9.40
POTASSIUM FELDSPAR	Maximum	66.6	46.7	33.3	52.0	41.0	51.3	31.7	44.5	78.2	43.3	80.0	54.7	71.8	42.7	37.0	53.5	51.4	49.7	46.3	14.6	29.3
	75 Percentile	29.7	30.3	25.3	35.5	38.6	34.5	23.6	30.3	24.3	28.0	41.3	49.0	52.5	42.3	37.0	43.0	39.0	37.3	17.7	12.7	10.0
	Median	18.7	23.3	13.7	28.0	25.7	14.7	20.0	21.5	12.0	16.0	32.5	37.7	38.6	36.0	28.0	30.8	28.7	23.3	5.7	6.0	3.7
	25 Percentile	6.0	20.0	0.7	16.4	18.3	10.0	3.3	15.7	2.6	6.6	17.4	30.6	37.6	33.0	8.8	22.7	20.7	11.6	3.0	2.3	0.4
	Minimum	0.0	0.5	0.0	1.0	12.3	3.0	1.0	0.5	0.0	0.0	0.1	1.3	20.4	2.7	2.4	0.0	5.3	0.7	0.0	0.0	0.0
	Mean	19.4	23.9	13.4	26.5	27.3	21.6	15.6	20.9	15.7	18.0	30.0	35.0	43.0	35.8	22.2	30.8	30.0	22.4	10.2	6.1	6.3
	Standard Deviation	14.43	9.08	13.54	13.46	10.19	17.50	10.73	12.91	15.27	13.58	17.29	15.26	12.20	14.65	15.63	17.22	12.40	14.10	13.23	5.85	8.33
PLAGIOCLASE	Maximum	74.7	60.5	53.3	68.0	45.3	57.6	60.5	78.0	71.9	62.8	77.3	77.0	44.6	82.3	72.0	66.7	59.5	74.6	60.0	52.4	53.0
	75 Percentile	53.7	44.7	50.0	44.6	40.3	44.7	55.5	56.7	54.6	52.0	47.0	36.8	34.3	35.2	72.0	57.3	43.6	47.6	57.1	43.4	44.7
	Median	42.3	38.3	49.7	39.3	37.7	36.2	41.7	38.3	46.0	39.3	34.1	32.6	27.5	28.0	41.2	34.8	35.0	41.6	47.0	41.0	35.0
	25 Percentile	36.0	32.3	29.7	30.6	28.0	34.7	35.3	36.3	37.3	32.0	25.0	26.0	16.0	24.3	28.0	20.7	27.7	32.7	43.5	38.7	23.5
	Minimum	7.5	22.0	26.0	7.8	21.4	21.7	28.3	29.0	13.7	25.7	7.3	16.0	4.2	14.7	21.7	8.7	16.3	15.3	23.4	22.5	0.7
	Mean	43.5	38.6	40.3	37.9	35.0	38.0	43.3	45.4	45.5	42.6	36.5	33.2	26.0	32.0	45.4	35.5	35.7	41.0	47.2	39.5	31.7
	Standard Deviation	12.82	8.90	12.0	12.39	8.21	11.18	11.7	15.99	12.07	11.74	15.57	14.08	12.35	14.50	22.00	18.44	10.15	13.10	10.36	8.92	16.00
FELDSPAR + MUSCOVITE	Maximum	81.0	73.6	59.4	88.6	69.0	73.0	70.2	81.4	92.6	73.9	94.0	85.3	80.0	92.1	80.8	77.5	83.3	80.4	74.7	59.4	55.4
	75 Percentile	68.9	66.3	58.6	68.7	68.0	66.2	63.0	77.3	68.0	69.0	73.2	72.7	71.7	70.3	80.8	72.4	71.0	70.2	67.0	58.0	50.0
	Median	63.7	62.7	57.0	65.0	62.0	60.6	60.0	63.0	62.3	59.7	67.4	69.0	68.6	67.6	67.3	65.3	66.7	64.4	58.6	43.6	44.0
	25 Percentile	58.3	59.6	50.7	62.0	60.0	54.7	54.7	59.3	55.0	52.0	61.6	66.5	65.9	62.8	66.4	62.4	61.0	58.4	50.0	41.03	31.0
	Minimum	28.0	46.4	43.4	25.9	52.0	44.0	50.0	54.0	30.7	51.0	38.6	49.0	63.0	50.3	59.0	58.3	50.3	45.3	45.3	24.8	8.4
	Mean	62.8	62.5	53.7	64.3	61.8	59.6	59.0	66.4	61.2	61.0	66.5	68.3	69.0	67.8	68.5	66.3	65.8	63.4	57.5	45.6	38.0
	Standard Deviation	8.67	5.77	6.04	10.08	5.98	9.56	6.39	10.12	10.61	7.80	9.34	8.58	4.55	8.45	7.86	6.26	7.81	9.23	9.53	11.94	14.87
MAFIC MINERALS[p]	Maximum	38.0	25.4	33.7	59.9	16.1	14.1	20.7	18.4	45.7	31.4	19.0	17.0	8.2	16.3	12.4	17.1	20.5	26.0	35.2	43.0	85.7
	75 Percentile	11.4	12.8	20.0	10.4	12.6	12.3	16.1	16.7	20.8	16.7	7.6	7.8	5.3	4.3	12.4	7.6	11.3	15.1	32.7	25.5	58.0
	Median	7.01	10.1	16.7	5.4	10.0	4.6	12.6	13.7	12.8	11.0	4.2	2.6	1.4	2.8	4.2	3.3	9.8	9.3	19.3	23.3	41.7
	25 Percentile	3.7	6.1	9.0	4.0	5.0	4.2	6.1	11.5	7.7	8.1	2.0	2.0	1.0	1.0	2.4	3.1	6.7	4.8	17.0	17.3	39.0
	Minimum	0.2	0.1	5.4	0.4	1.3	3.0	1.4	2.7	0.4	4.0	0.0	0.5	0.0	0.3	2.0	0.3	1.3	1.8	11.0	2.3	33.7
	Mean	8.5	10.2	15.8	8.5	8.9	7.2	11.2	12.6	14.4	13.1	5.4	4.5	2.7	3.2	5.6	5.2	9.1	10.2	22.1	21.8	48.6
	Standard Deviation	6.54	5.18	10.31	9.86	4.63	4.44	6.24	4.80	8.77	7.86	4.19	4.43	2.45	3.38	4.32	4.58	4.00	6.49	8.10	12.34	15.80

a - Felsic to intermediate metavolcanics in Amn.
b - Pink gr-Agr, includes few feldsparphyric samples.
c - Migmatitic pink gr-Agr.
d - Grey gr-Agr.
e - Granitoid layers in Amg.
f - Late granitoid intrusions in Amn.
g - Late granitoid intrusions in Amg.
h - Pink Ag (late massive granitic intrusions)
k - White Ag (late massive granitic intursions).
l - Foliated phase of Ag.
m - Chiefly massive, a few nebulitic samples.
n - Metasedimentary inclusions in Amg.
o - Mafic inclusions in Amg.
p - Mafic minerals are chiefly biotite, amphiboles, and magnetite. Garnet is common, chlorite less common, while pyroxene, sulphides, and allanite occur locally.

reverse. The amphibolite "matrix", like most amphibolite bodies in the complex, has strongly sheared margins with up to one metre thicknesses composed chiefly of biotite. Crystalline granitic rocks have been diapirically emplaced in nearby Mary River Group strata (e.g. *see* Fig. 33), and many (if not all) of the major contacts in the megabreccia may be secondary tectonic contacts.

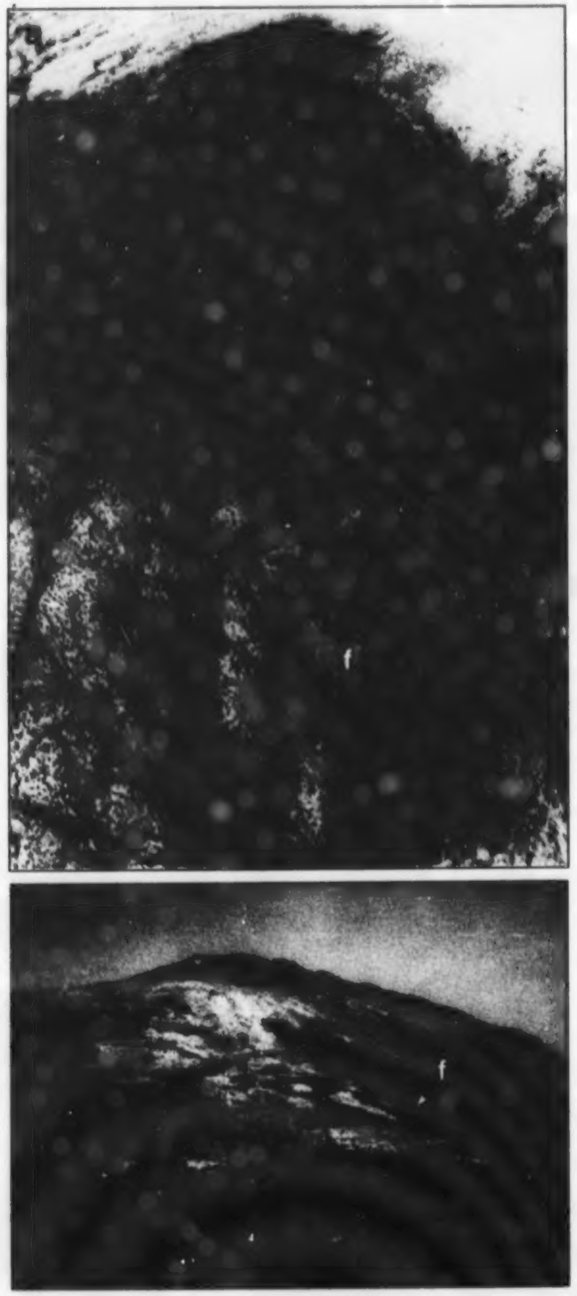

The complex in general has been intruded by numerous metamorphosed, northeast-trending amphibolite dykes (unit b), by felsic dykes, and by several small bodies of younger massive microcline granite-granodiorite (**Ag**) which contain inclusions of the older rocks (Jackson, 1978b) and truncate some amphibolite dykes. Most of the amphibolite and felsic dykes have strongly sheared margins and do not *seem* to intrude the overlying Mary River Group. Some amphibolite dykes *seen* in canyon walls *seem* to be vertical rafts floating in the younger granite with the lower parts of the dykes missing. The felsic dykes are chiefly foliated granodiorite, massive white pegmatite, granite, and aplite, and are generally emplaced in the order named. Locally they make up to 20% of the outcrop. Structures within the complex are complicated and many of the relics *seem* to be Mary River Group rocks that have been interfolded with, faulted into, and/or intruded into the complex to form a mélange-like mixture. The complex is too intricately associated with younger rocks to show on the map (Icebound Lake, NTS 37G) and is included in unit mu.

Contact relations

Map unit Agn probably includes some rocks that elsewhere have been included in units Amn, gr-Agr, **Amg**, and **Agp**. Contact relations with Amn, gr-Agr, and mu *seem* to be conformable. The relationship between Agn and **Amg** varies from concordant to strongly discordant. Unit **Agp** intrudes Agn locally. Unit Agn was mapped as a unit in the Mary River area because of the complexity of the geology in the unit, because the unit is overlain nonconformably by the Mary River Group (M) even though unit Agn contains a sizeable metarhyolite component and remnants of amphibolite and metasediments, and because the granitic rocks of unit Agn are intruded by late mafic and felsic dykes and irregular bodies that do not extend into the Mary River Group. Unit Agn has been intruded by mafic and ultramafic rocks (Mg, Mu) that also intrude and/or are coeval with the Mary River Group and by Aphebian granite (**Ag**) and Hadrynian diabases (**Hg**). Locally Agn is in fault contact with several map units including the Mary River Group. It is also in fault contact with, and overlain nonconformably by, the lower Paleozoic strata.

***Figure 18. a)** View north from helicopter at megabreccia south-southwest of Mary River No. 1 iron deposit. Light coloured fragments range from 2 to 275 m long. The fragment marked "f" is about 90 m long. The fragments comprise chiefly felsic metavolcanics and porphyritic intrusive metagranite and occur in an intrusive amphibolite matrix. A few relatively small blocks are mostly quartzite. Dark coloured rocks adjacent to and east of the breccia are mainly amphibolite and metaultramafite. Metasediments increase in proportion eastward (stratigraphically up) and include metapelite and metaconglomerate. Photograph by R. von Guttenberg, Strathcona Mineral Services. GSC 1991-310. **b)** View northeast at Mary River No. 1 iron deposit on the skyline. The megabreccia (f) shown in Figure 18a occurs in the near hillside. Photograph by G.D. Jackson. GSC 204194-S*

The relationship of the fine grained complex of felsic intrusive and extrusive rocks west of Mary River No. 1 iron deposit to the adjacent gneisses is not clear, and no widespread unconformity within or below it has been identified. Some of the felsic rocks appear to have been incorporated into various types of migmatite toward the north and west, others become coarser grained laterally and grade into gneissic granitoid rocks, and still others appear to have been changed into coarser more granitic rocks by potassium metasomatism and recrystallization.

Age

Several foliated to rodded samples from the vicinity of No. 4 iron deposit in the Mary River area (NTS 37G) yielded whole rock Rb/Sr isochron ages of 2476 ± 70 to 2642 ± 42 Ma, with initial ratios of 0.7063 to 0.7054 respectively (Jackson, 1978b; Wanless and Loveridge, 1978). These ages are considered to be metamorphic ages. The initial ratios are somewhat high and compatible with an emplacement age of about 2900 Ma (Wanless and Loveridge, 1978; *see* section on "Regional geochronology"). A Nd-depleted mantle model age of 2.98 Ga has been obtained by E. Hegner for an acid metavolcanic sample from the complex west of Mary River No. 1 iron deposit. These ages are similar to a zircon U-Pb age of 2851 Ma obtained for map unit gr-Agr (Table 51), also in map area 37G. These ages agree with field conclusions that units Agn, Amn, and gr-Agr are equivalents in part.

Additional Rb/Sr isochron-errorchron metamorphic ages for units Agn, gr-Agr and other Archean rocks in the same area range from 2635-1935 Ma (*see* Table 52; Jackson, 1978b), whereas most K-Ar mineral ages range from 1753-1615 Ma (*see* Table 53). Muscovite from the rodded monzogranite (gr-Agr) sample used for the 1642 Ma Rb/Sr isochron yielded a K-Ar age of 1659 ± 50 Ma (*see* Table 52, 53; Jackson, 1978b). These data indicate that the rocks of map unit Agn may have been subjected to several periods of metamorphism (*see* "Regional geochronology" section).

Origin

The origin of most of the rocks in this map unit is uncertain, but probably most are meta-igneous. The foliated and massive granitic intrusions that are considered to be part of the map unit may be chiefly shallow intrusions emplaced penecontemporaneously with the metamorphosed felsic volcanics. It seems likely that the metasedimentary and amphibolite relics may be older than the adjacent Mary River Group unless these rocks were all emplaced about the same time and subsequently intermixed by deformation. The nebulitic granitic migmatites and schlieren-bearing foliated granitic rocks may be, in part, felsic volcanic rocks that have been deformed and recrystallized beyond recognition. It is inferred from the common occurrence and composition of felsic volcanic clasts within conglomerate lenses in the Mary River Group that felsic metavolcanics may be more abundant in map units Agn and Amn than is presently recognized. Felsic to intermediate metavolcanic rocks within the overlying Mary River Group are finer grained, less recrystallized, contain more relict primary textures, and are slightly darker coloured, containing a greater proportion of mafic minerals than do the felsic metavolcanic rocks of the complex. Field evidence and petrographic studies indicate that the underlying felsic volcanic complex probably was not highly metamorphosed prior to the deposition of the Mary River Group in the Mary River region and at Eqe Bay. At Mary River, felsic volcanic clasts in the conglomerate within the basal Mary River Group metapelite-amphibolite unit and in conglomerates above the iron-formation in No. 4 and No. 1, 2, and 3A iron deposit areas still retain some primary structures. Some clasts also indicate a lower grade of metamorphism than indicated by their matrix and the associated metasediments. Felsic volcanic rocks have been recognized both unconformably below the Mary River Group and in the basal part of the group in the No. 1 iron deposit area, but not in the No. 4 iron deposit area, in spite of the fact that porphyritic felsic volcanic cobbles occur in conglomerate above the iron-formation in the No. 4 area. This conglomerate is stratigraphically below any known Mary River Group felsic metavolcanics in this locality and the felsic volcanic clasts resemble the felsic metavolcanics in the complex rather than the Mary River felsic metavolcanic rocks. Rocks of closely similar composition and texture to the felsic volcanic cobbles are abundant in the "basement" gneisses of the No. 4 area. These rocks would be identical if the very fine grained matrix of the felsic volcanic clasts were recrystallized and primary textures destroyed during this recrystallization. These features suggest that, locally at least, some of the rocks now mapped as granitic plutonic and migmatitic rocks may originally have been felsic volcanics.

The relative abundance of felsic metavolcanics in the complex south and west of Mary River No. 1 iron deposit, and the complexity of the geology suggest that this area may have been part of an older felsic volcanic vent area, upon which the megabreccia was superimposed.

The origin and age of the intrusive megabreccia are problematic. The presence of mafic and ultramafic rocks and minor metasedimentary rocks, similar to those in the Mary River Group stratigraphically below the iron-formation, are compatible with the possibility that the megabreccia formed during or after deposition of the Mary River Group. The absence of iron-formation in the megabreccia, the presence of metaconglomerate lenses containing abundant felsic metavolcanic clasts in the basal metapelite-amphibolite unit of the Mary River Group, and the absence of the megabreccia in the overlying Mary River Group are compatible with the megabreccia having formed in the basement complex before deposition of the Mary River Group. Subsequent intrusion, metamorphism, and deformation further complicated the geology.

The source of the potassium in the sheared, biotite-rich rims of the amphibolite most likely was provided from two possible sources: the adjacent granitic blocks or the parent rock of the amphibolite itself. In the former case the amphibolite was likely formed from a normal gabbro. In the latter case the parent rock of the amphibolite might have been a lamprophyre related to formation of a diatreme.

Nebulitic granitic migmatite (Amn)

Description

About two thirds of the Clyde River map area (NTS 27F) is underlain by variously shaped interconnected areas composed of nebulitic granitic migmatite. Southwest trends predominate slightly over other trends. In the western part of map area NTS 27F Amn underlies a belt that extends northerly to north of Scott Inlet (NTS 27G). Unit Amn is abundant in the southeast corner of the Conn Lake map area (NTS 37E) and underlies long narrow areas up to 125 km long concentrated in a zone that extends northwest from Conn Lake 260 km to Paquet Bay at the north edge of the Icebound Lake map area (NTS 37G), and into the Pond Inlet map area (Jackson et al., 1975). Lens-shaped areas up to 70 km long and underlain by unit Amn trend west from the western part of the Conn Lake map area to the western edge of the Steensby Inlet map area (NTS 37F), and form about 15-20% of this region.

Some of the areas in the Icebound Lake map area, shown as being underlain by undifferentiated gneisses (mu), are underlain chiefly by unit Amn. These areas are: south of 71°25′N latitude and east of 77°W longitude, between 71°30′ and 71°45′N latitude and west of 79°W longitude, and between Angajurjualuk Lake (NTS 37G) and Nina Bang Lake (NTS 37F). Some of the other areas shown as mu in the Icebound Lake map area (NTS 37G) are underlain by Amg (*see* section on "Banded migmatite (Amg)"). The rest of the areas of mu in the Icebound Lake map area as well as most of the areas shown as mu in the Buchan Gulf map area (NTS 37H) are underlain by intermixed Amg and Amn.

Unit Amn shows up on aeromagnetic maps in a similar manner to unit Agn, because the rocks are similar. The magnetic relief is low, commonly gently undulating, with poorly defined trends parallel to the regional structure, and positive areas rarely more than 300 nanoteslas above background. This unit stands out best north and east of Steensby Inlet (NTS 37F) where the topographic relief is low and hence has relatively little effect on the aeromagnetic pattern. Some of the positions of the interpreted contacts do not agree with the positions that might be chosen on the basis of aeromagnetics alone.

The rocks in map unit Amn are predominantly monzogranite and granodiorite in composition, with lesser tonalite (Fig. 17; 19; 20, in pocket). They are, in general, bimodal, and modal analysis plots show a major peak in the monzogranite field adjacent to granodiorite, and a lesser peak in the tonalite field. The overall mean lies in the granodiorite field adjacent to the monzogranite field. A few of the rocks are syenogranite, trondhjemite, and quartz monzonite to quartz diorite in composition. Few of the rocks have more than 20% mafic minerals and most have less than 12%. Quartz-alkali feldspar-plagioclase (Q-A-P) and quartz- feldspar-mafic (Q-F-M) mineral plots for individual map areas are presented in Figure 20A. The Q-A-P plots for Amn in map areas NTS 37G and 37E are weakly bimodal and show concentrations of points in the monzogranite and granodiorite fields. Unit Amn in map areas NTS 37H-27G and 37F give stronger bimodal plots with concentrations close to the monzogranite-granodiorite join and in the tonalite field. In map area NTS 27E-F, however, the Q-A-P plot is unimodal and shows one strong concentration in the monzogranite field. The bimodal nature of Amn in four of the map areas may be a reflection of the two main components: nebulitic granitic gneiss and the more potassium feldspar-rich massive granitic rocks. In general the rocks of this map unit are slightly more inhomogeneous, more nebulitic, and more mafic than the rocks in Agn.

The rocks of this map unit are chiefly fine- to medium-grained and finely foliated to medium banded and massive. Most fresh and weathered surfaces are white to medium grey, pinkish grey, or pink. Many of the rocks have a light ash-grey weathered surface. A few of the rocks are greenish grey, greyish black, or pinkish black to black, and yellowish brown or greyish brown to brown, and locally are mottled. Mineral lineations and aggregate rodding are common. Potassium feldspar megacrysts (porphyroblasts in the nebulitic granitic migmatites and blastophenocrysts in the massive granitic rocks) are common and most have been crushed, rotated, smeared out, and/or recrystallized to various degrees. Plagioclase porphyroblasts are present locally. Metamorphic textures prevail in unit Amn, and granular textures, hypidiomorphic mosaics, and triple junctions are common.

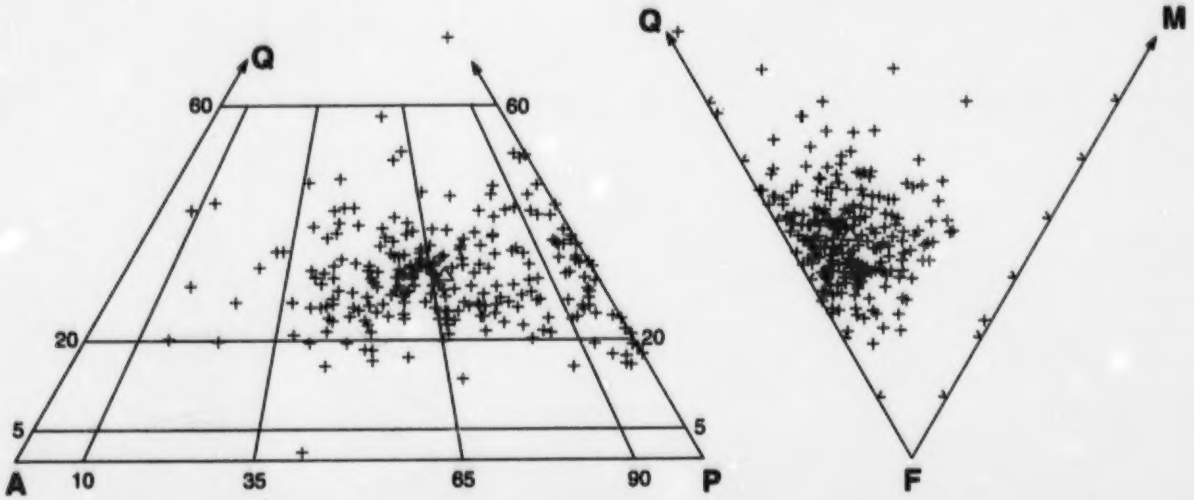

Figure 19. Quartz-alkali feldspar-plagioclase (QAP) and quartz-feldspar-mafics (QFM) plots for unit Amn. The mean position is shown by the small triangles.

The major minerals in unit Amn are plagioclase, quartz, and potassium feldspar. Locally the quartz content is very low and the plagioclase content is high (Fig. 17, 19, 20). Statistical data for these minerals, and for mafic minerals combined are presented in Tables 5 and 6. Biotite and hornblende are almost always present as minor components. Myrmekite occurs locally and clinopyroxene (chiefly diopside-hedenbergite) is uncommon. Hypersthene is ubiquitous in the granulite terrane.

Accessory amounts of apatite, allanite, zircon, sphene, and magnetite are usually present, and one or another may be present in amounts of up to 2%. Chlorite is common and epidote, muscovite (including sericite), hematite, pyrite, ilmenite, leucoxene, calcite, and albite are rare. Garnet was noted at several localities in map area NTS 27F but seems to be rare in the other map areas. The chlorite, some muscovite, epidote, albite, hematite, leucoxene, and possibly some of the sphene are retrograde metamorphic and/or alteration products.

Throughout almost all of the amphibolite facies terrane (*see* Fig. 99), the plagioclase is oligoclase (An_{15-32}), the potassium feldspar is microcline, and the hornblende is blue-green or rarely olive-green. Biotite is chiefly dark brown but ranges from greenish brown to dark reddish brown. The most common amphibolite facies assemblage is:

quartz+microcline+plagioclase+biotite±hornblende.

Other assemblages are:

quartz+plagioclase+biotite+hornblende,

quartz+microcline+plagioclase+muscovite±biotite, and

quartz+orthoclase+plagioclase+biotite+hornblende+clinopyroxene.

Plagioclase is oligoclase-andesine (An_{24-41}) in the granulite facies terrane (*see* Fig. 99) and is commonly antiperthitic. Most of the potassium feldspar is orthoclase and is commonly perthitic. Biotite is chiefly reddish brown and the hornblende is chiefly olive- to brownish-green. Bluish-green hornblende occur locally as rims on hypersthene (optically negative, few unpublished probe analyses), and is a retrograde product. Clinopyroxene is more common in the granulite than in the amphibolite terrane. Sphene is absent in the granulites but accessory rutile may be present in a few places. Several assemblages are present in the granulite facies terrane:

quartz+plagioclase+biotite+hornblende+hypersthene,

quartz+plagioclase+biotite+clinopyroxene+hypersthene,

quartz+orthoclase+plagioclase+biotite+hypersthene, and

quartz+microcline+plagioclase+biotite+hornblende+clinopyroxene+hypersthene.

Most of unit Amn is composed of banded nebulitic granitic migmatite gneiss (Fig. 21). The compositional differences between most bands are not pronounced, involving slight differences in mafic content and proportion of potassium feldspar to plagioclase (Fig. 21a). Locally, the composition is highly variable and structures within bands are complex. These rocks (Fig. 21b-d) are characterized by a wispy to streaky appearance, nebulitic schlieren, swirly "wildfolding" with no consistent pattern, fold noses disconnected from limbs, annealed fault planes, rotated blocks of nebulitic gneiss, granitic gneiss veins that contour the dislocated blocks, and thickening and thinning of bands (Fig. 21c). These features show that most of unit Amn was deformed plastically. A large proportion of the fold structures are of a recumbent isoclinal nature.

Thinly scattered bands of paragneiss, felsic metavolcanics (Amn^h; superscripts defined in Appendix 4), amphibolite (Amn^f), and pyroxene gneiss are common (Table 5; Fig. 17; Fig. 20E, Ja, Ka; Fig. 21c-f), but are rarely as much as 20 m thick. Bands of metamorphosed ultramafic rocks are rare. Distinct, rounded to angular fragments of paragneiss and amphibolite up to a few metres across, which differ markedly in composition from the enclosing rock, commonly make up less than 3% of the outcrop, and rarely make up to 30% of the outcrop locally. Some blocks obviously represent boudined layers, but many are so displaced and recrystallized that in isolated outcrops their origin is not obvious (Fig. 21e). Metamorphosed ultramafic and biotitite inclusions were reported from two or three localities. The following assemblages occur in the mafic rocks:

quartz+plagioclase+garnet+biotite,

quartz+plagioclase+biotite+hornblende, and

plagioclase+hornblende+clinopyroxene+hypersthene.

Layers and lenses of massive granitic rocks (Amn^i) and foliated granitic rocks (Amn^b), similar in composition to the nebulitic gneisses, are commonly interlayered with, of comparable thickness to, and generally appear to be intrusive into, the nebulitic granitic rocks (Fig. 20Ha). Contacts range from sharp and discordant to gradational. Pegmatitic intrusions and sweats and apparent feldspathization of more mafic components adjacent to the massive granitic rocks are ubiquitous. The massive granitic rocks have also been deformed and commonly possess an indistinct but pervasive foliation, and a few scattered schlieren.

Some of the nebulitic granitic rocks within this unit are thickly banded (Fig. 21a), with bands up to several hundred metres thick that are commonly banded internally (Fig. 21). This feature is well displayed in the Sam Ford Fiord-Gibbs Fiord region of the Clyde Inlet map area (NTS 27F). Along Gibbs Fiord the thickest bands are 200-300 m thick, and are

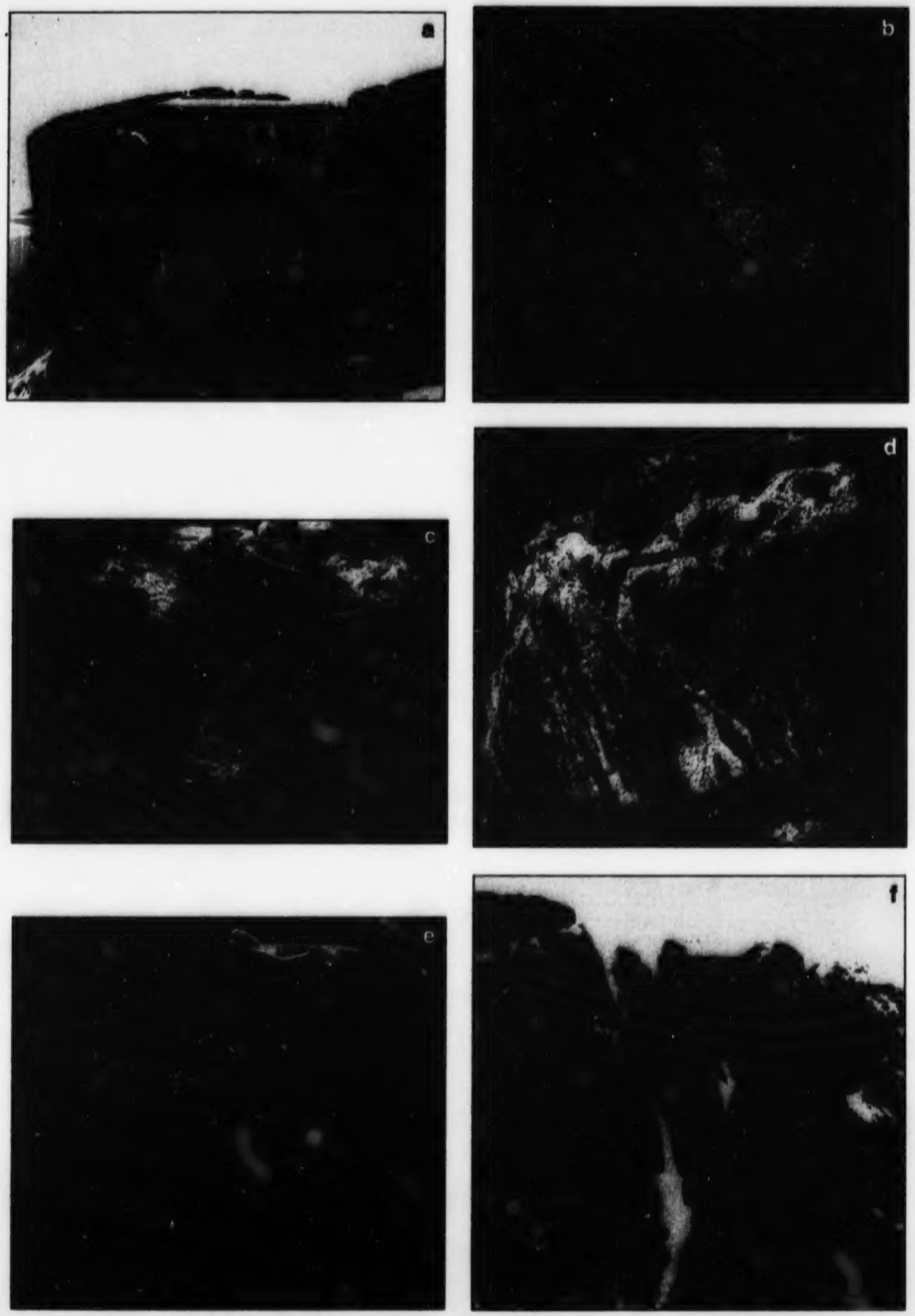

separated by planar surfaces, some of which appear to truncate structures in adjacent bands. Differential weathering of the bands, and the presence of thin seams of mafic rock separating some of the bands, accentuate these planes. These seams commonly have been deformed into series of boudins that in cases of more extensive deformation have evolved into beaded structures. Most of these thick bands dip at low to moderate angles. Individual bands may maintain uniform dips and thicknesses over long distances but the presence of steep dips locally, and the identification here and there of large isoclinal, overturned to recumbent folds, indicate that the structure is complex. At some localities the separating surfaces are remarkably planar, whereas elsewhere they are undulose, fork, and rejoin. Many of these surfaces may be shears or thrust planes.

Contact relations

Rocks of map unit Amn commonly appear to be concordant with the adjacent Archean and Aphebian metamorphic rocks (Agn, gr-Agr, Amg, Agp, M, etc.), the contact ranging from abrupt to gradational. In some places Amn and gr-Agr are difficult to differentiate. In many of the larger cliff sections, massive or foliated to faintly nebulitic granitoid rocks (Amn) at the base grade upward into more pronounced nebulitic migmatite, which in turn grades upward into well banded migmatite (Amg) in the upper part of the cliff. On some cliff faces, however, nebulitic granitic gneiss (Amn) is clearly shown to be intrusive into overlying amphibolite (Mb?) (Fig. 21f), banded migmatite (Amg) and other rocks.

Several domal areas of unit Amn are mostly surrounded by banded migmatite (Amg), the Mary River Group (M), and the Piling Group (AP). In several places, unit Amn seems to be basement to at least the Mary River and Piling group supracrustals and to contain infolded segments of these rocks. The main examples occur southwest of Cambridge Fiord (NTS 37H), southwest of Gibbs Fiord (NTS 37E), in the southeast corner of the Conn Lake map area (NTS 37E), and north of Steensby Inlet (NTS 37F). Elsewhere, however, banded migmatite (Amg) seems to underlie the nebulitic granitic migmatite (Amn). The supracrustal remnants in Amn could belong to a sequence that is older than the Mary River Group but in some places the remnants appear to belong to the Mary River Group.

Bodies of **Agp**, **Ag**, and **Ack** intrude unit Amn locally, although the relationships were not readily apparent at most places. Intrusive granitic, aplitic, and quartz-rich dykes and sills are common locally. Metamorphosed mafic dykes and sills are commonly highly deformed, and are most abundant in the fiord country of map area NTS 27F. They were also mapped in northwestern map area NTS 37E, in eastern and western map area NTS 37F and in northern and western map area NTS 37G.

Unit Amn is also commonly in fault contact with other map units and in several areas contains subhorizontal planar features that may include thrusts (e.g. western map area NTS 27F). Apparent reversals of stratigraphic relations in some places, therefore, may be due to the emplacement of thrust slices.

Nebulitic migmatites (Amn) have been intruded by basic dykes and sills (b) that have been metamorphosed to amphibolite and pyribolite. Several ages may be represented because some are little deformed and emplaced after Amn had undergone most of its deformation. Most, however, are much deformed, isoclinally folded and boudined, and some may have been emplaced prior to most of the deformation and recrystallization undergone by map unit Amn. Unit Amn is also intruded by Hadrynian diabase dykes (**Hg**).

Chemistry

A mean for spectrographic analyses of nebulitic granitic migmatite (Amn) is presented in column 1 of Table 48 (*see* section "Regional geochemistry"), and is similar to the means for foliated monzogranite-granodiorite in columns 2 (Amn^b) and 3 (gr-Agr). The patterns and modes displayed by individual elements in histograms (*see* Table 49, Fig. 96) are most similar to patterns for foliated monzogranite-granodiorite (Amn^b, gr-Agr), banded migmatite (Amg), and the leucosome in banded migmatite (Amg^j). There is also considerable similarity with the histograms for charnockite (Ack). Unit Amn least resembles younger massive granites (Agp, Amn^i, Amg^i, Ag).

Figure 21. a) *Very thickly banded nebulitic granitic gneiss* (Amn) *interbanded with and overlain by boudined banded migmatite, west end of Scott Island. The uppermost zone is the westward continuation of the sinistrally sheared nappe shown in Figure 105d. The abrupt subhorizontal boundaries between light coloured rocks above and dark rocks below may be thrust- or shear-planes. The cliff on the left is about 500 m high. Photograph by S.L. Blusson. GSC 185835.* ***b)*** *Nebulitic granitic gneiss* (Amn) *with folds and schlieren, south side of Clyde Inlet; Photograph by W.C. Morgan. GSC 186659.* ***c)*** *Nebulitic granitic gneiss* (Amn) *with amphibolite bands, detached and partly ingested amphibolite fragments, and contorted folds, near the head of Cambridge Fiord. Photograph by S.L. Blusson. GSC 185409.* ***d)*** *Agmatitic migmatite in* Amn *near the head of Cambridge Fiord, composed chiefly of granite; fine grained, grey gneiss with mafic borders due to depletion of quartzofeldspathic material; and minor amphibolite. Photograph by S.L. Blusson. GSC 185413.* ***e)*** *Scattered inclusions, chiefly of variously ingested amphibolite in* Amn, *north side of Clyde Inlet. Photograph by G.D. Jackson. GSC 204343-U.* ***f)*** *Nebulitic granitic migmatite* (Amn) *"intruding" a large inclusion of veined amphibolite* (Mb?), *west side of Clark Fiord, at the junction of NTS 37E and 37H. The cliff face is roughly 500 m high. Photograph by S.L. Blusson. GSC 185576*

. Many studies of granitic rocks have related compositions to origins of magma and tectonic environment of emplacement. Means of analyses so related by Pearce et al. (1984) and Whalen et al. (1987) are presented in Table 31. The mean analysis for Amn does not clearly favour any one type of granite or tectonic environment. It most closely resembles the mean for S-type (sedimentary protolith) and volcanic arc granitic rocks, but also resembles collision and I-type (igneous protolith) granites. Amn least resembles within-plate and A-type (recycled continental crust) and M-type (from subducted oceanic crust or mantle) granites. According to Pearce et al. (1984), however, S-type granites are chiefly a type of collision granite.

Eleven of the elements determined spectrographically are compared with other map units in Figure 95 (*see* section "Regional geochemistry"). The X-Y plots involving TiO_2, MgO, Zr, Ba, and Sr were made for several of the quartzofeldspathic map units (Fig. 22; *see* Fig. 26, 58, 63, 72). The plots for each map unit, in general, possess differences when compared with the other map units. Plots for Amn (Fig. 22) do not indicate any obvious trend when Zr is plotted against TiO_2, MgO, Ba, or Sr, so are not presented. The plots are relatively diffuse, but show a relatively restricted range in Zr content and a rather large variation in Ba which is probably related to variations in plagioclase content. Similarly the positive Ba-Sr correlation, which is similar for several other map units as well (Fig. 22; *see* Fig. 26, 58, 63, 72), may be related to variations in plagioclase and potassium feldspar content rather than indicating a differentiation trend. The diffuse nature of the plots may be related to several factors such as the presence of rocks of more than one age or origin, and the effects of more than one period of metamorphism.

Analyses for small bodies of foliated granitic rocks (*see* Amn^{b}: column 2, Table 46) within map unit Amn plot in the lower left corner of these X-Y plots in positions that are common to all of these plots (Fig. 22; *see* Fig. 26, 58, 63, 72). Hence these plots do not help to determine whether or not bodies of Amn^{b} are related to map unit gr-Agr.

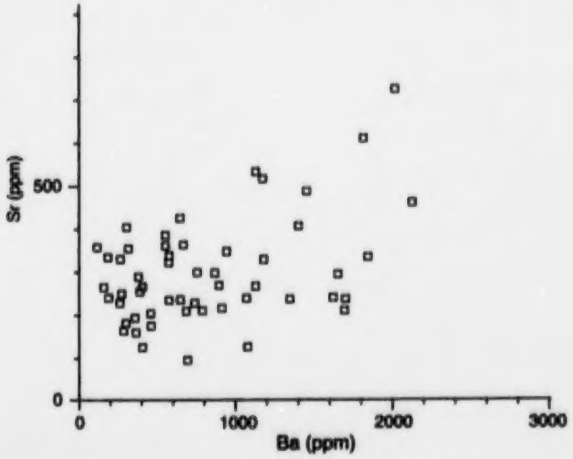

Figure 22. *Plot of Sr (ppm) versus Ba (ppm) for map unit* Amn.

Small, late massive hornblende-biotite granitic intrusions (Fig. 17, 20Ha; *see* Table 48; Appendixes 2-4) in map unit Amn (Amn^{i}) have a chemistry that most closely resembles that for collision granites of both I- and S-type, as well as that for the leucosome in banded migmatite (Amg^{j}) and the small late discordant granitic intrusions in banded migmatite (Amg^{i}). There are fewer similarities, however, between these granitic intrusions (Amn^{i}) and larger mappable bodies of late massive monzogranite (Ag). It is inferred from the data and field relations (*see* Table 48, columns 6, 7, 8, 9; Table 49; Fig. 63, 72), that some of the late massive granitic intrusions in Amn may be related to those in banded migmatite (Amg^{i}) or formed by fusion of unit Amn rocks; but that some Amn^{i} intrusions may be older and unrelated to the late massive monzogranite (Ag).

Analyses for remnants of intermediate to mafic rocks in Amn (Amn^{f}) show a dispersed pattern on the TiO_2-Zr plot of Pearce (1980), and plot in both the island arc and within-plate lava fields outside the MORB field (*see* Fig. 48a). These analyses also plot toward the Zr apex and chiefly outside the fields outlined by Pearce and Cann (1973) for their Ti/100-Zr-Sr/2 triangular plot (*see* Fig. 48a). This probably reflects the mobilization and movement of Sr out of the rocks during metamorphism. Increasing the Sr content in these samples would have the effect of moving the points toward the Sr/2 apex so that most of the points would probably plot in the calc-alkaline basalt field. The intermediate to mafic rocks in Amn (Amn^{f}) plot on the above two plots in positions similar to those obtained for mafic rocks in banded migmatite (Amg^{g}) and for Mary River Group mafic rocks (*see* Fig. 48a, b).

The analyses for intermediate to mafic rocks in Amn (Amn^{f}) plot chiefly in the calc-alkaline (CAB) and rift basalt (RB) field in a different TiO_2-Zr plot (*see* Fig. 49a) devised by Condie (1985). When compared with Condie's (1985) reference plots, the TiO_2 content of these remnants suggests an Archean age but the Zr content suggests that an Aphebian component may also be present. According to Condie (1985), Archean basalts do not contain TiO_2 2% or Zr 200 ppm. Some of the mafic remnants in Amn, however, contain up to 380 ppm Zr. Plots for the remnants occupy a similar field to that for mafic rocks in banded migmatite (Amg^{g}) and Mary River Group metagabbro (Mg). Plots for Mary River Group metabasalt (Mb) are less scattered than those for Amn^{f}, Amg^{g}, and Mg (*see* Fig. 49a, b).

A comparison of TiO_2 content with Fe/(Fe+Mg) yields a plot that indicates a crude differentiation trend for the intermediate-mafic remnants in Amn (*see* Fig. 50a). The orientation of the computed line differs from the lines obtained for mafic rocks in banded migmatites (Amg^{g}) and for Mary River Group mafic rocks. This indicates that the intermediate-mafic rocks in Amn (Amn^{f}) may not be correlatives of these other mafic rocks. From a visual inspection of the point distribution for Amn^{f}, however, one would anticipate a line that would be quite similar to those for mafic rocks in the Mary River Group and in banded migmatite.

Analyses for intermediate to mafic rocks in Amn (Amn^{f}) as well as a few for felsic volcanic remnants in Amn (Amn^{h}) are compared with similar rocks in the Mary River Group (Mb, Mg, Ma), and with mafic rocks (Amg^{g}) in banded migmatite (Amg) in a Jensen (1976) cation plot (*see* Fig. 46). The mafic rocks Amn^{f} and Amg^{g} plot about equally in the calcalkalic and tholeiitic fields and points on the right trend toward the komatiitic field. Plots for Amn^{f} and Amg^{g} in Figure 46 are similar to one another and, with those for Amn^{h}, are compatible with their being part of a continuous calc-alkaline-tholeiitic suite. Data for Mary River Group metamorphosed mafic and felsic volcanic rocks plot in different fields and may therefore represent different magma sources.

Age

A Rb/Sr errorchron age of 2159 Ma with an initial intercept of 0.7109 (Table 52) was obtained for five samples of nebulitic granitic gneiss (Amn) and three samples of foliated monzogranite (gr-Agr) taken from the Ayr Lake region (NTS 27F). The mean square of the weighted deviates (MSWD) of 126 obtained for this age (Fig. 23) is too large to place much credence in the age. It does however indicate a minimum age for both units, and may be indicative of a mid-Aphebian disturbance in the region (*see* "Regional geochronology" section). An Nd depleted mantle model age of 3.67 Ga (*see* Fig. 98) was obtained by E. Hegner for a sample of map unit Amn from the south-central part of map area NTS 37H. One of the nebulitic granitic gneiss samples used for the Ayr Lake 2159 Ma errorchron age yielded a model age of 3.38 Ga. A model age of 2.98 Ga was obtained for felsic metavolcanics in the basement to the Mary River Group at Mary River (NTS 37G). Ages of some components of complex gneisses associated with units Amn and Amg near the head of Cambridge Fiord (NTS 37H) are discussed in the section dealing with the age of unit Amg.

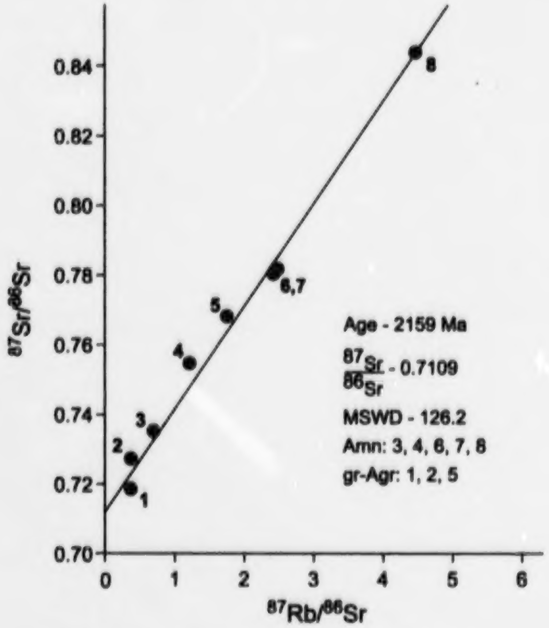

Figure 23. *Rb/Sr errorchron diagram for units* Amn *and* gr-Agr *in the Ayr Lake region (NTS 27F).*

Unit Amn is considered on the basis of the field evidence to be in part equivalent to units Agn and gr-Agr and probably, therefore, to contain some rocks of about the same age. The Nd model ages suggest that some of this sialic crust may be as old as 3.7 Ga, and that part of unit Amn is older than unit gr-Agr. Rb/Sr ages of 2642 Ma and 2697 Ma for similar rocks to unit Amn at the Mary River No. 4 iron deposit (Agn, in map area NTS 37G), and McBeth gneiss dome (NTS 27C), just south of the map area, are probably metamorphic ages and indicate minimum ages for map unit Amn. Rubidium-strontium and samarium-neodynium data for one sample from the McBeth dome both indicate an age of ca. 3.3 Ga (Jackson, 1978b; Jackson et al., 1990a). Uranium-lead zircon ages of ca. 2.77, 2.84, and 2.82 Ga have been reported for granitic components in gneisses south of the map area (Morgan, 1983; Scammell and Bethune, 1995a).

Biotites from four different localities within unit Amn represent both amphibolite and granulite facies terranes and have yielded K-Ar ages of 1703 to 1679 Ma (Table 51). These ages may be cooling ages related to the Hudsonian Orogeny.

Origin

Unit Amn undoubtedly includes rocks of more than one origin. Some of the massive granitic rocks are intrusive. The presence of contacts that seem to range from gradational to intrusive between nebulitic quartzofeldspathic gneiss and massive and foliated granite, and the intrusive nature of Amn locally into overlying amphibolite and other rocks, suggest that Amn may in part be a more contaminated equivalent of the Archean granitic intrusions gr-Agr, and Agp. It also suggests that some of the massive granitic rocks may have formed by a segregation process during an early anatexis of the nebulitic rocks. The remnants of supracrustal sequences, the presence of structures that resemble crossbedding at a few localities and the similarity in composition of the abundant schlieren to the matrix suggest that some of unit Amn may represent quartzofeldspathic metasediments and felsic metavolcanics. Apparent contact relations between unit Amn and the Mary River and Piling groups suggest that unit Amn may have undergone an anatectic event that predates deposition of these supracrustals, and is a component of the basement to them. The general lack of aluminosilicate minerals, such as sillimanite, and paucity of garnet in most of these rocks suggest that if some are metasediments then they were probably eroded and deposited with a minimum of chemical decomposition. Chemical data suggest that Amn may be related to unit gr-Agr, and that some of the rocks included in Amn may represent volcanic arc, collision, and within-plate tectonic environments. Because of the chemical differences discussed above, most of the mafic rocks in Amn are considered tentatively to represent a different, older igneous event than mafic rocks of the Mary River Group.

Foliated monzogranite-granodiorite (gr-Agr)

Description

Rocks assigned to this map unit underlie equidimensional, irregular areas up to 35 km across, and areas up to 65 km long that are elongated parallel to the regional trends (northwest in NTS 37G, east-west in NTS 37F, etc.). These rocks underlie about 15% of the Icebound Lake (NTS 37G) map area, about 10% of the Steensby (NTS 37F) and Clyde River (NTS 27E, F) map areas, and underlie small areas in the western and southern parts of the Conn Lake (NTS 37E) and Buchan Gulf-Scott Inlet (NTS 37H, 27G) map areas. Units gr-Agr and Amn have several similarities and in some areas of poor outcrop it is difficult to differentiate the two. A few of the rocks ascribed to gr-Agr in map areas NTS 37G and 37H may belong in unit Amn.

The aeromagnetic pattern resulting from this unit is similar to that from units Agn, Amn, and mu. In topographically flat areas such as north of Steensby Inlet (NTS 37F) and between Isortoq Lake (NTS 37F) on the west and the west edge of the Barnes Ice Cap (NTS 37E) on the east, the aeromagnetic pattern is nearly flat and featureless. Elsewhere the pattern is gently undulating and has a texture that varies from a subtle bird's-eye type to one with poorly defined trends parallel to the regional structure. Positive anomalies are rarely more than 300 nanoteslas, and then only in areas of relatively rugged terrain. One exception to this seems to be in the vicinity of Cockburn Lake (NTS 37F) where nanotesla values are slightly higher, and the aeromagnetic contour lines a little more closely spaced than one would expect for this unit and the topography of the area.

Unit gr-Agr is chiefly monzogranite and granodiorite in composition, and four varieties have been differentiated: pink, white to grey, porphyritic, and migmatitic (Fig. 17, 20D, 24). Banded migmatite is included in the unit locally. The structures and mineralogy are similar in all four varieties, although the mineral proportions vary. Pink foliated gr-Agr includes some rocks of syenogranite composition in map areas NTS 37E, 37F (Fig. 20Db, 24a), whereas granodiorite is relatively abundant in map areas NTS 37G and 27F, E (Fig. 20D). Porphyritic gr-Agr is chiefly pink monzogranite (Fig. 24b) and, like pink foliated gr-Agr in map areas NTS 27F, E (Fig. 20Dc), has a relatively restricted composition. White to grey foliated gr-Agr is chiefly granodiorite and tonalite (Fig. 24d). Some rocks of monzonite, quartz monzonite, syenodiorite, trondhjemite, and quartz diorite composition also occur in unit gr-Agr. Most of this map unit has less than 15% mafic minerals and rarely has more than 20% (Fig. 17, 20D, 24). Mafic minerals are most abundant in white to grey gr-Agr and in porphyritic gr-Agr.

Most of the rocks in gr-Agr are foliated and medium grained, but may range from fine- to coarse-grained and pegmatitic. Fresh and weathered surfaces are mostly light or medium grey to pink, and are rarely white, greyish black, or pinkish black. Some of the rocks have an ashy weathered surface. Colours are commonly uniform, but vaguely banded varieties in which alternate bands vary slightly in colour and composition are almost as common. Several of the rocks are mottled, and others have been reddened along cliff faces and fault zones and resemble younger massive granitic rocks from a distance. The rocks in granulite facies commonly have a resinous lustre and are greenish grey to yellowish brown.

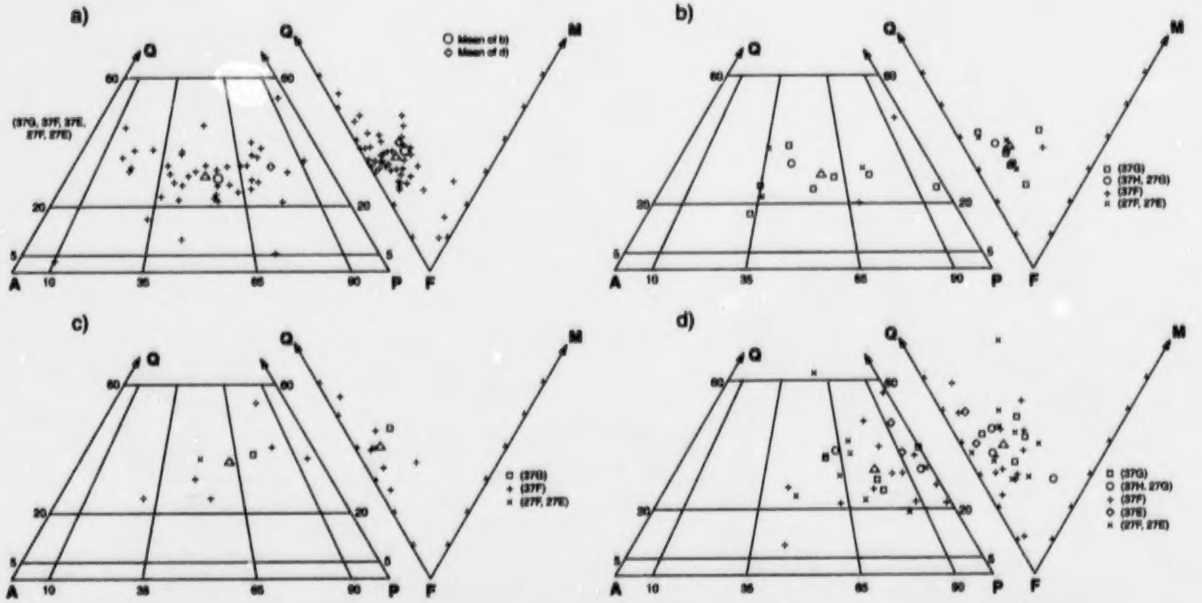

Figure 24. Quartz-alkali feldspar-plagioclase and quartz-feldspar-mafics plots for unit gr-Agr*:* ***a****) pink,* ***b****) porphyritic,* ***c****) migmatitic, and* ***d****) white to grey. The mean composition for each is shown by a triangle.*

Potassium feldspar megacrysts (chiefly microcline) occur in many of the rocks in map unit gr-Agr, and have been deformed into augen and further drawn into thin recrystallized lenses. In some places only the megacryst rims have been recrystallized, and a few megacrysts appear to have either escaped recrystallization, or perhaps were formed later. These augen commonly compose less than 10% of the rock and range up to 5 cm long. Small quartz megacrysts are also present in some of the rocks. Metamorphic granoblastic textures prevail and a few of the finer grained rocks have a salt-and-pepper texture.

Most mineral assemblages are compatible with the amphibolite facies, but some of the rocks are granulite facies. Quartz, microcline (orthoclase in the granulite facies), and oligoclase (An_{16-30}) are major constituents and are commonly associated with minor myrmekite. Perthitic microcline seems most abundant in the Steensby Inlet (NTS 37F) and Conn Lake (NTS 37E) map areas. Some of the oligoclase is antiperthitic. Dark brown to dark greenish-brown and dark reddish-brown biotite is the major mafic mineral and is accompanied by bluish-green and olive- to brownish-green hornblende in about one third of the thin sections examined from this unit. Both biotite and hornblende differ in colour between the amphibolite and granulite facies as they do in unit Amn. Clinopyroxene and garnet are very rare, but hypersthene (optically negative, some unpublished probe analyses) is common in the granulite facies. Chlorite is commonly present as an alteration product, and muscovite is present in a few places in more than trace amounts in about one sixth of the thin sections. Major accessory minerals in order of abundance are: apatite and magnetite-ilmenite, zircon, sphene, allanite, and epidote. Allanite is markedly more common in units Amn and gr-Agr than in any other map unit. Pyrite, pyrrhotite, limonite, hematite, leucoxene, and carbonate are rare. Retrograde minerals include chlorite, epidote, prehnite, sericite, leucoxene, and iron oxides. The most common mineral assemblage is:

quartz+microcline+oligoclase+biotite.

Common additional minerals are hornblende and/or epidote, or muscovite, or locally clinopyroxene. Hypersthene is the major mafic mineral in the granulites where orthoclase replaces microcline.

Most of map unit gr-Agr is composed of uniformly foliated rock that rarely contains inclusions and in which the quartzofeldspathic component contains parallel mafic folia 2 mm or less thick and up to 2 cm apart. Much of the unit is also vaguely and discontinuously banded, the alternating bands varying only slightly in colour and composition. The bands commonly are less than 10 cm thick and highly contorted, but locally are evenly spaced, continuous, or as much as 1 m thick. Swirly, indistinct nebulitic schlieren are common, but rarely make up more than 10 per cent of the rock. Contacts between different lithologies are commonly diffuse and each lithology may contain inclusions of the other. Mineral lineations and rodding of mineral aggregates are common and schlieren and sheared zones, locally 0.6-2 m apart, were seen in several places.

Amphibolite inclusions and bands up to 60 m thick are common, and include deformed dykes and sills (Fig. 20Ja, 25). The amphibolite bodies grade into agmatite locally. The most common assemblage is:

quartz+plagioclase+hornblende+biotite±
microcline±epidote

Hypersthene replaces hornblende as the major mafic mineral in the granulite facies.

Locally some of the granitic rocks are thinly laminated, or are fine grained with small phenocrysts of quartz and feldspar. These rocks are probably felsic metatuffs and metavolcanics of rhyolite to dacite composition. Small areas of undifferentiated porphyritic granitic rocks, lit-par-lit gneiss, banded migmatite, and various metasediments are included in the unit. Younger massive granitic rocks (granite to rarely quartz diorite in composition) occur as dykes, sills, irregular veins, and pegmatites.

Contact relations

Most contacts between map unit gr-Agr and map units Agn, Amn, Amg, and Agp are gradational, representing both primary compositional changes, and secondary, sheared contacts. Some rocks ascribed to gr-Agr may be the foliated or sheared equivalent of other units. For example, the large body of feldsparphyric, foliated monzogranite-granodiorite (gr-Agr) 25 km southwest of the head of North Arm in the Icebound Lake (NTS 37G) map area (Fig. 13) is considered to be the foliated, sheared equivalent of the massive feldsparphyric

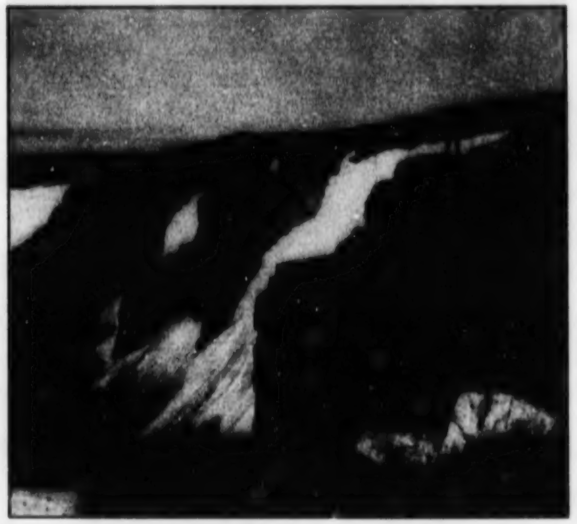

Figure 25. *Foliated monzogranite* (gr-Agr) *containing amphibolite inclusion below person in upper right corner and quartz vein in lower right foreground, west of Mary River No. 1 iron deposit (NTS 37G). Photograph by W.J. Crawford. GSC 1997-54A*

body of similar composition (Agp) immediately to the southwest. Also, a body of gr-Agr in the northeast corner of the Steensby Inlet (NTS 37F) map area is cored by map unit Agp.

Map unit gr-Agr is also commonly in sharp contact with many of the other map units. Some of these contacts are faults (including thrusts, e.g. Gibbs Fiord, northwest NTS 27F), whereas others are intrusive, with either gr-Agr being the intrusive unit or with younger units like Agp and Ag intruding gr-Agr. Foliated granitic rocks assigned to unit gr-Agr are probably overlain unconformably by the Mary River Group in the Mary River region and elsewhere.

Chemistry

Table 48 (*see* column 3, Group I) contains a mean for spectrographic analyses of map unit gr-Agr as well as a mean for foliated granitic rocks in unit Amn (Amn^b = column 2, Group I). The patterns and modes displayed by individual elements in histograms (*see* Table 49, Fig. 95, 96) are similar enough for units gr-Agr, Amn^b, and Amn to be considered as equivalents. However, they are at least equally similar chemically to the conformable leucosome in banded migmatites (*see* Amg^j = column 7, Group I of Table 48), and to charnockites (Ack = column 5, Group I). Both gr-Agr and Amn^b are least similar to unit Agp and have few similarities with unit Amp (*see* Table 49). The chemical dissimilarities between units gr-Agr and Agp do not support the field observation that some bodies of gr-Agr may be the sheared equivalents of Agp.

A comparison with chemical data (e.g. *see* Table 31) interpreted by Pearce et al. (1984) shows that map unit gr-Agr most closely resembles volcanic arc granites, and is more similar to arc granites from active continental margins that those from oceanic tholeiitic and calc-alkaline arcs. The unit resembles collision granites a little more than within-plate and ocean ridge granites.

Comparison with data presented by Whalen et al. (1987) indicates that the unit resembles I-type granites somewhat more than S-type granites. Also the I-type granites have several similarities with A-type granites and only a few similarities with M-type granites.

X-Y plots for units gr-Agr and Amn^b using the spectrographic data represented in Table 48 (*see* Table 48, Appendices 2, 3, and 4) for TiO_2, MgO, Zr, Ba, and Sr are shown in Figure 26. These plots are similar to, but less diffuse than, the plots for unit Amn. Therefore the same comments apply to both units gr-Agr and Amn, except that the plots for gr-Agr involving Zr also show a weak positive differentiation trend that is most obvious in the TiO_2 versus Zr plot (Fig. 26a).

Table 30 (*see* Table 30) presents major, minor, and trace element analyses for several map units in the map area, on Bylot Island, and south of the Piling Basin. These analyses, which include one for a foliated, rodded monzogranite from unit gr-Agr in the map area, are used to plot a variety of diagrams (*see* Fig. 69, 73) and to calculate several ratios (*see* Table 32). Most of the plots indicate that the sample from unit gr-Agr (symbolized by a triangle) is a calc-alkaline peraluminous I-type, continental margin (or within-plate) volcanic arc monzogranite with average potassium. Individual diagrams suggest it may be one of an anomalous, a mantle derived, an alkaline, or a metasomatic granite. This and a few other samples of foliated granitic rocks (*see* Fig. 74, 75) have relatively high differentiation indices and lie along linear trends that probably represent differentiation trends.

Age

A zircon U-Pb age of 2851 +20/-17 Ma (Fig. 27; *see* Fig. 98, Table 51) has been obtained for grey foliated tonalite (gr-Agr) that is considered to be unconformably overlain by the Mary River Group near the south edge of the Icebound Lake map area (NTS 37G). Its lower intercept age of 1711 Ma may reflect late Aphebian activity. Mary River Group felsic metavolcanics (Ma) from the same area have yielded a zircon U-Pb age of 2718 Ma (Table 51). E. Hegner (Hegner and Jackson, 1990; Jackson et al., 1990a) has obtained Nd depleted mantle model ages of 2.85 Ga for the grey tonalite sample noted above, 3.10 Ga for one of the foliated grey monzogranite (gr-Agr) samples from the Ayr Lake region (NTS 27F; used to obtain the 2159 Ma Rb/Sr errorchron age discussed below), and 2.83 and 2.86 Ga for samples of pink foliated granitic rocks from the Buchan Gulf (NTS 37H) and Clyde Inlet (NTS 27F) map areas respectively. These few data support field evidence that grey foliated granitic rocks may be older than the pink rocks.

The Rb/Sr errorchron age of 2159 Ma (Fig. 23) obtained for five samples of Amn and three samples of foliated monzogranite (gr-Agr) from the Ayr Lake region (NTS 27F) is considered to be a minimum age for both units (*see* Table 52, Fig. 98), and to be related to a mid-Aphebian disturbance (*see* "Regional geochronology" section). A somewhat older age is indicated for the gr-Agr samples than for the Amn samples.

Much of unit gr-Agr is considered on the basis of field evidence and age determinations to be in part equivalent to, and about the same age (3.1-2.85 Ga) as some of the rocks included in units Agn and Amn. These three units commonly underlie the Mary River and Piling groups (Jackson, 1966b, 1969, 1978a, 1978b; Jackson and Taylor, 1972). Zircon U-Pb ages of ca. 2.84 Ga for granitic cobbles in Mary River Group conglomerate and ca. 2.77 Ga for protolithic material in quartzofeldspathic gneisses have been reported for the Eqe Bay region just south of the map area (Scammell and Bethune, 1995a). These ages support the contention that granitic rocks as old as 2.85 Ga may be common in map units gr-Agr, Amn, and Agn.

Some small bodies of foliated granitic rocks included in unit gr-Agr, however, may be younger. Similar rocks, for example, intrude Mary River Group strata, and contain inclusions of rocks similar to those of the Mary River and Piling groups. Many of the intrusive quartzofeldspathic layers in banded migmatites formed in part from both the Mary River and Piling groups resemble the granitic rocks of this unit (gr-Agr). Also, the large body of feldsparphyric foliated monzogranite-granodiorite 25 km southwest of the head of North Arm (NTS 37G; Fig. 13, *see* Fig. 110) is considered to be the foliated, sheared equivalent of the massive porphyritic

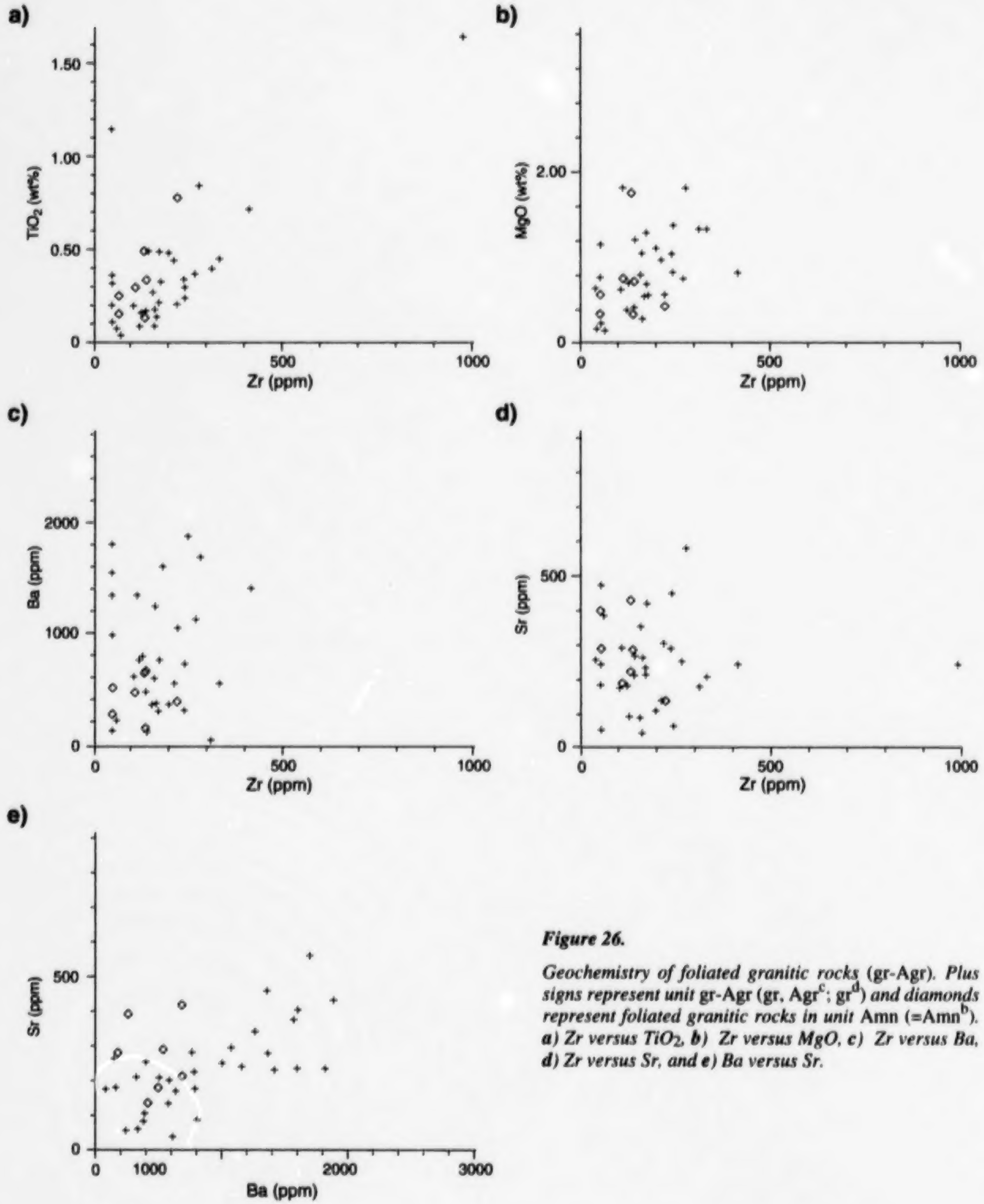

Figure 26.

Geochemistry of foliated granitic rocks (gr-Agr). *Plus signs represent unit* gr-Agr (gr, Agr^c; gr^d) *and diamonds represent foliated granitic rocks in unit* Amn (=Amn^b). ***a)*** *Zr versus TiO_2,* ***b)*** *Zr versus MgO,* ***c)*** *Zr versus Ba,* ***d)*** *Zr versus Sr, and* ***e)*** *Ba versus Sr.*

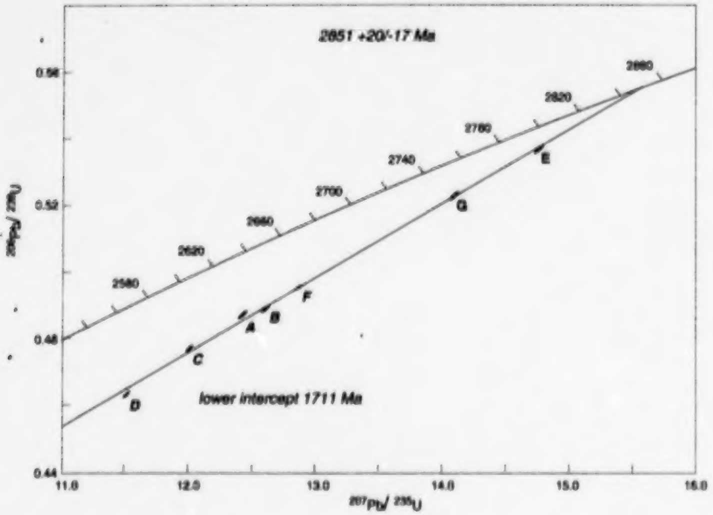

Figure 27.

Concordia diagram and U-Pb isotopic ratios for zircons from a foliated tonalite in map unit gr-Agr, *south-central Icebound Lake map area (NTS 37G). A-G identify plots of different zircon fractions. The sizes of the plots are commensurite with the laboratory errors. Data supplied by P.A. Hunt and the Geochronology Section, Geological Survey of Canada, Ottawa.* See *Jackson et al. (1990b).*

monzogranite-granodiorite (Agp) immediately to the southwest. Zircon from the latter has yielded a U-Pb age of 2709 Ma (*see* Table 51).

Rodded monzogranite (unit gr-Agr) in the Mary River area (*see* Table 53) yielded a muscovite K-Ar age of 1659 Ma which may be a metamorphic cooling age related to the Hudsonian Orogeny (*see* Fig. 98).

Origin

Most of unit gr-Agr is considered to be composed of Archean granitic intrusions that have been thoroughly recrystallized and deformed to varying degrees. The presence of remnants of metasediments, some of which have been metasomatized, and felsic metavolcanics suggest that these rocks may form a larger part of the unit than is presently recognized. There is, however, a paucity of minerals such as aluminosilicate minerals and garnets which are commonly associated with metasediments. Apparently gradational contacts in some places between units gr-Agr, Amn, and Agp suggest that these units may include interrelated rocks of the same age.

The chemical data are somewhat conflicting, but overall favour I-type granite emplaced in a calc-alkaline volcanic arc of an active continental margin rather than a collision environment. Following Pearce et al. (1984), the major ferromagnesian minerals present indicate the same environments, but favour a post-tectonic over syntectonic collision environment. Inferences made from the petrography, however, are contingent upon the metamorphic assemblages mirroring the primary assemblages.

Mafic dykes and sills (b)

Description

Thin tabular bodies up to more than 100 m thick, and a few small equidimensional bodies of metamorphosed mafic rocks occur throughout the map area, chiefly in map units Agn and Amn, and in Amg where they are less readily differentiated from the host rock (Fig. 28). In some regions these bodies seem to be little deformed, are both parallel to and cut across gneissosity and rock boundaries, intrude one another, bifurcate, and locally have finer grained margins. There seems little doubt that these mafic bodies are metamorphosed dykes, sills, and stocks, and may represent one or more swarms of intrusions.

In other regions, however, the tabular bodies are highly deformed (Fig. 28), isoclinally folded and refolded, transposed parallel to contacts and gneissosity in enclosing rocks,

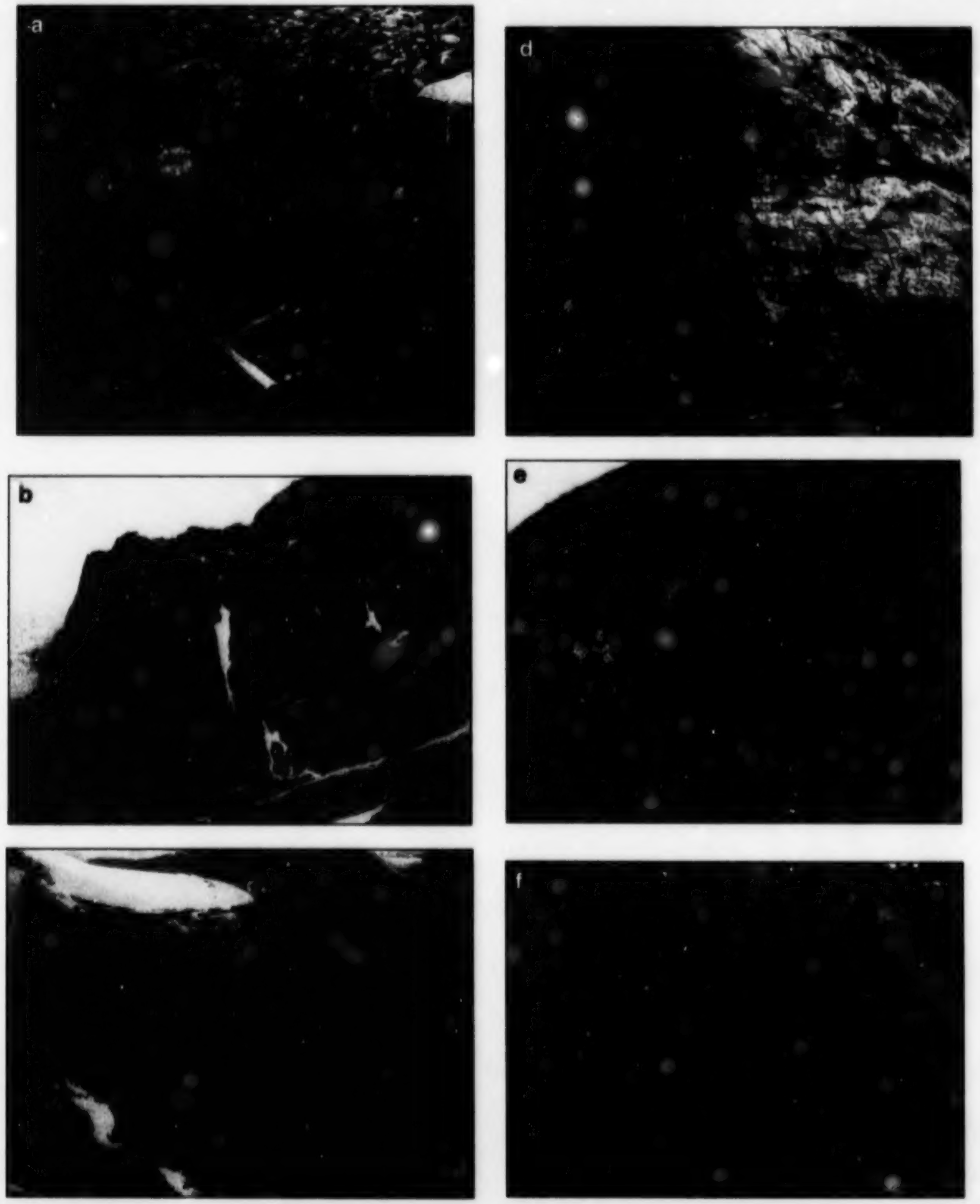

Figure 28. ***a)*** *Northeast-trending amphibolite dyke, 3 m thick, in gneissic tonalitic rock with quartz eyes west of Mary River No. 1 iron deposit (NTS 37G). The dyke has sheared, locally garnetiferous margins and zoned feldspar megacrysts up to 5 cm in diameter. Photograph by W.J. Crawford. GSC 1997-54B.* ***b)*** *View northeast at a folded amphibolite dyke in banded migmatite* (Amg) *along the east wall of Tromso Fiord (NTS 37H). The top of the cliff is 900 m above the fiord. Photograph by G.D. Jackson. GSC 186928.* ***c)*** *View west by north at a folded and boudined amphibolite dyke in banded migmatite* (Amg) *on the south wall of Cormack Arm (NTS 27F). Some of the boudins have been stacked one above the other in the axial zone of a fold (centre of photograph). The top of the cliff is 1100 m above the fiord. Photograph by G.D. Jackson. GSC 187019.* ***d)*** *Northwest wall of Clyde Inlet immediately northeast of Cormack Arm. Boudined, concordant, plastically deformed amphibolite bodies in banded migmatite* (Amg) *range from rounded and rotated to sharply angular (upper part of cliff). The cliff exposure is estimated to be roughly 400 m high. Photograph by G.D. Jackson. GSC 204343-W.* ***e)*** *East wall of Clyde Inlet just south of the map area shows plastically deformed and boudined amphibolite dykes in blastoporphyritic, nebulitic granitoid gneiss* (Amn). *Small thrust planes were developed during later brittle deformation. Granite dykes were emplaced along and subparallel to the thrusts. The cliff exposure is estimated to be roughly 300 m high. Photograph by W.C. Morgan. GSC 186653.* ***f)*** *Boudined and plastically deformed body in nebulitic granitoid gneiss* (Amn), *Inugsuin Fiord, just south of the map area. The exposure is estimated to be of the order of 100 m across. Photograph by G.D. Jackson. GSC 187001*

and locally so disrupted and attenuated as to have been drawn into aligned angular boudins and rounded beaded structures. Locally, chiefly in fold noses, the boudins appear stacked on top of one another (Fig. 28c-f). In such areas of intense deformation it is commonly difficult to determine whether the mafic body is an intrusion or a remnant of a larger intrusion or of an extrusive sequence of similar composition. Only tentatively, therefore, are all of the bodies assigned to this map unit assumed to be metamorphosed dykes, sills, and stocks.

Few of these bodies seem to have any obvious expression on the available aeromagnetic maps, perhaps because of their discontinuity. Some of the relatively thick and long bodies (up to about 6 km) are associated with positive and minor negative anomalies of as much as 120 nanoteslas.

The mafic bodies of map unit b are chiefly amphibolite, hornblende gneiss, hornblende-pyroxene gneiss, and minor pyroxene gneiss and biotitite. They range in composition from quartz diorite to gabbro, and their mafic content ranges from 30 to 90%. They commonly contain less quartz than the more nondescript mafic inclusions in map units Amn and gr-Agr (Fig. 17, 20Ja; Fig. 29, in pocket; Table 5). A large proportion of these mafic bodies have been intruded by granitoid rocks and pegmatites. At several localities, chiefly adjacent to younger granites and pegmatites, they seem to have been affected by metasomatism and to be partially feldspathized.

These old dykes and sills are green to black on the fresh and weathered surfaces, equigranular, fine- to medium-grained, and rarely coarse grained. Some are massive and structureless to megacrystic with locally zoned plagioclase megacrysts that range up to 5 cm or more in diameter and from wispy anhedral to euhedral (Fig. 28a). The megacrysts seem to be blastophenocrysts in some dykes and porphyroblasts in others. Most, however, are foliated and/or lineated, and many have a blotchy appearance with blobs of mafic minerals up to 7 mm or so in diameter disseminated in a fine grained plagioclase-rich matrix. Some dykes, locally at least, have an ophitic- to intergranular-like texture in which the plagioclase crystals are white, sugary, finely recrystallized aggregates; but it is uncertain whether this is a metamorphic or a relict igneous texture.

The major minerals are bluish- to brownish-green hornblende and plagioclase (An_{20-49}). The plagioclase is commonly fairly fresh, but locally, as in the Mary River area, plagioclase phenocrysts have been totally altered to either sericite with minor hornblende, biotite, quartz, and magnetite; or to sericite with minor clay minerals, celadonite-glauconite (X-ray identification), hornblende, and quartz. Olive-green to brown and reddish-brown biotite ranges from a major to a minor constituent and locally, sheared margins of these mafic bodies are composed chiefly of biotite for a thickness of a metre or more. Garnet also occurs locally in the margins, especially where the margins have been sheared. Minor quartz is common and clinopyroxene occurs locally. Hypersthene is a common minor component in granulite terrane. Accessory minerals include apatite, magnetite-ilmenite, martite, leucoxene, spinel, chlorite, anthophyllite, prehnite, kaolinite, sphene, and locally possibly rutile and zircon. Retrograde minerals are: chlorite, sericite, prehnite, celadonite-glauconite, leucoxene, martite, and clay minerals (e.g. kaolinite). Typical mineral assemblages include:

quartz+plagioclase+hornblende+biotite+spinel,

quartz+hornblende+anthophyllite+biotite+sericite,

plagioclase+hornblende, and

plagioclase+hornblende+biotite±cummingtonite or hypersthene.

The most spectacular display of old metamorphosed dykes and sills occurs in the Clyde River map area (NTS 27F, E). There, highly deformed dykes are concentrated in a 30 km wide belt that extends from Inugsuin Fiord northwest for 150 km to Gibbs Fiord (Fig. 28c-f). The dykes within the belt are chiefly subhorizontal to northeasterly trending and commonly outline fold structures overturned to the northeast and southwest. Some individual boudined dykes may extend the width of the belt. Small concentrations of similar deformed dykes occur to the northwest (Fig. 28b) on strike with this belt between upper Dexterity and Tromso fiords (NTS 37H) and about upper North Arm (NTS 37G), which is a total distance of 350 km. Dykes in this zone do not seem to intrude remnants of the Mary River and Piling groups.

Amphibolite intrusions up to 2.4 km long, and amphibolite dykes up to 50 m thick trend northwesterly north of No. 4 iron deposit (*see* Fig. 106) in the Mary River region of the Icebound Lake map area (NTS 37G). These bodies cut across the lineations and foliations of the enclosing rodded granitic Archean gneisses of Agn at a low angle, and have been traced into the lower part of the quartz-muscovite-biotite-feldspar schist unit at the base of the Mary River Group. They were not, however, found to intrude the upper part of this unit or any other formation of the Mary River Group (Jackson, 1966b, 1978b).

Twenty-five kilometres to the southeast the No. 1 iron deposit trends south-southwest for about 2 km before it swings abruptly to the southeast. An extremely complex zone west of this deposit includes Archean rocks (Agn) that are basement to the Mary River Group, migmatites derived from and containing relics of Mary River Group strata (Amg), and younger granitic intrusions (Ag). Amphibolite dykes (Fig. 28a) intrude the Archean rocks (Agn) and appear to intrude the younger granite, but in the canyon walls the amphibolite dykes are seen to be rootless inclusions in the younger granite. These amphibolite dykes do not intrude the Mary River Group. They range up to 90 m in thickness but are commonly 30 m or less and cut across the foliation of the older rocks. Southwest of the southeast-trending arm of the No. 1 iron deposit these dykes trend northwesterly to a little east of north. West of the main south-southwest-trending arm, the dykes trend northeasterly. The difference in trend in the two localities is greater than the difference in trend of the two arms of the No. 1 iron deposit, and at least two dyke trends may be present.

Similar dykes occur along the north half of the western border of map area NTS 37E, in adjacent east-central map area NTS 37F, and about the head of Steensby Inlet (NTS 37F). The trend of most of these dykes, like those in the Clyde River map area, is easterly to northeasterly.

Contact relations

The nature of individual contacts has been discussed above. Where seen they are almost always sheared. These old metamorphosed mafic bodies in map unit b are most abundant in map units Amn and Agn, and are abundant locally in Amg, where it is difficult to differentiate them from mafic rocks of the Mary River Group (Mg, Mb). They are uncommon in map unit gr-Agr, include rocks that are overlain unconformably by the Mary River Group, and are absent in map unit Agp and younger intrusions (e.g. Ag) except as inclusions of older rocks.

Chemistry

No samples that are considered with confidence to have been collected from a large old mafic tabular body have yet been analyzed. It seems likely, however, that some of the mafic inclusions in unit Amn (Amn^f) for which samples have been analyzed, represent remnants of map unit b. It is anticipated therefore that the chemistry for unit b will be similar to these mafic inclusions in unit Amn (e.g. *see* Fig. 48, 49, 50). The mafic remnants and inclusions in unit Amg probably include remnants of unit b as well as remnants of the Mary River Group.

Age

Crosscutting relations seen in the field indicate that at least two ages of metamorphosed mafic rocks are present in unit b. These bodies are considered to be older than the Mary River Group. Therefore the 2718 Ma U-Pb zircon age for Mary River Group felsic metavolcanics (Ma) in map area NTS 37G (*see* Fig. 54, Table 51) provides a minimum age. The U-Pb zircon age of 2851 Ma for unit gr-Agr in map area NTS 37G may be a maximum age. However, the paucity of unit b in unit gr-Agr compared with unit Amn suggests that some of units Amn and b may be older than gr-Agr.

Origin

Unit b is composed of metamorphosed mafic bodies that were emplaced mostly as quartz diorite to gabbro dykes and sills. As mapped, concentrations of these bodies seem to be aligned in northwest-trending belts parallel to the belt in Clyde River map area (NTS 27F). Possible groupings are:

a) Inugsuin to Gibbs fiords, Tromso Fiord, North Arm.

b) Northwest corner NTS 37E to northeast corner NTS 37F, Mary River No. 1 and No. 4 areas.

c) North end of Steensby Inlet.

On the other hand, most of the individual tabular bodies of unit b trend easterly to east-northeast. Possible groupings of this orientation are:

a) Mary River region to North Arm.

b) North end of Steensby Inlet to northeast corner NTS 37F and northwest corner NTS 37E, Tromso Fiord.

c) Several small belts or one large belt from Gibbs Fiord southeast to Inugsuin Fiord.

The tabular bodies of unit b are considered to be remnants of one or more dyke swarms. Fold structures outlined by these bodies are truncated in the upper part of several cliffs along fiords by decollement zones overlain by subhorizontally layered plastically deformed rocks (*see* Fig. 105a, d, e). The tabular bodies of unit b and their host rocks have been involved in at least one major thrusting event. Although more data are needed to determine the directions of movement, some data discussed later are taken to indicate that one relatively late direction of thrusting (compression) may have been in a northeast to southwest direction.

Mary River Group (M, AM)

General description

The Mary River Group is a metamorphosed and intensely deformed assemblage composed chiefly of felsic and mafic volcanics, pelites, and greywackes. Quartzite, iron-formation, ultramafic rocks, and anorthositic and gabbroic intrusions are commonly an integral part of the assemblage (Table of Formations). Metamorphic grade is chiefly upper amphibolite facies. It decreases to greenschist facies in the centres of several large bodies of the Mary River Group, and ranges from subgreenschist to granulite over distances of less than 10 km at one or two localities.

The group was named by Jackson (1966b) after the Mary River area (Fig. 1, *see* Fig. 99) where some of the highest grade iron deposits in the world are found (Tables 55, 56, 57). Many of the deposits range from pure hematite to pure magnetite) (Gross, 1966; Jackson, 1966a, b). Rocks assigned to this group outcrop throughout most of the map area. They are abundant in western and southern map area NTS 37G, in central map area NTS 37H, in northern and southeastern map area NTS 37F, and in north-central map area NTS 37E. They have been mapped in only a few small areas in map area NTS 27F.

Within and adjacent to the map area the Mary River Group outcrops in numerous lenticular, separated and interconnected, en echelon bodies up to 65 km long. These are concentrated in a large arc that crosses the Dexterity Granulite Belt (*see* Fig. 99, 114) and extends 160 km northeast from Eqe and Grant-Suttie bays (NTS 37C; Fig. 1, *see* Fig. 114) immediately south of map area NTS 37F to the north end of the Barnes Ice Cap and the vicinity of Conn and Bieler lakes (NTS 37E). From there it extends another 290 km westward and northwest to Nina Bang Lake (NTS 37F) and the Mary River-Tay Sound region (NTS 37G). Individual lenses trend chiefly easterly, northeasterly, and southeasterly, and rarely southerly. The largest areas underlain by the Mary River Group occur at Eqe and Grant-Suttie bays (northeast NTS 37C-southeast NTS 37F), in the Mary River-Tay Sound region (northwest NTS 37G), east of Nina Bang Lake (northwest NTS 37F), and at the north end of Barnes Ice Cap (NTS 37E). Scattered bodies up to 16 km long lie outside the main arc, chiefly in the vicinity of and southeast of Cockburn Lake (NTS 37F) where they are more abundant than shown on the published map (Jackson et al., 1978c; *see* "Aeromagnetic pattern"). Scattered bodies also lie along the upper reaches of the fiord region from North Arm (NTS 37G) southeast to Clark and Gibbs fiords (NTS 37E). In Clyde River map area (NTS 27F, E), rocks assigned to the Mary River Group underlie a small island northwest of Erik Point, occur locally northeast of the mouth of Cormack Arm, and occupy a small northwest-trending belt on the west side of Inugsuin Fiord.

The Mary River Group has been studied most extensively in the Mary River and Eqe Bay regions (Fig. 1; *see* Fig. 12, 99) (Gross, 1966; Jackson, 1966a, b, 1978b; Jackson and Taylor, 1972; Crawford, 1973; Morgan et al., 1975; Jackson and Morgan, 1978a, b; Jackson et al., 1978b, c, d, 1990b; Morgan, 1982, 1983; Bethune and Scammell, 1993, 1997; Scammell and Bethune, 1995a). The group contains similar rocks throughout the map area, and individual sections are commonly least complete in small areas underlain by the group. The Mary River and Eqe Bay regions are considered to be type areas for the Mary River Group. Incorporation of selected data from the Eqe Bay region, much of which is previously unpublished, provides a more complete description of the group, and contributes much toward our understanding of it and the contained high grade iron deposits. Additional data is contained in reports by Bethune and Scammell. However, detailed lithological descriptions provided here apply solely to the map area, unless specified otherwise.

Correlations

The rocks noted below outcrop in widely separated areas over a large region. They are considered tentatively to belong to one group because of close lithological and stratigraphic similarities, similar association of mafic and ultramafic rocks including anorthosite, similar relationships with surrounding rocks, and alignment along strike. Even the most reliable age determinations for these rocks are variable, ranging from 2742-2718 Ma, and additional accurate determinations are needed. Future work may show that more than one distinct group of rocks is included in the Mary River Group and that certain rocks should be excluded from the group.

Rocks elsewhere on Baffin Island that may be correlatives of the Mary River Group (*see* Fig. 114) outcrop locally on both sides of southern Milne Inlet, south of Milne Inlet (Fig. 1), and west of southern Navy Board Inlet (Blackadar, 1968a; Jackson et al., 1985; unit 2 of Jackson and Sangster, 1987). They also occur extensively adjacent to Eclipse Sound and Pond Inlet (unit sv of Jackson and Davidson, 1975, and Jackson et al., 1975). Immediately south of the map area (Fig. 1, *see* Fig. 112) the Mary River Group occurs in the Eqe and Grant-Suttie bays region (NTS 37C, 37D; Blackadar, 1958b, 1963; Jackson, 1969; Jackson and Taylor, 1972; Crawford, 1973; Morgan et al., 1975; Morgan, 1982, 1983; Bethune and Scammell, 1993; Scammell and Bethune, 1995a).

A similar succession occurs on the south side of Generator Lake at the southeast end of the Barnes Ice Cap (NTS 27C). Aeromagnetic data and most fieldwork (Eade, 1953; Jackson, 1969; Jackson and Taylor, 1972; Kranck, 1955; Morgan, 1983; Henderson, 1985a) indicate strongly that the Generator Lake sequence is probably part of the Piling Group.

The Mary River Group was correlated with Heywood's (1967) Prince Albert Group and their westward extension by Jackson (1966a, b, 1969; Jackson and Taylor, 1972) and subsequent workers (e.g. Schau, 1982; Ashton, 1988). The Prince Albert Group on and adjacent to Melville Peninsula has been studied by Heywood (1967), Campbell (1973, 1974), Heywood and Sanford (1976), Schau (1977, 1978, 1982), Frisch (1982), Henderson (1983), Schau and Heywood (1984), and Schau and Beckett (1986). Similar rocks have been reported on Baffin Island north of western Fury and Hecla Strait by Ciesielski (1983), and in a large coastal region of northwestern Greenland including the head of Inglefield Bredning (Nutman, 1984), Kap York (Dawes, 1976), and Melville Bugt (Dawes and Frisch, 1981). Some of the rocks in northwestern Greenland have yielded ages similar to those obtained for the Mary River and Prince Albert groups (e.g. Kalsbeek, 1986). Using the predrift position of Le Pichon et al. (1977), these similar rocks of similar age extend in a belt about 2000 km long (the Committee Orogen) from northwest Greenland southwest to west of the Baker Lake region (*see* Fig. 114).

The Mary River and Piling groups are in close proximity to one another north of Isortoq Fiord and Isortoq River (NTS 37F), and are in contact just south of the map area in the Koch Island map area (Morgan, 1982; Bethune and Scammell, 1993, 1997; Scammell and Bethune, 1995a). The impression gained from fieldwork is that, in general, the Mary River Group has been more metamorphosed and deformed, and may have undergone at least one more major period of deformation, granitic intrusion, and migmatization than the Piling Group. The presence of Piling quartzite and marble, the two basal units of the Piling Group, north of well developed Mary River strata suggests that an unconformity exists between Piling and Mary River strata. Yet where the two groups are in close proximity, they seem to have been similarly affected by metamorphism and deformation. Ages determined recently for the Piling Group indicate it is late Aphebian.

Aeromagnetic pattern

The magnetic expression of the Mary River Group is typified by narrow high anomalies up to 10 km long due mostly to the presence of iron-formation, iron ore, amphibolite, and ultramafic rocks. Most anomalies occur in belts within which individual anomalies are arranged in en echelon, beaded, and/or parallel fashion. Most anomalies for the Mary River Group are 900-1000 nanoteslas above average values for the map area, with some values up to 5000 nanoteslas above. Anomalies up to 7000 nanoteslas above occur northeast of the Mary River area, and an 11 000 nanotesla anomaly occurs on the west side of Nivalis Lake at the north end of the Barnes Ice Cap (NTS 37E), and in the vicinity of Oliver Sound just north of the map area (Jackson et al., 1975). Anomalies up to 24 000 nanoteslas above have been recorded for the Mary River region (NTS 37G) and up to 35 000 nanoteslas above between Eqe and Grant-Suttie bays (NTS 37C). The highest anomalies are commonly partially or completely surrounded by a zone containing an abnormally large negative anomaly. This is a normal expression of strong positive anomalies that does not indicate that the surrounding rocks are abnormally low in magnetite (e.g. *see* Fig. 111).

The size of aeromagnetic anomalies for the Mary River Group are obviously dependent chiefly on the magnetite content of the iron-formation, its lateral extent, and its orientation relative to the Earth's magnetic field. Topography combined with height of flight lines above ground can also be a significant factor locally. Some major anomalies in the Mary River and Eqe Bay areas are enhanced because many, if not most, of the magnetite-rich bodies (some of which are about 100 m across near Eqe Bay) occur at or near the tops of hills that rise as much as 200 m above the adjacent terrain. By contrast a large magnetite-rich body in a valley adjacent to the Rowley River in the northeast corner of Steensby Inlet map area (NTS 37F), where local relief is about 300 m, has virtually no magnetic expression.

Numerous additional supracrustal remnants, considered to be Mary River Group, noted by the author in Steensby Inlet map area (NTS 37F) in 1994, lie mostly in tectonic subdomain 2c in central map area NTS 37F (*see* Fig. 111, 112). At least twelve additional east-trending lenses in unit Amg occur over a distance of 35 km south-southeast from west of the north end of Cockburn Lake. Most lenses are associated with positive aeromagnetic anomalies, or are on strike with mapped Mary River Group. These rocks therefore may be not only more abundant in subdomain 2c in map area NTS 37F than shown on the published map (Jackson et al., 1978d), but may be as abundant there as in tectonic subdomain 2a. The relatively high magnetic background shown on the aeromagnetic maps for subdomain 2c may be more closely related to the abundance of Mary River Group remnants than to the abundance of granite facies rocks.

Contact relations

The Mary River Group is considered to overlie rocks of units Agn, Amn, gr-Agr, and b nonconformably in the Mary River region and at Eqe Bay (Jackson, 1966b, 1978b; Jackson and Taylor, 1972; Crawford, 1973; Morgan, 1982, 1983). Similar relations seem to be present throughout the map area, but the basal contact is commonly poorly exposed and invariably sheared, faulted, marked by mylonite, or folded. Generally the underlying gneiss complex is more complexly deformed than the Mary River Group which lies adjacent to different lithologies at different places. At some of these localities an additional episode of deformation appears to be represented in the underlying gneisses. Lateral and vertical gradations of Mary River Group strata into lit-par-lit anatectic gneisses and banded migmatites (Amg, locally into rocks resembling Amn) containing felsic and mafic intrusions, and relics of the Mary River Group, are common.

The basal contact south and west of the No. 1 iron deposit in the Mary River region is probably a nonconformity that has been obscured by subsequent development of a tectonic mélange in the contact zone (*see* "Contact relations" under "Metapelite-amphibolite unit"; Fig. 18, *see* Fig. 107; Fig. 4 of Jackson, 1966b). The presence of felsic metavolcanics in both the basement and in the Mary River Group complicate matters further, although the basement volcanics are more leucocratic, more deformed, and are at a slightly higher metamorphic grade at this locality. Likewise, sheared rocks, strike faults, and isoclinal folds in the Mary River Group obscure the basal contact along the north side of the No. 4 iron deposit area (*see* Fig. 106; Fig. 3 of Jackson, 1966b; Fig. 11 of Jackson, 1978b). The basal Mary River Group strata in this area are interpreted as metamorphosed regolith that grades into the underlying granitic rocks. It is capped by an unconformity that also approximates the position of the strike fault complex (*see* "Contact relations" under "Quartz-rich unit (Mq: 0 to 590 m)"; Fig. 106; Fig. 3 of Jackson, 1966b; Fig. 11 of Jackson, 1978b).

Basal contact relations are equally difficult to ascertain in the Eqe Bay region (Crawford, 1973; W.C. Morgan, pers. comm., 1988; Bethune and Scammell, 1993, 1997; Scammell and Bethune, 1995a), and throughout the map area. Emplacement of a quartz diorite intrusion along the northern border of the Mary River Group at Grant-Suttie Bay has obscured relations there (Crawford, 1973).

Most unconformities within the Mary River Group are assumed to represent relatively little time, because they seem to be developed only locally. Crawford (1973), however, notes that the conglomerate overlying his middle unconformity transects the stratigraphically lower 60 m thick conglomerate (*see* Table 7), and suggests that the upper conglomerate may represent an extensive period of erosion. The unconformity at the top of the proposed metamorphosed regolith (discussed below) north of the No. 4 iron deposit might represent a long or short time interval depending on the length of time between its formation and deposition of the overlying sedimentary rocks.

In the northwest corner of the map area, the Mary River Group is overlain unconformably by lower formations of the Neohelikian Bylot Supergroup. Strata correlated with the Neohelikian Fury and Hecla Formation west of northern Foxe Basin overlie the Mary River Group unconformably in the Eqe Bay area (Blackadar, 1958b, 1963; Crawford, 1973;

Morgan, 1982). Cambro-Ordovician strata unconformably overlie the Mary River Group along the western edge of the map area (NTS 37F, 37G).

The Mary River Group is intruded by metamorphosed mafic and ultramafic rocks that are considered to be largely coeval with it for reasons discussed below. At least two and probably three ages of granitic intrusions (Agp to Ag) were emplaced in the Mary River Group and the underlying basement complex about 2700 to 1800 Ma ago (*see* Table 51; Jackson, 1966b). The granites are associated with aplite dykes, pegmatites, numerous quartz veins, extensive deformation and migmatization, and remigmatization. Locally crystalline granitic rocks have been diapirically emplaced into the Mary River Group (e.g. *see* Fig. 33). Neohelikian and Hadrynian diabases intrude the Mary River Group at many places.

Table 7. Comparison of the generalized stratigraphy of the Mary River Group.

Mary River Region (Modified from Gross, 1966; Jackson, 1966a, b; 1978b)		**Eqe Bay Region (Modified from Crawford, 1973; Morgan et al., 1975; Morgan, 1982, 1983; *see* Bethune and Scammell, 1993, 1995, 1997; Scammell and Bethune, 1995a, b)**
Meta-anorthosite (0-20+ m) Metagabbro Metaultramafite (0-400 m?) Chiefly basic pillowed metavolcanics (150?-1000? m); local thin open framework meta-conglomerate-agglomerate in lower 30 m	--- --- ---	Meta-anorthosite (0-335 m) Metagabbro Metaultramafite Thick turbiditic metapelite-metapsammite, minor amphibolite, silicate- and oxide-facies iron-formation Closed framework polymictic pebble-boulder metaconglomerate (46 m)
Local disconformities?		*Unconformity*
Chiefly metasediments (metapelite-metagreywacke, 150?-840? m); local thin open- and closed-framework metaconglomerate-breccia		Porphyritic intrusive and extrusive meta rhyolite-dacite; some pyroclastics Metapelite and boulder metaconglomerate with lean iron-formation clasts to 30 cm
Local disconformities?		*Unconformity*
Silicate- and silicate-oxide-facies iron-formation (0-60 m) Lenses of metapelite-metagreywacke, metamorphosed mafic and ultramafic igneous rocks (0-160? m), local, thin, open framework metamorphosed breccia-conglomerate	--- ---	Interlayered and intergradational metapelite and lean silicate- and oxide-facies iron-formation Silicate-, silicate-oxide-, and oxide-facies iron-formation (122 m); local mafic metavolcanics Thin metapelite Mafic metavolcanics Magnetite-bearing metapelite over metamorphosed breccia-conglomerate (60 m)
Local disconformities		*Unconformity*
Oxide facies iron-formation, iron ore (10-152 m); minor silicate-oxide facies Porphyritic metarhyolite-dacite, (0-650+ m); pyroclastic lenses to 10+ m; some metasediments, mafic metavolcanics Quartz-rich unit (0-590+ m); metaorthoquartzite (0-130 m)	--- ---	Oxide- and silicate-facies iron-formation, iron ore (150-215 m) Thin metapelite (60 m) Mafic pillowed metavolcanics, metagreywacke (1070 m) Cherty quartzite (60 m)
Local unconformity		
Micaceous and aluminous metasediments, quartz-pebble metaconglomerate (0-460+ m) Metapelite-mafic metavolcanics (0-167+ m); metapelite over interlayered metapelite, mafic metavolcanics, lenses of boulder metaconglomerate to 10+ m	---	Pillowed mafic metavolcanics, amphibolite (305 m)
Note: The stratigraphy of the Mary River Group is variable, on the large and small scales, from one area to the next. The plus sign indicates that the thickness is considered to be greater than the value given.		

Stratigraphy

The stratigraphy of the Mary River Group, even locally, is poorly known. This is in large part due to the metamorphism and the complexity of the structural geology as is indicated to some extent on the published maps. Much of the folding is isoclinal and refolded folds and faults are common. Some idea of the abundant faulting and resulting repetition of formations is given by Figure 36 (*see* Fig. 36). Ductile thrusts and nappes abound along the northeast coast of Baffin Island, and the fish hook outcrop pattern of the refolded Mary River Group, especially in the Mary River region (*see* Fig. 106, 107), is suggestive of the presence of thrusts that may have imbricated the Mary River Group and subsequently been folded. A large variation in stratigraphy from one locality to the next (*see* Table 7) is especially evident in the Eqe Bay region (Crawford, 1973; Morgan et al., 1975; Morgan, 1982, 1983; Bethune and Scammell, 1993, 1997; Scammell and Bethune, 1995a).

Detailed information for a few areas combined with the reconnaissance data suggest a general stratigraphy for much of the map area that is in agreement with the few stratigraphic top determinations that are available. Assumptions on top directions were made from graded beds; rare crossbeds, volcanic pillows, and clast compositions in conglomerate and breccia lenses; and stratigraphic sequences determined at a few localities where the rocks are relatively low grade and little deformed (*see* Fig. 45a).

Roughly comparable thicknesses of Mary River Group strata are exposed in the Mary River and Eqe Bay regions where maximum preserved stratigraphic thicknesses are estimated to be in the 2000-4000 m range. Comparison of generalized stratigraphic sections for the two regions in Table 7 (*see* below) are based largely on the general similarities of the sections and on the assumption that the lowermost major quartzite and overlying iron-formation units are equivalent. The presence of local disconformities is indicated by the presence of conglomerate-breccia beds that contain clasts of underlying strata, and by locally identified erosion surfaces. Neither the conglomerate lenses nor the erosional intervals seem to be laterally extensive, although they may be more continuous in the Eqe Bay area (Crawford, 1973). Stratigraphic differences between the two regions reflect chiefly the variations in stratigraphic positions and sizes of the major felsic and mafic volcanic piles in each region.

There are two main iron-formation horizons in the Eqe Bay region (*see* Table 7) where the major felsic volcanic sequence overlies the main iron-formations and the major mafic volcanic sequence lies below them (Crawford, 1973; W.C. Morgan, pers. comm., 1988; *see* Bethune and Scammell, 1993; Scammell and Bethune, 1995a). In the Mary River region the iron-formation occurs as a single formation in some places but in others deposition of one or more shale-greywacke lenses has separated the iron-formation into at least two stratigraphic units (*see* Table 7). Locally, thin lenses of iron-formation occur above and/or below the main iron-formation(s). In some parts of the Mary River region, the major felsic and mafic volcanic piles occupy stratigraphic positions similar to those in the Eqe Bay area, but elsewhere the relative stratigraphic positions are reversed. In the map area, small thicknesses (up to about 200 m) are either measured or based on paced distances. Larger thicknesses are based on visual estimates, or determined by making use of mapped distribution, strikes and dips, elevations available on topographic maps, and barometric measurements.

Much of the stratigraphic variability of the Mary River Group is primary and is compatible with the conclusion that the Mary River Group was deposited in a volcanic arc environment on an active continental margin. However, much of the apparent variability is also clearly due to deformation and tectonic juxtaposition.

Because of uncertain knowledge and variability of the stratigraphy, many of the various rock types will be described irrespective of stratigraphic position but with their various stratigraphic occurrences noted where relevant. Petrographic data are provided in Tables 5 and 6, and in Figures 20Jb, c, 20Kb, c, and 29. Chemical data are presented in Appendices 2-6; Tables 9, 10, 14-17, 20, 23, 48, 55, and 56; and Figure 95. Chemical comparisons with the Piling Group and the Bylot Supergroup are provided in the section on "Regional geochemistry".

Metapelite-amphibolite unit

Description

Metapelites are abundant throughout the Mary River Group intercalated with other lithologies, and in several places occur in lenses thick enough to be mapped separately. In some places a metapelite-amphibolite-rich unit (0 to >167 m) underlies the quartz-rich unit that is commonly the basal unit of the Mary River Group. It was included with the quartz-rich unit on the maps because of the small map scale.

The metapelite-amphibolite unit includes minor finely foliated and/or lineated amphibolite, lesser amounts of metamorphosed ultramafics, conglomerates, and felsic volcanics, and a small amount of quartzite. The amphibolite and metaultramafic rocks occur chiefly as concordant sill-like bodies. Some are intrusions but others could equally well be extrusions. These and most other minor lithologies in this unit occur as major units at higher stratigraphic levels in the Mary River Group, and the reader is referred to the description of these rocks. Known coarse conglomerates and metapyroclastics are restricted mostly to this unit. Most lithologies within the unit seem conformable and intergradational. The metapelite-amphibolite unit in the Mary River No. 1 iron deposit area may be divided into a lower member of mixed lithologies, and an upper member composed chiefly of metapelites. At Eqe Bay about 300 m of pillowed mafic metavolcanics (amphibolite) occupy a similar stratigraphic position to the metapelite-amphibolite unit.

Lower member (0-45 m)

The lower member in the Mary River No. 1 iron deposit area consists of metapelites interbedded with concordant amphibolites that may be mafic metavolcanics and with minor metaultramafics that are locally discordant. Lenses of metaconglomerate, felsic metavolcaniclastics including some metapyroclastics, and minor quartzite are also present.

Metaconglomerate. Metaconglomerate lenses up to more than 10 m thick occur in the lower member south of No. 1 iron deposit (Fig. 30a). Other than a faint suggestion of bedding in a few places the conglomerate is massive and structureless. However, a secondary foliation, mineral lineation, and clast elongation has been superimposed. The conglomerate chiefly has an open framework, and is oligomictic.

Most of the clasts are from felsic volcanics, or shallow intrusive equivalents, and range in composition from rhyolite to quartz latite and dacite. Some quartzite, arkose, and pelite clasts are also present. It is not certain whether or not the rocks in the clasts were metamorphosed prior to deposition of the conglomerate. The clasts range in size up to 76 cm in diameter, and from angular to well rounded. Most are 5-30 cm in diameter. They are most commonly subrounded and range from equidimensional to about twice as long as they are wide due to tectonic elongation. The open framework nature of the conglomerate may have protected the clasts from severe deformation. The felsic metavolcanic clasts resemble the felsic metavolcanics in map units Agn and Amn more closely than those that form sequences within the Mary River Group. These clasts range in colour from off-white to light grey and in some cases buff, from very fine- to fine-grained, and are commonly friable and blastoporphyritic, with quartz and more rarely feldspar metaphenocrysts up to 1.3 cm in diameter, but commonly 0.6 cm or less, and scattered sparsely through a quartz-plagioclase matrix. Euhedral plagioclase crystals were seen in two or three thin sections. A porphyroclastic structure may be present locally. In addition to quartz and oligoclase-andesine (An_{21-34}), the major minerals include biotite, muscovite, and, locally, blue-green and colourless hornblende, orthoclase, and perthitic microcline. Minor minerals are chiefly chlorite, kaolinite, and epidote. Accessory minerals include apatite, zircon, magnetite, hematite, pyrite, limonite-goethite, and leucoxene. Some of the metavolcanic clasts contain irregular, thin, wispy, very fine grained, relatively dark, biotite-rich lenses with well defined boundaries that are probably recrystallized shards or lithic fragments. Metapelite clasts contain abundant quartz, biotite, muscovite, and variable amounts of cordierite, sillimanite, and/or andalusite.

The conglomerate matrix is light to medium grey, locally dark grey, weathering grey or locally buff. It is fine- to medium-grained and is commonly finely conglomeratic. Irregular, wispy, dark, relatively biotite-rich lenses up to several centimetres long, similar to those in the coarse clasts, also occur in the matrix. The matrix contains the same minerals as are found in the clasts, including quartz megacrysts or clasts, and ranges in composition from biotite-rich metapelite to a composition almost identical to the "felsic metavolcanic" clasts. Commonly, however, the matrix is darker, and contains more biotite and other mafic minerals and/or quartz, and less plagioclase than do the clasts.

The lower member is present locally in the Mary River No. 4 iron deposit area as well. At one place, 60 cm of conglomerate-breccia occur near the base of 5 m of biotite amphibolite and hornblende gneiss. Quartz-feldspar clasts up to 10 cm across are tectonically rodded and lensed, and occur in a biotite amphibolite matrix (*see* Fig. 30b).

A conglomerate that is somewhat similar lithologically to that described above occurs in the Eqe Bay area (Crawford, 1973) but is believed to occur at a stratigraphically higher position (Table 7). It is 46 m thick, apparently overlies rhyodacite-dacite porphyry and pillowed "intermediate" metavolcanics unconformably, and is overlain by a thick sequence of argillite, siltstone, and greywacke. The clasts are well rounded and lithologies represented by them include white and pink quartz, grey granitic rock, and pink weathering granite (Crawford, 1973).

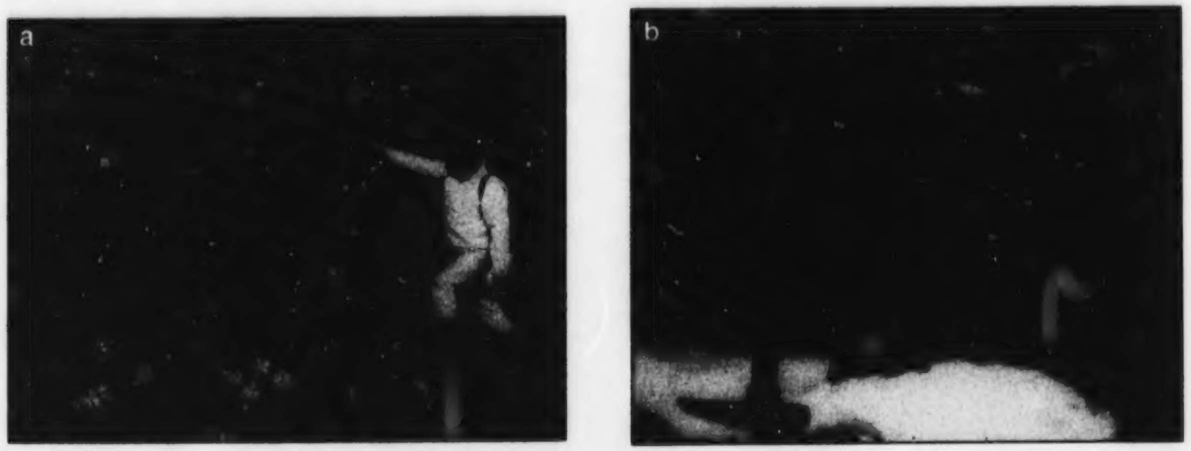

Figure 30. *Metaconglomerates in the lower member of the basal metapelite-amphibolite unit of the Mary River Group.* ***a)*** *Boulder metaconglomerate in the No. 1 iron deposit area. Photograph by G.D. Jackson. GSC 186879.* ***b)*** *Pebble conglomerate-breccia in the No. 4 iron deposit area. Photograph by G.D. Jackson. GSC 1997-54C*

Felsic metapyroclastics. Lenses of foliated, metamorphosed felsic pyroclastic rock, up to 10 m thick, also occur in the lower member south of No. 1 iron deposit. The fragments are similar in composition to the volcanic clasts in the conglomerate described above, but are friable. They are also more angular, include some pillow- and bomb-like clasts, range up to 1.2 m in length, and, except on the margins of the lenses, are more closely packed (Fig. 31a, b). Clasts are stretched, and some are fractured with component fragments having moved relative to one another. Structures and textures of some of these rocks, both megascopically and in thin section, resemble those of welded felsic pyroclastic rocks. The matrix is similar to that in the conglomerate but weathers brown and contains quartz eyes up to 1 cm in diameter, some of which may be pebbles.

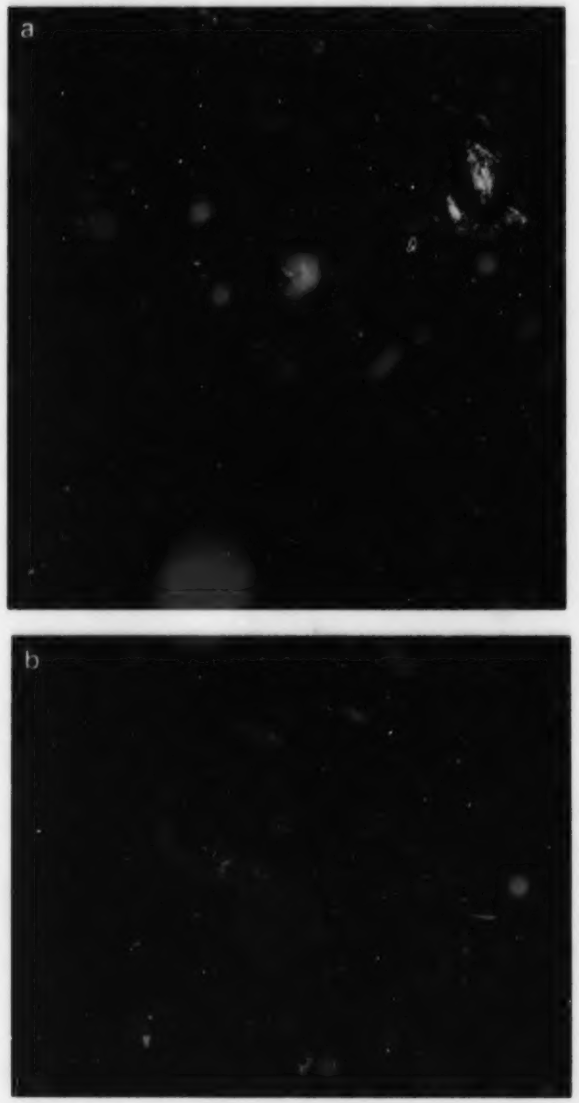

Figure 31. ***a)*** *Margin of a rhyodacite metapyroclastic (lahar?) lens in the lower member of the basal metapelite-amphibolite unit of Mary River Group, south of No. 1 iron deposit. The matrix is more mafic (biotite-rich) in the margin than in the middle of the lens. Photograph by G.D. Jackson. GSC 1997-54D.* ***b)*** *Volcanic breccia-conglomerate in the basal metapelite-amphibolite unit of Mary River Group, south of No. 1 iron deposit. Most large clasts are rhyodacite. Photograph by G.D. Jackson. GSC 186877*

Upper member (0 to >122 m)

The upper member is composed almost entirely of metapelite. Minor amphibolite, metasandstone, and a few thin lenses of pebble and cobble metaconglomerate are also present. Most of the conglomerate clasts were probably derived from felsic and mafic volcanic rocks. The upper and lower members are gradational, aluminosilicate minerals being more abundant in the upper member metapelites.

Metapelites at the various stratigraphic positions in the Mary River Group are similar to one another, and the stratigraphic position of pelites in isolated outcrops cannot be recognized. The description and mineral assemblages presented below apply generally to all the metapelites, except as noted.

General description. The metapelites are chiefly mica-rich paraschists (Fig. 32), paragneisses, and derived migmatites (lit-par-lit, etc.). Argillites, phyllites, metasiltstones, and metasandstones can be identified in low grade terrane as in the Mary River and Eqe Bay regions. The metapelites are overall commonly massive or indistinctly banded, but finely foliated and crinkled, with locally well developed mineral lineation, on a small scale. Primary structures are rarely

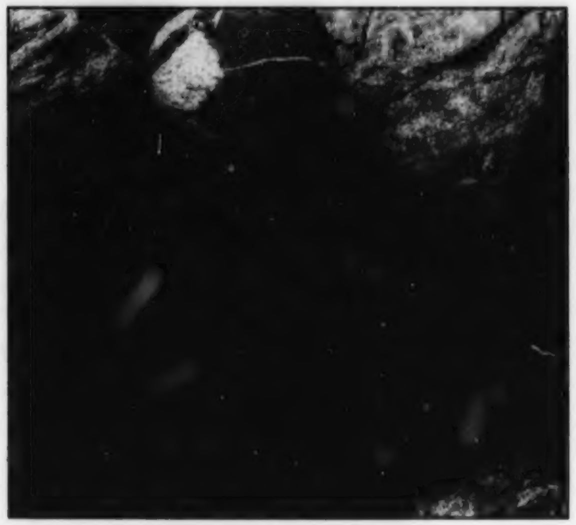

Figure 32. *Coarse cordierite in a biotite-rich matrix, metapelite of the upper member of the metapelite-amphibolite unit of the Mary River Group, south of No. 1 iron deposit (Nuluijaq Mountain). Photograph by W.J. Crawford. GSC 1997-54E*

preserved, but some laminations are graded, a feature that is probably related to primary graded bedding. Colours range from light grey to dark grey, black, and greenish black. Most are medium grained, but some are fine- or coarse-grained. Aluminosilicate minerals are common in matrices and as porphyroblasts (Fig. 32).

Metamorphic mineral assemblages. Statistical data for modal analyses of Mary River Group metapelites are included under Ms, AMs in Table 6. Selected representative modal analyses are also shown graphically under Ms in Figure 29. Most of the points shown on the triangles in Figure 20Kc are for metapelites. The Q-AD+-ST+ triangle in Figure 20Kc shows that minerals like amphibole, pyroxene, garnet, mica, and staurolite are more abundant than aluminosilicate minerals, cordierite, and chlorite. Prograde mineral assemblages for major localities (Fig. 1, *see* Fig. 99) are presented in Table 8, and include some interesting assemblages (e.g. no. 17, 20, 53). The metamorphic significance of the assemblages will be discussed in the section on "Metamorphism".

The most common major minerals are quartz, biotite, and muscovite. The muscovite occurs as both a prograde and a retrograde mineral, and in some cases it is difficult to determine which it is. Other common major minerals are: cordierite (Fig. 32), andalusite, sillimanite, plagioclase, garnet, and anthophyllite. Andalusite and cordierite occur locally in knots up to several centimeures in diameter. Plagioclase is chiefly oligoclase (An_{17})-andesine, but includes albite and labradorite (An_{52}). Hypersthene-bearing metapelites are not differentiated from other metasediments in granulite terrane. Minor minerals are: microcline, orthoclase, hornblende, staurolite, kyanite, cummingtonite-grunerite, and locally magnetite-ilmenite. Accessory minerals are: apatite, zircon, sphene, rutile, tourmaline, pistacite, clinozoisite, zoisite, allanite, calcite, graphite, magnetite-ilmenite, hematite, pyrite, and pyrrhotite. Microcline and orthoclase are least abundant in the Mary River region where anthophyllite is most abundant. Kyanite is generally rare, but is relatively common in the No. 1 iron deposit area of the Mary River region. Staurolite is uncommon except for scattered occurrences in the western part of the map area.

Chlorite, which ranges from a major constituent to an accessory mineral, is in most cases a retrograde alteration product. Other common alteration products are: serpentine, chiefly after cordierite, and kaolinite, chiefly after feldspars. Accessory retrograde alteration products include limonite-goethite-hematite, leucoxene, and prehnite.

Contact relations

At No. 1-3A iron deposits area (NTS 37G), there is considerable indirect evidence for the presence of a nonconformity between the Mary River Group and the adjacent granitic gneiss complex, but the basal contact, including that of the metapelite-amphibolite unit, is not exposed, poorly exposed, or faulted. West and south of No. 1 iron deposit the complicated gneiss-felsic metavolcanic-granite complex adjacent to the Mary River Group is intruded by several mafic dykes and by foliated granitic intrusions that do not intrude the Mary River Group (e.g. *see* Fig. 107; Fig. 4 of Jackson, 1966b). Younger massive granitic intrusions locally intrude the complex and the metapelite-amphibolite unit (Fig. 33). The presence of lenses of boulder conglomerate containing a large proportion of felsic volcanic clasts, and felsic pyroclastics as described above, and the compositions of the other clasts in conglomerate at or near the base of the metapelite-amphibolite unit at this locality support the inference that an unconformity is present.

Tectonism and intrusion have complicated the contact relations. Intricate interfolding and downfaulting of some Mary River Group rocks into the basement complex west of the Mary River No. 1 iron deposit area, for example (Fig. 18a; *see* Fig. 107; Fig. 4 of Jackson, 1966b), has resulted in a tectonic mélange, or megabreccia locally, that contains large rounded to angular blocks, up to about 275 m in length, of monzogranite-rhyolite, quartzite, feldspar-mica-quartz paragneiss, metapelite, and gneiss (*see* "Foliated monzogranite and granodiorite, nebulitic migmatitie (Agn)"). The matrix is chiefly amphibolite, but includes some metapelite and metaultramafite. The blocks, mineral lineations, and small fold axes invariably plunge northeast about 55° (Fig. 18). As noted in the section on "Structural geology", thrusts may be present in the No. 1-3A north and No. 4 iron deposit areas (*see* Fig. 36, 106, 107).

Truncation of amphibolite intrusions at the basal contact north of No. 4 iron deposit in the Mary River region (*see* Fig. 106), and presence of rounded cobbles and boulders of plutonic rocks in Mary River Group conglomerates at the No. 4 iron deposit area and at Eqe Bay support the conclusion that a basal unconformity is present at these localities as well.

A U-Pb zircon age of 2718 Ma for Mary River Group dacite and 2851 Ma for basement foliated trondhjemite-tonalite (Jackson et al., 1990b) also support the presence of an unconformity. Although similar Nd model ages of 2.87-2.85 Ga were obtained for these same samples, and for Mary River Group mafic volcanics, other gneisses mapped as mostly older than the Mary River Group in the map area have yielded Nd model ages of 3.67 to 2.83 Ga (Hegner and Jackson, 1990; Jackson et al., 1990a).

The metapelites of the metapelite-amphibolite unit at Mary River No. 1-3A iron deposits are gradational with the overlying metamorphosed siltstones and sandstones of the quartz-rich unit. The amphibolite and metaultramafic layers are locally discordant and are considered to be chiefly sill-like intrusions, but may also include extrusions.

Chemistry of pelitic rocks

Most of the spectrographic analyses listed under Ms in Appendices 2-4 are for samples of Mary River Group metapelites; some are metasiltstone-metagreywacke and two or three are arkosic. Means of the spectrographic analyses are given in column G of Table 47 and column 26 of Table 48. Of the 46 samples analyzed, 16 contain 7.4 or more per cent Al, and most of these contain aluminosilicates. An average of these 16 samples is compared with that for the remaining 30 in Table 10. The averages for some elements are distinctive

Table 8. Some common prograde mineral assemblages in Mary River Group metapelites.

Assemblage	1	2	3	4	5	6	7	8	9	10	11	12	13	14	15	16	17	18	19	20	21	22	23	24	25	26	27	28
Quartz	+	±	+	+	+	±	+	+	+	+	+	+	+	+	+	+	+	+	+		+	+	+	+	+		+	+
Plagioclase						±			±			±					±				+	+	+	+				+
K-feldspar																							+	+				
Biotite			+	+	+	+		+	+	+	+	+	+	+	+	+	+	+		+	+	+	+	+	+	+	+	+
Muscovite	+				+			+	+	+	+	+										+	±					+
Anthophyllite	+	+				+																					+	
Grunerite	+																											
Hornblende																												
Garnet			+	+									+	+	±										+	+	+	
Andalusite								+			+	+	+	+			+	+	+							+		
Sillimanite								+				+		+	±	+	l									+		+
Kyanite	+										+						e?			+	+							
Staurolite			+										+				±e?											
Cordierite	+	+	±	+		+		±	+	+	+	+	+	+		+	+	±	+	+		±	±	+		+		
Spinel																												
Beryl																												
Calcite																												
Chlorite		±					+			±															+			
Talc							+																					
Magnetite		±	+	+		±	+								+			±	+							+		
Graphite									±	±																		
Locality (Fig. 99)	2	2	2, 9	2	2	1	1	1	1	1, 4	1	1	1	1, 3	1	1	1	1	1	1	1	1	1	1	1	3	3	3, 9
Assemblage	**29**	**30**	**31**	**32**	**33**	**34**	**35**	**36**	**37**	**38**	**39**	**40**	**41**	**42**	**43**	**44**	**45**	**46**	**47**	**48**	**49**	**50**	**51**	**52**	**53**	**54**	**55**	**56**
Quartz	+	+	+	+	+	+	+	+	+	+	+	+	+	+	+	+	+	+	+	+	+	+	+	+	+	+	+	
Plagioclase	?	+	+		+	+	+	±		+	+	+			+	+	+	+	+	+	+					±		
K-feldspar		+	+		+	+	+	+		+					+	±	±	±										
Biotite	+	+	+	+	+	+	+	+	+		+	+	±		+	+	+	+		+	+	+	+		+	+		
Muscovite	+	+					±				+		+	+				±		+				+			+	
Anthophyllite																												
Grunerite										+																		
Hornblende			+	+						+											+				+	+		
Garnet		±		+	+	+	+		+			+			+	+	+	+	+			±		+				+
Andalusite	+																										+	
Sillimanite	l	+			+		+	+	+		+	+	+	+	+	±		+	+			+		+	+			
Kyanite																												±
Staurolite														±					+			+	+	+	+			+
Cordierite	±	±				+		+			+		+	+	+				+			+	+	+	+			
Spinel									+																			
Beryl																											+	
Calcite																				+								
Chlorite																												
Talc																												
Magnetite									+	+	+		+	+				±			±					+		
Graphite																												
Locality	4	4	4	4	5	8	8	8	8	5	5	5	5	5	6b	6b	6a	6a	6a	6a	6a	6a	6a	6a	6a	6a	6a	6a

* - Includes data from Crawford (1973) and Morgan (1982)
1 - Mary River No. 1-3A deposit areas (37G)
2 - Mary River No. 4 deposit area (37G)
3 - Turner River - Glacier Lake (37G)
4 - Central, south-central Icebound Lake map area (37G)
5 - Upper Rowley River (NE 37F)
6a - Eqe Bay belt (NE 37C, NW 37D, SW 37E)*
6b - Isortoq Fiord belt (NE 37C, 37E, 37F)*
8 - West, north, and east of northern Barnes Ice Cap (37E), in Dexterity Granulite Belt
9 - Drever Arm (37H)
? - uncertain.
l - late
e - early
+ - Mineral is present.
± - Mineral is present in some assemblages, not in others. Two minerals represented by ± in an assemblage indicates there are four combinations represented, etc.

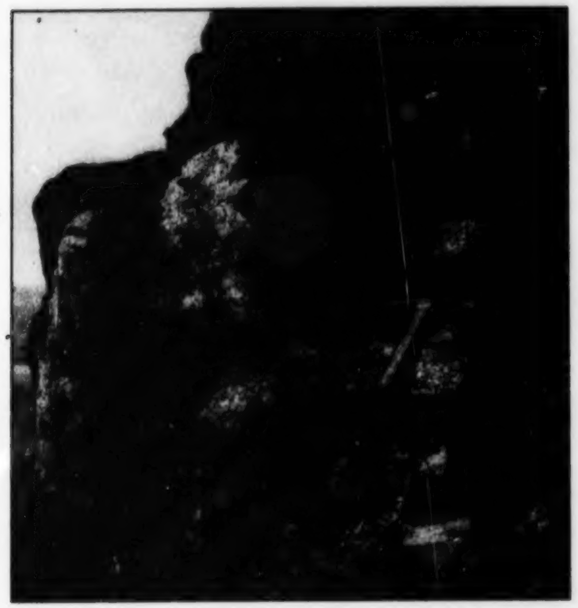

Figure 33.

Massive, jointed, white to pale pink granite intruding biotite schist and amphibolite south of No. 1 iron deposit at Mary River. A 3 cm reaction zone occurs at the contact, and thin quartzo-feldspathic segregations occur in the schist adjacent to the contact. The schist and segregations were deformed when vertical movement along some of the joints in the granite pushed the granite blocks up into the schist. Photograph by G.D. Jackson. GSC 118327

Table 9. Analyses (in weight per cent) of Archean and Proterozoic shales and metapelites.

	Archean pelitic rocks				Aphebian pelitic rocks				Neohelikian	?
	Archean Average 1	Archean Average 2	Mary River 3	Mary River 4	Aphebian Average 5	Aphebian Average 6	Piling 7	Piling 8	Arctic Bay 9	Mid-Late Proterozoic 10
SiO_2	58.0	64.2	65.2		62.6	58.4	50.7			57.7
TiO_2	0.73	0.48	0.34	0.63	0.73	0.79	1.25	0.50	0.28	0.88
Al_2O_3	16.9	15.8	12.1	12.7	15.6	16.6	14.8	11.8	8.2	17.0
$Fe_2O_3{}^a$	7.6	6.4	10.2	6.2	6.1	9.8	18.7	4.9	4.4	7.74
MnO	0.09	0.07	0.08	0.08	0.06	0.15	0.22	0.045	0.10	0.11
MgO	3.33	2.45	4.42	2.49	2.42	4.12	7.07	2.17	1.58	2.38
CaO	2.07	4.02	1.51	>1.1	0.50	2.34	3.90	>1.1	0.46	1.20
Na_2O	2.5	2.84	1.28	>0.8	1.40	1.57	1.83	>0.8	0.54	0.93
K_2O	2.73	2.32	1.69		4.65	3.08	0.69			4.18
P_2O_5	0.16	0.14	0.10		0.13	0.09	0.08			0.09
CO_2	1.1	0.04	0.00		0.10	0.59	0.01			1.10
C	0.7				1.6					
S	0.66		0.10		0.63		0.01			
SO_3		0.08				0.20			1.08	
H_2O	3.4	1.68	2.44		3.6	2.85	1.82		6.19	
Total	99.97	100.52	99.46		100.12	100.58	101.08			101.27
Samples	406	247	2	46	326	460	2	8	16	34(1226*)
V	0.0130		0.0090	0.001	0.0188		0.030	0.016	0.0046	
Co	0.0035		0.0010		0.0022		0.0047			
Cr	0.0133		0.014	0.0072	0.0105		0.035	0.035	0.0028	
Cu	0.0056		0.0046	0.0031	0.0075		0.042	0.0030	0.0025	
Ni	0.0052		0.0049	0.003	0.0057		0.018			
Sr	0.0199			0.019	0.0069			0.0094	0.0040	
Sc	0.0016				0.0016					
Zr			0.021	0.020			0.015	0.020	0.027	
Ba								0.052	0.015	
Rb	0.0091				0.0174					
Na/K	0.81	1.1	0.68		0.27	0.46	4.3		0.20	
Sr/Rb	2.2				0.40					

* = number of individual samples in composites; 1 - Southern Superior Province; after Cameron and Garrels (1980); 2,6,10 -Russian Platform; after Ronov and Migdisov (1971); 3 - Mary River Group, Eqe Bay, Baffin Island; after Crawford (1973); 4 - Mary River Group, this memoir, column G-Table 47, column 26-Table 48; 5 - Adjacent to southern and eastern edge of southern Superior Province, after Cameron and Garrels (1980); 7 - Piling Group, Generator Lake, Baffin Island, after Crawford (1973); 8 - Piling Group, this memoir, column H-Table 47, column 28-Table 48; 9 - Arctic Bay Formation, this memoir, column I-Table 47, column 32-Table 48; ^{a} - All Fe as Fe_2O_3 for comparison. About 90% of the Fe in columns 3 and 7 occurs as FeO.

Table 10. Average of spectrographic analyses (in weight per cent) for Mary River Group metapelites and metagreywackes from Appendix 2.

	a	b
Ti	0 .33	0 .41
Al	8.0	6.0
Fe	3.5	4.7
Mn	0 .047	0 .072
Mg	1.2	1.7
Ca	(+)	(+)
Na	(+)	(+)
Ba	0 .066	0 .052
Co	(-)	(-)
Cr	0 .0066	0 .0078
Cu	0.0020	0 .0037
La	(-)	(-)
Ni	0 .003	0 .003
Sr	0 .022	0 .017
V	0 .0087	0 .012
Zr	0 .019	0 .021
Pb	(-)	(-)
No. of samples	16	30

Notes: a: High-Al metapelites; b: Metapelites-metagreywackes (+), (-): the amount of element present is greater or less than, respectively, the limit of reliable determination.

(Al, Mn) but for most may not be significant when the analytical error and sampling technique are considered. These results, and an average of two complete metapelite analyses from the Eqe Bay area are compared with means for other Archean metapelites and with Proterozoic pelitic rocks in Table 9. Means for metapelites of the Mary River Group at Eqe Bay (column 3) and the Piling Group at Generator Lake (column 7) have high iron contents. Their alumina is high compared with most sedimentary iron-formations and is much higher than that for Aphebian shaly iron-formations analyzed by Cameron and Garrels (1980). They could be called ferruginous metapelites, or aluminous facies iron-formation if the iron content exceeds 15%.

Averages of spectrographic analyses for 11 common elements are plotted with standard deviations in Figure 95 (*see* below). These plots show that the Mary River Group metapelites and metagreywackes (M,Ms) contain more Fe, Ti, Mn, Sr, Ba, and Al than similar rocks in the Piling and Eqalulik groups. Eqalulik Group contains the most Zr.

Analyses for the four Baffin Island samples (Table 9: two from the Mary River Group, two from the Piling Group) are listed individually and more fully in Appendices 5 to 7 along with analyses and structural formulae for contained biotite, chlorite, garnet, staurolite, and anthophyllite. The average of the two Mary River Group samples resembles that of the Piling Group average, except the Mary River has more SiO_2 and K_2O and the Piling has more CaO, TiO_2, iron oxides, and MgO.

Pettijohn (1975) concluded that most elements in pelitic rocks show no significant differences related to age, and this seems to be so in the map area (Table 9). He did note, however, that older rocks (Archean-(?)Aphebian) show ferrous oxide to exceed ferric oxide, while the reverse is generally true in younger rocks (? Helikian and younger). This seems to be the case on the Russian Platform (Ronov and Migdisov, 1971) and for some metapelites and for aluminous facies iron-formation of the Mary River (Ms, Mif, AMif) and Piling (APs, APif) groups (Tables 9, *see* Table 14; Appendices 5, 6). Pettijohn (1975) considered this difference to reflect the greater proportion of metamorphosed older rocks. However, the sampled Mary River and Piling rocks are both metamorphosed to similar metamorphic grade. Therefore the difference in the proportion of iron oxides is probably related to something other than the degree of metamorphism. Differences in oxygen content of the atmosphere are commonly suggested for differences in the degree of oxidation of Archean and Early Proterozoic sedimentary rocks. A slight decrease in total iron and in sodium with decreasing age was also noted by Pettijohn (1975). This, however, does not appear to be true for iron in and adjacent to the map area (Table 9; Appendices 5, 6). The sodium in the Mary River and Piling metapelites is about the same, the Piling sample in Table 9 being anomalously high in sodium. The sodium is a little lower in the Neohelikian Arctic Bay shales than in the older metapelites (Table 9; Appendix 6). The analyzed Archean Mary River metapelites have a sodium content and an Na/K ratio about half that quoted for some other Archean metapelites, and similar to quoted values for Aphebian metapelites elsewhere (Table 9).

Cameron and Garrels (1980) have discussed compositions of Archean and Aphebian shales. Values of CaO, CO_2, and Sr for Mary River metapelites are all low compared to Archean values reported by these authors and resemble the values they report for Aphebian pelites. It is also noteworthy that the Ca content of Aphebian shales on the Russian Platform (Ronov and Migdisov, 1971) is similar to that for Archean shales analyzed by Cameron and Garrels (1980). One problem with the Aphebian samples reported on by Cameron and Garrels (1980) seems to be that some depositional environments may be proportionally misrepresented. For example, most of their Labrador Geosyncline samples are shown to have been obtained from the shelf or miogeoclinal region (Menihek, Attikamagen formations) with the basinal or eugeoclinal region being underrepresented. Because the Aphebian contains a higher proportion of mature sediments than the Archean, overrepresentation of shelf sediments should exaggerate this difference. Presence of both noncalcareous and calcareous shales in the Neohelikian Bylot Supergroup for example, representing different depositional environments, demonstrates the need for great care in selection of samples, and large sample collections for such comparisons to be statistically meaningful. The author is in agreement with Pettijohn (1975), who cautioned that differences attributed to most secular changes are small, and might be more properly attributed to sampling, nonisochemical diagenesis and metamorphism, differences in depositional environments (basin versus platform, marine versus continental) and source rocks, and to related tectonic settings. However, some elements, such as Fe, Na, and atmospheric oxygen do seem to show a change with time.

Origin

General lack of obvious primary structures in the metapelites and associated amphibolites, felsic pyroclastics, conglomerates, and immature sandstones, together with a variable gross stratigraphy and discontinuous lensoid nature of the unit that is gradational with more widespread stratigraphically overlying units, suggest that the metapelite-amphibolite unit was deposited rapidly and discontinuously in response to catastrophic events. However, primary structures may well have been present and obliterated by the intense deformation and by metamorphism. The metapelites have been deposited in a variety of environments, probably chiefly in interconnected marine basins. Those in the metapelite-amphibolite unit were probably deposited in lakes and nearshore marine depressions formed when drainage was interrupted by mafic and felsic volcanism similar to the recent Mount St. Helen's eruption. The high iron and alumina content of some of the pelites suggest they may be a mixture of clastic and chemical exhalative deposits. The welded appearance of some of the volcaniclastics, the shapes of volcanic clasts, and similar compositions of matrices and clasts indicate that the felsic volcanics in this unit are chiefly lahar and ash flow deposits in which quartz fragments were rounded during emplacement. One of the largest conglomerate lenses at No. 1 iron deposit area resembles some avalanche deposits (S.L. Blusson, pers. comm., 1968).

Metamorphosed felsic volcanic rocks may be more common than mafic volcanic rocks in gneisses considered to be older than the Mary River Group. Two possibilities concerning the timing of Mary River Group felsic volcanism seem most likely. One is that it, and the rest of the volcanics in the Mary River Group, represent part of a regional volcanic episode that includes the volcanism recorded in the rocks underlying the Mary River Group. In this case the unconformity at the base of the Mary River Group would probably be one of a series of local unconformities each representing a short time span.

The second possibility is that the felsic volcanics in the metapelite-amphibolite unit represent the initiation of renewed volcanism and plutonism in the region after a lengthy period of dormancy. This is the conclusion preferred here for the following reasons:

1. The mature nature of some of the metasediments at and near the base of the Mary River Group as discussed below is compatible with a considerable period of erosion prior to deposition of the group.
2. The structures in the rocks underlying the Mary River Group are more complex than those of the group, and contain mafic and felsic dykes that do not seem to intrude the group.
3. The felsic clasts in the conglomerate and pyroclastic lenses resemble the underlying more leucocratic felsic volcanics rather than Mary River Group felsic volcanics while the matrices are more mafic and locally at least more closely resemble the Mary River felsic volcanics.

Quartz-rich unit (Mq: 0 to >590 m)

Description

The quartz-rich unit includes the lowermost Mary River Group strata recognized throughout most of the Mary River region (*see* Fig. 106, 107), locally in a few other areas in the Icebound Lake map sheet (NTS 37G), west of Coutts Inlet (NTS 37H), along the upper Rowley River (NTS 37F), north and northwest of the Barnes Ice Cap (NTS 37E), and in some parts of the Eqe Bay region (Crawford, 1973; Morgan, 1982). It is relatively rare north of the map area (Jackson et al., 1975). The unit is lensoid, and has a maximum estimated thickness of about 590 m in the Mary River region. Generally this unit can be separated into two lensoid members, a lower feldspar-mica-quartz schist member, and an upper quartzite member (Table of Formations). These members are commonly intergradational but in some places, as in the No. 4 iron deposit area, they seem to be separated by a local(?) unconformity (*see* "Contact relations"). Where the schist is absent the quartzite is unconformable on the gneisses. The quartzite is generally conformable and gradational with overlying iron-formation. Similar lithologies also occur above the iron-formation in several places, but not as persistently. In several other areas the stratigraphic position of similar lithologies cannot be determined.

Lower member (0 to >460 m)

This member ranges from 0 to more than 460 m thick in the Mary River region and locally may be much thicker. The apparently gradational nature of the lower contact together with complex deformation and metamorphism make it difficult to estimate the thickness of this member. Most of the member is composed of feldspar-mica-quartz schist. This is the rock type most commonly present at the base of the Mary River Group in the iron deposit areas (Gross, 1966; Jackson, 1966b, 1978b), and is present in most occurrences of the quartz-rich unit. The feldspar-mica-quartz schist generally grades downward into granitic rocks, chiefly medium- to coarse-grained potassium feldspar porphyroblastic gneisses. A rodded rock that could be either a metaconglomerate or a flaser gneiss predominates locally. Minor lithologies include metapelite, metagreywacke, metasiltstone, metaconglomerate, conglomeratic schist, felsic metavolcanics, and local quartzite. Contacts between lithologies are gradational. Intrusive amphibolite and metaultramafic rocks occur locally.

The rocks of the lower member are mostly light to dark grey, pinkish grey, and locally greenish black to black. They are chiefly medium grained, but inequigranular and range from fine- to coarse-grained. They are also schistose, commonly along two planes. A well developed lineation of individual mineral grains and/or mineral aggregate rodding is also common in the Mary River area and a few other areas. The schistosity consists of thin mica folia alternating with quartz and quartz-feldspar lenses and bands commonly less than 1.3 cm thick.

Rodded varieties of feldspar-mica-quartz schist predominate in the lower member in the vicinity of No. 1-3A iron deposits at Mary River (*see* Fig. 107), are abundant in the No. 4 iron deposit area and are present at several other localities. R. Von Guttenberg (Strathcona Mineral Services Ltd., pers. comm., 1993) considers these to be mostly deformed felsic metavolcanic rocks, possibly metapyroclastic rocks. In these rocks quartz and quartz-plagioclase lenses and rods up to 2 cm in diameter and several centimetres long (elongation up to more than 6:1) occur in a mica-rich matrix. Individual rods are a mosaic-aggregate of grains when viewed through the microscope. Some rods have sparse fine mica laminations which are either parallel to the rock foliation or have been rotated several degrees. Some of the schist has small quartz granules or quartz eyes that are also mosaic aggregates, but which have swirly dust trails indicating rotation.

Lenses of metaparaconglomerate and conglomeratic schist are common at various stratigraphic horizons in the feldspar-mica-quartz schist. The clasts range from granule size to several centimetres in diameter, are subangular to well rounded, and are commonly rodded or "stretched". The clasts are generally sparsely scattered through the schist and composed of fine- to coarse-grained quartz aggregates, quartz-plagioclase, and granitic material. At some localities the plagioclase is poorly twinned poikiloblastic albite, which contains abundant tiny rounded quartz inclusions, and which is partially altered to kaolinite, biotite, and muscovite. Larger clasts are rarely composed entirely of quartz. Those that are entirely quartz are rarely, if ever, larger than quartz aggregates in the subjacent relatively coarse grained granitic gneisses. The matrix in the conglomeratic lenses is typical feldspar-mica-quartz schist except that it commonly has a more "gritty" weathered surface.

Modal analyses for this member are included with those for metapelites and some metagreywackes under Ms in Figure 20Kc (QAP, QFM), Figure 29, and Table 6. Chemical data are likewise presented in Appendices 2-4, Figure 95, and Tables 47 (column G) and 48 (column 26).

Any one of quartz, micas, or feldspars may form up to about 70% of the rock, although quartz is commonly the most abundant. Biotite is generally more abundant than muscovite, and microcline and plagioclase are about equally abundant overall. Most of the plagioclase (An_{17-52}) is oligoclase-andesine; it is labradorite in a few places and is albite locally at No. 4 and No. 1 iron deposit areas. Garnet, chlorite, cordierite, sillimanite, andalusite, hornblende, actinolite, hypersthene, and spinel occur as minor constituents locally, and rarely as major constituents. One of the major differences between this and the underlying metapelite-amphibolite unit is the abundance of feldspars and general lack of cordierite and aluminosilicate minerals in this unit. Accessory minerals include: apatite, calcite, chlorite, zircon, sphene, epidote (mostly pistacite), allanite, ilmenite, leucoxene, magnetite, pyrite, limonite-goethite, serpentine, kaolinite, orthoclase, and possibly prehnite and rutile. Metapelite assemblages include cordierite- and/or aluminosilicate-bearing assemblages similar to those noted in the metapelite-amphibolite unit (Table 8). The most common assemblages are:

quartz+microcline+plagioclase (oligoclase-andesine)±biotite±muscovite and

quartz+biotite+muscovite±garnet.

Albite- or orthoclase-bearing assemblages, which are of minor local extent, include:

quartz+microcline+albite+muscovite and

quartz+microcline+orthoclase?+biotite+muscovite.

Locally preserved thin conglomerate lenses, laminations in relatively low grade metasiltstone-metapsammite-metagreywacke, and quartz and feldspar phenocrysts in felsic volcanic lenses are generally the only primary rock features observed. Low angle trough crossbeds and channels occur in granite-pebble conglomerate blocks adjacent to outcrop (Fig. 34b) southeast of the No. 4 iron deposit in the Mary River area.

Upper member (0-130 m)

The upper member is mostly quartzite, and has a maximum thickness of about 130 m in the Mary River region and elsewhere in the map area. An estimated thickness of 230 m in the No. 4 iron deposit area (NTS 37G) is for deformed quartzite that has been repeated by folding. Generally the member is not more than 80 m thick in the map area and in the Eqe Bay region (Crawford, 1973). The upper quartzite member is continuously developed in some areas, but is commonly more lensoid and discontinuous than the overlying iron-formation. Some of the lenses were probably deposited as discontinuous quartz arenite and/or chert. Others probably represent the boudining or dismemberment of a once continuous unit by folding and faulting. The presence of quartzite clasts in conglomerate lenses within the Mary River Group suggests that some lenses might be erosion remnants of a once more continuous unit. Modal analyses for this member are shown under Mq in Figure 20Kb, Figure 29, and Table 5. Chemical data are presented in Appendices 2-4, Figure 95, and Tables 47 (column K) and 48 (column 25).

Most of the quartzite in the Mary River Group belongs to this member, but quartzite occurs locally at other stratigraphic positions as well. It occurs in the lower part of the underlying feldspar-mica-quartz schist member, in the basal metapelite-amphibolite unit, and in the metasediments above the iron-formation. In other localities, as for example east of Icebound Lake (NTS 37G), the stratigraphic position of quartzite within the Mary River Group is unknown. Quartzite lenses also occur in the migmatites, granitoid gneisses, and in younger massive granite, chiefly adjacent to or associated with Mary River Group relics. These are also tentatively considered to be Mary River Group strata.

Most of the member consists of glassy quartzite with more than 90% quartz, that is white to pale grey on the fresh and weathered surfaces. Some is medium grey, pale pink, rusty brown, buff, and green. Rusty weathering is related generally to contained pyrite and/or carbonate. The quartzite is predominantly medium- to coarse-grained but ranges from very fine- to very coarse-grained and massive. Layering is absent to indistinct in most of the member, and commonly occurs only locally near the lower and upper contacts. Where present it ranges from very thin bedded to very thick bedded (*see* Table 2), from faintly to prominently laminated, and locally is sheared and rodded. Other than the conglomerate lenses, no primary structures such as crossbedding, which would indicate clastic deposition, have been identified. Some of the quartzite is very fine grained and thinly laminated and may be metachert. The fact that some of the quartzite grades upward into oxide facies iron-formation which is probably, in part at least, a chemical precipitate, also suggests that some metachert is present. Crawford (1973) noted that the quartzite near the base of his Eqe Bay section "...shows a distinct ribbon-like layering typical of chert associated with volcanic assemblages".

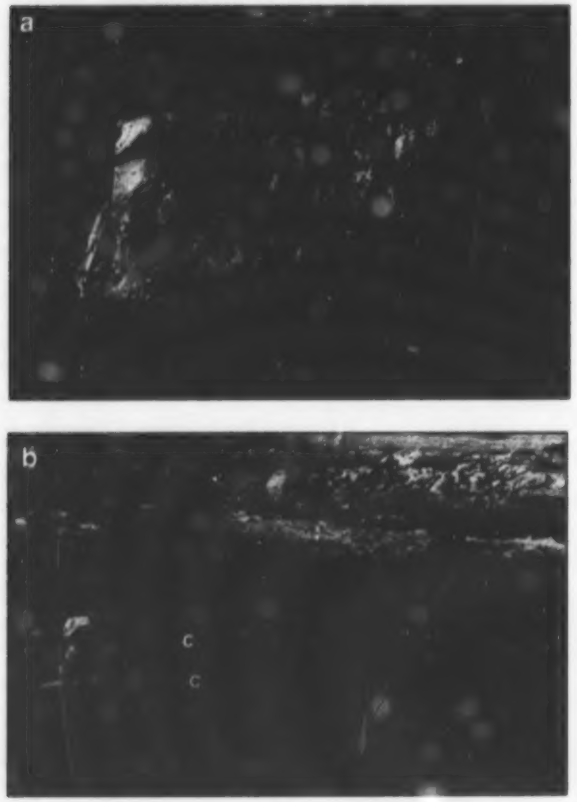

Figure 34. *Granite-pebble conglomerate in feldspar-mica-quartz schist, in the upper part of the lower member of the quartz-rich unit in the lowermost part of the Mary River Group, southeast of No. 4 iron deposit, Mary River area.* ***a)*** *Block 65 cm long of paraconglomerate containing "stretched" pink granite clasts up to 20 cm long. Photograph by W.J. Crawford. GSC 1997-54F.* ***b)*** *Block 2.5 m long of granite clast conglomerate. Clasts are up to 7 cm long and are less deformed than in a). Note the low angle trough crossbeds on the right and two channels (c) on the left. Photograph by W.J. Crawford. GSC 1997-54G*

Much of the member has the composition of subarkose and, locally, arkose. Lenses of micaceous schist occur chiefly in the lower part of the member where it grades into the underlying feldspar-mica quartz schist member. Thin conglomeratic lenses containing quartz granules and pebbles are rare. The uppermost quartzite is gradational with the iron-formation and some thin beds contain disseminated iron oxide. In the No. 4 iron deposit area at Mary River for example, the quartzite contains thin magnetite-hematite bands and grades upward into iron oxide facies iron-formation. Also, at other localities in the same area, hematite veinlets, up to 1.3 cm across, occur in the quartzite, and brecciated quartzite is locally enriched in limonite, goethite, and hematite. Milky vein quartz occurs with the quartzite locally and is as much as 15 m thick south of No. 3A iron deposit where it contains inclusions and lenses of amphibolite and ultramafite.

Metapelite, up to a few metres thick, occurs between the quartz-rich unit and the overlying iron-formation and iron ore west of No. 1 iron deposit at Mary River (NTS 37G).

Quartz is the dominant mineral in the upper member but potassium feldspar, plagioclase, biotite, and muscovite form much of the rock locally. Minor constituents locally are magnetite, garnet, hornblende, hypersthene, staurolite, cordierite, chlorite, fuchsite, and kaolinite. Accessory minerals include: allanite, apatite, zircon, sphene, hematite, limonite, pyrite, calcite, clinozoisite, anthophyllite, cummingtonite, sillimanite, and spinel. Quartzite west of Coutts Inlet contains a little disseminated hematite and is associated with a rusty to vivid orange-red gossan-like zone that may also extend to the east side of the inlet. The water at the downstream edge of the valley glacier flowing past this quartzite is stained blood-red with hematite, so that iron-formation (and possibly high grade iron oxide) probably occurs adjacent to this quartzite.

A few rounded zircon grains seen in thin sections are probably detrital, and indicate that some of these rocks are clastic. The quartz itself is completely recrystallized. The more pure the quartzite, the larger the grain size, the more strained the quartz, and the more irregularly sutured are the grain boundaries, some of which are also granulated. In one thin section, rounded grains of mosaic, sutured quartz grains up to 1 cm in diameter, in a muscovite-biotite matrix, are also invaded by the matrix. The grains have been formed in the rock by synmetamorphic deformation.

Contact relations

The quartz-rich unit is the most common basal unit of the Mary River Group. The basal contact is rarely well exposed but the greater deformation displayed in the adjacent granitic gneisses suggests that the quartz-rich unit overlies the gneisses unconformably. At several localities, however, such as at No. 2-3A and No. 4 iron deposits in the Mary River region where the lower schist is present, this basal contact is conformable and gradational, a feature that is probably due to the presence of either a metamorphosed regolith or a shear zone. Locally conglomeratic, lensoid, feldspar-mica-quartz schist (the lower member of the quartz-rich unit) grades northward, away from the Mary River Group north of No. 4 iron deposit, into a foliated to platy monzogranite to granodiorite rock of uncertain origin (*see* Fig. 106; Fig. 3 of Jackson, 1966b; Fig. 11 of Jackson, 1978b). Northward across this transition zone, the biotite content decreases and muscovite increases. Farther northward, muscovite and schistosity decrease and the potassium feldspar content increases, hornblende replaces some of the biotite, and the rock grades into a pink to grey granitoid that contains megacrysts, probably porphyroblasts, of potassium feldspar. The mafic content decreases northward in this granitoid and the microcline is commonly fresh while the plagioclase is partly altered.

The granitoid rocks and the feldspar-mica-quartz schist are intruded north of No. 4 iron deposit by northwesterly trending amphibolite dykes (map unit b) and larger intrusions up to 2 km long (*see* Fig. 106; Fig. 11 of Jackson, 1978b). These intrusions are homogeneous, fine grained, composed of about equal amounts of plagioclase and hornblende, and not known to contain relict primary textures like some of the Mary River Group mafic intrusions. They generally transect the foliations and lineations of the enclosing rocks at a low angle. The intrusions were traced upward to the base of the upper quartzite member, but were not found intruding the quartzite or the iron-formation. The gneisses north of No. 4 iron deposit display a variety of foliation trends, while various types of lineations plunge chiefly southeast. Southward, toward the north side of the Mary River Group, the foliations, lineations, and the amphibolite intrusions swing eastward to become subparallel to the north margin of the group. Here a shear zone containing a steep, complex fault zone occurs along the north side of the upper quartzite member of the quartz-rich unit (Jackson, 1966b, 1978b). The main fault seems to be a strike fault along which there has been strike-slip movement.

Chemistry

Some of the spectrographic analyses listed under M and Ms in Appendices 2-4 are for samples of Mary River Group feldspar-mica-quartz schist. Their analyses are similar to those for metapelite and metagreywacke, and are averaged together in column 26 of Table 48, which is closely similar to averages for metasediments in banded migmatite (Amg^{m}-column 27), felsic metavolcanics in nebulitic granitoid migmatite (Amn^{h}-column 21) and for Mary River Group felsic metavolcanics (Ma-column 22). The amounts of Fe, Mg, Mn, and Ni for the average (column 26) are intermediate in value between averages for granitic rocks (groups I, II, and III in Table 48) and averages for mafic rocks (group IV, column 17). The averages for Piling Group metapelites and metagreywackes (APs - column 28) and the Neohelikian Arctic Bay pelites (NAB - column 32) are quite distinct from those for M, M^{l}, and M^{s} (column 26), and for Amg^{m} (column 27). Column 25 (Mq) of Table 48 is an average for some quartz-rich rocks in the Mary River Group but few of the samples were from good metaorthoquartzite.

Origin

The presence of minor interbedded metapelite, thinly scattered metaconglomerate and quartzite lenses, local low grade metasiltstone and metasandstone, and rare crossbedding and channelling are taken to indicate that most of the lower feldspar-mica-quartz member is a conglomeratic metasediment. The quartz-rich rodded varieties of feldspar-mica-quartz schist in the Mary River area are highly tectonized and are most likely either metaconglomerate or highly deformed shale interlaminated to very thinly interbedded (Table 2) with chert or quartz arenite. Because of their association with metaconglomerate they are also tentatively considered to be metaconglomerate. They are commonly most abundant where the upper quartzite member is thin or missing and may in part be younger than the quartzite member.

The abundance and varied proportion of feldspars and mafic minerals (chiefly micas), as shown on a Q-A-P plot for chiefly metapelites and feldspar-mica-quartz schists (Fig. 20Kc), indicate that their compositions are mainly equivalent to arkosic and lithic arenite. Their igneous equivalent compositions range from quartz-rich granitoids and monzogranite to tonalite. The modal compositions of the strata, and the presence of minor felsic volcanic lenses, and granite clasts in the conglomerates indicate that sources were chiefly felsic plutonic and volcanic rocks. Available chemical data suggest that some of these rocks may be a mixture of felsic and minor mafic detritus. Its lensoid nature, apparently poor sorting, and common lack of bedding is indicative of relatively rapid deposition of the lower member, possibly in part in an alluvial fan or related to felsic volcanism.

Locally, as described under "Contact relations", the lower, feldspar-mica-quartz schist unit is conformable and gradational with adjacent granitic gneisses, both having been intruded by amphibolite that does not extend into the overlying Mary River Group. The relationships suggest the following possibilities:

1. The intrusive amphibolites north of the Mary River Group are older than the group, as in the No. 1 iron deposit area:
   a) A major unconformity exists between the lower feldspar-mica-quartz schist and the overlying upper quartzite, both in the No. 4 and No. 1 iron deposit areas, and the feldspar-mica-quartz schist in question should not be included in the Mary River Group.
   b) The lower feldspar-mica-quartz schist at these localities is chiefly a metamorphosed regolith with an unconformity (assumed to be local) of minor time significance at the base of the overlying quartzite. Any changes in K content could be due to either potassium metasomatism or to weathering, and the feldspar-mica-quartz schist probably belongs to the Mary River Group.

2. The amphibolites are younger than the Mary River Group and:
   a) intruded parallel to and along pre-existing structures that bend parallel to the Mary River Group as it is approached, and the intrusions did not intrude the quartzite and iron-formation.
   b) intruded the quartzite and iron-formation but were offset along the east-west fault zone. The southern extensions may underlie crosscutting drift-covered gullies and the amphibolites may have been feeders for the Mary River mafic volcanics.
3. The lower feldspar-mica-quartz schist at the localities in question is chiefly a sheared granitoid rather than a paragneiss. The amphibolites were emplaced after most of the shearing, which may have been related to thrusting, took place.

The third possibility seems least likely because if the whole 460 m of feldspar-mica-quartz schist were sheared granitoid, one would expect the amphibolite bodies to be more dismembered than they are. Many of the mafic metavolcanics overlie the iron-formation in the Mary River region. If the amphibolites in the feldspar-mica-quartz schist north of No. 4 iron deposit and in the felsic volcanic complex west of No. 1 iron deposit represent Mary River Group igneous events, and were feeders to the mafic volcanics, then one would expect the quartzite and overlying iron-formation to be intruded by these intrusions. This, however, does not seem to be the case.

The tentative conclusion is that 1(b) best fits the available data. Thus, in the map area, the lower feldspar-mica-quartz member is considered to be in part a metamorphosed regolith. At some localities this may apply to only the lower part whereas in others, such as north of No. 4 iron deposit, it applies to virtually all of it.

The contact between the two members ranges from locally unconformable to gradational as noted above. The upper quartzite member is gradational with the overlying iron-formation, and also seems conformable with locally overlying metapelite.

The upper quartzite member is considered tentatively to be mostly a metamorphosed sedimentary orthoquartzite because of the occurrence of a few detrital zircon grains and rare metaconglomerate lenses; its locally gradational contact with the underlying metasediments, which it overlaps in places to lie directly on gneisses, indicate deposition probably occurred during a marine transgression. Its discontinuous lensoid nature may represent the way the quartzite was deposited, or may be a result of partial erosion after deposition. The presence of some thinly laminated, very fine grained quartzite, and the upward gradation in some places of quartzite into overlying oxide facies iron-formation indicate that some of the quartzite may be metachert, although vein quartz occurs locally. The change upward from clastic to, at least in part, chemical deposition suggests continuing marine transgression and deepening water during sedimentation.

Felsic metavolcanics (Ma)

Description

Rocks considered to be metamorphosed felsic to intermediate volcanics occur in the Mary River Group at many localities and at various stratigraphic positions, but are indicated by symbol Ma only on the Icebound Lake map sheet (NTS 37G). The felsic metavolcanics are commonly interlayered with metasediments that are, in part, volcaniclastic, and with mafic metavolcanics. Both the metavolcanics and metasediments are commonly partially migmatized by anatexis and are intruded by fine grained granitic rocks, emplaced at shallow levels, of similar composition and textures to the felsic volcanics.

The stratigraphic position of the felsic metavolcanics varies from place to place, and these rocks occur both above and below the iron-formation. In the Turner River area (30 km northeast of the Mary River No. 1 iron deposit) of the Mary River region they occur chiefly below the iron-formation, are the major component in a section of strata over 610 m thick (Table 7), and include some excellent examples of metamorphosed crystal tuff (R. Von Guttenberg, Strathcona Mineral Services Ltd., pers. comm., 1993). Along the south-central edge of the Icebound Lake map sheet (NTS 37G), felsic metavolcanic zones up to 425 m thick are interlayered with mafic metavolcanic (amphibolite) zones up to 75 m thick in an 800 m section adjacent to metasediments that may, in part, be laterally equivalent to the volcanic sequence. Felsic to intermediate metavolcanics and shallow intrusions of similar composition seem to occur chiefly above the iron-formation in the Eqe Bay region (Crawford, 1973), but also occur in the lower part of the section (Morgan et al., 1975; Morgan, 1982; Bethune and Scammell, 1993; Scammell and Bethune, 1995a).

The differences between felsic metavolcanics of the Mary River Group in the Mary River area and those in the underlying complex are subtle. The Mary River felsic metavolcanics are slightly darker and more mafic, finer grained, less metamorphosed, and less deformed than the underlying felsic metavolcanics, from which they are separated by clastic sediments, including conglomerate. The relationships of the felsic metavolcanics in the Turner River area are obscured by drift, faulting, and granitic intrusions. Some older felsic metavolcanic rocks may be included with the Mary River Group.

The felsic metavolcanics range from rhyolite to quartz latite and dacite, but are chiefly rhyolite and rhyodacite (Fig. 35). The related fine grained intrusions are chiefly monzogranite and granodiorite in composition. Modal data for Ma are presented in Figure 20E, Figure 29 (Mav), and Table 55. Limited spectrographic data are given in Appendices 2 and 3, and Tables 47 and 48.

The felsic metavolcanics are chiefly light to medium grey, but range to dark grey and locally pinkish grey on fresh and weathered surfaces. Some weathered surfaces are buff to light brown, or have a slight ashy appearance. These rocks are chiefly very fine- to fine-grained although a few are medium grained.

Both the felsic metavolcanics and intrusions are blastoporphyritic and contain undeformed to moderately stretched quartz, plagioclase, and/or microcline metaphenocrysts up to 0.65 cm in diameter that rarely make up to 30% of the rock (Fig. 35). Those composed of quartz have been recrystallized into mosaics. The feldspar metaphenocrysts have also been recrystallized and contain abundant mica inclusions, but some have retained euhedral shapes. Some of the microcline appears fresh and may occur as secondary porphyroblasts. Thin clots, lenses, and wispy zones and laminae up to several centimetres long, ranging from thinly scattered to closely packed, are common in some of the felsic volcanics. Most are slightly darker than the matrix and resemble flattened shards, lapilli, and small blocks of volcanic rock although some metapelite lenses may also be present. These rocks probably are ash and lapilli tuffs, welded tuffs, and ignimbrites.

Major minerals are quartz and oligoclase-andesine (An_{17-25}). Albite occurs locally. Microcline and brown to brownish-green biotite range from minor to major components while muscovite and green hornblende are major constituents in a few places. Other minor minerals, at least locally, are chlorite and pistacite. Accessory minerals include apatite, zircon, magnetite, sphene, allanite, calcite, kaolinite, and rarely, rutile and chloritoid.

The felsic metavolcanics and some of the related intrusions range from massive to very thinly banded and are commonly foliated with a weakly to strongly developed mineral lineation. Most of the foliation is due to scattered, thin biotite folia in a massive quartz-feldspar matrix, or thin biotite laminae separating quartz-feldspar lenses and bands up to a few centimetres across. An intense aggregate rodding and granulation has been developed locally. The rods and matrix have similar compositions but some rods have more mafic rims.

Contact relations

The basal contact was not seen at localities where these felsic metavolcanics seem to form the basal unit of the Mary River Group. However, the greater structural complexity of the adjacent gneisses suggests the basal contact is an unconformity

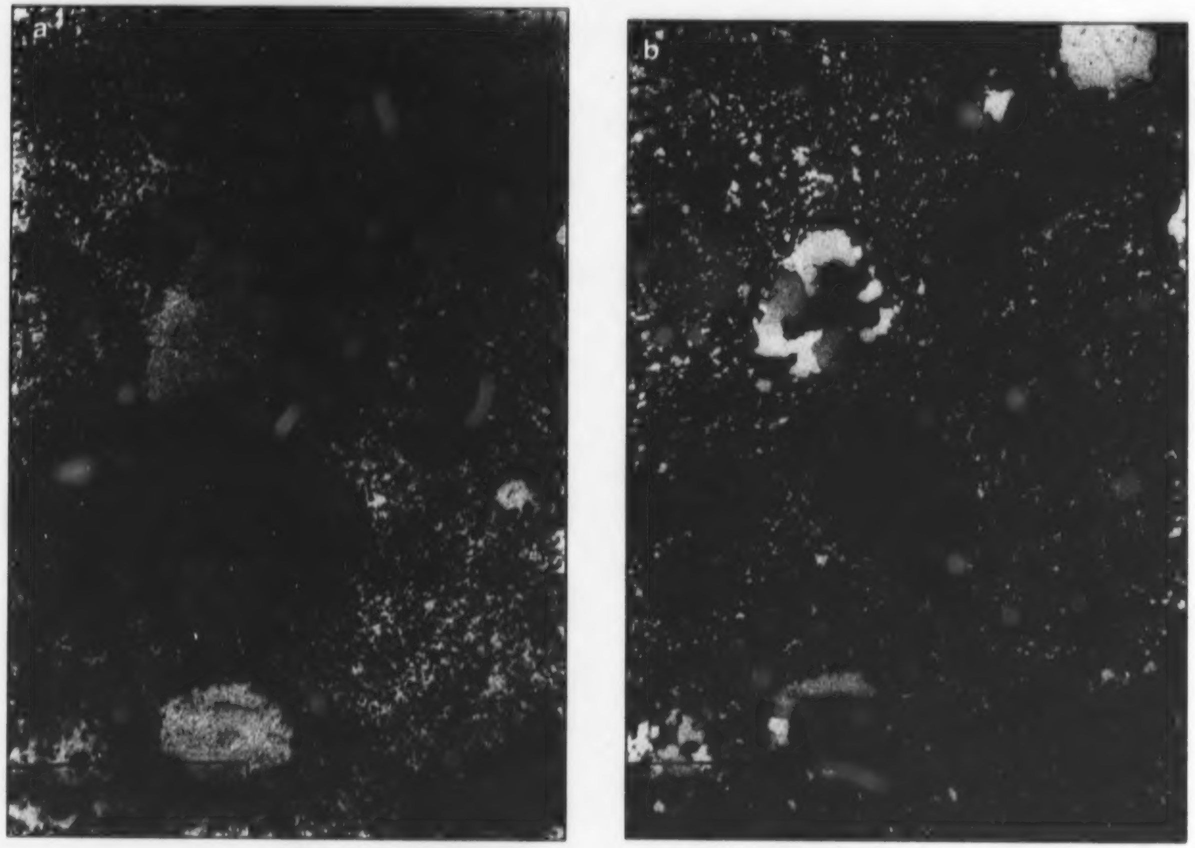

Figure 35. *Photomicrographs of metamorphosed rhyodacite* (Ma) *of the Mary River Group in eastern Mary River region. Phenocrysts of quartz, albite, and minor potassium feldspar (chiefly microcline) in a fine quartz-feldspar-biotite matrix. Mafic clots are mostly biotite.* ***a)*** *Plane-polarized light; note resorbed phenocryst margins and indefinite circular fine grained aggregates;* ***b)*** *Crossed nicols.*

and/or a fault. Contacts between the felsic metavolcanics and other adjacent Mary River Group strata, where not faulted, seem conformable and commonly gradational. In addition to the granitic intrusions, which are related to the felsic volcanics, the volcanics are also intruded by coarser granite and pegmatite, and by mafic and ultramafic intrusions. The intrusions range from concordant sills to sharply discordant bodies.

Chemistry

Only a few spectrographic analyses are available for the Mary River felsic metavolcanics (*see* Table 48 – column 22). The mean analysis is very similar to that for felsic metavolcanics associated with the underlying nebulitic granitic migmatite (*see* Table 48 – column 21, Amn^h; *see* Fig. 46). However, the Al, La, Ni, and Sr contents are discernibly lower in the Mary River felsic metavolcanics. Comparable differences for these elements are not obvious among the various older Archean granitic plutonic rocks (*see* Table 48 – columns 1, 4, ?5) or between these rocks and the younger Aphebian (and (?) Late Archean) granitic plutonic rocks (Table 48 – columns ?5, 6, ?7, 8, 9). Few samples from the shallow intrusions related to the Mary River felsic metavolcanics were analyzed. In contrast, the Aphebian plutonic rocks contain less Ti, Fe, Cu, V, and Zr than both felsic volcanic units and the Archean granitic plutons.

Iron-formation (Mif, AMif)

Description

Iron-formation is a minor but conspicuous rock unit in virtually all of the larger areas underlain by the Mary River Group (e.g. *see* Fig. 106, 107), and also occurs in isolated remnants associated with other Mary River strata in granitic intrusions, granitic gneisses, and migmatites. Considerable iron-formation occurs as virtually the only remaining recognizable primary lithology where the Mary River Group has been thoroughly migmatized during intense regional metamorphism. Mary River Group iron-formation was identified at only one locality in the Clyde River map sheet (NTS 27F), on the west side of Inugsuin Fiord. The aeromagnetic expression of the Mary River Group and the contained iron-formation has been discussed in the introductory remarks on the Mary River Group.

Within the map area, the iron-formation in the Mary River Group occurs in or somewhat below the middle part of the group as preserved (Table of Formations). Generally, iron-formation strata occur in only one stratigraphic interval at any one locality, and iron-formation strata are thinly interlensed with overlying metapelite-metagreywacke and underlying quartzite. The interlensed iron-formation is most commonly oxide facies, as much as 3 m thick but rarely greater than 60 cm, and generally up to 6 m (rarely 30 m) above the top of the main iron-formation.

In several places, several stratigraphic intervals of iron-formation alternate with other rock types in sections up to several hundred metres thick (Table of Formations, Table 7, Fig. 36; Gross, 1966; Jackson, 1966b, 1978b). In some other places, one or two lenses or layers of metamorphosed shale, siltstone, greywacke, and/or mafic volcaniclastics and flows as much as 100 m thick but generally not more than 15 m, occur in the iron-formation. In other cases relatively thick continuous iron-formations in one area may represent the same episode of iron-formation deposition as iron-formations interlayered with other sediments and/or volcanics in another area.

As much as 240 m of metagreywacke, amphibolite, ultramafics, and intrusive granite occur locally between iron-formations in the Mary River area. Although most of the interlayering of iron-formation with other lithologies is primary, much is secondary and has been imposed by faulting, folding, and/or emplacement of intrusions.

The structural complexity of the geology throughout the region makes it difficult to determine stratigraphic relations between and within formations, and how much of the stratigraphic variability within the Mary River Group, including the iron-formation, is primary. On the basis of detailed mapping for his thesis, Crawford (1973) concluded there are three main iron-formations in the Eqe Bay region. W.C. Morgan (pers. comm., 1988), on the basis of subsequent regional studies, considers two more likely.

The iron-formation is up to 195 m, but commonly not over 90 m, thick, and thins and dies out locally. Lenses of secondary high grade iron oxide are up to 152 m thick and 2-3 km long. Most significant thickness variations occur over distances of at least several kilometres, and are in part a depositional feature related possibly to a masking of iron-formation deposition by the deposition of an abnormal amount of clastic and/or volcanogenic material in some areas. Some of the apparent iron-formation lenses may not be totally isolated but may merge with the main body of iron-formation. Thickness variations would also be more abrupt when observed perpendicular to the long axes of lensoid bodies. Most observed thickness changes are a result of partial migmatization, syndepositional erosion (lean iron-formation clasts in overlying conglomerate), and, perhaps most importantly, by tectonism.

Compositionally the iron-formation may be divided into four main facies: oxide, silicate, aluminous (pelitic), and carbonate. Beds composed of virtually pure iron oxide are common. Silicate-oxide facies iron-formation is the only common compound type, and is a major component locally. It is discussed with the silicate facies. A few per cent sulphide minerals, chiefly pyrite or pyrrhotite, commonly associated with graphite, occur in a few places, chiefly in oxide and aluminous (pelitic) facies iron-formation, but is present in sufficient amounts locally to consider the rock a sulphide facies iron-formation.

The terminology for iron-formation facies used here is one that is commonly used in the literature (James, 1954; James and Sims, 1973), except for the term aluminous facies iron-formation. This term is used here for sedimentary iron-formation that has at least several per cent (> about 5%) Al_2O_3 compared with the other sedimentary iron facies, which commonly have less than 1% (James, 1954; *see* Tables

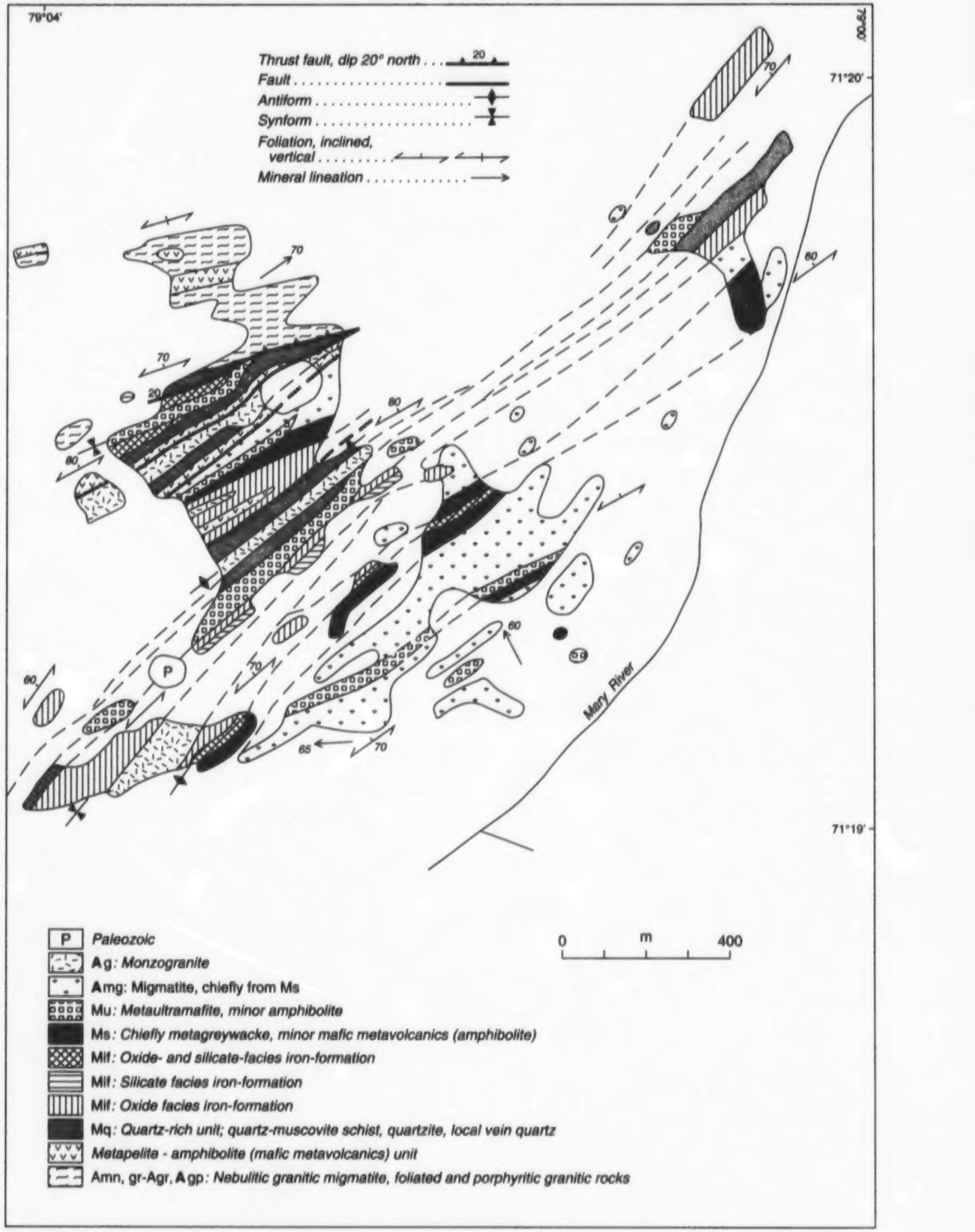
79°04'
79°00'
71°20'
71°19'
Thrust fault, dip 20° north
20
Fault
Antiform
Synform
Foliation, inclined, vertical
Mineral lineation
70
60
80
20
65
P
Mary River
P Paleozoic
Ag: Monzogranite
Amg: Migmatite, chiefly from Ms
Mu: Metaultramafite, minor amphibolite
Ms: Chiefly metagreywacke, minor mafic metavolcanics (amphibolite)
Mif: Oxide- and silicate-facies iron-formation
Mif: Silicate facies iron-formation
Mif: Oxide facies iron-formation
Mq: Quartz-rich unit; quartz-muscovite schist, quartzite, local vein quartz
Metapelite - amphibolite (mafic metavolcanics) unit
Amn, gr-Agr, Agp: Nebulitic granitic migmatite, foliated and porphyritic granitic rocks
0
m
400

Figure 36. *Details of field relations between iron-formation and associated rocks east of No. 3A iron deposit in the Mary River area (NTS 37G).*

14-17, 55, 56; Appendix 5). Magnesium oxide, CaO, K_2O, and Na_2O are also relatively abundant. Presence of these elements results in abundant cordierite, biotite, muscovite, plagioclase, hornblende, and/or sillimanite in metamorphic assemblages; most of these rarely occur in the other iron-formation facies.

The different facies are conformable with, and grade into, one another vertically over short distances of up to a metre or so. Lateral facies gradations are also commonly evident. With very minor exceptions, rocks in the various iron-formation facies are considered here to be metamorphosed equivalents of primary sedimentary facies on the basis of field relations, chemistry, and the conclusions of many (including the author) who have studied the metamorphism of iron-formations and/or have followed iron-formations from unmetamorphosed or very low grade terrane into high grade terrane.

In general, most of the iron-formation comprises oxide facies strata, although locally silicate (including silicate-oxide) facies rocks are equally abundant or predominate. Aluminous iron-formation is abundant locally. In some parts of the Mary River region, silicate (including silicate-oxide) and aluminous facies rocks together are as much as 60 m thick. Carbonate facies iron-formation, up to about 1 m thick, was seen in only a few places. Modal analyses for samples representing several of the facies are presented in Figures 29 and 38 (*see* below). Figure 38 shows how most Mg-Fe-silicate-bearing assemblages (CG+) don't contain large amounts of alumina minerals (MV+). Oxide facies strata plot along or close to the Q-OQ line, and silicate facies plot along or close to the Q-CG+ line, etc.

The stratigraphy of the iron-formation seems to vary from one locality to another, but in general oxide facies rocks predominate in the lower part of the iron-formation, while silicate (including silicate-oxide) and aluminous facies iron-formations occur interbedded with oxide facies zones in the upper part. Carbonate iron-formation is associated with oxide and silicate facies.

Most of the iron-formation is laminated to thin bedded (Table 2; Fig. 37), with beds ranging up to 10 cm, but commonly no more than 1.3 cm thick. Laminae compositions are generally uniform, and contacts abrupt and sharp. Locally, beds range up to very thick bedded and massive (Table 2), and some iron-rich beds in the oxide facies exceed 12 m in thickness. Most of the banding in the iron-formation is sedimentary layering. Other primary sedimentary features such as intraformational breccia, slump, and other deformational features were recognized by Gross (1966) in the Mary River area, and are present elsewhere as well (e.g. Crawford, 1973).

The iron-formation is predominantly equigranular and fine to medium grained but ranges from very fine to very coarse. The oxide and carbonate facies are chiefly granoblastic while the silicate and aluminous facies commonly have a lineated and/or a schistose fabric. Some of the pelitic facies have a pegmatitic texture.

The iron-formation is commonly highly deformed on a small as well as a large scale, and provides good examples of parallel, chevron, flow, and "refolded" folds (Fig. 37b). Brecciation and aggregate rodding are well developed locally, especially in the oxide facies where small-scale folding and faulting has formed quartz-rich boudined lenses and rods around which the iron oxide has recrystallized. Structurally such rocks are similar to the underlying rodded feldspar-mica-quartz schists. Silicate minerals commonly have a well developed lineation parallel to aggregate rodding and small-scale fold axes. In some areas the lineation orientations vary considerably from one locality to the next, in others they are remarkably consistent. These features show that some of the brecciation is secondary, rather than primary, and is related to metamorphism and deformation. Amphibole spherulites, up to 5 cm or more in diameter, rosettes, and stellate and hourglass structures are well developed locally.

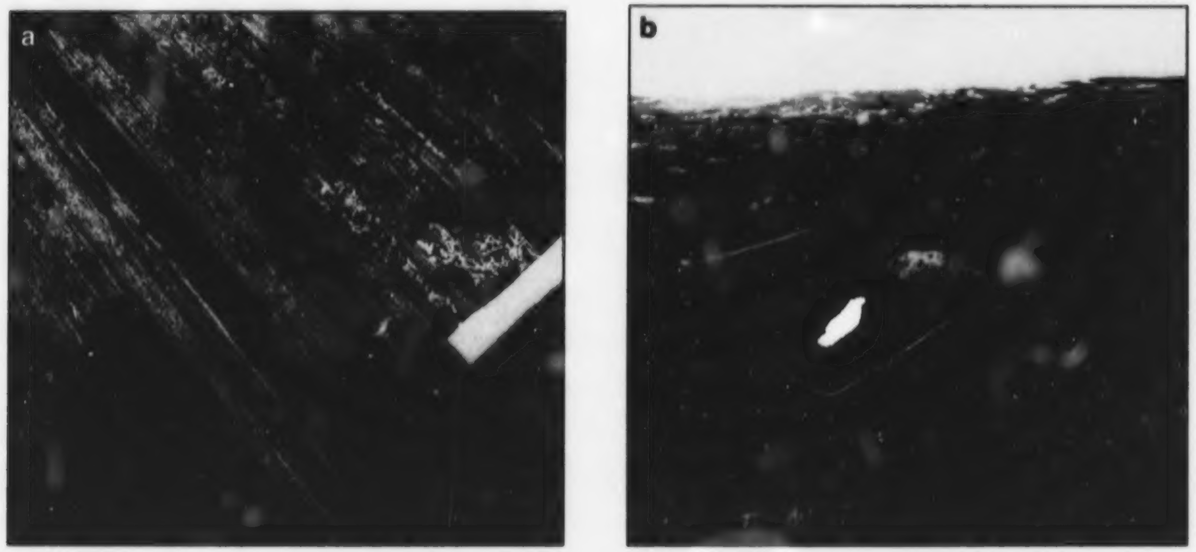

Figure 37. a) *Laminated, slaty, oxide facies (magnetite) iron-formation with quartz veinlets and segregations, south-central map area NTS 37G. Photograph by S.L. Blusson. GSC 185506.* ***b)*** *Very thin bedded, folded, oxide facies (magnetite) iron-formation. View south along faulted tight synform overturned to east, south-central map area NTS 37G. Photograph by W.J. Crawford. GSC 186253*

The iron-formation is locally leached and/or enriched, and is strongly altered adjacent to a few of the Hadrynian diabase dykes. Oxide facies iron-formation is leached and the iron oxide altered to limonite-goethite for a distance of several metres adjacent to a large Hadrynian (Hg) diabase dyke in the Mary River No. 4 iron deposit area. A metre-thick tourmaline dyke occurs in the leached rock. A possible source for the boron is the Neohelikian (1.27 Ga?) Bylot Supergroup to the northwest, especially the contained evaporitic sabkha deposits (Jackson et al., 1980, 1985; Jackson and Iannelli, 1981). The boron may have been picked up during horizontal flow of magma during the emplacement of the dyke swarm (Borden or Franklin) as proposed by Fahrig (1987). Heat from the dykes at the time of intrusion probably mobilized water enabling it to leach the iron-formation. The affected iron-formation is commonly vuggy and is weathered various shades of rust. Some stained subhorizontal weathered surfaces, however, may be the exhumed erosion surface at the base of the Paleozoic strata. Local iron oxide enrichment, other than the major iron deposits, consists of iron oxide both disseminated and in veins up to 0.5 m thick. In some places smaller veins branch off the main vein in lit-par-lit fashion.

Most of the enrichment iron is specularite, but some is magnetite and some is earthy hematite. Quartz veins up to 15 m thick are common locally.

Oxide facies and high grade iron oxide

Oxide facies iron-formation occurs in units that are commonly up to 52 m thick, although one unit is 195 m thick in the No. 4 iron deposit area (Fig. 1, 3, *see* Fig. 106). In any major occurrence of iron-formation, at least one zone of nearly pure iron oxide is commonly present, chiefly in oxide facies strata. Some examples are: 0.4 m north of Inugsuin Fiord (NTS 27F); 15-20 m in the northeast corner of the Steensby Inlet map area (NTS 37F); and 30 m northeast of Grant-Suttie Bay (NTS 37C). The thicker zones in the Mary River region range from 30 to 152 m thick and have been traced for distances of up to 4 km (Baffinland Iron Mines Limited, 1964; Gross, 1966; Jackson, 1966b). A variety of metamorphosed small dykes and sills up to 1 m across and composed chiefly of magnetite, occur locally in probably every major iron- formation occurrence. They occur chiefly in iron oxide facies rocks, but also in quartzite, and in several places with quartz veins. Small-scale hematite enrichment also occurs locally in fine grained, massive, pink granite-syenite in northeastern part of map area NTS 37G/6.

Interbeds of silicate iron-formation and/or amphibolite up to 8 m thick, and quartz veins up to 3 m thick, occur locally in oxide facies iron-formation. As much as 1 m of carbonate iron-formation is present at one locality in the No. 4 iron deposit area. A few per cent of pyrite-pyrrhotite occur in a 1.5 m thick zone in oxide iron-formation at the No. 1 iron deposit.

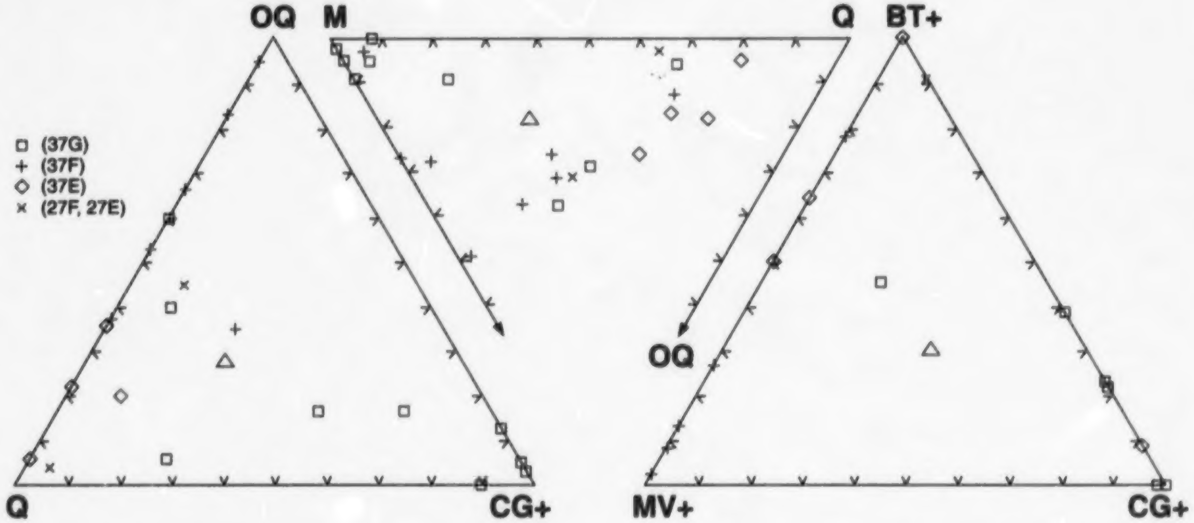

Figure 38. *Triangular plots for modal analyses of iron-formation. The mean is shown by the triangle. Q = quartz; M = mafics (all constituents except Q and OQ). OQ = magnetite+hematite+chromite+leucoxene+opaque+pyrrhotite+pyrite+chalcopyrite+sulphide (undifferentiated)+spinel. CG+ = cummingtonite+anthophyllite+grunerite+enstatite+hypersthene. MV+=muscovite+plagioclase+cordierite+sillimanite+andalusite+microcline. BT+ = biotite+garnet+chlorite+hornblende+diopside+epidote.*

Oxide facies. The oxide facies iron-formation is composed predominantly of alternating white to light grey, quartz-rich and steel-grey magnetite- and/or hematite-rich beds (Fig. 37). Small amounts of various silicate minerals may also be present. Aphanitic to very fine grained red jasper beds occur in the Eqe-Grant-Suttie bays area which, in the author's experience, resembles the thin bedded jaspilite member of the Sokoman iron-formation of the Labrador Geosyncline. A faint reddish tint remains in some quartz-rich beds in the Mary River region and granule-like shapes are outlined by iron oxide in a few others. Some carbonate is present locally.

The oxide facies generally comprises 10-70% of oxide-rich laminae that contain up to 50% iron. Magnetite predominates over hematite although hematite predominates locally. Specularite and martite are the two most common forms of hematite, and in the Mary River area, at least, both have formed from magnetite (Baffinland Iron Mines Limited, 1964; Gross, 1966). Still younger earthy hematite predominates locally, especially in zones of nearly pure iron oxide. Minerals that commonly occur as minor or accessory constituents include quartz, limonite-goethite, chlorite, anthophyllite, cummingtonite-grunerite, green and light brown biotite, apatite, and green and blue-green hornblende. Less common accessory minerals include: zircon, muscovite, carbonate, plagioclase, pyrite, garnet, tourmaline, cordierite, sillimanite, hypersthene, and chalcopyrite.

High grade zones. High grade zones are commonly composed of individual beds up to 3 m thick, but which locally range up to 15 m thick. A faintly defined, thin compositional layering is present in many places (Fig. 39b). These high grade zones are chiefly fine- to medium-grained, massive, dense, recrystallized rocks that only locally are friable, porous, vuggy, and contain postmetamorphic iron oxides. Isolated high grade remnants within the migmatites and gneisses are chiefly medium to coarse grained and are almost invariably magnetite.

The high grade zones within the Mary River Group range from nearly pure magnetite through a mixture of magnetite and hematite to nearly pure hematite, with magnetite predominating overall (Fig. 39). Specularite-rich zones seem to be related to faults and complex fold structures.

Mary River high grade iron deposits. The iron deposits in each of the No. 1-3A and No. 4 areas (Fig. 1, *see* Fig. 106, 107) occur on the north limbs of each of two pairs of adjacent complex synforms. In both areas the north synforms trend westerly and the south synforms northwesterly. They were formed by the deformation of previously formed synforms and merge westward into a single complex synformal structure (e.g. *see* Fig. 106; Jackson, 1966b, 1978b). Locally the top of the iron ore seems to be stratigraphically consistent whereas the base is in contact with various lithologies. In some places this is clearly a fault contact, and in others a replacement contact but in some places it could be an unconformity as well (Gross, 1966; Jackson, 1966b). The ore grades laterally into adjacent rock types in some places whereas there is an abrupt contact in others.

In both the No. 1-3A and No. 4 areas the iron deposits occur in the upper part of the iron-formation as it outcrops, whether the iron-formation is right side up or overturned. Where the iron-formation is right side up the high grade iron occurs stratigraphically in the upper part of the iron- formation associated with silicate- and aluminous-facies iron-formation, amphibolite, and serpentinite. Where the iron-formation is overturned the high grade iron occurs stratigraphically in the lower part of the iron-formation associated chiefly with oxide facies iron-formation, and minor quartz-rich rocks, ultramafics, and amphibolite.

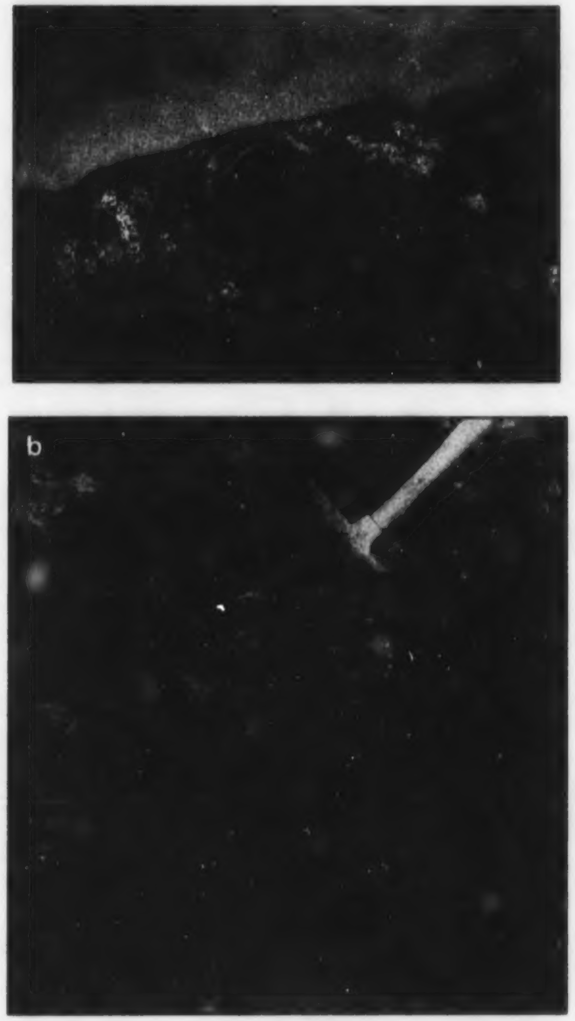

***Figure 39.** a) Folded magnetite "ore" surrounded, and partially assimilated by, migmatitic pink granite near at the east end of the north synform in No. 4 iron deposit, Mary River area. Photograph by W.J. Crawford. GSC 1997-54H. **b)** Blue, vuggy, clinker-like hematite ore, No. 2 iron deposit, Mary River area. Horizontal white lines are mostly remnants of primary chert beds, cut by quartz veinlets. Photograph by G.D. Jackson. GSC 118309*

The No. 1, 2, 3, and 3A iron deposits (e.g. Fig. 36, 40, *see* Fig. 107) are somewhat different than the other magnetite-hematite zones in that they are chiefly very fine- to fine-grained, relatively vuggy (Fig. 39b), and are composed chiefly of hematite. The ore is brecciated locally and contains clasts up to 15 cm across. No. 1 iron deposit, which is the largest found to date, is predominantly magnetite at its north end and also at its south end in the vicinity of Mary River, where it is discontinuous. Over most of its length it ranges from a magnetite-hematite mixture to hematite. Much of the hematite ore is very fine grained, vuggy, locally brecciated, and is little, if at all, metamorphosed. This hematite ore seems identical to the hematite pods that formed by oxidation of sulphide, and which are associated with the lead-zinc mine at Nanisivik (Jackson and Iannelli, 1981). In the author's experience, the hematite ore is also very similar to some of the Schefferville ore in the Labrador Geosyncline. In the northern part of the deposit the iron oxide zone appears to be gradational with chlorite-hornblende schist at one place, while at another the layering in quartz-iron oxide formation ends abruptly at the contact with the high grade zone, which also contains inclusions of low grade iron-formation. Quartz-garnet-staurolite-chlorite schist separates iron ore and oxide iron-formation in No. 3 and 3A iron deposits which also contain minor secondary carbonate.

Baffinland Iron Mines Limited (1964, 1966) identified magnetite as the earliest oxide to have formed, among the iron oxides now present in the No. 1 iron deposit and showed that it had undergone partial martitization prior to local formation of specularite under conditions of relatively high pressure and temperature. Goethite and limonite are important locally and are later than the martite. Traces of cummingtonite-grunerite, anthophyllite, clinochlore (var. leuchtenbergite), quartz, garnet, pyrite, pyrrhotite, chalcopyrite, and covellite were also found in the high grade deposit.

Local postmetamorphic leaching and enrichment of the iron-formation is most extensive in the No. 1 iron deposit (NTS 37G) where vuggy hematite, hematite breccia, and minor goethite were formed. Leaching of silicate minerals, formation of goethite pseudomorphs of garnet, and kaolinization of other silicate minerals (Gross, 1966) is further evidence of postmetamorphic alteration.

In the No. 4 iron deposit area, hematite-goethite enrichment zones up to about 60 cm thick, outside the ore zones, occur in oxide facies and oxide-silicate facies rocks. The laminated nature of the rock has been preserved and enrichment seems to have occurred chiefly by alteration and/or replacement of the quartz- and silicate-rich laminae. Both the quartzite and oxide facies iron-formation have undergone silica leaching and goethite-earthy hematite enrichment along the south side of the major "refolded" synformal structure present at the junction of the two converging synforms (*see* Fig. 106).

Silicate (and silicate-oxide) facies

These rocks are typically thin laminated to thin bedded (10 cm). Thicknesses range up to 112 m for both facies interbedded and to 58 m for either facies by itself. In the silicate facies rocks, white to light grey quartz-rich layers commonly alternate with iron silicate-rich layers, most of which are composed chiefly of straw-coloured cummingtonite-grunerite. Green actinolite-rich layers are common and dark

***Figure 40.** View northwest at Nuluijaq Mountain and the L-shaped Mary River No. 1 iron deposit. (See Fig. 18 of south end.) Photograph by W.J. Crawford. GSC 1997-54I; GSC 1997-54J*

Table 11. Stratigraphy of iron-formation and associated rocks in Mary River iron deposits area.

(a) Amphibolite (mafic metavolcanics)	150+ m	
Metagreywacke	330 m	
Silicate-oxide I.F.	1.5 m	(18-60 m[1])
Laminated oxide I.F.	4.5 m	
Silicate-oxide I.F.	12 m	
Oxide I.F.	20 m	
Metaultramafite	33-46 m	
Hematite "ore" (magnetite increases up)	30-76 m	
Biotite schist	23 m	
Quartzite	0.18 m	
Feldspar-mica-quartz schist	*	
Fault zone	*	
Flaser gneiss	*	
Sheared granodiorite feldspar porphyry	*	
Average I.F.	about 110 m	
(b) Oxide I.F.	3 m	
Silicate I.F.	6 m	
Oxide I.F.	6 m	
Silicate I.F.	6 m	
Massive "ore"	9 m	
Oxide I.F.	3 m	
I.F.	33 m	
(c) Intrusive pink granite	*	
Quartz-biotite-feldspar schist, amphibolite	*	
Silicate, aluminous, and oxide I.F.	12-18 m	
Amphibolite, paragneiss	0-several m	
Chlorite schist (metaultramafite)	few m	
Oxide I.F., iron "ore"	1-8 m	
Silicate-oxide and aluminous I.F.	0-several m	
Oxide I.F., minor silicate I.F.	40 m	
Amphibolite, biotite schist, paragneiss	5-90 m	
Oxide I.F., iron "ore"	3-50 m	
Amphibolite, talc schist (metaultramafite)	0-20 m	
Feldspar-mica-quartz schist	0-60 m	
Granitic gneisses	*	
Average I.F.	about 100 m	
(d) Metagreywacke, mafic metavolcanics	few 100 m	
Metaultramafite	0-30 m	
Oxide I.F., iron "ore"	30-80 m	
Silicate I.F., aluminous I.F.; minor amphibolite, metaultramafite	30-115 m	
Quartzite	60-130 m	
Oxide and/or silicate I.F.	0-20 m	
Sheared, rodded feldspar-mica quartz schist, amphibolite dykes	30-460 m	
Average I.F.	about 140 m	

1 Iron-formation elsewhere in this area ranges from 18-60 m thick

* Thickness not measured

Note (a), (b) represent individual sections in the No. 1-3A deposits area; (c), (d) each are syntheses of at least two sections in the No. 4 deposit area.

I.F. = iron-formation

green hornblende-rich layers are of minor importance. Some beds are a mixture of quartz, cummingtonite, and either actinolite or hornblende. In many places the amphibole crystals penetrate quartz grains, indicating that some amphiboles may have formed by a reaction involving silica, iron oxide, and the breakdown of a carbonate mineral. The weathered surface of silicate rocks is commonly a rusty brown that tends to mask the banded nature of the rocks.

In silicate-oxide facies rocks, dark steel-grey magnetite-rich layers alternate with the straw-coloured and/or green iron silicate- and quartz-rich layers. Hematite-rich layers are rare and have been observed chiefly in strongly lineated or sheared varieties. Some layers are composed of intermixed magnetite and iron silicates, some of which also contain quartz. Some of the silicate-oxide facies rocks contain as much as 60% iron oxide, but generally the iron oxide is less than 30%. A few layers up to 10 cm thick in the vicinity of No. 4 iron deposit contain 40% magnetite, 10% pyrite, and some clinopyroxene. Silicate-, silicate-oxide-, and oxide-facies iron-formation grade into one another by variations in the proportion of layers in which quartz, iron silicates, and iron oxides dominate, and by variations in the amounts of these minerals in layers where they are intermixed.

Some iron amphiboles (chiefly cummingtonite) occur in spherulites up to 5 cm in diameter that form 30% of the rocks and make up most of the rock locally. Diopside-hedenbergite, tremolite, actinolite, hornblende, garnet, and rarely epidote may also occur in major amounts in some beds. Garnet occurs chiefly as euhedral porphyroblasts up to 3 cm in diameter. Hypersthene-ferrohypersthene is a major component in some of these rocks in the granulite facies. Anthophyllite seems to be rare but occurs as a major and minor component locally in the Mary River and Eqe Bay areas. Chlorite is a major component locally, and is a common minor and accessory mineral. Plagioclase is uncommon and occurs as a minor and accessory component in a few places. Common accessory minerals include limonite-goethite, pyrite, and carbonate (chiefly parankerite). Apatite, zircon, light green and light brown biotite, and sericite are less common and chalcopyrite and leucoxene were seen in two places. The more common mineral assemblages are shown in Table 12.

A few of the assemblages, such as No. 18 in Table 12, and the diopside-carbonate-bearing assemblages, may have been carbonate, silicate-carbonate, or oxide-carbonate facies rocks prior to metamorphism. Hornblende is commonly green to blue-green and is ferrohastingsite in some places (Crawford, 1973). The biotite is light green or light brown. Some biotite and chlorite may be later alteration products.

Aluminous (and aluminous-oxide) facies

Aluminous sedimentary iron-formation (Fig. 41), although not uncommon in the Precambrian, has received relatively little attention, especially in metamorphic terranes where it has probably been described with other iron-formations such as the silicate facies or, where the iron content is lower, has been considered to be ordinary pelitic rocks. Within the map area, rocks assigned to this facies, as defined above, contain reasonably distinct assemblages that locally form a large part of the iron-formation. Therefore, the name "Aluminous iron-formation facies" is ascribed to this rock type in order to distinguish it from the apparently more common alumina-free to alumina-poor silicate facies described by James (1954) and others.

Table 12. Some common prograde mineral assemblages in Mary River Group silicate- and silicate-oxide-facies iron-formation.

Assemblage	1	2	3	4	5	6	7	8	9	10	11	12	13	14	15[2]	16[2]	17[2]	18[2]
Quartz	+	+	+	+			+	+	+	+		+	+	+	+			+
Magnetite	±		+		+	+	+	+	+	+	+	+	+	±	+	+	+	
Hematite																		+
Anthophyllite									+						+			
Cummingtonite	+	+		+	+	+	±					±				+		
Tremolite										+	+							
Actinolite								+										
Hornblende												+	+					+
Diopside				+				±		+			+					
Hypersthene[1]			+											+				
Garnet		+	+		±	+												
Carbonate				±							+		+					
Biotite					±						+				+			
Muscovite							±											
Chlorite		±				+	+											
Albite																	+	
Plagioclase															+	+		
Epidote																	+	

1 - Includes some ferrohypersthene; 2 - Uncommon assemblages; + - Mineral is present; ± - Mineral is present in some assemblages, not in others. Two minerals represented by ± in an assemblage indicates there are four combinations represented, etc.

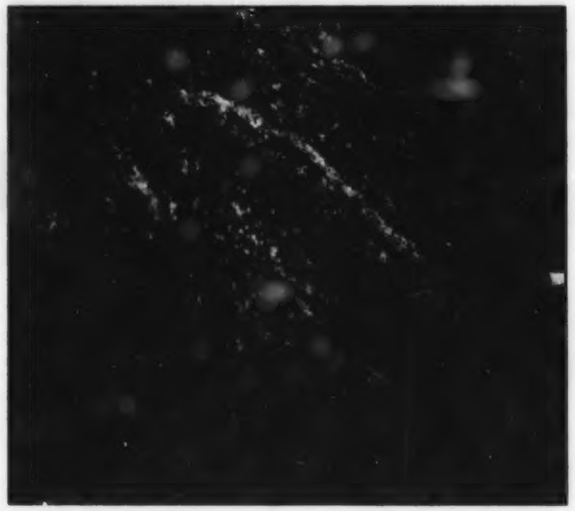

Figure 41. Folded and sheared aluminous iron-formation at Eqe Bay. Photograph by W.J. Crawford. GSC 204343-0

Within the map area, the aluminous facies iron-formation occurs in thin units not more than 30 m thick. It is commonly laminated to thin bedded, like most of the iron-formation. Typically it is composed of alternating light to medium grey quartz- and/or cordierite-rich layers and greenish-grey iron silicate-rich layers. The weathered surface is commonly rusty and the banded nature of the rock is masked, or less pronounced, than in the oxide and silicate facies. Common major components include quartz, cordierite, anthophyllite, garnet, biotite, and magnetite. Some of these rocks contain up to 50% iron oxide (chiefly magnetite), both disseminated through the rock and concentrated in bands, and could be considered as aluminous-oxide facies. Most, however, contain 5-20% magnetite in addition to iron-bearing silicates. Muscovite, plagioclase, cummingtonite-grunerite, hornblende, and sillimanite are also common and locally abundant. Epidote occurs as an accessory mineral in a few places and as a major component in one or more places. Chlorite is a common secondary accessory mineral, and also occurs as a major component of metamorphic assemblages in a few places. Other common accessory minerals are apatite, zircon, muscovite, pyrite, hematite, and limonite-goethite; tourmaline, serpentine, microcline, and chalcopyrite occur in a few places. With decrease in iron content, aluminous facies iron-formation grades into ordinary metapelites. In general, hypersthene does not seem to occur in this facies even when coexisting rocks do have hypersthene. The presence of cummingtonite-sillimanite instead (assemblage 12, Table 13) suggests the

Table 13. Some common prograde mineral assemblages in Mary River Group aluminous facies iorn-formation.

Assemblage	1	2	3	4	5	6	7	8	9[1]	10[1]	11[1]	12[1]	13[1]
Quartz	+	+	+		+	+	+	+	+		+	+	+
Magnetite	+	+	+	+	±	+	+	+	+	+	+	+	+
Cordierite	+	+	+	+				±					
Sillimanite			+	+				+				+	+
Anthophyllite	+	±					+						
Cummingtonite												+	
Hornblende									+				
Garnet		+		+	+	+			+				+
Biotite	±	+		+	+	+	+	+					+
Muscovite			+		+	+		+			+		
Plagioclase							O	O	A	A	+		
Spinel													+
Epidote										+			
Chlorite						+				+			
Pyrite									+				

A - Albite; O - Oligoclase; 1 - Uncommon to rare; + - Mineral is present; ± - Mineral is present in some assemblages, not in others. Two minerals represented by ± in an assemblage indicates there are four combinations represented, etc.

absence of high pressures during the formation of granulites at those localities. Some of the more common mineral associations are shown in Table 13.

Carbonate facies

Carbonate-rich rocks form a very minor part of the iron-formation at several localities, although accessory carbonate is common. However, iron silicate crystals, chiefly several types of amphibole, penetrate into quartz grains in many places. Some of these amphiboles probably formed by a reaction involving silica, iron oxide, and the breakdown of a carbonate mineral. Ca-bearing minerals such as tremolite-actinolite, hornblende, diopside-hedenbergite, and epidote are locally abundant. The above features suggest that carbonate minerals and carbonate facies iron-formation were more abundant prior to metamorphism.

The carbonate-rich rocks occur chiefly as laminae and very thin beds interlayered with the more common iron-formation lithologies over thicknesses of a few centimetres to one or two metres. Carbonate-rich beds up to one metre thick were seen at two localities south and southeast of No. 4 iron deposit and at a few other places. The beds are themselves faintly to well laminated and contain up to 50% magnetite, concentrated chiefly in laminae but also disseminated. A few secondary hematite laminae also occur south of No. 4 iron deposit. Where those rocks contain abundant iron oxide they are more properly called carbonate-oxide facies. The carbonate beds commonly have been plastically deformed and the associated magnetite laminae boudined and offset. The carbonate beds are fine grained and range from grey, pinkish grey, and greenish grey on the fresh surface, to grey to brown on the weathered surface. X-ray determinations indicate that most of the carbonate is a ferruginous dolomite and that some is calcite. Some of the calcite seems to have been introduced. Several optical determinations on carbonates from the Mary River region indicate that the calcite has $N_o = 1.658$ and that most of the dolomite is parankerite with $N_o = 1.697$, but that some may be magnesiodolomite with $N_o = 1.690$-1.695. The dolomites generally are slightly altered to limonite-goethite. Chlorite, tremolite-actinolite, quartz, and diopside are major components locally in silicate-carbonate facies rocks. Accessory minerals include apatite, biotite, pyrite, and locally, chalcopyrite. Mineral assemblages include:

parankerite+magnetite,

parankerite+actinolite+magnetite+quartz±diopside, and

parankerite+chlorite+quartz+magnetite±calcite± (tremolite-actinolite).

Sulphide facies

Sedimentary sulphide-rich zones, like carbonate-rich zones, form a very minor part of the iron-formation. They are discontinuous, up to about 1.5 m thick, and are associated chiefly with the oxide facies, but also occur in silicate- and aluminous-facies iron-formation and in other metasedimentary rocks of the Mary River Group. Small-scale secondary sulphide mineralization also occurs in the same rocks and locally may be mistaken for sedimentary sulphide. Locally the sulphide is concentrated in alternating layers in the iron-formation, or disseminated throughout part of the iron-formation. In either case the rusty weathered surface tends to mask the rock structures and textures.

Sulphide-rich layers are fine to medium grained, and are composed chiefly of quartz, chlorite, biotite, pyrite, and/or pyrrhotite and magnetite. The sulphide may make up to 55% of the rock, but commonly has magnetite associated with it and is rarely the only opaque mineral present. Apatite, calcite, muscovite, and chalcopyrite are common accessory minerals. Very small amounts of sphalerite, galena, and arsenopyrite occur locally. Mineral assemblages include:

quartz+magnetite+pyrite and/or pyrrhotite,

quartz+chlorite+pyrite+magnetite±muscovite±pyrrhotite,

quartz+actinolite+pyrite+pyrrhotite+magnetite, and

quartz+chlorite+cummingtonite+pyrite+magnetite.

Contact relations

Generally, the contacts between iron-formation and adjacent strata are faulted, sheared, or mylonitized across a metre or more. However, where tectonism is absent, the various primary iron-formation facies are conformable and gradational to interbedded with one another, including much of the high grade iron, and with adjacent units of the Mary River Group. Commonly the lower contact is gradational and iron-formation is interbedded with quartzite, probably including metachert, and with argillite, metapelite, and metagreywacke that occur at several places between the iron-formation and underlying quartzite. The iron content in these rocks increases toward the iron-formation. The upper contact is commonly interbedded with metapelite, metagreywacke, and meta-arkose. Mafic and possibly ultramafic metavolcanics are also interbedded at the lower and upper contacts, and have been recrystallized to biotitite for up to a metre from the contact. This is especially common adjacent to faulted or sheared contacts. The lower contact of some of the high grade iron ("ore") in the No. 4 iron deposit area is transgressive, due to faulting, the presence of an unconformity, or to the replacement nature of the iron enrichment.

The iron-formation, and some high grade iron in the No. 1-4 iron deposits areas, were intruded by mafic and ultramafic dykes and sills that were later metamorphosed (Jackson, 1966b). Most of these intrusions are considered to be penecontemporaneous with the Mary River Group mafic metavolcanics and ultramafics because of spatial association and chemical similarities discussed below. The iron-formation, like the rest of the Mary River Group, has been intruded by at least two ages of granitic intrusions (Fig. 39a; Jackson, 1966b), earlier mostly white to pale grey, and later chiefly pink.

Chemistry

Chemical data for Mary River Group iron-formation, high grade iron oxide, and some contained minerals (including chemical formulae) are provided in Appendices 2-5, 7; Tables 14-17, 47, 48, 55, 56; and Figure 95 (*see* below). The data provided to Crawford (1973) are included. A few analyses of oxide facies and high grade iron samples were also carried out for W.J. Crawford at Bondar-Clegg in Ottawa to compare with analyses for splits of the same samples analyzed at the Geological Survey of Canada. The iron and manganese values for the two sets of analyses are in good agreement but some of the Al_2O_3, TiO_2 and MgO results are not. There is generally better agreement for whole rock and hematite samples than for magnetite samples. Crawford (1973) considered these differences to reflect erratic distribution of elements and minerals in the rock. However, the differences were also probably due to sample splitting and mineral separation difficulties caused by the fine grained, poikiloblastic nature of some minerals. Al-bearing silicate minerals are more closely associated with magnetite than hematite, are themselves slightly magnetic, and commonly contain magnetite inclusions, making separation difficult.

Fryer (1971a) has reported Rb-Sr and some trace element data (chiefly REEs) for samples from the Mary River No. 1-4 iron deposit areas. Some differences between the major iron-formation facies in major element content, other than silica and iron, are summarized in Table 16. Mean values and corresponding standard deviations for the major facies and minerals are given in Table 17. Obviously SiO_2, Fe_2O_3, and FeO are major components throughout most of the iron-formation. Magnesium oxide is a major component in the silicate, aluminous, and carbonate facies, and Al_2O_3 is a major component in the aluminous facies. Iron is generally significantly lower in the aluminous facies than in the other major facies; however, minor components, CaO, Na_2O, K_2O, H_2O, and especially TiO_2 and S, and trace elements are all most abundant in the aluminous facies.

Silica seems to be concentrated in magnetite and hematite when the silica content of the rock is less than about 0.5%. The apparent silica content in these minerals generally does not exceed 0.8% in iron ore and in the oxide facies. As much as 5% is reported in these minerals from the silicate, silicate-oxide, and aluminous facies. These silica values are due to contamination of silica and/or various silicate minerals. Hematite is absent from most silicate-, silicate-oxide-, and aluminous-facies rocks because of the oxidation state of these facies. Generally, where hematite is present in these facies, it is clearly a later mineral.

Much of the high grade iron deposits is pure hematite and/or magnetite. Some assays of high grade iron indicate more iron than the chemical formulas for magnetite and hematite allow (*see* Table 56). Baffinland Iron Mines Limited (1964, 1966) postulated that the presence of free iron might be the reason for this, but it seems more likely that the analyses in question may be slightly inaccurate. The high grade iron deposits have a chemistry similar to the oxide facies. In silicate- and silicate-oxide-facies rocks, hypersthene has much more Fe_2O_3 than FeO, which is the reverse of the various amphiboles (grunerite, anthophyllite, hornblende).

The minor and trace element content of the iron-formation is generally low, and many of the values are near the lower limit of reliable determination. Some elements such as Cu and Cr seem to be concentrated in the magnetic separates from the Davis Tube tests (Tables 14-17, 56; Appendix 5). These concentrates are not considered in the following discussion. Examination of the spectrographic data in

Appendices 2-4 and Tables 17 and 48 indicate that most of the elements vary by factors of 3-10 in the iron-formation. Some elements (Mn, Fe, Cr, Ni) vary by a factor of 50 or more in the silicate facies (Table 17). Trace elements are most abundant in the aluminous facies (e.g. Ti, S, V, Y, Zr, Cr, Ba). Oxide and silicate facies have comparable lesser amounts.

It is obvious from the mineral analyses given in the tables noted above that some minerals such as biotite (high Co, Cr, Ti, Ni), chlorite (high Cu, Mn, Ni, Sr), and magnetite (high Cr, Ni, Ti, V) commonly contain greater varieties and/or quantities of trace elements than the coexisting minerals that were analyzed. Except for a few elements, coexisting magnetite (high Ti) and cummingtonite (high Mn) have similar trace element patterns.

Crawford (1973) concluded there was little or no correlation of chemical variation with increasing metamorphic grade, and that the silicate iron-formations have both low MgO/(FeO + Fe_2O_3) ratios and a fairly high oxidation state. Figures 48 and 49 in Crawford (1973) are MgO-FeO-Fe_2O_3 plots that demonstrate some of these points. However, the anthophyllite-bearing iron-formation contains the smallest proportion of Fe_2O_3 and ferrohypersthene-bearing iron-formation the highest, with grunerite schists plotting in between them, close to the point for hypersthene. This suggests that at least the oxidation state may have been modified during metamorphism. Some of Crawford's (1973) other conclusions listed below also bear on whether, or how much, the present facies compositions are a reflection of the primary compositions which are further discussed in "Origin".

1. Magnetites from the Mary River and Rowley River areas have uniform MgO, FeO, Fe_2O_3, and MnO content, which may represent the original ore composition.
2. More highly oxidized iron-formations throughout the region have a much lower content of these oxides, which may represent weathering and enrichment prior to emplacement of the volcanics that overlie the Mary River iron-formation (Table of Formations).
3. Only Mg shows a distinctly proportional distribution in coexisting magnetites and grunerites.
4. The Fe^{2+}, Mg, and Ti in magnetites decrease with increasing Fe^{3+} in silicate facies and are constant in oxide facies.
5. The Mg and Mn in grunerites increase, and Fe^{2+} decreases, with increasing Fe^{3+}.
6. Magnetites from the silicate facies have a lower Fe^{3+} content than those from the oxide facies.

Table 14. Analyses (weight per cent) of Mary River Group (Mif, Amif) iron "ore" and iron-formation.

Sample	J74/1	A9-65	A10-65	J51H-65	B118/2 Conc⧫	J112/1*	J248/5*	B127/2	B275/1*	Avg. 1	Avg. 2
Map area	$37G^{a}$	$37G^{a}$	$37G^{a}$	$37G^{a}$	$37G^{b}$	$37F^{c}$	$37F^{c}$	$37F^{c}$	$37E^{d}$	37F,G	37E-G
Analysis-Lithology	1-Q	2-P	3-P	4-P	5-Q	6-Q	7-Q	8-P	9-Q	10-P	11-Q
Fe_2O_3(T)	100.6	98.1	99.7	100.2	92.00	100.70	84.10	100.6	101.30	99.65	96.68
SiO_2	2.4	0.6	0.2	0.1	9.79	0.23	11.32	0.8	0.36	0.4	3.58
Al_2O_3	0.18	0.62	0.37	0.26	0.18	0.50	0.50	0.79	0.87	0.51	0.29
TiO_2	0.01	0.00	0.00	0.00	0.014	0.009	0.028	0.02	0.014	0.005	0.015
Fe_2O_3	69.2	98.1	99.7	99.1	62.40	69.44	75.30	97.6	70.58	98.63	69.88
FeO	28.2	0.7	0.0	0.2	26.6	28.11	7.91	1.16	27.68	0.52	22.98
MnO	-	-	-	-	-	-	-	-	-	-	-
MgO	0.18	0.01	0.05	0.01	1.20	0.36	0.22	0.24	0.50	0.06	0.32
CaO	0.01	0.01	0.06	0.03	0.100	0.021	0.060	0.09	0.080	0.045	0.04
Na_2O	0.00	0.00	0.00	0.00	NF	0.05	0.05	0.00	0.00	0.00	0.03
K_2O	0.00	0.00	0.00	0.00	-	0.05	0.05	0.03	0.00	0.01	0.03
P_2O_5	0.00	0.00	0.00	0.00	0.12	0.02	0.04	0.00	0.06	0.00	0.03
S	0.00	0.00	0.02	0.00	0.10	0.04	0.09	0.00	0.08	0.00	0.05
≡O	0.00	0.00	0.01	0.00	-	-	-	0.00	-	0.00	-
CO_2(T)	0.00	0.00	0.00	0.00	-	0.06	0.12	0.00	0.00	0.00	0.05
H_2O(T)	-	-	-	-	-	0.00	0.04	-	0.00	-	0.01
H_2O^+	0.02	0.39	0.28	0.00	-	-	-	0.18	-	0.21	-
H_2O^-	0.04	0.01	0.04	0.02	-	-	-	0.02	-	0.02	-
Soluble Fe_2O_3	-	-	-	-	90.50	100.5	83.10	-	100.3	-	97.97
Total	100.24	100.44	100.71	99.72	100.5	98.89	95.73	100.93	100.22	100.43	97.30
Ba	-	-	-	-	0.00071	0.00070	0.00078	-	0.00066	-	0.00078
Co	0.0021	NF	NF	NF	<0.002	0.0023	0.0030	NF	0.0023	NF	0.0024
Cr	<0.0020	<0.0020	<0.0020	0.0021	0.0070	<0.002	0.015	<0.0020	<0.0020	<0.0020	<0.0020
Cu	<0.0010	<0.0010	<0.0010	<0.0010	0.0021	0.0062	0.0032	<0.0010	0.0025	<0.0010	0.0032
Mn	0.17	0.026	0.078	0.011	0.0077	0.070	0.013	0.0056	0.13	0.030	0.096
Ni	0.0026	0.0036	0.0045	0.0040	0.040	0.018	0.077	0.0021	0.024	0.0036	0.030
Pb	NF	NF	NF	NF	-	-	-	NF	-	NF	-
Sr	-	-	-	-	0.0047	0.0058	0.0056	-	0.0059	-	0.0058
Ti	0.0042	0.0042	0.0050	0.0038	0.0046	0.0026	0.028	0.0042	0.0070	0.0043	0.0104
V	0.0013	<0.0010	0.0015	0.0011	<0.0020	NF	0.0035	0.0025	0.0037	0.0013	0.0021
Zr	NF	<0.0070	<0.0070	<0.0070	0.017	0.018	0.018	NF	0.017	<0.0070	0.013

Major elements determined by conventional chemical and atomic absorption methods. Minor elements determined by quantitative optical emission spectroscopy methods expected to be accurate to 15% of reported values. Mo, Nb, Sc, Sn, Ta, W, and Zn were looked for but not found in some samples, and may be present in amounts below the limit of quantitative determination in others.

NF - Not found.
- - Not determined.
a - Mary River area.
b - Ravn River area.
c - Rowley River area.
d - Northwest Barnes Ice Cap.
R - Hematite-oxide iron-formation.
S - Magnetite-hematite oxide iron-formation.
T - Mg-bearing silicate-oxide (magnetite ± hematite) iron-formation.
U - Mg- and Al-bearing silicate-oxide (magnetite ± hematite) iron-formation.
Avg. 1 - Average of samples 2, 3, 4, 8 (hematite-rich "ore").
Avg. 2 - Average of samples 1, 6, 7, 9 (magnetite-hematite "ore").

Table 14. (cont.)

Sample	C21/1	C21/2*	C19/1 Conc⧫	B118/2*	B293/2*	B278/6	C122E 035	C19/1*	Avg. 3	C70/1 65	Avg. 4	Avg. 5
Map area	$37C^{e}$	$37C^{e}$	$37C^{f}$	$37G^{b}$	$37F^{c}$	$37E^{d}$	$37C^{f}$	$37C^{f}$	$37C^{f}$	$37G^{a}$	$37C^{f}$	$37C^{f}$
Analysis-Lithology	12-P	13-P	14-Q	15-S	16-R	17-S	18-R	19-S	20-S	21-T	22-U	23-T
Fe_2O_3(T)	92.6	88.60	90.00	48.95	51.41	41.9	51.1	55.85	57.70	64.7	22.7	48.83
SiO_2	6.8	11.42	10.10	49.36	46.81	57.3	47.9	43.33	42.1	27.1	54.1	46.18
Al_2O_3	0.67	0.25	0.16	0.00	0.10	0.71	0.53	0.35	0.73	0.07	10.11	0.64
TiO_2	0.02	0.022	0.009	0.013	0.013	0.01	0.01	0.014	0.025	0.02	0.40	0.02
Fe_2O_3	92.0	87.20	62.80	28.97	50.21	26.9	50.3	47.87	38.65	39.7	7.4	23.97
FeO	0.56	1.26	24.45	17.97	1.08	13.5	0.77	7.18	17.10	22.5	14.3	23.1
MnO	-	-	-	-	-	-	-	-	-	-	0.19	-
MgO	0.02	0.02	0.09	0.20	0.05	0.88	0.03	0.18	0.48	5.71	5.03	3.52
CaO	0.04	0.093	0.038	0.400	0.024	0.23	0.02	0.071	0.260	2.63	1.86	0.50
Na_2O	0.00	0.00	0.05	0.04	0.04	0.00	0.09	0.09	0.00	0.00	1.02	0.04
K_2O	0.00	0.00	0.02	0.02	0.02	0.00	0.00	0.06	0.00	0.02	0.89	0.00
P_2O_5	0.00	0.07	0.04	0.16	0.02	0.00	0.00	0.04	0.00	0.00	0.06	0.02
S	0.00	0.13	0.04	0.08	0.09	0.00	0.01	0.14	0.01	0.04	0.24	0.07
≡O	0.00	-	-	-	-	0.00	0.00	-	0.01	0.01	0.09	0.03
CO_2(T)	0.00	0.00	0.54	0.96	0.22	0.00	0.00	0.38	0.01	0.00	0.00	0.02
H_2O(T)	-	0.00	0.00	0.22	0.00	-	-	0.04	-	-	-	-
H_2O^+	-	-	-	-	-	0.22	0.21	-	0.50	1.48	3.42	1.24
H_2O^-	0.02	-	-	-	-	0.00	0.01	-	0.03	0.04	0.01	0.04
Soluble Fe_2O_3	-	87.40	90.00	42.75	50.55	-	-	54.95	-	-	-	-
Total	100.13	100.47	98.34	98.39	98.68	99.75	99.88	99.75	99.89	99.30	98.94	99.33
Ba	-	0.00047	0.00067	0.00075	0.00061	-	-	0.00099	-	-	-	-
Co	NF	0.0021	0.0023	<0.002	NF	NF	NF	<0.0020	NF	NF	0.0020	NF
Cr	0.0067	0.016	0.014	0.017	0.028	<0.0010	<0.0020	0.015	<0.0020	<0.0020	0.0185	0.0014
Cu	<0.0010	0.0037	0.0028	0.0037	0.0045	0.00086	<0.0010	0.0051	<0.0010	<0.0010	0.0036	<0.0010
Mn	0.0020	0.0042	0.017	0.016	NF	0.34	0.031	0.032	0.023	0.17	0.096	0.29
Ni	0.0029	0.12	0.064	0.081	0.15	<0.0010	<0.0020	0.10	<0.0020	<0.0020	0.006	0.0011
Pb	NF	-	-	-	-	NF	<0.020	-	NF	NF	NF	NF
Sr	-	0.0036	0.0037	0.0028	0.0028	-	-	0.0030	-	-	-	-
Ti	0.0047	0.0036	0.0021	0.0046	0.0052	NF	0.0036	0.0064	0.014	0.0019	0.259	0.012
V	0.0018	0.0047	NF	NF	NF	NF	0.0013	NF	0.0020	<0.0010	0.013	0.0019
Zr	NF	0.014	0.015	0.0094	0.0092	<0.0070	NF	0.0089	NF	NF	0.0167	0.0078

e - Isortoq Fiord.
f - Eqe Bay.
* - Head sample (i.e. millhead) for Davis Tube Test.
⧫ - Concentrate from Davis Tube Test (*see* Johnson and Maxwell, 1981): these samples were too impure to be considered as mineral concentrates (*see* Table 15).
<0.010 - Present but less than 0.010
P - Hematite-rich "ore".
Q - Magnetite-hematite "ore".
Avg. 3 - Average of two samples, not listed in table, of oxide facies (magnetite + hematite) iron-formation from Eqe Bay.
Avg. 4 - Average of two samples, not listed in table, of Mg- and Al-bearing silicate-oxide (magnetite ± hematite) iron-formation from Eqe Bay.
Avg. 5 - Average of six samples, not listed in table, of Mg-bearing silicate-oxide (magnetite ± hematite) iron-formation from Eqe Bay.
Fe_2O_3(T) - All iron reported as Fe_2O_3.
≡O - Oxygen equivalent of reported sulphur, is subtracted from total.

Table 15. Analyses (weight per cent) of mineral concentrates from Mary River (Mif, Amif) iron-formation and iron "ore".

Sample	J74/1	C70/1-65	J112/1♦	J248/5♦	B127/2	B293/2♦	B275/1♦	B278/6	Avg.^{h}	C21/2♦	Avg.^{k}	A9-65	A10-65	A9-65
Mineral	**Magnetite**	**Magnetite^{x}**	**Magnetite**	**Magnetite**	**Magnetite^{x}**	**Magnetite**	**Magnetite**	**Magnetite^{x}**	**Magnetite**	**Magnetite**	**Magnetite**	**Maghemite^{x}**	**Hematite**	**Hematite^{x}**
Map area	37G^{a}	37G^{a}	37F^{c}	37F^{c}	37F^{c}	37F^{c}	37E^{d}	37E^{d}	37-E-G^{acd}	37C^{e}	37C^{e,f}	37G^{a}	37G^{a}	37G^{a}
Map unit	iron "ore"	silicate I.F.	iron "ore"	iron "ore"	iron "ore"	iron "ore"	iron "ore"	oxide I.F.	iron "ore" I.F.	iron "ore"	I.F. iron "ore"	iron "ore"	iron "ore"	iron "ore"
Fe_2O_3(T)	102.39	100.59	102.00	101.50	102.13	100.00	100.70	101.87	101.40	101.70	93.27	99.27	99.16	100.20
SiO_2	0.08	0.83	0.12	0.09	0.77	**	0.06	0.40	0.34	1.48	7.23	0.64	0.65	0.64
Al_2O_3	0.21	0.09	0.20	0.25	0.36	**	0.55	0.17	0.23	0.25	0.415	0.57	0.30	0.49
TiO_2	0.01	0.01	0.008	0.009	NF	**	0.009	NF	0.006	0.026	0.147	0.01	0.01	0.01
Fe_2O_3	70.55	67.46	70.02	69.30	69.42	50.30	68.70	67.61	66.67	65.74	64.53	86.74	86.59	98.21
FeO	28.65	29.81	28.76	28.95	29.43	44.70	28.76	30.83	31.24	32.35	26.67	11.27	11.31	1.79
MnO	0.26	0.07	-	-	0.08	-	-	0.34	0.09	-	0.065	0.02	0.12	0.03
MgO	0.09	0.27	0.32	0.36	0.12	**	0.52	0.11	0.26	0.10	0.404	0.02	0.08	0.02
CaO	0.02	0.18	0.021	0.020	NF	**	0.040	0.03	0.044	0.120	0.15	0.03	0.03	0.03
Na_2O	-	-	-	0.04	-	**	0.03	-	-	-	-	-	-	-
K_2O	-	-	-	0.02	-	**	0.00	-	-	-	-	-	-	-
P_2O_5	-	-	0.02	0.02	-	**	0.02	-	0.01	0.05	-	-	-	-
S	0.02	0.03	0.04	0.12	0.02	**	0.06	0.03	0.05	**	0.12	0.03	0.02	0.03
=O	0.01	0.01	-	-	0.01	-	-	0.01	0.01	-	0.049	0.01	0.01	0.01
CO_2(T)	-	-	0.64	0.88	-	**	0.08	-	0.23	-	-	-	-	-
H_2O(T)	-	-	0.00	0.00	-	**	-	-	-	-	-	-	-	-
Soluble Fe_2O_3	-	-	100.40	101.00	-	**	100.50	-	100.63	101.70	-	-	-	-
Total	99.88	98.74	100.15	100.06	100.19	95.00	98.83	99.51	99.17	100.12	99.68	99.32	99.09	101.24
Ag	NF	NF	-	-	NF	-	-	NF	NF	-	<0.00050	<0.00050	<0.00050	<0.00050
B	<0.050	<0.050	-	-	<0.050	-	-	<0.050	<0.050	-	<0.050	<0.050	<0.050	<0.050
Ba	<0.0010	<0.0010	0.00084	0.00077	<0.0010	0.00099	0.0035	<0.0010	<0.0010	0.00084	0.0010	<0.0010	0.0011	<0.0010
Ca	<0.020	0.13	0.026	0.033	NF	0.067	0.034	0.018	0.044	0.037	0.104	0.021	0.020	<0.020
Co	0.0021	NF	0.0030	0.0034	0.014	0.0031	0.0024	<0.0020	0.0043	0.0080	<0.0020	<0.0020	<0.0020	<0.0020
Cr	<0.0020	NF	<0.0020	0.012	NF	0.22	<0.0020	<0.0020	0.004	0.11	0.006	<0.0020	<0.0020	<0.0020
Cu	<0.0010	NF	0.0039	0.0051	NF	0.015	0.0030	<0.0010	0.004	0.012	<0.0010	<0.0010	<0.0010	<0.0010
Ga	<0.010	<0.010	-	-	<0.010	-	-	<0.010	<0.010	-	<0.010	<0.010	<0.010	<0.010
Mn	0.20	0.058	0.076	0.032	0.061	0.090	0.14	0.26	0.115	0.086	0.040	0.019	0.092	0.027
Ni	<0.0020	NF	0.017	0.048	0.024	0.090	0.021	<0.0020	0.033	0.22	0.02	0.0041	0.0043	0.0038
Sc	NF	NF	NF	NF	NF	NF	NF	NF	NF	NF	NF	NF	NF	NF
Sr	NF	NF	0.0060	0.0058	NF	0.0049	0.0056	NF	0.0028	0.0054	NF	NF	NF	NF
Ti	0.0051	0.0042	0.0017	0.0038	NF	0.012	0.0022	0.0022	0.0039	0.0045	0.088	0.0071	0.0043	0.0093
V	NF	NF	NF	0.0037	NF	0.0032	0.0041	NF	0.001	0.0041	<0.0010	NF	NF	NF
Y	0.0013	NF	-	-	NF	-	-	NF	NF	-	NF	NF	NF	NF
Yb	0.00056	0.00055	-	-	0.00057	-	-	0.00053	0.00050	-	NF	0.00052	<0.00050	<0.00050
Zr	<0.010	<0.010	0.019	0.016	<0.010	0.016	0.019	<0.010	<0.010	0.017	<0.010	<0.010	<0.010	0.010

NF = Not found
- = Not determined
** = Insufficient sample
I.F. = iron-formation

a = Mary River area
c = Rowley River area
d = Northwest Barnes Ice Cap
Fe_2O_3(T) = all iron reported as Fe_2O_3

e = Isortoq Fiord
f = Eqe Bay
=O = oxygen equivalent of reported sulphur, is subtracted from total

h = Average of eight preceding magnetite analyses, all from map area
k = Average of ten magnetites not listed in table, one from Isortoq Fiord and nine from Eqe Bay (Fig. 1)

Major oxides determined by conventional chemical, spectrochemical, atomic absorption, and other methods. Minor elements determined by quantitative optical emission spectroscopy methods, expected to be accurate to 15% of reported values. Nb, Sb, Ta, W, and Zn were either not found or not determined. Be, Mo, Pb, and Sn were not found in or not determined for most samples, but may be present below the limit of quantitative determination in some.

Table 15. (cont.)

Sample	J51H-65	B127/2	Avg.^{m}	Avg.^{n}	C70/1-65	Avg.^{o}	C115W 03N	C56W 47S	C115W 03N	B278/6	C180W 36N	JDC 13-3	JDC 13-3
Mineral	**Hematite**	**Hematite^{x}**	**Hematite**	**Hematite**	**Cummingtonite^{x}**	**Grunerite**	**Grunerite^{x}**	**Anthophyllite**	**Hornblende^{x}**	**Hypersthene^{x}**	**Chlorite**	**Almandine^{x}**	**Biotite^{x}**
Map area	37G^{a}	37F^{c}	37F,G^{ac}	37C^{ef}	37G^{a}	37C^{f}	37C^{f}	37C^{f}	37C^{f}	37E^{d}	37C^{f}	37C^{f}	37C^{f}
Map unit	iron "ore"	iron "ore"	iron "ore"	iron "ore", oxide I.F.	silicate I.F.	silicate I.F.	aluminous I.F.	silicate I.F.	silicate I.F.	oxide I.F.	aluminous I.F.	aluminous I.F.	aluminous I.F.
Fe_2O_3(T)	100.08	99.37	99.88	98.01	24.73	32.82	43.74	8.54	15.35	39.18	28.58	41.11	24.86
SiO_2	0.64	0.43	0.57	1.97	53.86	56.19	50.00	86.77	75.56	50.24	28.34	36.78	34.68
Al_2O_3	0.30	0.87	0.55	0.19	0.09	0.53	0.49	0.18	1.64	0.09	20.23	19.73	18.82
TiO_2	0.01	0.01	0.01	0.01	NF	0.01	0.01	0.01	0.02	NF	0.62	0.22	1.55
Fe_2O_3	99.25	99.37	98.94	97.54	9.87	1.80	NF	0.45	1.48	26.05	2.51	NF	1.13
FeO	0.75	NF	0.85	0.42	13.37	27.91	39.63	7.28	12.48	11.81	23.46	37.31	21.35
MnO	0.01	NF	0.01	0.04	0.79	0.57	0.63	0.19	0.40	3.10	0.48	1.15	0.02
MgO	0.01	0.01	0.01	0.01	12.22	8.94	6.80	4.11	3.93	9.76	11.13	2.50	7.82
CaO	0.03	0.04	0.03	0.02	5.87	1.32	0.20	0.16	1.77	1.03	0.84	0.95	0.09
Na_2O	-	-	-	-	0.16	0.10	0.15	0.16	0.14	0.50	0.38	0.07	0.38
K_2O	-	-	-	-	0.02	0.02	0.02	0.04	0.07	0.02	0.23	0.04	8.40
P_2O_5	-	-	-	-	-	-	-	-	-	-	-	-	-
S	0.02	0.02	0.02	0.02	0.03	0.08	0.18	0.05	0.03	0.03	0.08	0.03	0.03
=O	0.01	0.01	0.01	0.01	0.01	0.03	0.07	0.02	0.01	0.01	0.03	0.01	0.01
CO_2(T)	-	-	-	-	-	-	-	-	-	-	-	-	-
H_2O(T)	-	-	-	-	2.64	1.24	2.40	-	-	-	9.72	<0.01	4.10
Soluble Fe_2O_3	-	-	-	-	-	-	-	-	-	-	-	-	-
Total	101.01	100.74	101.00	100.21	98.91	98.68	100.44	99.38	97.51	102.62	97.99	98.77	98.36
Ag	<0.00050	<0.00050	<0.00050	<0.00050	NF	<0.00050	NF	-	-	<0.00050	NF	-	NF
B	<0.050	<0.050	<0.050	0.25	<0.050	<0.050	<0.050	-	-	<0.050	<0.050	-	<0.050
Ba	<0.0010	<0.0010	<0.0010	<0.0010	<0.0010	<0.0010	<0.0010	-	-	<0.0010	0.0068	-	0.21
Ca	<0.020	0.027	<0.020	<0.020	>5.0	0.95	0.14	-	-	0.74	0.60	-	0.061
Co	<0.0020	<0.0020	<0.0020	<0.0020	NF	<0.0020	<0.0020	NF	NF	NF	<0.0020	0.0023	0.0067
Cr	0.0021	<0.0020	<0.0020	0.0046	NF	<0.0020	<0.0020	<0.0010	<0.0010	<0.0020	0.014	0.023	0.045
Cu	<0.0010	0.0022	<0.0010	<0.0010	0.0057	<0.0010	<0.0010	0.00094	0.0010	0.0013	0.0046	0.00075	0.0017
Ga	<0.010	<0.010	<0.010	<0.010	NF	<0.010	NF	-	-	<0.010	NF	-	-
Mn	0.0092	<0.0020	0.012	0.026	0.61	0.55	0.49	0.15	0.31	2.4	0.37	0.89	0.016
Ni	0.0033	<0.0020	0.0027	<0.0020	NF	<0.0020	<0.0020	<0.0010	0.0022	<0.0020	0.015	0.0012	0.026
Sc	NF	NF	NF	NF	NF	<0.00050	NF	-	-	NF	<0.00057	0.0051	0.0051
Sr	NF	NF	NF	NF	NF	NF	NF	-	-	NF	0.014	-	NF
Ti	0.0049	0.0051	0.0064	0.0052	NF	0.0050	0.0050	0.0075	0.011	<0.0010	0.37	0.13	0.93
V	NF	0.0018	NF	<0.0010	NF	<0.0010	NF	NF	NF	NF	0.0071	0.015	0.062
Y	NF	NF	NF	NF	NF	<0.0010	NF	-	-	0.0015	NF	-	NF
Yb	<0.00050	0.00051	0.0050	<0.00050	NF	<0.00050	<0.00050	-	-	<0.00050	<0.00050	-	<0.0005
Zr	<0.010	<0.010	<0.010	<0.010	<0.010	<0.010	<0.010	<0.0070	<0.0070	<0.010	<0.010	0.020	<0.010

m = Average of three preceding hematites, all from map area.
n = Average of two hematites not listed in table, one each from Isortoq Fiord and Eqe Bay.
o = Average of four grunerites from Eqe Bay.

♦ = Magnetic concentrate from Davis Tube Test (*see* Tables 12 and 57; Johnson and Maxwell, 1981).
x = Minerals with same sample numbers are coexisting; e.g. C70/1-65, magnetite and cummingtonite; C115W 03N, grunerite and hornblende.
<0.050 = Probably present, but below the indicated level of quantitative determination.

Table 16. Summary of chemical differences between major iron-formation facies (weight per cent).

	Iron ore, oxide I.F.	Silicate I.F., silicate-oxide I.F.	Aluminous I.F.
Al_2O_3	<1	<1	ca. 10
Fe_2O_3	high	variable	low
MnO	<0.1	<0.5	<0.2
MgO	<1	3-6	2-11
TiO_2	<0.03	<0.03	0.06-1.6
CaO	<0.3	<2.7	1-6
Na_2O	<0.1	<0.1	0.7-3
K_2O	<0.03	<0.03	<1.3
H_2O	-	-	0.5-2
CO_2	<1	-	-

- = Not determined for enough samples to indicate a value or limit.
I.F. = iron-formation.

Analyses for Rb-Sr age determinations and for trace element studies (mostly REEs) in the Mary River area have been discussed by Fryer (1971a, b). Six samples of magnetite, hematite, and the oxide facies (supplied by G.A. Gross, Geological Survey of Canada) were analyzed for Co, Cr, Sc, Th, As, La, Ce, Nd, Eu, Sm, Ho, Yb, and Lu. Some of Fryer's (1971a, b) conclusions and comments are:

1. The absolute trace element abundances are very low.
2. Analyses from the Mary River area are notable for their diversity.
3. A minimum in the Nd to Gd range of rare-earth elements indicates that these rocks are relatively enriched in the heavy rare-earth elements as compared to Archean basalts.
4. A distinct positive europium (Eu) anomaly is present in five of the six samples analyzed.

A brief comparison was made between the chemical data for the Mary River iron-formation and high grade iron, and some data available for the Aphebian Sokoman iron-formation of the Labrador Geosyncline (Schwellnus, 1957; Fryer, 1971a, b). The trace element variations seem to be as great from one outcrop to the next in a given locality as from one locality to the next. Without doing a statistical analysis, there appears to be as great a variation in results of different workers for the same area as there appears to be between the Mary River and Sokoman iron-formations, although the trace element content may be slightly lower in the Sokoman iron-formation. Fryer (1971a, b) found that, unlike the Mary River iron-formation, the Sokoman does not have a positive Eu anomaly. However, G.A. Gross (pers. comm., 1991) has obtained similar patterned positive Eu anomalies for the oxide facies of both these iron-formations.

Classification and origin of the iron-formation

General comments

Many studies have dealt with the types and origins of iron-formation. An excellent summary of the more prominent work up to about 1962 has been provided by Gross (1965). Many subsequent studies have been discussed by Gross (1980, 1991) and Gross and Yeo (1987). The best reviews are symposia volumes by James and Sims (1973), Trendall and Morris (1983), and Appel and LaBerge (1987).

Most ferruginous sediments are either chemically precipitated, thinly banded chert and iron minerals, or ironstones containing oolitic chamosite-iron carbonate-goethite beds with variable clay and clastic detritus. There are two principal types of siliceous iron-formations, Algoma and Lake Superior (Gross, 1965, 1980).

The lithological nature (grain size, layering, composition, and relative proportion of facies) and extent of both types are quite similar, especially where deposition of the two types extends into deep shelf environments as depicted by Gross (1980, 1983). The major differences between the two types of iron-formation are in the associated rocks and the depositional environments, rather than in the iron-formations themselves. The Algoma type occurs with volcanic and greywacke rock lithologies along volcanic arc and rift zones etc., and the Lake Superior type occurs with quartzite, dolomite, and black shale in continental shelf environments. Gross and McLeod (1980) and Gross (1986) have shown that there are statistical differences in the chemical compositions of Algoma-type and Superior-type iron-formations, but the range of values for each element precludes differentiation solely on the basis of chemistry at present.

It is generally accepted that extensive banded iron-formations are predominantly chemical precipitates from well mixed, chemically homogeneous seawater, but agreement is lacking as to the source of iron and silica and the depositional environment. Most authors consider marine deposition in shelf to partially restricted and interconnected basins to be most likely, although lacustrine (Hough, 1958) and restricted evaporite basin environments (Trendall, 1973) have been postulated. As noted by Dimroth (1975), many of the banded iron-formations are detrital chemical sediments and have been deposited in depths of water ranging from below storm wave base to peritidal. Other banded iron-formations are exclusively to largely subtidal (Simonson, 1985), and include turbidites (Dimroth, 1975; Shegelski, 1987).

Two main sources for iron and silica are most likely. One is natural weathering of continental land masses (MacGregor, 1927; Towe, 1983; Lepp, 1987, Reimer, 1987). The second source includes hydrothermal, effusive, fumarolic, and exhalative processes related to volcanism (Van Hise and Leith, 1911; Gross, 1965, 1991; Simonson, 1985; Shegelski, 1987; Kimberley, 1989). Most of the recent chemical studies that include rare-earth elements favour the second main source (e.g. Derry and Jacobsen, 1990). The trace element content of metalliferous deposits formed on the present ocean floors directly from volcanogenic emanations (Gross, 1987; Gross and McLeod, 1987) is much higher than that generally found in banded iron-formations. This suggests that chemically precipitated iron-formations, if related chiefly to exhalative processes and related processes, were deposited at some distance from the vents, after thorough mixing in the ocean.

It is now commonly accepted that banded iron-formations (including the oxide facies) are of remarkably uniform and similar composition, are abundant throughout the geological record from at least 3.8 Ga ago, and that Archean iron-formations are much more abundant than formerly realized (Gross, 1973, 1983, 1991; Gole and Klein, 1981; James and Trendall, 1982; Appel, 1987; Zhai and Windley, 1989). Comparison of REE patterns show that similar iron-formations have similar REE patterns (e.g. positive Eu anomalies for the oxide facies) regardless of age. It has now been well demonstrated that one must be careful to compare the same facies (chemical with chemical, clastic with clastic, etc.) (Laajoki and Lavikainen, 1977; Graf, Jr., 1978; Derry and Jacobsen, 1990; G.A. Gross, pers. comm., 1991). These similarities imply similar genetic histories, and to some, that biogenic factors and the composition of the atmosphere had only a limited influence on the precipitation of the iron-formations from a well mixed homogeneous reservoir (Graf, Jr., 1978; Gole and Klein, 1981; Gross, 1983; Crocket and Bowins, 1985). However, others have proposed that free oxygen was available in the atmosphere to help precipitate iron as early as 3.8 Ga (MacGregor, 1927; Dimroth and Kimberley, 1976; Clemmey and Badham, 1982; Towe, 1983). Others contended that iron-oxidizing micro-organisms in the water precipitated iron and silica (LaBerge, 1973; Holm, 1987; LaBerge et al., 1987; Robbins et al., 1987).

Several models that espouse natural weathering as the main source for iron and silica consider the iron to have been removed in the reduced state, accompanied by silica, with the alumina left behind. It is then proposed that the iron was transported shoreward, after having accumulated in anoxic basins, by regionally upwelling seawater that brought iron-bearing minerals to the surface where they were oxidized and then redeposited (Borchert, 1960; Holland, 1973; Braterman and Cairns-Smith, 1987). In Towe's (1983) model, the early Earth (pre-3.8 Ga) was enveloped in a moist greenhouse atmosphere (H_2O, CO_2). Oceans as such did not exist initially. Extensive weathering and erosion under these conditions moved large amounts of iron and silica into anoxic ocean basins that enlarged as the Earth cooled and continents grew. Earlier formed redbeds would have been cannibalized. Some iron may have been transported by pore water in clastic sediments. Gross (1986) considered that iron and silica from hydrothermal effusive sources were deposited as iron-formation by direct chemical precipitation, flocculation, and by reworking of previously deposited material.

Iron-bearing carbonate and iron hydroxides or iron oxides are commonly considered to be the major primary minerals in banded iron-formations (Van Hise and Leith, 1911; Gross, 1980; LaBerge et al., 1987; Lepp, 1987). Replacement of carbonate by chert has been proposed as the origin for some iron-formations (Kimberley, 1974; Dimroth, 1977; Lepp, 1987). Primary oxides and hydroxides were probably modified by diagenesis, and most Precambrian iron-formations have been metamorphosed to some degree. Although the metamorphism of many iron-formations was probably isochemical (Gole and Klein, 1981) both diagenesis and metamorphism would destroy the evidence for the reducing or oxidizing nature of the depositional environment, the presence of redbeds in the Archean, and other primary features (Dimroth and Kimberley, 1976; Clemmey and Badham, 1982; Schau and Henderson, 1983; Rainbird et al., 1990).

There is an increasing awareness that many iron-formations and associated metal deposits are cogenetic and are primary stratafer (e.g. Gross, 1991: iron-bearing strata) deposits formed in response to hydrothermal and exhalative processes (King, 1969; Gross, 1986; Gauthier et al., 1987; Shegelski, 1987). Gross (1991) referenced an extensive literature, and considered three principal facies groups – iron-formation, manganese, and polymetallic Fe-Cu-Zn-Pb-Au-Ag-REEs-Ni-Mo-Sn-W-Sb – to be part of one genetic group.

Iron-formation

The iron-formation within the Mary River Group is a good example of the Algoma type as defined by Gross (1965, 1980), and has been so classified by Gross (1966, 1983) and Crawford (1973). Stratigraphy and composition are variable. The iron-formation is lensoid on the large scale, and is closely associated with various mafic and felsic metavolcanics, ultramafic rocks, and metamorphosed greywacke, siltstone, and metapelite (Gross, 1966; Jackson, 1966b, 1978b). Undisputed oolitic or granular textures have not been recognized in the iron-formation. However, remnants of thin bedded red jasper beds occur at Eqe Bay, and remnants of jaspery rock containing granule-like outlines occur locally in the Mary River area. Remnants of iron-formation in migmatite, some far from known well developed iron-formation, partially ingested iron-formation in granite, and presently unexplained aeromagnetic anomalies that resemble iron-formation anomalies suggest that the iron-formation was originally much more continuous and extensive than at present. This is typical of Algoma types as depicted by Gross (1973) for other shield areas. In addition to volcanic rocks, the Mary River iron-formation is underlain locally and variously by meta-arkose, metaconglomerate, metapelite, metaorthoquartzite, metachert, and rare carbonate rocks that could have been deposited in environments that range from terrestrial to neritic. Sedimentary features that could have formed in moderate to high energy environments, shallow water, or both occur chiefly in the associated rocks and include coarse to fine conglomerate-breccia and volcaniclastic lenses, channels associated with crossbeds, and graded beds. The iron-formation itself contains thin conglomerate-breccia

Table 17. Averages (weight per cent) and standard deviations for analyses of iron-formation facies and derived mineral concentrates from the Mary River Group (1-16), and the Piling Group (17, 18).

	High grade iron (1-3)			Oxide facies (4-7)				Silicate-oxide facies (8-12)					Aluminous facies (14-18)				
Lithology	**Rock**	**Magnetite**	**Hematite**	**Rock**	**Rock**	**Magnetite**	**Hematite**	**Rock**	**Rock**	**Magnetite**	**Cummingtonite**	**Hypersthene**	**Rock**	**Rock**	**Magnetite**	**Rock**	**Anthophyllite**
Source	1	2	3	4^{a}	5	6^{b*}	7^{b}	8^{a}	9^{c}	10^{cx}	11^{c}	12^{d}	14^{a}	15^{b}	16^{b}	17^{e}	18^{e}
No. of samples	10	5	4	56	6	2	1	26	8	7	6	1	14	2	1	2	1
Fe_2O_3 (T)	**96.65**	**100.76**	**99.86**	**54.05**	**53.79**	**86.27**	**96.22**	**51.49**	**49.95**	**96.30**	**33.29**	**39.18**	**22.64**	**25.3**	**96.93**	**15.95**	**27.62**
	6.07	1.52	0.37	24.76	4.31	11.72		23.61	13.70	8.45	11.21		17.93	13.86		7.57	
SiO_2	**3.42**	**0.45**	**0.59**	**43.71**	**45.27**	**14.38**	**3.29**	**45.78**	**45.19**	**5.26**	**54.77**	**50.24**	**47.62**	**49.40**	**2.72**	**55.00**	**49.14**
	4.65	0.32	0.11	25.12	3.86	11.02		22.77	14.49	7.49	5.93		16.43	8.91		4.10	
Al_2O_3	**0.50**	**0.32**	**0.48**	**0.65**	**0.41**	**0.48**	**0.13**	**0.65**	**0.58**	**0.19**	**0.45**	**0.09**	**12.33**	**13.86**	**1.08**	**13.84**	**7.72**
	0.24	0.14	0.28	0.49	0.31	0.08		0.27	0.40	0.09	0.31		4.17	4.74		3.05	
TiO_2	**0.012**	**0.01**	**0.01**	**0.03**	**0.02**	**0.03**	**0.01**	**0.02**	**0.02**	**0.04**	**0.01**	**NF**	**0.76**	**0.64**	**1.12**	**0.78**	**0.60**
	0.01	0.0	0.0	0.06	0.01	0.01		0.01	0.02	0.09	0.0		0.61	0.01		0.21	
Fe_2O_3	**85.32**	**79.14**	**98.96**	**42.37**	**42.44**	**57.56**	**96.05**	**34.02**	**26.30**	**64.92**	**3.41**	**26.05**	**10.78**	**5.95**	**64.59**	1.10	**2.16**
FeO	**9.58**	**19.45**	**1.08**	**10.49**	**10.20**	**25.83**	**0.15**	**15.69**	**21.83**	**29.01**	**27.44**	**11.81**	**10.65**	**17.4**	**29.10**	**13.50**	**22.91**
	12.91	9.02	0.62	8.48	8.21	4.24		9.58	6.60	2.61	11.53		6.49	5.66		6.08	
MnO	-	**0.10**	**0.01**	**0.16**	-	**0.04**	**0.07**	**0.28**	-	**0.10**	**0.61**	**3.10**	**0.29**	-	**0.19**	**0.18**	**0.10**
	-	0.10	0.01	0.30	-	0.02		0.32	-	0.11	0.31		0.35	-		0.02	
MgO	**0.16**	**0.06**	**0.01**	**1.01**	**0.24**	**0.40**	**0.01**	**1.55**	**3.46**	**0.41**	**9.13**	**9.76**	**8.74**	**4.25**	**0.40**	**8.12**	**12.03**
	0.17	0.05	0.01	1.39	0.22	0.07		1.20	1.54	0.20	2.40		6.02	0.18		3.49	
CaO	**0.05**	**0.03**	**0.03**	**0.37**	**0.17**	**0.19**	**0.03**	**0.56**	**0.77**	**0.09**	**1.89**	**1.03**	**2.52**	**1.00**	**0.22**	**4.19**	**1.09**
	0.03	0.005	0.01	0.52	0.16	0.14		0.66	0.92	0.06	2.49		3.16	0.54		2.86	
Na_2O	**0.01**	-	-	**0.01**	**0.04**	-	-	**0.008**	**0.03**	-	**0.12**	**0.50**	**0.16**	**1.12**	-	**0.52**	**0.35**
	0.02	-	-	0.03	0.04	-		0.03	0.04	-	0.08		0.25	0.02		0.25	
K_2O	**0.01**	-	-	**0.01**	**0.02**	-	-	**0.003**	**0.001**	-	**0.02**	**0.02**	**1.15**	**1.70**	-	**0.39**	**0.33**
	0.02	-	-	0.08	0.02	-		0.008	0.01	-	0.01		1.02	1.69		0.46	
P_2O_5	**0.02**	-	-	**0.14**	**0.04**	-	-	**0.16**	**0.01**	-	-	-	**0.17**	**0.05**	-	**0.06**	-
	0.03	-	-	0.14	0.06	-		0.05	0.02	-	-		0.09	0.05		0.04	
S	**0.04**	**0.02**	**0.02**	**0.02**	**0.06**	**0.02**	**0.01**	**0.17**	**0.07**	**0.16**	**0.10**	**0.03**	**0.19**	**0.27**	**0.08**	**0.0**	**0.03**
	0.05	0.005	0.005	0.02	0.06	0.00		0.36	0.12	0.34	0.10		0.37	0.30			
=O	**0.001**	**0.01**	**0.007**	-	**0.01**	**0.01**	**0.0**	-	**0.02**	**0.06**	**0.03**	**0.01**	-	**0.10**	**0.03**	**0.0**	**0.01**
	0.004	0.0	0.005	-	0.00	0.0		-	0.05	0.13	0.04		-	0.11			
CO_2(T)	**0.02**	-	-	**0.35**	**0.26**	-	-	**0.09**	**0.02**	-	-	-	**0.64**	**0.00**	-	**0.0**	-
	0.04	-	-	1.26	0.38	-		0.12	0.05	-	-		1.13				
H_2O(T)	**0.11**	-	-	**0.51**	**0.26**	-	-	**1.01**	**1.23**	-	**2.20**	-	**4.03**	**3.21**	-	**1.50**	**1.6**
	0.15	-	-	0.41	0.23	-		0.89	0.72	-	0.34		1.59	0.83		0.25	

Table 17. (cont.)

	High grade iron (1-3)			Oxide facies (4-7)				Silicate-oxide facies (8-12)					Aluminous facies (14-18)				
Lithology	**Rock**	**Magnetite**	**Hematite**	**Rock**	**Rock**	**Magnetite**	**Hematite**	**Rock**	**Rock**	**Magnetite**	**Cummingtonite**	**Hypersthene**	**Rock**	**Rock**	**Magnetite**	**Rock**	**Anthophyllite**
Source	1	2	3	4^{a}	5	6^{b*}	7^{b}	8^{a}	9^{c}	10^{cx}	11^{c}	12^{d}	14^{a}	15^{b}	16^{b}	17^{e}	18^{e}
No. of samples	10	5	4	56	6	2	1	26	8	7	6	1	14	2	1	2	1
Total	**99.25**	**99.57**	**101.18**	**99.83**	**99.33**	**98.92**	**99.75**	**99.97**	**99.49**	**100.12**	**100.12**	**102.62**	**100.03**	**98.75**	**99.47**	**99.18**	**98.05**
Ba	**0.0007**	**<0.001**	**<0.001**	**0.003**	-	**0.003**	**<0.001**	**0.002**	-	**<0.001**	**<0.001**	**<0.001**	**0.027**	-	**0.0024**	-	**0.0052**
	0.0002			0.001	-	0.001		0.001	-				0.038	-		-	
Co	**0.002**	**0.009**	**<0.002**	**0.0003**	-	**<0.002**	**<0.002**	**0.003**	**NF**	**<0.002**	**<0.002**	**NF**	**0.003**	**0.003**	**<0.002**	**0.0049**	**0.0082**
	0.0	0.009		0.0003	-			0.0002					0.002	0.001		0.0007	
Cr	**0.005**	**0.006**	**0.003**	**0.002**	**0.13**	**<0.002**	**<0.002**	**0.0014**	**0.001**	**<0.002**	**<0.002**	**<0.002**	**0.021**	**0.028**	**0.11**	**0.136**	**0.057**
	0.006	0.009	0.004	0.003	0.20			0.001	0.0005				0.04	0.004		0.119	
Cu	**<0.001**	**<0.001**	**0.004**	**0.001**	**0.002**	**<0.001**	**<0.001**	**0.001**	**<0.001**	**<0.001**	**0.0018**	**0.0013**	**0.006**	**0.006**	**0.0023**	**0.0019**	**0.0018**
			0.002	0.001	0.002			0.001			0.0021		0.006	0.002		0.0002	
Mn	**0.051**	**0.079**	**0.012**	**0.12**	**0.02**	**0.026**	**0.052**	-	**0.22**	**0.07**	**0.48**	**2.4**	**0.22**	**0.125**	**0.092**	**0.16**	**0.081**
	0.059	0.074	0.013	0.23	0.01	0.016		-	0.12	0.08	0.24		0.27	0.063		0.042	
Ni	**0.026**	**0.049**	**0.002**	**0.002**	**0.056**	**<0.002**	**0.002**	**0.005**	**<0.005**	**<0.002**	**<0.002**	**0.002**	**0.016**	**0.011**	**0.0075**	**0.025**	**0.048**
	0.04	0.091	0.001	0.006	0.063			0.007	0.005				0.035	0.001		0.004	
Sr	**0.005**	**NF**	**NF**	**0.0008**	-	**NF**	**NF**	**0.001**	-	**NF**	**NF**	**NF**	**0.008**	-	**0.0037**	-	**0.0034**
	0.001			0.0005	-			0.0007	-				0.013	-		-	
Ti	**0.007**	**0.005**	**0.006**	-	**0.008**	**0.016**	**0.0046**	-	**0.01**	**0.007**	**0.005**	**<0.001**	-	**0.47**	**0.67**	**0.48**	**0.36**
	0.007	0.002	0.002	-	0.005	0.008		-	0.01	0.006	0.003		-	0.057		0.085	
V	**0.002**	**NF**	**NF**	**0.001**	**NF**	**<0.001**	**<0.001**	**0.001**	**0.001**	**0.004**	**NF**	**NF**	**0.01**	**0.024**	**0.073**	**0.022**	**0.036**
	0.001			0.001				0.0009	0.0009	0.0004			0.008	0.0		0.004	
Y	-	**NF**	**NF**	**0.0006**	-	**<0.001**	**NF**	**0.0006**		**NF**	**NF**	**0.0015**	**0.003**	-	**NF**	-	**NF**
	-			0.0004	-			0.0005	-	-			0.002	-		-	
Yb	-	**0.0005**	**0.0004**	**0.0**	-	**<0.0005**	**<0.0005**	-	-	**<0.0005**	**<0.0005**	**<0.0005**	-	-	**0.00063**	-	**<0.0005**
	-	0.0001	0.0002	0.0	-			-	-				-	-		-	
Zn	-	-	-	**0.004**	**NF**	**NF**	**NF**	**0.003**	-	**NF**	**NF**	-	**0.012**	**NF**	**NF**	**NF**	**NF**
	-	-	-	0.008				0.002	-				0.01				
Zr	**0.008**	**<0.01**	**<0.01**	**0.005**	**NF**	**<0.01**	**<0.10**	**0.0004**	**<0.007**	**<0.01**	**<0.01**	**<0.01**	**0.013**	**0.014**	**<0.01**	**0.011**	**<0.01**
	0.008			0.001				0.0002					0.007	0.007		0.01	

Notes: For each element the upper figure (bolded) is the average and the lower is the standard deviation. Unless otherwise noted averages and standard deviations represent several localities within the map area and Eqe Bay area.

a - Average analysis and standard deviation for Mary River area (37G/5) only, supplied by G.A. Gross, Geological Survey of Canada, Ottawa.
b - Eqe Bay area only (37C).
c - Chiefly Eqe Bay area (37C).
d - Northwest Barnes Ice Cap (37E).
e - Piling Group iron-formation, Generator Lake area (27C).
Fe_2O_3(T) - all iron reported as Fe_2O_3.

* - High silica in individual samples (22%, 7%) due to poor separation.
x - High silica value of 22% in one sample (poor separation). The other six samples range from 0.40% to 4.6% with an average and standard deviation of 2.49% and 1.7% respectively.
(T) - All iron as Fe_2O_3, all C as CO_2, $H_2O(T) = H_2O + H_2O$.
NF - Not found.
- - Not analyzed.
=O - Oxygen equivalent of reported sulphur, is subtracted from total.

lenses, graded beds, and possibly rare granules or ooliths. Most greywacke-type metasediments associated with the iron-formation are probably turbidites.

The association and local interbedding of the Mary River Group iron-formation with felsic and pillowed mafic volcanics, ultramafic rocks, and graded metagreywackes together with the variable stratigraphy of the Mary River Group demonstrates deposition in a volcanogenically active, unstable marine environment such as a volcanic arc. A similar conclusion was reached by Gross (1983). The author agrees with Crawford (1973) that a period of volcanic and tectonic quiescence must have occurred which permitted the iron-formation to be deposited so widely, otherwise the Si-Fe-Mg-Ca chemical sediments of the oxide and silicate facies would have been drowned in clastics, something that seems to have happened only locally for the most part. Presence of a quartz-rich unit, albeit discontinuous, the upper quartzite member of which is gradational with the overlying iron-formation, also indicates a period of weathering and erosion during a period of relative stability. The paucity of Al and low level of trace elements in most of the Mary River iron-formation (this memoir; Fryer, 1971a, b) (oxide and silicate facies) is additional evidence for a period of erosion, weathering, and movement of Fe, Si, Mg, and Ca by some process during which the Al and trace elements were geochemically partitioned. The Mary River oxide facies iron-formation was tentatively considered by Fryer (1971a, b) to be a product of normal weathering, because it is not enriched in Cr (Tables 14, 17; *see* Table 48, Fig. 95). The nature of the rocks associated with the Mary River iron-formation, and worldwide association of iron-formations and metal deposits, suggest that the chemical sediments in the Mary River iron-formation were probably derived both from weathering of older crust and recently emplaced volcanic rocks, and from hydrothermal-exhalative processes related to the volcanism.

Aluminous facies iron-formation is a common, generally minor, component of the iron-formation that occurs at various stratigraphic positions in the Mary River Group. Locally most of the iron-formation is composed of this facies. Contacts of aluminous facies iron-formation with oxide facies iron-formation, and with metapelite-metagreywacke, are mostly gradational. The interlayering of the metapelite-metagreywacke with iron-formation indicates that the alumina in this iron-formation facies probably represents a clastic component that has been deposited in varying amounts with chemical precipitates. Variations in the composition of the aluminous facies indicate that this clastic component could range in composition from a shale or greywacke to a laterite. However, a few of the aluminous facies lenses in the Mary River No. 4 iron deposit area may be chemically altered sedimentary and/or mafic igneous rocks. Some of the contacts are sharp while others are discordant but drift covered, and could be either fault or intrusive contacts. Local leaching and enrichment, and metasomatism (K, Na), is also present in this area. The recognition of minor secondary sulphide in the iron-formation raises some doubt as to how much of the sulphide facies is a primary sedimentary rock. It is not known whether the secondary sulphide is remobilized primary sulphide, or whether it came from an external source.

There is a crude positive correlation between Al, Mg, Ca, Na, K, Ti, Co, Cu, and Ni in the aluminous facies (Tables 14, 16, 17; Appendix 5). The higher values of the elements noted above could represent both the clastic content, probably derived from felsic (e.g. K), mafic, and ultramafic (e.g. Ni) rocks, and the deposition of proximal volcanogenic exhalative material with little or no chemical partitioning. The aluminous facies, and volcanic rocks and metagreywacke interbedded with the iron-formation, demonstrate that tectonism and volcanism were still active locally during iron-formation deposition.

The Mary River iron-formation clearly has a variable thickness and cannot be traced continuously. In some places its continuity is broken by faulting and folding, migmatization, and ingestion by younger granite. In others it thins and dies out. Elsewhere its deposition may have been masked by an influx of clastic material or by volcanism, or it was eroded shortly after deposition. The Mary River Group and its correlatives that occur in the Committee Orogen may have extended continuously from Northwest Greenland southwest across Baffin Island to Melville Peninsula and the Woodburn Lake area (*see* Fig. 114, this memoir; Jackson, 1966b; Jackson and Taylor, 1972; Schau, 1982; Schau et al., 1982; Taylor, 1985), a distance of 2000 km. It is reasonable to assume, from its distribution throughout the belt, that much of the iron-formation was deposited in a laterally continuous fashion, in several coeval extensive basins and smaller basins, with and without interconnections. This is compatible with conclusions reached by Crawford (1973), Goodwin (1973), Gross (1983), and Towe (1983). Lack of shallow water indicators in the Mary River iron-formation and presence of graded bedding may be related to its deposition in relatively deep water. The apparent thinning and absence of iron-formation and underlying quartzite to the north is taken to suggest that a shoreline may have existed somewhere to the south during deposition.

High grade iron

Crawford (1973) considered all high grade iron deposits in the region to be premetamorphic. Field data, however, indicate that several generations of high grade iron deposits (almost entirely iron oxide) are present in the Mary River iron-formation and may be separated into two main categories: premetamorphic to synmetamorphic (metamorphosed), and postmetamorphic. Hematite granules and cobbles in the basal Cambrian Gallery Formation in the Mary River area (Jackson, 1966b), and in northwestern Baffin Island (Lemon and Blackadar, 1963) indicate that Precambrian high grade iron oxide had been unroofed and was being eroded at that time. The clasts are in large part martite, pseudomorphous after magnetite. The iron oxide is fine to coarse grained and resembles the metamorphosed high grade iron rather than the postmetamorphic high grade iron.

Most of the high grade iron deposits are medium- to coarse-grained iron oxide, chiefly magnetite, that occur both in the iron-formation and in migmatite. Locally these deposits have been intruded and partially assimilated by metamorphosed mafic and ultramafic rocks, and by both metamorphosed and unmetamorphosed granitic rocks. These deposits were recrystallized during metamorphism, were deformed with the associated rocks, and clearly belong to the first category. Most of these deposits are concordant layers and lenses, some of which have gradational contacts with overlying and underlying strata. It seems likely that at least some of these concordant beds are primary. However, although clasts of lean banded iron-formation have been found in Mary River Group conglomerate, breccia, and agglomeratic beds above the iron-formation, no high grade clasts have been identified.

Some relatively large lenses of fine- to coarse-grained, premetamorphic to synmetamorphic, high grade iron deposits, chiefly in the Mary River and Eqe Bay regions, have discordant relations with adjacent rocks and contain relics of low grade banded iron-formation. Most of these lenses are composed of magnetite, but some specularite lenses occur along faults and shear zones. Also, metamorphosed magnetite and hematite veins occur in iron-formation and in other rocks in the same regions, and small metamorphosed mafic and ultramafic dykes and sills occur in high grade iron deposits at Mary River. These relations indicate that some of the relatively large high grade iron formed by secondary enrichment, not long after the iron-formation was deposited, and prior to emplacement of mafic and ultramafic intrusions related to the Mary River igneous activity that was penecontemporaneous (discussed below) with sedimentation. Some metamorphosed high grade iron deposits in the Mary River area occur chiefly in the upper part of the iron-formation as it outcrops regardless of whether or not the iron-formation is overturned (*see* "Oxide facies", *see* Fig. 106). This suggests that some deposits are replacement types formed after considerable deformation, but before the main metamorphism.

Parts of the high grade bodies, especially in the No. 1-3A iron deposits at Mary River and some in the Eqe Bay region, are probably postmetamorphic. Very fine- to fine-grained massive magnetite and massive to porous, blue, "clinker-like" hematite lack any indication of high grade metamorphism and intense deformation. Although fine grained hematite in No. 2-3A iron deposits becomes coarser grained to the east, it is not certain whether the clinker-like hematite also does or whether it lenses out instead. In view of the intense deformation undergone by the iron-formation it does not seem likely that the clinker-like hematite at No. 1 iron deposit is predeformation high grade iron oxide that somehow escaped being affected by metamorphism and deformation. The age of these high grade bodies is uncertain other than that they are post-2.6 Ga and likely post-1.9 Ga. The author finds this unmetamorphosed high grade iron oxide to be megascopically similar to unmetamorphosed late Phanerozoic ore in the Schefferville region of the Labrador Geosyncline, and to be identical to hematite ore pods in the Neohelikian (ca. 1.27 Ga) Society Cliffs Formation near Nanisivik, 270 km northwest of Mary River (Blackadar, 1970; Olson, 1977, 1984; Jackson et al., 1978a). The hematite pods near Nanisivik probably formed by oxidation of pyrite-pyrrhotite pods that were emplaced when the Nanisivik lead-zinc ore was emplaced. The lead-zinc ore is intruded by a Hadrynian (Franklin-723 Ma) diabase dyke, which gives an upper limit for the age of the ore but not the time of oxidation of the sulphide to hematite.

The presence of high grade, fine grained, red earthy to blue, soft hematite and hematite breccia; alteration of garnet to form goethite pseudomorphs; goethite deposition; and leaching and kaolinization of silicate minerals, have been noted in or adjacent to the No. 1 iron deposit (Gross, 1966). These features all indicate that some leaching and enrichment have taken place in relatively recent time. Some of the leached and enriched strata south of No. 4 iron deposit are too delicate to have survived glaciation and are either Recent or occur at an old erosion surface beneath Paleozoic strata that has recently been stripped off. Gross (1966) considered that this activity occurred prior to glaciation, and was arrested when the present stage of permafrost developed.

Nature of metamorphism

Metamorphism of the iron-formation was probably not entirely isochemical, but there were probably no large-scale changes other than in H_2O and CO_2 content, and the local leaching and iron enrichment processes that produced high grade iron deposits. Crawford (1973) considered the metamorphism to be isochemical, and that variations in present oxidation state, and highly erratic variations in major and minor elements in the high grade deposits, were primary features or related to leaching and enrichment prior to metamorphism.

Several features of the iron-formation and high grade iron suggest that in some places at least the degree of oxidation was altered during metamorphism and/or deformation, and that metamorphism was not isochemical. Some of Crawford's (1973, Fig. 48) data suggest that the degree of oxidation of iron may have increased crudely with increasing metamorphic grade. Also the high grade iron deposits are invariably specularite wherever they have been highly sheared.

Studies of iron-formations in the Lake Superior region and in the Labrador Geosyncline show that silicate and silicate-oxide facies generally increase in relative abundance with an increase in metamorphic grade (Mueller, 1960; Kranck, 1961; Jackson, 1962; Floran and Papike, 1978; Klein, 1983). This is commonly accompanied by a decrease in carbonate content, which suggests a breakdown of carbonate minerals. The presence of Mg-Fe and Ca-Mg-Fe silicates that contain negligible amounts of other elements, and of Ca and Mg in the oxide facies and high grade iron suggests that ferruginous carbonates may have broken down during metamorphism with escape of CO_2. Commonly, as metamorphism increases, the proportion of carbonate decreases in iron-formation with a consequent increase in silicates. Spherulites and rosettes of amphiboles may form from nodular carbonates, for example. The presence of amphibole needles extending into quartz indicates that such a reaction has occurred. Fryer (1971a, b) concluded that carbonate complexing was probably important in the marine geochemistry of the rare-earth elements, and it seems likely that carbonates, now very minor, were originally more abundant in the iron-formation. Trace elements in the carbonates would be largely transferred to the silicates.

The sharp contacts between interbedded laminae rich in magnetite and/or hematite, iron silicates, quartz, magnetite+iron silicates, iron silicates+carbonate, and carbonate have been interpreted by Crawford (1973) and others as being indicative of isochemical metamorphism of iron-formation. This is probably true generally, at least for the major oxides, although abruptness of some laminae contacts may have been accentuated by metamorphism. Although the major element composition of most of the iron-formation has probably not changed significantly since deposition, there has probably been considerable removal of water from the original hydrous gel of the chemical precipitate. This water may have flushed out, or at least altered, much of the minor and trace element content. The presence of quartz veins and iron oxide veins concentrated in and adjacent to the iron-formation, and the discordant nature of some high grade iron deposits, both attest to movement of material, and probably a loss, gain, and/or exchange of some elements, at least locally.

Metasediments (Ms)

Description

Although the various metasedimentary lithologies were differentiated at individual outcrops, the reconnaissance nature of the fieldwork together with the interbedding of the lithologies, the complex structures, and the various degrees of anatexis that are commonly present, make it difficult to delineate individual lithologies on the maps, and to determine their precise stratigraphic positions.

This unit is composed chiefly of metasiltstone- and metagreywacke-type schists and gneisses (Fig. 42). Metapelites are almost invariably present, locally abundant, and similar to those already described. Meta-arkosic rocks, although regionally a minor component, are abundant in a few places. Minor impure biotite-rich and muscovite-rich quartzite, amphibolite, felsic and mafic metavolcanics, and local white quartzite, metaconglomerate, metamorphosed tuff-agglomerate, mylonite, and marble are also present. Lit-par-lit gneiss is abundant, and commonly all of the metasediments have been recrystallized to schist or gneiss. Most of the minor lithologies are similar to major components in other units and, except for the metamorphosed conglomerate-breccia-tuff and marble, are described elsewhere. The rocks of this unit are generally at least 150 m thick. They are estimated to range from 300-1200 m thick between No. 1 and No. 4 iron deposit areas, and are probably considerably thicker south of Tay Sound (NTS 37G) and in the Eqe Bay area.

Modal analyses for these rocks are presented, along with those for metapelites, in Figures 20Kc and 29, and in Tables 5 (included in unit M) and 6. Chemical data are given in Appendices 2-4 and 6, in Tables 47 and 48, and in Figure 95.

Metasiltstone-metagreywacke, meta-arkose

These metasediments seem to be more abundant stratigraphically above the main iron-formation than below it in both the Mary River-Tay Sound region (NTS 37G) in the northwestern part of the map area, and in the Eqe Bay region just south of the map area. The stratigraphy is less well known between these two regions (Fig. 1, 12, *see* Fig. 113, 114) in the east-trending Nina Bang-Maino Lakes belt (northern NTS 37F) and north of the Barnes Ice Cap (NTS 37E), but the same relationships are considered to hold there also. The metasiltstones-metagreywackes and associated metasediments generally form layered sequences between mafic metavolcanics. The thickness of these sequences varies from place to place, but overall the amounts of metasiltstone-metagreywacke and mafic metavolcanic rocks seem to be about equal and together form most of the Mary River Group.

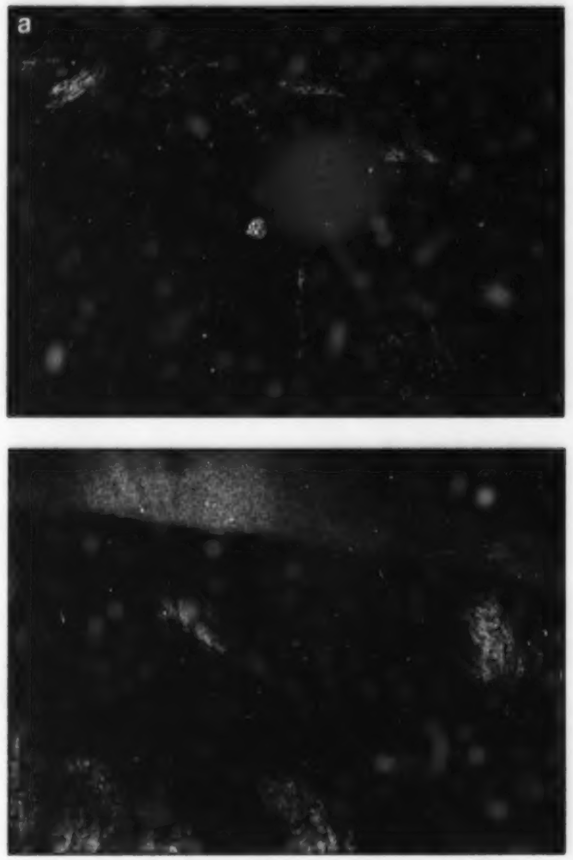

Figure 42. ***a)*** *Migmatitic, fine grained biotite-hornblende paragneiss and minor arkosic paragneiss, southwest of the head of Cambridge Fiord (NTS 37H). Pen for scale at centre right. Photograph by W.J. Crawford. GSC 186321.* ***b)*** *View northwest at amphibolite and paragneiss in an isoclinal fold dipping northeast with what seems to be a detached granitic block in its core. Chiefly banded migmatite* (**Amg**) *to the southwest (left) and nebulitic granitic rocks* (**Amn**) *to the northeast (right). Near the head of Gibbs Fiord (NTS 37E), in a region containing thrusts and nappes. Photograph by S.L. Blusson. GSC 185714*

Primary layering is mostly thinly laminated to thin bedded, but some rocks range up to very thick bedded and massive (Table 2). The more common individual lithologies predominate in zones up to 150 m or more thick that are interlayered with zones in which other lithologies predominate. Graded bedding is preserved in several of the less intensely deformed and metamorphosed areas, but crossbeds are rare. The rocks are completely recrystallized, and generally metamorphism and deformation have obliterated primary sedimentary structures. Some of the present layering is locally lensoid and discontinuous, and is secondary, related to shearing, flow banding, and anatexis.

Metasiltstones and metagreywackes are probably the most abundant metasediments in the Mary River Group. They and the minor meta-arkoses are chiefly fine- to medium-grained and equigranular, commonly with a salt-and-pepper appearance. However, they range from very fine- to coarse-grained and include porphyroblastic and augen gneisses containing megacrysts of plagioclase, potassium feldspar, garnet, quartz, and locally, aluminosilicate minerals. Most fresh rock surfaces are light to dark grey, but some are various shades of greyish green to green, off-white and pink to grey, mottled pinkish grey, and brownish grey. Weathered surfaces are chiefly grey to brown, greenish grey, or rusty coloured.

The major minerals in these rocks are quartz, plagioclase (albite-labradorite), microcline, orthoclase, biotite, muscovite, hornblende, garnet, and, locally at least, chlorite, clinozoisite-epidote, hypersthene, and clinopyroxene. Common minor and accessory minerals include chlorite, zircon, apatite, pyrite, magnetite, sphene, kaolinite, and clinozoisite-epidote. Less common are calcite, rutile, hematite, pyrrhotite, graphite, chalcopyrite, sillimanite, staurolite, cordierite, and rarely spinel and prehnite. Assemblages are presented in Table 18.

Metamorphosed conglomerate-breccia-tuff

Metaconglomerate lenses have been found chiefly in the Mary River and Eqe Bay regions during relatively large-scale mapping in those regions, and may be more abundant elsewhere than is known presently. Several lenses of polymictic metaconglomerate-breccia in metasiltstone-metagreywacke rocks (Fig. 43) and in basic metavolcanics of the Mary River Group contain a greater variety of clasts, including iron-formation, than do metaconglomerate and metavolcaniclastic lenses in the metapelite-amphibolite and quartz-rich units described above.

Most of the metaconglomerate lenses in the Mary River area are about 1-2 m thick, 5-30 m stratigraphically above the main iron-formation, and contain clasts up to 20 cm in diameter. Layering in the metaconglomerate lenses and in the adjacent rock is commonly ill defined. Most clasts are rounded and have been deformed and considerably elongated, locally parallel to mineral and fold-axis lineations. Some clasts were brecciated rather than stretched during deformation (Fig. 43). Some breccia lenses are composed chiefly of angular clasts. Most clasts are composed of very fine- to fine-grained felsic metavolcanics (and shallow granitic intrusions?) of rhyolite to dacite composition containing metaphenocrysts of altered oligoclase-andesine in a finely recrystallized quartz-feldspar matrix (Fig. 43). Some plagioclase metaphenocrysts are euhedral, and most have partially resorbed margins. Some very finely recrystallized areas resemble shards. These clasts seem to have been preserved from complete recrystallization by the buffering action provided against stress by the matrix.

Coarse grained quartzite and fine grained quartz-rich clasts are common and locally form the bulk of the clasts. Most of the fine grained quartz-rich clasts are laminated, and are chiefly metachert, lean quartz-silicate- and lean quartz-silicate-oxide-iron-formation. Amphibolite (mafic metavolcanic?), metapelite, and metasiltstone-metagreywacke clasts are abundant or predominate locally, but are less common than quartzite clasts. Meta-arkose, pink granite, and lean oxide iron-formation clasts have also been identified.

Similar metaconglomerates overlie iron-formation in the Eqe Bay area. According to Crawford's (1973) description (*see* Bethune and Scammell, 1993; Scammell and Bethune, 1995a), they are thicker and more continuous than those in the Mary River area. A massive flat-pebble metaconglomerate zone overlies oxide iron-formation and contains rectangular clasts of lean iron-formation and lensoid clasts of greenish volcanic rock. A second boulder metaconglomerate zone overlies argillite and chiefly silicate iron-formation, and contains lean iron-formation clasts up to 0.3 m across in a matrix of rounded carbonate grains and minor acicular chloritoid needles. According to Crawford (1973), this boulder metaconglomerate overlies pebble metaconglomerate directly and unconformably at one locality.

Matrix types, in order of decreasing abundance, are metapelite-metagreywacke, amphibolite (perhaps mafic metatuff), and minor meta-arkose. One metagreywacke-type matrix is composed of quartz, plagioclase, hornblende, and biotite. Metamorphism and deformation makes it difficult to ascertain the true nature of some of these conglomerate-breccia lenses. They are all concordant with present layering and most were probably deposited as a result of normal weathering and erosion in a moderately stable environment. However, some layering and some metaconglomerate lenses may be tectonic, or a result of explosive volcanism.

Carbonate rocks

Calcite beds generally up to 5 cm thick occur in Mary River metasediments locally at several places. Thicker beds are rare. One calcite-rich bed about 1 m thick (Fig. 44a) occurs in metasediments near iron-formation in the northeast corner of the Steensby Inlet map area (NTS 37F). The other major component is diopside, while minor minerals are prochlorite, serpentine, and green spinel. Locally, calcite is present in amounts up to several per cent in the metasediments, and seems to be a primary constituent. The abundance and local

Table 18. Some common prograde mineral assemblages[1] in metasiltstone-metagreywacke, and minor meta-arkose (unit Ma) of the Mary River Group[2].

Assemblage:	1	2	3	4	5	6	7	8	9	10	11	12	13	14	15	16	17	18	19	20	21	22	23	24	25	26	27	28	29	30	31
Quartz	+	+	+	+	+	+	+	+	+	+	+	+	+	+	+	+	+	+	+	+	+	+	+	+	+	+	+	+	+	+	+
Albite					+	+	+																								
Oligoclase-labradorite																	+		+	+	+	+					+	+		+	+
Plagioclase	+		+											+	+	+							+	+							
K-feldspar					+	+	±									+			+	+	±	±						+		+	
Clinozoisite	+										±	+																			
Epidote		+	+																			±									
Prehnite	+																														
Chlorite		+	+	±				+	+	+				±			+	±													
Biotite	+				+	+	+			+	+	+	+	+	+			+	+	+	+	+		+	+	+	+	+	+	+	±
Muscovite	+		+	+	+	+				+	+	+		+	+	±		±	+	+								±			
Cummingtonite								+																							
Actinolite										+														+							
Hornblende					+				+		+		+							+		+	+	+							
Clinopyroxene																															+
Hypersthene																														+	+
Garnet						+				+	+		±						+						+	+	+	±	+		
Spinel																													+		
Cordierite																										+					
Staurolite																									+						
Sillimanite																											±	+	+		
Calcite										+	+	+			+		+	±													
Magnetite								+	+					+			±								+	+			+		
Graphite								+	+																						

1 - Assemblages listed occur within a thin section. Some represent many thin sections, others only a few.

2 - The assemblages range in a general way, from subgreenschist for No. 1 to granulite facies for No. 30, 31 assemblages.

+ - Mineral is present. ± - Mineral is present in some assemblages, not in others. Two minerals represented by ± in an assemblage indicates there are four combinations represented, etc.

predominance of metamorphic tremolite-actinolite, hornblende, epidote, and feldspar (Fig. 44b) in the Mary River metasediments (Ms) suggest carbonate minerals may have been more extensive prior to metamorphism than now, and combined with silica during metamorphism to form Ca-Mg-Fe-silicate minerals.

Contact relations

The metasediments within this unit (Ms) are gradational with one another and with adjacent metasediments in the Mary River Group such as the iron-formation. Gradations into lit-par-lit anatectite and feldspar-megacrystic gneisses are common along the margins of larger areas underlain by Mary River rocks, and throughout many of the smaller remnants still recognizable as Mary River. The metasediments seem to be conformable with interlayered mafic metavolcanics but the contacts are commonly obscured or sheared. The presence of metamorphosed conglomerate-breccia lenses that contain clasts of Mary River Group rocks suggests that at least local disconformities may be present.

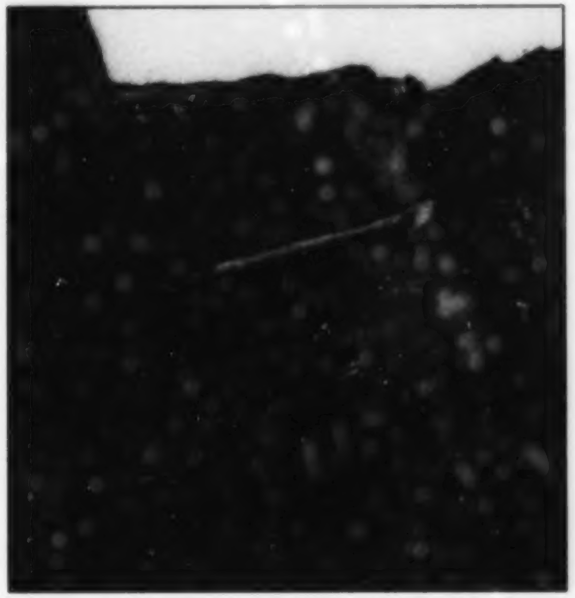

***Figure 43.** Metamorphosed conglomerate-breccia southeast of No. 1 iron deposit, Mary River area (NTS 37G). Angular fragments and stretched rounded clasts to 15 cm across represent both clastic and tectonic fragments of fine- to coarse-grained quartz, very fine grained feldspar, and medium grained plagioclase-hornblende. Stretching is greatest in a vertical direction and seems to vary in intensity over short distances. Note the fragment to the left of the hammer handle that has been brecciated in situ. Metagreywacke-type matrix. Photograph by G.D. Jackson. GSC 118326*

Chemistry

Some of the spectrographic analyses listed under M and Ms in Appendices 2-4, are for specimens of Mary River Group metasiltstone-metagreywacke and two or three analyses are for arkosic samples. Analyses for these samples are included with some for metapelites in column b of Table 10. Comparison of individual and average analyses suggests that the analyses are not greatly different than those for ordinary metapelite and metasiltstone-metagreywacke, and that most of the conclusions reached for the metapelites in the metapelite-amphibolite unit are valid for these rocks as well. The reader is referred to that discussion for more details.

Origin

Preservation of abundant graded beds in some areas and general lack of crossbeds suggest that most of the metasiltstones and metagreywackes may be turbidites. Their large regional

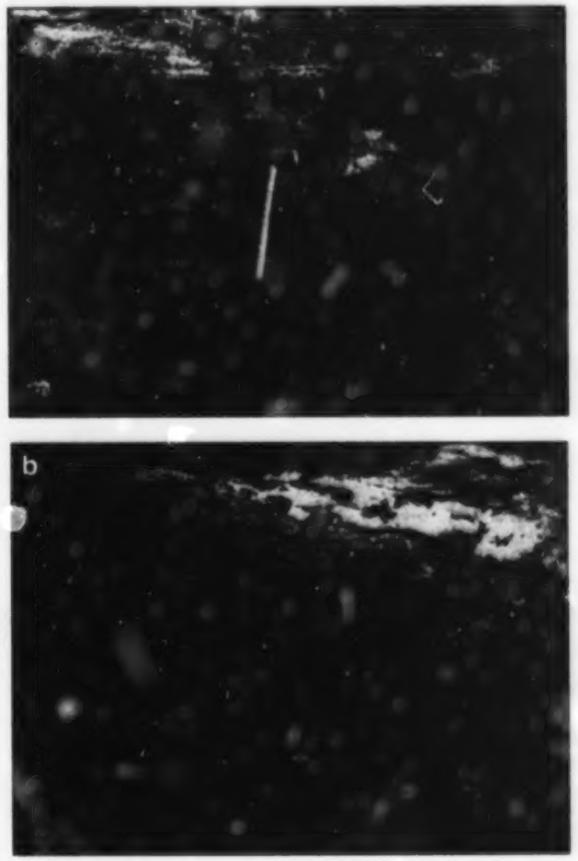

***Figure 44. a)** Quartz-rich calc-silicate rock in the northeast corner of map area NTS 37F. Note recumbent folds. Photograph by G.D. Jackson. GSC 186918. **b)** Hornblende crystals in an epidote-hornblende-plagioclase rock in the Mary River area (NTS 37G). The block is about 60 cm long. Photograph by W.J. Crawford. GSC 1997-54K*

extent, association with pillowed mafic volcanics and rare calc-silicate and carbonate lenses suggests marine deposition in a volcanically active region. Most of the metamorphosed conglomerate-breccia lenses have gradational contacts with adjacent metasediments. The angular nature of many of the clasts in these lenses (Fig. 43) indicates relatively little transport prior to deposition. The lenses may have formed in response to local episodic uplift related to faulting (rifting?) and erosion, or during explosive volcanism. Their lensoid nature, variable stratigraphic position, immaturity, and clast angularity suggest that these coarse clastics do not mark a well established ancient shoreline.

The felsic metavolcanic clasts in the metaconglomerates in the Mary River area resemble the felsic metavolcanics in the basement complex (Agn) more closely than the felsic metavolcanics in the Mary River Group. Megascopically, many of these clasts texturally resemble the massive to foliated components of the white to pale grey medium grained granitic gneisses that occur in the basement complex. The finely crystalline quartz-rich material in the metavolcanics may have been recrystallized to medium grained quartz in the coarser gneisses. Therefore a considerable part of the granitic basement rocks (Agn, Amn, gr-Agr) may be recrystallized felsic volcanics (*see* "Origin" in section "Nebulitic granitic migmatite (Amn)").

Another interesting feature of the metamorphosed conglomerate-breccia lenses is the apparent absence of high grade iron-formation clasts, although lean cherty iron-formation clasts are present and hematite-ore clasts are abundant in the basal Paleozoic conglomerate. This absence of ore clasts suggests that either primary high grade material was not uncovered during the formation of the conglomeratic lenses or that few, if any, of the high grade deposits are primary and had not been formed when the metaconglomerates were deposited.

Mafic metavolcanics (Mb, AMb)

Description

As much as 2000 m of chiefly mafic metavolcanics may be present between No. 1 and No. 4 iron deposits in the Mary River area (NTS 37G), and greater thicknesses may be present south of Tay Sound (NTS 37G) and just south of the map area in the Eqe Bay area (NTS 37C; Crawford, 1973; Bethune and Scammell, 1993; Scammell and Bethune, 1995a). Elsewhere mafic metavolcanic rocks (Fig. 45) predominate in zones up to about 300 m thick, although most are not more than 150 m thick. The mafic metavolcanic zones commonly alternate with metasediment-rich zones, chiefly metasiltstone-metagreywacke. Minor metasediments (chiefly metamorphosed siltstone-greywacke and metapelite; some hornblende gneiss (possibly metatuff), local iron-formation, quartzite, and conglomerate-breccia) and local felsic metavolcanics (rhyolite-dacite) occur in the mafic metavolcanic-rich zones. Minor metamorphosed mafic and ultramafic sills and dykes are also present. These minor lithologies are as described elsewhere in this memoir.

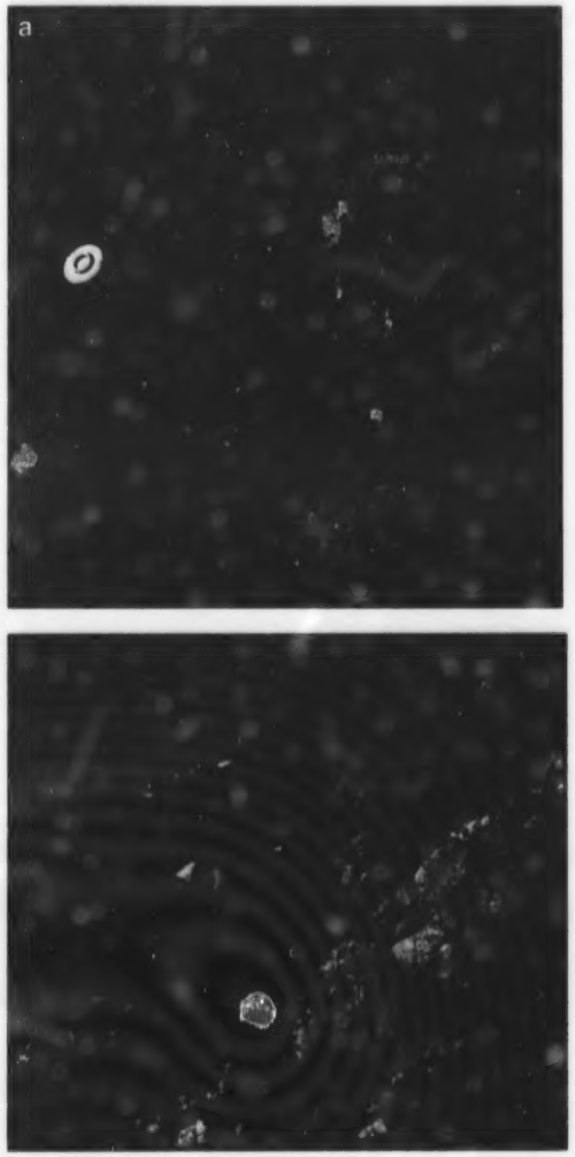

Figure 45. ***a)*** *Pillowed mafic metavolcanics near the No. 4 iron deposit in the Mary River area (NTS 37G). The pacer is about 5 cm in diameter. Photograph by G.D. Jackson. GSC 118280.* ***b)*** *Mary River Group amphibolite with minor quartz-biotite-feldspar paragneiss overlying massive, fractured pink granite along a fault, between No. 1 and No. 4 iron deposits, Mary River area (NTS 37G). Photograph by W.J. Crawford. GSC 1997-54L*

Modal analyses for mafic metavolcanics are provided in Figures 20Jb and 29. Chemical data are provided in Appendices 2-4, and in Tables 20, 47 (column S), and 48 (column 13). Figures 46-50 and 95 show plots of several different elements and oxides.

Most of the mafic metavolcanics are of basaltic composition, but include some andesite (Crawford, 1973), and felsic varieties occur locally. Small amounts of pyroclastics accompany the flows in many places. The metavolcanics are chiefly fine- to medium-grained and medium to dark greyish green and

Table 19. Some common metamorphic mineral assemblages in Mary River Group mafic metavolcanics (Mb, AMb)[1].

Assemblage:	1	2	3	4	5	6	7	8	9	10	11	12	13	14	15	16	17	18	19	20	21	22
Albite		+			+	+	+	+	+	+												
Oligoclase-bytownite												+	+		+	+	+	+	+		+	
Plagioclase																						
Microcline																			+			+
K-feldspar																					+	
Quartz				+		+	+	+	+	+	+	+				+	+	+	+	+	+	
Anthophyllite												+										
Cummingtonite																						
Actinolite		+	+	+					+													
Hornblende						+	+				+			+	+	+	±	+	+	+	+	
Diopside																						
Hypersthene																						
Garnet																						
Biotite	±	+	+	+	+		+				±					±	+			+	±	
Muscovite	+		+				±	+									+	+				
Chlorite	+				+	+	+	+	+	+	+	+	+	±	+							
Clinozoisite									+									+			±	
Epidote		+			+	±				+			+	±		±	±		±	±		+
Prehnite	+																					
Pumpellyite	+																					
Talc																						
Calcite			+	+				+							+	±					±	
Magnetite																				±		

Assemblage:	23	24	25	26	27	28	29	30	31	32	33	34	35	36	37	38	39	40	41	42	43	44
Albite																						
Oligoclase-bytownite	+	+	+	+	+	+	+	+	+		+	+	+	+	+	+	+	+	+	+	+	+
Plagioclase																						
Microcline					+						±					±	±					
K-feldspar																						
Quartz	+			+	+			±	+		±	+	+	±					+		+	+
Anthophyllite							+															
Cummingtonite								+	+													
Actinolite																						
Hornblende		+	+			+	+	+	+	+	+	+		+	+	+	+	+	+	+	+	
Diopside										+	+	+	+	+	+	+	+	+		+	+	+
Hypersthene																		±	+	+	+	+
Garnet			+	+		+															+	+
Biotite	+	+		+	+		+		+		+		+	+	±				+	+		+
Muscovite						+	±							+				+				
Chlorite																						
Clinozoisite															±		+					
Epidote	±					+				+		+				+						
Prehnite																						
Pumpellyite																						
Talc										+		±										
Calcite												+				+	+					
Magnetite									+												+	

1 - The assemblages range in a general way, from subgreenschist for No. 1 to granulite facies for No. 44 assemblage.
+ - Mineral is present. ± - Mineral is present in some assemblages, not in others. Two minerals represented by ± in an assemblage indicates there are four combinations represented, etc.

Table 20. Analyses of Mary River Group metabasalt and some other mafic rocks.

Source	Crawford		This memoir: Group IV, Table 48		
	1973	Mb	Mg	Amn^f	Amg^g
SiO_2	54.38	(+)	(+)	(+)	(+)
Al_2O_3	11.90	10.6	9.6	11.1	11.9
TiO_2	0.79	0.77	0.77	0.87	0.90
Fe_2O_3	6.79				
FeO	2.90(9.0*)	9.1*	10.0*	7.8*	8.4*
MnO	0.20	0.19	0.14	0.17	0.17
MgO	7.96	6.1	5.8	4.6	5.0
CaO	10.21	(+)	(+)	(+)	(+)
Na_2O	1.89	(+)	(+)	(+)	(+)
K_2O	0.24				
P_2O_5	-				
CO_2	1.25				
$H_2O(T)$	0.16				
Total	98.67				
Ni	0.0046	0.023	0.011	0.0077	0.0061
Cu	0.0106	0.0065	0.0074	0.0042	0.0044
Co	0.0024	0.0039	0.0033	(-)	(-)
Zr	0.0075	0.014	0.023	0.026	0.023
Cr	0.01-0.03	0.052	0.033	0.017	0.019
Ba	0.01-0.03	0.014	0.0033	0.056	0.053
Zn	0.001-0.003	(-)	(-)	(-)	(-)
Sr	0.001-0.003	0.012	0.018	0.025	0.036
Samples	1	18	8	11	24

Notes: Crawford's (1973) sample is Mary River metabasalt (Mb) from the Eqe Bay area.
Mb - Mary River Group metabasalt.
Mg - Mary River Group metagabbro.
Amn^f - intermediate to mafic rocks in nebulitic granitic megmatite (Amn).
Amg^g - mafic rocks in banded migmatite (Amg).
* - all iron as FeO.
(+), (-) - above and below limit of method of detection.

grey to locally black and pinkish black on fresh and weathered surfaces. Weathered surfaces are also commonly stained brownish. Ropy surfaces are preserved in a few places where metamorphic grade and deformation are relatively low. The metavolcanics are variously massive, pillowed, foliated to very thinly banded, or schistose (Fig. 45). Most pillows are 1 m or less across, and are rarely vuggy. Much of the banding is considered to be secondary and to represent transposed bedding and smeared-out agglomerate clasts and pillows. Some of the rocks contain vague layers that range from laminations to very thick and massive beds up to roughly 20 m thick. The thinner layers may represent mylonite, flow banding in sills, and layering within pyroclastic beds, while the thicker layers may represent individual flows, pyroclastic beds, and sills. Amygdules, chiefly quartz, and vesicles are common and many of the rocks have a blotchy texture in which irregular to ovoid and euhedral plagioclase-rich areas are interspersed through the mafic rock. Sparsely scattered anhedral to euhedral cream-coloured plagioclase phenocrysts up to 5 cm across occur in several beds. In thin section these are found to be composed of a mixture of quartz, chlorite, sericite, epidote, clay minerals, celadonite, and altered plagioclase. Channel-like structures were seen in a few places. Most of these rocks have been highly deformed and contain drag folds and complex fold structures, mineral lineations, and aggregate rodding of agglomerate clasts and pillows.

The mafic metavolcanics have been metamorphosed chiefly to amphibolite (Fig. 45b) and hornblende and/or pyroxene gneiss, some of which are magnetite-bearing. Other minor associated rock types include: hornblendite, pyroxenite, biotite, meta-anorthosite, and metagabbro. The basic metavolcanics are commonly feldspathized and migmatized to varying degrees, especially adjacent to their margins. Other common features are quartzofeldspathic sweats, lit-par-lit gneisses, plagioclase, and potassium feldspar as disseminated porphyroblasts and in veinlets, partial assimilation of mafic volcanics in the marginal zones of granitic intrusions, and shearing and conversion of amphibolite to biotitite for a distance of up to 1 m from the sheared contact with granitic rocks.

Blue-green to brownish-green hornblende is the most abundant, and plagioclase, some of which is zoned, is the second most abundant constituent in the mafic metavolcanics. The plagioclase ranges from albite to bytownite. Oil immersion work indicated that most of the plagioclase in the feldsparphyric rocks is andesine-labradorite (An_{30-56}).

Minor and accessory components, which occur locally as major components, include biotite, chlorite, actinolite, hypersthene, diopside, garnet, and epidote-clinozoisite. Pumpellyite was identified by X-ray in one sample from a flow or sill. Other common minor constituents are quartz, microcline, orthoclase, and cummingtonite. Accessory minerals include calcite, sphene, rutile, allanite, apatite, pyrite, pyrrhotite, chalcopyrite, magnetite, ilmenite, leucoxene, serpentine, kaolinite, and rarely tourmaline. Metamorphic mineral assemblages are shown in Table 19.

Contact relations

The mafic metavolcanics are conformable with adjacent metasediments of the Mary River Group and grade into migmatites (layered, agmatite, homogenized mixtures) and megacrystic gneisses containing feldspar porphyroblasts. At least locally the mafic metavolcanics also grade into ultramafic rocks and into anorthosite. Presence of clasts of metamorphosed Mary River Group rocks in the conglomerate-breccia lenses suggests the existence of local disconformities somewhere in the group. As with the Mary River Group in general, fault (Fig. 45b) and intrusive contacts with other rocks are common. Both deformed and undeformed pegmatites occur in Mary River Group amphibolite.

Chemistry

The Mary River mafic metavolcanics are considered to be chiefly basalts, although limited chemical data are available. Crawford (1973) provided one analysis (Table 20) for metabasalt from the Eqe Bay area which plots in the subalkaline field of Irvine and Baragar (1971). Its high silica and ferric iron content was noted by Crawford (1973), who considered the analysis to represent altered and oxidized andesitic basalt. It could also be called a tholeiitic or quartz basalt. The Mary River Group has probably undergone at least two regional metamorphisms (Jackson, 1966b; this memoir), which could have modified the chemistry.

The metabasalts plot, with two exceptions, in the tholeiitic field of the Al_2O_3 versus FeO/(FeO+MgO) diagram used by Naldrett and Cabri (1976) to aid in differentiating tholeiitic and komatiitic volcanics. Incomplete data suggest, following Arndt et al. (1977), that about one third of the metabasalts may be tholeiites, about one fifth are pyroxenitic komatiites, and the remainder (almost half) may be basaltic komatiites.

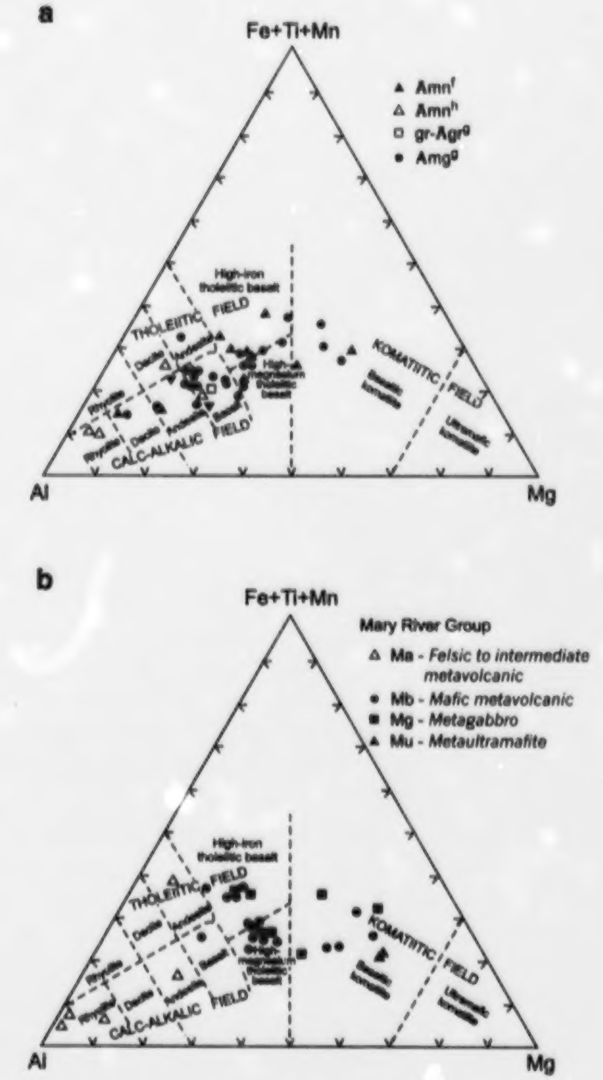

***Figure 46.** Jensen (1976) (Fe+Ti+Mn)-Al-Mg cation plots. **a)** Intermediate to mafic metaigneous rocks (Amn^f) and felsic to intermediate metavolcanic rocks (Amn^h) – both in nebulitic granitic migmatite (Amn); mafic igneous component (gr-Agr^g) in foliated monzogranite-granodiorite (gr-Agr); mafic igneous component (Amg^g) in banded migmatite (Amg). **b)** Felsic to intermediate metavolcanics (Ma), mafic metavolcanics (Mb), metagabbros (Mg), and metaultramafics (Mu) in the Mary River Group (M, AM).*

Most of the analyzed metabasalts also plot in the magnesium tholeiitic basalt field of Jensen's (1976) cation diagram (Fig. 46b), and outline a distinct area that extends from the high-iron tholeiitic field well into the basaltic komatiite field. Analyses of Mary River Group gabbroic intrusions (Mg), ultramafics (Mu), and felsic volcanics (Ma) are also shown on Figure 46b. Lack of complete Mu analyses limits the points available for the ultramafics, but it is obvious from Figure 46b and the partial analyses (Appendix 2a) that they will plot in the ultramafic field. The relationships of the points shown in Figures 46b and 47 support the inference from field relations that the Mary River Group basalts, gabbros, ultramafics, and anorthosites form part of a continuous series. Limited data available for Mary River Group felsic volcanics suggest that Mary River Group felsic and mafic volcanics are bimodal, a common feature of Archean volcanic associations. The picture is distinct from the one presented in Figure 46a for felsic to mafic components in nebulitic granitic migmatite (Amn, which may be basement) and in banded migmatite (Amg) which resembles that for a continuous calc-alkaline-tholeiitic sequence. The different trends and patterns obtained for the mafic remnants in the nebulitic granitic gneisses (*see* sections on "Chemistry" for units Amn and Amg), suggest in part at least, a different, possibly older source.

The averages for Mary River metabasalt (unit Mb) and metagabbro (unit Mg) in Tables 20 and 48 (*see* Table 48) are very similar, as are the two averages for mafic rocks in nebulous granitic migmatite (Amn^f) and banded migmatite (Amg^g). These two groups are also similar to one another, although units Mb and Mg, having more Fe and Mg, but less Al and Ti, may represent a less differentiated magma.

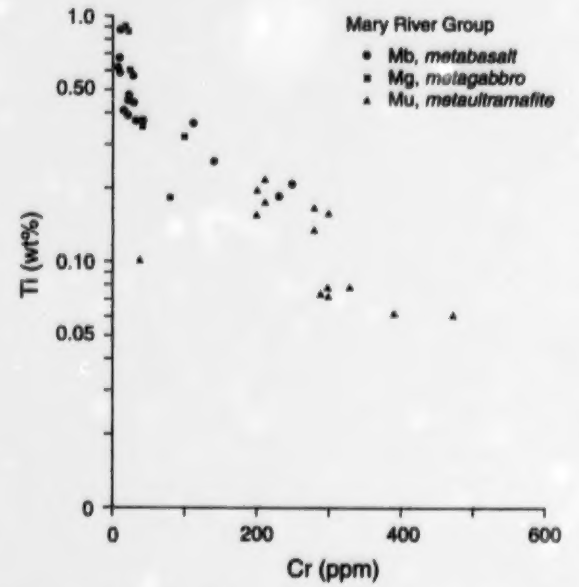

***Figure 47.** Log Ti (weight per cent) versus Cr (ppm) for mafic and ultramafic rocks of the Mary River Group.*

Mafic and ultramafic rocks in the map area are compared in terms of 11 elements in Figure 95 (*see* Fig. 95). The Mary River Group ultramafics differ considerably from the mafic rocks. Within the mafic rocks the mafic metavolcanics (Mb) and metagabbro intrusions (Mg) are similar to one another and show greater dissimilarities with the remnants of mafic rocks present in nebulitic (Amn^f) and banded (Amg^g) migmatite, although the differences are not marked. The Al and Sr are most abundant in mafic remnants in banded migmatite (Amg^g) and least abundant in units Mb and Mg. Iron, however, is most abundant in units Mb and Mg.

Most analyses of Mary River Group metabasalt plot in a small area on the TiO_2-Zr diagram of Pearce (1980) that lies within the arc lava field and barely extends into the within-plate lava field (Fig. 48b). The same analyses plot toward the Zr apex chiefly outside the fields outlined by Pearce and Cann (1973) in their Ti/100-Zr-Sr/2 diagram. These analyses do not obviously tail off toward the Sr/2 apex as do the points for mafic rocks in the migmatites (Fig. 48a, b), and it is a moot point whether or not they originally contained more Sr. If so they would probably have plotted in the calc-alkaline basalt field.

Analyses for Mary River Group metagabbro are plotted on the same diagrams (Fig. 48b) and occupy similar fields but are more dispersed. However, the closest similarity is on the Pearce (1980) TiO_2-Zr diagram between the mafic remnants in banded migmatite (Amg^g) and the metabasalt (Mb).

Metabasalt analyses plot chiefly in the calc-alkaline and rift basalt field (Fig. 49b) in a TiO_2-Zr diagram devised by Condie (1985). Mary River Group metagabbro plots in the same field but more diffusely with respect to Zr. Comparison of the Zr and the TiO_2 content with plots by Condie (1985) for basalts of different ages suggests an Archean age for the Mary River metabasalts and metagabbros.

A comparison of TiO_2 content with Fe/(Fe+Mg) (Fig. 50b) indicates well defined differentiation trends for both the Mary River Group metabasalts (Mb) and metagabbros (Mg). The computed lines (Fig. 50, Table 21) are remarkably similar for the metabasalts (Mb) and for mafic remnants in banded migmatite (Amg^g). The orientations of the lines for the metagabbro (Mg) and the mafic remnants in nebulitic granitoid migmatite (Amn^f) differ from the other two lines and from each other (Fig. 50a). However, as noted previously, a visual inspection of the points for Amn^f suggests a line similar to that for the metagabbro (Mg).

The chemical data available suggest that many of the mafic remnants in banded migmatite (Amg) may be from Mary River Group metabasalt, and to a lesser extent, from Mary River Group metagabbro. The different trends and patterns obtained for the mafic remnants in the nebulitic granitic gneisses suggest, in part at least, a different, possibly older source.

Metamorphosed ultramafic rocks (Mu, Amu)

Description

Most of the ultramafic rocks in the map area occur with or adjacent to Mary River Group rocks (e.g. *see* Fig. 106, 107). Although ultramafic rocks occupy various stratigraphic positions within the Mary River Group, they occur chiefly within the iron-formation or adjacent to it in the overlying strata. Ultramafic rocks are most abundant in the southern half of the Icebound Lake map area (NTS 37G), but are present also in the Eqe Bay area (Morgan et al., 1975; Morgan, 1982) and in most other areas containing Mary River Group rocks. Ultramafic rocks are rare north of the map area where paragneisses that are correlated with the Mary River Group outcrop on southeastern Bylot Island and in a large area that extends westward from southeast of Pond Inlet to Eclipse Sound and from there northwest to west of Navy Board Inlet (Daniels, 1956; Jackson and Davidson, 1975; Jackson et al., 1975, 1985). Ultramafic rocks in or adjacent to Mary River Group strata are chiefly serpentinites that contain various amounts of other minerals, especially amphiboles. Ultramafic rocks in the granitic gneisses and migmatites are mostly metamorphic hornblendites and pyroxenites that are assumed to be more highly metamorphosed equivalents of the Mary River Group serpentinites, but may include older rocks as well. Modal analyses of Mary River Group ultramafics are shown in histograms (Fig. 29) and in triangular plots (Fig. 51). Partial chemical analyses are provided in Tables 23 (column Mu), 47 (column T), and 48 (column 19). Plots for some elements are shown in Figures 46b, 47, 48b, and 95 (*see* below).

Most of the ultramafic rocks occur as tabular intrusions, that range from concordant sills to slightly discordant bodies up to 200 m in thickness (*see* Fig. 106, 107). Many concordant contacts are abrupt, but some ultramafic rocks are gradational with Mary River Group metabasalt and are probably flows. Rough estimates suggest that some bodies may be 1000 m or more thick, but the rocks are invariably strongly deformed and faulted, and the present thickness may not be primary. Moderately to highly discordant ultramafic dykes are common and some bodies resemble deformed laccoliths. Several plugs were noted, most less than 10 m in diameter, although some may be as large as 200 m (*see* Fig. 105). One plug, 60 m in diameter, intrudes iron-formation in the Mary River region and has a sheared chlorite margin 3 m thick. Contacts between isolated hornblendite and pyroxenite bodies and enclosing gneisses range from concordant to discordant. Some of these concordant contacts have been transposed by shearing and plastic deformation. Most of the ultramafic rocks are in the amphibolite metamorphic facies, contain a secondary foliation, and, locally at least, are banded and contain mineral lineations and aggregate rodding.

The ultramafic rocks range from aphanitic to very coarse grained and pegmatitic. Fresh surfaces of the ultramafic rocks are chiefly medium- to dark-green and greenish grey, and are

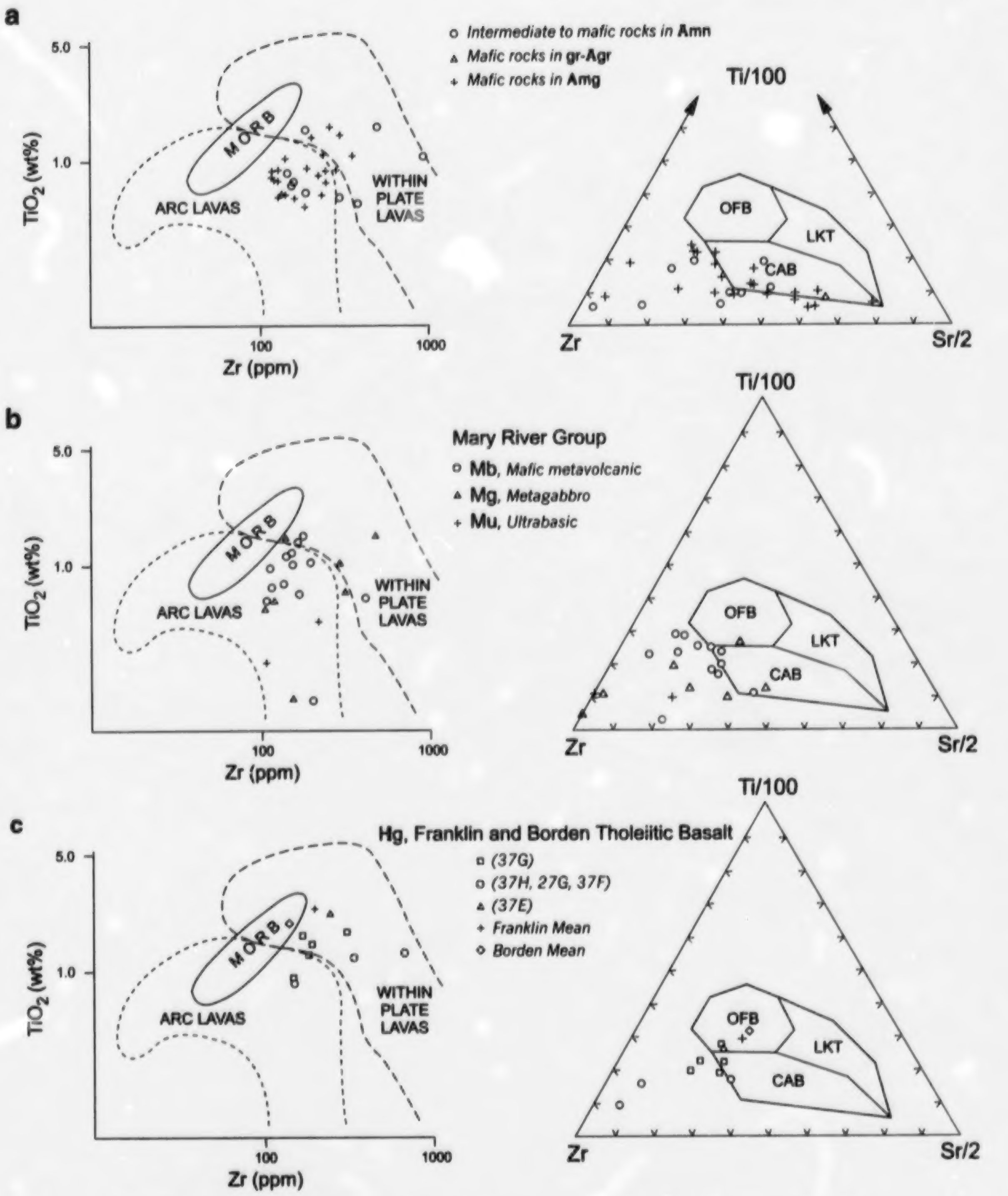

Figure 48. *TiO_2 versus Zr (Pearce, 1980) and Ti/100-Zr-Sr/2 (Pearce and Cann, 1973) diagrams. MORB = mid ocean ridge basalt, OFB = ocean floor basalt, LKT = low potassium tholeiite, CAB = calc-alkaline basalt.*

commonly blotchy, with lighter blotches of talc or amphibole up to 5 cm across in a darker serpentine-chlorite matrix, and similarly sized darker serpentine-chlorite blotches in a lighter talc or amphibole matrix. Fresh surfaces may also be light green and dark greenish black to black. Weathered surfaces are chiefly rough or hackly, and where the rocks are serpentinous may reflect the primary texture of the rock. Colours of weathered surfaces are chiefly light- to medium-grey or greenish grey, light- to dark-brown and olive-brown, and locally yellowish brown to orange-brown. Grain sizes of these rocks range from aphanitic to very coarse grained and pegmatitic or blastoporphyritic.

The ultramafic rocks are chiefly massive, with layering, where present, being greater than 10 m thick (Table 2). Some compositional layering ranges from about 1 mm up to 1 m thick. In one cumulate zone, light brown, high-weathering enstatite-rich bands as much as 3 mm thick alternates with dark green-weathering serpentinite bands up to 2 cm thick (Fig. 52a, b). In another cumulate zone, magnetite-ilmenite (+chromite locally) is abundant at the base of layers and lenses up to 60 cm thick, but decreases upward in abundance and grain size. Magnetite phenocrysts (up to 6 mm) occur sporadically in the ultramafics. South of No. 2 and 3 iron deposits in the Mary River area (NTS 37G), the ultramafic rocks contain zones up to 10 m thick that weather variously light to dark green, and yellowish- to brownish-orange to brown. It is not certain whether this banding is secondary or a primary feature in a layered intrusion, but in the same general area serpentinite on the margins grades vertically into amphibolite in the middle of a concordant folded body.

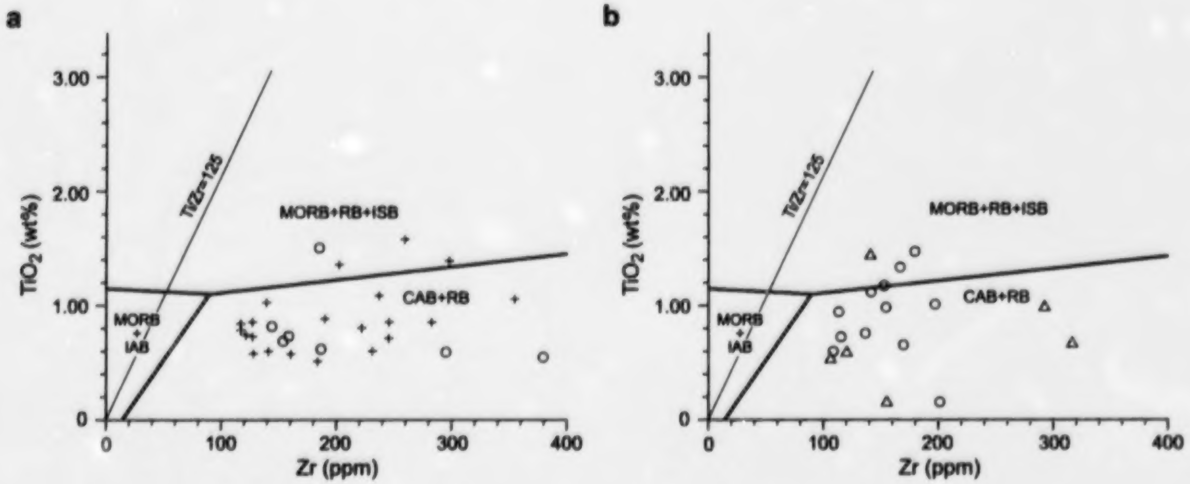

Figure 49. *TiO_2 versus Zr diagrams after Condie (1985). MORB = mid ocean ridge basalt, RB = rift basalt, ISB = island basalt, IAB = island arc basalt, CAB = calc-alkaline basalt.* ***a)*** *circle = intermediate to mafic rocks in* Amn (=Amn^f)*, plus sign = mafic rocks in* Amg (=Amg^g). ***b)*** *circle = Mary River Group metabasalt* (Mb), *triangle = Mary River Group metagabbro* (Mg).

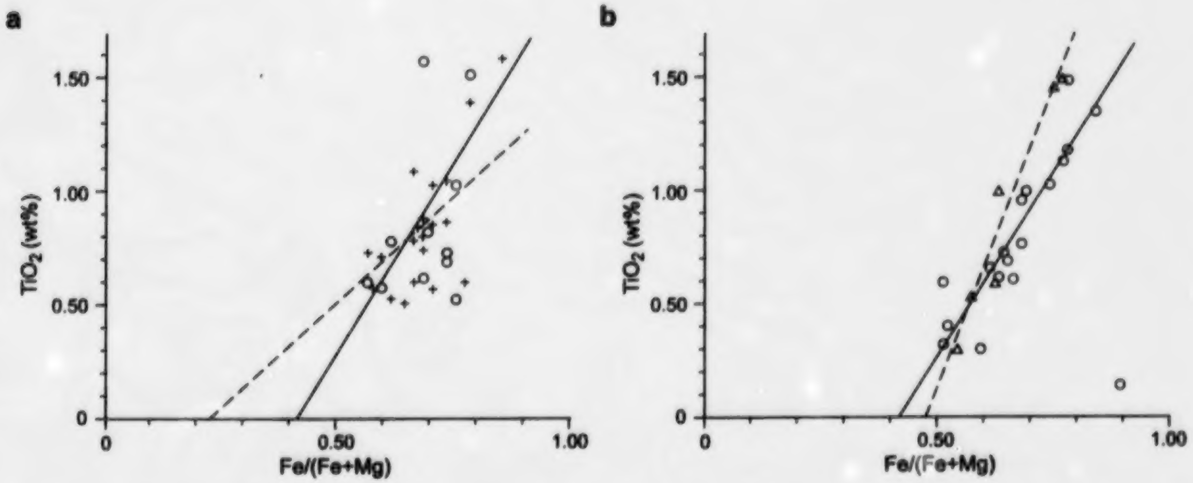

Figure 50. *TiO_2 (weight per cent) versus Fe/(Fe+Mg) diagrams. Symbols as in Figure 49. In* ***a)*** *the dashed regression line is for the circles and the solid regression line is for the plus signs. In* ***b)*** *the dashed regression line is for the triangles and the solid regression line is for the circles.* (See also *Table 21.)*

Table 21. Regression line constants (y=Mx+b) and statistics for TiO_2 versus Fe/(Fe+Mg) plots for map units Amn^f, Amg^g, Mb, Mg, and Hg.

Map unit	No. of samples	M	b	Correlation coefficient	Variance
Amn^f	11	1.815	-0.386	0.363	0.125
Amg^g	22	2.812	-1.095	0.667	0.043
Amn^f+ Amg^g	33	2.476	-0.858	0.558	0.065
Mb	17	3.132	-1.271	0.909	0.022
Mg	6	5.098	-2.417	0.973	0.016
Hg	9	2.826	-0.761	0.659	0.113
Hg*	11	3.101	-0.849	0.561	0.186

*Includes means for Borden and Franklin dykes (Table 44).

Several ultramafic sills and/or flows up to 15 m thick alternate with slightly thinner amphibolite (mafic metavolcanic) and a few metasedimentary bands across about 200 m of section above and east of the falls on Mary River in the No. 1 iron deposit area (NTS 37G). The rocks are highly drag folded, and at least in part interfolded, so the true number of sills or flows present is uncertain. In the same area vuggy-weathering ultramafic rocks contain pillow-like outlines east of No. 3 iron deposit.

In a few places in this region, and elsewhere, the weathered surface resembles that of a pyroclastic or brecciated rock, although actual clast boundaries were not noted on fresh surfaces (possible random spinifex texture). Locally weathered and fresh surfaces show a texture resembling deformed spinifex texture (O.R. Eckstrand, pers. comm., 1975), with lath-shaped crystals up to 10 cm long.

The Mary River Group ultramafics are commonly intruded by metabasalt and metagabbro dykes (Mg) that are concentrated in the Mary River Group and so are considered tentatively to be penecontemporaneous with the metabasalts and metaultramafics. Locally, ultramafic rocks have intruded mafic rocks and contain inclusions of massive and blotchy

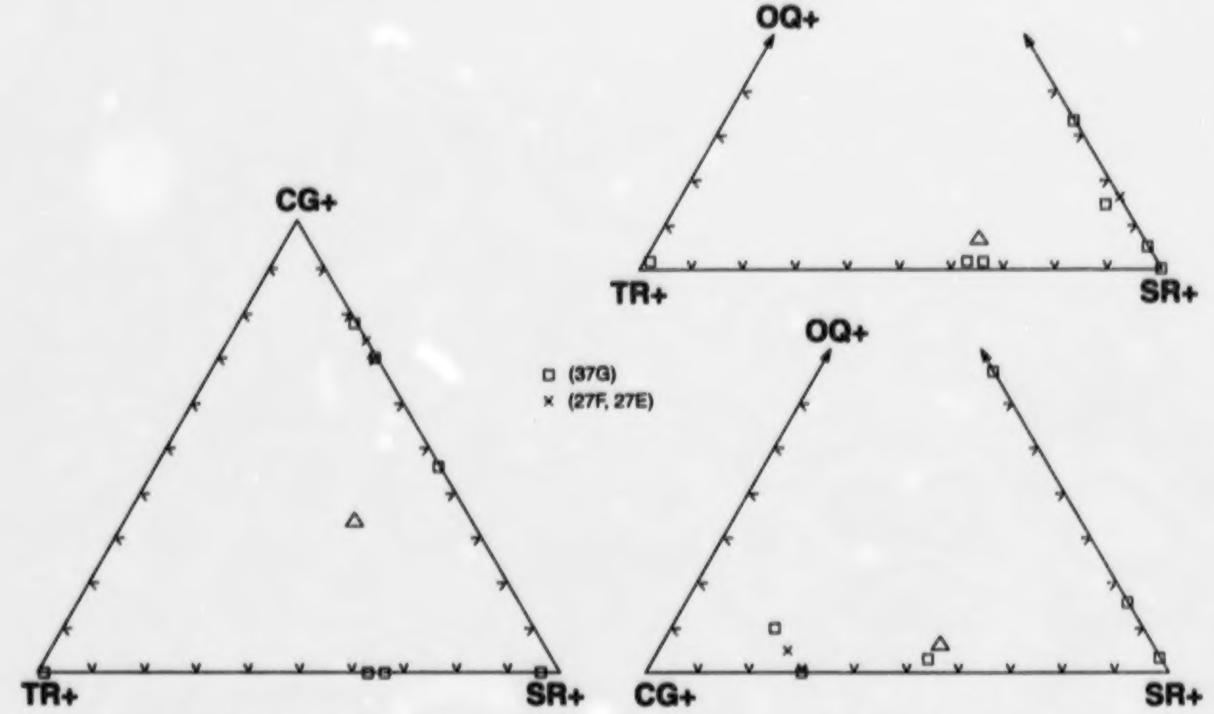

Figure 51. *Modal analysis plots for ultramafic rocks. The mean is shown by the triangle. OQ+ = magnetite+hematite+chromite+spinel+leucoxene+opaque+pyrrhotite+pyrite+undifferentiated sulphide+chalcopyrite. CG+ = cummingtonite+anthophyllite+grunerite+enstatite+hypersthene. TR+ = tremolite-actinolite+hornblende+clinopyroxene+diopside+augite. SR+ = serpentine+chlorite+talc+olivine.*

amphibolites (metagabbro, anorthositic metagabbro, metaultramafite) up to 6 m across, some of which contain plagioclase aggregates up to 8 cm across.

Locally, the ultramafic rocks (chiefly serpentinite) are intruded by serpentinite, pyroxenite (chiefly enstatite), and amphibolite dykes up to about 1 m thick. One 60 cm thick pyroxenite (enstatite) dyke has 60 cm thick reaction zones on either side composed largely of coarse fibrous talc (Fig. 52c, d). The ultramafic host rock had been altered to serpentinite, perhaps diagenetically, before heat from the emplaced enstatite dyke drove water out of the adjacent serpentinite.

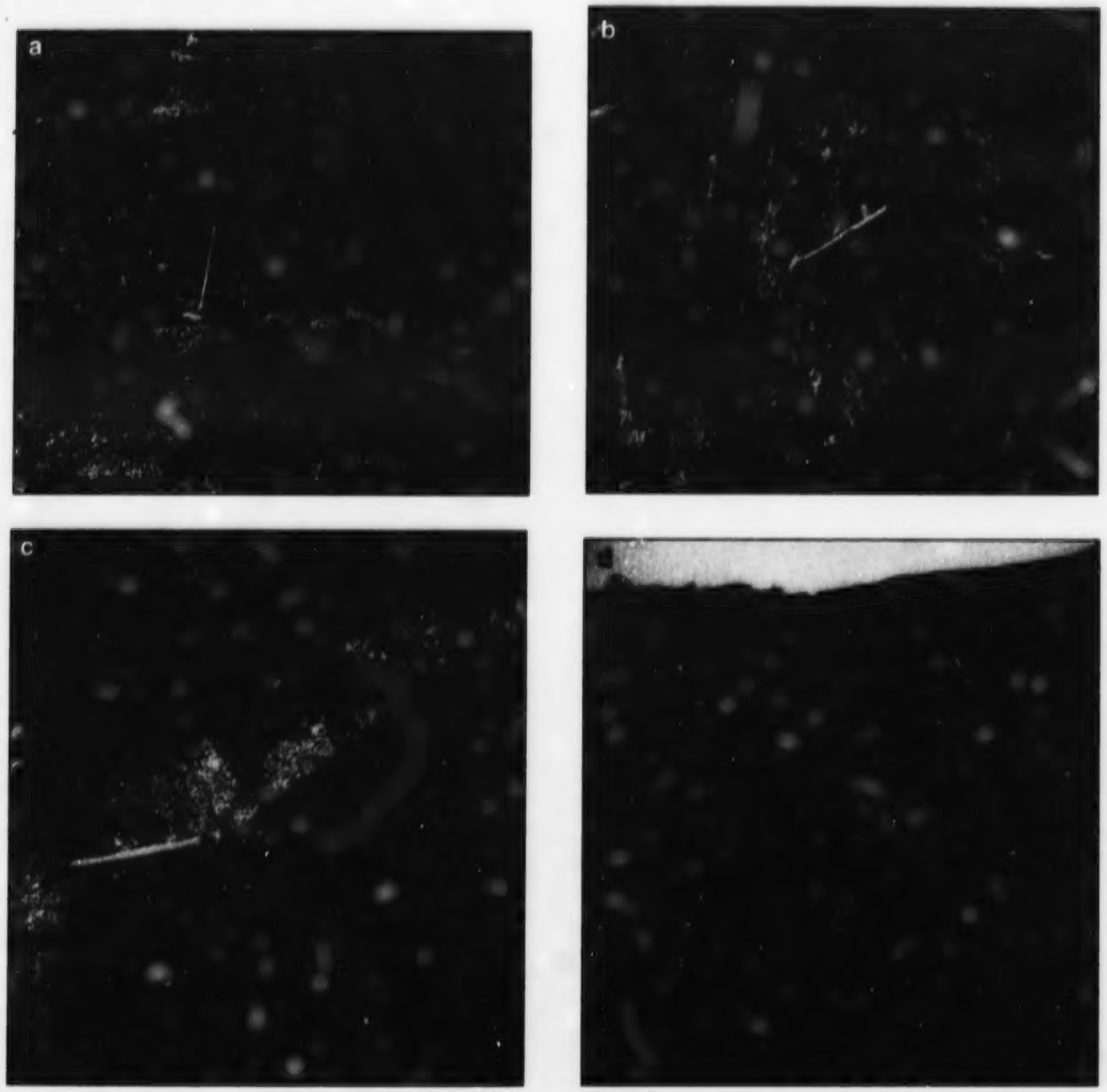

Figure 52. *Outcrops southeast of Mary River No. 1 iron deposit (NTS 37G).* ***a)*** *Dehydration fractures on the surface of massive serpentinite. Photograph by G.D. Jackson. GSC 186831.* ***b)*** *Thinly banded ultramafic intrusion in metabasalt. Photograph by G.D. Jackson. GSC 118314.* ***c)*** *Serpentinite dyke in massive serpentinite. Photograph by G.D. Jackson. GSC 118330.* ***d)*** *South-dipping, 60 cm thick pyroxenite (enstatite) dyke in serpentinite to right of hammer. Reaction zones on either side of the dyke are up to 60 cm thick and contain coarse talc and actinolite. The north side of the dyke is bordered by a 15 cm zone that contains veinlets up to 1 cm thick of cross-fibre chrysotile asbestos. Photograph by G.D. Jackson. GSC 118331*

Adjacent to the enstatite dyke on one side is a 15 cm thick zone that contains veinlets up to 1 cm thick of light brown, resinous cross-fibre chrysotile asbestos. Cross-fibre chrysotile asbestos also occurs in a series of lenses and veinlets up to 2 mm thick and up to 2 cm apart just north of Mary River Falls. Some of the veinlets are rimmed by talc. These talc-rimmed veinlets appear to be largely a surface weathering phenomenon and to extend only about 5 cm into the ultramafic rock. Dark serpentine and enstatite veinlets are common.

Deformed veins of quartz and others of carbonate occur in the ultramafic rocks locally in the Mary River area, where granite gneiss inclusions have also been seen in the ultramafics (Baffinland Iron Mines Limited, 1964). Also, iron-formation has been caught up in an ultramafic intrusion that changes along strike from a sill to a dyke. The intrusion is enriched locally in martite and quartz, probably from assimilated iron-formation.

The serpentinites are composed chiefly of antigorite and/or chrysotile with varying amounts of chlorite and talc. Chlorite-, talc-, chlorite-talc-, and garnet-chlorite-schists are common; tremolite-actinolite and anthophyllite schists are less common. Anthophyllite rosettes and spherulites occur in a few of the rocks. Relics of olivine, enstatite, cummingtonite, green spinel, and chromite have been noted in these rocks, and along with some of the magnetite, are assumed to represent the primary mineral assemblage, although the cummingtonite and green spinel are more likely to be a relic of earlier metamorphism and some metamorphic cummingtonite is present locally. Other minor minerals are hornblende, magnetite-ilmenite, epidote, biotite, and rarely, feldspar (chiefly sparsely scattered plagioclase). Locally, poikiloblastic hornblende crystals up to 8 mm long are pseudomorphous after pyroxene. The minerals mentioned above, as well as quartz, leucoxene, apatite, sphene, and local tourmaline, may occur as accessory minerals. Zircon is an abundant accessory at one locality at No. 1 iron deposit in the Mary River area. Some mineral assemblages of the lower grade ultramafic rocks are given in Table 22.

Chemistry

Most of the fourteen ultramafic samples analyzed are from the Mary River region (NTS 37G) and the headwater region of Rowley River (northeast NTS 37F). Most of the elements determined are less abundant in the ultramafics (Mu) than in the other mafic rocks (Mb, Mg, Amn^f, Amg^f; gr^g, *see* Appendix 4). However Mg, Co, Cr, Ni, and Pb are about an order of magnitude greater (Table 48, Fig. 46b, 47, 95). Some elements (Al, Na, Cu, Cr) vary considerably in value whereas others do not (Fe, Mn, Co, Ni, Pb). This may have something to do with the nature and proportion of primary mineral phases that were present originally, metamorphism and metasomatism, and the possibility that ultramafics of more than one type or source are present. The chemistry, modal analyses (Fig. 29, 51), and field observations suggest that the most abundant primary minerals in the ultramafics were probably olivine and orthopyroxene (enstatite), perhaps in roughly equal proportions.

Table 22. Some lower grade metamorphic mineral assemblages in Mary River Group metaultramafics (Mu).

Assemblage:	1	2	3	4	5	6	7	8	9	10	11	12	13	14	15	16
Serpentine	+	+	+	+	+	+	+	+	+	+	+					
Chlorite	+	+	+	+				+		+		+	+	+		+
Talc	±				+				+	+			+	±		
Actinolite	+	+	+	+		+	+		+			+				
Anthophyllite																±
Cummingtonite										+	+					
Hornblende														+	+	
Garnet																+
Quartz		+														
Calcite									+							
Magnetite	+	+	+	+	±	+			+	+		+		+	+	
Chromite							+					+				
Pyrrhotite														±		
Pyrite				+												
Relict minerals:																
Olivine			+						+							
Enstatite									+	+						
Pyroxene				+												
Cummingtonite									+							
Spinel (Mg)								+								
Chromite-magnetite								+								

+ - Mineral is present. ± - Mineral is present in some assemblages, not in others. Two minerals represented by ± in an assemblage indicates there are four combinations represented, etc. The relict minerals include primary minerals and possibly earlier metamorphic minerals (e.g. cummingtonite).

Plots using the Jensen (1976) cation diagram and Ti versus Cr (Fig. 46b, 47) suggest that there may be a continuous gradation between the ultramafic (Mu), basaltic (Mb), and gabbroic (Mb) intrusions. Eleven of the samples analyzed contain more than 15% MgO, and these probably plot in the ultramafic komatiite field (Fig. 46b, Appendix 2) considering the high content of Mg-bearing minerals present (Fig. 29). Only two of the fourteen samples contain measurable Zr (Fig. 48b). The analysis for one sample plots barely in the tholeiitic field of Naldrett and Cabri (1976), and the other in the komatiitic field.

Mary River Group ultramafics are compared with Recent and Archean ultramafic rocks from different environments in Table 23. Columns 1-4 are analyses of the Marum ophiolite in the Papuan ultramafic belt, which is a representative of a relatively little disturbed orogenic or alpine tectonite (Jaques et al., 1983). Ocean-floor or abyssal ultramafics (spinel harzburgite, lherzolite) are represented by analyses presented in columns 5 and 6, while analyses for Archean Al-depleted komatiites are given in columns 7-10. Comparing Mary River Group ultramafics with the analyses for alpine and abyssal ultramafics shows that Ti and Sr are markedly greater in the Mary River ultramafics, and the maximum values for Al, Na, and Cu are also relatively high. Mary River Group ultramafics bear a closer resemblance to the alpine ultramafics, especially lherzolite, than the abyssal ultramafics; but they bear a still closer resemblance to Al-depleted komatiites.

Smith and Erlank (1982) distinguished two groups of komatiites. Group I contains $Al_2O_3/TiO_2=20$ and $CaO/Al_2O_3=10$ (in weight per cent). This is the most widespread group, especially in the Archean. Group II contains $Al_2O_3/TiO_2=10$ and $CaO/Al_2O_3>1$ and is the most abundant in the Barberton greenstone belt. The $Al_2O_3/TiO_2=15$-24 for eleven of the fourteen Mary River Group ultramafic samples, which indicates a similarity with Group I komatiites. However, the general chemistry, especially the low Al_2O_3 and TiO_2 contents, are more similar to Barberton komatiites (chiefly Group II) and only a minority of komatiites in other regions such as at Abitibi and in Munro Township (Arndt et al., 1977). The alumina, iron, and titanium are low compared to many komatiites (Table 23).

Metagabbro (Mg, AMb)

Metamorphosed mafic sills and dykes up to about 60 m thick intrude the Mary River Group and seem to be associated chiefly with the mafic metavolcanics, metaultramafics, and meta-anorthosites of the Mary River Group. A few scattered, small, metamorphosed, mafic, plug-like, and lens-shaped intrusions up to 6.5 km long, but mostly less than 0.3 km long, occur within the Mary River Group, and in adjacent gneisses. Locally, small mafic dykelets appear to intrude massive to faintly foliated quartz monzonite (Ag) and to have been tectonically drawn out into thin wisps. These various mafic intrusions were observed mainly in the Mary River region (NTS 37G), about 13 km southwest from the head of Quernbiter Fiord (NTS 37H) and in the Isortoq River-Eqe Bay region (NTS 37C, F). These intrusions may also, of course, occur in the older granitic gneisses and, as has been mentioned above, are similar to older mafic dykes (b) within these gneisses. These two groups (b, Mg) of mafic intrusions are commonly similar to one another, have not been properly dated, and at present can be differentiated in the field only on the basis of whether or not they intrude other Mary River Group rocks. In the Mary River region, for example, the older mafic dykes (b) in the basement gneisses (Agn, Amn) are truncated at the contacts with the Mary River Group (Jackson, 1966b, 1978b). The younger metagabbros (Mg) intrude the Mary River Group as well as the basement gneisses. East of No. 3 iron deposit, serpentinite (Mu) contains inclusions of blotchy metagabbro (Mg) up to 6 m across that are sheared around their margins. The serpentinite is in turn intruded by a deformed sill-like metagabbro (Mg) with relict ophitic texture and plagioclase metaphenocrysts along one side. The serpentinite and two metagabbros are considered here to be penecontemporaneous (*see* section on "Origin of igneous rocks (Ma, Mb, Mg, Mu, Mn)").

Table 23. Spectrographic analyses of Mary River Group ultramafics compared with those of some alpine and abyssal ultramafics, and with those of komatiite (weight per cent).

	Mu		Alpine				Abyssal		Komatiite			
	Average	(range)	1	2	3	4	5	6	7	8	9	10
Ti	0.12	(0.058-0.21)	NF	0.018	0.03	0.012	0.012	0.029	0.19	0.26	0.20	0.25
Al	1.9	(0.34-3.6)	0.021	0.94	0.42	2.2	0.62	0.74	3.1	3.8	1.9	1.7
Fe	6.4	(5.5-7.8)	5.1	3.6	4.8	8.2	6.4	5.8	5.8	8.7	8.7	8.7
Mn	0.13	(0.069-0.17)	0.085	0.11	0.15	0.14	0.11	0.09	-	-	0.14	0.14
Mg	>9.0		30.11	13.7	13.9	21.6	27.3	27.7	15.9	15.5	18.9	19.7
Ca	>1.0		0.036	12.7	10.9	3.3	0.81	0.66	5.1	4.1	4.1	3.4
Na	0.13	(<0.01-0.45)	0.0014	0.067	0.052	0.082	0.015	NF	0.19	0.12	-	-
Co	0.010	(0.0067-0.016)	NF	-	-	-	-	-	-	-	0.013	0.012
Cr	0.27	(0.036-0.47)	0.42	0.31	0.20	0.31	0.15	0.40	-	-	0.28	0.27
Cu	0.002	(<0.001-0.013)	0.0004	0.0005	0.0001	0.0031	-	-	-	-	-	-
Ni	0.17	(0.089-0.24)	0.25	0.040	0.025	0.16	0.17	0.25	-	-	0.19	0.22
Sr	0.0024	(<0.001-0.0096)	NF	0.0007	0.0006	0.0021	-	-	0.0033	0.0031	-	-
V	0.0084	(<0.003-0.016)	0.0001	0.0085	0.0070	0.0037	-	-	-	-	0.010	0.0096
Pb	0.10	(0.073-0.13)	-	-	-	-	-	-	-	-	-	-
Zn	<0.07		0.0040	0.0026	0.0034	0.0073	-	-	-	-	-	-
Sc	-		0.0002	0.0056	0.0049	0.0013	-	-	0.0021	0.0026	0.0019	-

Notes- Mu: Mary River Group ultramafics (Table 47-14 samples).
1-4: Individual samples of alpine ultramafics from the Marum ophiolite, Jaques et al. (1983); 1 = dunite, 2 = wehrlite, 3 = olivine pyroxenite, 4 = lherzolite.
5,6: Averages from Dick and Fisher (1984) of 50 abyssal spinel harzburgites and lherzolites.
7,8: Representative analyses from Ludden and Gélinas (1982), for some komatiites in Lamotte Township, Abitibi.
9,10: Average analyses from Smith and Erlank (1982), for some komatiites in the Barberton greenstone belt.
NF: Not found.
-: Not determined.

Mary River Group mafic intrusions (Mg) are of dioritic to chiefly gabbroic composition and have been metamorphosed to amphibolite, hornblende gneiss, and locally, pyroxene gneiss. Modal analyses for Mary River Group metagabbros are shown in Figure 29 and presented in triangular plots of Figure 20Jc. Chemical data are presented in Appendices 2-4, Tables 20, 47 (column S), and 48 (column 14), and Figures 4650 and 95.

The Mary River metagabbros (Mg) are green to black on fresh and weathered surfaces, are chiefly equigranular, fine- to medium-grained, and locally coarse grained. Most are foliated and/or lineated, but some are massive and may have a blotchy texture in which mafic blobs up to about 6 mm across are disseminated in a finely recrystallized plagioclase-rich matrix. Locally, an ophitic- to intergranular-like texture is present in which the plagioclase crystals have been recrystallized to fine, white, sugary aggregates. The origin of this texture is uncertain (cf. Morgan and Taylor, 1972). Wispy to rounded porcelaneous plagioclase metaphenocrysts, commonly 10 cm or less in diameter, occur mainly along one edge of the intrusions (Fig. 53a), suggestive of crystal differentiation.

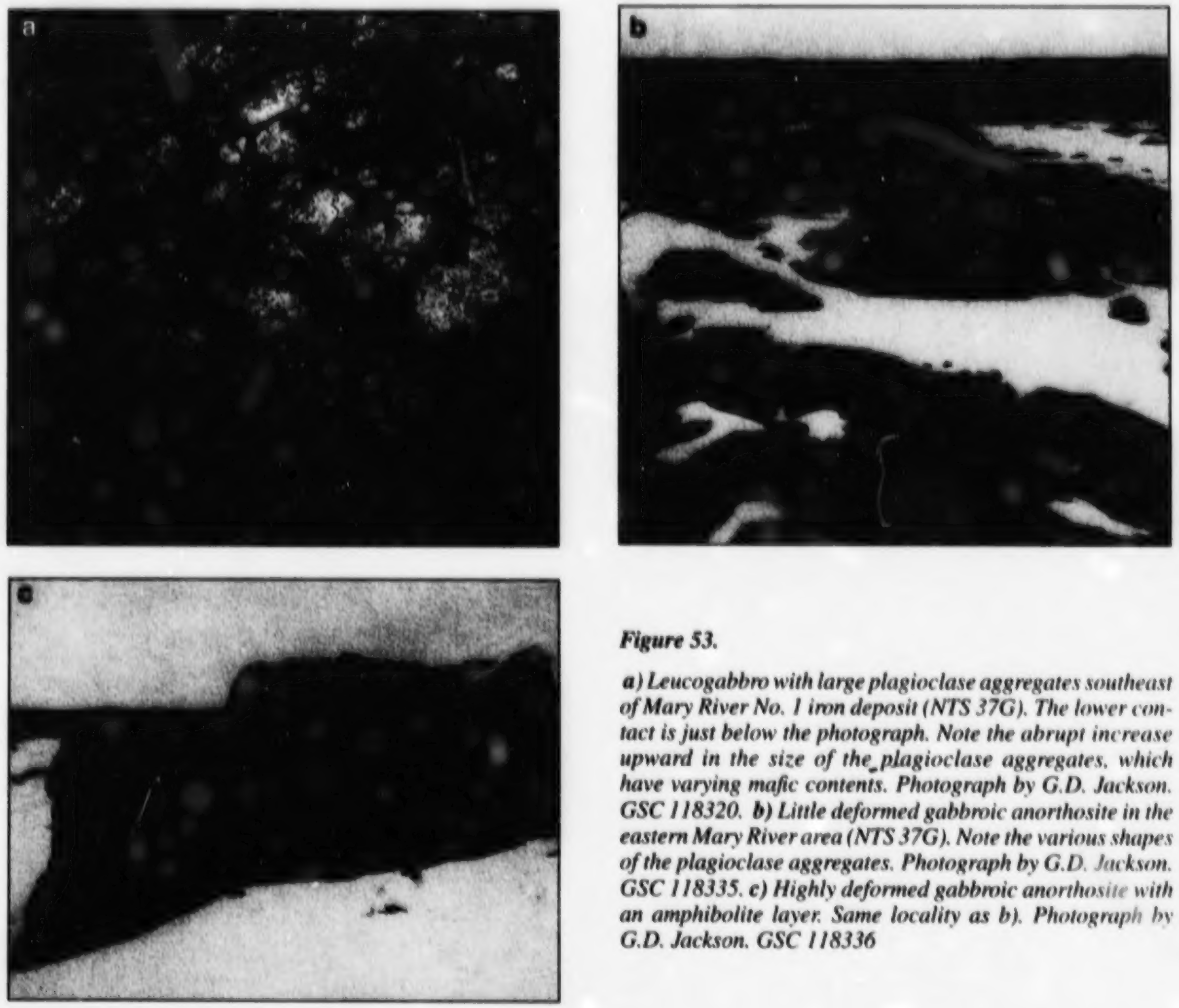

Figure 53.

***a)** Leucogabbro with large plagioclase aggregates southeast of Mary River No. 1 iron deposit (NTS 37G). The lower contact is just below the photograph. Note the abrupt increase upward in the size of the plagioclase aggregates, which have varying mafic contents. Photograph by G.D. Jackson. GSC 118320.* ***b)** Little deformed gabbroic anorthosite in the eastern Mary River area (NTS 37G). Note the various shapes of the plagioclase aggregates. Photograph by G.D. Jackson. GSC 118335.* ***c)** Highly deformed gabbroic anorthosite with an amphibolite layer. Same locality as b). Photograph by G.D. Jackson. GSC 118336*

Porphyritic metagabbro grades locally into anorthosite, indicating that the two lithologies have a common magma source and/or may be part of a differentiated intrusion.

Mafic minerals predominate in Mary River Group metagabbros (Mg), and consist mostly of medium- to dark-green, bluish-green, and brownish-green hornblende. Biotite and epidote-clinozoisite are common minor constituents, and predominate locally. The biotite ranges from orange to brownish green, brown, and reddish brown, and is especially abundant in recrystallized sheared margins. Epidote and clinozoisite seem to be much more common in the Mary River Group intrusions (Mg) than in older metagabbros (b). Anthophyllite, cummingtonite, and actinolite occur in several places, and chlorite is common, locally in major amounts. In many cases the chlorite is a retrograde mineral derived from earlier metamorphic minerals, as is also some of the actinolite, epidote, and sericite. Diopside and hypersthene are common in the high grade areas, and muscovite occurs in a few places. Plagioclase is commonly a major component and predominates locally. Much of it is andesine or labradorite, but ranges from albite to bytownite. Phenocrysts are chiefly labradorite-bytownite. Many of the larger grains, especially, are altered in varying degrees to sericite, epidote, amphibole, chlorite, and/or kaolinite. A few per cent of quartz and traces of sphene occur in many, if not most, of these rocks. Other accessory minerals include apatite, calcite, magnetite, ilmenite, goethite-hematite, pyrite, pyrrhotite, leucoxene, orthoclase, microcline, zircon, allanite, zoisite, and talc. Garnet with an orthopyroxene inclusion occurs in a chlorite-biotite-muscovite rock in the No. 1 iron deposit area (NTS 37G). Some mineral associations are shown in Table 24.

The contact relations, chemistry, and origin of the Mary River metagabbros (Mg) are discussed above and below in sections dealing with Mary River metabasalts (Mb) and ultramafics (Mu).

Meta-anorthosite (Mn)

Metamorphosed anorthosite-gabbroic anorthosite-gabbro is a minor map unit in the Mary River (NTS 37G) area and just south of the map area in the Eqe Bay (NTS 37C, D) region. Anorthosite intrusions also occur at one or two localities in the southwestern part of the Conn Lake map area (NTS 37E), in the Buchan Gulf map area (NTS 37H, included in Mb), and along the eastern edge of the Steensby Inlet map area (NTS 37F). They are all concordant, sill-like bodies, and most range from 3 to 60 m in thickness. A large foliated sill east of Grant-Suttie Bay has a maximum thickness of about 340 m, and a discontinuous length of about 25 km in a northeasterly direction (Morgan, 1982). The sill may be folded and its true thickness may be considerably less. Most sills have relatively thin metagabbroic (amphibolite) borders that grade into glomeroporphyritic (to 1 m diameter) anorthosite and gabbroic anorthosite over short distances with an increase in the number and size of plagioclase blastophenocrysts. Some anorthosite may be a minor part of larger differentiated sills. The anorthosites are associated chiefly with the mafic and ultramafic rocks of the Mary River Group as noted above (*see* sections "Mafic metavolcanics (Mb, AMb)" and "Metamorphosed ultramafic rocks (Mu, Amu)".

Table 24. Some metamorphic mineral assemblages in Mary River Group metagabbro (Mg: 1-20) and meta-anorthosite (Mn: 21-27) map units.

Assemblage:	1	2	3	4	5	6	7	8	9	10	11	12	13	14	15	16	17	18	19	20	21	22	23	24	25	26	27
Plagioclase	+	+	+	+	+	+	+	+	+	+			+			+	+	+	+	+	+	+	+	+	+	+	+
K-feldspar							±					±										±					+
Quartz	±						±	+		+				+		+	±	+	+	+				+	+	+	+
Anthophyllite						+																					
Cummingtonite																+							+				
Actinolite													+	+										±r			
Hornblende	+	+	+	+	+	+	+				+	+				+	+	+	+		+		+	+	+	+	±
Diopside			±				±l										+	±	+	+				+			
Hypersthene															±i		+		+	+							
Biotite		±				+	+	+	+	+			+	+	+	+	+	+		+	±			+			+
Muscovite										+	±			+	+	±						+	+		+	+	+
Sericite					±																						
Garnet															±l												
Chlorite									+						+							+					+
Epidote							±	+	+		+	+									+	+		+	+		±
Clinozoisite				±																						+	

l - relict; i - inclusion in garnet; r - retrograde; + - mineral is present; ± - mineral is present in some assemblages, not in others.
Two minerals represented by ± in an assemblage indicates there are four combinations represented, etc.

The mafic borders to, and mafic bands within, the anorthosites are typical amphibolites composed chiefly of hornblende (50-90%) and plagioclase (10-40%). The central parts of some anorthositic bodies are virtually all plagioclase (e.g. Eqe Bay sill), but most contain about 5-20% mafic minerals, chiefly hornblende with minor biotite and chlorite. As much as 5% quartz may also be present. Generally, the anorthositic bodies are more properly called gabbroic anorthosite. Modal analyses for anorthositic rocks are plotted on triangular diagrams in Figure 20Jc and are shown graphically in Figure 29. Chemical data for one sample is given in Table 48 (column 20). Data for this sample and for one sample from the Eqe Bay sill are listed in Appendix 2.

The meta-anorthosites are massive to very thick bedded rocks upon which a metamorphic foliation and rodding of plagioclase blastophenocrysts have been superimposed; however, primary textures are preserved in much of the rock. Amphibolite layers up to 10 m thick but commonly 3 m or less, occur at intervals of up to 45 m in the anorthositic rocks, and are similar in composition to the mafic borders. A few rusty zones are also interspersed in the anorthosite. The origins of the central mafic bands are uncertain. Thin metamafic dykes, a few pink to red syenite-syenodiorite rocks, and in the Eqe Bay area, calcite-rich rock (perhaps a vein) are associated with the anorthosite.

The meta-anorthosites are white to pale grey and pale greenish grey on fresh surfaces and white on weathered surfaces. They are fine to very coarse grained and blastoporphyritic, except where the rock is virtually entirely plagioclase. The plagioclase blastophenocrysts range from 6 mm to about 1 m in length, and in general increase from a minimum size at the margin to a maximum size only a short distance in from the margin. The blastophenocrysts vary from wispy to irregular, square, rectangular, circular, and oval (Fig. 53b, c). Many appear to have been partially resorbed; others resemble pillows, even to the extent of having what seems to be a small protuberance on one side that resembles that on the bottom side of pillows. Blastophenocrysts are a minor component in the mafic border zones, but increase uniformly over short distances toward the anorthosite to commonly make up 80-95% of the rock, and may themselves contain up to 10% mafic inclusions. The plagioclase crystals are commonly partially crushed and recrystallized into fine, anhedral, untwinned aggregates, and the twinning in the remainder commonly has a fuzzy or blurred appearance. Many of the smaller metaphenocrysts were probably originally part of a single larger crystal. Optically determined plagioclase compositions range from oligoclase to bytownite (An_{22-89}), but most are in the andesine-labradorite field. Several refractive index determinations by oil immersion gave $N_y = 1.555\text{-}1.571$, and N_x, as large as 1.576; these values indicate an anorthite content of 44-90%. The plagioclase blastophenocrysts in anorthosite are rimmed by amphibolite of similar composition to that in the mafic bands and border zones. Most amphibolites throughout the metamorphosed anorthosite-gabbroic anorthosite-gabbro intrusions contain smaller plagioclase blastophenocrysts ranging from about 6 mm to 2 cm. Locally the meta-anorthosite grades into pockets of metagabbro with up to 40% mafic minerals, chiefly hornblende.

The plagioclase has been highly sericitized and/or epidotized in several places, and some of the epidote has allanite cores. Green to chiefly blue-green hornblende is the principal mafic mineral. It has been retrograded to actinolite in a few places, and is commonly accompanied by minor epidote, brown biotite, muscovite, and, in a few places, diopside. Quartz is commonly present in amounts ranging from traces to 4%. In addition, the following minerals are commonly present in amounts less than 1%: sphene, apatite, magnetite, ilmenite, hematite, leucoxene, calcite, microcline, clay minerals, pyrite, and rarely garnet, pyrrhotite, chalcopyrite, fuchsite, malachite, and zircon. Some mineral assemblages are listed in Table 24.

The single spectrographic analysis for an anorthosite from southwestern map area NTS 37E in Table 48 shows high Al, Ca, and Na contents as well as very low values for most other elements. A sample of anorthosite from the large Eqe Bay sill yielded a very similar analysis (Appendix 2).

Origin of igneous rocks (Ma, Mb, Mg, Mu, Mn)

Gradations of metabasalts into both ultramafic rocks and plagioclase-rich mafic rocks, and of metagabbro into meta-anorthosite, and intrusions of mafic and ultramafic rocks into the volcanic rocks and into each other, suggest that the igneous rocks of the Mary River Group have a spatial affinity for one another and were emplaced during deposition to shortly after deposition of the metasediments of the group. The chemical data (Fig. 46-50) and field relations are also compatible with the suggestion that the Mary River Group felsic, mafic, and ultramafic rocks are probably part of a single major magmatic event. The mafic and ultramafic rocks may be part of a chemically continuous comagmatic series, and locally at least, such as at Mary River and Eqe Bay, may have been derived from a single magma chamber. In general the tholeiitic basalts were extruded first. These were followed by emplacement of ultramafic extrusions and intrusions, followed by emplacement of gabbros and the cumulate porphyritic ("football") anorthosite. This sequence of emplacement is similar to that determined for other Archean complexes such as the Fiskenaesset complex (Windley, 1971). Subordinate felsic volcanism (2.718 Ga) occurred penecontemporaneously with the mafic-ultramafic igneous activity, possibly from a different magma source. Meagre chemical data (Appendix 2a, Fig. 46) suggest that the felsic and mafic volcanics are bimodal.

The above igneous activity was followed closely by emplacement of feldspar-phyric monzogranite-granodiorite (Agp - 2.709 Ga) and possibly some charnockite (Ack) plutons. If similar but undated granites that intrude the Mary River Group are the same age, and if the two ages noted are valid (*see* respective sections on "Age"; Jackson et al., 1990b), then the Mary River Group was intruded by the granite about nine million years after deposition.

The metabasalts (Mb) were deposited in an unstable, volcanically active, marine environment for the same reasons noted in discussing the origin of the iron-formation (Mif). Presence of a sialic basement and chemical data for the metabasalts suggest deposition in a rift-related calc-alkaline to tholeiitic continental margin volcanic arc or possibly back arc environment.

The presence of obviously discordant intrusive contacts, inclusions of various rock types, rhythmic and graded layering, and dry enstatite intrusions in serpentinite show that most of the ultramafic bodies may be shallow intrusions. Presence of gradational contacts with amphibolite (possibly metabasalt), brecciated rocks, chemical compositions, and rare pillows and probable spinifex texture suggest that some of the ultramafics are komatiites extruded into water.

Chemical composition of the ultramafics, the nature of the associated Mary River Group, and the presence of sialic basement, granite gneiss inclusions in the ultramafics, and some granitic intrusions that are only slightly younger, suggest that the Mary River ultramafics were emplaced in an alpine (orogenic) continental island arc environment.

The blastoporphyritic meta-anorthosites in the map area are similar to anorthositic rocks found throughout the world in chiefly Archean metamorphic terranes (e.g. Windley, 1984), as part of layered mafic igneous complexes, formed by the differentiation of tholeiitic(?) magma, and commonly associated with supracrustal assemblages. Within the map area, however, some of the anorthositic bodies seem to be associated with very little mafic differentiate. Myers (1975a, b) has noted a similar relationship, and has suggested that if the parent magma was an oceanic tholeiite, then a mafic-rich fraction must have separated from the magma before intrusion of anorthosite into the host rock. Thus the differentiation now seen in such an individual body represents only a fraction of the total differentiation process.

Age of the Mary River Group (M, AM)

Attempts to determine the age of the Mary River Group within and adjacent to the map area by K-Ar dating proved unsuccessful (*see* Table 53), but did provide information on regional uplift. Rubidium-strontium isochron ages also proved inconclusive. An isochron age of 1971 ± 97 Ma for the group (*see* Table 52) is considered to be the age of late Aphebian metamorphism and deformation (*see* Fig. 98), to which a K-Ar age of 1865 ± 60 Ma for biotite from a felsic volcanic clast in conglomerate may also be related (*see* Table 53).

A precise U-Pb zircon age of 2718 +5/-3 Ma (Fig. 54; *see* Table 51; Jackson et al., 1990b) has been obtained for Mary River Group felsic metavolcanics (dacite) in the south-central part of the Icebound Lake map area (NTS 37G). The zircons used were small and euhedral, and the 2718 Ma age is considered to be a reliable primary age for the felsic metavolcanics from which they were derived.

Uranium-lead zircon ages of 2752 ± 30 and 2888 ± 35 Ma have been obtained for felsic metavolcanics in the Eqe Bay area just south of the map area; these are also considered to belong to the Mary River Group (Morgan, 1982; *see* Table 51). These two ages are each based on two points, for which analyses were determined on relatively large numbers of pure zircon grains unsorted as to type. The two samples were collected along strike about 8 km apart, seem to be from the same stratigraphic unit (*see* Morgan, 1982; W.C. Morgan, pers. comm., 1991), and should be of the same age. However, felsic metavolcanics are present in the basement to the Mary River Group and Morgan's (1982) 2888 Ma age is similar to 2851 +20/-17 Ma for the foliated tonalite that is basement to the adjacent 2718 Ma Mary River Group felsic metavolcanic in the map area. Locally the basement felsic metavolcanics are difficult to differentiate from Mary River Group rocks. The four points together for Morgan's (1982) two samples indicate an age of 2742 Ma, which is similar to a zircon age of 2734 +59/-45 Ma obtained for amphibolite (considered to be Mary River Group; *see* Fig. 64) in migmatite near the head of Cambridge Fiord (NTS 37H), as discussed in the section on the age of banded migmatite (Amg). The 2752 and 2888 Ma ages reported by Morgan (1982) are considered to be less reliable than the 2718 Ma age for the above reasons, and also because of recent technique improvements. Scammell and Bethune (1995a, b) have reported U-Pb zircon ages for the Equ Bay area of 2759-2725 Ma for felsic metavolcanics in the Mary River Group. They have also obtained ages of 2726-2702 for granite-intermediate intrusions, one of which intrudes Mary River Group mafic metavolcanics. More than one age of felsic volcanics may be present in the Mary River Group, and volcanic activity may have persisted for more than 100 Ma. However, on the basis of present knowledge the Mary River Group is probably 2759-2718 Ma.

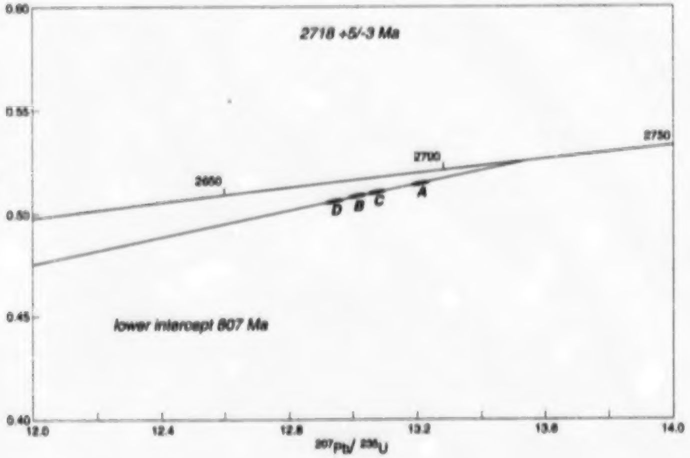

Figure 54.

Concordia diagram and U-Pb isotopic ratios for zircons from a rhyodacite quartz porphyry (Ma) *in the Mary River Group, south-central Icebound Lake map area (NTS 37G). Data supplied by P.A. Hunt and Geochronology Section, Geological Survey of Canada, Ottawa. A-D identify plots of analyses of different zircon fractions. The sizes of the plots are commensurate with the laboratory errors.*

The U-Pb zircon ages for felsic metavolcanics and intrusions on Melville Peninsula indicate that the Prince Albert Group, considered here on the basis of stratigraphy and regional trends to be equivalent to the Mary River Group, may be 2953-2879 Ma (Frisch, 1982; Henderson, 1983; *see* Table 51, Fig. 98). These ages were also determined several years ago and it is uncertain whether or not the 2953 Ma age is for rocks of the Prince Albert Group (T. Frisch, pers. comm., 1993). The age of 2879 Ma for felsic metavolcanics is still considered valid. The above ages from Baffin Island and Melville Peninsula, if valid, indicate that Archean greenstone sequences of at least two distinct ages, 2752-2718 Ma and 2879 Ma may be present. The Woodburn Lake Group at the southwestern end of the Committee Orogen (Fig. 114) west of Baker Lake, has been tentatively correlated with the Prince Albert and Mary River groups (Ashton, 1988). Several U-Pb zircon ages for the Woodburn Lake Group support this correlation: 2705+53/-30 Ma for felsic quartz-feldspar porphyry and a minimum age of 2575 Ma for rhyolite (Ashton, 1988), 2798 +24/-21 Ma with a lower intercept of 1513 +41/-40 Ma for dacite porphyry (Tella et al., 1985), 2796-2752 Ma for metadacite and 2769 ± 11 Ma for zircons in metagraywacke (Roddick et al., 1992).

Gneisses in the Melville Bugt region of North-West Greenland contain remnants of supracrustal rocks similar to the Mary River Group. The gneisses have yielded several Rb-Sr errorchron and U-Pb zircon ages of 2710-2600 Ma (Kalsbeek, 1986; Dawes et al., 1988).

Hegner (Hegner and Jackson, 1990; Jackson et al., 1990a; Jackson and Hegner, 1991) obtained a Nd-depleted mantle model age of 2.86 Ga for the same sample of Mary River Group dacite that gave a U-Pb zircon age of 2.718 Ga, and an age of 2.87 Ga for Mary River Group metabasalt at Eqe Bay. These two model ages are similar to the Nd model age of 2.85 Ga and U-Pb zircon age of 2.851 Ga obtained for foliated tonalite that is considered basement to the Mary River Group. The similarity of these ages raises the question of whether or not the Mary River Group dacite zircon age of 2.718 Ga (Jackson et al., 1990b) is primary or metamorphic. Assuming it is a valid primary age then at least some of the magma for Mary River Group felsic volcanics was probably derived from 2.85 Ga granitic plutons. Perhaps the presence of older relict 2.85 Ga zircons in younger magma that itself was regenerated at somewhat different times throughout the Committee Fold Belt (*see* Fig. 114), is one reason for the different ages obtained for the various supracrustals. The model age of 2.98 Ga for felsic volcanics in the basement to the Mary River Group at Mary River is considerably older than the 2.86 Ga model age obtained for Mary River dacite in the same area (NTS 37G), but is similar to the 2.95 Ga age from Melville Peninsula and may identify an older volcanic component in the basement to the Mary River Group.

Origin of the Mary River Group

The widespread association of locally interbedded felsic and pillowed mafic volcanics, extrusive and intrusive alpine-type (orogenic) ultramafics, gabbro and anorthosite, and graded greywacke, together with the variable stratigraphy of the Mary River Group, indicates an unstable marine depositional environment in which volcanism was active. The presence of penecontemporaneous to slightly younger (**Agp**) granitic intrusions in the map area also indicate igneous activity and instability. The occurrence of conglomeratic quartz-rich sediments and quartzites in the lower part of the sequence, overlain by a discontinuous quartz-rich unit and widespread iron-formation, most of which is a chemical sediment, indicate the quartzite and iron-formations were deposited during an interval of relatively widespread stability and volcanic quiescence.

The chemistry of granitic intrusions that are older, penecontemporaneous, and slightly younger (**Agp**) than the Mary River Group in the map area most closely resembles that for volcanic arc granites and collision granites, emplaced along an active continental margin. The chemistry of Mary River mafic metavolcanics (**Mb**) is most similar to that for calc-alkaline arc and rift basalts. The chemical data, together with the association of rock types and the presence of an older sialic basement (**Agn**, **Amn**) suggest that the regional setting was a rift-related continental arc or back arc. This is in agreement with Gross (1980, 1983), who considered the Mary River iron-formation to have been deposited in a volcanic arc environment.

Porphyritic monzogranite-granodiorite (Agp)

Description

Mappable intrusions of porphyritic monzogranite-granodiorite are scattered sparsely throughout the map area, but were not identified in map areas NTS 27E, 27G, or in southern map area NTS 37G. The largest body of **Agp** extends west-northwest for about 52 km in north-central map area NTS 37G and has an area of about 700 km^2. The rest of the **Agp** intrusions range up to 30 km in length. A small body of **Agp** occurs in the core of a foliated granitic body (gr-Agr) in northeastern map area NTS 37F. Most bodies of **Agp** are elongated parallel to local foliations and are the rock type that most commonly seems to be gradational with charnockitic rocks (Ack). Intrusions of **Agp** show up on the aeromagnetic maps in similar fashion to late granitic intrusions (**Ag**, **Ack**), and coincide with patterns that are slightly more pronounced than **Ag** patterns, but less pronounced than **Ack** patterns. Modal analyses are shown in Table 6 and Figure 17, and are

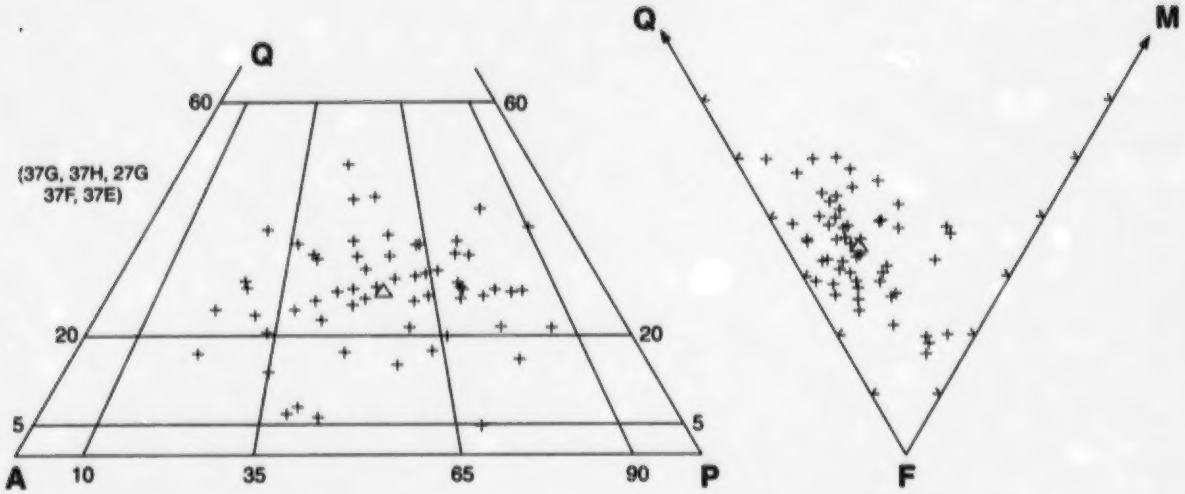

Figure 55. Quartz-alkali feldspar-plagioclase and quartz-feldspar-mafic plots for unit **Agp***. The small triangle gives the mean value.*

***Figure 56.** Foliated, locally deformed porphyritic monzogranite intruded by thin pegmatite in map area NTS 37G. The exposure is about 1.3 m across. Photograph by W.J. Crawford. GSC 186256*

plotted on QAP and QFM diagrams in Figures 20Fa-d and 55. Chemical data are included in Tables 30, 47 (column C), 48 (column 4), and 49, and in Figures 58, 69, 73, 74, 75, and 95.

Unit **Agp** intrusions are chiefly medium grained (fine- to coarse-grained), and light pinkish grey, but range from white to grey, pink, mottled pink, and red. Some gneissic varieties are black locally.

Major minerals are quartz, plagioclase (An_{17-34}), and perthitic microcline (Table 30, Fig. 17, 20Fa-d, 55). The microcline occurs as phenocrysts (locally includes porphyroblasts?) as much as 6 cm long, and in the matrix (Fig. 56). Minor myrmekite is common. Mafic minerals are chiefly brown biotite and blue-green to olive-green hornblende, and commonly make up as much as 25% of the rock. Biotite predominates over hornblende in most of the intrusions. Hornblende, however, predominates over biotite by as much as 3:1 in small homogeneous intrusions adjacent to granulites on the west side of Tromso Fiord (NTS 37H) and at the head of Clark Fiord (NTS 37E).

Muscovite occurs locally and sericite, chlorite, light green hornblende, epidote, and kaolinite-montmorillonite are chiefly retrograde products; orthoclase occurs adjacent to granulite terrane. Accessory minerals are: sphene, apatite, allanite, zircon, leucoxene, pyrite, magnetite, and goethite. The most common mineral assemblage is:

quartz+microcline+plagioclase+biotite±hornblende.

Rarely, orthoclase is present rather than microcline.

Most of the **Agp** intrusions are monzogranite and granodiorite (Fig. 20Fa-d, 55), but include some quartz monzonite (NTS 37G) and syenogranite (NTS 37G, 37H-27G). Most also plot in the middle part of the QAP diagram, crudely approximating the position of minimal granitic melts. Mineralogically, there is little difference between the map areas other than that the intrusions in map area NTS 37G contain less quartz and those in map area NTS 37E vary least in mafic content (Fig. 20Fa-d).

Unit **Agp** intrusions are chiefly homogeneous and massive to faintly foliated. Some of the rocks, however, are faintly laminated to very thinly banded and locally have a mineral lineation and a few scattered lenses and schlieren or skialiths of paragneiss and amphibolite. Banded migmatitic, granitic, nebulitic, porphyroblastic, augen, and flaser gneisses, as well as blotches of potassium feldspar, occur locally. Several of the **Agp** intrusions contain crushed or fractured zones as much as 2 m thick in which the feldspar megacrysts have been granulated and mafic minerals have been recrystallized to chlorite and minor biotite. Unit **Agp** is intruded by dykes of massive granite, pegmatite, and aplite.

Contact relations

Where observed the contacts are usually sharp and well defined. Some marginal zones of plutons contain schlieren of adjacent rocks and are migmatitic, and these intrusive rocks (**Agp**) range from massive to strongly foliated and sheared parallel to the contacts. Faulted contacts are common and interleaving of granitic and host rocks occurs locally.

In a few places, unit **Agp** plutons intrude rocks that are considered to belong to the Mary River Group. The relationship between unit **Agp** and the Piling Group in the southeast corner of the Conn Lake map area (NTS 37E) suggests that both have been deformed together. Unit **Agp** has not been reported as intruding the Piling Group, and is considered here to be older than the Piling Group. Contacts with charnockitic rocks (**Ack**) seem to be gradational and to represent increasing metamorphic grade toward the charnockites. Bodies of **Agp** are intruded by Aphebian massive granites (**Ag**), by pegmatites and granite dykes, and by Hadrynian diabase dykes (**Hg**). A few metamorphosed basic dykes may be present locally.

Chemistry

A mean for spectrographic analyses of porphyritic monzogranite-granodiorite (**Agp**) is given in Table 48 (column 4). The analyses in groups I-III are in general similar. However, according to the modes and patterns displayed by individual elements in histograms (*see* Table 49, Fig. 95), unit **Agp** is least similar to other quartzofeldspathic map units. It is moderately similar to unit **Amp**, a migmatite with potassium feldspar porphyroblasts. Unit **Agp** is relatively dissimilar to charnockitic rocks **Ack**, which is somewhat surprising considering the two units appear to be intergradational in the field. However, Ti, Cu, and Zr values are virtually identical in the two units.

Chemical data in Tables 30 and 48 have been compared with chemical data interpreted by Pearce et al. (1984) and others (e.g. *see* Tables 31, 32). The data are conflicting, but unit **Agp** seems to be slightly more similar to volcanic arc granites than to other types, and to active continental margin granites than to other arc granites. However, there are almost as many similarities to collision, ocean ridge, and within-plate granites.

Comparison with data in Whalen et al. (1987) shows map unit **Agp** is more similar to I-type granites than to S-type granites. There are several similarities with M-type granites, and unit **Agp** is least similar to A-type granites.

Spectrographic analyses for eleven elements are compared with other map units in Figure 95 (*see* Fig. 95). The values for **Agp** and **Ack** are comparable, and values for Sr, Zr, Ba, and Fe are higher than for other granitic rocks. Plots for both units **Agp** and **Ack** comparing Zr with TiO_2, MgO, Ba, and Sr, and Ba with Sr are given in Figure 58. These plots show a larger range of Zr values for both **Agp** and **Ack** than for several other granitic units (gr-Agr, Fig. 26; **Ag**, *see* Fig. 72; late massive granites in **Amg**, *see* Fig. 63). The plots for **Agp** and **Ack** show what seems to be a positive differentiation trend that has been modified, perhaps by metamorphism.

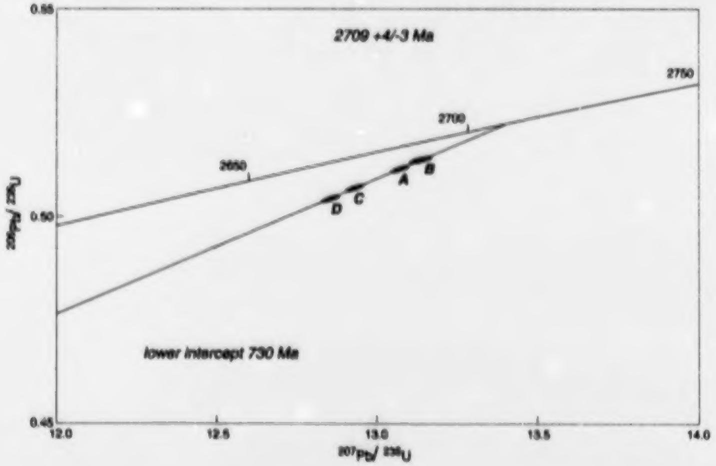

Figure 57.

Concordia diagram and U-Pb isotopic ratios for zircons from porphyritic foliated monzogranite (**Agp**) *in north-central Icebound Lake map area (NTS 37G). Data supplied by P.A. Hunt and Geochronology Section, Geological Survey of Canada, Ottawa. A-D identify plots of analyses of different zircon fractions. The sizes of the plots are commensurate with the laboratory errors.*

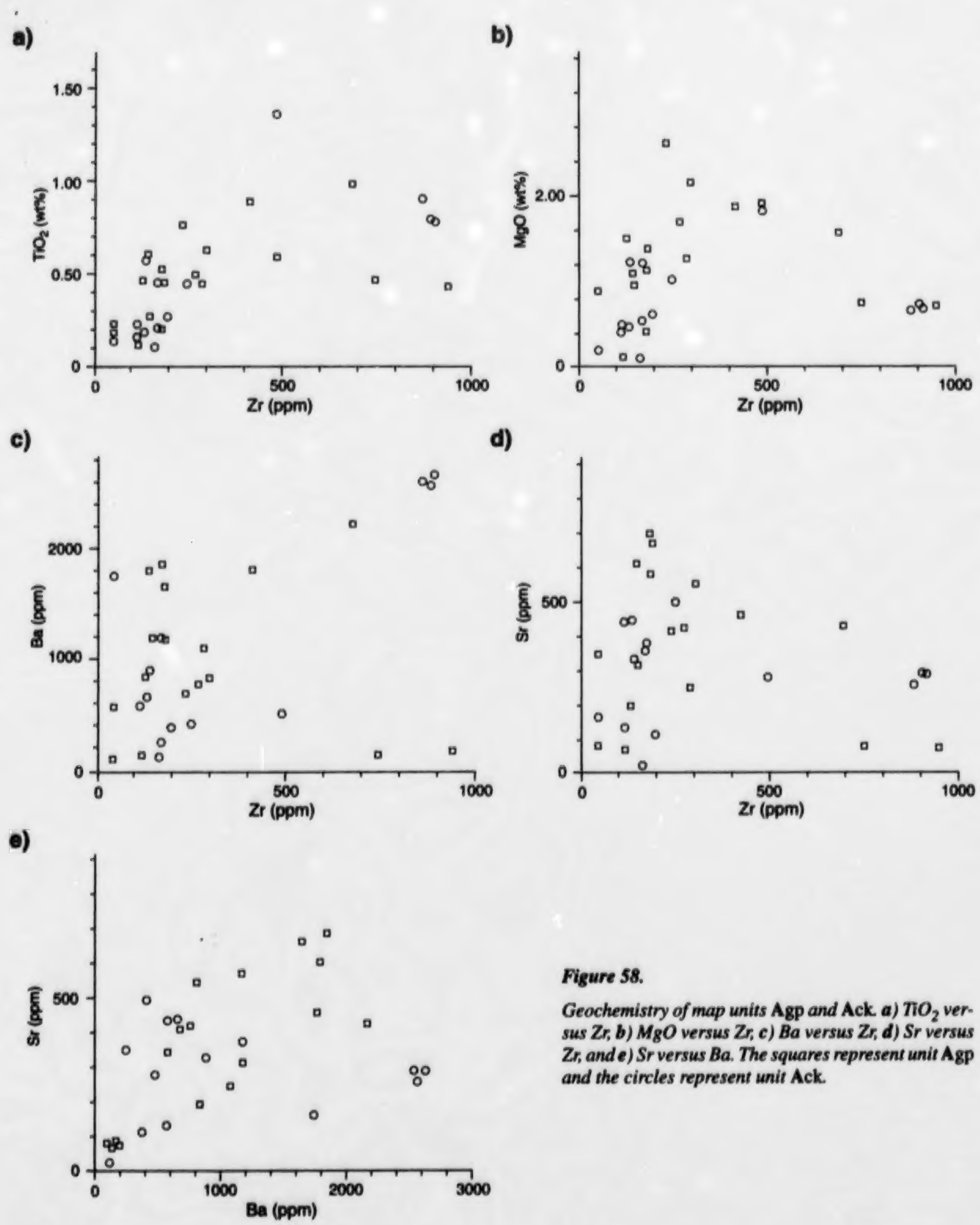

Figure 58.

Geochemistry of map units Agp *and* Ack. *a)* TiO_2 *versus Zr, b) MgO versus Zr, c) Ba versus Zr, d) Sr versus Zr, and e) Sr versus Ba. The squares represent unit* Agp *and the circles represent unit* Ack.

Patterns for both units are more similar to one another than to the plots for the other granitic rocks. This similarity supports the field observation that Agp and Ack are intergradational.

One chemical analysis for massive monzogranite (Agp) is compared with other granitic rocks, chiefly charnockites (Ack), in Table 30. Plots in Figures 69 and 73, and indicator ratios in Table 32, for the most part, indicate that the sample is a K-rich alkaline or calc-alkaline, metaluminous volcanic arc monzogranite that plots along the granite calc-alkaline continental margin trend (*see* Fig. 69f). The sample also plots in the anomalous granite field of Figure 69k, in the metaluminous field of Figure 73g, and close to the differentiation trend for magma from crustal fusion in Figure 73h. The sample's position in Figure 73f presumably indicates that the sample is metasomatic. Figures 69j and 73c indicate that the sample is an I-type granite, although the indicator ratios in Table 32 are contradictory as to whether the sample of Agp is an I-type or an S-type granite.

Figure 74 (*see* Fig. 74, below) shows that the sample has a relatively low differentiation index. The analysis for map unit Agp and analyses for other granitic map units in the map area are plotted for comparison in Figures 74 and 75 where they outline linear trends that resemble positive and negative differentiation trends.

Age

A U-Pb zircon age of 2709+4/-3 Ma (Fig. 57) has been obtained for the large porphyritic monzogranite body in north-central Icebound Lake map area (NTS 37G). The collinearity of the points and their proximity to the concordia curve indicate that this is a reliable age, and Agp plutons are now considered to be Archean, although some similar younger plutons could also be present. The same sample provided a Nd T_{DM} (DePaolo) model age of 2.90 Ga.

Before this zircon age was available, unit Agp was considered to be Aphebian. The main reasons for this earlier conclusion are that some bodies of Agp intrude the Mary River Group and these rocks are relatively undeformed as compared with older Archean granitic rocks. A U-Pb zircon age of ca. 2.72 Ga for similar plutonic rock in the Eqe Bay area (Scammell and Bethune, 1995a) is further support for a late Archean age for unit Agp.

Origin

The Archean (2709 Ma) porphyritic monzogranite-granodiorite intrusions of unit Agp are penecontemporaneous or slightly younger than the Mary River Group felsic metavolcanics (unit Ma, 2718 Ma). Their close spatial relationships and age similarities (both U-Pb zircon and Nd T_{DM}) suggest a magmatic and tectonic relationship, although there is not a strong similarity in their chemistry (*see* Table 48).

The chemistry of unit Agp (e.g. *see* Tables 30, 48) is somewhat conflicting with, but the data plot in similar fields to, unit gr-Agr, and also favours emplacement of alkaline to calc-alkaline I-type granite in an active continental margin of a volcanic arc environment. Petrographic data, following the conclusions of Pearce et al. (1984), are in agreement with the chemistry but could equally well apply to post-tectonic collision granite. The 200 Ma difference in the U-Pb zircon and Nd T_{DM} model ages suggests that either the monzogranite represents magma that did not crystallize until 200 Ma after it separated from the mantle, or it was remelted and reintruded at the later date.

APHEBIAN AND/OR ARCHEAN

Relatively little is known about map units bg, sv, and mu. The first (bg) is chiefly homogeneous quartz-biotite-feldspar gneiss. The second (sv) is mostly paragneiss and lit-par-lit gneiss. The third (mu) consists mostly of a variety of gneisses that have not been subdivided. The rocks in all three map units have been highly metamorphosed and are at least as old as Aphebian.

Homogeneous quartz-biotite-feldspar gneiss (bg)

This unit occupies a belt, 50 km long and 15 km wide, that extends north from Clark Fiord (Buchan Gulf-Scott Inlet, NTS 37H-27G). It also occupies a small area on the north coast of Sillem Island (NTS 27F, G). No aeromagnetic maps are available for this region. A few modal analyses plot on granodiorite-tonalite fields of the QAP triangle and toward the feldspar apex of the QFM triangle (Fig. 20Ka).

Most fresh and weathered surfaces are grey, but weathered surfaces may also be grey-black, and rarely pinkish grey. Medium grained rocks predominate but some are fine grained.

Quartz, oligoclase, and microcline make up 60 to 90% of these rocks, with microcline itself ranging from 1 to 20%. Plagioclase and some potassium feldspar megacrysts, up to 1.5 cm across, occur scattered throughout much of the rock, are granulated in some places, and locally make up to 20% of the rock. Brown biotite and hornblende make up most of the remainder of the rocks. Accessory minerals are magnetite, sphene, and rarely, epidote and allanite. Amphibolite inclusions make up less than 1% of the outcrop at one locality.

Most of this unit is massive and relatively uniform in composition, especially as seen from the air. In detail, however, some of the rock is weakly foliated to schistose, tightly folded on a small scale, and contains internal dislocations and healed shears. The rocks are migmatitic in a few places and in others resembles a nebulitic granitic migmatite (Amn).

A shear zone probably separates unit bg from unit Amn to the southwest just north of the elbow in Clark Fiord (NTS 27G). Sixteen kilometres east-southeast of Duart Lake (NTS 37H), there is an abrupt change from unit bg to unit mu along what may be a fault zone. A few pink granitoid dykelets intrude these rocks in places.

A mean for three spectrographic analyses (Table 48, column 12) shows relatively high Cu, La, and Sr compared with most other rocks in the map area. Values for other elements seem quite normal.

The origin and age of unit bg is uncertain, and it may contain rocks of more than one origin. Much of it may be a metamorphosed Archean granitic pluton, but some of it could be an arkosic metasediment of uniform composition or nebulitic granitic migmatite (Amn).

Paragneiss, lit-par-lit gneiss (sv)

Paragneiss and lit-par-lit gneiss underlie a small elongated area that trends southeast for about 12 km from a small bay about 20 km southwest of Cape Eglinton (Fig. 1, NTS 27F). The rocks consist chiefly of quartzofeldspathic paragneisses, lit-par-lit gneisses, and minor felsic-intermediate metavolcanics. As seen from the air, small amounts of quartzite or marble may be present locally. No aeromagnetic maps are available for the area.

The rocks are fine- to medium-grained, very pale- to medium-grey, and locally pinkish grey. Compositional banding ranges from fine folia to thin bands 10 cm thick. Some are crushed and others seem to be blastomylonitic. Isoclinal microfolds (hand specimen size) are also present.

The major minerals are plagioclase, quartz, and potassium feldspar. Minor potassium feldspar porphyroblasts are common and the felsic-intermediate metavolcanics contain quartz eyes. Hornblende is more abundant than biotite, and together they form about 20% of the rock. Minor garnet is present and allanite is an accessory mineral.

The age of this unit is uncertain. It could be an outlier of the Mary River or Piling groups, or of some other supracrustal sequence. The presence of felsic-intermediate metavolcanics suggests an affinity with the Mary River Group.

Undifferentiated gneisses, mixed rocks (mu)

This unit occurs chiefly as irregular bodies within a wedge-shaped region that is about 100 km wide in the western part of the Icebound Lake map area (NTS 37G) and extends eastward to the southern part of the Buchan Gulf map area (NTS 37H), and the northwestern corner of the Conn Lake map area (NTS 37E). Elsewhere, areas up to 16 km across occur adjacent to Scott Inlet (NTS 27G), north of Scott Inlet in the Bruce Mountains (NTS 37H), east and west of the Barnes Icecap (NTS 37E), and in the area of Nina Bang Lake (NTS 37F).

Aeromagnetic maps of the areas underlain by unit mu show patterns that range from nondescript to bird's-eye to linear parallel to the regional trend. Peak values are seldom as high as 500 nanoteslas above the average local nanotesla value.

Ground, airborne, and airphoto observations indicate that this unit consists of: (1) a heterogeneous assemblage of granitoid gneisses (Agn, Amn, gr-Agr, Amg, Amp), each type being impersistent; (2) some undifferentiated metasediments and amphibolites that have been variously deformed and granitized; and (3) minor amounts of agmatite, veined gneiss, gneissic mafic plutonic rocks, and massive and porphyritic granitic rocks and pegmatite.

Ground observations are lacking in most of the areas underlain by this unit in the Steensby Inlet (NTS 37F), Conn Lake (NTS 37E), and Scott Inlet (NTS 27G) map areas. Several ground observations in the Icebound Lake (NTS 37G) and Buchan Gulf (NTS 37H) map areas, together with more recently acquired field observations for much of northern map area NTS 37G, permit a few generalizations to be made. In map area NTS 37G the following areas shown as mu are underlain chiefly by nebulitic granitic migmatite (Amn):

(a) south of 71°25′N latitude, east of 77°40′W longitude;
(b) 71°30′-71°45′N latitude, west of 79°W longitude; and
(c) along the southern boundary west of 79°W longitude, including the area in the northwestern corner of NTS 37F.

Areas listed below are underlain mostly by banded migmatite (Amg):

(a) north of 71°25′N latitude, east of 76°45′W longitude;
(b) south of 71°30′N latitude, 77°40′-79°W longitude; and
(c) north of 71°45′N latitude, west of 78°30′W longitude.

The rest of the areas in the Icebound Lake map area and most of the Buchan Gulf map area seem to be underlain mainly by discontinuous bodies of Amn and Amg, or of relatively intimately intermixed Amn and Amg. A small, but important complex area of basement rocks (Agn) west of No. 1 iron deposit at Mary River, and not differentiated from mu on the Icebound Lake (37G) map area, is described with map unit Agn.

APHEBIAN

Piling Group

Regional description

Moderately to intensely deformed metasediments of the Piling Group occupy a belt as much as 130 km wide south of the map area, which extends across Baffin Island from Longstaff Bluff on the west to Home Bay on the east. This belt forms the eastern Foxe Fold Belt, as originally defined by Jackson and Taylor (1972). Piling Group strata range in metamorphic grade from greenschist to granulite (Jackson and Morgan, 1978a).

The general stratigraphy was established, and the group named, by Jackson and co-workers (Jackson, 1969, 1971; Jackson and Taylor, 1972) after Piling Lake and Piling Bay, in the general vicinity of which are some excellent outcrops. The first descriptions of the Piling Group were provided by Kranck (1951, 1953, 1955) and by Eade (1953); Kranck used "Clyde series" to refer to some of these rocks. Brief mention was also made by Gray (1966) and Forester and Gray (1967).

W.C. Morgan, in a systematic study of the western Piling Group and its basement, provided new information on stratigraphy, metamorphism, and deformation, assigned names to the formations, and mapped that part of the Foxe Fold Belt adjoining the Steensby Inlet (NTS 37F) and Conn Lake (NTS 37E) map areas to the south (Morgan et al., 1975, 1976; Morgan, 1982, 1983). Strata in the Eqe Bay area (NTS 37C) were re-examined by Bethune and Scammell (1993, 1997; Scammell and Bethune, 1995a).

Henderson continued the study eastward and mapped the region that adjoins the Clyde River (NTS 27E-F) map sheet to the south (Henderson et al., 1979; Henderson and Tippett, 1980; Henderson 1985a, 1985b). Bedrock studies of relatively restricted areas include those by Chernis (1976), Tippett (1978, 1979, 1980), and Brisbin (1979). Cameron (1986) has interpreted the geochemistry of lake water and sediment samples collected in western Baffin Island between 68°-70°N latitude. Anomalies for various elements including an extremely high As anomaly are considered to be locally derived from the underlying Piling Group. Recently Henderson carried out a more detailed study of the Piling Group in the Dewar Lakes area (Henderson et al., 1988, 1989; Henderson and Henderson, 1994).

The Piling Group contains three major lithological sequences, the relationships between which are clearest south of the map area (Jackson and Taylor, 1972). The lowermost is a relatively thin sequence that contains three formations: the basal Dewar Lakes Formation composed of basal quartzite and muscovite schist, the Flint Lake Formation composed of calc-silicates and marble, and at the top, the Astarte River Formation composed of rusty quartz-rich schist (Morgan et al., 1975, 1976; Morgan, 1982, 1983). The rusty schist is chiefly a sulphide facies iron-formation but grades locally into silicate- and oxide-facies iron-formation. The middle sequence, which is best developed south of the map area, consists of a thin sequence of pillowed metabasalt and associated mafic sills, and ultramafic sheets that are most abundant on the west coast of Baffin Island. This igneous sequence dies out northward and seems to occur only sporadically on the north side of the Foxe Fold Belt. In this region, including the map area, the rusty schist at the top of the lowermost unit seems to occupy the same stratigraphic position as the igneous sequence. Amphibolite associated with quartzite, oxide facies iron-formation, rusty schist, and metagreywacke on the south side of Generator Lake (NTS 27C; Fig. 101) may represent the reappearance of the mafic igneous sequence along the north side of the Foxe Fold Belt. It seems less likely that the amphibolite and associated rocks represent the Mary River Group, although outcrop is relatively poor in this area (*see* "Correlations" in section "Mary River Group (M, AM)"). The uppermost sequence is composed chiefly of metagreywacke with graded bedding and minor metapelite, forming a monotonous, well bedded turbiditic-flysch sequence (Jackson, 1971; Jackson and Taylor, 1972) more than 3000 m thick (Morgan et al., 1976) and named the Longstaff Bluff Formation. This sequence becomes lighter coloured and more quartzofeldspathic upward in some areas, as the proportions of shale and mafic components decrease.

Rafts and schlieren of amphibolite, metasediments, and minor ultramafite probably derived from the Piling Group are abundant in the migmatite zone lying immediately south of the main Piling belt, and also occur in migmatites south to Cumberland Sound. Amphibolite bands and lenses are relatively minor along the northern edge of the belt, but may increase in abundance chiefly northeastward and eastward.

Modal analyses for Piling strata are provided in Figure 29 and Tables 26 and 27, and shown in triangular plots in Figure 20Kd-e. Chemical data are provided in Tables 9 (columns 7 and 8), 17 (columns 17 and 18), 47 (column H), and 48 (column 28). Additional data are given in Appendices 2, 5, and 7. These data are referred to in the appropriate sections. Chemical comparisons with the Mary River Group and the Bylot Supergroup are provided in the section on "Regional geochemistry".

Occurrence in map area

Discontinuous swirly belts of Piling Group, as much as 40 km long, outcrop chiefly within two terranes along the southern edge of the map area covered by this memoir, and probably represent a stratigraphic thickness of several hundred metres. One terrane is about 32 km across in the southeast corner of the Steensby Inlet map area (NTS 37F), and extends south into the Koch Island map area (NTS 37C; Morgan et al., 1975; Morgan, 1982; Bethune and Scammell, 1993). It is about 80 km northwest of the nearest known Piling Group strata in the Lake Gillian map area (NTS 37D) to the south. The second terrane, about 72 km long, extends from the southeast corner of the Conn Lake (NTS 37E) map area, eastward into the southwest corner of the Clyde River (NTS 27F) map area, and southward into the northeast corner of the Lake Gillian (NTS 37D; Morgan, 1983) and northwest corner of the McBeth Fiord (NTS 27C; Henderson, 1985b) map areas. Piling Group strata in the eastern terrane have been traced discontinuously southward to the major Piling basin.

A few small areas of supracrustal rocks lie along Walker Arm, Sam Ford Fiord, and Clyde Inlet (NTS 27F). Most are too small to show on the maps, and it is uncertain as to which group of rocks they belong. Kranck (1955) has described schlieren and bands of diopside-hornblende-magnetite-bearing garnet skarn from about 3 km west of the head of Gibbs Fiord (NTS 37E) in which pyrrhotite, pyrite, and minor chalcopyrite are common. These rocks were considered by Kranck (1955) to be remnants of the rusty quartz schist and iron-formation unit of the Piling Group.

In the eastern terrane described above, individual bodies of Piling Group strata are commonly elongated northwest, subparallel to Franklin diabase dykes in the Clyde River (NTS 27F) map area, and east-west in the Conn Lake (NTS 37E) map area. The Piling Group appears to have little magnetic expression in the map area except for iron-formation which is chiefly sulphide facies; oxide facies is thin and rarely present. Although the aeromagnetic pattern roughly parallels the regional rock trends it seems to be related chiefly to the diabase dykes and to reflect a topographic effect. The Piling Group commonly occupies areas of relatively low topographic relief, which appears to further reduce its generally low magnetic expression.

Table 25. Partial sections of lower Piling Group near the head of Sam Ford Fiord (NTS 27F), southwest.

A: West side of fiord (this memoir)		B: East side of fiord (Kranck, 1955)	
Fine grained, pink layered quartzofeldspathic augen gneiss		**Gneiss, commonly migmatitic**	
THRUST FAULT		**THRUST FAULT**	
Flint Lake Formation		**Dewar Lakes Formation**	
White marble	12.2 m	Quartzite	6.1 m
Dark green calc-silicate gneiss	1.8 m		
White to grey marble	16.8 m	**Flint Lake Formation**	
		Salmon-red limestone marble	12.2 m
Astarte River Formation			
Garnetiferous pegmatitic gneiss		**Astarte River Formation**	
Rusty pyrrhotite-bearing schist	4.6 m	Rusty pyrrhotite-bearing schist	3.7 m
Garnetiferous biotite-quartz-feldspar augen gneiss			
		Flint Lake Formation	
Flint Lake Formation		Calcareous mica schist, minor skarn	13.7 m
Off-white limestone marble	0.6 m	Coarsely crystalline, white to pale violet marble	12.2 m
Dark grey to green calc-silicate gneiss Orange to pink limestone marble, brecciated locally	6.1 m	Skarn with diopside, chondrodite, tremolite, wollastonite, phlogopite	4.6 m
Pure white dolomitic marble	2.7-4.6 m	**Dewar Lakes Formation**	
Serpentine-spotted marble Impure quartzite, faserkiesel gneiss Light green skarn, calc-silicates	3.7 m	White glassy quartzite (thickness varies)	8.5 m
			61.0 m
Dewar Lakes Formation		? ? ? ?	
Pink pegmatite quartzite	0.6 m	Gneiss, commonly migmatitic	
White metaorthoquartzite	3.0 m		
Grey layered quartzite	0.3 m		
	52.4-54.3 m		
? ? ? ?			
Pink to grey, well-layered, homogeneous quartzofeldspathic gneiss, nonmigmatitic (meta-arkose?)			

In the western terrane described above (e.g. NTS 37F), the Piling Group lenses commonly occur in close proximity to Mary River Group lenses, and derived migmatites contain relics of both groups. Both groups contain iron-formation although that in the Mary River Group is chiefly oxide facies and thicker and more continuous than that in the Piling Group, which is chiefly sulphide facies. The aeromagnetic pattern in this area is discontinuous, swirly, has low magnetic expression except where iron-formation is present, and reflects in part the presence of faults and northwest-trending diabase dykes, and numberous remnants of the Piling and Mary River groups. Additional Piling Group remnants, not shown on the Steensby Inlet map sheet (Jackson et al., 1978d), were noted by R. Berman and the author in 1992, and by the author in 1994.

Piling Group strata within the map area are variously folded into upright to horizontal, chiefly isoclinal structures. Marble beds commonly show evidence of extreme plastic deformation, and evidence of brittle deformation is equally common in quartzites, calc-silicate rocks, and pegmatites. Piling Group strata, chiefly quartzite, marble, and rusty schist, are structurally underlain and overlain in several places by basement nebulitic granitic gneisses adjacent to subhorizontal and low-angle thrusts, and in nappes. Structures and lithologies are truncated along one or both sides of the faults. Some of the recumbent folds and thrusts have themselves been moderately to highly deformed so they are difficult to delineate.

Stratigraphy

A generalized stratigraphic section for the Piling Group in the map area is provided in the Table of Formations. Two partial sections are shown in Table 25 for Piling strata on both sides of Sam Ford Fiord (NTS 27F), which lie along the thrust-faulted axial portion of an isoclinal syncline overturned to the southwest, with overthrusting in that direction. The precise positions of the fault and fold axial plane are uncertain, which makes the primary stratigraphy of these rocks uncertain, but a crude correlation is evident across the inlet. Formation names were assigned to the Piling Group by Morgan (1983) after the maps for areas NTS 37E and 37F were published.

Dewar Lakes Formation (ADL, APq)

This formation (Morgan, 1983) is commonly the basal unit (*see* Table 25) of the Piling Group and can be subdivided into three members, although all three are rarely present at any one locality within the map area. From bottom to top these are: quartzofeldspathic paragneiss, muscovite-quartz schist, and quartzite. All three members occur in contact with the underlying basement gneisses which are chiefly nebulitic granitic migmatite (Amn), suggesting depositional onlap. South of the map area the Dewar Lakes Formation is much thicker, locally at least, in the eastern, than in the western, Piling Group. The formation is continuous throughout much of the Piling terrane, but it is absent in some places where overlying formations lie directly on the basement. Modal analyses are plotted in Figures 20Kd and 29.

Quartzofeldspathic paragneiss

Quartzofeldspathic gneiss occurs locally as the basal Piling unit and is overlain conformably by quartzite and/or marble in several places, as for example on Sam Ford Fiord. In some places the quartzofeldspathic gneiss seems to be conformable and gradational with both overlying quartzite or marble and underlying nebulitic granitic migmatite, and may include a metamorphosed regolith.

The quartzofeldspathic gneiss is discontinuous, but is at least 30 m thick on Sam Ford Fiord (NTS 27F). These rocks are fine- to medium-grained, and are commonly well banded, well foliated, or both, the foliation being defined chiefly by elongate quartz grains and parallel mica crystals and folia. Fresh and weathered surfaces are pink to light grey. Major minerals are quartz, plagioclase, and microcline. The plagioclase is chiefly altered oligoclase that shows evidence of retrogression. Most of the microcline occurs in clear, irregular-shaped grains and is probably of metamorphic origin. Some perthitic, and porphyroblastic grains are also present. Minor minerals include brown to reddish-brown biotite, muscovite, and garnet. Accessory minerals include zircon, apatite, magnetite, hematite, graphite, sphene, allanite, metamorphic epidote rimmed by magnetite, and secondary or retrograde chlorite and, locally, muscovite. Typical assemblages are:

> quartz+potassium feldspar+oligoclase+biotite+(muscovite or garnet), and
>
> quartz+andesine+biotite+garnet.

A few of the points plotted on Figure 20Kd represent quartzofeldspathic paragneiss and muscovite-quartz schist. Their positions in the QFM plot indicate an arkosic composition, and the member is considered to be chiefly meta-arkose or grit.

Muscovite-quartz schist

This lithology occurs at the base of the Piling Group at many localities to the south, but in this map area it is rare at that stratigraphic position, and is only 1-2 m thick in some places. This lithology also occurs as conformable interbeds within the quartzite, marble, and metagreywacke. Where present at the base of the Piling Group, this member seems conformable with both the underlying basement gneisses and the overlying quartzite.

These rocks are commonly finely foliated or sheared, off-white to light grey, and fine- to medium-grained. Major minerals include quartz, oligoclase, and muscovite. Minor constituents include biotite and potassium feldspar.

Quartzite

The previously described quartzofeldspathic paragneiss and muscovite-quartz schist are absent in most places in the map area and in many places to the south, so that the quartzite is commonly the basal member of the Piling Group and the main or only member of the Dewar Lakes Formation. The basal contact is sheared at many localities, and in a few places, faint banding in both the underlying gneiss and in the quartzite ends abruptly at the contact, which may be a fault. Contact with the overlying Flint Lake Formation is commonly conformable, and either gradational or with several lithologies being interbedded in the transition zone (Table 25). Thicknesses in most places range from several centimetres to about 10 m in the map area, but may be greater locally, and are greater south of the map area. The quartzite seems to be continuous in most of the area but locally has been deposited discontinuously in topographic lows.

Most of the quartzite member is white to rarely pink, fine- to medium-grained, locally coarse grained, and has a somewhat varied composition. The quartzite is generally jointed, ranges from massive to layered, and is sheared in some places. A finely foliated to thinly banded impure grey quartzite up to 0.3 m thick commonly lies at the base of the member whether it overlies the basement gneisses directly or overlies the quartzofeldspathic gneiss. This impure quartzite grades upward into metaorthoquartzite that contains minor interbedded feldspathic quartzite, meta-arkose, and muscovite-quartz schist. Marble, calc-silicate rocks, and aluminosilicate-bearing metasandstones are interbedded with the quartzite chiefly in its upper part. On Sam Ford Fiord the top of the quartzite contains 0.3-0.6 m of rock that ranges from quartzite containing potassium feldspar porphyroblasts to pink pegmatite. Rare crossbeds and metaconglomerate occur south of the map area (Morgan et al., 1976).

Major minerals include quartz and locally, potassium feldspar, plagioclase, and muscovite. Plagioclase is chiefly oligoclase, but ranges to bytownite in the cores of some sillimanite nodules (faserkiesel) which range up to 5 cm across. These nodules range from chiefly quartz-sillimanite and quartz-sillimanite-plagioclase to those composed chiefly of plagioclase and containing minor fibrous and spherulitic sillimanite. The cores of the faserkiesel are composed of calcic plagioclase, whereas more sodic plagioclase forms the outer rims of the nodules. Some of these outer rims contain minor to locally abundant quartz and potassium feldspar. Quartz-sillimanite segregations have also been noted in the area to the south (Eade, 1953; Forester and Gray, 1967; Morgan et al., 1976).

Carbonate and calc-silicate minerals are abundant locally. Minor and accessory minerals include biotite, phlogopite, hornblende, orthopyroxene, garnet, magnetite, zircon, and apatite.

Flint Lake Formation (AFL, APs)

Carbonate and related calc-silicate rocks form a distinctive map unit that conformably overlies the quartzite unit and locally the nebulitic granitic migmatitic gneisses with apparent conformity (Fig. 59a,b). The marble unit has been intensely deformed plastically, whereas in many places quartzitic and calc-silicate interbeds, and intrusive pegmatites, have been brecciated and the fragments mixed heterogeneously in a marble matrix. Although commonly angular, the fragments are locally well rounded. At some localities, where quartzite and marble have been interfolded, quartzite beds have been fractured along fold limbs and the ends separated during attenuation. Marble has deformed plastically around the quartzite fragments so that quartzite rods occur along fold axes and elongated quartzite fragments along fold limbs.

The marble is composed chiefly of equidimensional, equigranular, fine- to coarse-grained carbonate crystals. Fresh and weathered surfaces are chiefly white to grey and are also commonly buff or greenish. Distinctive orange to salmon-pink marble occurs at many localities, chiefly in the central part of the unit, but it is not known whether or not it marks a specific stratigraphic horizon. Calc-silicate bands are also equigranular and range from fine- to coarse-grained and locally pegmatitic. They are commonly pale green to green and greyish green but may also be white on the fresh and weathered surfaces. The unit is well layered, from very thin banded to massive (*see* Table 2), with some massive or only faintly banded marble bands ranging up to 18 m thick. Calc-silicate rocks are commonly interbanded with the marble and occur in beds up to 2 m or more thick, but most are 0.6 m or less. They commonly consist of carbonate and silicate minerals intimately intermixed in varied proportions. Differential weathering results in many of these beds having a rough, hackly weathered surface.

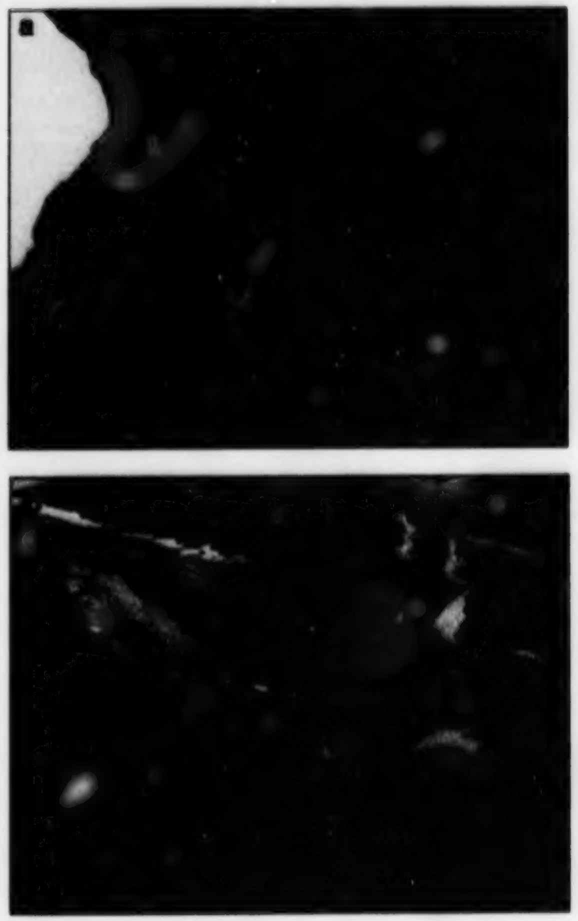

Figure 59. ***a)*** *Cave in pink marble of the Flint Lake Formation, southeast corner of map area NTS 37E. Photograph by W.J. Crawford. GSC 186519.* ***b)*** *Isoclinal fold of Flint Lake marble overturned to the south (dips 5-10°N) with a central thin band of contorted metapelitic rock. Discordant migmatitic granitic gneiss occurs in the foreground and concordant migmatitic granitic gneiss occurs at the top of the photo. The width of the marble outcrop is uncertain, possibly about 200 m. Hadrynian diabase occurs on the right. Southwest corner of map area NTS 27F. Photograph by S.L. Blusson. GSC 185695*

Garnet-bearing rocks seem to be largely of two types. One type is predominantly white calc-silicate rock and contains relatively few mineral species, chiefly white to pale coloured grossularite with diopside, carbonate, and minor quartz. One such rock in the southeast corner of the Steensby Inlet map area (NTS 37F) contains about 85% grossularite with minor diopside. Both minerals contain less than 2% iron. Minor quartz is also present. These rocks originally may have been a carbonate or siliceous carbonate with various amounts of intermixed clay minerals. The second type of garnet-bearing rock is common in the western terrane (NTS 37F) and contains red garnet, probably almandine-pyrope, that ranges from a major to a very minor component. Other major components include quartz, plagioclase, potassium feldspar, muscovite, and biotite. Minor and accessory minerals include cordierite, sillimanite, muscovite, and iron oxides. This second type may represent sediments ranging from a siliceous mud to muddy sand.

Other lithologies present in the Flint Lake Formation include minor interbeds of quartzite (including metachert), muscovite-quartz schist, amphibolite, pyroxene gneiss, metapelite-metagreywacke, and rusty graphitic sulphide schist. Pegmatites in the formation are rich in calcic plagioclase, with minor microcline and quartz, and probably are largely internally derived. The marble unit ranges up to 61 m thick, and possibly considerably more locally. Much greater thicknesses occur south of the map area, which may reflect, in part at least, primary sedimentary thickness.

Major minerals include calcite and dolomite in the pure marbles. In impure marbles and calc-silicate rocks, major minerals include calcite, dolomite, quartz, diopside, scapolite, plagioclase, and locally, epidote, muscovite, potassium feldspar (chiefly microcline), and garnet (Fig. 20Ke, 29). The plagioclase where identified is mostly oligoclase-andesine, but bytownite occurs locally.

Minor minerals may include any of the above and/or amphibole (hornblende, tremolite, actinolite), biotite, phlogopite, garnet (pyrope-almandine, grossularite), olivine, serpentine, talc, and locally, spinel, hypersthene, chondrodite, clinohumite, and wollastonite. Accessory minerals may include any of the above and/or apatite, magnetite, tourmaline, sphene, allanite, zircon, and alteration products such as chlorite and goethite-hematite. Cross-fibre chrysotile asbestos occurs in veins up to 1 cm thick in calc-silicates in the southeast corner of the Conn Lake (NTS 37E) map area. Some assemblages of carbonate and calc-silicate rocks and a few minor assemblages are given in Table 26.

Spectrographic analyses of more than a dozen marble samples and eight samples of calc-silicate rocks, most from south of the map area (e.g. Appendices 2-4), indicate that calcite is almost twice as abundant as dolomite in both marbles and in calc-silicate rocks. As much as 2.5% Fe also occurs in both rock types, while Ba, which is commonly less than 0.05%, exceeds the limit of determination at 0.3% in a couple of places. Calc-silicate rocks contain up to 11.5% Al (e.g. Appendix 2). Dolomite marble at one locality contains 0.13% Pb, but Pb and Cu were not detected in most of the samples, and Zn not at all.

Astarte River Formation (APif, APs)

A zone composed chiefly of mica-graphite-sulphide-quartz schist overlies the marble unit with apparent conformity in many places. Within and south of the map area, this sulphide-bearing schist grades along strike into oxide- and silicate-facies iron-formation, and locally into only slightly metamorphosed very finely recrystallized pyrrhotite-bearing chert (Jackson, 1969, 1971; Jackson and Taylor, 1972; Crawford, 1973). The sulphide-bearing schist, therefore, is considered to be metamorphosed sulphide facies iron-formation. This formation was too thin to be separated from the Longstaff Bluff Formation in map area NTS 37E and 27F but is shown separately on Map 1450A (Jackson et al., 1978d; NTS 37F)(APif), partly on the basis of aeromagnetic data.

This rusty quartz schist unit is somewhat discontinuous and within the map area is commonly 15 m or less thick although measured thicknesses range up to 33 m. Much thicker sections were observed at a few localities, but it reaches its maximum development in the northern parts of the areas mapped by Morgan (1983) and Henderson (1985a) and seems to become thicker toward the northeast.

The sulphide facies iron-formation contains beds of other iron-formation facies which also become more abundant toward the northeast, the most common type being oxide facies iron-formation. Beds of silicate- and silicate-oxide-facies iron-formation, and thin interbeds of aluminous facies iron-formation are also present. Phyllite, mica schist, metagreywacke, and impure quartzite are common minor lithologies interbedded with the sulphide facies iron-formation. Amphibolite occurs locally.

The sulphide facies strata are commonly fine- to coarse-grained, thinly foliated to thinly banded, and highly weathered. Fresh surfaces range from off-white to dark grey and green whereas weathered surfaces are brown, bright yellow, orange, or red, and locally dark grey to green. The rustiness of the weathered surface commonly imparts a relatively

Table 26. Some prograde metamorphic mineral assemblages in the Flint Lake Formation (**AFL**, **Aps**) of the Aphebian Piling Group.

Assemblage:	1^a	2^a	3^a	4^a	5^a	6^a	7^a	8^a	9^a	10^a	11^a	12^b	13^b	14^b	15^b	16^b	17^b
Carbonate	+	+	+	+	+	+	+	+	±		+					+	
Diopside		+	+		+	+	+	+	+	+						+	+
Hypersthene											+						+
Plagioclase			+					+		±			+	+	+	+	+
Potassium feldspar			+		+		+	+					+	+	+	+	
Scapolite	+		+		+	+		+								+	
Tremolite	+							+									
Actinolite			+														
Hornblende											+					+	
Amphibole		+					+										
Olivine		+									+						
Serpentine				+													
Grossularite									+	+							
Garnet		+										+	+	+	+		
Phlogopite	+	+		+													
Muscovite								+			+		±		+		
Biotite												+	+	+	+	+	
Quartz						+		+	+	+		+	+	+	+	+	+
Sillimanite														±	+		
Cordierite															+		
Allanite			+		+												
Sphene			+			+	+										
Epidote								+								+	
Tourmaline			+		+												
Magnetite	+						+										

a - carbonate and calc-silicate assemblage; b - metapelite and metagreywacke assemblage; + - mineral is present; ± - mineral is present in some assemblages, not in others. Two minerals represented by ± in an assemblage indicates there are four combinations represented, etc.

massive appearance. Weathering-out of sulphides and recrystallization have resulted in a vuggy appearance and destruction of primary and/or metamorphic banding in some of the rock.

Quartz, probably recrystallized chert in large part, is the most abundant mineral. Fine graphite and as much as several per cent pyrrhotite occur most commonly disseminated through the rock or in concordant bands, less commonly in veinlets. Minor pyrite and accessory chalcopyrite occur with the pyrrhotite. Minor biotite and muscovite are present in most places and predominate locally; feldspar and hornblende are also common locally. A typical sulphide facies assemblage is:

quartz+pyrrhotite+pyrite+chalcopyrite+graphite+
(biotite and muscovite)/

Oxide facies iron-formation is composed of interbedded quartz- and magnetite-rich bands. Thin interbeds of aluminous iron-formation contain quartz, biotite, muscovite, garnet, magnetite, and hematite. Silicate facies iron-formation bands contain varied amounts of quartz and iron silicates. Silicate-oxide facies iron-formation contains iron silicates and magnetite intermixed with quartz, with these minerals concentrated in alternate bands. The major iron-silicate minerals in silicate- and silicate-oxide-facies iron-formations are cummingtonite, hypersthene, and garnet. Accessory minerals include zircon, tourmaline, and retrograde chlorite. Assemblages of silicate and silicate-oxide facies include:

quartz+garnet+hypersthene+magnetite, and

quartz+cummingtonite±magnetite.

Three samples of sulphide facies iron-formation from south of the map area were analyzed spectrochemically (Appendix 2; APs, samples 01004, 01005, 01702). They contain 0.004-0.007% Cu, but Pb and Zn were not detected. A fourth sample (*see* section on "Economic geology") contains about 13% Zn, 0.06% Cu, 0.05% Pb, and 1.37 g/t Ag.

Amphibolite, mafic gneiss (APs)

Thin bands and lenses of amphibolite and mafic gneiss occur chiefly in the lower part of the Longstaff Bluff Formation and especially near or at the contact with the underlying Astarte River Formation. They also occur within the Astarte River Formation and the Flint Lake Formation. Some are likely of sedimentary origin. Most, however, are probably metamorphosed mafic sills or flows and/or pyroclastics. They are considered to be the northern extension of the metabasalts, metagabbro sills, and metaultramafites that define the middle unit of the Piling Group along the south edge of the Foxe Fold Belt (Jackson, 1969; Jackson and Taylor, 1972; Morgan et al., 1975; Henderson et al., 1979, 1989; Tippett, 1980). These Aphebian mafic-ultramafic rocks are distinguished from similar Archean rocks (e.g. Mb, Mg, Mu) by association with the Piling Group. Amphibolites may increase slightly in abundance eastward from Generator Lake south of the map area (e.g. Kranck, 1955; Gray, 1966). Thin metamorphosed ultrabasic layers, rarely seen associated with the amphibolites in the map area, include pyroxenite, hornblendite, and serpentinite. These rocks are included with the Astarte River and Longstaff Bluff formations on geological maps for NTS 37E, 37F, and 27F.

The amphibolites are commonly dark grey to greyish green or black, medium grained and foliated or massive, and locally lineated. Hornblende, plagioclase, and biotite are the major minerals. Although commonly a minor component, quartz is also a major mineral locally. Hypersthene is a minor constituent at several localities and potassium feldspar occurs locally. Accessory minerals include apatite, zircon, magnetite, ilmenite, and hematite. Some assemblages are:

plagioclase (labradorite-bytownite)+hornblende±quartz,

plagioclase (andesine)+hypersthene+biotite+quartz, and

plagioclase+hornblende+biotite+quartz±hypersthene.

Longstaff Bluff Formation (APs)

A thick turbidite sequence of metamorphosed sandstone, siltstone, and minor shale conformably overlies the rusty, graphitic quartz schist unit. Thin beds of similar lithologies also occur in the other Piling Group units. The most abundant rock type is probably quartz-feldspar-mica schist and paragneiss in which primary bedding is preserved, and metamorphic grade ranges from greenschist to granulite. Argillite-, phyllite-, and aluminosilicate-bearing schist and lit-par-lit gneiss are also common. A few interbeds of quartzite, meta-arkose, marble, calc-silicate rocks, amphibolite, and sulphide-, silicate-, and oxide-facies iron-formation are also present. These lithologies occur mainly in the lower part of the formation, except for meta-arkose, which is also present in the upper part. Rocks similar to the grey felsic metavolcanics of the Mary River Group were rarely noted. A large number of pegmatites and aplite dykes intrude the unit and the pegmatites, at least, are probably in large part internally derived.

Most of the sandstones resemble greywacke in the field. However, the modal analyses available (Fig. 20Kd, 29) for the map area, and for south of the map area where primary clastic grains are preserved in greenschist facies, suggest that compositions range from greywacke to minor arkose and rare quartz arenite, and that feldspathic greywacke and subgreywacke are abundant. This formation is as much as a few hundred metres thick within the map area, a small fraction of its maximum thickness to the south of more than 3000 m.

The strata of this formation are very thin- to thick-bedded (Table 2), very fine- to medium-grained (Wentworth scale), and chiefly medium- to dark-grey. Some beds are greenish grey or brownish grey, and a few mica-rich beds have a purplish cast. Weathered surfaces commonly are a grey to brownish-grey. Graded and massive bedding were the only primary structures positively identified in the map area, although crossbedding, scours, and ripple marks have been identified to the south (Forester and Gray, 1967; Morgan et al., 1976).

Major minerals are chiefly quartz, plagioclase (oligoclase-andesine), potassium feldspar (chiefly locally perthitic microcline, local orthoclase), biotite, and muscovite. Minor minerals are garnet, sillimanite, cordierite, and locally, carbonate, graphite, hornblende, diopside, and hypersthene. Kyanite, which occurs south of the eastern Piling area (Eade, 1953; Kranck, 1955; Forester and Gray, 1967) has not been identified in the map area. Accessory minerals include zircon, apatite, magnetite, hematite, pyrrhotite, and pyrite. Some representative mineral assemblages for the Longstaff Bluff Formation are given in Table 27. Several assemblages for Piling Group metapelites from the vicinity of Generator Lake (northwest NTS 27C) just south of the map area are included in Table 27 for comparison with those in the map area, to accompany the chemical analyses (Table 17; Appendices 5-7) and P-T determinations (*see* Table 60) from this area, and for comparison with Mary River Group metapelites.

Six of the nine samples (01201, 01202, 01300, 01501, 01503, 10702) from field map unit APs (Appendix 2; Table 9, *see* Tables 47, 48) are mostly shale and siltstone from the Longstaff Bluff Formation metamorphosed to greenschist and amphibolite facies. Sample 03600, probably from the same formation, is a granulite facies garnet-rich gneiss. As much as 0.0072% Cu was detected while Pb (0.013%) was found in one sample. Zn was not detected.

Contact relations

The Piling Group rests unconformably on Archean granitic rocks, a relationship that is not evident at many localities and which is best demonstrated in the area to the south of the map area where, in several places, structures in underlying gneisses are more complex than in the overlying Piling Group and appear to be truncated at the contact. Morgan et al. (1976) identified lenses of basal conglomerate in a few places. At one locality just south of the map area, about 0.6 m of sandy schist separates marble from granitic gneiss. The schist contains rounded, flattened granitic fragments up to 0.6 m across. Both the fragments and contact may be tectonic. Within the map area, structures on both sides of the basal contact either seem parallel or are truncated along faults.

The formations overlying the basal Dewar Lakes Formation onlap the basement at several localities and some of these contacts appear to be gradational. These basal Piling Group strata, like similar Mary River Group strata (*see* above) are also considered tentatively to be a metamorphosed regolith.

At other localities, the rocks on both sides of the basal contact are fine grained, thinly banded, and parallel to the contact, and are probably blastomylonite. Elsewhere thin bands of homoclinal and isoclinal Piling Group strata are bounded by granitic and migmatitic gneisses on both sides, and occur in nappes and thrust slices with thrusts on one or both sides (Fig. 59b).

The Piling Group has been highly migmatized, except in the low grade central part of the Foxe Fold Belt, and has been deformed together with underlying basement rocks throughout the belt (Jackson and Taylor, 1972). In general, most of the related pegmatites are muscovite-rich and are probably locally derived. Metamorphism, anatexis, and deformation increase outward from a greenschist facies core area in central Baffin Island (Jackson and Morgan, 1978a) to granulite facies to the north and south. Within the map area, relics of Piling Group-like strata occur in migmatites north of Inugsuin Fiord, along Sam Ford Fiord, near the head of Gibbs Fiord, in the southern part of the Steensby Inlet map area, and northeast of Ayr Lake (NTS 27F). These widely separated

Table 27. Some prograde metamorphic mineral assemblages in the Longstaff Bluff Formation (Aps) of the Aphebian Piling Group, in and just south of the map area.

Assemblage:	1^a	2^a	3^a	4^a	5^a	6^a	7^a	8^b	9^b	10^b	11^b	12^b	13^b	14^b
Quartz	+	+	+	+	+	+	+	+	+	+	+	+	+	+
Potassium feldspar	+	+									+	+		
Plagioclase	+	+			+	+	+	+	+		+	+	+	
Biotite	+		+	+	+		+	+	+		+	+	+	+
Phlogopite		+												
Muscovite	±		+	+				+			+	±	+	+
Cordierite	+									+				
Sillimanite	+	±						+		+		+	+	+
Garnet	+				+			±		+		±	+	
Anthophyllite										+				
Cummingtonite									+					
Tremolite		+											±	
Hornblende				+				±	+					
Diopside				+		+								
Hypersthene						+	+							
Clinozoisite				±										
Tourmaline											+			+
Magnetite	±				+	+	+	±	±			±		

a - map area; b - Generator Lake area (NTS 27C, NW) just south of map area; + - mineral is present, ± - mineral is present in some assemblages, not in others. Two minerals represented by ± in an assemblage indicates there are four combinations represented, etc.

relics indicate that the Piling Group was deposited much farther north, and over a much broader region than is generally recognized.

To date, direct evidence that granitic bodies other than pegmatites and small dykes are intrusive into Piling Group strata has been found mostly south of the map area, where chiefly sill-like bodies of monzogranite and monzocharnockite increase in abundance and thickness south toward the Cumberland Batholith (Jackson and Taylor, 1972; Jackson and Morgan, 1978a; Jackson et al., 1990b).

Granite intrusions, other than pegmatites, into Piling Group strata were also noted in several places by both Eade (1953) and Kranck (1955), and occur in the map area as far north as Gibbs Fiord (northeast NTS 37E, northwest NTS 27F). Piling strata are also intruded by Hadrynian diabase dykes (**Hg**).

Although they outcrop together at several localities, the relationship between the Piling and Mary River groups has not been determined in the field. In areas where they outcrop together (NTS 37E, 37F, 27F; Morgan, 1982), both groups seem to be equally deformed, similarly metamorphosed, and caught up in similar structures. Elsewhere, each group has undergone several episodes of deformation (Jackson, 1966b; Jackson and Taylor, 1972; Morgan et al., 1975, 1976; Henderson et al., 1979, 1988, 1989; Henderson and Tippett, 1980; Tippett, 1980).

Chemistry

Chemical data for Piling metapelites and a few contained minerals are compared with Mary River and other metapelites in Table 9 and Appendix 7. A discussion of these analyses is presented in the section on the "Chemistry of pelitic rocks" for the Mary River metapelite-amphibolite unit. In Table 48, spectrographic data for Piling metagreywacke-metapelite (APs -column 28) are compared with similar strata in the Mary River Group (M, M^{l}, M^{s} - column 26). In general the Piling Group strata contain more Cr and V, and less of most of the other elements listed, than do the Mary River Group strata. Columns 29 and 30 in Table 48 compare Piling (column 30 - APm) carbonates with Mary River Group (column 29 - Ms^{n}) carbonate-rich strata.

Two analyses of Piling aluminous facies iron-formation from Generator Lake (NTS 27C), south of the map area, and a few contained minerals, are compared with some analyses for the Mary River iron-formation, in Appendix 5. The Piling and Mary River aluminous iron-formation facies are similar chemically (cf. Table 17), except that the Piling Group facies contains more Al, Na, Co, Cr, and Ni. Similar differences are shown by analyses of anthophyllite and cummingtonite-grunerite, the Piling Group minerals containing more Al, Ti, Mg, Na, Co, Cr, and Ni, and less total Fe (Tables 15-17; Appendices 4, 5, 7) than the Mary River minerals.

The greater Na content in the Aphebian Piling Group aluminous facies iron-formation compared with equivalent rocks in the Archean Mary River Group is contrary to the trend of decreasing Na content with decreasing age commonly found in shales (Pettijohn, 1975). Some chemical differences between Piling Group and Mary River Group paragneisses may be due to differences in the chemistry of source rocks and proportions of material supplied by them (*see* section on "Origin" below), as well as the factors noted in the respective sections on the chemistry of pelitic rocks of the Mary River and Piling groups.

Age

Age determinations related directly to the age of the Piling Group are mostly for rocks south of the map area. Rocks considered to be basement to the Piling Group, in and south of the map area, have given U-Pb zircon ages of 2888-2709 Ma (Table 51; Morgan, 1982, 1983; Jackson et al., 1990b; Scammell and Bethune, 1995a, b).

Along the north side of the Foxe Fold Belt, south of the map area, blocks of what are considered tentatively to be Piling Group metagreywacke and amphibolite are largely enveloped in white, massive granitic rocks and pegmatites that intrude the basement granitic gneisses in the core of the McBeth gneiss dome adjacent to the core's north contact. Extensive mobilization and pegmatite emplacement are almost universal in both Piling and basement rocks adjacent to the contact, and the enveloping massive granitic rock and pegmatites are considered to be younger than the granitic gneisses. The latter have yielded a Rb-Sr errorchron age of 2697 Ma (MSWD 4.69). Data for samples of amphibolite, biotite paragneiss, and massive monzogranite in the dome indicate an overprint errorchron age of 2033 Ma (Jackson, 1978a; Wanless and Loveridge, 1978). In the southern part of the Foxe Fold Belt Rb-Sr data for Piling metabasalts indicate an age of about 2.2 Ga (W.C. Morgan, pers. comm., 1980). It was not certain whether this represents a primary or a metamorphic age. Uranium-lead zircon ages of 1895-1806 Ma for pegmatites and granitic and charnockitic rocks that intrude the Piling Group, and U-Pb monazite metamorphic ages of 1845-1810 Ma indicate minimum ages for the group (*see* Table 51; Henderson, 1985b; Jackson et al., 1990b; Henderson and Henderson, 1994; Scammell and Bethune, 1995a, b).

An Nd T_{DM} model age of 2.43 Ga has been obtained for metapelite in the Longstaff Bluff Formation and 1.93 Ga for a mafic metavolcanic in the amphibolite-mafic gneiss-ultramafic unit of the Piling Group. The 2.43 Ga Nd model age for metapelite probably represents a mixture of basement detritus and material derived from late Early Proterozoic juvenile crust and is therefore considered to be a maximum age. The 1.93 Ga Nd model age for the mafic metavolanic is comparable to a U-Pb zircon age of 1.883 Ga obtained for a diorite sill in the mafic metavolcanics by Henderson and Parrish (1992). They also report two populations of detrital zircons in the quartzite of the basal Dewar Lakes Formation. The older one, 2850-2840 Ma, is similar in age to some felsic rocks in northern Baffin Island (*see* Table 51, Fig. 98). The younger population, 2180-2160 Ma, is similar to a few Rb-Sr ages (*see* Fig. 98) and provides a maximum age for this formation. The age of the Piling Group therefore is presently constrained between 2.16 and 1.88 Ga.

The above ages, when considered with some Nd T_{DM} model ages for the Lake Harbour and Hoare Bay groups (Hegner and Jackson, 1990; Jackson et al., 1990a, b; Jackson and Hegner, 1991) suggest the Piling, Lake Harbour, and Hoare Bay groups are all about 1.9 Ga. Recent zircon data indicate the Lake Harbour Group was deposited between 1934 and 1845 Ma (Scott and Gauthier, 1996; Scott, 1997). Presence of gradational contacts and/or interfingering of lithologies along the contacts of all the formations of the Piling Group at several localities indicates that there is probably not a significant time break between the shelf sediments of the Dewar Lakes and Flint Lake formations and the overlying formations.

Correlations

Eade (1953) and Kranck (1955) remarked on the similarity of strata now included in the Piling Group to strata in south Baffin Island (Lake Harbour Group), on Cumberland Peninsula (Hoare Bay Group), and in southwestern Greenland (Isortoq Group). The Piling Group was correlated with the Penrhyn Group by Jackson (1969, 1971), and a correlation between the Piling and Lake Harbour groups was suggested by Jackson and Taylor (1972). They also suggested that the Piling and Hoare Bay groups might be equivalent because of the apparent gradation between the two assemblages and the alignment of their regional trends, cautioning that the two formations were deposited in different depositional environments, and that the Hoare Bay Group had closer lithological similarities with the Mary River Group, since determined to be Archean. Similarity of Nd T_{DM} model ages, and the tectonic setting of the Piling, Hoare Bay, and Lake Harbour groups in the fold belts surrounding the Cumberland Batholith in the Baffin Orogen have been used to further support the correlation of these three groups (Hegner and Jackson, 1990; Jackson et al., 1990a, b; Jackson and Hegner, 1991). Remnants of Piling Group and Piling Group-like strata including quartzite and lesser amphibolite metaultramafics, and iron-formation have been mapped from the Ekalugad Fiord-Home Bay map area (NTS 27B; Henderson, 1985b) southeast along both sides of the Penny Ice Cap to the Hoare Bay Group on Cumberland Peninsula (e.g. Jackson and Taylor, 1972). As with Piling and Mary River group strata in map areas NTS 37C and 37F, the relations on northern Cumberland Peninsula between commonly amphibolite-poor Piling Group strata and greywacke-metabasalt-ultramafite rocks of the Hoare Bay Group (e.g. Jackson and Taylor, 1972) are obscured by deformation and metamorphism. Although the general change in lithologies seems too abrupt for the two groups to be correlative, the presence of remnants of amphibolite, rusty schist, and ultramafite in Piling Group remnants, and in migmatites across Baffin Island south of the Foxe Fold Belt, suggest the abruptness of the change may be more apparent than real and related in part to deformation and metamorphism.

The Piling Group has been correlated with the stratigraphically similar Karrat Group of central West Greenland by Taylor (1982), a correlation proposed strongly to Taylor by the present author for their earlier paper (Jackson and Taylor, 1972). Anderson and Pulvertaft (1985) and Henderson and Pulvertaft (1987) also accept this correlation.

Origin

The basal Dewar Lakes Formation (chiefly quartzite) and overlying Flint Lake Formation (chiefly marble) are blanket deposits that generally, but not always, occur together. The Dewar Lakes quartzite is commonly thin, but locally, on eastern Baffin Island south of the head of McBeth Fiord, is probably in excess of 330 m thick, presumably infilling depressions in the underlying gneisses or active graben areas. The known occurrences of the Flint Lake Formation and possibly correlative marble to the south (including marble in the Lake Harbour Group) lies west of a very irregular line that extends northward from the east side of Frobisher Bay to upper Cumberland Peninsula, Dewar Lakes, McBeth Fiord, east of Barnes Ice Cap, and west to northern Steensby Inlet. It is inferred from the distribution and thickness variations of these two formations that a basement high, perhaps an island, may have existed in eastern and/or just east of Baffin Island as far north as the Barnes Ice Cap, and north of Steensby Inlet. The Dewar Lakes and Flint Lake formations are shelf sediments that were probably deposited in an encroaching Aphebian sea, either in the northerly part of an epicontinental sea or on the margin of a passive continental margin. Although marked changes in the thickness of the Dewar Lakes quartzite suggests rifting, the apparent paucity of conglomerates indicates that rifting, if present, was not intense at that time.

Deposition of the various iron-formation facies of the rusty-weathering Astarte River Formation, as well as the lenses of similar lithologies in the underlying marble and overlying metagreywacke units, heralded a marked change in depositional conditions, tectonic environment, and sedimentary source material. The presence of very finely recrystallized chert in relatively low grade rocks of this formation suggests that much of the quartz elsewhere in this formation is also probably finely to coarsely recrystallized chert. It is inferred from the presence of chert and similarity to other iron-formations interpreted to be chemical deposits, that this formation is mainly a chemical deposit that contains variable amounts of shaly and sandy material. Deposition was chiefly below wave base, probably in a more restricted environment than for the underlying and overlying formations. The stratigraphic position of this unit, and of the lithologically similar lenses in adjacent strata, seems to coincide with that of the metabasalt-ultramafic unit along the south side of the Foxe Fold Belt. The rusty, sulphide-bearing quartz schist unit is probably, in part at least, an exhalative deposit formed in a basin restricted by volcanism and crustal instability.

The emplacement of the amphibolite-mafic gneiss unit (metabasalts, mafic and ultramafic intrusions), together with the abrupt thickening of the Dewar Lakes quartzite referred to above, are taken to represent increased rifting, either along the passive margin of an incipient ocean opening, or intracontinental rifting in an epicontinental sea.

The metagreywacke of the Longstaff Bluff Formation has a higher mafic content than the adjacent Archean granitoid gneisses, one of the major sediment sources for the unit. It is assumed on the basis of the composition of the formation and the age determinations discussed above, that a component was also supplied from penecontemporaneous to slightly older mafic-ultramafic and felsic extrusive and intrusive rocks that were rapidly uplifted and actively eroded. Relics of older supracrustals in the basement could also have been a minor source. The general lack of conglomerate and of structures other than bedding, together with the monotonous regularity of the bedding and the apparent predominance of silty to sandy sediment, indicates that the formation is probably a sandy turbiditic flysch deposited below storm base.

The Longstaff Bluff Formation is similar in lithology and probably in age to the Omarolluk Formation of the Belcher Group (Dimroth et al., 1970), which Hoffman (1987) has suggested is a foredeep deposit. Both formations are thick turbidite flysch concretion-bearing sequences that become less mafic upward, and were deposited, at least locally, above a mafic volcanic sequence. They were deposited in rapidly subsiding areas and mark a relatively abrupt change from shelf deposition to deposition possibly in a foredeep (foreland basin), or a back arc basin. The extent of the Piling Group is considered to favour a foredeep related to a collision of two continental masses rather than to intracontinental thrusting. As discussed subsequently in the section on the Baffin Orogen, it is suggested that the shelf sediments were deposited on a continental mass that subsequently rifted and separated only slightly before closing together again. The seemingly minor amount of mafic-ultramafic rocks, apparent onlap onto granitic basement, and common occurrence of basement below the Piling Group would seem to argue against the Longstaff Bluff Formation being a trough (oceanic) deposit as concluded by Grocott (1989), at least in the northern part of the Foxe Fold Belt. However, more field studies are required before more definite conclusions can be made. The greater thickness of Piling Group-derived migmatite (chiefly Longstaff Bluff) preserved south rather than north of the Foxe Fold Belt may be a function of relative uplift and erosion, but the Piling Group, or at least the Longstaff Bluff Formation, may also originally have been thicker to the south.

It seems likely, therefore, that initial deposition of the Piling Group was on sialic crust after a long period of erosion following the Kenoran Orogeny, in an encroaching early Aphebian epicontinental sea. Deposition extended at least 1400 km from south of Committee Bay east to western Greenland and at least 800 km from Steensby Inlet to the south edge of Baffin Island if suggested correlations are correct. Shelf deposition gave way to deep water (foredeep) deposition as conditions became more unstable, especially where belts of volcanism developed in rifted regions, such as in the Dewar Lakes region of central Baffin Island.

The facies distribution, as presently known, with amphibolite and ultramafic rocks occurring chiefly in the southern Foxe Fold Belt or south of it, suggests that any major rifting or suture zone would lie somewhat to the south. Henderson et al. (1989) consider the metabasalts in one small area to be allochthonous and to have been thrust from the south.

Banded migmatite (Amg)

Description

Unit Amg is the most abundant map unit in the map area. Irregular bodies up to 35 km across, with variable trends, occur chiefly in a broad belt that extends northwest through the coastal region of map area NTS 27F, and constitute about one quarter of that map area. To the northwest and west, unit Amg underlies about two-thirds of map areas NTS 37H and 37F and half of map area NTS 37E. In all three map areas the other rock units tend to occur as lenses surrounded by unit Amg. Trends, although variable, are chiefly northwest-southeast in map area NTS 37H and pronouncedly east-west in map areas NTS 37E and 37F. A few scattered areas of unit Amg have been delineated in map unit NTS 37G, the largest being a 65 km long east-trending lens adjacent to the southern boundary of the map area. However, Amg occurs intermixed with other lithologies throughout map area NTS 37G in areas shown as mu. The following areas in map area NTS 37G are underlain chiefly by unit Amg: southeast corner, north of 71°25'N and east of 77°W, north of 71°30'N and west of 79°W (*see* Fig. 13), south of 71°31'N, and between 78°30'W and 77°W. The Amg bodies in map area NTS 37G also have various trends, but east trends predominate along the southern edge and northwest trends elsewhere.

Unit Amg displays similar but stronger and more varied aeromagnetic patterns than do Agn and Amn. Most patterns range from elongated and gently undulating, to a strong bird's-eye pattern. Belts, slightly above background and containing a subsidiary bird's-eye pattern, are most common in map areas NTS 37E and 37F. Individual anomalies range up to 1200 nanoteslas (nT) above background, and anomaly patterns are obviously modified by high local relief. Where data are available, most higher anomalies are related to supracrustal-basic igneous rocks, to local topography, or both. In areas below granulite grade the magnetic relief is low to moderate and highs are rarely more than 400 nT above background. Background values are commonly 100-400 nT higher, patterns are more strongly developed, and local anomalies commonly range up to 800 nT above background in granulite terrane as compared with lower grade terrane.

Unit Amg is chiefly banded migmatite (Fig. 60). The term migmatite is used here in a broad sense for a complex of variously interlayered and intermixed rocks. Granitoid rocks of several ages form the bulk of the map unit and range from well banded gneisses to massive crosscutting granites. Metasediments, amphibolites and minor ultramafics (metamorphosed extrusions and intrusions), and some acidic metavolcanics range from sparse, minute, contorted wisps to, locally, the bulk of the map unit, and display a complete range in degree of assimilation. Contacts between the various components range from sharply discordant and sharply conformable to gradational. Modal analyses for unit Amg are presented in Figures 17, 20B, 20C, 20E, 20Hb, 20Jd, and 62, and in Tables 5 and 6. Chemical data are shown in Tables 47 (columns D, E, R) and 48 (columns 7, 8, 10, 16, 27) and in Figures 48, 49, 50, 63, and 95.

The layers in unit Amg characteristically have widely divergent compositions and range from less than one centimetre to a few hundred metres thick, most being very thin- to thin-banded (Table 2; Fig. 60, 61). Most thicker layers also commonly display an internal banding. The layering ranges from parallel layers of similar thickness to highly irregular and variable layers. Layers are commonly persistent over large distances although they are highly contorted in most places. The mafic component tends to be the more fragmented and discontinuous (Fig. 61e-f). It ranges from unsegmented layers to angular and rounded variously shaped boudins and xenoliths, and highly swirled schlieren. Giant rotated boudins up to 200 m or so in diameter were seen in several fiord walls (NTS 37F, 37H).

The rocks in most areas are lineated and dips are commonly low to moderate. Steep dips occur locally and are most abundant in the western part of the map area. The rocks are highly deformed and faulted. Flowage features are common (Fig. 60, 61) and large-scale, undulating, inclined to isoclinal recumbent folds are especially well displayed in the fiord region of map area NTS 37H. Some folds are probably nappes. Shear planes and cataclastic rocks occur at several localities.

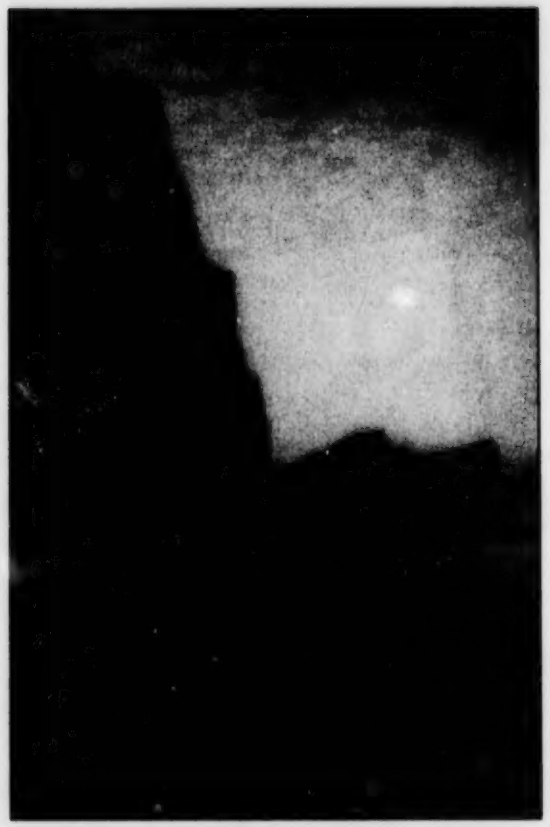

Figure 60. *Banded migmatite* Amg *outcropping in "The Mitres", Buchan Gulf (NTS 37H). View northeast along the axes of recumbent fold structures. One axis is marked by white granitic rock near the top. Elevation is about 610 m. Photograph by W.J. Crawford. GSC 186355*

Unit Amg lithologies range from very fine- to coarse-grained but are chiefly medium grained. Granitoid gneiss and foliated to massive homogeneous granites are chiefly white to grey, pinkish grey, and pink. The homogeneous granites are, less commonly, red. Granitoid gneisses are highly deformed on a small scale, being commonly swirly and nebulitic. Mafic rock lenses and inclusions are ubiquitous. Granitized replacement areas range from discordant, irregular masses, veins, and dykes to concordant layers and lenses. Their contacts range from sharp to diffuse. Evidence of mobilization is commonly extensive, and inclusions are common in some of the homogeneous granites.

Locally, banded migmatites are intruded by still younger concordant and discordant bodies of chiefly pink granite, pegmatite, aplite, and minor syenite. These latest granites rarely contain inclusions, and form as much as 60% of the rock (e.g. Clyde Inlet, NTS 27F; Bruce Mountains and Isortoq River, NTS 37E; Cockburn River system, NTS 37F; central NTS 37G; and southwestern NTS 37H). They range from concordant sheets to anastomosing networks of crosscutting veins and dykes (Fig. 61a) that include stockwork structures and agmatites. In areas of low relief, horizontal sheets of late granite could be mistaken for stocks or small batholiths, but the relations are evident in the fiord country, where relatively few small stock-like bodies are present.

In the granulite facies, all of the granitic rocks, even the latest granites and pegmatites, have a greasy lustre, indistinct contacts, and contain hypersthene. This indicates that even the latest granites were emplaced before granulite metamorphism.

The granitoid gneisses and concordant homogeneous granites (synmigmatite) range from syenite to tonalite and quartz diorite. Although the average composition for granitoid gneisses is granodiorite in the entire map area (Fig. 17, 20B, 62a; Tables 5, 6), the most common lithology is probably tonalite, except in map area NTS 27F where it is granodiorite. Homogeneous concordant (leucosome) granite, however, is chiefly monzogranite (Fig. 20C, 62b; Table 6). In addition, modal plots commonly show a "gap" between the monzogranite-granodiorite rocks and the tonalites. The discordant granites, which probably include both homogeneous and late granites, are chiefly syenogranite and monzogranite (Fig. 20Hb; Tables 5, 6); tonalites are rare or absent.

Quartz, plagioclase (An_{15-37}), and potassium feldspar are the major minerals of the granitic rocks in Amg (Fig. 17; Table 6). Porphyroblasts and augen of potassium feldspar up to 5 cm long are common and those of garnet, hornblende, and pyroxene occur locally. Myrmekite is common and is abundant locally. Cordierite was noted at two localities. In the granulite facies the potassium feldspar is chiefly perthitic orthoclase, and major mafic minerals are red-brown biotite, hypersthene (includes bronzite), olive-green hornblende, and locally, garnet and clinopyroxene. In the amphibolite facies the potassium feldspar is microcline, the biotite is brown, and the hornblende is blue-green. Garnet and minor clinopyroxene are also present and some massive granites contain as much as

5% magnetite. Accessory minerals in the granitic rocks include magnetite-ilmenite, leucoxene, zircon, apatite, sphene, allanite, pyrite, pyrrhotite, and hematite, and rare chalcopyrite, malachite, atacamite, and rutile. Retrograde minerals include hornblende, epidote, chlorite, sphene, and rare prehnite.

Major mineral associations for the granitic rocks both below and in granulite grade are given in Table 28.

Metasediments (Fig. 20Ka) in Amg are chiefly grey to dark grey metapelites and metagreywackes. Minor quartzite, oxide- and silicate-facies iron-formation, and local calc-silicate rocks are also present. Their characteristics are similar to those of the Mary River and Piling groups. Primary bedding has probably been transposed in many places. Acidic to intermediate metavolcanics have been identified in a few places (Fig. 17, 20E; Table 6) and locally contain metatuffs up to 35 m thick (e.g. south-central NTS 37G).

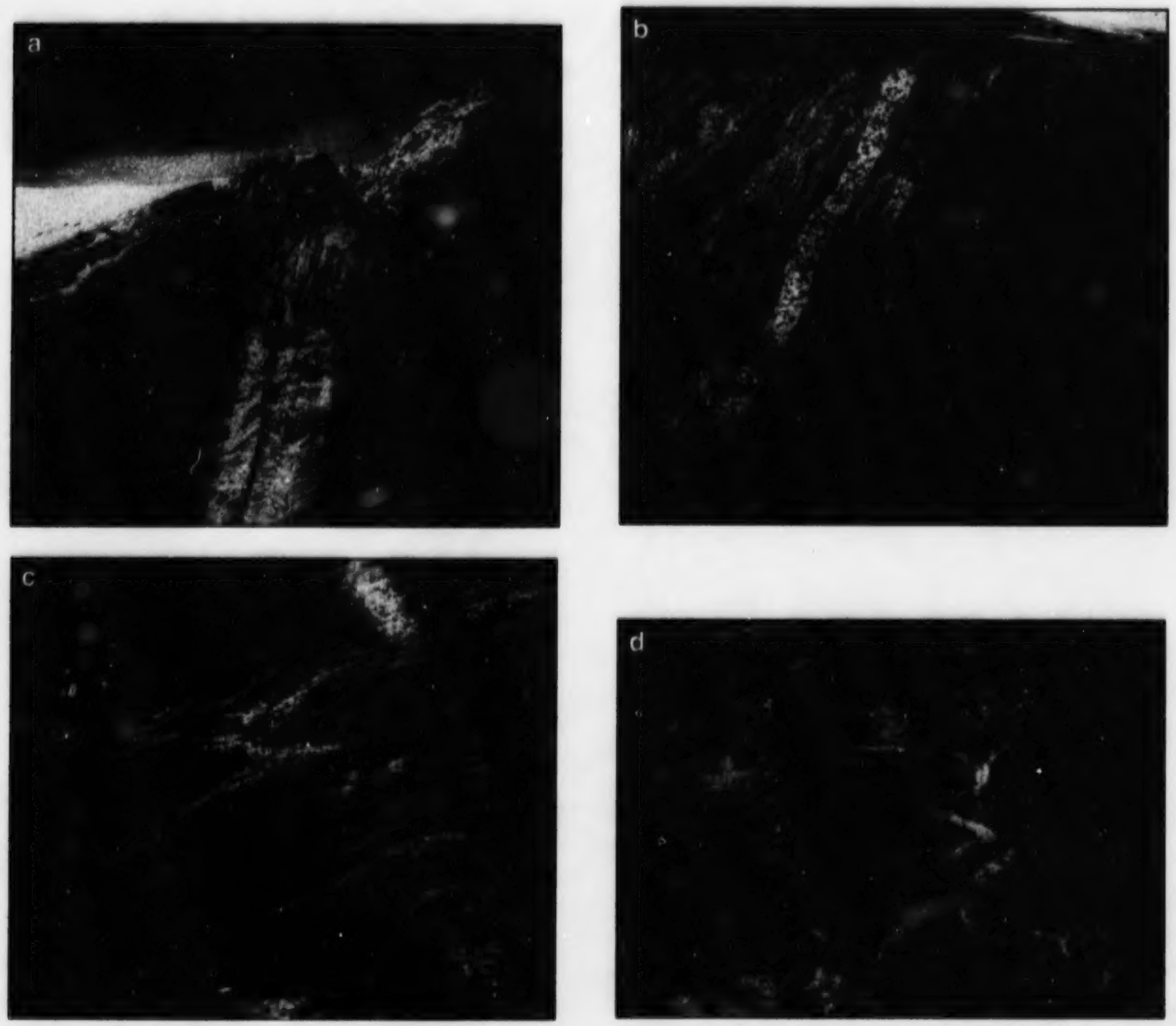

Figure 61. a) *Veined migmatite and agmatite, Coutts Inlet (NTS 37H, northwest). Elevations to 1350 m. Photograph by W.J. Crawford. GSC 186300.* ***b)*** *Banded migmatite with thin pegmatite. The edge of a 6 m thick migmatized amphibolite dyke occurs on the right at the head of Gibbs Fiord (NTS 37E, northeast). Photograph by S.L. Blusson. GSC 185707.* ***c)*** *Thinly banded migmatite showing plastic deformation and small shears (NTS 37H). Photograph by A. Davidson. GSC 203059-T.* ***d)*** *Plastically deformed migmatitic gneiss, Livingston Island, Buchan Gulf (NTS 37H, north-central). Photograph by W.J. Crawford. GSC 186356.*

Amphibolite layers, inclusions, and large disrupted bodies are dark green to black, medium- to coarse-grained, schistose, and foliated to banded. Some are massive and may contain vestiges of primary igneous texture. Others are highly deformed, and include metamorphosed dykes and sills similar to the swarm in map area NTS 27F; chilled margins are preserved locally. Some acidic and basic metavolcanics contain layered tuffs and are interbedded with metasediments and granitic rocks. The origin of most amphibolite bodies, however, is not known. Compositions are similar to amphibolites of the Mary River Group (Table 6; Fig. 17, 20J, 29). Amphibolite bodies are commonly recrystallized to biotite along their margins. Biotite, garnet, and pyroxene are common, both in the matrix and as porphyroblasts. Ultramafic remnants are fairly common and include hornblendite, pyroxenite, and serpentinite.

Feldspar porphyroblasts are most abundant in the metasediments where local "sweats" are also common. Locally, however, sparse feldspar porphyroblasts occur in amphibolite, commonly connected by paper-thin feldspar veinlets.

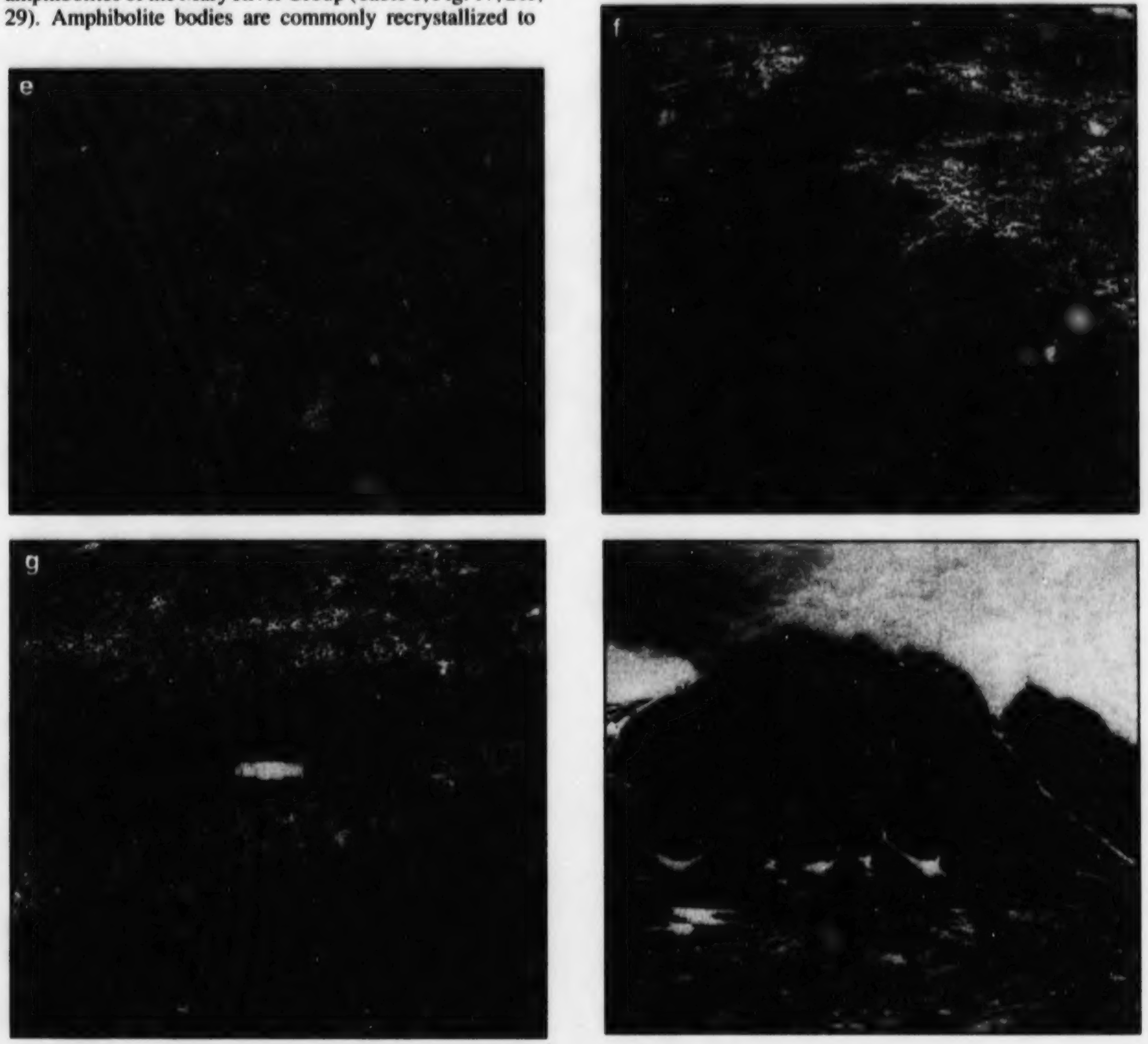

Figure 61. e) *Agmatitic migmatite containing fragments of amphibolite (NTS 37E, west edge). Photograph by S.L. Blusson. GSC 185495.* ***f)*** *Agmatite formed by partial ingestion of an amphibolite body by gneissic granodiorite in migmatite, head of Gibbs Fiord (NTS 37E). Photograph by S.L. Blusson. GSC 185710.* ***g)*** *Partial homogenization of banded migmatite* (Amg) *by subgranulite facies metamorphism, west coast of Adams Island (NTS 37H). Photograph by G.D. Jackson. GSC 186938.* ***h)*** *Banded migmatite* (Amg) *with isoclinal recumbent folds in cliff. Boudined amphibolite occurs in the foreground. Height of cliff is about 730 m. View west, at the mouth of Royal Society Fiord. Photograph by W.C. Morgan. GSC 186599*

Major mineral assemblages for the amphibolites both below and in granulite grade are given in Table 28.

Contact relations

Banded migmatites (Amg) grade locally into nebulitic gneisses of unit Amn and into feldsparphyric gneisses of unit Amp. Unit Amg is gradational, or interfingers, with the Mary River and Piling groups, and with unit gr-Agr. Many contacts with older map units appear transgressive on the map because of the discordant nature of anatexis or intrusion of dykes and sills into the host rocks. Fault contacts are also common. Banded migmatite has been intruded by dykes metamorphosed to amphibolite (b), by Hadrynian diabases (**Hg**), by Archean granites (**Agp**), and by mid-late Aphebian granites (**Ag**) and charnockites (**Ack**). Banded migmatite includes supracrustal remnants, in part anatectized, that were derived from the Mary River and Piling groups. It also contains reworked portions of the basement to the supracrustals (Agn, Amn, and possibly gr-Agr), and the younger synanatectic to postanatectic granitic bodies.

Chemistry

The mean for spectrographic analyses of banded migmatite (Amg, Amg^a; Tables 47, 48) resembles that for nebulitic granitic migmatite (Amn) more than those for other granitic rocks in the map area. This is to be expected considering the hybrid nature of both map units. Means for the concordant (chiefly leucosome) granitic component (Amg^j) and the late crosscutting granitic component (Amg^i) of unit Amg were compared with chemical data interpreted by Pearce et al. (1984) and Whalen et al. (1987). The concordant granites (Amg^j) resemble volcanic arc granites much more than other tectonic granites and resemble I-type more than S-type. The discordant granites resemble volcanic arc and collision granites about equally, and are somewhat less similar to ocean ridge granites. They also resemble I-type much more than S-type. There is no indication that many of these concordant or discordant granites are A- or M-types.

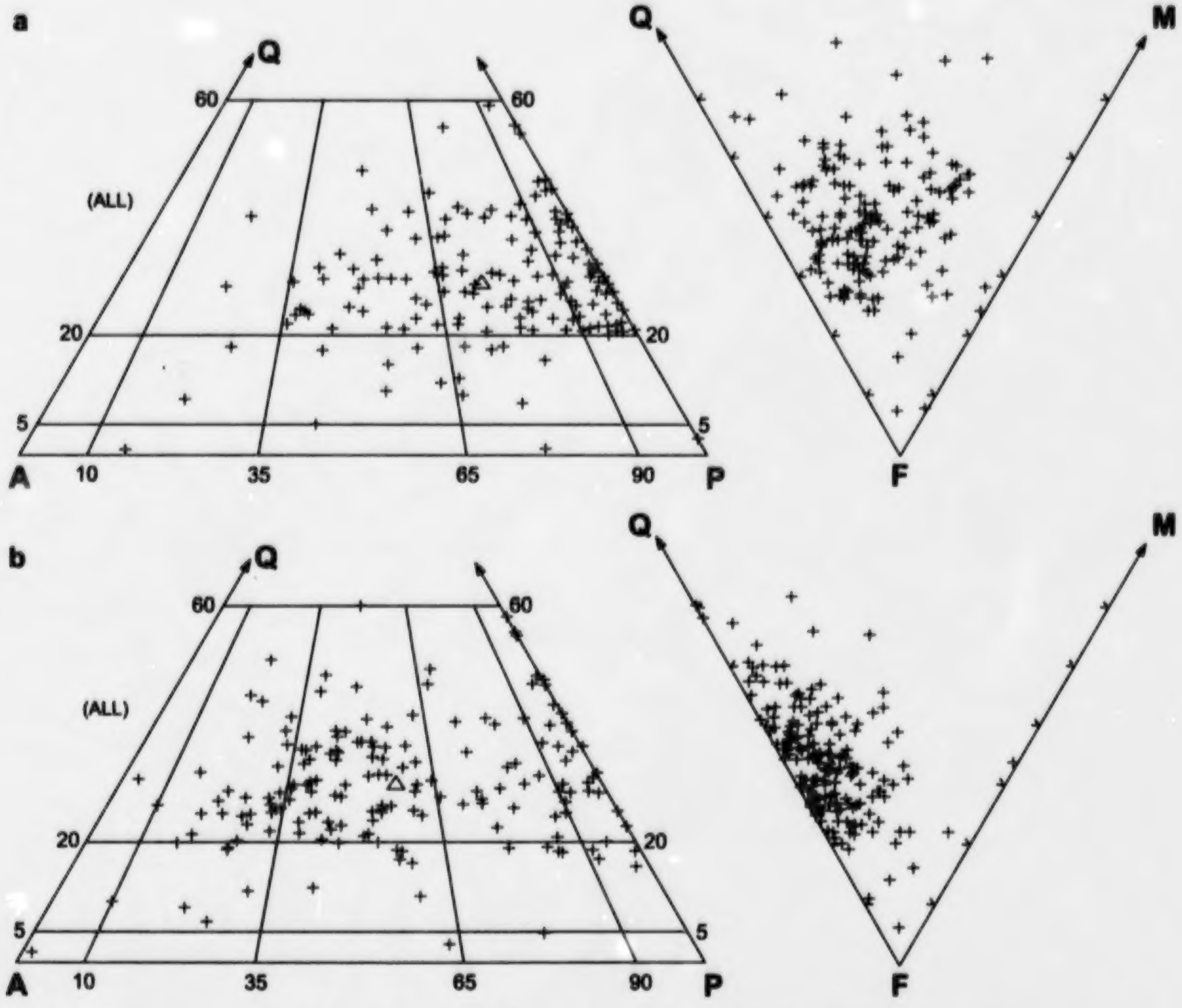

Figure 62. *Quartz-alkali feldspar-plagioclase and quartz-feldspar-mafic plots for* ***a)*** *unit Amg, and* ***b)*** *concordant (leucosome) granitic component* (Amg^j) *in Amg. The mean is shown by the small triangle.*

Table 28. Most common mineral assemblages for granitic rocks (Amg^i, Amg^j) and amphibolites (Amg^g) in banded migmatite (Amg).

Assemblage:	1^a	2^a	3^a	4^a	5^a	6^a	7^b	8^b	9^b	10^b	11^c	12^c	13^c	14^c	15^c	16^d	17^d	18^d
Quartz	+	+	+	+	+	+	+	+	+	+			+	+	+	±	+	
Microcline	+	+	+	±											+			
Orthoclase							+	+									±	
Plagioclase	+	+	+	+	+	+	+	+	+	+	+	+	+	+	+	+	+	
Scapolite											±							
Biotite	±	+		+	+		+		+	+	+	+	+		+	+	+	
Hornblende		+	+	+	±	+	±		+		+	+	+		+	+		+
Clinopyroxene	±				±			±	+		+		+	+	+	+		
Hypersthene						+		+	+						+	+	+	
Olivine																		+
Garnet													±	+				
Epidote			±	±										+				
Rutile								+										

a - granitic rocks below granulite facies, b - granitic rocks in granulite facies, c - amphibolite below granulite facies, d - amphibolite (pyribolite) in granulite facies; + - mineral is present; ± - mineral is present in some assemblages, not in others. Two minerals represented by ± in an assemblage indicates there are four combinations represented, etc.

Figure 63 shows that plots for Amn^i (late granitoid component in Amn), Amg^i (late granitoid component in Amg), and Amg^j (concordant leucosome in Amg), involving Zr, TiO_2, MgO, Ba, and Sr, are similar. They are also much more similar to one another than to Amn, gr-Agr, Agp, Ack, and Ag (Fig. 22, 26, 58; *see* Fig. 69). Components Amn^i, Amg^i, and Amg^j are discussed further in the "Chemistry of Ag, Ack" section of "Late granitic intrusions (Ag, Ack)".

Compared with mafic remnants in Amn (Amn^f), analyses for remnants of mafic rocks in Amg (Amg^g) plot in a similar but relatively small field on the TiO_2-Zr plot of Pearce (1980) that lies chiefly in the arc lava field, and extends into the within-plate lava field (Fig. 48a). A pattern similar to but more dispersed than that for Amn^f is given by these analyses for Amg^g on the Ti/100-Zr-Sr/2 diagram of Pearce and Cann (1973). They plot from near the Zr apex through the lower part of the calc-alkaline basalt field (Fig. 48a). This spread is probably due to movement of Sr during metamorphism. These plots are also similar to those obtained for Mary River Group mafic rocks (Fig. 48b).

Analyses of Amg^g plot chiefly in the calc-alkaline and rift basalt field in Condie's (1985) TiO_2-Zr diagram (Fig. 49a) as discussed in sections on the chemistry of Amn and of Mary River Group metagabbro (Mg) and metabasalt (Mb).

Comparison of TiO_2 with Fe/(Fe+Mg) (Fig. 50a) indicates a crude differentiation trend for the mafic remnants in Amg (Amg^g) that is similar to the trends obtained for Mary River Group metabasalt (Mb) and metagabbro (Mg), but differs from the trend obtained for mafic remnants in Amn (Amn^f) (Fig. 50a, b; Tables 20, 21). A comparison of histograms, however, shows close similarity of Amg^g, Amn^f, and Mb (*see* Table 49).

Age and origin

Two mineral K-Ar ages (*see* Table 53) for Amg rocks are 1630 Ma (NTS 37E) and 1669 Ma (NTS 37H). A metamorphic Rb-Sr isochron age (Table 52) of 1971 Ma (Jackson and Morgan, 1978a) obtained for the Mary River Group at Mary River, a Rb-Sr errorchron age of 2159 Ma obtained from samples of Amn and gr-Agr from map area NTS 27F (Jackson, 1984), and a Rb-Sr errorchron overprint age of 2033 Ma on Archean gneiss and Piling Group strata from the McBeth gneiss dome to the south (NTS 27C; Jackson, 1978a), are probably all metamorphic ages related to the migmatization and remobilization that affected the rocks of Amg in the late Aphebian.

Undifferentiated gneisses (mu) near the head of Cambridge Fiord (NTS 37H) are similar to both units Amn and Amg. On the strength of recent age determinations they are tentatively placed in unit Amg. Hybrid leucocratic gneisses of uncertain origin (possibly Amn) contain an early amphibolite component (Fig. 21c) that has undergone at least two stages of anatexis involving earlier grey and later pink granitic intrusions. Uranium-lead zircon age determinations gave upper and lower intercept ages of 2734 +59/-45 Ma and 1800 Ma, respectively, for the amphibolite and 2522 +11/-10 Ma and 1525 Ma, respectively, for the latest granite (*see* Table 51; Fig. 64). Most of the determined points are quite discordant and the zircons from the granite contain older cores and considerable uranium. The ages are not considered to be accurate, although the amphibolite is probably as old or older than the Mary River Group felsic metavolcanics (2718 +5/-3 Ma, Fig. 54; *see* Table 51), and is tentatively considered to represent the Mary River Group mafic intrusions.

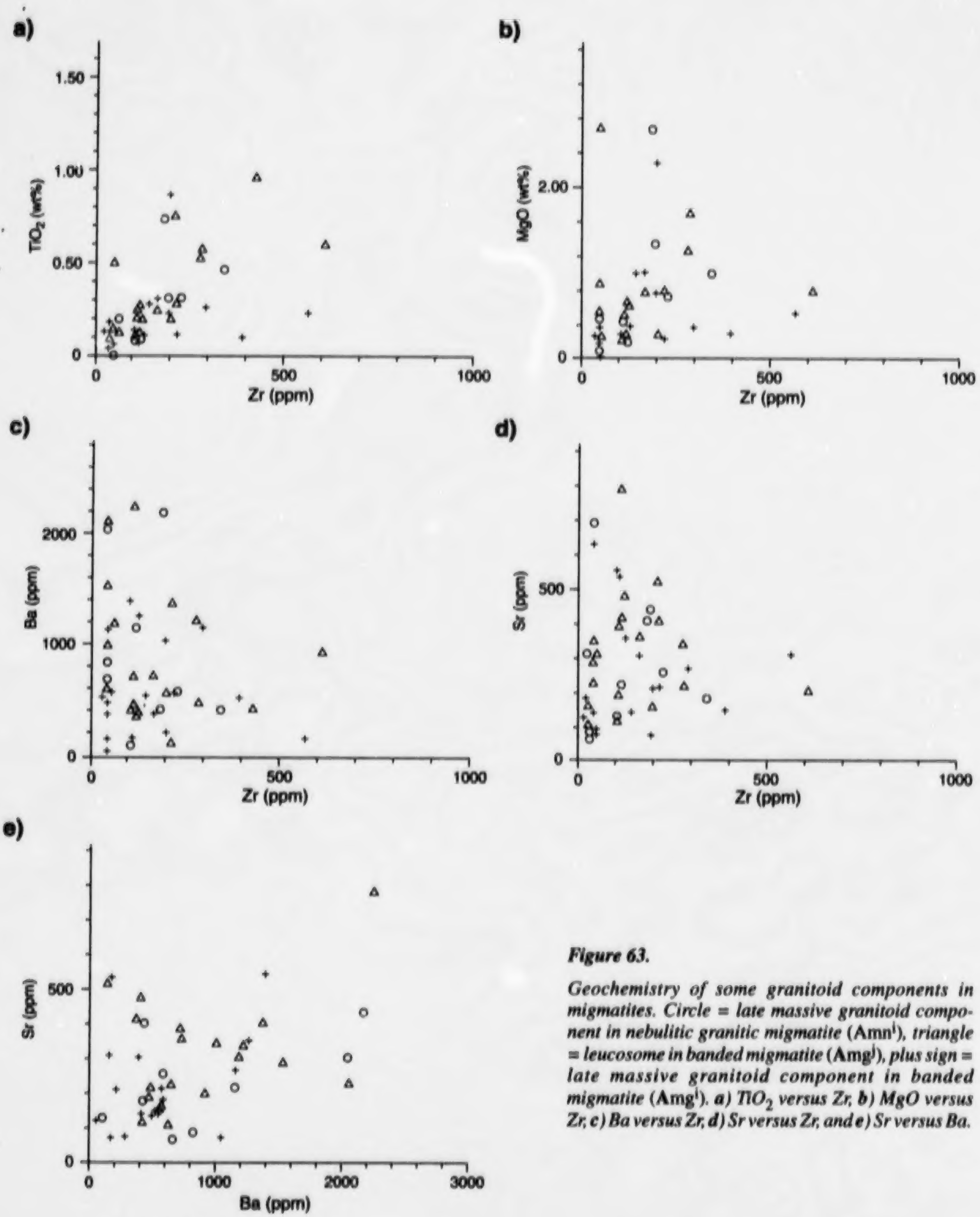

Figure 63.

Geochemistry of some granitoid components in migmatites. Circle = late massive granitoid component in nebulitic granitic migmatite (Amn^{l}), *triangle = leucosome in banded migmatite* (Amg^{j}), *plus sign = late massive granitoid component in banded migmatite* (Amg^{l}). ***a)*** *TiO_2 versus Zr,* ***b)*** *MgO versus Zr,* ***c)*** *Ba versus Zr,* ***d)*** *Sr versus Zr, and* ***e)*** *Sr versus Ba.*

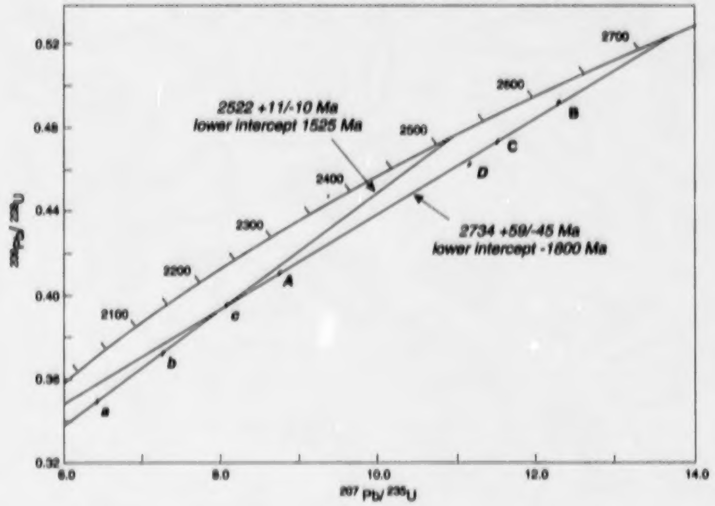

Figure 64.

Concordia diagram and U-Pb isotopic ratios for zircons from amphibolite (points A-D: 2734 Ma) and granite (points a-c: 2522 Ma) in unit **Amg** *(formerly* mu*) near the head of Cambridge Fiord (NTS 37H). Data supplied by P.A. Hunt and Geochronology Section, Geological Survey of Canada, Ottawa. A-D identify plots of analyses of different zircon fractions. The sizes of the plots are commensurate with the laboratory errors. Zircons from two samples are plotted, hence two lines.*

The 2522 +11/-10 Ma age probably approximates the age of emplacement of the latest granite, and is interpreted as a minimum age for the first (late Archean) anatexis to affect the amphibolite. The lower intercept age of 1800 Ma, Rb-Sr ages of 1971 and 2033 Ma noted above, and data from elsewhere on northern Baffin Island (*see* Tables 51-53, Fig. 98), indicate that the latest anatexis probably occurred about 2000-1800 Ma ago and involved partial remobilization of older granite and Archean crust.

Field relations show that unit **Amg** contains components of all other Archean and Aphebian map units in the map area, and therefore contains rocks of metaigneous (intrusive and extrusive) and sedimentary origin. These components have been affected by migmatization and anatexis, and in many places are intricately intermixed. They probably range in age from at least 2.9-1.8 Ga and probably include much Archean banded migmatite, and considerable granite of about 2.7 Ga (Tables 51, 52). However, the most intense period of regional migmatization, metamorphism, deformation, and granite emplacement seems to have occurred between 2.1-1.8 Ga, and affected most, if not all, of the pre-existing rocks to some degree. Therefore **Amg** is considered to be chiefly Aphebian in age.

The chemical similarities between concordant (**Amg^{j}**) and late discordant (**Amg^{l}**) granitic components in **Amg**, coupled with their differences – which result in **Amg^{j}** resembling volcanic arc granites while the later **Amg^{l}** resembles both volcanic arc and collision granites – invite the suggestion that the granitic rocks are all related to one major ocean closing and collisional event. However, it is not yet known if **Amg^{j}** and **Amg^{l}** are related to the same event or are even of the same age.

Most of the mafic remnants in **Amg** (**Amg^{g}**) may represent the Mary River Group, but older mafic remnants (possibly **Amn^{f}**) may also be present.

Porphyroblastic migmatite (Amp)

Description

Porphyroblastic migmatite is one of the least abundant rock units in the map area. The largest body extends northeast-southwest for about 60 km in the southern adjoining corners of map areas NTS 37E and 37F. A 27 km long body extends east-west along the northern border of map area NTS 37F and extends a few kilometres north into map area NTS 37G. Several smaller bodies occur in northwestern map area NTS 37F and three small northwest-trending bodies up to 30 km long occur in southwestern map area NTS 37H. Unit **Amp** was not identified in areas large enough to be differentiated in map areas NTS 27E-G.

A strong bird's-eye pattern is shown on the aeromagnetic maps for areas of **Amp** in southwestern map area NTS 37H. Local anomalies commonly are as much as 300 nanoteslas (nT) above background and show some orientation subparallel to foliation. However, some of the pattern and the anomaly values are influenced by the relatively rugged topography in this area. Elsewhere, in map areas NTS 37E, 37F, and 37G, **Amp** is represented on aeromagnetic maps by a very weak pattern of undulations and poorly developed bird's-eye pattern. Local anomalies are rarely more than 100 nT above background and there is a faint orientation parallel to the general foliation.

Unit **Amp** is chiefly banded granitic migmatites (**Amg**) in which potassium feldspar porphyroblasts constitute as much as 50% or more of the rock (Fig. 65) and are developed over an area large enough to be shown on the map. Commonly the rock is more homogenized and granitized than in **Amg** so that structures are less distinct. Locally the rock is difficult to differentiate from blastoporphyritic orthogneiss, which is a minor component of **Amp**. Foliations are variable and lineations are common. Well displayed folds in southwestern map area NTS 37E and southeastern map area NTS 37F trend

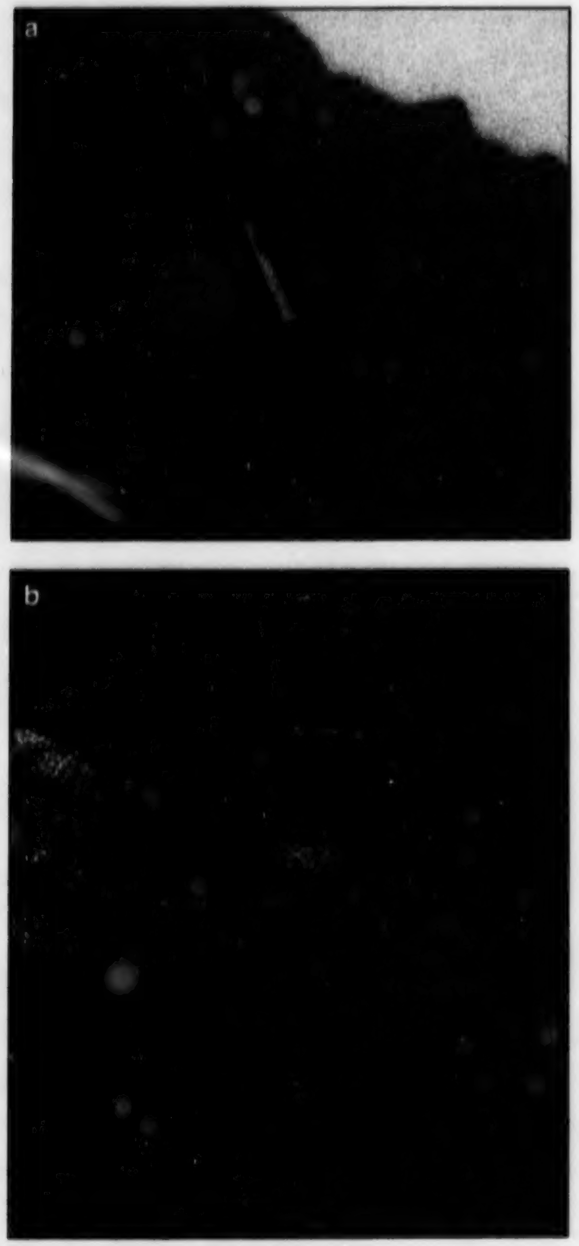

***Figure 65. a)** Anatectic Mary River Group biotite paragneiss with potassium feldspar porphyroblasts in an early stage of unit* Amp *development and occurs in the southeast corner of map area NTS 37F. Photograph by S.L. Blusson. GSC 185485. **b)** Porphyroblastic migmatite west of the head of Cambridge Fiord (NTS 37H). Photograph by G.D. Jackson. GSC 204194-M*

southwest parallel to a major fault east of Isortoq Lake (NTS 37F). Petrographic data for Amp are provided in Table 6 and in Figures 17 and 66. Chemical data are given in Tables 47-49, and Figure 95.

The granitoid gneisses are chiefly thin banded, but range from finely foliated to thick banded and massive (Table 2). Colours are white to grey and pink; amphibolite bands are commonly black. Unit Amp gneiss ranges from syenitic to quartz diorite but is mostly monzogranite (Table 4, Fig. 66).

Most banded, porphyroblastic, granitic migmatites are complexly deformed and contain abundant schlieren of more mafic rocks. Potassium feldspar porphyroblasts are concentrated in cores of some small folds. Locally the gneisses are mostly paragneisses and amphibolite. Flaser gneiss was seen in a few places, and granitoid gneiss grades locally into relatively homogeneous granitized areas and is intruded by younger granites.

The major minerals are quartz, microcline, plagioclase (An_{19-24}), brown biotite, and locally, hornblende. Microcline porphyroblasts are up to 4 cm long. Minor minerals include garnet, myrmekite, and epidote. Chlorite, epidote, and prehnite occur as retrograde minerals. Accessory minerals are apatite, epidote, prehnite, allanite, zircon, sphene, magnetite, leucoxene, pyrite, and sulphide. Common mineral assemblages are:

quartz+microcline+plagioclase+(biotite or hornblende),

quartz+microcline+plagioclase+biotite+
hornblende±garnet, and

quartz+plagioclase+biotite.

The major mafic assemblage is:

plagioclase+biotite+hornblende.

At several places Amp is in gradational contact with Amn and Amg. It is in fault contact with the Mary River Group in map areas NTS 37E and 37F, and locally has a gradational contact with Mary River strata.

Chemistry

A comparison of means for spectrographic analyses of quartzofeldspathic units (Groups I-III, Table 48) indicates that Amp most closely resembles units Amg and Amn, the other two hybrid map units. A comparison of individual element histograms (Table 49, *see* Fig. 95) shows that Amp does not strongly resemble any other quartzofeldspathic unit, and that it is most similar to Amn and Agp.

As one might suspect, a comparison with the tectonic interpretation of Pearce et al. (1984) gave conflicting results. Comparison with the data and interpretation presented by Whalen et al. (1987) indicates that Amp resembles M-type granites more closely than other types.

Age and origin

The age of Amp is uncertain. Because field evidence indicates that most of the unit has been formed from unit Amg and from Mary River Group strata by the mobilization and/or addition of potassium, it is inferred that the formation of porphyroblasts may be related to the last major tectonometamorphic event at ca. 2.1-1.8 Ga. The mean positions for the modal plots in Figures 62 and 66 indicate that Amp probably contains more potassium than Amg. The source of the potassium is uncertain. It could have been derived locally or perhaps from the granulites and charnockites during metamorphism, although these rocks contain as much potassium as their lower grade counterparts. In the granulite facies, Amp would probably be difficult to differentiate from charnockite.

Late granitic intrusions (Ag, Ack)

Late granitic intrusions (Ag, Ack) are abundant in a broad, poorly defined arcuate belt that extends southeasterly from the northwest corner of map area NTS 37G to eastern map area NTS 37F, from where the belt extends easterly through northern map area NTS 37E and northeasterly through eastern map area NTS 37H. These late intrusions range from abundant dykes and sills to small equidimensional stocks and large irregular batholiths up to 50 km long and 1000 km^2 in area. The largest intrusions occur at each end of the belt and in western map area NTS 37E. Most of the intrusions are elongated parallel to the local structures but not necessarily parallel to regional structures (e.g. NTS 37G, 37H). Their emplacement either predates or is coincident with the formation of the dominant trend in their host structural domain (*see* Fig. 110). Intrusions are elongated to the southeast in map area NTS 37G and southeast to northeast elsewhere. Intrusions large enough to delineate on the maps are rare outside the arcuate belt. Most of these late granitic intrusions are intimately associated with, and smaller than the older Archean plutons (*see* maps, Fig. 112). Petrographic data for Ag and Ack are provided in Tables 6 and 29 and in Figures 17, 20Ga-c, 68, and 69a, b. Chemical data are presented in Tables 30, 47, and 48, and in Figures 69c-k, 72-74, and 95.

Most contacts of the late granitic plutons are poorly exposed. Most of the few that were observed closely are sharp and clearly defined, and most obscured contacts are probably similar. Marginal parts of the plutons, however, commonly contain schlieren of country rock and are migmatitic. The intrusive rocks range from massive and discordant to weakly and strongly foliated (possibly sheared) subparallel to the contacts. Interleaving of granitic rocks with host rocks along the contacts (Fig. 67f), and faulted contacts are also common.

The shapes of the late granitic intrusions are not defined by the magnetic patterns on the aeromagnetic maps although parts of some of the larger intrusions (e.g. NTS 37G) coincide with slightly higher background nanotesla values. A few small intrusions coincide with anomalies of at least 300 nanoteslas (nT) above background. Most of the intrusions coincide with a poorly defined bird's-eye pattern in which the local anomalies range up to 200 nT above background. A relatively fine bird's-eye pattern coincides with some Ack in north-central map area NTS 37E. Elsewhere some of the intrusions coincide with relatively featureless magnetics where the local anomalies are less than 100 nT above background. As elsewhere, topography has played a part in shaping the magnetic patterns.

Streckeisen's (1974, 1976, 1979) classifications of granitic and charnockitic rocks have been followed in this memoir, except for a few modifications to the charnockitic nomenclature (Fig. 15). Therefore the names used here will not coincide in every case with those used on the map legends which were completed, using Brown's (1952) classification, before Streckeisen's (1974, 1976) classifications became widely accepted. For example, granite on the maps is chiefly

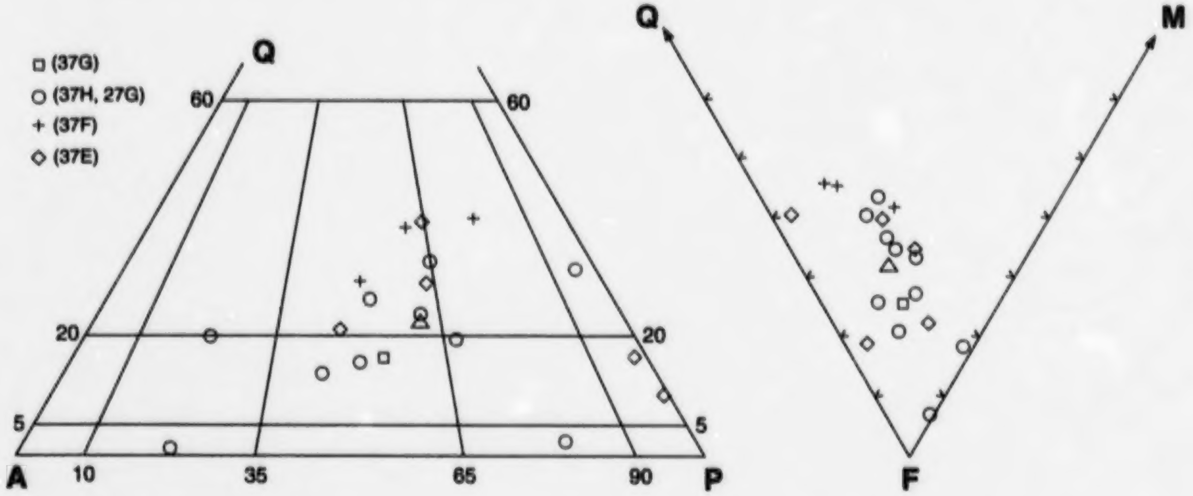

***Figure 66.** Quartz-alkali feldspar-plagioclase and quartz-feldspar-mafic plots for unit* Amp. *The mean is shown by the small triangle.*

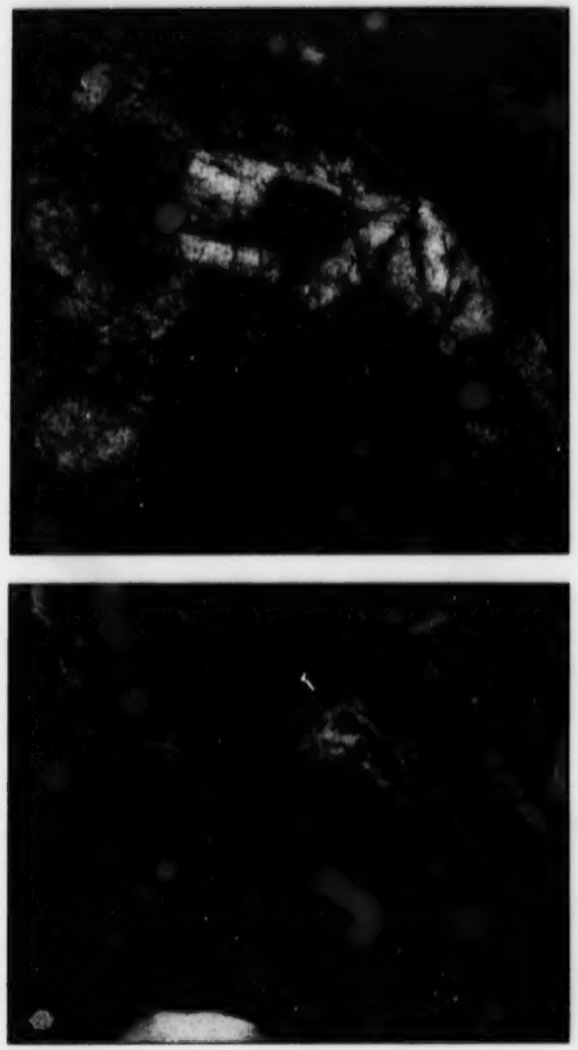

Figure 67. ***a)*** *Large feldspar crystals in massive pink pegmatitic granite* (**Ag**)*, Mary River area (NTS 37G). Photograph by G.D. Jackson. GSC 118352.* ***b)*** *Pink massive granite* (**Ag**) *with hornblendite agmatite, Mary River area. Photograph by G.D. Jackson. GSC 118343.* ***c)*** *Detached segments of folded massive light pink pegmatite* (**Ag**?) *in biotite amphibolite, Mary River area. Photograph by W.J. Crawford. GSC 1997-54M.* ***d)*** *Pink pegmatite* (**Ag**) *intruding amphibolite* (**Mb**) *with quartzite at the base, Mary River area. The left side of the cliff is about 5 m high. Photograph by W.J. Crawford. GSC 1997-54N.* ***e)*** *Folded massive pink pegmatite* (**Ag**) *in amphibolite* (**Mb**)*, Mary River area. Photograph by G.D. Jackson. GSC 118354.* ***f)*** *Massive to faintly foliated pink granite* (**Ag**?) *interleaved at the base with migmatite, and intruded by small hornblendite dykelets (h). The section of cliff is about 15 m high. West coast, Dexterity Island (NTS 37H). Photograph by G.D. Jackson. GSC 186948.* ***g)*** *Intensely contorted red muscovite pegmatite* (**Ag**?) *at The Bastions, Buchan Gulf (NTS 37H). Photograph by W.J. Crawford. GSC 186347*

syenogranite and minor quartz syenite in the text; quartz monzonite on the maps is chiefly monzogranite and minor quartz monzonite in the text; what was formerly called granodiorite also includes some tonalite, trondhjemite, and quartz monzodiorite; and syenodiorite on the maps has been replaced by monzodiorite-quartz monzodiorite in the text. This is discussed more fully in the "Introduction" under "Present investigations".

Massive monzogranite (Ag)

Description

Unit **Ag** intrusions are abundant in western map area NTS 37G (Fig. 67), common in northern map area NTS 37F, and rare in the rest of the map area. Massive monzogranite is the most abundant rock type (Fig. 20Ga-c, 68). Unit **Ag** is mostly medium grained but ranges from fine grained to coarsely pegmatitic (Fig. 67). Most of unit **Ag** is light to dark pink, but red, white to dark grey, and mottled colours are also present. The bulk of unit **Ag** intrusions comprise quartz, locally perthitic microcline, and plagioclase with a few per cent of myrmekite, brown to reddish-brown biotite, muscovite, local blue-green hornblende, and rare garnet. Most of the plagioclase is oligoclase (An$_{15-28}$) but some of **Ag**, especially in map area NTS 37G, contains albite (An$_{0-7}$). Orthoclase is present instead of microcline locally. Retrograde minerals are chiefly chlorite, epidote, sericite, and locally talc and clay minerals. Accessory minerals are apatite, zircon, allanite, iron oxide (magnetite, hematite, limonite), garnet, leucoxene, and pyrite. Some common mineral assemblages are given in Table 29.

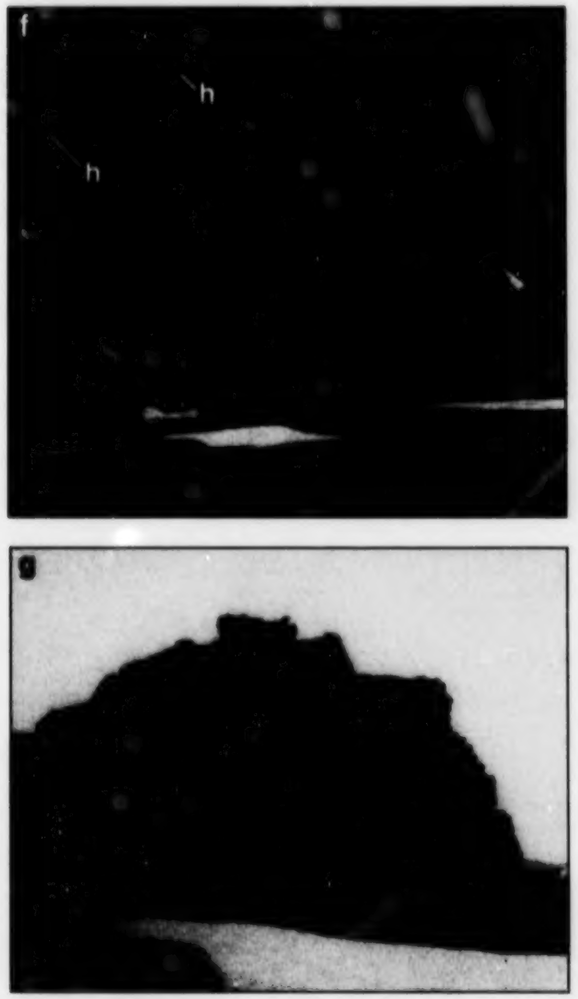

Figure 67. *(cont.)*

Late massive granitic rocks range in composition from syenogranite to tonalite, but most plot in the middle of the QAP triangle in the position of minimal granitic melts. Syenite, quartz syenite, quartz monzodiorite, and quartz diorite are rare (Fig. 20Ga-c, 68). Foliated phases define a linear trend from syenogranite toward the plagioclase apex of the QAP triangle (Fig. 68c), which seems to be unique for quartzofeldspathic rocks in the map area.

A few small, pink syenite-monzodiorite dykes and stocks occur at various localities, and include diatreme breccias as much as 20 m in diameter in west-central map area NTS 37G. The diatreme breccias contain small angular fragments of pink syenite, and Mary River Group lithologies (ferruginous argillite-mylonite, quartz, serpentine) in a pink crystalline calcite matrix (Jackson, 1966b). The syenitic intrusions and the diatreme breccias are included with the late granitic rocks because they are too small to differentiate on the published maps. Their ages, however, are uncertain, other than that they are late- or post-regional metamorphism, and some syenitic rocks are intergradational with late granitic rocks.

Although chiefly massive and homogeneous, **Ag** intrusions also commonly display faint foliation and coarse feldspar segregations locally. Flow structures are outlined locally by potassium feldspar phenocrysts as much as 5 cm long, some of which have been sheared. In a few places the massive granites contain scattered inclusions and schlieren, or grade into nebulitic gneisses, deformed gneisses that locally are well banded, and possibly into contorted felsic metavolcanics.

Contact relations

Unit **Ag** intrudes **Agp** in map area NTS 37G, is much less sheared and foliated than **Agp**, its contacts are more distinct, and the contained minerals tend to be less altered than those in **Agp**. Unit **Ag** (Fig. 67) also intrudes units **Agn**, **Amn**, and the Mary River Group (**M**,**AM**). Pegmatites and small granitic bodies that intrude the northern Piling Group are considered tentatively to represent unit **Ag**. Granitic dykes, pegmatites, and aplites also intrude unit **Ag**. Their contacts are mostly sharp but some are gradational and these intrusions are probably a late phase of the plutonic event represented by unit **Ag**.

Within the map area, and throughout most of Baffin Island, contacts of late massive granitic intrusions **Ag** and late pegmatites and aplites are almost always sharp and distinct, except in granulite facies terrane. There the contacts become

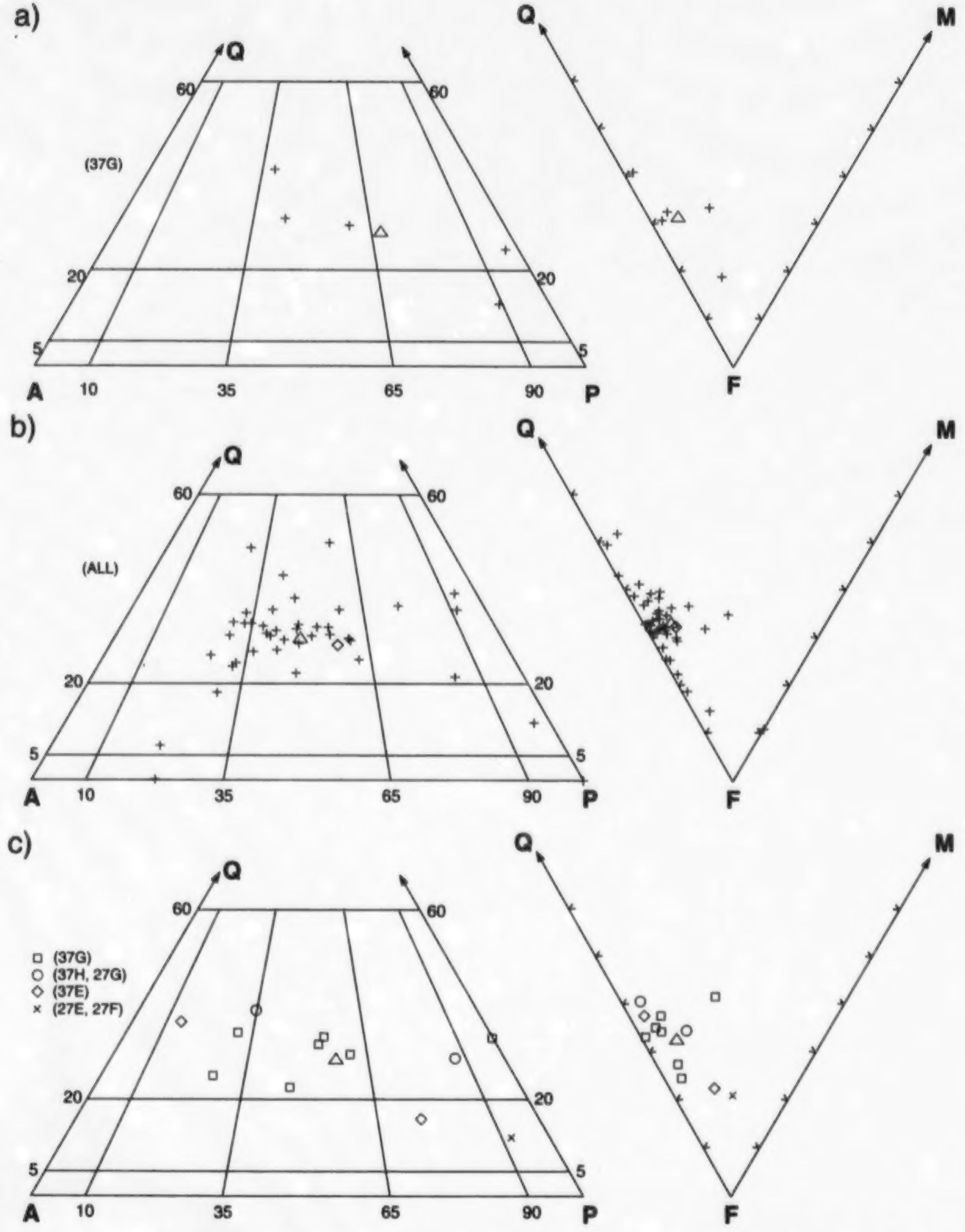

Figure 68. Quartz-alkali feldspar-plagioclase and quartz-feldspar-mafic plots for map unit **Ag**. ***a)*** *white massive granite,* ***b)*** *pink massive granite for the entire map area, and* ***c)*** *foliated phase of pink massive granite. The small triangle indicates the mean composition. The diamond in b) indicates the mean composition for foliated late granite shown in c).*

Table 29. Common mineral assemblages in massive granites (**Ag**) and charnockites (**Ack**).

Assemblage:	1^{a}	2^{a}	3^{a}	4^{ab}	5^{ab}	6^{c}	7^{c}	8^{c}	9^{c}	10^{c}	11^{c}	12^{c}
Quartz	+	+	+			+	+	+	+	+	+	+
Microcline	+	+		+								
Orthoclase			+									
Potassium feldspar						+	+	+	+	+		
Plagioclase	+	+		+	+	+	+				+	+
Muscovite					±							
Biotite	+	±	+			+	+	+	+	+	+	+
Hornblende		+					+	+	+		+	
Clinopyroxene				+	+	±		±	+			
Hypersthene						+	+		+		+	
Garnet			+							+	+	
Rutile									±			
Carbonate				±	+							

a - massive granite (**Ag**), b - syenitic assemblage (**Ag**), c - massive charnockite (**Ack**);
+ - mineral is present; ± - mineral is present in some assemblages, not in others. Two minerals represented by ± in an assemblage indicates there are four combinations represented, etc.

blurred or less distinct, and somewhat gradational due in part to minor recrystallization of metamorphic minerals (e.g. hornblende, pyroxene, garnet) across the contact. In addition, these late intrusive rocks have different colours in granulite than in lower grade terrane. In granulite terrane the late intrusions have a greasy resinous lustre, similar to the other granulites. White granites take on a light grey to greenish-grey colour while pink to red colours become less distinct in the contact area and are absent in good granulite grade terrane.

Charnockites (Ack)

Description

Massive hypersthene-bearing granitic plutons (charnockites) occur almost entirely within an irregular, discontinuous belt of rock in the granulite metamorphic facies (Dexterity Granulite Belt), which extends from Steensby Inlet (NTS 37F) map area northeast through Conn Lake (NTS 37E) map area to Buchan Gulf (NTS 37H) map area, where the largest intrusion, the Dexterity Fiord Batholith, occurs. This belt contains 18-20 charnockitic intrusions, chiefly hypersthene monzogranite (monzocharnockite – Fig. 15) and hypersthene granodiorite (granoenderbite), and forms the southern and eastern component of the arcuate belt of granitic intrusions outlined previously. The intrusions at both ends of the charnockite belt are elongated parallel to the belt but the rest of them are elongated northwest-southeast, parallel to the regional structure but at a sharp angle to the belt (*see* Fig. 99, 112). A small charnockitic body lies south of the belt east of Beiler Lake (southeast NTS 37E) in a small window of granulites. The charnockite outcrops are relatively deeply weathered, and commonly display spheroidal shapes.

Most of unit **Ack** is medium grained but ranges from fine grained to coarsely pegmatitic. Colours range from grey-green to grey, lavender, pale pink, and brown, and most of the rock has a greasy or resinous lustre and is dark weathering. Major minerals are quartz, locally antiperthitic plagioclase (An_{20-35}), and perthitic potassium feldspar. The latter is chiefly orthoclase but microcline is also common. The rest of the minerals make up 10-20% of the rock (Table 6; Fig. 17, 70). Minor minerals are chiefly red-brown to brown biotite, hypersthene, olive- to yellow-green hornblende, diopsidic clinopyroxene, myrmekite, and locally, garnet. Some of the hornblende, chiefly blue-green, has formed from hypersthene. At one locality, in the large intrusion along Dexterity Fiord (NTS 37H), hypersthene is rimmed by diopside, which in turn is rimmed by blue-green hornblende. Some biotite is also retrograde and in several places is poikiloblastic and occurs in wormy intergrowths with quartz. Some garnet is also poikiloblastic. Other retrograde minerals are chlorite, muscovite, sphene, and kaolinite. Accessory minerals are apatite, magnetite, hematite, zircon, rutile, pyrite, and carbonate. Some representative assemblages are given in Table 29.

Compositions of **Ack** range from hypersthene syenogranite (syenocharnockite) and hypersthene quartz monzonite (quartz mangerite) to hypersthene tonalite (enderbite) and hypersthene quartz diorite (quartz norite). Thin layers and variously shaped small bodies of hypersthene syenite are rare. The patterns displayed on the QAP and QFM plots by **Ack** are similar to those for **Agp**, but resemble those for **Amn** and the concordant granitic component in **Amg** most closely (Table 6; Fig. 15, 17, 19, 55, 62, 66, 68, 69a-b, 70).

Charnockite plutons are generally well jointed, somewhat crushed, and range from massive to strongly foliated. Minor, locally abundant components include layered gneisses, migmatitic rocks, strongly lineated and sheared rocks, boudined layers, nebulitic schlieren, and feldspar megacrysts of one or more generations. Potassium feldspar and plagioclase phenocrysts, augen, and porphyroblasts are as much as 5 cm long. Feldspar aggregates up to 70 cm in diameter, and large granulite facies pyribolite masses are also present. Late pegmatites and aplites commonly intrude the charnockites.

Contact relations

The large northeast-trending pluton along Dexterity Fiord, the Dexterity Fiord Batholith (NTS 37H), is chiefly massive, very slightly crushed charnockite, but the margins are foliated, sheared, and slightly to highly migmatitic, especially the southeast margin. In some places the foliation is deformed into tight, steeply inclined mesoscopic folds. Remnant pyribolite, biotite-hornblende gneiss, nebulitic migmatite, massive and foliated charnockites, and pegmatites occur in the migmatitic phase. Foliations on both sides of the Dexterity Fiord Batholith dip chiefly to the northwest but at both ends dip northeast, so the body may plunge northerly.

Several steeply dipping, massive to banded pyribolite bodies (Fig. 71) in the Dexterity Fiord Batholith may include both Mary River Group remnants and metamorphosed intrusive dykes (Mb, Mg, b). Other charnockitic plutons range from massive with minor marginal foliation or sharp contacts, to strongly foliated and nebulitic or schlieren- bearing throughout.

One interesting feature of the charnockite plutons is that they are known to occur only in granulite facies terrane (Jackson and Morgan, 1978a). Also, some of the contacts between charnockite plutons and certain other map units are gradational. These features have been observed from northwestern Baffin Island (including Bylot Island) at least as far south as Cumberland Sound, and have been discussed in more detail by Jackson and Morgan (1978a). Gradational relationships have been observed between charnockite (Ack), porphyritic monzogranite (Agp), and monzogranite (Ag) and also seem to be present between Ack and foliated granite (gr-Agr) and nebulitic granitic gneiss (Amn).

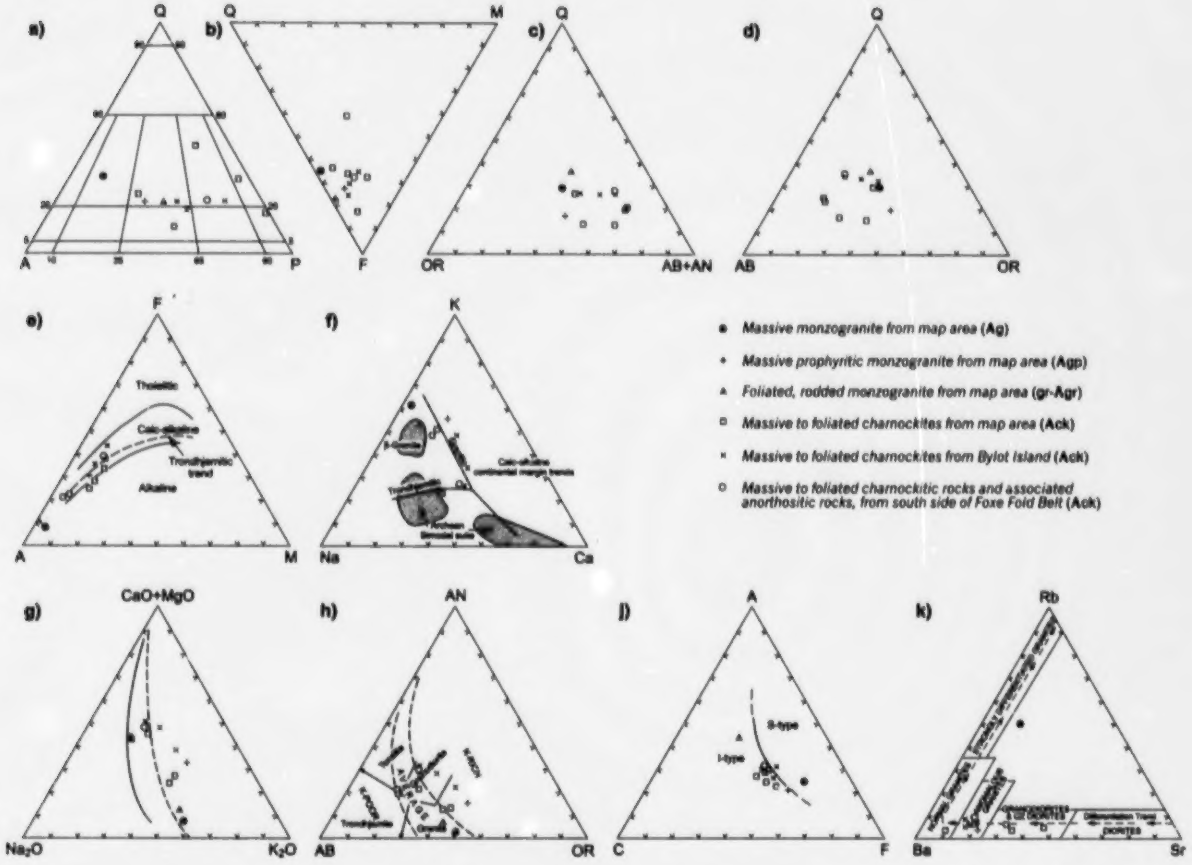

***Figure 69.** Triangular plots for selected charnockite and granite analyses presented in Table 30. **a)** Modal quartz-alkali feldspar-plagioclase plot showing Streckeisen's (1976) classification. **b)** Modal quartz-feldspar-mafics plot. **c)** Normative quartz-orthoclase-albite+anorthite plot. **d)** Normative quartz-albite-orthoclase plot. **e)** A-F-M plot after Coleman and Donato (1979). **f)** K-Na-Ca plot after Barker et al. (1981). **g)** CaO+MgO-Na_2O-K_2O plot after Smith (1978), solid line = alkalic trend, dashed line = average calc-alkaline trend. **h)** Normative anorthite-albite-orthoclase plot, K content after Irvine and Baragar (1971), classification from Barker (1979). **j)** ACF (A=Al_2O_3-Na_2O-K_2O, C = CaO, F = FeO+ gO) plot after Baker and Drucker (1985). **k)** Rb-Ba-Sr plot after El Bouseily and El Sokkary (1975).*

Similar relations were observed in the map area where charnockite plutons (Ack) are gradational mostly with porphyritic monzogranite (Agp). These relations are best displayed in the Conn Lake (NTS 37E) map area. Unit Agp and Ag plutons lose their pink colour in the contact area and acquire colours characteristic of charnockite. Textures are similar on both sides of the contact and the presence or absence of hypersthene is used to arbitrarily place the contact in these cases. Thin section studies to date have not found evidence that hypersthene is absent in Agp and Ag plutons because of retrogression. Well crystallized brown hornblende occurs on both sides of the contact areas, and the hypersthene isograd passes through these rocks into adjacent map units (e.g. Amg; Amn; M, AM), insofar as regional

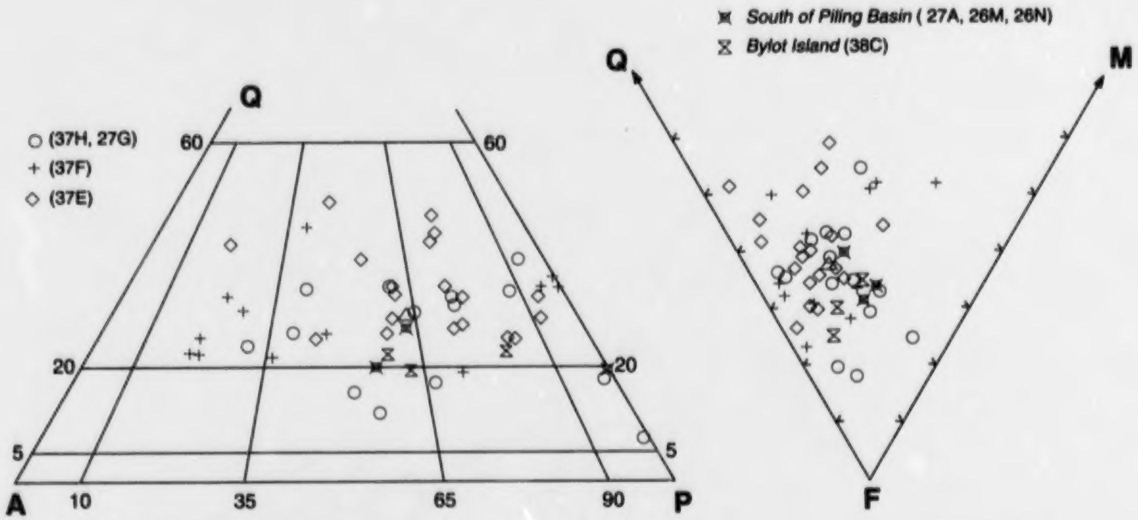

***Figure 70.** Quartz-alkali feldspar-plagioclase and quartz-feldspar-mafic plots for map unit* Ack. *The small triangle indicates the mean composition.*

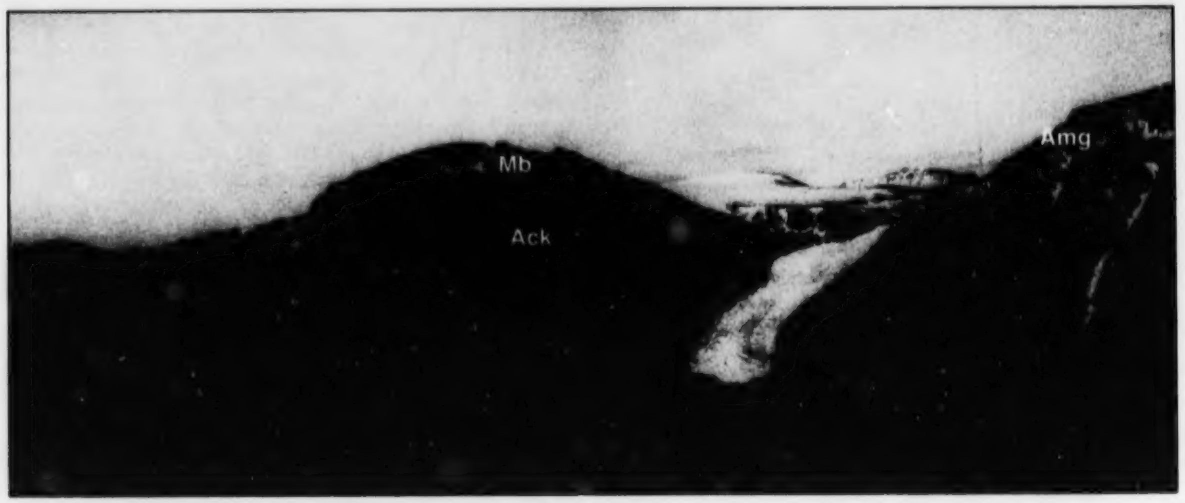

***Figure 71.** Charnockite* (Ack) *with an inclusion of Mary River Group pyribolite* (Mb?) *left of valley glacier, and overlain by banded migmatite* (Amg) *on the right. View northeast across Dexterity Fiord (NTS 37H). The cliff is about 2 km away and peaks in distance to 1475 m high. Photograph by G.D. Jackson. GSC 186957-8*

mapping can determine, without offset. Metamorphic hypersthene has not yet been differentiated from primary hypersthene in the charnockites.

Chemistry of Ag, Ack

Chemical data for one sample of late massive granite (Ag) and five charnockite (Ack) samples from the map area (NTS 37E, 37H) are compared with other granitic rocks in Table 30. Means of spectrographic data are provided in Table 48.

According to modes and patterns displayed by individual elements in histograms (*see* Table 49, Fig. 95, 96), units **Ag**, **Amp**, and **Agp** show relatively low similarity with other quartzofeldspathic map units. Unit **Ag** is similar to late granitic intrusions (**Amg**^{i}) in banded migmatite (**Amg**), and is somewhat less similar to foliated granitic rocks (**Amn**^{b}) and late granitic intrusions (**Amn**^{i}) in **Amn**, and concordant (leucosome) granitic rocks (**Amg**^{j}) in **Amg**.

The charnockites (**Ack**) and units **gr-Agr** and **Amg**^{j} show greater similarity with various quartzofeldspathic units and with one another than the above mentioned units do. Charnockite (**Ack**) is also at least as similar to units **Amg**^{i}, **Amn**^{i}, and **Amn**^{b} as is **Ag**. Both **Ag** and **Ack** show relatively little similarity to one another and to **Agp**. This is rather surprising considering that fieldwork and other chemical data indicate that these rocks are intergradational, in some places at least.

Chemical data for **Ag** and **Ack** have been compared with chemical data (e.g. Table 31) interpreted tectonically by Pearce et al. (1984) and by Whalen et al. (1987). An active continental margin type of volcanic arc environment is indicated for both **Ag** and **Ack** but the results are somewhat indefinite for **Ag**, which has several similarities with a continent-continent type of collision environment. The mineralogy of both **Ag** and **Ack** favour volcanic arc granites, but is also similar to that of post-tectonic collision granites, and has probably been modified by metamorphism. Although both **Ag** and **Ack** resemble I-type granites most, they also have some similarity with M-, A-, and S-types.

Eleven spectrographically determined elements are compared for most map units in Figure 95. The massive granitic rocks are shown together in one section of this figure, and three groups may be distinguished. Unit **Ag** in map area NTS 37D, just south of the map area, seems most distinctive. The second group comprises **Amn**^{i}, **Amg**^{i}, **Amg**^{j}, and **Ag** in the map area. The third group comprises **Agp** and **Ack**, which is in agreement with these two units commonly grading into each other in the field.

Figure 72 compares Zr, TiO_2, MgO, Ba, and Sr values for **Ag**. These plots show much more restricted fields and values, except for Ba, than do similar comparisons made for: **Agp** and **Ack** (Fig. 58); **Amn**^{i}, **Amg**^{i}, and **Amg**^{j} (Fig. 63); **gr-Agr** (Fig. 26); and **Amn** (Fig. 22). The smaller fields suggest a relatively uniform and restricted range in composition for **Ag**. Although this is borne out by the statistics in Appendix 4 for most of the elements plotted in Figure 74, some of the other elements seem as varied as in the other map units. The positive correlation trend shown by the Ba-Sr plot may be related to variations in plagioclase and potassium feldspar content rather than being a differentiation trend.

The analyses listed in Table 30 for **Ag**, **Ack**, and other granitic rocks are also used for several plots. Those in Figures 69 and 73 show both **Ag** and **Ack** from the map area as plotting in calc-alkaline, subalkaline, and alkaline fields. The monzogranite sample (**Ag**^{a} – Table 30) is indicated to be a strongly differentiated, normal peraluminous syenogranite with normal K. It plots in the S-type (Fig. 69j) field of Baker and Drucker (1985) but in the I-type field (Fig. 73c) of White and Chappell (1983). It also plots in the peraluminous field (Fig. 73g) of Jensen (1985). A diagram from Pearce et al. (1984) suggests that the **Ag** sample is a syncollision granite (Fig. 73d), while it plots at the extreme end of the granitic calc-alkaline continental margin trend (Fig. 69f) of Barker et al. (1981).

In Figures 69 and 73, charnockites within the map area tend to plot a little differently than those from Bylot Island and south of the Piling Group in the Cumberland Batholith. Those analyzed from the map area range from quartz monzonite to monzogranite and tonalite. They plot in the I-type fields (Fig. 69j, 73c) of both Pearce et al. (1984) and White and Chappell (1983), and along both the trondhjemite and granitic calc-alkaline continental margin trends (Fig. 69f) of Barker et al. (1981). According to Figure 73d (Pearce et al., 1984), they are volcanic arc granites. The charnockites from the map area plot as both normal and anomalous granitic rocks in Figure 69k, as average to K-rich in Figure 69h, and as metaluminous in Figure 73g. Those samples that plot outside the normal field in Figure 73f have supposedly been affected by metasomatism. Figure 73h (Harvey, 1983) shows that most charnockite samples do not obviously plot along either the mantle or the crustal fusion differentiation trend. However the sample for **Agp** and three of the charnockitic samples from the map area do plot close to the crustal fusion trend.

Indicator ratios provided in Table 32 favour a peraluminous S-type granite for **Ag**. The ratios indicate strongly that charnockite (**Ack**) in the map area is a metaluminous I-type granite. Although the charnockites on Bylot Island and in the Cumberland Batholith are also probably I-type granites (Bylot = D162/1, B196, D137/1; Cumberland Batholith = S3), the indications are weaker and the rocks range from metaluminous to peraluminous.

The diagrams in Figures 74 and 75 outline linear trends that are probably positive and negative differentiation trends. The lone sample for **Ag** has a high differentiation index (as indicated also by Fig. 69k) and plots along linear trends with the other granitic rocks.

Ages of late massive granitic intrusions (Ag, Ack)

Reliable ages of larger plutons representing **Ag** and **Ack** have not yet been obtained in the map area nor in much of Baffin Island, although several attempts have been made. At least three ages of leucocratic phases of **Ag**, superseded an amphibolite phase (*see* section on "Age of the Mary River Group (M, AM)") in migmatite near the head of Cambridge Fiord

Table 30. Analyses, CIPW norms, and modal analyses for selected charnockites (Ack) and other granitic rocks.

Sample	B284		B281/1		M180		C170		B321		D231/1	
Map area	37E		37E		37E		37E		37E		37H	
Map unit	Ag^{a}		Ack^{b}		gr-Agr^{c}		Ack^{b}		Agp^{d}		Ack^{b}	
SiO_2	74.8		66.2		74.3		67.9		63.6		62.4	
Al_2O_3	13.2		15.7		13.2		16.0		15.2		16.6	
TiO_2	0.11		0.41		0.07		0.38		0.82		0.59	
Fe_2O_3	0.1		1.9		0.6		1.0		2.1		2.2	
FeO	0.9		1.8		0.4		2.0		2.7		3.0	
MnO	0.02		0.05		0.01		0.05		0.06		0.08	
MgO	0.35		1.63		0.07		1.50		1.46		2.07	
CaO	0.40		3.74		1.13		3.92		2.78		4.17	
Na_2O	3.7		4.9		3.5		4.9		3.0		4.4	
K_2O	5.67		2.43		4.49		2.31		5.67		3.39	
P_2O_5	0.01		0.14		0.01		0.14		0.30		0.33	
S	0.00		0.00		0.00		0.00		0.00		0.00	
CO_2	0.1		0.3		0.1		0.1		0.1		0.2	
H_2O	0.3		0.0		0.2		0.2		0.7		0.5	
TOTAL	99.7		99.2		98.1		100.4		98.5		99.9	
B	<0.0050		<0.0050		<0.0050		<0.0050		<0.0050		<0.0050	
Ba	0.026		0.094		0.10		0.063		0.16		0.073	
Ce	<0.015		<0.015		<0.015		<0.015		<0.015		<0.015	
Co	<0.0010		<0.0010		<0.0010		<0.0010		<0.0010		<0.0010	
Cr	<0.00050		0.0011		<0.00050		0.0014		0.0011		0.0015	
Cu	<0.00070		0.0018		<0.00070		0.0012		0.0016		0.0020	
La	0.0068		0.0050		NF		0.0052		0.0093		0.0075	
Mo	<0.0050		<0.0050		<0.0050		<0.0050		<0.0050		<0.0050	
Ni	<0.0010		0.0012		<0.0010		<0.0010		<0.0010		0.0012	
Sr	0.011		0.053		0.023		0.078		0.047		0.037	
V	0.0024		0.0057		0.0022		0.0056		0.0063		0.0075	
Y	<0.001		<0.0010		NF		<0.0010		0.0025		<0.0010	
Yb	<0.00015		<0.00015		<0.00015		<0.00015		0.0002		<0.00015	
Zr	0.0049		0.013		0.0079		0.032		0.032		0.0078	
Sc	0.00066		0.00080		NF		0.0017		0.0012		0.0013	
Li	0.0035		0.0011		0.0009		0.0015		0.0010		0.0017	
Rb	0.0360		0.0055		0.0081		0.0087		0.0081		0.0074	
U	0.186		NF		0.070		0.012		0.067		0.004	
Th	NF		NF		NF		NF		0.0033		NF	
CIPW norms												
Quartz	30.05		19.25		35.40		20.16		18.09		12.43	
Corundum	0.51		0		0.86		0		0		0	
Orthoclase	33.72	66.53	14.47	70.04	27.12	62.15	13.62	69.8	35.46	72.32	20.14	73.2
Albite	31.51		41.79		30.01		41.37		25.95		37.44	
Anorthite	1.30		13.78		5.02		14.81		10.91		15.62	
Diopside	0		1.34	1.67	0		1.62	2.49	0.28	0.44	0.96	1.42
Hedenbergite	0		0.33		0		0.87		0.16		0.46	
Enstatite	0.88	2.31	3.47	4.46	0.18	0.35	2.98	4.82	3.59	5.87	4.74	7.38
Ferrosilite	1.43		0.98		0.17		1.84		2.28		2.64	
Magnetite	0.15		2.78		0.84		1.45		3.11		3.21	
Ilmenite	0.21		0.78		0.14		0.72		1.20		1.13	
Apatite	0.02		0.33		0.02		0.33		0.73		0.79	
Calcite	0.23		0.69		0.23		0.23		0.23		0.46	
Differentiation Index	95.78		75.51		93.40		75.16		77.51		70.01	
Crystallization Index	1.91		17.55		5.14		18.51		13.71		19.90	
K/Rb	131		367		460		221		601		380	
Rb/Sr	3.27		0.104		0.362		0.112		0.172		0.200	
Ba/Sr	2.36		1.77		4.35		1.06		3.40		1.97	
K/Ba	181		22		37		23		30		39	
Modal analyses												
Quartz	33		35		22		30		21		15	
Orthoclase			10				4		41			
Microcline	53				37						1	
Plagioclase*	12(24-29)		30(18)		40(20-24)		59(24)		31(26)		66(26-34)	
Myrmekite					P		P		P		P	
Biotite	1.8		8		0.9		1		2		8	
Hypersthene	T?		T?		T?		T?				5	
Clinopyroxene			1								1	
Hornblende			14				5		3		T	
Garnet							T					
Fe-Ti oxide	0.2		T		0.1		0.8		1		2	
Apatite			T				0.2		1		2	
Zircon	T		T		T		T				T	
Allanite							T					
Sphene	T		1				0.1					
Rutile			T									

All chemical results in weight per cent. Major oxides determined by X-ray fluorescence (XRF); H_2O, FeO, and CO_2 by rapid chemical methods. Minor elements determined chiefly by quantitative optical emission spectroscopy methods expected to be accurate to within 15% of value reported. Ag, As, Be, Sb, and Zn may be present in amounts below the limit of quantitative determination. Li, Rb, and Cs were determined by atomic absorption spectroscopy. U and Th were determined by XRF methods.

NF - Not found.
* - Optically determined plagioclase composition shown in parentheses.
a - Massive to faintly foliated monzogranite.
b - Massive to foliated granoenderbite (hypersthene granodiorite) with K-feldspar phenocrysts and metaphenocrysts. D137/1 is garnetiferous.

Table 30 (cont.)

Sample	D236	J263/3	D162/1^k	B196^k	D137/1^k	S3^h
Map area	37H	37H	38C	38C	38C	
Map unit	Ack^e	Ack^f	Amg^f	Ack^g	Ack^b	Ack^h
SiO_2	70.4	64.5	66.7	64.0	66.4	67.2
Al_2O_3	15.0	16.9	15.6	14.6	15.6	15.7
TiO_2	0.39	0.67	0.82	0.92	0.64	0.50
Fe_2O_3	1.4	1.6	1.0	1.3	1.0	0.53
FeO	1.4	1.4	3.5	4.5	3.6	4.0
MnO	0.03	0.04	0.05	0.08	0.06	0.06
MgO	0.79	0.84	1.45	1.29	1.20	1.28
CaO	2.20	2.35	4.31	4.08	3.01	3.95
Na_2O	3.4	4.3	3.4	2.9	2.7	3.4
K_2O	4.92	5.47	2.42	3.13	4.27	2.38
P_2O_5	0.18	0.14	0.08	0.24	0.14	0.17
S	0.00	0.00	0.00	0.00	0.00	0.00
CO_2	0.2	0.2	0.2	0.3	0.1	0.04
H_2O	0.2	0.1	0.5	0.8	0.7	0.5
TOTAL	100.5	98.3	100.0	98.2	99.4	99.7
B	<0.0050	0.0053	0.0050	0.0051	0.0051	0.0055
Ba	0.15	0.33	0.100	0.12	0.11	0.109
Ce	0.018	0.035	<0.015	<0.015	0.018	<0.015
Co	<0.0010	<0.0010	0.0012	0.0021	<0.0010	0.0011
Cr	<0.00050	0.00062	0.0018	0.0014	0.0011	0.0040
Cu	0.00088	<0.00070	0.0015	0.0019	0.0010	0.0007
La	0.010	0.018	0.0078	0.0071	0.010	0.0092
Mo	<0.0050	<0.0050	<0.0050	<0.0050	<0.0050	<0.0050
Ni	0.0010	0.0010	0.0010	0.0012	<0.0010	0.0022
Sr	0.040	0.038	0.028	0.026	0.022	0.027
V	0.0049	0.0059	0.0086	0.011	0.0068	0.0068
Y	<0.0010	0.0019	<0.0010	0.0024	0.0024	0.0034
Yb	<0.00015	<0.00015	<0.00015	0.00024	0.00018	0.00024
Zr	0.017	0.057	0.026	0.036	0.026	0.037
Sc	0.00055	0.0016	0.0022	0.0026	0.0021	0.0024
Li	0.0004	0.0010	0.0011	0.0028	0.0028	0.0015
Rb	0.0131	0.0126	0.0094	0.0073	0.0114	0.013
U	0.024	0.032	NF	0.011	0.029	0.028
Th	NF	NF	NF	NF	NF	NF
CIPW norms						
Quartz	26.50	13.66	25.18	23.97	24.90	25.90
Corundum	0.97	0.44	0.21	0.30	1.65	0.66
Orthoclase }	28.98 }	32.91 }	14.37 }	19.00 }	25.56 }	14.17 }
Albite }	28.68 } 66.11	37.04 } 79.6	28.90 } 62.96	25.20 } 61.43	23.14 } 62.26	28.99 } 61.53
Anorthite }	8.45 }	9.65 }	19.69 }	17.23 }	13.56 }	18.37 }
Diopside }	0	0	0	0	0	0
Hedenbergite }	0	0	0	0	0	0
Enstatite }	1.96 } 2.78	1.62 } 1.84	3.63 } 7.99	3.30 } 9.26	3.03 } 7.93	3.21 } 9.49
Ferrosilite }	0.82 }	0.22 }	4.36 }	5.96 }	4.90 }	6.28 }
Magnetite	2.02	2.36	1.46	1.94	1.47	0.77
Ilmenite	0.74	1.30	1.56	1.79	1.23	0.96
Apatite	0.43	0.34	0.19	0.58	0.34	0.41
Calcite	0.45	0.46	0.46	0.70	0.23	0.09
Differentiation index	85.13	85.13	68.66	68.48	75.25	69.91
Crystallization index	9.82	9.82	22.23	19.54	15.68	20.62
K/Rb	311	311	214	356	311	71
Rb/Sr	0.328	0.328	0.336	0.281	0.518	0.481
Ba/Sr	3.75	3.75	3.57	4.62	5.00	4.04
K/Ba	27	27	20	22	32	18
Modal analyses						
Quartz	23	23	18	19	20	20
Orthoclase						18
Microcline	40	40	28	12	29	
Plagioclase*	25(22)	25(22)	47(31)	53(36)	41(36)	49(33-42)
Myrmekite	P	P	P		P	P
Biotite	8	8	0.3	1	1	3
Hypersthene	T	T	5.5	4.5	5	8
Clinopyroxene	T	T				
Hornblende	T	T		5		0.3
Garnet				3	3	
Fe-Ti oxide	1	1	1.0	2	1	1
Apatite	1	1	0.2	0.5	T	0.6
Zircon	1	1	T	T	T	0.1
Allanite			T			
Sphene						
Rutile						

c - Foliated and rodded monzogranite.
d - Massive monzogranite with K-feldspar phenocrysts.
e - Massive monzocharnockite (hypersthene monzogranite).
f - Massive to faintly foliated quartz mangerite (hypersthene quartz monzonite) in Amg. D162/1 is part of layered sequence.
g - Foliated monzocharnockite (hypersthene monzogranite) with K-feldspar megacrysts.
h - Granoenderbite (hypersthene granodiorite). Average of three samples from charnockitic suite along north edge of Cumberland Batholith south of Foxe Fold Belt, central Baffin Island. J116(26M) is foliated quartz mangerite with K-feldspar phenocrysts; E 158 (26 N) is massive enderbite, J 214/1 (27 A) is massive to faintly foliated quartz noritic andesine anorthosite.
k - Samples from charnockitic complex of Bylot Batholith on Bylot Island (complex also contains anorthosite).
P - Present, amount included in other minerals.
T - Trace

Table 31. Comparison of average compositions of various granite types with charnockite (Ack) in map area.

Type:	ORG	VAG	WPG	CG	M	I	S	A	Ack^{bfg}	Ack^e
Samples:	51	120	86	56	17	991	578	148	7	1
SiO_2	72.3	70.6	72.9	72.3	67.2	69.2	70.3	73.8	65.4	70.4
TiO_2	0.33	0.30	0.28	0.26	0.49	0.43	0.48	0.26	0.63	0.39
Al_2O_3	14.0	13.4	12.4	14.6	15.2	14.3	14.1	12.4	15.9	15.0
Fe_2O_3	3.43[1]	2.91[1]	3.33[1]	1.85[1]	1.94	1.04	0.56	1.24	1.4	1.4
FeO					2.35	2.29	2.87	1.58	2.8	1.4
MnO	0.06	0.07	0.10	0.04	0.11	0.07	0.06	0.06	0.06	0.03
MgO	0.76	0.81	0.11	0.79	1.73	1.42	1.42	0.20	1.40	0.79
CaO	1.79	1.86	0.57	1.59	4.27	3.20	2.03	0.75	3.65	2.20
Na_2O	6.88	4.25	4.53	3.33	3.97	3.13	2.41	4.07	3.9	3.4
K_2O	0.13	2.54	4.72	4.66	1.26	3.40	3.96	4.65	3.4	4.92
P_2O_5	0.12	0.08	0.04	0.11	0.09	0.11	0.15	0.04	0.17	0.18
H_2O etc.[2]	0.45	2.16	0.53	0.60	-	-	-	-	0.60	0.40
Total	100.3	99.0	99.5	100.1	98.6	98.6	98.3	99.1	99.3	100.5
Ba	0.0125	0.0305	0.0369	0.0417	0.0263	0.0538	0.0468	0.0352	0.12	0.15
Rb	0.0002	0.0063	0.0151	0.0228	0.00175	0.0151	0.0217	0.0169	0.0089	0.0074
Sr	0.0086	0.0194	0.0036	0.0158	0.0282	0.0247	0.0120	0.0048	0.040	0.040
Zr	0.0331	0.0115	0.0641	0.0101	0.0108	0.0151	0.0165	0.0528	0.038	0.017
Y	0.0077	0.0026	0.0078	0.0018	0.0022	0.0028	0.0032	0.0075	0.001	0.001
U	-	-	-	-	0.00004	0.0004	0.0004	0.0005	0.013	0.024
La	0.00336	0.00206	0.00921	0.00263	-	-	-	-	0.0087	0.010
Sc	-	-	-	-	0.0015	0.0013	0.0012	0.0004	0.0018	0.0006
V	-	-	-	-	0.0072	0.0060	0.0056	0.0006	0.0074	0.0049
Ni	-	-	-	-	0.0002	0.0007	0.0013	0.0001	0.0010	0.040
Cr	-	-	-	-	-	-	-	-	0.0012	0.0005
Cu	-	-	-	-	0.0042	0.0009	0.0011	0.0002	0.0014	0.0009

Note: ORG, VAG, WPG, CG from Pearce et al. (1984). ORG = ocean ridge granites, VAG = volcanic arc granites, WPG = within-plate granites, CG = collision granites. M, I, S, A from Whalen et al. (1987). M = granites from melted subducted oceanic crust or overlying mantle, I = granites from igneous protoliths, S = granites from sedimentary protoliths, A = granites from lower, dehydrated continental crust (anorogenic), **Ack^{bfg}**, **Ack^e** from Table 30 (this memoir). All values in weight per cent. 1 - all iron as Fe_2O_3. 2 - is loss on ignition (LOI) for averages from Pearce et al. (1984), is $H_2O + CO_2 + S$ for **Ack^{bfg}** and **Ack^e**, no values given for averages provided by Whalen et al. (1987). -: not determined or not given.

(NTS 37H). Uranium-lead analyses of zircons separated from the latest phase, pale pinkish-grey to white monzogranite (Ag), give an upper intercept of 2522 +11/-10 Ma and a lower intercept of 1525 Ma (Fig. 64; Table 51). The data have been interpreted as representing a mixture of Proterozoic igneous zircons and Archean xenocrysts or cores or both, and the formation of a Proterozoic felsic melt from an Archean protolith (Jackson et al., 1990b).

Remarkably similar results were obtained for zircons from a pink massive monzogranite (Ag) intrusion, 50 m across that intrudes migmatite northwest of the map area (NTS 48D). The data yield an upper U-Pb intercept of 2500 Ma and a lower intercept of 1522 Ma (Table 51). These data also are interpreted as indicating a mixture of Proterozoic magmatic zircons that crystallized from a felsic melt, possibly in the late Aphebian between 1850-1600 Ma, and Archean cores or xenocrysts or both. Here too the data indicate formation of a Proterozoic melt from an Archean protolith (Jackson et al., 1990b). The same sample (from map area NTS 48D) has provided a Nd T_{DM} model age of 2710 Ma (Hegner and Jackson, 1990; Jackson et al., 1990a), which is similar to the U-Pb zircon age of 2709 Ma obtained for a large Archean granitic pluton (Agp) with large feldspar phenocrysts in north-central map area NTS 37G (Table 51). The sample from the latter intrusion, however, provided a Nd model age of 2900 Ma. Two other granitic plutons from the map area, considered tentatively to be Aphebian, have given Archean Nd T_{DM} model ages. One, a large pink granitic pluton in northwestern map area NTS 37G, has provided an Nd model age of 2820 Ma; the other, a grey to pinkish-grey granitic pluton about half way along the south edge of map area NTS 37H, has an Nd model age of 2830 Ma.

A postkinematic granite in the Eqe Bay area (bordering the map area south of eastern map area NTS 37F) was emplaced at ca. 1819 Ma (U-Pb zircon; Scammell and Bethune, 1995b). Farther south, the Piling Group in the southern part of Foxe Fold belt has been intruded by: a granite pegmatite sill at 1876 Ma (U-Pb zircon; Henderson and Henderson, 1994), on the west coast of Baffin Island by pink massive granite at ca. 1840 Ma (Geochronology subdivision, Geological Survey of Canada, unpub. data, NTS 37A), and by syntectonic granites (U-Pb monazite) and syn- to post-tectonic pegmatites (U-Pb zircon) at ca. 1812-1806 Ma (Table 51; Henderson and Loveridge, 1981; Henderson and Henderson, 1994).

One K-Ar age of 1679 Ma (Table 53) has been obtained for muscovite from a pegmatite that intrudes the Mary River Group in the No. 4 iron deposit area of western map area NTS 37G. In general, most K-Ar mineral ages north and south of the map area, and most Rb-Sr mineral ages south of the map

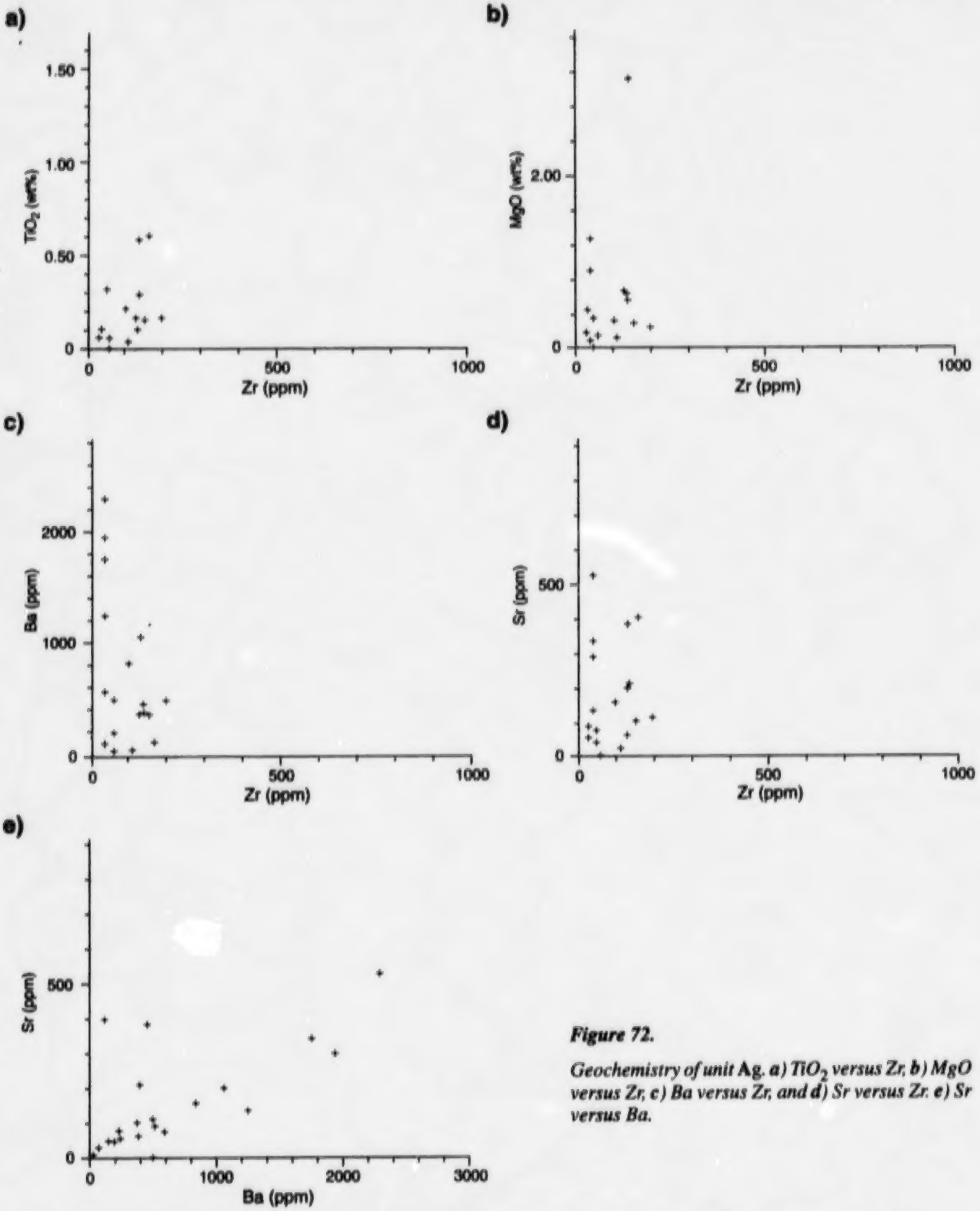

Figure 72.

Geochemistry of unit **Ag.** ***a)*** *TiO$_2$ versus Zr,* ***b)*** *MgO versus Zr,* ***c)*** *Ba versus Zr, and* ***d)*** *Sr versus Zr.* ***e)*** *Sr versus Ba.*

Figure 73. *Data from Table 30 shown on selected plots used to classify granitic rocks;* ***a)*** *after Brown (1981);* ***b)*** *after Irvine and Baragar (1971);* ***c)*** *after White and Chappell (1983);* ***d)*** *after Pearce et al. (1984): WPG = within plate granites, syn-COLG = syn-collision granites, VAG = volcanic arc granites.* ***e)*** *after Ewers and Scott (1977);* ***f)*** *after Hughes (1972);* ***g)*** *after Jensen (1985);* ***h)*** *after Harvey (1983): a - differention trend for mantle-derived granite magma; b - trend for granite magma derived by fusion of the crust.*

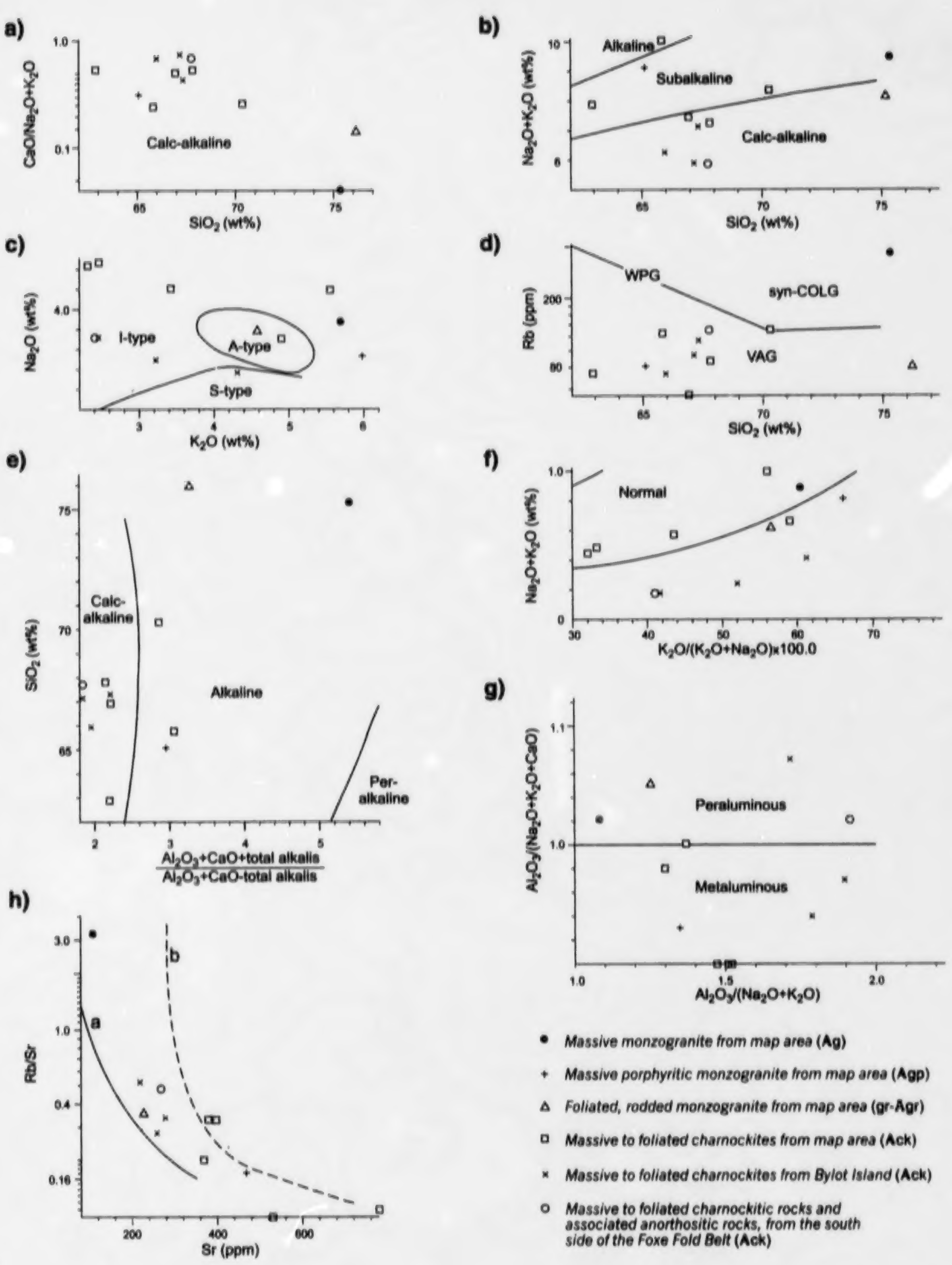

Table 32. Selected ratios (a) calculated from analyses in Table 30.

Sample		B284	B281/1	M180	C170	B321	D231/1	D236	J263/3	D162/1	B196	D137/1	S3
Map unit		Ag^a	Ack^b	gr-Agr^c	Ack^b	Agp^d	Ack^b	Ack^e	Ack^f	Amg^f	Ack^g	Ack^b	Ack^h
(b)	$\frac{Fe^{3+}}{Fe^{3+} + Fe^{2+}}$	0.09 S	0.49 I	0.57 I	0.31 I	0.41 I	0.40 I	0.47 I	0.51 I	0.21 I,S	0.21 I,S	0.20 I,S	0.11 S
(c)	$\frac{Al_2O_3}{Na_2O + K_2O + CaO}$	1.02 I,S,P	0.90 I,M	1.04 I,S,P	0.91 I,M	0.93 I,M	0.90 I,M	1.01 I,P	0.98 I,M	0.97 I,M	0.94 I,M	1.07 S,P	1.02 I,S,P
(d)	$\frac{Al}{Na + K + Ca/2}$	1.06 I,S	1.27 S	1.19 S	1.30 S	1.21 S	1.30 S	1.26 S	1.20 S	1.50 S	1.46 S	1.50 S	1.58 S
(e)	$\frac{Al_2O_3}{Na_2O + K_2O}$	1.08 P	1.47 M	1.24 P	1.52 M	1.35 M	1.52 M	1.37 P	1.30 M	1.90 M	1.79 M	1.72 P	1.92 P
(f)	$K = \frac{Na_2O + K_2O}{Al_2O_3}$	0.93	0.68	0.80	0.66	0.74	0.66	0.73	0.77	0.53	0.55	0.58	0.52
(g)	$\frac{K_2O}{Na_2O + K_2O}$	0.50 I,S	0.25 I	0.46 I	0.24 I	0.56 S	0.34 I	0.49 I,S	0.46 I	0.32 I	0.42 I	0.51 I,S	0.32 I
(h)	$\frac{C}{ACF}$	0.19 S	0.37 I	0.38 I	0.37 I	0.31 I,S	0.33 I	0.33 I	0.36 I	0.33 I	0.32 I,S	0.27 S	0.30 I,S

Notes: In C/ACF, C = CaO, A = Al_2O_3-Na_2O-K_2O, F = FeO + MgO. I = igneous, S = sedimentary, P = peraluminous, M = metaluminous. (a) - weight per cent used in iron ratio, atomic proportions in other element ratios, and molecular proportions in oxide ratios. (b) Chappell (1978): S <0.2, I >0.2. (c) Chappell (1978): S >1.03, I <1.03. (d) Pitcher (1982): S >1.05, I <1.1. (e) Jensen (1985), (when (c) <1.0): metaluminous >1.0, subaluminous ~1.0, peralkaline <1.0. If (c) >1.0 = peraluminous. (f) Kovalenko (1977): K = agpaitic coefficient. (g) Baker and Drucker (1985): I <0.5, S >0.5. (h) Baker and Drucker (1985): S <0.3, I >0.3. Other symbols as in Table 30.

area range from 1810-1609 Ma (e.g. Tables 52, 53; Fig. 98; Henderson, 1985a, b). Attempts have not yet been successful to determine the age of unit Ack in the map area, although the granulite metamorphism in the southwest end of the Dexterity Granulite Belt, bordering map area NTS 37F on the south, has been dated at ca. 1827-1821 Ma (U-Pb zircon and monazite; Scammell and Bethune, 1995b). Five U-Pb zircon ages for charnockite south of the map area and the Foxe Fold Belt range from 1895 to 1853 Ma (e.g. Table 51; Jackson et al., 1990b). Two of these same samples have provided three monazite metamorphic ages that range from 1854-1831 Ma. Three of the same samples have Nd T_{DM} model ages of 2440, 2460, and 2700 Ma (Jackson et al., 1990a; Jackson and Hegner, 1991). Attempts to date some charnockite zircons have yielded clustered, discordant data points opposite about 1880-1850 Ma on concordia, suggesting a partial resetting of older zircons. Potassium-argon mineral and Rb-Sr whole rock ages for charnockite range from 1877 to 1685 Ma (e.g. Tables 52, 53; Jackson et al., 1990b, Table 6). North of the map area, on Bylot Island, one K-Ar age of 1660 Ma has been obtained for phlogopite in anorthosite associated with charnockites that have Nd model ages of 2780 and 2730. Charnockite and granite on southeast Ellesmere Island have given U-Pb ages of 2.0-1.9 Ga (Fig. 98), and slightly older Nd model ages (Jackson et al., 1990a). These compare with Nd model ages for charnockite in the map area of 2880 Ma for the large Dexterity Fiord Batholith on the east coast (NTS 37H) and 2910 Ma for a small body of charnockite (north-central NTS 37E) that is gradational with the granite in south-central map area NTS 37H, which has a Nd model age of 2830 Ma (Jackson et al., 1990a; Hegner and Jackson, 1990).

Most of the late massive granitic and charnockitic intrusions (Ag, Ack) are considered to be penecontemporaneous late Aphebian plutons emplaced during the last major metamorphic event at about 2.0-1.8 Ga, either during or prior to the granulite metamorphism. The relatively old Nd model ages obtained for some, as well as field relations, suggest that some are Archean plutons such as Agp (Zr-2709 Ma) and gr-Agr (Zr-2851 Ma), which were also metamorphosed during the 2.0-1.8 Ga interval and are inadvertently shown as Aphebian on the maps. Only two of the several samples from Baffin Island that have U-Pb zircon ages of 2850 Ma or older have also been analyzed for Sm-Nd. Although both have Archean Nd model ages that are at least as old as the Zr, it is premature to assume that older Archean Nd model ages, such as 3180 Ma for a massive pink granite south of the Steensby Inlet (NTS 37F) map area or 3270 Ma for a homogeneous foliated granite in the Cumberland Batholith, can be used to separate Archean plutons from Aphebian plutons formed from melted Archean crust.

Aphebian Rb-Sr ages obtained for some gneisses in north-central Baffin Island (Fig. 98, Table 52) might be related to the ages of late massive granites and pegmatites that intrude the gneisses for which ages were obtained. These ages are discussed further in individual sections for the rocks that were dated and in the section on "Regional geochronology". They include a Rb-Sr isochron age of 1971 ± 97 Ma for the Mary River Group in the Mary River area (NTS 37G), and errorchron ages of 2033 Ma for some gneisses in the McBeth gneiss dome (NTS 27C) and of 2159 Ma for some gneisses in the Ayr Lake area (NTS 27F). These ages, if reasonably accurate, suggest that some Aphebian granites in Baffin Island

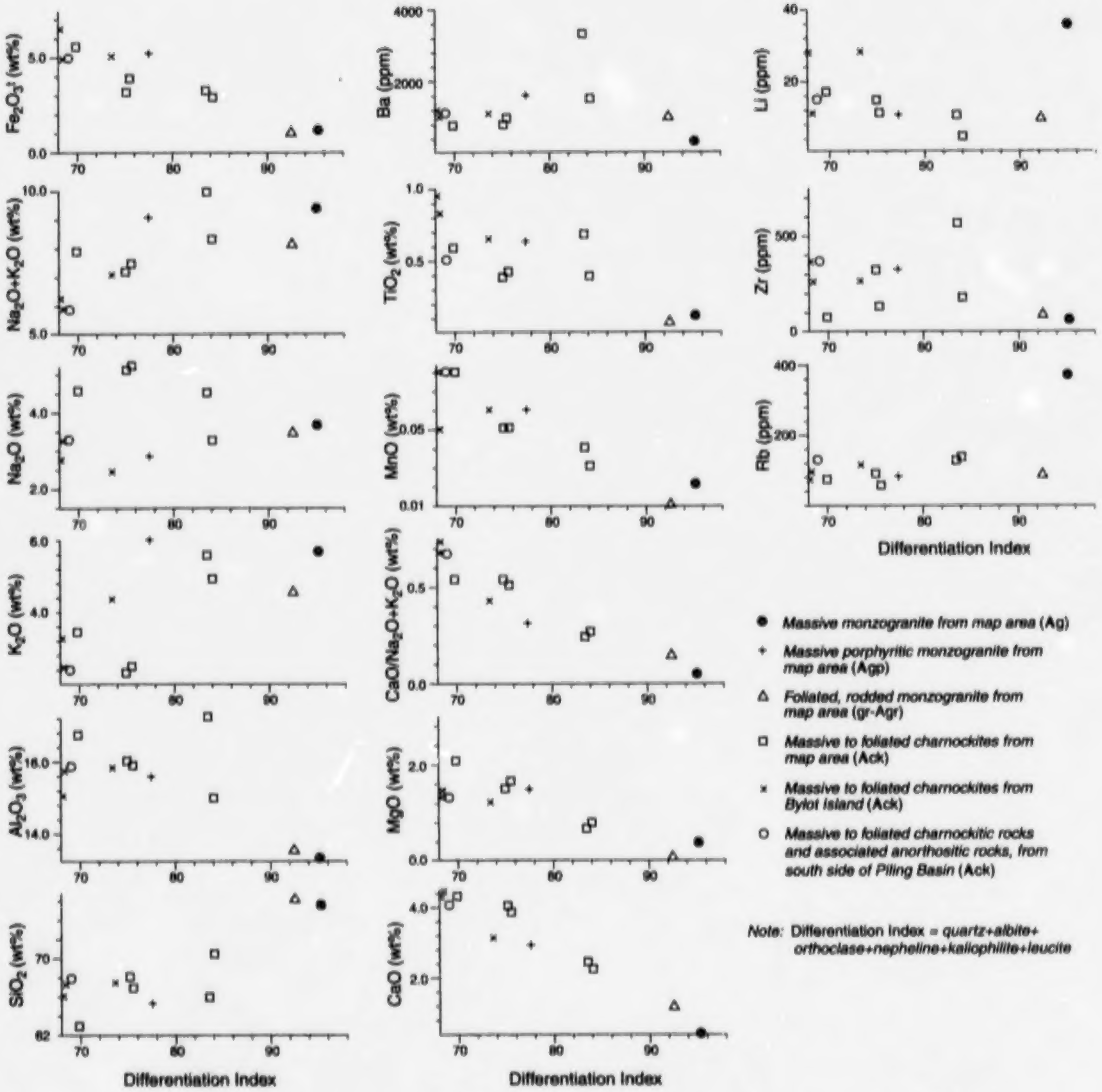

Note: Differentiation Index = *quartz+albite+orthoclase+nepheline+kaliophilite+leucite*

Figure 74. Plots of selected oxides and elements against differentiation indices for analyses in Table 30.

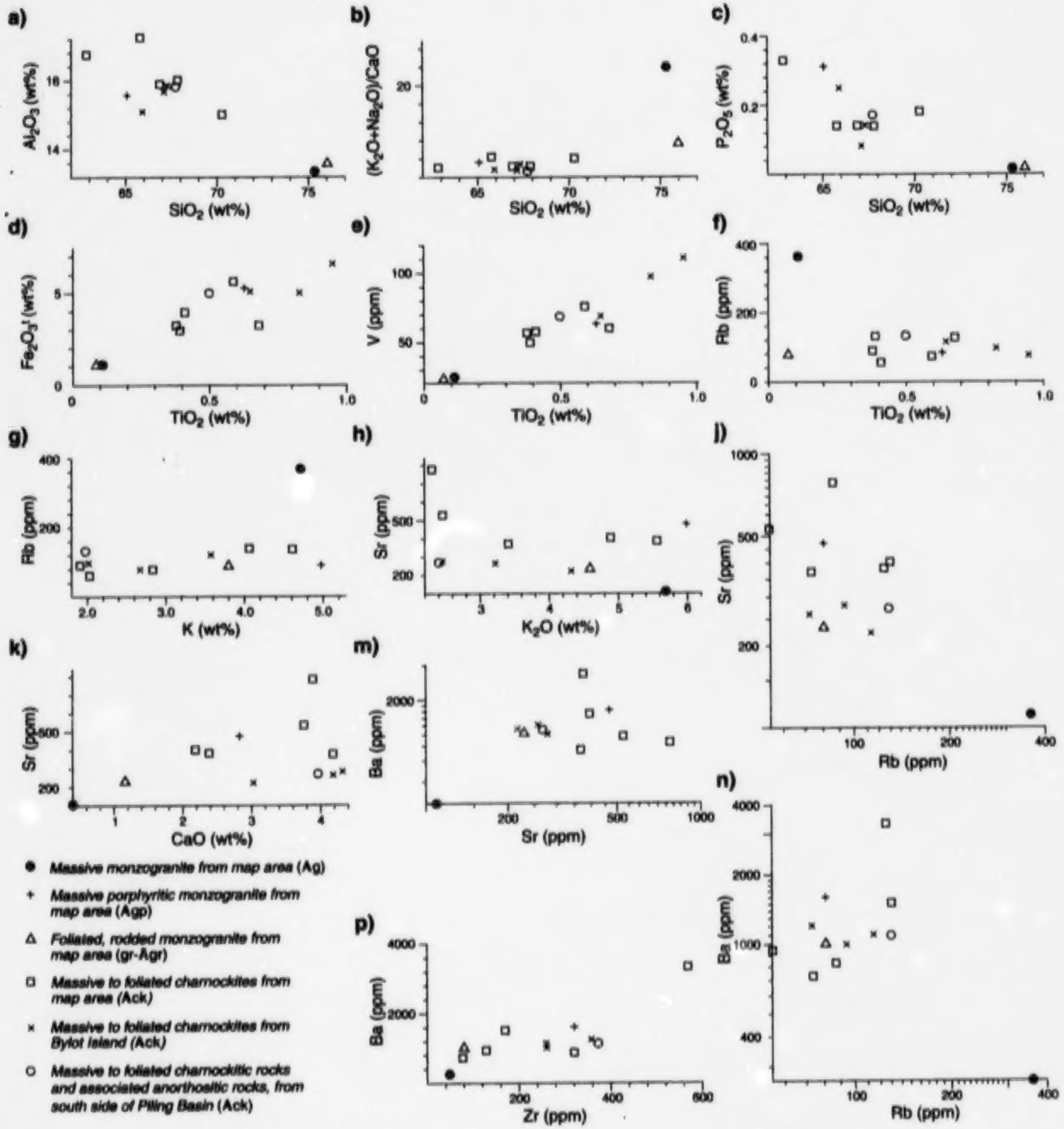

Figure 75. *Plots of selected oxides and elements for some analyses in Table 30.*

north of the Dexterity Granulite Belt may be closer in age to the granitic plutons of the Thelon Tectonic Zone (2.0-1.9 Ga in Henderson and van Breemen, 1992) than to those of the Baffin Orogen (1.9-1.8 Ga in Jackson et al., 1990b).

Origin of late massive granitic intrusions (Ag, Ack)

Field relations indicate that unit **Ag** is late tectonic or post-tectonic with regard to the last deformation, but was emplaced prior to the granulite metamorphism which, according to ages determined for rocks chiefly south of the map area, peaked at about 1854-1821 Ma. The data from U-Pb zircon and Nd model ages and from modal QAP plots indicate that the Aphebian monzogranite plutons in northwestern Baffin Island are recrystallized melts formed from Archean protoliths, which is supported by the close spatial field association of Archean and Aphebian granitic plutons (*see* Fig. 112).

Most chemical data discussed above show a strong similarity between units **Agp** and **Ack** and support the field data which indicate that some unit **Ack** plutons are metamorphosed and deformed Archean **Agp** (2709 Ma) and **Ag** intrusions. The spread of points noted in several chemical and QAP diagrams may be a reflection of the varied primary ages of **Ack** plutons. Some unit **Ack** plutons contain more xenoliths than are common in **Agp** and especially in **Ag** plutons. These plutons, as also suggested by other field observations and Nd model ages, may represent Archean sialic crustal material that was remobilized and emplaced during or before the last regional metamorphism and deformation. The charnockitic plutons are chemically similar to late Aphebian orthopyroxene granites-granodiorites on southeastern Ellesmere Island. Frisch (1988) considers similar high K_2O, Ba, Rb, Rb/Sr, and Ba/Sr, low K/Rb, normative corundum, and peraluminous nature to represent dry melts formed from a felsic parent. Unlike southeastern Ellesmere Island, however, late Aphebian migmatites in the map area were overprinted by the granulite metamorphism which probably accompanied the emplacement of some charnockitic plutons. The granulite metamorphism postdates the Piling Group and may be the same age or slightly younger (1.83-1.82 Ga) than the granulite metamorphism south of the Foxe Fold Belt that is associated with the Cumberland Batholith of the Baffin Orogen (i.e. 1.90-1.83 Ga).

Comparisons with tectonically interpreted chemical data favour an I-type granite emplaced in an active continental margin type of volcanic arc setting for both **Ag** and **Ack**. The continental volcanic arc setting is similar to that obtained for the Archean felsic intrusions in the map area (e.g. **gr-Agr**) and for the Mary River Group metabasalts (**Mb**). It seems likely therefore that the Aphebian plutons may also have inherited the volcanic arc signature from the protoliths. Late Aphebian granitic plutons in the Cumberland Batholith to the south (e.g. Table 31) also have a volcanic arc signature, and it is also possible that any Aphebian juvenile crust added to the map area may have formed in that environment as well.

The map area lies on the southeast side of the Archean Committee Orogen, which lies between two late Aphebian tectonomagmatic zones, the Thelon Tectonic Zone (2.0-1.9 Ga) to the northwest, and the Baffin Orogen (1.90-1.84 Ga) to the southeast (*see* Fig. 112). Considerable late Aphebian juvenile crust was emplaced in both (Hegner and Jackson, 1990; Jackson et al., 1990a; Jackson and Hegner, 1991; Henderson and van Breemen, 1992). Late Proterozoic granites emplaced in the map area (**Ag** and **Ack**) and elsewhere in the Committee Orogen on northern Baffin Island, formed from melts derived from Archean crust, and contain little if any juvenile Proterozoic crust. The Aphebian plutons may have formed in response to crustal thickening due to intracrustal thrusting possibly first northwestward-southeastward and then southwestward. The northeast-trending, charnockite-bearing Dexterity Granulite Belt that extends past the north end of the Barnes Ice Cap is parallel to both the Thelon Tectonic Zone and the north edge of the Foxe Fold Belt of the Baffin Orogen (*see* Fig. 99, 101, 114). The charnockite-granulite belt also lies just north of the Isortoq Fault Zone which marks a former southeast-dipping thrust zone along the southern border of the Committee Orogen. For reasons discussed below (Isortoq Fault Zone), it is suggested that the charnockites and the Dexterity Granulite Belt originated in a compressive regime at about 1.825 Ga, followed by extension.

NEOHELIKIAN

Bylot Supergroup

Introduction

As much as 1900 m of late Proterozoic (Neohelikian) strata, belonging to the Bylot Supergroup, outcrop in the northern part of map area NTS 37G in the vicinity of Tay Sound and Paquet Bay (Fig. 13, 76; Jackson et al., 1978b). Descriptive data and most interpretations presented below are modified from Olson (1970, 1977), Geldsetzer (1973a, b), W.L. Davison (pers. comm., 1977), Jackson et al. (1978b, 1980), Iannelli (1979, 1992), and Jackson and Iannelli (1981). Iannelli (1979) gathered most of the raw data on cycles, particularly for the Arctic Bay Formation; the data were processed, as presented, by the author.

Within the map area, Bylot Supergroup strata are restricted to the Milne Inlet Trough of Borden Rift Basin which is part of the North Baffin Rift Zone (Jackson and Davidson, 1975; Jackson et al., 1975, 1978b; Jackson and Iannelli, 1981). The Milne Inlet Trough is the most southerly and largest of three grabens, separated by two horsts, within Borden Rift Basin. Only the southeastern part of Milne Inlet Trough lies within the map area (Fig. 13, *see* Fig. 110).

Bylot Supergroup strata nonconformably overlie the amphibolite- to granulite-grade Archean-Aphebian gneiss complex, and are intruded by northwest-trending Hadrynian Borden and Franklin diabase dykes. A few Neohelikian Mackenzie dykes may also be present (Fahrig et al., 1971; Jackson and Sangster, 1987). The Bylot Supergroup is overlain unconformably by early Paleozoic strata west of the map area (Blackadar, 1968a, 1970) and by Cretaceous-Eocene strata north of the map area (Jackson, 1969; Jackson and Davidson, 1975; Jackson et al., 1975; Miall et al., 1980).

Some of the gneisses below the nonconformity are stained red and contain hematite-rich seams along joint surfaces. A thin, lensitic, sporadically occurring regolith up to 3 m thick is gradational with the underlying gneiss complex. It is friable, varicoloured (purple to pink, green, and yellow), and recessive. In most places the gneisses at the nonconformity are fresh and the erosion surface is undulating with as much as 6 m of local relief. Local draping and pinching out of sedimentary beds occur, commonly over several metres, adjacent to the small basement topographic highs, where some draped beds dip as much as 40 degrees. Dips as steep as 65 degrees occur locally in Bylot Supergroup strata adjacent to faults, but dips of more than 10 degrees are uncommon throughout the Milne Inlet Trough.

The nomenclature for the Neohelikian succession was set up originally by Lemon and Blackadar (1963) and Blackadar (1965, 1970). The complete succession was named the Bylot Supergroup by Jackson and Iannelli (1981), who reorganized the formations into three groups, instead of the two recognized previously (Fig. 76). The three groups – lower clastic (Eqalulik), middle carbonate platform (Uluksan), and upper clastic (Nunatsiaq) – are commonly, but not everywhere, separated by intrabasin disconformities. Only the lower, Eqalulik Group, and the lower part of the middle Uluksan Group are present within the map area (Table of Formations).

Attempts to determine the age of the Bylot Supergroup have been noted by Jackson and Iannelli (1981). Seventeen whole rock K-Ar ages determined for Nauyat volcanics near the base of the Eqalulik Group have a mean age of 946 Ma. In addition, 6 of 14 samples analyzed yield a 1129 Ma Rb-Sr errorchron age, which is in agreement with whole rock K-Ar ages reported for similar volcanics in the Fury and Hecla Basin 200 km to the south (Chandler and Stevens, 1981; Chandler, 1988) and with which the Nauyat volcanics have been correlated (Jackson and Iannelli, 1981; Chandler, 1988). Most whole rock K-Ar ages of the underlying gneisses are 1600 Ma or older, and those for the younger Hadrynian diabase dykes are 1050-438 Ma (Table 53; Jackson, 1978b; Jackson and Iannelli, 1981). The best indication available of the age of the Bylot Supergroup is probably provided by the Mackenzie paleomagnetic poles obtained by Fahrig et al. (1981), who concluded that the age of the pole for the Nauyat and Adams Sound formations is about 1220 Ma, and that the pole for samples from the lower Strathcona Sound Formation (lower Nunatsiaq Group) is about 16.5 Ma younger. Refinements to the polar wander path (*see* section on "Cyclicity" below) suggest that the age difference may be 24-31 Ma rather than 16.5 Ma (Table 42). Jackson and Iannelli (1981) agreed with Fahrig et al. (1981) that the Nauyat volcanics are a Mackenzie igneous event. Although the author has been unable to find a sample coarse enough to use for dating baddeleyite, LeCheminant and Heaman (1991) have shown with U-Pb baddeleyite ages that 1270 Ma is a good average age for Mackenzie igneous events. Ages obtained to date range from 1272 ± 2 Ma to 1267 ± 2. Therefore 1270 Ma is considered to be a more reliable age for the Nauyat and Adams Sound formations and their paleomagnetic pole than the 1220 Ma suggested by Fahrig et al. (1981). Using data discussed under "Cyclicity" of the Arctic Bay Formation it is estimated that the preserved Bylot Supergroup was deposited within 80 Ma between 1270-1190 Ma. Considering the depositional environments this is considered to be a maximum. A Sm-Nd age for Nauyat volcanics near the base of the lowermost Uluksan Group and an age for glauconite in the upper (Elwin) formation of the Nunatsiaq Group might help to better establish the age of the Bylot Supergroup.

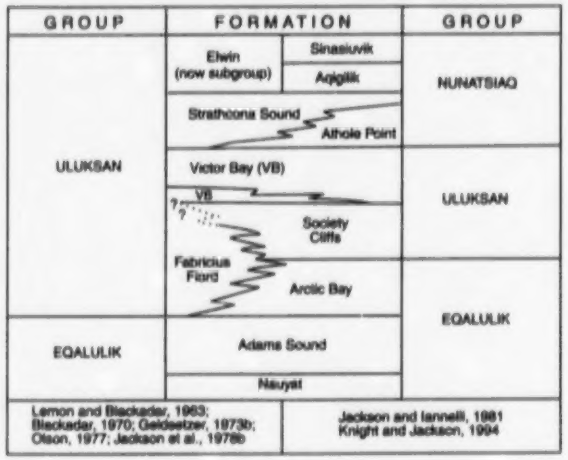

Figure 76. *Evolution of the stratigraphic nomenclature for the major units of the Bylot Supergroup. Knight and Jackson (1994) elevated the Elwin Formation to a subgroup containing the lower Aqigilik and the upper Sinasiuvik formations.*

The Bylot Supergroup has been correlated with several other Neohelikian sequences by Jackson and Iannelli (1981) who document several similar earlier correlations. These include the Fury and Hecla Group to the south, the Aston and Hunting formations to the west, and the Thule Group to the north. Chandler (1988) has recently discussed at considerable length the similarities and differences between the Fury and Hecla Group and the Bylot Supergroup, which he also considers to be of Mackenzie age. Although he supports the general correlation made by Jackson and Iannelli (1981), he prefers several alternative correlations within the sequences.

Modal analyses for Bylot Supergroup strata are provided in Figure 29. Chemical data are provided in Tables 9 (column 9), 47 (column I), and 48 (columns 31, 32) and Appendix 2. Chemical comparisons with the Mary River and Piling groups are provided in the section on "Regional geochemistry".

Eqalulik Group (NAS, NAB-L, NAB-U)

Following Lemon and Blackadar (1963), the Arctic Bay Formation was considered to be the basal formation of the Uluksan Group by Jackson et al. (1978b; map area NTS 37G). In the revised nomenclature followed here, the Arctic Bay Formation has been reassigned to the Eqalulik Group (Table of Formations; Fig. 76; 77, in pocket; Jackson and Iannelli, 1981).

Adams Sound Formation (NAS)

The Adams Sound Formation, lowermost formation of the Bylot Supergroup in the map area, outcrops discontinuously about the margins of the Milne Inlet Trough (northern NTS 37G) and in a small outlier about 30 km southeast of the main outcrop area, but still within the trough (Fig. 13; Jackson et al., 1975, 1978b, 1980; Iannelli, 1979; Jackson and Iannelli, 1981). The Adams Sound Formation is composed chiefly of quartz arenite with subordinate feldspathic sandstone, conglomerate, and minor shaly to silty strata. The formation is 9-45 m thick in most places. Locally, especially in the west, it may range from 70-122 m thick (Fig. 77). About 2-30 m are present in the small outlier to the southeast (Jackson et al., 1978b).

Adams Sound strata commonly overlie the basement rocks nonconformably (Fig. 77, 78), or are in fault contact with adjacent rocks. At several localities, however, Adams Sound strata are relatively thin or are missing completely and Arctic Bay Strata overlie basement rocks directly. The Adams Sound Formation grades into the overlying Arctic Bay strata. The contact is placed at the horizon above which shale ceases to be a negligible lithology and increases upward in abundance, either gradually or abruptly.

Throughout most of Borden Basin and in the western part of Milne Inlet Trough within the map area (Fig. 13, 77, and 79 (sites A-C)), Adams Sound strata may be subdivided into three intergradational members: a lower redbed member, a middle member composed of redbeds interbedded with light coloured beds, and an upper light coloured member that occurs everywhere the formation is present (Jackson and Iannelli, 1981). Ripple marks (oscillation, current, interference), including megaripples up to 5 m in wavelength, and planar, trough, and festoon crossbeds are abundant (Fig. 79). Loaded beds and bulbous load casts and channels occur locally. Three modal analyses are shown in Figure 29. Too few samples are reported on for the indicated differences between Adams Sound, Piling, and Mary River quartzites to be taken as real.

Lower member. About 8-20 m of lower member strata are present at and adjacent to section locality C (Fig. 13, 77, 79) and considerably more is present at locality A where the position of the upper contact of the member is uncertain. Most of the member is fine- to medium-grained, equigranular, medium bedded to massive quartz arenite. Bedding ranges from planar to gently undulating. Most strata are pink to maroon and purple; a few are white to yellow-orange, brown, and green. Polymictic orthoconglomerate and paraconglomerate beds and lenses, seen mainly in the eastern part of the member, contain rounded to well rounded clasts up to cobble size (25 cm) composed of quartz, quartz arenite, and various basement lithologies.

The small outlier 30 km southeast of the main area is floored by a thin bimodal conglomerate that contains quartz granules, pebbles, or cobbles in a siltstone-greywacke matrix. At one locality, the Adams Sound Formation is only about 2 m thick and consists of red to purple, medium- to coarse-grained quartz arenite and subarkose. At another locality, about 30 m of quartz arenite overlies the conglomerate and becomes more impure at the top where it grades into the overlying Arctic Bay Formation.

Middle member. This member ranges from 9-20 m thick in the vicinity of locality C (Fig. 13, 77, 79) but is considerably thicker at locality A. The member consists mostly of thin bedded to massive quartz arenite in which red and pink beds alternate with white to grey, buff-brown, and yellowish-green beds. Conglomerate beds and lenses are minor, similar to those in the lower member, and are more brightly coloured than the associated quartz arenite. Clasts are well rounded and range from disc-like to ovoidal and spheroidal.

Upper member. The upper member, 15-82 m thick, constitutes the entire formation in the eastern part of the main outcrop area (Fig. 13, 77, 79), and generally consists of quartz arenite with as much as 15% conglomerate lenses and beds. The strata are planar to undulating, thin bedded to massive, and are chiefly white to grey, buff, yellow, orange, and brown. Minor green and pink to red and purple colours are

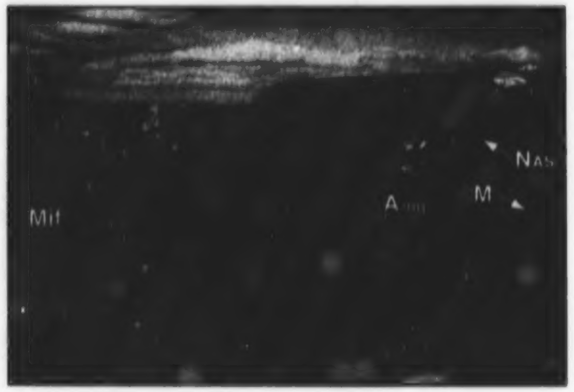

Figure 78. *Adams Sound Formation* (NAS) *on the right resting nonconformably on banded migmatite* (Amg) *and the Mary River Group* (M, AM). *Mary River iron-formation* (Mif) *occurs on the left. View north toward the head of Tay Sound (NTS 37G). Photograph by S.L. Blusson. GSC 185519*

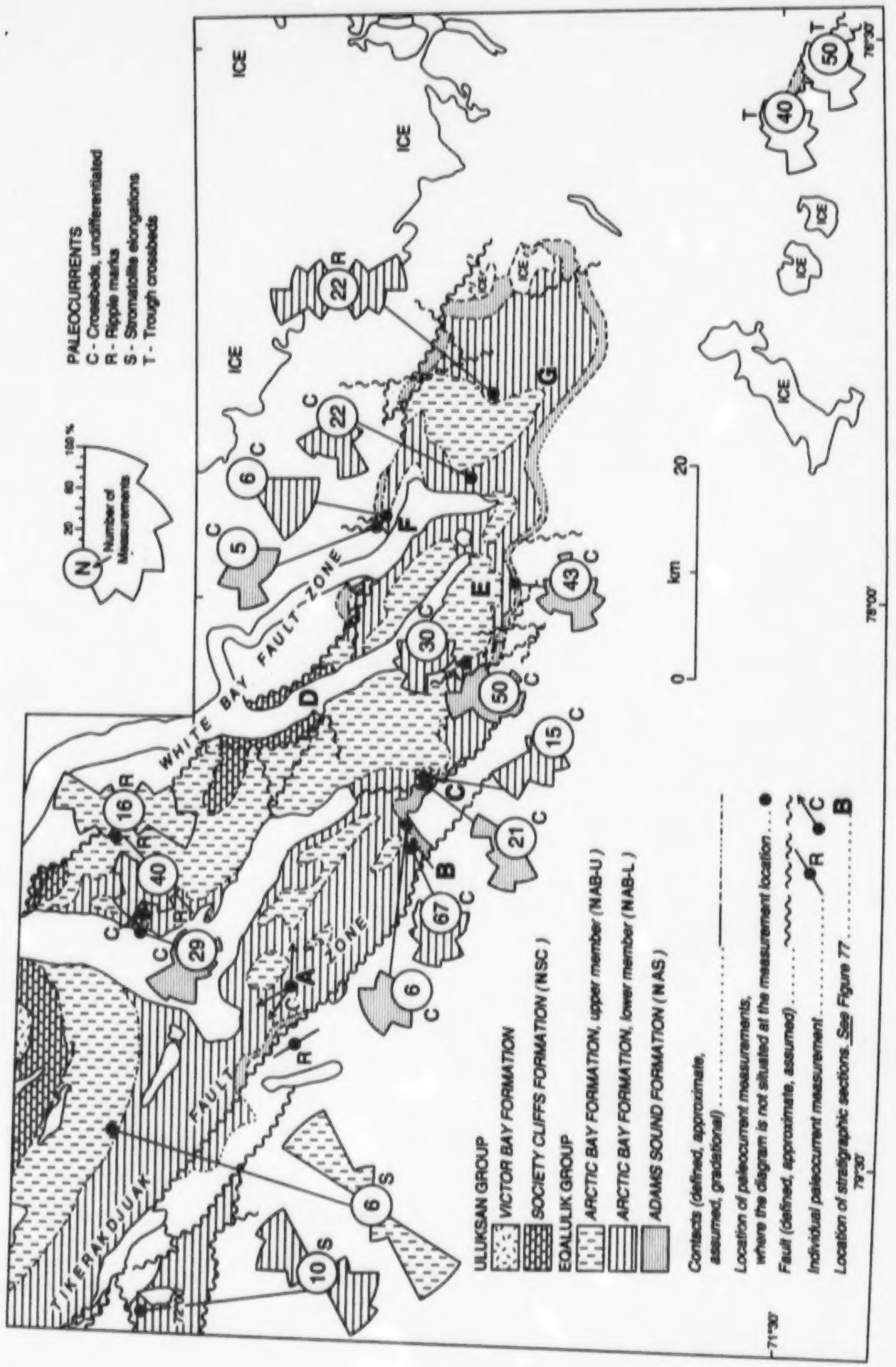
PALEOCURRENTS
C - Crossbeds, undifferentiated
R - Ripple marks
S - Stromatolite elongations
T - Trough crossbeds
N
Number of Measurements
20
60
100%
ULUKSAN GROUP
VICTOR BAY FORMATION
SOCIETY CLIFFS FORMATION (NSC)
EQALULIK GROUP
ARCTIC BAY FORMATION, upper member (NAB-U)
ARCTIC BAY FORMATION, lower member (NAB-L)
ADAMS SOUND FORMATION (NAS)
Contacts (defined, approximate, assumed, gradational)
Location of paleocurrent measurements, where the diagram is not situated at the measurement location
Fault (defined, approximate, assumed)
Individual paleocurrent measurement
Location of stratigraphic sections. See Figure 77
km
0
20
WHITE BAY FAULT-ZONE
FAULT ZONE
TIKERAKDJUAK
ICE
A
B
C
D
E
F
G
71°30'
72°00'
73°30'
75°00'
76°30'

Figure 79. Crossbed measurements for the Eqalulik Group. See Figure 13 for geological relations and Figure 77 for stratigraphy.

Table 33. Adams Sound Formation (NAS) element concentrations in weight per cent*.

Source	No. of samples	Fe	Ba	Cr	Cu	Ni	Pb	Sr	V	Zn	Zr	Ca	Mg	Ti	Mn
1.	4	0.25 (1)	0.040	NF	NF	NF	NF	0.0016 (2)	NF	NF	0.019 (3)	0.026	NF	0.030 (2)	NF
3.	2	0.56	0.0088	NF	NF			0.0028 (1)	NF		0.016 (1)	0.026	0.033	0.025	NF
5.	2						0.068			0.13					

Source: Sources are keyed to the "Notes" of Table 37. Samples used in this project (Source 1) are from the Adams Sound Formation upper member.

* : Spectrographic analyses from Appendices 2 and 3.

(1) : Number of samples of total population used for determination, where less than total number of samples.

NF : Not found.

Blanks indicate no data given.

commonly present. Abundant secondary iron staining locally outlines liesegang bands at the top of the member; malachite staining is rare.

Most of the sandstones are equigranular, fine- to coarse-grained quartz arenite with scattered quartz granules and pebbles locally. Subarkose and arkose occur chiefly in conglomerate as interbeds and as matrix in the conglomerate. Calcareous interbeds of siltstone and very fine grained quartz arenite occur locally at the east end of the outcrop area. Shale chips occur sporadically and contain graphite at one locality.

Quartz is the principal component. In thin section the quartz grains are chiefly well rounded to rounded, but range to angular in shape, include grains of variously strained quartz and of quartz arenite, and have silica overgrowths. Potassium feldspar and plagioclase are major components locally, but commonly are present only in minor amounts. The potassium feldspar seems to be mostly microcline. Minor amounts of biotite, muscovite, chlorite, clay minerals, graphite, and hematite-goethite, and traces of detrital sphene, occur locally. The hematite-goethite, chlorite, clay, and at least some of the "muscovite" are probably secondary.

Conglomerate lenses and beds commonly occur at the base of and at various horizons in the upper member, and range from oligomictic to polymictic orthoconglomerate and paraconglomerate. In general, conglomerate abundance and clast coarseness and variety decreases northwestward and upward in section whereas clast roundness increases in the same directions. Conglomerate-based fining-up cycles occur locally in the southeast part of the outcrop area. Conglomerate-capped coarsening-up cycles occur in as much as 28 m of relatively immature upper member strata present in the outlier to the southeast where basal redbeds are present (Iannelli, 1979). East of Paquet Bay the upper member consists of a lower conglomerate sequence 9-24 m thick, and an upper conglomerate-poor sequence 8-21 m thick (Fig. 13; Fig. 77, sections F, G).

Conglomerates contain up to 90% clasts that are up to 25 cm in diameter, most of which are rounded to well rounded and range from discoidal (oblate) to prolate ellipsoidal and spheroidal. Some clasts are subangular. Most of the conglomerates are quartz-clast orthoconglomerates that contain clasts of igneous quartz and earlier quartz arenite. Clasts representing various basement lithologies and contained minerals (granite, feldspar, biotite gneiss, banded gneiss, etc.) increase in abundance eastward and downward in section, but rarely constitute more than 15% of the clasts.

Crossbeds and ripple marks as described for the formation are abundant in the upper member. Planar crossbeds have a maximum height of 2.4 m, and locally have graded foreset beds and clasts aligned along foreset and bottomset beds (Iannelli, 1979). Ripple marks have a maximum wavelength of 1.2 m. Graded beds and channels are common, while load structures occur at several places. Synaeresis, mudcracks, tool marks, and raindrop casts are rare.

Results of four spectrographic analyses carried out on Adams Sound Formation upper member samples from the vicinity of section E (Fig. 13, 77, 79) are compared in Table 33 with results for the formation elsewhere in Milne Inlet Trough (*see* Fig. 95). The few analyses recorded indicate a general similarity in trace element chemistry for samples from the map area and on Borden Peninsula (source 3, Table 33) to the northwest. High values of Pb and Zn in two samples from the Nanisivik mine area (source 5, Table 33), 180 km to the northwest, may be related to the emplacement of the Pb-Zn-Ag ore in the Society Cliffs Formation at Nanisivik.

Interpretation. Adams Sound paleocurrents locally are chiefly unimodal and westerly to northwesterly directed along the southern side of the Milne Inlet Trough and southwesterly directed along the north side (Fig. 77, 79; Iannelli, 1979; Jackson and Iannelli, 1981). The paleocurrent directions, the fining of strata upward, northwestward, and away from the margins toward the centre of Milne Inlet Trough, and the onlap of the overlying Arctic Bay strata (Fig. 80) onto basement gneisses along the north and south sides of Milne Inlet Trough all indicate that Adams Sound Formation strata are channel deposits deposited by a northwesterly flowing stream restricted largely to the present trough area. The predominance of conglomerates in the lower member, the common occurrence of conglomerate-based fining-up cycles and coarsening-up conglomerate-capped cycles in the middle and upper members, the abundance of quartz arenite, and only minor occurrence of shaly to silty strata are taken to indicate that the strata are chiefly braided fluvial deposits. Iannelli (1979) concluded that the lower member contains proximal braided stream deposits, and that the distal braided stream deposits of the middle member and the lower part of the upper member are overlain by intertidal to subtidal sandstones of the upper part of the upper member and the overlying basal Arctic Bay member.

The restricted occurrence of the Adams Sound Formation, the deepening of the depositional basin coupled with the absence of underlying strata beneath onlapping overlying Arctic Bay and Society Cliffs strata, and the presence of conglomerate lenses in strata that coarsen northward toward the White Bay Fault Zone on the northeast side of Milne Inlet Trough in particular support the contention that syndepositional faulting occurred during deposition of Adams Sound Formation and overlying Bylot Supergroup strata (e.g. Jackson et al., 1975). The numerous faults within and bounding the Milne Inlet Trough suggest that the trough originated by faulting and that Adams Sound sedimentation was affected more by periodic faulting than by eustatic changes in sea level. As source areas were worn down and the area subsided, shallow marine water reworked and redeposited the uppermost Adams Sound strata. Periodic regressions resulted in formation, at least locally, of conglomerate-capped coarsening-up cycles in deltaic, fan delta, or barrier beach environments. Pebbly sands are common to dominant components of delta plain and delta front environments where delta distributaries are of the braided type. The presence of some calcareous siltstones and very fine grained quartz arenites at the east end of the Milne Inlet Trough indicate that the sediments may have been deposited in a lacustrine or supratidal environment.

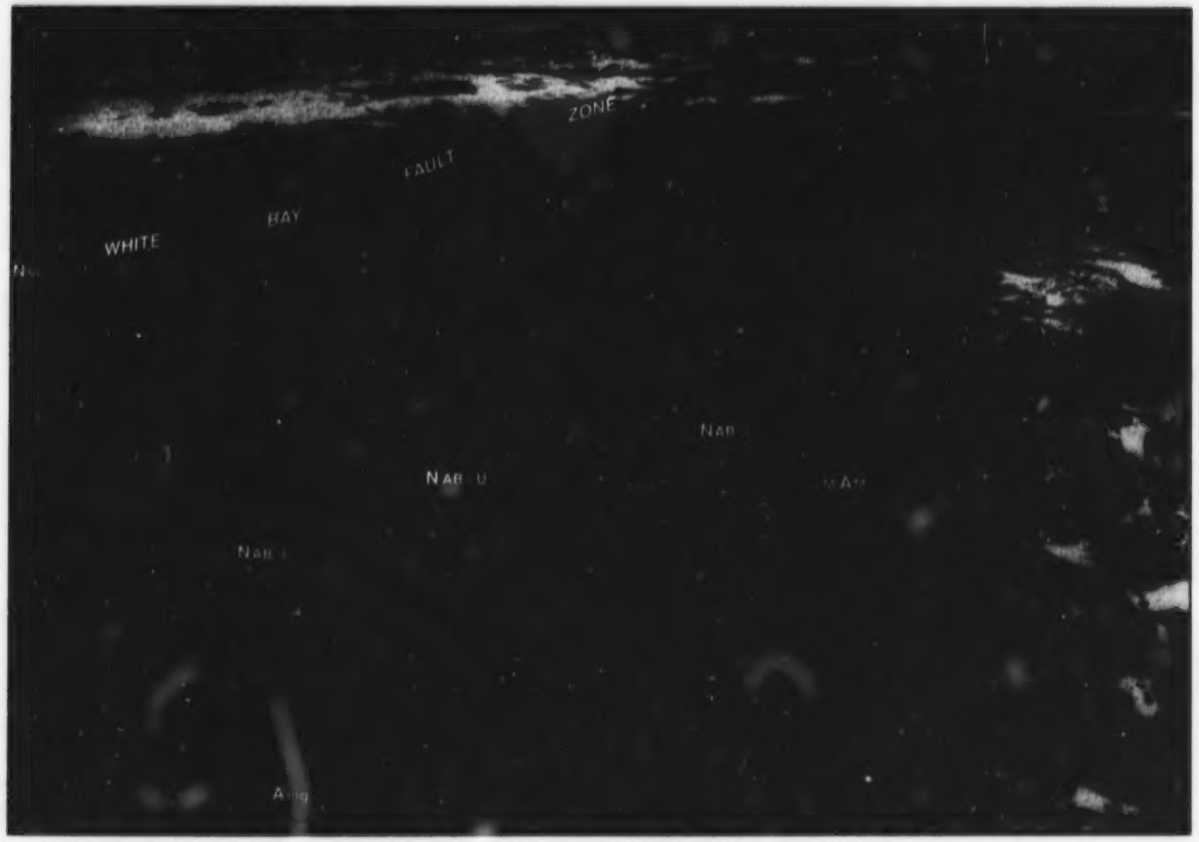

Figure 80. *View northeast toward the west arm of Paquet Bay. Arctic Bay strata* (NAB-U, NAB-L) *in the middle of the photograph overlie banded migmatite* (Amg) *in the left foreground and the Mary River Group* (M, AM) *in the right foreground. The escarpment in the distance marks the White Bay Fault Zone. Society Cliffs* (NSC) *strata occur on the left edge of the photo between the two arms of Paquet Bay. Compare with Figure 13. National Air Photo Library (NAPL) oblique airphoto T343L-216.*

Table 34. Major lithologies (volume per cent) in Arctic Bay Formation (NAB).

Member	Shale	Siltstone	Quartz arenite	Dolostone	Limestone
AB_4	68	8	13	9	2
AB_3	74	16	10		
AB_2	60.7	10	29	0.3	
AB_1	39	15	46		
Arctic Bay (1)	66	10	18	5	1
Formation (2)	67	9	15	7.5	1.5

(1) Weighted according to lithology thicknesses measured.
(2) Weighted according to member thickness, using 790 m for AB_4

Arctic Bay Formation (NAB, NAB-L, NAB-U)

Arctic Bay strata constitute most of the exposed Bylot Supergroup in the northern part of the Icebound Lake map area (Fig. 13, 77), where excellent outcrops are sparsely distributed in gullies and on hillsides (Jackson et al., 1978b, 1980; Iannelli, 1979). Dark shale predominates throughout most of the formation. The formation was originally divided by Jackson et al. (1975, 1978b) into a lower (NAB-L) member and an upper (NAB-U) member (*see* Table of Formations, Fig. 13). Subsequently Jackson et al. (1978a, 1980) and Jackson and Iannelli (1981) delineated four intergradational members (AB_1-AB_4; Table of Formations, Table 34, Fig. 77) recognizable throughout Borden Rift Basin, although the shale content is relatively low southeast of Milne Inlet. Within the map area the lower member (NAB-L; Fig. 81-83) comprises new members AB_1-AB_3, which are here considered to be submembers. The upper member (NAB-U) is equivalent to AB_4, and contains significantly more dolostone than the lower member (Table 34).

Description. Black to grey micaceous and carbonaceous shale predominates (66% – Table 34) and is thinly to thickly interbedded in varied proportions with siltstone (10%) and quartz arenite (18%). Dolostone (5%) and limestone (1%)

Figure 81. *Interlayered shale, siltstone, and lensitic, very fine- to medium-grained quartz arenite in the lower Arctic Bay member* (AB_2 *submember) south of the head of Tay Sound (NTS 37G). The shaly layers contain synaeresis. The lens cover is about 5 cm in diameter. Photograph by T.R. Iannelli. GSC 1997-540*

Figure 82. *View west at lower Arctic Bay strata* (AB_2 *of* NAB-L), *south of the west arm of Paquet Bay. Alternating black shales and shaly sandstones predominate on the large hill. A few dolostone and quartz arenite beds occur on the right. Note helicopter on the left for scale. Photograph by G.D. Jackson. GSC 186898, 186899, 186901*

occur chiefly in the upper Arctic Bay member (NAB-U = AB_4). Conglomerate lenses occur locally. The major lithologies are similar throughout the formation, are deposited in cycles, and vary in their relative proportions vertically and, to a lesser extent, horizontally. There is also some variation in the cyclic arrangement of the lithologies. Most of the formation is composed of coarsening-up cycles in which most minor clastic lithologies are well sorted, but do include minor intergradational and poorly sorted intermixed lithologies (Fig. 82, 83). Arctic Bay strata are planar to undulatory, locally lensitic, and thin laminated to massive. Bedding commonly thickens upward within cycles and within members. Minor white micaceous minerals (chiefly illite), other clay minerals, gypsiferous efflorescence, and sparsely disseminated pyrite are common and are most abundant in shale and least abundant in quartz arenites and carbonates. Sparse hematite-limonite spots are ubiquitous and probably represent oxidized iron sulphides. Two modal analyses for lower Arctic Bay strata are shown in Figure 29; one is for a siliciclastic carbonate and the other is for siltstone.

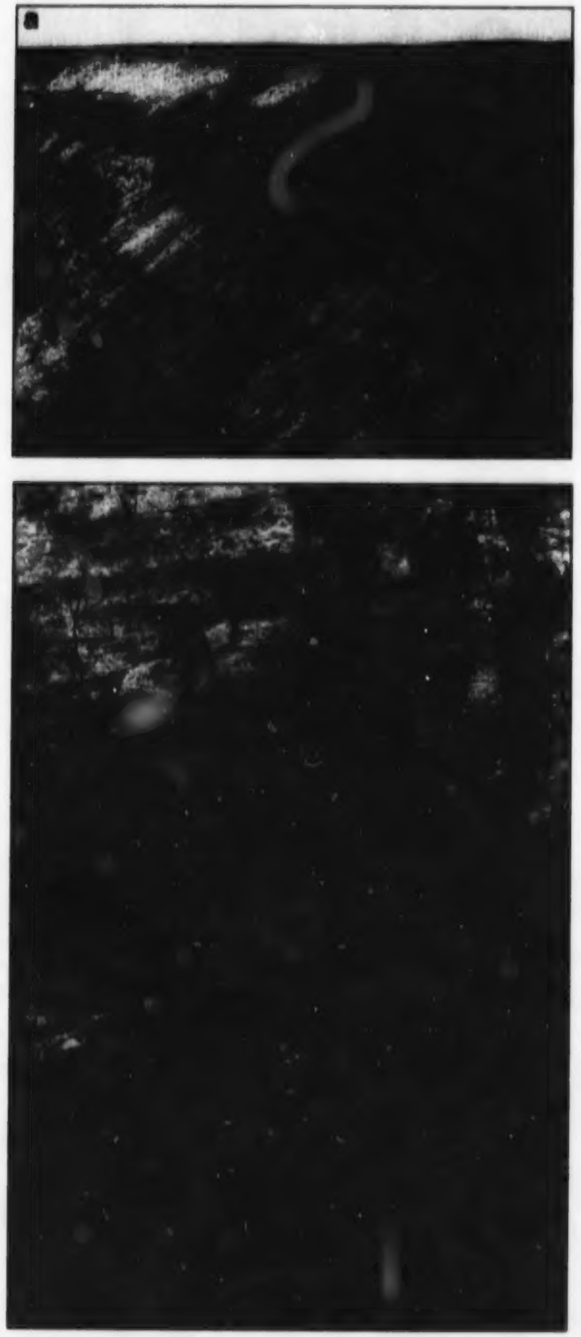

Figure 83. Coarsening- and thickening-upward cycles in the AB_2 *submember of the lower Arctic Bay member* (NAB-L, *NTS 37G).* ***a)*** *Section about 70 m thick, east of the head of Paquet Bay (NTS 37G). Cycles are 3-10 m thick and contain a lower part of laminated and massive shale with minor siltstone that grades upward into interlayered thin- to thick-bedded (Table 2) siltstone and fine- to coarse-grained quartz arenite. Upper parts of some cycles are almost entirely quartz arenite. Photograph by T.R. Iannelli. GSC 1997-54P.* ***b)*** *Upper part of a coarsening upward cycle, south of the head of Tay Sound, that overlies 2 m of shale (below view of photograph). The lower 3 m of the exposure contains laminated shale, siltstone, and very fine grained quartz arenite that is interlayered with very thin- to medium-bedded, medium- to coarse-grained quartz arenite. The top 5 m is medium- to thick-bedded, fine- to medium-grained quartz arenite. The hammer is about 35 cm long. Photograph by T.R. Iannelli. GSC 1997-54Q*

The Arctic Bay Formation is gradational with the underlying Adams Sound Formation, but south and east of Tay Sound and in the small outlier to the southeast, it overlaps the underlying Adams Sound Formation to lie nonconformably on the basement gneisses (Fig. 80). In most places, where it is well exposed, Arctic Bay Formation can be seen to be in fault contact with the overlying Society Cliffs Formation (Fig. 13). At one locality however, just west of Paquet Bay, these two formations seem to be confomable and gradational. Just north of the map area, along Tay Sound, a slightly undulatory disconformity between the two formations (Jackson et al., 1975; Iannelli, 1979) is assumed to represent only a small time interval. Complete sequences of the Arctic Bay Formation cannot be measured in the map area because of the disontinuity of outcrop, faulting, and the absence of the uppermost strata in most of the area. Thickness estimates, taking into account structure and elevations from topographic maps, suggest a thickness for the formation of 835-1100 m in the southeast and about 1460 m in the northwest (Table 35). Assessment of thickness data for partial sections indicate thicknesses ranging from more than 763 m, to more than 912 m in the southeast. The Arctic Bay Formation thickens northwestward toward the basinal area that was centred about Milne Inlet during Arctic Bay and overlying Uluksan Group sedimentation (Jackson and Iannelli, 1981; Jackson and Sangster, 1987). Jackson et al. (1975) originally estimated the formation to be 1220-1460 m thick immediately north of the map area. Iannelli (1979) concluded from more detailed work that Arctic Bay strata are 610-710 m thick in and immediately north of the map area.

Table 35. Thicknesses (m) for the Arctic Bay Formation (NAB).

A-Estimates from attitudes and topographic maps			
Unit	**Southeast**	**Centre**	**Northwest**
NAB-U (AB_4)	670	790	
NAB-L (AB_{1-3})	190	300	550-700
NAB (AB_{1-4})	835-1100		1460
B-Range of thicknesses obtained for partial sections			
Unit	**Minimum**	**Maximum**	**Mean**
NAB-L: AB_3	49	113	70
AB_2	58	183	88
AB_1	8	28	17
NAB-L (AB_{1-3})	143	303	185

Shale, the most abundant lithology in the formation (66%, Table 34) is chiefly carbonaceous (includes local graphite) and black to dark grey. Some shale is greyish shades of brown, green, purple, and blue. Minor purple to maroon shaly strata occur in lower Arctic Bay strata in the outlier 30 km southeast of the main outcrop area (NTS 37G). Most weathered surfaces are rusty. The shale is fissile and chiefly thin laminated to thin bedded. Minor partings and interbeds of silty to sandy shale, siltstone, and quartz arenite are common. Shale intraclasts and thin conglomeratic lenses are sparse. Preliminary studies of shale samples from the Bylot Supergroup northwest of the map area by R.N. Delabio of the Geological Survey of Canada's X-ray diffraction laboratory have identified quartz, feldspars, dolomite, calcite, chlorite, kaolinite, and illite.

Siltstone is mostly dark to light grey, and greyish shades of green, brown, and blue are also common. Buff to yellow, black, and off-white colours are uncommon to rare. Minor maroon to purple siltstone occurs in basal Arctic Bay strata in the small outlier southeast of the main outcrop area. Weathered surfaces are commonly rusty. Thin- to medium-bedded siltstone predominates. Quartz and feldspar are abundant (Fig. 29) while muscovite, biotite, clay minerals (including illite?), calcite, dolomite, and pyrite have been identified in the field.

Calcareous, dolomitic, shaly, and sandy beds are common, and together with quartz arenite, shale, carbonate, and/or conglomerate interbeds, commonly constitute up to 15% of siltstone units. Conglomerate interbeds, possibly intraformational conglomerate, contain chiefly subangular to rounded, flat to ovoid and spherical siltstone granules and pebbles set in a siltstone matrix.

Sandstone is predominantly dark grey to white. Greyish shades of green-brown, yellow, and locally, red and blue and mottled sandstone are common. Purple sandstone occurs in the basal Arctic Bay strata in the small outlier. Weathered surfaces commonly have a rusty tinge. Most of the sandstone is thin- to medium-bedded, fine- to medium-grained quartz arenite, although impure quartzose, silty, and shaly sandstone and subarkose occur locally. One thin section of fine grained, impure sandstone shows 75% quartz, 10% plagioclase, 11% clay minerals, and 3% biotite. Muscovite, microcline, and magnetite are also present. Minor interbeds of shale, siltstone, and conglomerate are common, and the conglomerate clasts have a variety of shapes and compositions (*see* the two following paragraphs on conglomerates). Muscovite, biotite, chlorite, quartz, potassium feldspar (microcline in thin sections), plagioclase, hematite, magnetite, pyrite, carbonate, and locally glauconite have been seen in the field.

Siliciclastic conglomerate beds and lenses are greyish shades of green and brown, and also include some purple-brown beds in the outlier to the southeast where conglomeratic strata are interbedded with sandstone in zones up to 7 m thick. Elsewhere, conglomerate-bearing zones are commonly 1 m thick or less and thin- to thick-bedded. Most conglomerate beds are lensitic, occur with sandstone as a capping to coarsening-up cycles, and seem to be most abundant in the outlier and near the margins of the Milne Inlet Trough. Shaly, silty, and sandy strata occur interbedded with conglomerate and as matrix material, the sandy matrices ranging from quartz arenite to arkose and sublitharenite.

Most of the conglomerates are oligomictic granule-pebble-clast paraconglomerates and orthoconglomerates that contain subangular to well rounded intraclasts of shale or siltstone, or well rounded quartz-quartz arenite clasts. Rounded dolostone clasts in a quartz arenite matrix are rare, and at one locality one of the shale-siltstone clasts seems to have been replaced by dolomite and calcite. A few conglomerates are polymictic and contain clasts of siltstone, shale, quartz arenite, quartz and/or feldspar, and gneiss up to 10 cm in diameter.

Carbonate rocks are light to dark grey, greyish green, and bluish grey on fresh surfaces. Weathered surfaces range from light grey to chocolate brown, but are characteristically a distinctive orange-brown. Carbonates are typically thin bedded and occur in zones up to 3 m thick (maximum 10 m). The carbonates range from clay to fine sand in crystal grain size, and are commonly siliciclastic. Some beds grade laterally from being partially disrupted to flat clast conglomerate with clasts up to cobble size in a carbonate matrix (Fig. 82, 84). Imbricate structure is present locally. The carbonate strata are predominantly dolostone, but minor limestone is common and locally is thinly interbedded with dolostone. Minor shale, silt, and sand-size siliciclastic material is commonly interbedded with or disseminated in the carbonates. Disseminated quartz grains are commonly subrounded to well rounded and constitute most of the siliciclastic material. Plagioclase and muscovite were seen in one thin section of carbonate which contains dark coloured areas of relatively coarsely recrystallized carbonate. The dark colour may indicate the presence of organic carbon. Sparry calcite wedges and lenses and microspar occur sporadically.

Most carbonate beds are stromatolitic. Columnar stromatolites range from unbranching to various branching types (vertical to inclined) up to nearly one-half metre high (e.g. Iannelli, 1979). Other types range from planar cryptalgal laminites to low domal, hemispherical, and bulbous types.

Sedimentary structures are common in the siltstone, quartz arenite, and dolostone beds, but are rare in AB_3 submember (Table 36). Most common are straight to undulating, lunate, and bifurcating ripple marks, trough- and planar-crossbeds (Fig. 79), a variety of load structures (chiefly tubular and bulbous), desiccation cracks, synaeresis cracks (Fig. 81), and convolute bedding.

Table 36. Sedimentary structures in the Arctic Bay Formation (**NAB**).

	AB_1					AB_2					AB_3					AB_4					
Structures	1	2	3	4	5	1	2	3	4	5	1	2	3	4	5	1	2	3	4	5	**Legend**
Brecciation, rip-up clasts																R					1-Shale
Cavities, vugs			R							R										R	2-Siltstone
Concretions																R	R				3-Sandstone
Convolute bedding		C				M	M	M								R	M	R			4-Conglomerate
Herringbone crossbeds			R					R													5-Carbonate
Planar crossbeds		C	A			M	M	A	M												
Trough crossbeds	M	C	A								R					R	M	C		R	R-Rare
Desiccation cracks						M	C									C	R	C	R	C	M-Minor
Graded bedding																		R			C-Common
Imbricate structure									R	R											A-Abundant
Injection features																				R	
Load structures	R	M	C		M	A	C	C			R					M	C	M	R	M	
Microfaults																		R		R	
Molar tooth																R				M	
Ripple marks	M	A	A			C	C	A	M		M	C				C	A	A	R	A	
Mega ripple marks								R										R	R		
Runsell structure						R	R		R												
Scour channels, marks			R			R	R	M	R								R	R			
Slumps						R	R													R	
Stromatolites																				C	
Synaeresis cracks	R	C	C			A	A	A	M		R	M				C	A	A	R	A	
Tepees																				M	
Tool marks								R													

Table 37. Arctic Bay Formation (NAB) element concentrations in weight per cent.

Source	Total no. of samples	Fe	Ba	Cr	Cu	Ni	Pb	Sr	V	Zn	Zr	Ca	Mg	Ti	Mn	B
Upper member																
1.	11	2.2 (9)	0.014	0.0041 (5)	0.0035 (8)	0.0054 (2)	NF	0.0055 (9)	0.0071 (5)	0.090 (1)	0.029 (9)	0.14 (8)	1.2	0.16 (10)	0.18 (6)	
2.[c]	4	2.6			0.0055		0.0043			0.019						
2.	13	1.9			0.0037		0.0020			0.0060						
4.	1			NF	0.00040	NF		0.0010	0.0010					0.0020	0.020	0.00040
Lower member																
1.	5	2.4 (4)	0.018	0.0052 (2)	0.0032 (3)	NF	NF	0.0045 (3)	0.012 (2)	NF	0.033	0.25	0.49	0.21	0.011 (4)	
4.	1			0.00040	0.00080	0.00080		0.020	0.0010					0.0040	0.040	0.00040
Upper and lower members combined																
1.	16	2.3 (13)	0.15	0.0044 (7)	0.0034 (11)	0.0054 (2)	NF	0.0052 (12)	0.0066 (7)	0.090 (1)	0.030 (14)	0.18 (13)	0.95	0.18 (15)	0.12 (10)	
3.	3	7.2	0.0031	NF	0.0040 (2)			0.0077 (2)	0.0024 (1)		0.0079 (1)	2.0	4.1	0.065	0.86	
5.	2						0.031			0.23						

Notes

1. This memoir.
2. Graf (1974) (from three sites on Borden Peninsula).
3. Blackadar (1970) (Borden Peninsula).
4. Lemon and Blackadar (1963) (Borden Peninsula).
5. Clayton and Thorpe (1982) (Nanisivik area).

NF = Not found.
c = Upper contact zone with Society Cliffs Formation (4.6 to 9.1 m thick).
(9) = Number of samples of total population used for determination, where less than total number of samples.

Chemistry. Values for major and minor elements determined spectrographically for Arctic Bay samples from the map area are shown in Tables 9, 37, 47 (column I), and 48 (column 32), in Appendices 2-4, and in Figure 95. Data for the Arctic Bay Formation on Borden Peninsula to the northwest have been provided by Lemon and Blackadar (1963), Blackadar (1970), Graf (1974), Olson (1977, 1984), and Clayton and Thorpe (1982).

The reader is referred to comparisons of Arctic Bay shaly rocks made with Mary River and Piling metapelites in the section on "Chemistry of pelitic rocks" in the "Mary River Group (M, AM)". The available evidence (Table 37) suggests that there may be a greater difference in the content of some elements such as Cu, Pb, and Zn between different localities of the Arctic Bay Formation than between lower and upper Arctic Bay strata at a given locality. If this is so, then stratigraphic position may not be of primary importance in searching for mineralized zones within the Arctic Bay Formation. Other elements such as Ni and Mn are more abundant in the upper Arctic Bay member than in the lower. It has yet to be determined whether these variations are primary or secondary. The relatively high Pb and Zn values in the Nanisivik area are probably related to the ore present in the Society Cliffs Formation, and indicate that the mineralization

Table 38. Major unit assemblages in Arctic Bay Formation (NAB) cycles.

Assemblage	Lithology
1	Shale and/or shale with minor siltstone
1,2	Shale interbedded with siltstone (up to ±50%)
1,3	Shale interbedded with quartz arenite
1,2,3	Interbedded shale, siltstone, quartz arenite
2,3	Interbedded siltstone and quartz arenite
3	Quartz arenite
2,3,4D±1	Interbedded calcareous siltstone, quartz arenite, dolostone, ±siltstone±shale
3,4D	Quartz arenite interbedded with dolostone
4D	Dolostone
1 or 3,4L	Limestone interbedded with minor shale or quartz arenite
4L	Limestone

Table 39. Most common Arctic Bay Formation (**NAB**) cycles.

Cycle[1] (*See* Table 38)	*	AB_1	Lower Member (NAB-L)[2] AB_2	AB_3	Upper Member (NAB-U)[2] AB_4	Total
(1) (1,2)					(7)-10.4	(7)-10.4
(1) (1,3) (3)			(1)-11.3		(2)-10.2	(3)-10.6
(1) (1,2,3)	5		(3)-10.1	(3)-17.8	(9)-6.7	(15)-9.6
(1) (1,2,3) (2,3)	5		(2)-14.2		(13)-11.1	(15)-11.5
(1) (1,2,3) (3)	1	(3)-12.6	(34)-11.2	(5)-7.3	(7)-10.4	(49)-10.8
(1) (1,2,3) (2,3,4D±1)	8				(9)-12.5	(9)-12.5
(1) (2,3)			(3)-6.1		(2)-6.0	(5)-6.1
(1) (2,3) (3,4D)					(2)-7.2	(2)-7.2
(1) (3)	3		(8)-8.8		(13)-6.1	(21)-7.1
(1) (2,3,4D±1)	7		(1)-10.1		(9)-9.1	(10)-9.2
(1) (2,3,4D±1) (4D)	9				(8)-8.8	(8)-8.8
(1) (2,3,4D±1) (4D) (2,3,4D±1)					(2)-13.7	(2)-13.7
(1) (3,4D)			(1)-9.8		(4)-4.5	(5)-5.6
(1) (4D)	2				(33)-9.0	(33)-9.0
(1) (4D) (2,3,4D±1)					(2)-8.2	(2)-8.2
(1) (4D) (4L)					(2)-13.4	(2)-13.4
(1) (1 or 3,4L)			(1)-3.7		(2)-3.2	(3)-3.4
(1) (1 or 3,4L) (4L)					(2)-3.5	(2)-3.5
(1) (4L)					(7)-7.8	(7)-7.8
(1) (4L) (4D)					(2)-16.6	(2)-16.6
(1,2) (1,2,3) (3)			(2)-10.1	(1)-7.6		(3)-8.4
(1,3) (3)		(1)-2.6	(1)-4.3		(1)-0.9	(3)-2.6
(1,2,3) (2,3)	9	(1)-9.1	(2)-6.4	(2)-4.0	(3)-11.1	(8)-7.9
(1,2,3) (3)	4	(3)-7.9	(11)-4.8	(2)-7.0	(2)-2.8	(18)-5.3
(4D) (3)					(2)-2.4	(2)-2.4
Total		(8)-9.2	(70)-9.3	(13)-9.2	(145)-10.8	(236)-9.7

1 - The lowest unit for each cycle is given first, followed by successively higher units. For example, cycle (1)(1,3)(3) has a lower shale unit (1), a middle unit of interbedded shale and quartz arenite (1,3), and an upper quartz arenite unit (3).
2 - The columns for each submember (e.g. AB_1) and the total column contain two figures. The first one, in brackets, is the number of cycles measured; the second one is the average thickness in metres.
* - The cycles are ranked according to the number of cycles measured in sections. Cycle (1)(1,2,3)(3) is ranked 1 because it was encountered and measured the most frequently (49 times).

there is not restricted to this formation, and that bedrock analyses should be useful in outlining areas for more detailed prospecting.

Cyclicity. Most of the Arctic Bay Formation is composed of stacked coarsening- and thickening-up cycles as shown in Tables 38-41 (Fig. 82, 83). Throughout Milne Inlet Trough, from Tremblay Sound eastward (Fig. 77; Jackson and Iannelli, 1981), basal units are composed of shale or silty shale, and are the thickest units in the cycles. Basal units grade upward into coarser grained, thicker bedded units within which the overall grain size also increases upward. Most commonly the basal shale unit of an overlying cycle overlies the relatively coarse top unit of the underlying cycle abruptly, although some basal contacts are gradational across a few centimetres. Some shallowing-up cycles are present (Fig. 84), and fining-up cycles are rare and relatively thin. Scour channels are not common (Table 36); a few occur at the base of upper sandstone units. The preponderance of coarsening-up assemblages coupled with the general absence of comparable fining-up intervals indicates that these coarsening-up intervals are stacked coarsening-up cycles. Channels and discordances are rare at the base of the cycles because the gradation upward is from fine to coarse, and the abrupt change in grain size is from coarse to fine, the reverse of that found in Bouma cycles. In this section, the types of cycles are identified, their abundances and thicknesses determined, and an estimate is made as to how long it may have taken to deposit a cycle. The major units within the cycles range in composition from single lithologies to assemblages of several intimately interbedded lithologies (Table 38). Except for some of the cycles adjacent to the fault zones bordering the Milne Inlet Trough, the major cycle units may be shown as various assemblages of four end members: 1 – shale, 2 – siltstone, 3 – quartz arenite, 4 – carbonate (4D = dolostone, 4L = limestone; Table 38). Shale more often than not contains minor siltstone. Arkose is common only where adjacent to the margins of Milne Inlet Trough. Dolostone is the predominant carbonate, although limestone is significant in some units.

Table 40. Composition of Arctic Bay Formation (NAB) by units in cycles.

Member[1]	Assemblage[2]										
	(1)	(1,2)	(1,3)	(1,2,3)	(2,3)	(3)	(2,3,4D±1)	(3,4D)	(4D)	(1 or 3, 4L)	(4L)
AB$_4$ (186) 8.3 m	63% (167) 5.9 m 0.3-22.3	1% (13) 1.4 m 0.3-3. 0	1% (11) 1.5 m 0.3-7.0	9% (59) 2.3 m 0.3-12.0	4% (31) 2.0 m 0.9-6.4	4% (39) 1.5 m 0.2-4.6	9% (51) 2.9 m 0.3-10.4	2% (13) 1.8 m 0.3-5.5	5% (64) 1.3 m 0.3-4.6	1% (12) 1.6 m 0.6-3.2	1% (18) 1.2 m 0.2-4.0
AB$_3$ (14) 10.0 m	57% (9) 8.9 m 3-21.9	8% (2) 5.3 m 5.2, 5.5		25% (13) 2.7 m 0.9-6.4	3% (2) 1.8 m 1.8, 1.8	7% (8) 1.2 m 0.2-3.7					
AB$_2$ (75) 9.2 m	52% (55) 6.5 m 0.3-15.2	2% (4) 3.6 m 0.6-9.4	1% (2) 2.7 m 2.4, 3.0	19% (56) 2.3 m 0.6-11.6	5% (11) 2.9 m 0.3-13.3	20% (58) 2.3 m 0.3-7.6	0.2% (1) 1.5 m	0.3% (2) 1.0 m 0.3, 1.8		0.2% (1) 1.2 m	
AB$_1$ (10) 9.0 m	30% (5) 5.4 m 3.4-8.2		2% (1) 1.8 m	34% (7) 4.4 m 1.5-6.9	9% (2) 4.1 m 2.1, 6.1	25% (8) 2.8 m 0.6-12.8					

[1] In this column, the number in brackets represents the number of cycles. The measurement below each represents the average thickness of the cycle.

[2] *See* Table 38. 63%/(167)/5.9 m/0.3-22.3 = average % of member composed of each assemblage/number of unit assemblages measured/mean thickness of assemblage in metres/range of thicknesses of assemblages in metres. Spaces indicate no data.

Table 41. Summary of cycle compositions for Arctic Bay Formation – volume per cent assemblage occurrences in cycle units.

Member		AB$_1$			AB$_2$				AB$_3$			AB$_4$			
Units		1[1]	2	3	1	2	3	4	1	2	3	1	2	3	4
ASSEMBLAGE SEE TABLE 38	(1)	42	22		87				81			96			
	(1,2)				3	<1			5	15		<1	5		
	(1,3)	4			1	2						1	1	1	
	(1,2,3)	36	36		8	55	2	100	14	62		2	33	1	
	(2,3)	14	5	32	1	9	15			11		<1	7	21	9
	(3)	4	37	68		30	82			12	100		10	13	6
	(2,3,4D±1)					1							17	37	60
	(3,4D)					1	<1						3	5	12
	(4D)												17	12	13
	(1 or 3, 4L)					1							3	5	
	(4L)												4	5	
% of member[2]		48	47	5	62	23	15	1	72	25	3	65	21	10	3
Avg. thickness (m)		4.2	4.3	1.5	5.7	2.1	2.5	1.1	7.2	2.4	0.9	5.5	1.8	1.9	2.9
Range (m)		1.5-8.2	1.5-12.8	0.6-3	0.3-15.2	0.3-11.6	0.3-13.3		2.1-21.9	0.5-6.4	0.2-2.7	0.3-22.3	0.3-7.3	0.2-9.9	0.3-3.7
Cycles measured		10	10	3	74	74	41	1	14	14	6	186	186	82	17

[1] Numbers 1 to 4 here represent the first to fourth units of the various sedimentary cycles. Unit (1) occurs as the first unit in AB$_1$ cycles 42% of the time and as the second unit 22% of the time etc.

[2] This figure is the volume per cent of each member that the indicated unit represents. Unit 1 is 48% of AB$_1$.

Assemblage 1, predominantly shale, is the most abundant assemblage in the cycles (Tables 39-41). More than two thirds of the cycles represent eight cycle types, the average thicknesses of which range from 9-11.5 m. Most cycles have two or three units, but as many as seven units within a cycle have been recognized. Cycles with more than three units are commonly complex cycles that may, for example, contain subsidiary fining-up cycles within an overall coarsening-up cycle. The most common cycles are (1) (1,2,3) (3); (1) (4D); (1) (3); (1,2,3) (3); (1) (1,2,3); (1) (1,2,3) (2,3); (1) (2,3,4D±1); and (1) (1,2,3) (2,3,4D±1) (Tables 38, 39). Units of assemblage 1 constitute 30-63% (Table 40) of Arctic Bay Formation submembers (e.g. AB1; *see* Table of Formations) and 42-97% of the first units of cycles, which are commonly the thickest units of the cycles. The second units of cycles comprise the greatest variety of assemblage types of which (1,2,3) is the most common, constituting 9-34% of submembers and 33-62% of second units in cycles. The most common assemblage in the third unit is (3), which constitutes 4-25% of submembers and 13-100% of third units in cycles. However, in the AB$_4$ submember, (2,3,4D±1) is the most common third unit assemblage with (2,3) the second most common. Average thicknesses of first units in cycles range from 4.2-7.2 m in the four Arctic Bay members (Table 41). Second units average 1.8-4.3 m, and third units 0.9-2.5 m. Unit assemblage (1) is the single most abundant in submembers AB$_2$-AB$_4$ (*see* Table of Formations), and the second most abundant in submember AB$_1$. Unit assemblage (1,2,3) is the most abundant in submember AB$_1$ and the second most abundant in AB$_3$ and AB$_4$. Assemblage (3) is the second most abundant in AB$_2$.

Figure 84. *Shallowing-up cycle in the upper Arctic Bay member* (NAB-U) *in Tay Sound area just north of the map area. The lower unit has 3 m of laminated black shale, interbedded in the upper part with overlying laminated to medium bedded limestone and dolostone, some of which is stromatolitic. The carbonate contains beds of flat pebble to granule clast carbonate conglomerate, gypsum partings, and a variety of sedimentary structures. Photograph by T.R. Iannelli. GSC 1997-54R*

Cycle time spans. About 1800 m of strata are estimated to lie between the lower Nauyat and Adams Sound formations and upper Strathcona Sound Formation strata (*see* Fig. 76). Fahrig et al. (1981) determined paleomagnetic poles at the base and top of the above sequence, and concluded that these two poles have a difference in age of 16.5 Ma.

Recently determined U-Pb zircon and baddeleyite age determinations have provided precise ages for mafic dyke swarms and paleomagnetic poles determined for their primary magnetization. Pole positions for Mackenzie (1270 Ma) and Sudbury (1238 Ma) dykes are very similar (Buchan and Halls, 1990), so their average age (1254 Ma) and pole position is used for the base of the Bylot Supergroup. Abitibi diabases at 1141 Ma (Buchan and Halls, 1990) provide the next youngest accurate date on the polar wander path, but the pole position is presently being recalculated. Using the available position indicates an age span of 31 Ma rather than 16.5 Ma determined by Fahrig et al. (1981) for the interval between the two poles. The Logan sills provide an accurate pole position as well as an accurate age of 1109 Ma (Fahrig et al., 1981). These data combined with the Mackenzie-Sudbury data indicate a span of 24 Ma for the same interval.

The rocks sampled by Fahrig et al. (1981) outcrop about 180 km northwest of the map area, and the 1800 m interval includes about 400 m of Adams Sound strata and about 350 m of strata in each of the Arctic Bay, Society Cliffs, Victor Bay, and lower Strathcona Sound formations (Table 42). The Arctic Bay Formation is mostly shale, the Adams Sound Formation mostly quartz arenite, the Society Cliffs and Victor Bay formations mostly carbonate, and the lower Strathcona Sound Formation mostly shale and siltstone with some sandstone. Compaction of siltstone, sandstone, and carbonate rocks are considered here to be negligible. Rates reviewed by Potter et al. (1980), however, indicate compaction of 200 and 260% (average is 230%) for shale. The decompacted thicknesses noted in Table 40 are based on the amounts of shale present. Sedimentation rates

Table 42. Some sedimentation rates for the Bylot Supergroup, and deposition intervals for the Arctic Bay Formation and its average cycle.

Formation	Thickness^1		Sedimentation rate cm/ka		Deposition interval	
	Present	Decompacted	A^2	B^2	A^2	B^2
A: Area of paleomagnetic studies						
Lower Strathcona Sound	350 m	530 m	80	62		
Victor Bay	350 m	430 m	8	6.2		
Society Cliffs	350 m	350 m	8	6.2		
Arctic Bay	350 m	690 m	8	6.2	8.6 Ma	11.1 Ma
Upper Adams Sound	400 m	400 m	8	6.2		
Total	1800 m	2400 m				
B: Arctic Bay Formation, in NTS 37G						
Minimum thickness	835 m	1560 m	18	14	99 900 a^3	128 900 a^3
Maximum thickness	1460 m	2730 m	32	25	57 100 a^3	73 700 a^3
Average cycle	9.7 m	18.1 m				

[1] From Jackson and Iannelli (1981).

[2] Age span of 24 Ma used for A and 31 Ma used for B.

[3] Is the same for average cycle of 9.7 m present thickness, or for 18.1 m decompacted.

(Table 42) were based on suggested sedimentation rates for various sediments in different environments (e.g. Schwab, 1976; Kukal, 1990), and the likely time span represented by each formation. The sedimentation rates given in columns A and B (Table 42) compare with 5-50 cm/ka reported by Schwab (1976) for rift basins and aulacogens. The rate of 8 cm/ka yields an interval of 8.6 Ma, and the rate of 6.2 cm/ka yields an interval of 11.1 Ma, for deposition of the Arctic Bay Formation.

Within the map area, the Arctic Bay Formation is considered to have been deposited in the same time interval as at 180 km to the northwest where Fahrig et al. (1981) made their paleomagnetic measurements. Considering its minimum and maximum thicknesses, and referring only to a time span of 8.6 Ma for the Arctic Bay Formation (Table 42), these figures indicate that it took 57 100 to 99 900 years to deposit the average cycle. The corresponding average subsidence (= sedimentation) rates are 18 cm/ka - 32 cm/ka. These figures are somewhat different than the 18 000-39 000 years/cycle and 27-46 cm/ka obtained by Grotzinger (1986) for shallowing cycles in the Aphebian carbonate-dominated Rocknest Formation, Wopmay Orogen. However, cycles in the Arctic Bay Formation may be more varied in thickness and in composition than those in the Rocknest Formation, and range from <1 m to >24 m in thickness (1-45 m decompacted) or 3150 to 248 100 years/cycle. Grotzinger (1986) concluded that the Rocknest cycles' period is consistent with a glacioeustatic origin for cyclicity, and that alpine or very limited continental glaciation would have been required. Arctic Bay cyclicity is considered to be related chiefly to basin fault activity, although eustatic sea level changes may also have been a factor.

Lower Arctic Bay member (NAB-L=AB$_1$+AB$_2$+AB$_3$). This member outcrops mostly in the southern part of the Milne Inlet Trough (Fig. 13, 77, 79, 80). Measured thicknesses are mostly of incomplete sections and range from 143-303 m. Estimated thicknesses range from 190-700 m (Table 35). The lower member thickens northwestward toward Milne Inlet, and the compositions and thicknesses of the contained three submembers vary from one locality to another (Fig. 77).

AB$_1$ *submember.* The AB$_1$ submember (*see* Table of Formations), the basal unit of the lower Arctic Bay member, is composed chiefly of thin- to thick-bedded, grey to green, locally white quartz arenite (46%) and siltstone (15%). Minor layers and lenses of grey to green and black shale are common, and predominate locally where interbedded with siltstone. The average shale proportion in the submember is about 39% (Table 34).

The AB$_1$ submember is commonly underlain by as much as 30 m of Adams Sound conglomeratic quartz arenite in the outlier southeast of the main outcrop area (Jackson et al., 1978a, 1980). The Adams Sound Formation dies out locally, near the head of Tay Sound and to the northwest along the south border of the Milne Inlet Trough. The AB$_1$ submember overlies as much as 2 m of regolithic material and is as little as 1.5 m thick at these localities. Basal quartz cobble (to 20 cm) conglomerate with a siltstone-greywacke matrix grades upward into light purple quartz arenite and subarkose.

In general, cyclic deposition is poorly developed in the AB$_1$ submember, although in most places a basal coarsening-up sequence grades upward into a fining-up sequence, which is overlain chiefly by coarsening-up cycles. Cycles (1) (1,2,3) (3), and (1,2,3) (3) are the most common of those measured. Cycles range from 2.6-20 m thick and the contained units average 2.6-12.6 m thick (Tables 39-41).

The AB$_1$ submember is 8-28 m thick throughout most of the southeastern Milne Inlet Trough (Table 35). Ripple marks, crossbeds, and load structures are the most common structures (Table 36). Crossbeds are chiefly northwesterly directed, but locally are bimodal-bipolar northwest-southeast (Fig. 77, 79; Iannelli, 1979; Jackson et al., 1980).

AB$_2$ *submember.* This submember contains about 60% shale, 10% siltstone, 30% quartz arenite with minor subarkose, and rare dolostone and conglomerate (Fig. 81; Table 34). The submember includes coarsening-up cycles 5-21 m thick. Internally gradational three-unit ((1) (1,2,3) (3)) cycles predominate and average 11.2 m thick (Table 39). The basal (1) units are composed of shale containing sparse siltstone and quartz arenite, are 0.3-15.2 m thick (average ca. 6.5 m) (Table 40), and rarely contain structures. The middle (1,2,3) units consist of shale interbedded with siltstone and quartz arenite, the latter two of which increase upward to compose about 50% of the rock types in the unit (Iannelli, 1979). Unit thicknesses range from 0.6-11.6 m and average about 2.3 m. Cycles (1) (1,2,3) (3) are capped by unit (3) quartz arenite and minor subarkose containing a few shale-siltstone lenses and partings (Iannelli, 1979). Limestone and dolostone occur locally (Table 38-41). Upper unit thicknesses range from 0.3-7.6 m, averaging 2.3 m (Table 40). Several two-unit cycles (e.g. (1) (3); (1,2,3) (3); Table 39) are also present in the submember. Granule- to cobble-conglomerate (clasts to 10 cm) occurs with sandstone in the upper units of AB$_2$ submember cycles in the small southeastern outlier (Jackson et al., 1978b, 1980). Upper units in the lower part of AB$_2$ submember are mostly conglomerate at this locality.

The AB$_2$ submember is 58-183 m thick (Table 35). It varies in thickness considerably, but is thickest to the west. Ripple marks, synaeresis cracks, load structures, and crossbeds are common in AB$_2$ submember (Table 36). Most crossbed measurements for the Arctic Bay Formation have been determined for AB$_2$ strata, and indicate chiefly southwesterly to northwesterly directed currents (Fig. 77, 79; Iannelli, 1979; Jackson et al., 1980). Bimodal and bipolar trends occur locally.

AB$_3$ *submember.* AB$_3$ strata are composed chiefly of grey to black carbonaceous shale (74%) that occurs in sequences up to 61 m or more thick. A white gypsiferous efflorescence commonly coats weathered surfaces. Minor siltstone (16%) and quartz arenite (10%; Table 34) are interbedded with the shale. Cycles, rarely well developed, include (1) (1,2,3) (3), (1) (1,2,3), and a few others (Table 39). Sedimentary structures are uncommon (Table 36). Thicknesses for the submember range from 49-113 m, and are largest in the west (Fig. 77; Table 35).

Upper Arctic Bay member (NAB-U = AB$_4$). The upper Arctic Bay Member constitutes most of the Arctic Bay Formation east of Milne Inlet including the map area (Fig. 13, 77). This member outcrops chiefly on the northern side of the Milne Inlet Trough (Fig. 13), and has not been subdivided. Grey to black, locally green shale is the major lithology (68%, Table 34). Siltstone (8%), quartz arenite (13%), dolostone (9%), limestone (2%), and local conglomerate are interbedded with the shale. Pyrite and dolomite nodules occur locally.

The upper Arctic Bay member in the map area is estimated to be 670-790 m thick (Table 35), based in part on a measured partial section of 665 m (Fig. 77). Previous estimates and measurements have indicated thicknesses from greater than 305 m to 615 m (Jackson et al., 1975, 1980; Iannelli, 1979). Deposition of the member was cyclic, but unlike the AB$_2$ submember, about two thirds of the cycles contain only two units (Table 39). Cycles are 1.8-23.8 m thick. Although the cycles are much more varied than those in the lower member, basal units of upper member cycles are also almost entirely shale (1) and average 5.5 m (0.3-22.3 m; Table 41) thick. Second units average 1.8 m (0.3-7.3 m) and third units average 1.9 m thick (0.2-9.9 m, Table 41).

More than half of the two- and three-unit cycles are shallowing-up cycles (Fig. 84) in which carbonate is prominent in the second or third units or both (Tables 39-41). The upper dolostone unit in one third of the two-unit shallowing-up cycles ((1) (4D)), and in some of the three-unit cycles, is 0.3-4.6 m thick (average 1.3 m) (Table 40). Other shallowing-up cycles include: (1) (2,3,4D±1); (1) (3,4D); (1) (1 or 3,4L); (1) (4L); (1) (1,2,3) (2,3,4D±1); and (1) (2,3,4D±1) (4D). The middle unit of three-unit cycles (e.g. (1,2,3); (2,3,4D±1)) are commonly relatively thin although composed of several interbedded lithologies.

Almost one half of the cycles are coarsening-up cycles, such as (1) (1,2,3) (2,3), (1) (1,2,3) (3), (1) (1,2,3), (1) (3), etc. (Table 39, 40). In these cycles, basal shale and silty shale grade upward into interbedded siltstone and quartz arenite with or without shale. The upper unit in the three-unit cycles is quartz arenite with or without interbedded siltstone. Several coarsening-up cycles adjacent to the White Bay Fault Zone (Fig. 13) contain a lower sandy shale unit that grades upward through fine grained arkose into conglomeratic arkose and granule to pebble and cobble conglomerates described above. A few fining-up cycles are interspersed with these arkose cycles which grade basinward into fining- and coarsening-up clastic-carbonate cycles (Jackson and Iannelli, 1981). Sedimentary structures are common in the upper Arctic Bay member (Table 36). Crossbeds, desiccation cracks, load structures, ripple marks (straight, undulose, lunate, etc.), and synaeresis cracks are most common. Crossbed and ripple mark measurements indicate west- to northwest- and southeast-directed paleocurrents (Fig. 77, 79; Iannelli, 1979; Jackson et al., 1980). Stromatolites are common in the carbonates and include planar, low domal, hemispheroidal, bulbous, and unbranching and expanding branching columnar types. Low biohermal mounds containing stromatolitic and brecciated dolostone are also present.

Interpretation. The presence of herringbone and other bimodal-bipolar crossbeds (minor, Fig. 79), coarsening-up cycles, and the lithologies present indicate that AB$_1$ and AB$_2$ strata were deposited in environments ranging from clastic shoreline to deltaic and intertidal (Iannelli, 1979; Jackson and Iannelli, 1981). The amount of siltstone and sandstone associated with the dark monotonous AB$_3$ shales decreases westward. The lithologies present, the paucity of structures, and thickening toward the west indicate that AB$_3$ strata were deposited in predominantly subtidal environments with a deepening basin westward. Abundance of shale-dolarenite shallowing-up cycles associated with coarsening- and fining-up cycles, and the lithologies and the structures present suggest that most upper Arctic Bay (AB$_4$) strata were deposited in mixed clastic shoreline, shallow carbonate basin, deltaic, and intertidal to shallow subtidal environments. The fault-fringing arkose-conglomerate-capped cycles may have formed in marine deltas and alluvial fan deposits that interfinger basinward with the shallowing-up cycles. As discussed above, the overall cyclicity and distribution of lithologies is considered to indicate deposition in response to fault movements rather than eustatic sea level changes.

The nature of the coarsening-up cycles also shows that they are shallowing-up cycles. The uppermost quartz arenite units probably include beach sands.

Several features taken together indicate that although deposition of the Arctic Bay Formation within the map area overlapped the underlying Adams Sound Formation, it still centred to a large extent about the Milne Inlet Trough. These features are:

a) the chiefly westerly directed paleocurrents with trends angled toward central Milne Inlet Trough (Fig. 79);
b) the onlap of Arctic Bay strata over Adams Sound strata onto basement gneisses on both sides of Milne Inlet Trough, and the probable onlap of Society Cliffs strata onto the basement just north of the map area, between Tay Sound and Paquet Bay (Jackson and Iannelli, 1981); and
c) the fining of coarser grained Arctic Bay gritty and locally conglomeratic strata away from the present fault-bounded margins toward the centre of Milne Inlet Trough.

The interbedded nature of most of the quartz arenite with shale or siltstone or both, and the rarity of fining-up sequences indicate that most of the quartz arenite was not deposited in sand bars or as storm surge ebb deposits, although these deposits may be represented in the middle of Milne Inlet Trough. It seems most likely that the coarsening-up cycles, abruptly terminated at their tops, were initiated by a sudden deepening of the depositional basin followed by gradual progradation outward from the basin margins. The evenness and continuity of bedding, as seen over large areas in cliff facies, is taken to suggest a more regional control for the cycles than only migrating delta fronts. Repeated abrupt deepening of the depositional basin allowed deposition of basinal mud to predominate once more until the prograde sedimentation of coarser clastics gradually took over again as the basin was filled or became shallower. The coarsening-up cycles therefore are also probably shallowing-up cycles.

Movement along the listric White Bay Fault Zone on the north side of Milne Inlet Trough (Fig. 13) was especially pronounced during deposition of the Strathcona Sound and Athole Point formations northwest of the map area (Jackson and Iannelli, 1981). The presence of conglomerate lenses in the Arctic Bay up through to Athole Point formations along this fault in and north of the map area is also attributed to syndepositional faulting. The asymmetrical downdropping of the north side of Milne Inlet Trough relative to the south side is evident in the field as well as on the aeromagnetic maps for the map area (*see* Fig. 111), and occurred at least in part during deposition of the Bylot Supergroup.

Uluksan Group

The Uluksan Group comprises the Society Cliffs Formation (NSC) and the conformably overlying Victor Bay Formation (NVB, *see* Jackson et al., 1975), both composed chiefly of a variety of shelf carbonates (Jackson and Iannelli, 1981). Only the Society Cliffs Formation outcrops in the map area (Fig. 13, 76, 77).

Society Cliffs Formation (NSC)

Strata of this formation underlie a small area on either side of the west arm of Paquet Bay (Fig. 13, 80). These strata are highly contorted adjacent to the White Bay Fault Zone, where they have been downfaulted against basement gneisses to the northeast. Society Cliffs strata are gradational with the underlying Arctic Bay strata. The contact is taken where grey- to buff-weathering dolostone becomes more abundant upward than orange-brown-weathering dolostone (Fig. 77). Varicoloured (green, red, black, brown) shales and siltstones make their appearance at about the same stratigraphic position. Throughout most of Borden Basin the change in the colour of the dolomite weathered surface coincides with an abrupt increase in the abundance of dolostone to about 40%. The Society Cliffs Formation has been divided into two intergradational members: a lower SC$_1$ member containing interbedded shale, siltstone, sandstone, and dolostone, and an upper SC$_2$ dolostone member. Within the map area, the dolostone content increases gradually upward in the lower member and increases abruptly at the SC$_1$-SC$_2$ contact.

More than 265 m of Society Cliffs strata have been measured at Paquet Bay, where more than 305 m are probably present (Fig. 77). Thicknesses of 580-610 m have been measured immediately north of the map area (Jackson et al., 1975, 1980; Iannelli, 1979). Ripple marks, synaeresis, and desiccation cracks are abundant. Load structures, convolute bedding, and slump structures are common. Minor structures include molar tooth, vugs (lined with calcite, dolomite, or quartz crystals), tepees, and flat clast conglomerate. Rip-up clasts, concretions, small-scale pull-apart and injection features, chert-filled mud cracks, and microfaults are also present. Stromatolites are abundant in the dolostones; planar to small domal, hemispheroidal, chevron shapes (conophyton), and short columnar forms are the most common.

No chemical data are available for this formation in the map area, but samples from Borden Peninsula, particularly the Nanisivik mine area, have been analyzed for minor and trace elements and for various isotopes (e.g. Olson, 1977, 1984; Ghazban et al., 1986). Bedrock samples that are not visibly mineralized do not contain abnormally high mineral values (Lemon and Blackadar, 1963; Blackadar, 1970; Graf, 1974). Water samples from streams flowing along the contact between the Arctic Bay and Society Cliffs formations contain high Zn values, reflecting the mineralization that occurs at this horizon (Olson, 1977). Dolomitization and sulphide mineralization of the Society Cliffs Formation has been discussed by Geldsetzer (1973b).

Lower member (SC$_1$). Planar to undulose, laminated to thin bedded shale and siltstone are the most abundant lithologies in this member. They are commonly light to dark green or grey on fresh and weathered surfaces, but are also black, red to purple, and locally brown, and resemble shaly sequences associated with evaporitic deposits. Sandstones are abundant and are fine- to coarse-grained, thin bedded, and buff to pink, grey, white, and green. They are mostly quartz arenite but subarkose, arkose, and subgreywacke are also present. Finely crystalline dololutite to dolarenite is also common. The dolostone ranges from laminated to thin bedded and massive, and light grey to buff; some is orange-brown, and rarely it is blue-grey. Some of the dolostone has a petroliferous odour. Flat-pebble conglomerate lenses occur locally. Gypsiferous laminae are very rare. The lower member is at least 170 m thick (Fig. 77), and more than 233 m are probably present. As much as 460 m of the member immediately north of the map area has been interpreted as coastal gypsiferous sabkha deposits (Jackson et al., 1975; Iannelli, 1979; Jackson et al., 1980).

Deposition of carbonate-capped shallowing-up cycles (Fig. 84) was initiated during upper Arctic Bay (AB$_4$) sedimentation. Abundance of these cycles increases stratigraphically upward in the AB$_4$ member, and the entire lower Society Cliffs (SC$_1$) member comprises these cycles. The lower part of the SC$_1$ member is composed mostly of three-unit cycles 14-19 m thick. The basal unit (11-15 m) is composed chiefly of shale or shale and siltstone. Minor dolostone and quartz arenite interbeds are common. The middle unit of the cycle (1.5-3 m) is laminated to medium bedded and is composed of shale, siltstone, quartz arenite, and dolostone, all variously interbedded. The upper unit (1.5-3 m) is composed chiefly of laminated to medium bedded dolostone, but some dolostone is thick bedded. Thin beds of siltstone, quartz arenite, red or green shale, and gypsum laminae or seams are rare. Small discordances are present at the bottom of some lower shale-siltstone units. Desiccation cracks, ripple marks, and several of the other structures noted above may be present in any of the three units but are most common in the middle unit. Convolute bedding and slump and load structures are most abundant in the lower unit, the deformed bedding of which is truncated in some places by undeformed beds of overlying units. Brecciated zones, rip-up clasts, and beds and lenses of flat clast conglomerate are common in the upper parts of the upper unit. Although the basal unit of the cycles contains a relatively large amount of shale, the features noted above indicate that these are shallowing-up cycles (e.g. James, 1984).

Upper SC$_1$ strata are arranged in two-unit cycles (7-13 m) in which the middle unit of the three-unit cycles is absent. Also, in some basal units (5.5-9 m), the dolostone and sandstone components are equal to the shale and siltstone. Upper units are 1.8-4 m thick.

Upper member (SC$_2$). Upper member strata in the map area are almost entirely light- to medium-grey dolostone. The dolostone is finely crystalline, planar to undulose bedded, dololutite to dolarenite, and is commonly stromatolitic. Minor amounts of flat pebble conglomerate, and a few thin grey to black shale beds and partings are also present. The basal unit, 4.6 m thick, is medium to thick bedded. It is separated from 20 m of thick bedded to massive dolostone by 5.2 m of thin- to medium-bedded dolostone. About 30 m of SC$_2$ strata have been measured and more than 75 m are estimated to be present in the map area; but 165-250 m occur immediately to the north of the map area (Iannelli, 1979; Jackson et al., 1980).

Interpretation. The shallowing-up cycles of the lower Society Cliffs member (SC$_1$) are interpreted to have been deposited in response to repeated abrupt deepening of the basin (or rising of sea level) followed by a prograde filling of the basin to yield a series of shallowing-up cycles. The presence of polymictic conglomerates in, and apparent onlapping onto basement gneisses of, lower Society Cliffs strata between Tay Sound and Paquet Bay, a few kilometres north of the map area (Jackson et al., 1975), is taken as support for the conclusion that the repeated basin deepening was due largely to faulting, along or adjacent to the White Bay and Tikerakdjuak fault zones (Fig. 13). Jackson and Iannelli (1981) concluded that the Navy Board High, the northwest extension of the basement on the north side of Milne Inlet Trough, was uplifted slightly during Society Cliffs sedimentation. The relatively large amount of siliciclastic material in the lower units of the cycles, compared with cycles described by James (1984), is attributed to influx from an uplifted source area. Similar relations were described from the Bylot Island area to the north (Jackson et al., 1985) where arkoses and shales were deposited in upper Uluksan Group strata as a result of uplift of the Byam Martin High. The basal units of the SC$_1$ cycles are interpreted as chiefly subtidal deposits that periodically interrupted carbonate deposition. The abundant soft sediment deformation is probably related to rapid sedimentation and instability of the basin due to faulting. The middle unit is chiefly intertidal assemblages, and the upper unit, intertidal to supratidal dolostone.

The transition from chiefly siliciclastic sedimentation in the upper Arctic Bay Formation to chiefly carbonate sedimentation in the lower Society Cliffs Formation coincided with a general shallowing trend, the erosion and lowering of source areas in an arid tropical region as indicated by the paleomagnetic poles determined by Fahrig et al. (1981), and the presence of varicoloured shales and gypsum and sabkha deposits (Jackson et al., 1980). The basin was partially restricted with a depot centre northwest of the map area (Jackson and Iannelli, 1981) so that conditions were probably ideal for carbonate deposition to take over from siliciclastic deposition while the nature of the cyclic sedimentation (shallowing-up) remained the same. The SC$_1$ deposition in the partially restricted basin occurred in environments that ranged from supratidal to intertidal and lagoonal or tidal flat pools, and possibly alluvial plain. Abrupt deepening of eastern Milne Inlet Trough, probably by faulting, improved water circulation and led to SC$_2$ carbonate deposition with rare siliciclastic material, chiefly black shale. Little of the SC$_2$ member is exposed in the map area, and much of the evidence for deeper water deposition comes from north of the map area. The abrupt termination of redbeds and sabkha deposition, which continued to be deposited in Eclipse Trough to the north (Jackson and Iannelli, 1981; Jackson et al., 1985), rarity of conglomerates and siliciclastic breccias, together with the presence of local unconformities, the variety of stromatolites, and the development of bioherms, suggests deposition in shallow subtidal to intertidal environments.

History of Milne Inlet Trough

The evolution of Milne Inlet Trough is intimately associated with the evolution of Borden Rift Basin as a whole, for which more comprehensive accounts are provided by Blackadar (1970), Geldsetzer (1973a, b), Jackson et al. (1975, 1985), Olson (1977), and Jackson and Iannelli (1981, 1989).

Bylot Supergroup deposition began during marine transgression of a northwesterly dipping peneplain underlain by an Archean-Aphebian granitoid-metamorphic complex. Deposition of the basal Adams Sound quartz arenites was restricted to a narrow fault-controlled channel in eastern Milne Inlet Trough that merged northwestward into an alluvial braidplain and a shallow marine shelf (Iannelli, 1979; Jackson and Iannelli, 1981). Nauyat plateau tholeiitic basalts were extruded near and at the base of the sequence west and north of the map area and are spatially related to faults. Within the map area the basal sequence is the Adams Sound Formation. The restriction of Adams Sound braided fluvial deposits to a narrow channel, their overlap by Arctic Bay and Society Cliffs strata, the presence of fault-associated basalts to the west and north, and the abundance of sedimentary cycles that coarsen toward the present margins bounded by the White Bay and Tikerakdjuak fault zones suggest Milne Inlet Trough originated as a graben. Thinning of Nauyat basalts toward the map area and their absence in the map area, together with the general lack of volcaniclastic material in contemporaneous and younger sedimentary rocks, suggest that volcanics probably were not deposited in the map area.

Periodic regional subsidence resulted in marine transgression from the northwest and deposition of the dominantly marine Arctic Bay Formation. The relatively abrupt change from deposition of fluvial and shelf sandstones of the Adams Sound Formation to basinal shales of the Arctic Bay Formation, together with the persistence of coarsening- and shallowing-up cycles and rarity of fining-up cycles in the Arctic Bay and lower Society Cliffs formations, the coarsening of clastics toward the present boundary faults, the abrupt facies changes and even more pronounced coarsening toward faults, west and northwest of the map area in laterally equivalent strata (Iannelli, 1979; Jackson and Iannelli, 1981), and the development of a depot centre in the Milne Inlet area during Arctic Bay sedimentation (Jackson and Iannelli, 1981), are compatible with the conclusion that syndepositional faulting was relatively active during Arctic Bay deposition, especially during deposition of the upper member, and during lower Society Cliffs Formation deposition. Carbonate layers increase upward in abundance and in thickness in the upper Arctic Bay member, and were the forerunners of the thick platform carbonates of the overlying Society Cliffs and Victor Bay formations. The coarsening of Arctic Bay and younger formations toward the margins of the present graben indicate that deposition of these formations was still controlled somewhat by the original graben. However, the onlap of the Arctic Bay and Society Cliffs formations also indicates that successively younger strata were deposited over progressively broader regions. An abrupt change to deeper water subtidal-intertidal carbonate deposition marks the lower-upper Society Cliffs Formation contact, and probably deposition of upper Society Cliffs strata over a much broader region. West of Milne Inlet, however, this abrupt change occurs stratigraphically lower at the Arctic Bay-Society Cliffs contact along which a disconformity is also commonly present (Jackson and Iannelli, 1981). These features are also taken to indicate syndepositional faulting, that varied in timing and intensity throughout the basin, resulting in formation of subbasins.

Movement chiefly along northwest-trending faults has occurred throughout Baffin Island from Neohelikian time or earlier to the present (Jackson et al., 1975; Jackson and Morgan, 1978a; Jackson and Iannelli, 1981). Several features in Borden Basin indicate that faulting, chiefly along the northwest-trending faults but also along northerly trending syndepositional faults, were active during deposition of the Bylot Supergroup (Jackson et al., 1975; Jackson and Iannelli, 1981, 1984, 1989; Galley et al., 1983):

a) the spatial relationship of the Nauyat ocean-floor type subaerial basalts to the faults;
b) juxtaposition of coarse clastic facies and thicker sections adjacent to the faults (Fig. 13);
c) juxtaposition of different facies indicating different environments; and
d) truncation of steep faults within the Bylot Supergroup by overlying strata that are not faulted;
e) the stratigraphy and lithologies of some formations vary markedly from one to another of the three main grabens of Borden Rift Basin, and between localities in individual grabens.

Movement along some individual faults alone has spanned much or all of the time between the Neohelikian and the present time. For example, movement along the Central Borden Fault Zone has clearly displaced Cambro-Ordovician strata in the map area south of Mary River. On Borden Peninsula, 200 km to the northwest, Bylot Supergroup strata coarsen and thicken toward the fault zone while another 150 km to the west it passes under the lower Paleozoic strata on Brodeur Peninsula without displacing them (Jackson et al., 1990a). Lack of evidence for significant horizontal offset, and the nature of the faults themselves in Borden Basin and the Mary River region, suggest that the fault movement is mostly dip-slip (Jackson and Sangster, 1987). The Milne Inlet graben is tilted downward to the northeast whereas minor blocks within the graben are tilted northeast and southwest indicating that at least some of the major faults are listric.

Representatives of the northwest-trending faults noted above include the White Bay and Tikerakdjuak fault zones which border Milne Inlet Trough, the Central Borden Fault Zone which extends through the Mary River area, and the Nina Bang Fault Zone which passes by the head of Steensby Inlet (*see* Fig. 112). Effects of the regional northwest faults are considered to be traceable from Milne Inlet Trough northwest to Somerset and Cornwallis islands and southeast through the map area to Home Bay on the east coast of central Baffin Island, a distance of at least 1200 km (Jackson and Iannelli, 1981). This zone probably passes through the easternmost metamorphic saddle in the granulite metamorphic belt that extends northeast across Baffin Island at the north end of the Barnes Ice Cap (Fig. 3 – Jackson and Morgan, 1978a, b). Within the map area the Milne Inlet Trough coincides approximately with a line that parallels the long axis of Baffin Island. This line separates more highly deformed gneisses to the northeast from those less highly deformed to the southwest (*see* Fig. 112-114). As concluded earlier, this line, which is also evident on the aeromagnetic maps (*see* Fig. 111), may approximate the western limit of intense activity during a mid-late Aphebian (ca. 1810 Ma) orogenic event involving southwest-directed overthrusting. It is concluded therefore that Milne Inlet Trough probably developed along a pre-existing structural boundary. Gneissosity and orientation of metamylonites locally are parallel to the bounding, more brittle fault zones, which is in agreement with the above conclusion.

In most places the basement gneisses nonconformably underlying the Eqalulik Group are in the upper amphibolite metamorphic facies. Locally, outside the map area, the underlying gneisses are granulites, some of which have been retrograded along fault zones. Probably most of the granulites now exposed in northern Baffin Island were at or near the surface as Neohelikian sedimentation began.

Geldsetzer (1973a, b) concluded that the Bylot Supergroup was deposited as a megacycle on a stable shelf during regional subsidence, interrupted by four regional upwarps. He considered the grabens to have occurred later. However, Jackson and Davidson (1975) and Jackson et al. (1975) concluded that sedimentation had occurred in an active rift zone, and that faulting has continued to Recent time. Olson (1977, 1984) considered Milne Inlet Trough (Fig. 13) to be an aulacogen, while Fahrig et al. (1981) concluded from paleomagnetic data and K-Ar ages that the Nauyat volcanics represented a Mackenzie igneous event, and that the associated sediments were of similar age. Jackson and Iannelli (1981) concurred with both conclusions and noted several features of Borden Rift Basin that are common to aulacogens. They also noted that mafic volcanics and/or sills of about Mackenzie age, based chiefly on paleomagnetic data and Rb-Sr and K-Ar ages, occurred with several sedimentary sequences along the northwest edge of the Canadian-Greenlandian Shield from the northern Canadian Cordillera to northeast Greenland. A U-Pb baddeleyite age of 1270 Ma has since been determined for some of the Mackenzie igneous events (LeCheminant and Heaman, 1991). It was also noted that present distribution and thicknesses indicate that several of the inferred basins were once interconnected or were parts of the same larger basin or both, and that in some basins marine encroachment was from the west or northwest. Similarities were noted between the orientation and size of Neohelikian horsts and grabens and those along the North American Atlantic coast related to the early Mesozoic opening of the Atlantic Ocean. The above features, along with some others, and Baragar's (1977) conclusion that the Coppermine volcanics represent a mantle plume, led Jackson and Iannelli (1981) to suggest that the rifting and Mackenzie mafic igneous activity was related to the opening of the Poseidon Ocean now considered to have occurred at about 1270 Ma. The similarity of the chemistry of several of the Mackenzie mafic igneous rocks was demonstrated by Galley et al. (1983). Jackson and Iannelli (1984, 1989) concluded that Borden Rift Basin evolved over a short period of time. They first considered a three-stage mantle plume-related model but modified this to four: Rift - I, Downwarp - I, Rift - II, Downwarp - II. The second rift stage may be related to the ocean's closing, which could, however, also have closed later at 1.1-1.0 Ga. This age, based on Rb-Sr and K-Ar data for the Nauyat volcanics and associated gneisses (Jackson and Iannelli, 1981; Jackson et al., 1990b) and on K-Ar data for volcanics in the Fury and Hecla Basin to the south (Chandler and Stevens, 1981), may approximate the time of subgreenschist metamorphism and formation of small southeast-directed overthrusts in the Bylot Supergroup.

A variety of changes in facies and thickness trends define a zone that extends northward along Milne and Navy Board inlets, and is aligned with the Nares Strait Fault between Ellesmere Island and Greenland. Based in part on this feature it has been proposed that some movement between Greenland and Baffin Island probably occurred along this zone when the Borden and Thule basins were formed at about 1270 Ma (Jackson and Iannelli, 1981, 1984; Galley et al., 1983; Jackson et al., 1985; Jackson, 1986). Also, Borden and Thule basins, and Somerset Island (Aston, Hunting formations) are probably parts of a single basin or basin complex. Fahrig (1987) agreed that the Poseidon Ocean opened during the Mackenzie Igneous events. While Chandler (1988) supported the conclusion by Jackson and Iannelli (1981) that the Poseidon Ocean opened to the west or northwest, he disagreed with their suggestion that the Fury and Hecla Strait area is also a Neohelikian rift zone. He asserted that there is no evidence of failed arm formation in the strait area itself.

Mackenzie dykes

A few northwest-trending dykes on northwestern Baffin Island are considered here to be Mackenzie dykes on the basis of paleomagnetic poles and K-Ar whole rock ages. Three paleomagnetic poles reported by Fahrig et al. (1971: sites 10, 11, 23) plot very close to the mean Mackenzie pole position. Site 10 lies in the northwest corner of the Conn Lake (NTS 37E) map area (Jackson and Morgan, 1978b), and site 11 in the southwest corner of the Buchan Gulf-Scott Inlet (NTS 37H) map area (Jackson et al., 1978b). Site 23 lies southeast of Barnes Ice Cap (27C; Henderson, 1985a). Potassium-argon whole rock ages of 1035 ± 80 Ma and 994 ± 80 Ma were obtained for a diabase at or near site 10 (Table 53). It has been the author's experience and that of others (e.g. W.R.A. Baragar, pers. comm., 1993; W.F. Fahrig, pers. comm., 1988) that whole rock K-Ar ages obtained for diabase dyke swarms commonly range from too young to almost the age of crystallization; they very rarely yield the actual age of crystallization or an older age. This, of course, is contingent on the dykes not having been affected by a significant thermal event after emplacement. The ages noted above do suggest that the dyke is not Hadrynian, although available chemical data suggest the Baffin dykes have some chemical differences (e.g. high Ca, low K) when compared with Mackenzie dykes. Finally, some of the late Proterozoic diabases on northwest Baffin Island are considerably more altered than most and contain relatively stubby baddeleyite; a few are deformed. These features may be related to the age of the dykes.

HADRYNIAN

Borden and Franklin diabase dykes (Hg)

Description

Nearly all of the Hadrynian dykes are vertical or nearly so, range up to at least 200 m thick, and are gabbros in which granophyric phases are rare. Most trend northwesterly in an irregular to en echelon fashion, vary in thickness along strike, and locally branch or bifurcate (Fig. 85, 86). These dykes crosscut each other at several localities. Some dyke segments are relatively straight and have a uniform thickness for several kilometres. At a very few localities these late dykes extend, or widen out, into small, pod-like mafic intrusions. Some dykes pinch out upward in the cliffs along the eastern fiords (Fig. 85). The dykes are more easily weathered than the gneisses, but commonly stand in relief above the more easily weathered Neohelikian Bylot Supergroup strata (Fig. 86).

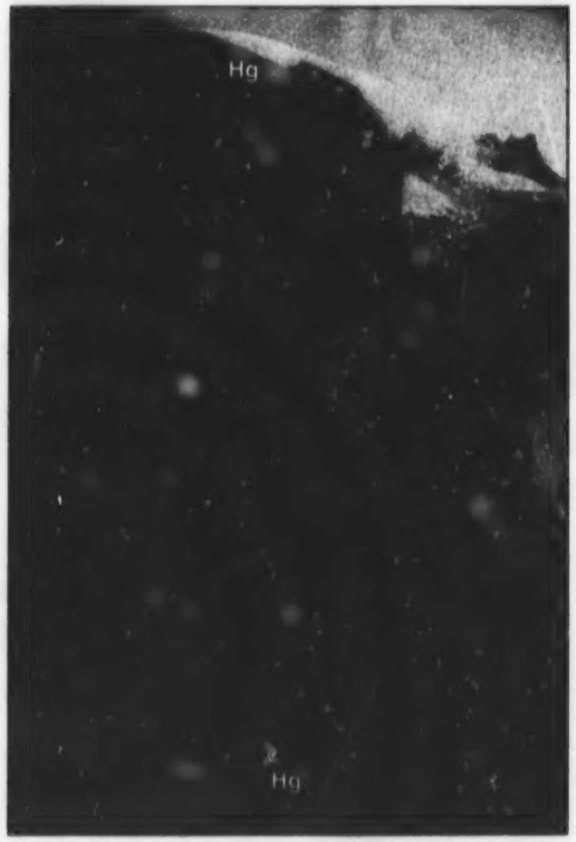

***Figure 85.** Vertical diabase dykes* (**Hg**) *in horizontally banded gneisses* (**Amg**) *of the west wall of Gibbs Fiord, east end of Sillem Island, northwest corner of map area NTS 27F. Note the small dykes extending into the gneisses in an apparent gap (g) between dykes in the lower part of the photo, and the irregular dyke contact at the top of the cliff. Elevations to 1070 m. Photograph by S.L. Blusson. GSC 185778*

In general, the major dykes show up well on aeromagnetic maps, most having a slight positive anomaly that ranges locally up to about 280 nanoteslas above background (flight lines about 305 m above ground). Some dykes are represented by negative anomalies, even in areas where background values are relatively low.

Fresh dyke surfaces are medium to dark grey to green, rarely black. Weathered surfaces are light to medium brown, locally rusty, and commonly show spheroidal weathering. Most dykes are medium grained with intergranular to ophitic textures and aphanitic to fine grained chilled margins, although some show little change in grain size even at the contact. Plagioclase crystals are oriented parallel to the walls of a few dykes and relatively thin dykes (<20 m) are fine grained.

Mineral assemblage data for the Hadrynian dykes are presented in Table 43, and Figures 29, 87, and 89. Plagioclase (37-70% anorthite according to optics) is the most abundant mineral and commonly is 30-50% of the mode (5-75% range). A small amount of quartz (13% in one dyke) occurs in many dykes. Mafic minerals are commonly 50-70% (25-90% range). Pigeonite, the most common mafic mineral, ranges from 14 to 40%. Opaques make up to 11% of the dykes and are chiefly magnetite-ilmenite with minor pyrite, pyrrhotite, and, rarely, hematite. Minor brown-green hornblende and/or reddish-brown biotite occur in most dykes, commonly with minor, later blue-green hornblende and green biotite. Secondary chlorite is also common and serpentine is rare. Zircon, apatite, calcite, kaolinite-pyrophyllite, and less commonly leucoxene, iddingsite, and potassium feldspar, occur as accessory minerals.

A late diabase dyke northeast of the Mary River area contains considerable hornblende and chlorite and locally up to 25% epidote and 10% orange-red garnet. The epidote and garnet may reflect material ingested by the magma. The dyke is intruded by a small syenitic dykelet, which could be a granophyric phase of the diabase, or perhaps related to small local late syenite plugs in the Mary River region (NTS 37G).

Commonly, dykes have columnar jointing, have been crossfaulted, and the adjacent country rock has been baked. Contact effects in country rocks are most obvious in the Neohelikian Bylot Supergroup (NTS 37G) with some carbonate rocks being finely recrystallized and bleached. In the No. 4 iron deposit area of the Mary River region, near the middle of the west edge of map area NTS 37G, the Mary River iron-formation on either side of a large diabase has been altered for several metres. The magnetite has been

Table 43. Modal analyses of Hadrynian diabases (Hg) according to swarm (*see* Fig. 89).

Sample **Area**	**B365/3** **27G**	**C196/1** **27F**	**B146/3** **37G**	**B158/3** **37G**	**J146A** **37G**	**B125/2** **37G**	**C219A/1** **37G**	**J151/1** **37G**	**C267/1** **37G**	**J133/2** **37G**	**C26/2** **37G**	**D11/1** **37F**	**M90/1** **37F**
Swarm*	1a	1b	2a	2a	2a	2b	2b	2b	3a	3a	3b	4	5
Quartz	5	5	5	13	T	6	1	2	-	-	-	2	-
Plagioclase	52	60	60	55	65	48	70	52	60	70	55	59	55
(An)	(40-65)	(35-65)	(55-85)	(40-70)	(65)	(37-63)	(40-80)	(63-69)	(54-56)	(54)	(60-62)	(60-70)	(46-63)
Clinopyroxene[1]	24	15	25	14	25	30	21	32	20	20	40	25	40
Hornblende	4	5	-	13[2]	-	5	2	-	-	2[2]	-	3	-
Biotite	4	2	-	3	-	2	-	-	-	-	-	1	-
Chlorite	T	3	-	-	-	-	-	4	15[3]	3	-	4	2
Magnetite[4]	11	10	10	2	10	9	7	10	5	5	5	6	3
Zircon	-	T	-	-	-	-	-	-	-	-	-	T	-
Apatite	-	T	-	-	-	-	-	-	-	-	-	T	-
Mafic	43	35	35	32	35	46	30	46	40	30	45	39	45

Notes: 1 - Pigeonite in most samples.
2 - Chiefly retrograde blue-green hornblende.
3 - Chiefly serpentine.
4 - Commonly includes ilmenite, hematite, pyrrhotite, or pyrite.

T - Trace amount.
- - Not present.
* - Lower case letters are used to indicate samples from the same dyke, or samples from dykes in the same swarm that are on strike with each other (see text).

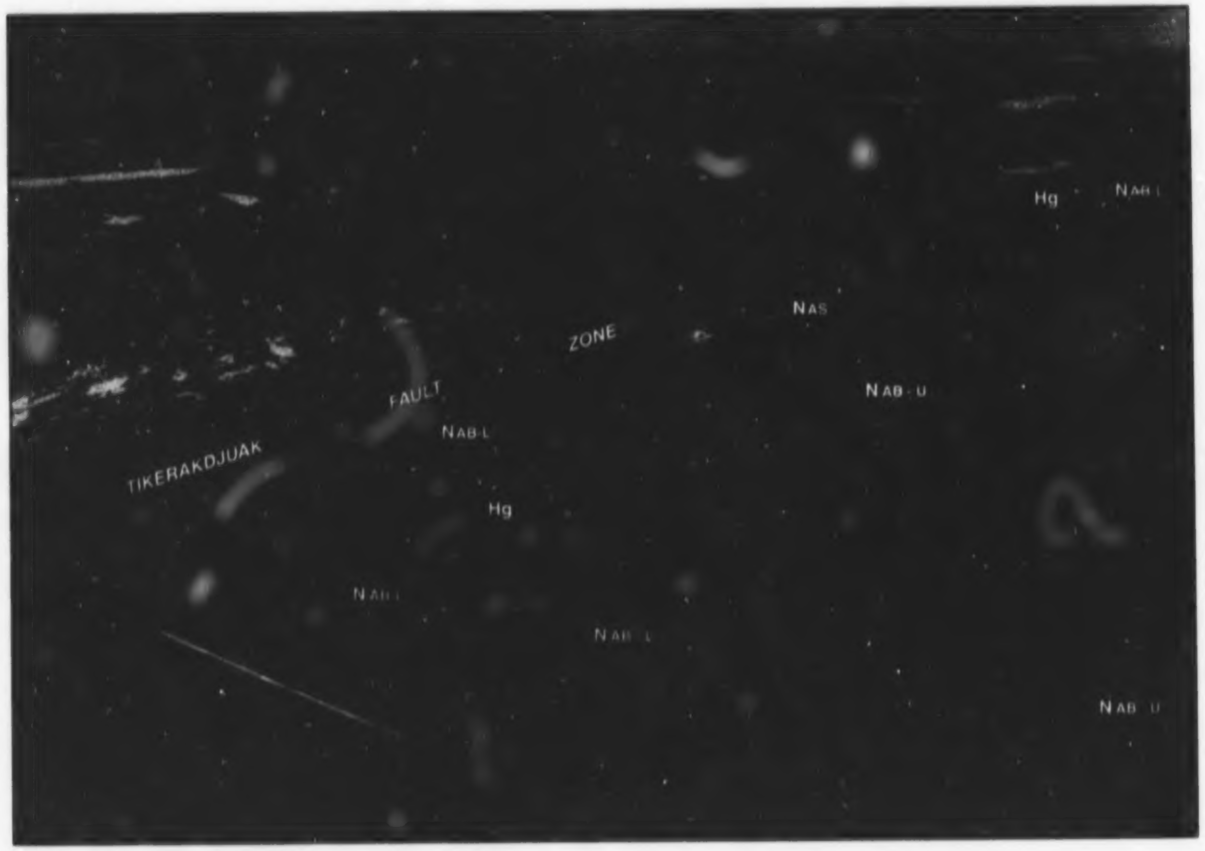

***Figure 86.** View southwest across Milne Inlet Trough, south of Tay Sound (NTS 37G). Branching and en echelon diabase dykes* (**Hg**) *intrude and stand out in relief above more easily weathered, gently folded Arctic Bay strata* (**NAB-L, NAB-U**). *The latter and the Adams Sound Formation* (**NAS**) *are downfaulted along the north side of the Tikerakdjuak Fault Zone, marked by a string of lakes subparallel to the dykes on the left. National Air Photo Library (NAPL) oblique airphoto T343R-212.*

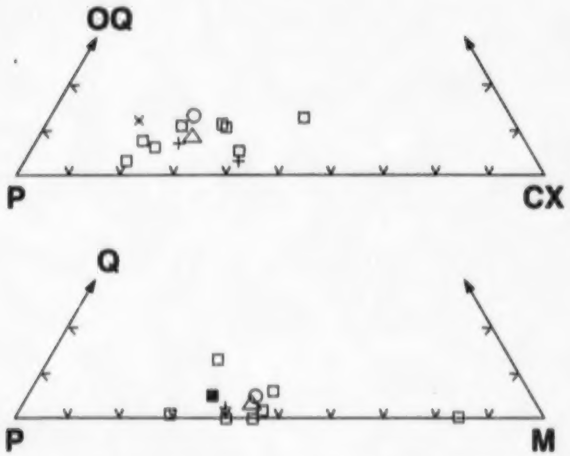

Figure 87. Modal plots for Hadrynian diabase (**Hg**). *Opaque (OQ) - plagioclase (P) - clinopyroxene (CX), and quartz (Q) - plagioclase (P) - mafic (M). The square represents samples from map area NTS 37G, the circle from NTS 37H, 27G, the plus sign from NTS 37F, and the cross from NTS 27F. The triangle is the mean composition.*

changed to hematite, mostly earthy hematite, and the silicate minerals have been bleached yellowish brown. A tourmaline dyke, 1 m thick, is also present. Possibly, this particular alteration is early Paleozoic in age and reflects proximity to the erosion surface separating overlying Paleozoic strata, since stripped off, from underlying Precambrian rocks.

Chemistry

Chemical data from W.F. Fahrig (pers. comm., 1985) are presented in Table 44 for Franklin and Borden dykes as differentiated by Christie and Fahrig (1983). It is not known whether variations within the map area from the corresponding Baffin average are meaningful. Analyses for both groups of dykes tend to vary in the same direction, i.e. less MgO and K_2O but more CaO and Na_2O in the map area. There seem to be some meaningful differences between the two groups. Borden dykes have less MgO and more Na_2O, K_2O, and Al_2O_3 than Franklin dykes, which lends support to the suggestion that Borden dykes are slightly more differentiated than Franklin dykes, and may be separable from them on the basis of mineral composition and chemistry, as well as paleomagnetism.

Spectrographic data for **Hg** samples are given in Appendices 2 and 3, and data from the means for Franklin and Borden dykes in Table 44 are presented in Figure 48c. The data plot chiefly in the within-plate lava field in the TiO_2-Zr diagram of Pearce (1980). Data for the same samples plot along a line extending from near the Zr apex to the boundary between the ocean floor basalt and calc-alkaline basalt field in the Ti/100-Zr-Sr/2 plot of Pearce and Cann (1973). Figure 48 shows that the Hadrynian dyke data are less scattered than those for several Archean mafic rocks, and that the Hadrynian rocks have more Ti. They may also have a little more Zr than Mary River Group mafic rocks and about the same amount as is present in the mafic remnants in several Archean-Aphebian quartzofeldspathic map units.

The TiO_2 plotted against Fe/Fe+Mg (Fig. 88) yields a differentiation trend that has a similar slope to that for Mary River metabasalt and mafic remnants in banded migmatite (Table 21), but the TiO_2 content is greater in the Hadrynian dykes. Additional chemical data are presented in Figure 95.

Ages

Late Proterozoic diabase dykes intrude older rocks throughout Baffin Island and are part of a huge swarm that extends in a giant arc from northern Quebec and Labrador northwest through Baffin Island and Melville Peninsula and then westerly to the Coronation Gulf region. The K-Ar ages for the dykes and sills range from 470 to 1025 (revised from 1040) Ma (*see* Table 53; Fahrig et al., 1971; Robertson and Baragar, 1972; Fahrig and Schwarz, 1973; Jackson, 1978a, b; Jackson and Iannelli, 1981; Christie and Fahrig, 1983; Palmer et al., 1983; Chandler, 1988). Paleomagnetic results indicate that most of these dykes belong to the Franklin igneous event, which W.F. Fahrig (pers. comm., 1985) considered to be about 750 Ma. However, U-Pb baddeleyite ages of 716 +4/-5 Ma and 720 ± 8 Ma were determined recently for two Hadrynian Franklin dykes (swarm 2 – *see* below) on Borden Peninsula, northwestern Baffin Island (Pehrsson and Buchan, 1999), and a baddeleyite age of 723 Ma was determined for a Franklin dyke (swarm 5 – *see* below) on southern Cumberland Peninsula (e.g. Heaman et al., 1990). The Franklin swarm, therefore, is about 723 Ma.

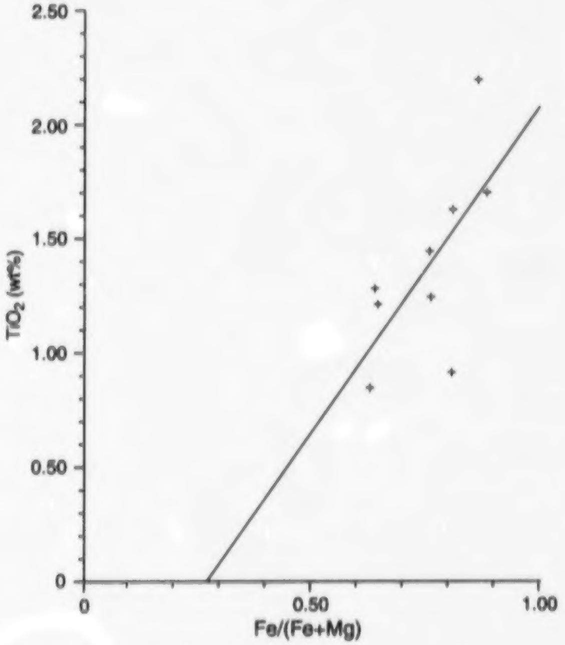

Figure 88. Plot of TiO2 versus Fe/(Fe+Mg) for Hadrynian diabase (**Hg**).

Table 44. Mean chemical analyses of Franklin and Borden dykes (**Hg**) in weight per cent.

	Franklin		Borden	
	Baffin Island	**Map area**	**Baffin Island**	**Map area**
Samples	64	13	24	5
SiO_2	49.5	49.4	50.2	49.4
Al_2O_3	14.3	14.5	15.0	16.2
TiO_2	2.12	2.37	2.04	1.93
Fe_2O_3	3.27	3.75	3.72	3.81
FeO	9.63	9.94	9.40	9.61
MnO	0.21	0.20	0.19	0.19
MgO	5.76	5.11	4.86	3.98
CaO	9.96	10.2	9.11	10.1
Na_2O	2.21	2.51	2.48	2.92
K_2O	0.82	0.52	1.03	0.54
P_2O_5	0.21	0.18	0.23	0.10
Cr_2O_3	0.033 (24)	0.030 (1)	0.022 (18)	-
CO_2	0.068 (55)	0.11 (8)	0.10 (22)	0.10 (3)
H_2O	1.45	1.15	1.23	0.92
S	0.082 (44)	0.020 (1)	0.047 (18)	-
Total	99.62	99.99	99.66	99.80
Co	0.004 (56)	0.005 (8)	0.004	0.004
Cr	0.010 (56)	0.007 (8)	0.009	0.004
Cu	0.014 (56)	0.026 (8)	0.024	0.030
Zn	0.013 (44)	0.000 (7)	0.012 (18)	0.000
U	0.037 (56)	0.044 (8)	0.036	0.036
Ni	0.009 (24)	0.011 (1)	0.009 (18)	-
Sr	0.023 (37)	0.027 (7)	0.022 (10)	0.021
Rb	0.004 (44)	0.004 (1)	0.005 (18)	-
Ba	0.028 (44)	0.012 (7)	0.034 (18)	0.012
Zr	0.015 (33)	0.020 (7)	0.015 (17)	0.014
Yb	0.000 (36)	0.001 (8)	0.000	0.000
Y	0.010 (55)	0.002 (8)	0.001	0.003

Note: Analyses provided by W.F. Fahrig (Geological Survey of Canada). Where all of the sample population does not contribute to a mean value the number of contributing samples is shown in parentheses.
- = not determined.

Christie and Fahrig (1983) used paleomagnetic data and K-Ar ages to distinguish what they consider to be an older group of dykes in northwestern Baffin Island, and which they named the Borden dykes. Christie and Fahrig (1983) considered the Borden dykes to be about 950 Ma, very close to the mean of 946 Ma reported for 17 whole rock K-Ar ages for the Nauyat volcanics in the same region. The Nauyat K-Ar ages, however, may have been reset by a low grade thermal event associated with the closing of the Poseidon Ocean (Jackson and Iannelli, 1981), which probably preceded the emplacement of Hadrynian diabase dykes.

Both Borden and Franklin dykes trend chiefly northwest, but both groups also include northerly trending dykes, most of which are smaller and intersect their northwest-trending, slightly older counterparts. The author has always found the identical nature of the trends of the two dyke swarms to be puzzling, and Pehrsson and Buchan (1999) appear to have solved the problem. The U-Pb baddeleyite ages of 723 Ma and 729 Ma recently reported by them are for two dykes that Christie and Fahrig (1983) considered to be Borden dykes. In addition, after re-evaluation, Pehrsson and Buchan (1999) have concluded that Borden dyke paleomagnetic signatures result from superposition of a steeply directed Cretaceous-Eocene chemical overprint on either a normal or a reversed primary Franklin component. K. Buchan (pers. comm., 1993) also suggests that the selective magnetic overprinting of specific dykes may be related to slight chemical differences between dykes, which is compatible with the chemical differences noted above. The author concurs with Pehrsson and Buchan (1999) that the Borden dykes of Christie and Fahrig (1983) are Franklin dykes, and that the name Borden should no longer be used.

Regional relations

Regional mapping and aeromagnetic data (e.g. maps for map area; Fahrig and West, 1986) show that the Hadrynian dykes of Baffin Island may be considered to be concentrated in four major swarms and at least three subsidiary swarms; in some areas adjacent swarms may merge. Five of these seven swarms pass through the map area. From northeast to southwest these swarms are:

1. northeast Baffin Island: mouth of Inugsuin Fiord – northeast corner of Borden Peninsula (major);

2. east-central Baffin Island: Home Bay – along east side of Barnes Ice Cap – Arctic Bay (major; includes the two dykes reported on by Perhsson and Buchan, 1994);
3. central Baffin Island: Broughton Island – along west side of Barnes Ice Cap – Mary River area – Fabricius Fiord (subsidiary);
4. west-central Baffin Island: Cumberland Peninsula – Penny Ice Cap – southern Steensby Inlet (major);
5. west Baffin Island: western Cumberland Peninsula – head of Cumberland Sound – west coast of Baffin Island – southern Steensby Inlet (major; includes the Cumberland Sound dyke dated by Heaman et al., 1990);
6. southwest side of Cumberland Sound – Fury and Hecla Strait (subsidiary); and
7. Hudson Strait (subsidiary).

The seven swarms outlined above are on strike with, or adjacent to, major fault zones that have been active in mid- to late-Proterozoic and/or Phanerozoic time (e.g. Fahrig et al., 1971; Jackson and Morgan, 1978a). Minor swarms and single dykes occur between the seven swarms and, in the map area, are commonly at least 7 km apart.

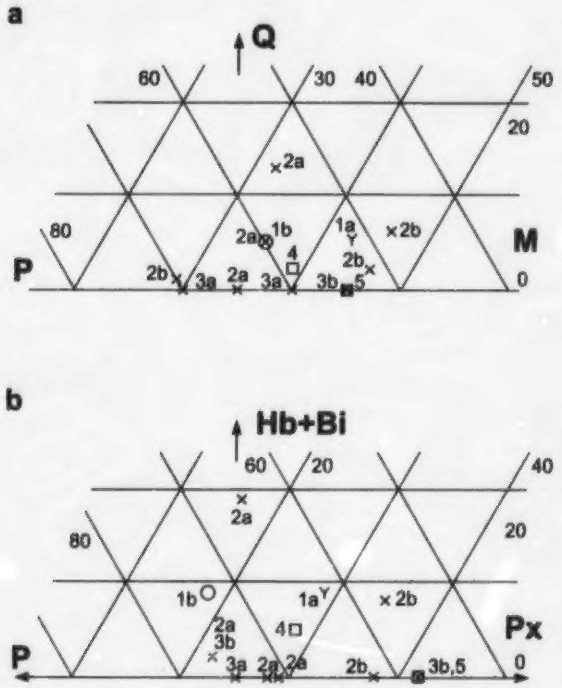

Figure 89. Modal plots for selected Hadrynian diabases according to swarm (see text for designators). ***a)*** *Quartz (Q) - plagioclase (P) - mafic (M).* ***b)*** *hornblende+biotite (Hb+Bi) - plagioclase (P) - pyroxene (Px). The circle represents Clyde River-Cape Hewett (NTS 27F, 27G), the X represents Icebound Lake (NTS 37G), the Y represents Scott Inlet (NTS 27G), and the square represents Steensby Inlet (NTS 37F).*

On Baffin Island, only dykes from swarms 2, 3, and 4 have been studied by Fahrig and his co-workers (Fahrig et al., 1971; Fahrig and Schwarz, 1973; Christie and Fahrig, 1983). Borden dykes were identified by Christie and Fahrig (1983) only in the northwest end of swarm 2, east-central Baffin Island, where they are intimately interspersed with Franklin dykes, and dyke trends are not diagnostic. However, W.F. Fahrig (pers. comm., 1985) considers the major northwest-trending dykes in swarm 2 to be Borden dykes.

Within the map area, Borden and Franklin dykes did not appear to be separable with any confidence, except paleomagnetically. In general, physical features (size, colour, weathering, texture) are similar for all of the late Proterozoic dykes unless stated otherwise. However, it was thought that petrography and chemistry might be useful in differentiating them. The modal analyses in Table 43 are numbered from 1 to 5, in accordance with the swarm, as listed above, from which they were derived. Number M90/1 is from a dyke west of Steensby Inlet that is on strike with swarm 5 to the southeast. Also, lower case letters are used to indicate samples that are either from the same dyke or from dykes that are along strike, beginning from the northeast. Thus, "2a" dykes occur in the east-central Baffin Island belt but are northeast of "2b" dykes, which lie in the same belt. The same system of numbering is used in Figure 89.

Although there seems to be no major mineralogical differences between dykes of different swarms, those of the northeast (1) and east-central (2) Baffin Island swarms contain more quartz, iron oxides, hornblende, and biotite, but less clinopyroxene and chlorite than dykes in the subsidiary swarm (3) and swarm (4) and possibly swarm (5). Also, Figure 89 shows that the dykes from the same swarms tend to plot in distinct fields. These differences suggest that the dykes of swarms 1 and 2 may be slightly more differentiated than the others, and that chances of finding Borden dykes in belt 1 may be relatively good. However, both Franklin and Borden dykes may be represented by "2a" and "2b" dykes in Table 43 and Figure 89. In light of the findings of Pehrsson and Buchan (1999), and pending determination of U-Pb baddeleyite ages for diabase dykes from the other swarms, it is suggested that the slight mineralogical and chemical differences noted above, if valid, may reflect penecontemporaneous emplacement of Franklin dyke swarms. To date, the oldest K-Ar ages obtained for the dykes come from the western half of Baffin Island (Jackson et al., 1978b, c, d; Jackson and Morgan, 1978b; Jackson and Iannelli, 1981). This point, and the indication that the most differentiated dykes are to the northeast in swarms 1 and 2, raise the suggestion that the swarms may young slightly eastward and that Greenland may have separated slightly from Canada at this time, although these dykes are relatively sparse in the eastern part of Baffin Island.

Fahrig et al. (1971) and Christie and Fahrig (1983) suggested that the Baffin Hadrynian dykes were emplaced at shallow depth in an extensional environment. Fahrig (1987) related the emplacement of several large mafic dyke swarms to ocean openings and closings, and concluded that most swarms form in an extensional failed-arm environment during early spreading, with dyke material moving largely in a horizontal direction. There is little or no evidence of a Franklin ocean opening, although distribution of 723 Ma mafic rocks in the Coronation Gulf-Victoria Island area (Pearson-Franklin node) suggested to Fahrig (1987) that there may have been a spreading point in the Arctic region.

Fahrig (1987) also commented on the observations by several persons that mafic dykes in certain regions are much less abundant and thinner within granulite facies rocks than in adjacent lower grade areas. This relationship seems to be valid in the Cumberland Sound region of Baffin Island, but in the map area there seems to be, in general, little difference, and the presence of major late fault zones seems to be much more important than metamorphic grade. Using the granulite facies rocks to imply depth of dyke emplacement would seem to assume the dykes were emplaced while the granulites were still at granulite facies depth. Evidence on northern Baffin Island shows granulite facies rocks had already been elevated and eroded by 1.2 Ga, and were probably not far from the surface when the Franklin dykes were emplaced. However, it certainly seems likely that it is relatively difficult to emplace dykes into plastic dense rocks at depth.

EARLY PALEOZOIC STRATA

Introduction

Most of the data for early Paleozoic strata in map area NTS 37G (Fig. 90, in pocket) were collected in 1965 by W.J. Crawford (Jackson, 1966a, b). These data have been supplemented by data for map areas NTS 37F and 37G from Operation Bylot (Jackson et al., 1978b, d) and from Trettin (1968, 1975). As much as 400 m of early Paleozoic sedimentary rocks, representing four formations and two groups (Table of Formations; Fig. 90), are preserved along the western edge of the map area. These strata underlie a low flat area containing a few low mesas in map area NTS 37F. Local relief increases northward and in map area NTS 37G, broad mesas rise to 200 m above intervening valleys.

The early Paleozoic strata were deposited on an erosion surface that represents a time hiatus across which the rocks differ in age from about 200 Ma to more than 2000 Ma, and the relations vary from regional disconformity to angular unconformity, and nonconformity. A thin grey to reddish, clay-bearing, locally arkosic regolithic zone up to about 2 m thick caps the Archean-Aphebian rocks locally below the Gallery Formation in the Mary River area (NTS 37G). Early Paleozoic carbonate containing small spherical concentric structures, probably oolites and pisolites, was deposited in cracks on the exposed erosion surface in the same area.

Fossils collected from the Paleozoic strata have been examined by T.E. Bolton and G.W. Sinclair, and the strata may range in age from Early Cambrian to Late Ordovician (Tables 45, 46; Bolton and Sinclair, 1967; Trettin, 1975; Bolton et al., 1977). Within the map area these strata are preserved in several southeast-trending grabens, half-grabens, and related depressions in the eastern part of the Foxe-Baffin structural depression (Trettin, 1975), and grade northwestward into thick geosynclinal strata of the Innuitian Mobile Belt. Paleozoic strata within the map area have little magnetic expression, their main effect being to "smooth out" the aeromagnetic pattern of the underlying rocks.

Stratigraphy and nomenclature of the early Paleozoic rocks have been provided chiefly by Blackadar (1956), Lemon and Blackadar (1963), and by Trettin (1969, 1975), who also refer to previous studies of these rocks. As noted by Trettin (1975), his map unit O_{ls} in northern Foxe Basin region is similar to member B of the Baillarge Formation of northwestern Baffin Island. Therefore map unit O_{ls} is included in the Baillarge Formation in this memoir (Table of Formations; Fig. 90). The similarity of the Turner Cliffs and Ship Point formations made it impractical to effectively differentiate these formations on the maps (based on reconnaissance mapping), as section data were too dispersed. The subdivisions in Figure 90, described below, are believed to coincide reasonably with those delineated by Trettin (1975) who has discussed regional correlations of these strata (*see* Sanford, 1977).

Admiralty Group

The Admiralty Group comprises the siliciclastic Gallery Formation and the overlying siliciclastic dolomites of the Turner Cliffs Formation. The group may attain a maximum thickness of about 110 m along the west edge of the Icebound Lake map sheet (NTS 37G), but may be absent west of Steensby Inlet (NTS 37F). Trettin (1975) concluded that the Gallery Formation is probably of upper Early Cambrian age, but could be as young as Late Cambrian; and that the Turner Cliffs Formation is most likely Middle Cambrian but could be as young as lower Early Ordovician, which is indicated by the faunas noted in Tables 45 and 46.

Gallery Formation (COGA)

Gallery Formation strata outcrop chiefly along and south of the Central Borden Fault Zone in the western part of map area NTS 37G, and consist chiefly of crossbedded (Fig. 90, 91), locally ripple marked, equigranular, very thin bedded quartz-rich sandstone. The Gallery Formation, where exposed, ranges from 10 to 70 m thick and may be separated into two intergradational members: a lower predominantly red conglomeratic member up to 30 m thick, and an upper greyish member up to 40 m thick. Red and grey strata may be interbedded in both members. Conglomerate beds are abundant in the lower part of the formation and minor shale, siltstone, and siliciclastic dolostone occur locally.

The sandstone consists mostly of subrounded to well rounded grains, although angular to subangular grains predominate in some places. Quartz has been derived from veins and strained metamorphic crystals. Feldspar is abundant, consisting mainly of plagioclase. Clay is common as pseudomorphs of feldspar. Minor hematite, some goethite, and accessory zircon are also common. The strata are friable to well indurated and are cemented by quartz, dolomite, and locally by calcite and clay minerals. Hematite is the main

Table 45. Ordovician faunas identified by Bolton and Sinclair (1967). *See* Figure 90 for locations.

Formation-Member	GSC Location	Fossils	Age/Stage
Baillarge (OBA) Member B	77280	*Protrochiscolithus* sp. *Catenipora* spp. *Calapoecia* sp. Favositid - large corallites, recrystallized *Maclurites* sp. cf. *Cyrtocerina* sp.	Late Ordovician
	77293	*Hormotoma* cf. *major* (Hall)	Edenian?
	77291	*Cyrtophyllum pattersoni* (Roy) - Bolton et al. (1977), Pl. 6, fig. 8, hypotype, GSC 42936 *Maclurites* sp. *Lambeoceras* sp. Indet. straight cephalopod	Edenian
	77290	*Protrochiscolithus* sp. *Catenipora* sp. *Calapoecia* sp. *Rhynchotrema* sp.	Late Ordovician (as 77280)
	77292	*Endoceras* sp. Orthoconic cephalopod	Early Edenian?
	77279	*Receptaculites* sp. *Maclurites* spp. - seven specimens (steinkerns) *Ephippiorthoceras*? sp. - larger than normal *Richardsonoceras* sp. *Narthecoceras*? sp. or very slender spyrocerid *Endoceras*? sp. *Illaenus* sp. *Isotelus* sp. *Krausella* sp.	Probably Early Edenian
Baillarge (OBA) Member A	77295*	*Streptelasma* sp. or *Grewinkgia* sp. *Receptaculites* sp. *Rhynchotrema* sp. cf. *R. increbescens* (Hall) *Maclurites* spp. *Fusispira* sp. *Trochonema* sp. Small snail indet. *Endoceras* sp. - large form *Ephippiorthoceras*? sp. "*Orthoceras*" sp.	Probably Early Edenian
	77289	Gastropod - high spired whorls similar to forms in 77282	Canadian (Early Ordovician)
Ship Point (OSP) Member B	77282	Borings indet. *Hormotoma* sp. - high spired: similar to forms in Washington Land, Greenland, and east coast, northern Ellesmere Island in Poulsen's (1946) gastropod limestone. However, there are two lithologies in collection, and *Hormatoma* may be out of place	Canadian (Early Ordovician)
	77285	*Maclurites* sp. *Tripteroceras*? sp.	Ordovician
Turner Cliffs- Ship Point Member A (COTCSP-A)	77294	*Stromatocerium*? sp. High spired gastropods similar to those in 77282 and 77289	Canadian (Early Ordovician)

* Location uncertain, probably at one of the two locations indicated on section A(C10), Figure 90.

SUMMARY

An Early Ordovician age is indicated for localities 77282, 77289, and 77294. A Middle Ordovician late 'Barneveld' stage is suggested for localities 77279 and 77295. Localities 77293, 77291, and 77292 may be slightly younger still – late 'Barneveld' or early Edenian. The youngest collections (Late Ordovician) are from localities 77280 and 77290.

Table 46. Paleozoic faunas identified in the field (excludes fossils noted in Table 45). *See* Figure 90 for locations.

Fauna	Locality															
	1	2[1]	3[1]	4	5	6	7	8	9a,b	10	11[2]	79[3]	88[3]	91[3]	92[3]	93[3]
Algae								b								
Receptaculites		d	e										e	e	e	e
Spicules								b								
Corals												e				
Horn corals		d														
Favositid														e		
Brachiopods				e						b	e		e			
Gastropods (spiral)	b							b								
Hormotoma						b[4]	c									
Maclurites		d	e	e	d										e	e
Cephalopods								b								
Orthocone cephalopods		d	e								e					e
Worm burrows									a							

1. GSC loc. 77295 (Table 45) may be from one of these two localities.
2. Location not shown, is west of Steensby Inlet (37F), at 79°12'W longitude, 70°13'N latitude.
3. These numbers are the last two digits of GSC localities 77279, 77288, etc. in Table 45.
4. Possibly is Lophospira?

a = Gallery Formation.
b = Turner Cliffs Formation, Ship Point Formation, Member A.
c = Ship Point Formation, Member B.
d = Baillarge Formation, Member A.
e = Baillarge Formation, Member B.

cement in a few places. Both trough and planar crossbeds are present, and range up to 1 m in height (rarely up to 3 m locally).

Lower member strata are mostly bright- to dusky-red, brownish-pink, and purple, medium grained to granular, quartz arenitic to subarkosic and locally arkosic, conglomeratic sandstones that are interbedded with conglomerate beds up to 3 m thick. Channel conglomerates occur locally. Conglomerate clasts are chiefly flattish, rounded to well rounded, commonly yellowish stained, quartz clasts up to 5 cm across, but locally range up to 15 cm in diameter and include some clasts of subangular quartz, vein quartz, sandstone, and conglomeratic sandstone. Subangular to well rounded, fine- to medium grained iron oxide clasts predominate locally near Mary River No. 1 and No. 4 iron deposits. The oxide is invariably hematite that is in part martite.

Figure 91. Brownish-pink to white, crossbedded quartz arenite of the Gallery Formation at the base of section E (Fig. 90). Outcrop about 5 m high. Crossbeds are easterly directed. Hoodoos are capped by resistant quartz arenite here, and elsewhere by gneiss boulders (NTS 37G, west). Photograph by W.J. Crawford. GSC 1997-54S

The upper Gallery Formation member is chiefly light- to medium-grey, with some buff, brown, and white, very fine- to very coarse-grained sandstones. Red patches occur locally. Quartz arenite predominates but some subarkose is present and ferruginous lenses up to 5 cm thick occur locally. Conglomeratic beds and lenses containing rounded quartz pebbles are common. In general, the sandstones become finer grained and more dolomitic and calcareous up-section toward the Turner Cliffs Formation.

The few crossbeds measured for the Gallery Formation (Fig. 90, 91; Trettin, 1975, p. 8) indicate that easterly-, westerly-, and northerly-directed paleocurrents predominated during sedimentation. In addition to abundant crossbeds and common ripple marks, load casts were seen at the base of some beds. Worm burrows, 3 mm in diameter and 10 cm long, are abundant locally (Table 46). Early work by Trettin (1969, p. 16) suggests that this horizon may be lower Turner Cliffs, but in a subsequent study, Trettin (1975, Fig. 5, p. 8-9) concluded that they probably occur in upper Gallery Formation strata. The lower Gallery Formation member according to Trettin (1975) is probably mostly nonmarine and in large part fluvial. The upper member was considered by Trettin (1975) to be a mixture of intertidal, bar, beach, and supratidal deposits, with the marine component increasing upward in the member.

Turner Cliffs Formation (COTC)

The Turner Cliffs Formation outcrops from Central Borden Fault Zone (NTS 37G) south to Nina Bang Lake (NTS 37F), but is not differentiated from Ship Point strata on the covering maps (unit COTCSP; NTS 37F, 37G). Turner Cliffs strata range from 13-90 m in thickness, commonly being about 30 m.

Turner Cliffs strata are chiefly very thin- to thick-bedded microcrystalline dolostone. Buff to yellow, brown, and light grey colours predominate. In general, the lower beds are composed mostly of siliciclastic grains, although dolostone is abundant in some sections. Minor thin beds and lenses of dolostone flat clast conglomerate occur throughout the formation. Well rounded dolostone clasts range up to 18 cm in diameter, and some have oxidized rims. Quartz clasts up to 3 cm have also been observed. Dolostone breccia occurs locally. A few sandstone beds up to 6 m thick contain quartz arenite (quartz-cemented) and dolomite-cemented quartz sandstone.

The dolostone contains variable amounts of disseminated silt and very fine- to medium- and locally very coarse-grained quartz and minor feldspar (Fig. 92). Glauconite and pyrite are common and some glauconite rims oolites. Fossils are relatively rare, and those seen are recorded in Tables 45 and 46. Trough and planar crossbeds, symmetrical ripple marks, and mud cracks are moderately common.

The lower contact is taken at an abrupt but seemingly conformable and gradational change upward from closed framework quartz arenites of the Gallery Formation to Turner Cliffs Formation chiefly open framework sandstones, siliciclastic dolostones, and dolostones. Trettin (1969) had suspected a disconformity to be present but later (Trettin, 1975) considered relations to be conformable.

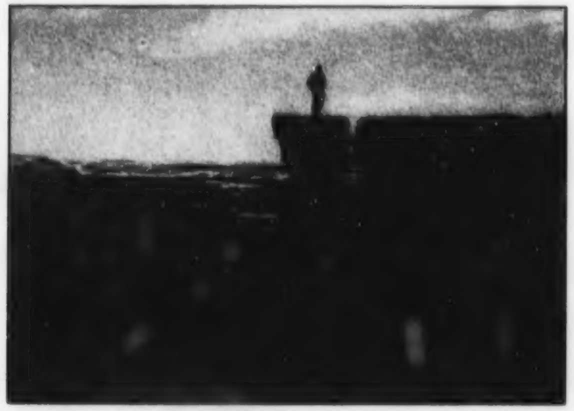

Figure 92. Thin- to medium-bedded siliciclastic dolostone interbedded with dolomitic quartz sandstone, typical of Turner Cliffs and Ship Point (member A) strata southeast of section B1 (Fig. 90). View southeast along the edge of a large mesa. The area on the left is largely drift covered but includes outcrops of the Gallery Formation, the Mary River Group, and a variety of gneisses. Low hills in the distance are capped by Paleozoic strata. Photograph by W.J. Crawford. GSC 1997-54T

Following Lemon and Blackadar (1963), and Trettin (1969, 1975) the upper Turner Cliffs contact is placed at the base of the uppermost distinctive sandstone unit that occurs regionally. This places the Turner Cliffs-Ship Point contact somewhat higher stratigraphically (sections D and E of Fig. 90) than indicated by Trettin (1975) in his section 14 (Inuktorfik –northeast 1). Although this contact seems conformable in the map area, Trettin (1975) has concluded from several lines of reasoning that a disconformity (erosional hiatus) is probably present.

Most Turner Cliffs strata are probably intertidal shallow marine deposits with a few interbedded supratidal and shallow subtidal strata (Trettin, 1975). The flat clast conglomerates most likely represent storm deposits. A sedimentary basin may have existed at the present site of Foxe Basin just south of the map area throughout Admiralty Group deposition (Trettin, 1975). If so, Trettin concluded it was a minor feature compared to the contemporaneous Admiralty Basin on Borden Peninsula northwest of the map area (Trettin, 1969, 1975).

Ship Point Formation (OSP)

The Ship Point Formation outcrops from the Central Borden Fault Zone in the north (NTS 37G) to west of Steensby Inlet in the south (NTS 37F). It is not differentiated from Turner Cliffs strata on the maps for the area north of Nina Bang Lake (unit COTCSP, NTS 37G). As redefined by Trettin (1975), the Ship Point Formation ranges from about 70-165 m thick in the map area and has been divided into two intergradational members. The lower member, A, 10-30 m thick, is composed of interbedded dolomitic sandstone, dolomite, and quartz arenite; the upper member, B, 60-135 m thick, is composed chiefly of silty to sandy dolostone.

Most of member A is composed of very fine- to very coarse-grained, laminated to medium bedded, dolomite-cemented, open framework quartz sandstone, and lesser microcrystalline dolostone (Fig. 92), most of which contains minor, but a variable amount of silt and sand (mostly quartz with a few feldspar grains). Minor calcite occurs as cement. Buff to pale yellow, orange, brown, and grey colours are common. At most localities, the basal unit of member A is 1.5-6 m of white to light grey, very fine- to very coarse-grained, very thin- to thick-bedded quartz arenite interbedded with minor dolomitic sandstone and dolostone. Similar quartz arenite units up to 3.5 m thick, most of which are dolomitic at least in part, occur throughout the member. Locally, the quartz arenite component is absent or only a minor component (Fig. 90, 92). Thin beds of dolostone flat pebble (to 3 cm) conglomerate are present at several horizons, and dolostone breccia occurs locally. Small amounts of pyrite are common. Replacement chert, vugs, ooids, stromatolites, and coated grains occur chiefly in the upper part of the member (Trettin, 1975). Trough and planar crossbeds are common, especially in the sandstones. Mud cracks and ripple marks occur sporadically, and stylolitic structures are rare.

The bulk of member B is aphanitic to finely crystalline, very thin- to medium-bedded dolostone, most of which contains a minor but variable amount of quartz silt, and quartz sand with very minor feldspar. Dolostone flat pebble (to 2.5 cm) conglomerate occurs sporadically in the north but seems more common west of Steensby Inlet. Chert, nodular dolomite, vuggy dolomite, and dolomite breccia (possibly solution breccia) occur locally. Colours commonly range from pale to medium yellow, orange, brown, grey, and olive. Bioturbation, small amounts of pyrite, and a variety of fossils are common (Fig. 90; Tables 45, 46; Trettin, 1975).

Ship Point Formation strata range from upper Early to lower Middle Ordovician in age (Tables 45, 46; Trettin, 1975; Bolton et al., 1977). The variation in grain size, predominance of dolomitic quartz sandstone, abundance of dolostone flat pebble conglomerate, and crossbedding indicate that member A strata were deposited in shallow intertidal marine to supratidal environments. Predominance of dolostone together with decrease in structures and dolostone flat pebble clonglomerate suggest somewhat deeper intertidal environments for member B.

Brodeur Group

Baillarge Formation (OBA)

The Baillarge Formation is the only representative of the Brodeur Group present and caps several mesas along the western edge of the map area. Trettin's (1975) O$_{ls}$ map unit west of Steensby Inlet is included here in the Baillarge Formation and probably outcrops a little more extensively than shown on geological map for NTS 37F (Jackson et al., 1978d). The Baillarge Formation is composed of microcrystalline fossiliferous limestone and dolostone, about 100 m of which are preserved south of Central Borden Fault Zone (Tables 45, 46; Fig. 90). Two intergradational members have been differentiated, a lower member "A" about 15 m thick, and an upper member "B" at least 85 m thick.

Member A is composed of laminated to thin bedded, light grey to buff, shaly to silty limestone, dolomitic limestone, and minor dolomite. Minor, very fine grained sandy material occurs locally in the carbonate strata which are also locally burrowed, or nodular.

Member B has been partially dolomitized and is composed of very thin- to thin-bedded dolomitic limestone, dolostone, and limestone (Fig. 93). Colours are chiefly light to medium brown, but include minor buff to grey strata. The upper strata of member B are shaly to silty (Fig. 90). Nodular strata, chert, and burrows occur locally. Reassessment of field data indicates that breccia, mud chip conglomerate, and sandstone are rare or absent. Shaly and silty material are more rare than in member A. Where present, coarser grains (sand to fine pebble) are commonly fossil fragments (Fig. 94).

Figure 93. Nodular, very thin bedded, microcrystalline, grey-weathering limestone in member B of the Baillarge Formation, section D (Fig. 90). Photograph by W.J. Crawford. GSC 1997-54U

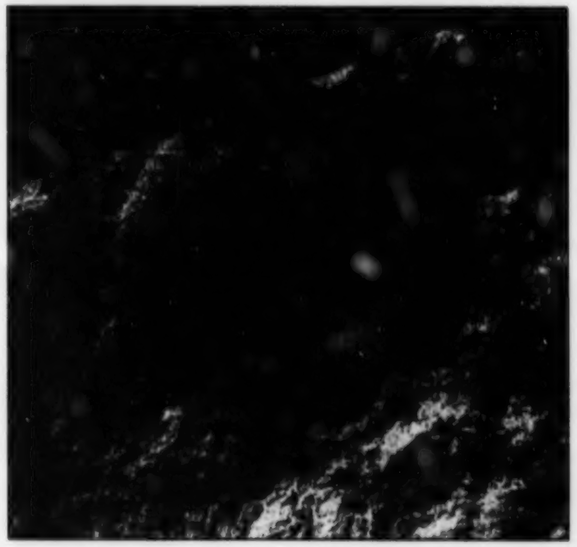

Figure 94. Receptaculites sp. 60 cm in diameter, from the middle of member B of the Baillarge Formation, section B2 (Fig. 90). Photograph by W.J. Crawford. GSC 1997-54V

A regional disconformity probably separates the underlying Ship Point Formation from the Baillarge Formation (Trettin, 1969, 1975). The latter are truncated by the present erosion surface. The Baillarge Formation ranges in age from late Middle Ordovician to Early Silurian (Trettin, 1969, 1975; Bolton et al., 1977), but the strata within the map area are probably all of Ordovician age (Tables 45, 46).

The absence in the map area of crossbeds, mud cracks, ripple marks, and intraformational conglomerate, together with an abundant marine fauna, indicate that the Baillarge Formation was deposited in a subtidal shelf environment more akin to the quiet environment deduced by Trettin (1975) for map unit O_{ls}, south of the map area, than the lagoonal and shallow, locally restricted environment deduced by Trettin (1969) for the laterally equivalent Baillarge Formation northwest of the map area. However, Baillarge lower member A can still be distinguished, although through facies changes it has become more similar to member B. Trettin's (1975) conclusion that the thinning and disappearance of member A occurs in the Inuktorfik Lake area due to facies changes seems correct.

Trettin (1975) noted that fossils show map unit O_{ls} is limited to the Ordovician, and that O_{ls} strata are more similar to member B strata of the Baillarge Formation than to member A. Trettin's (1975, Fig. 3) correlation chart shows map unit O_{ls} to be equivalent to both member A and the Ordovician part of member B of the Baillarge Formation. Unit O_{ls} strata overlie the Ship Point Formation directly west of Steensby Inlet, and meagre lithological data for that area indicate that these O_{ls} strata may be equivalent to Baillarge member A to the north.

Paleogeological setting

The regional geological setting during deposition of these early Paleozoic rocks has been discussed by Trettin (1975). Much of the map area is included in diagrams by Sanford (1977), which indicate that Ordovician marine strata were deposited over all of Baffin Island, at least as far north as the map area.

Admiralty Group strata were deposited in fluvial and chiefly shallow marine environments between the contemporary Admiralty Basin to the northwest on Borden Peninsula (Trettin, 1969) and possibly a minor contemporary basin to the south that was ancestral to the present Foxe Basin (Trettin, 1975). Following a retreat of the sea, Ship Point strata were deposited during a second marine transgression; then a second withdrawal of the sea was followed by a third marine transgression and deposition of the Baillarge Formation of the Brodeur Group.

The early Paleozoic rocks are downfaulted against Precambrian rocks, and preserved in a broad, shallow, complex graben structure (Trettin, 1975) in which bedding attitudes vary from one disturbed block to the next. Within the map area, faults bounding and intersecting the Paleozoic strata trend chiefly southeast. Paleozoic strata in the northern part of the map area are preserved in the southeastern end of the Phillips Creek Trough (Jackson et al., 1975), bounded on the north by Central Borden Fault Zone and on the south by Nina Bang Fault Zone. The Paleozoic rocks west of Steensby Inlet occur in a subsidiary graben, named here the Neergaard Graben, that occurs along the northeast side of a major horst area, the Steensby High (Jackson et al., 1975). Vertical displacement of Paleozoic strata along some of these faults may be as much as 300 m (Trettin, 1975), and along the Central Borden Fault Zone in the Mary River area is probably at least 600 m.

The age(s) of the Paleozoic-displacing faults is uncertain, but two major episodes seem likely: Early Devonian and Cretaceous-Recent (Jackson et al., 1975; Trettin, 1975; Sanford, 1977; Jackson and Morgan, 1978a; Jackson and Iannelli, 1981). Some of the faults parallel lines of weakness or structural trends in the basement gneisses and may have been active since mid-Aphebian (+2000 Ma) time. The Central Borden Fault Zone, for example (or a fault parallel to it), was active during Borden Basin sedimentation 1270-1200 Ma ago (Trettin, 1969; Jackson and Iannelli, 1981). Vertical movement of at least 600 m has subsequently occurred along the fault following early Paleozoic sedimentation. In addition, larger clasts (ca. 15 cm diameter) in the Gallery Formation are chiefly quartz, but include some of hematite ore and occur only adjacent to Central Borden Fault Zone. Therefore, a fault or fault line scarp may have existed along the fault as early Paleozoic sedimentation began. No positive evidence has been found by the author and co-workers, or by Trettin (1975) or Sanford (1977), of early Paleozoic syndepositional faulting, although Trettin (1975) and Sanford (1977) noted the upwarping along Boothia Uplift and Melville Arch.

CRETACEOUS-RECENT (T, KT$_4$)

Glacial geology was discussed in the "Introduction". Only a few small areas underlain by strata previously thought to be of Cretaceous-Paleogene age, but now considered to be more likely Pleistocene-Recent, are included here.

Strata underlying a small area south of Rimrock Lake (NTS 37E; Jackson and Morgan, 1978b) and several small coastal areas in the vicinity of Scott Inlet (NTS 27G; Jackson et al., 1978c) were, tentatively, considered to be of Cretaceous-Paleogene age and correlated with the Eclipse Group of Bylot Island and the Pond Inlet region of northwestern Baffin Island (Jackson and Davidson, 1975; Jackson et al., 1975; Miall et al., 1980). Most observations of these strata were made at low level from a helicopter during Operation Bylot. Cretaceous-Tertiary strata in Baffin Bay contain an oil seep about 40 km seaward from the mouth of Scott Inlet (MacLean et al., 1981; Loring, 1984; Grant et al., 1986). The host strata have been traced southeastward to the Home Bay and Padloping Island areas (MacLean and Williams, 1983). The Cretaceous strata are marine with perhaps some nonmarine strata to the southeast.

Rimrock Bed (T)

A small outcrop of laminated, buff to brown, silty shale up to 0.1 m thick and composed chiefly of (clastic?) limestone, occurs on a hill summit south of Rimrock Lake about 26 km northwest of Barnes Ice Cap (NTS 37E). The exposure has been named the "Rimrock Bed" by Andrews et al. (1972) who have discussed the strata in detail, and are confident that the "Bed" is in place and nonconformably overlies basement gneisses (Amg). Based chiefly on palynology studies, they have assigned a Paleogene age to the Rimrock Bed, and concluded it was deposited during a warm climate in a fresh water swamp or a marginal marine marsh. The "Bed" is similar in age and lithology to strata within the Eclipse Group with which it has been tentatively correlated by Jackson and Morgan (1978b). The relationships of the Rimrock Bed to early Paleozoic and Pleistocene strata are not exposed in the map area but are assumed to be unconformable.

Scott Inlet area (KT$_4$)

Six small areas of horizontally bedded, poorly consolidated to unconsolidated strata occur on an elevated, largely drift-covered, wave-cut beach underlain by basement gneisses in the vicinity of Scott Inlet (NTS 27G; Jackson et al., 1978c). The strata may have a maximum thickness locally of about 15 m. As seen from the air, these deposits resembled some of the Cretaceous-Eocene Eclipse Group strata to the north (Jackson and Davidson, 1975; Jackson et al., 1975), and were tentatively correlated with the Eclipse Group.

Two of the five localities north of Scott Inlet were examined in 1980 by D.C. Umpleby (pers. comm.) of Atlantic Geoscience Centre. He found the deposits to consist chiefly of buff to grey, immature quartzofeldspathic sands with some silt and minor clay and peat. His initial impression was that the deposits are Quaternary. A palynological analysis of peat samples collected by Umpleby has been made recently by Burden and Holloway (1985). They found indications of mid-late Cretaceous marine deposition in one sample, and Quaternary nonmarine deposition in another. Both samples also contain characteristically Mesozoic taxa. Burden and Holloway (1985) concluded that the deposits are probably Quaternary, for which some material came from erosion of nearby Cretaceous strata.

The sixth locality in the Scott Inlet area occurs at Cape Smith, east of Scott Island (NTS 27G; Jackson et al., 1978c). The stratified deposit here is considered by Miller et al. (1977) to be an ice-marginal marine delta. Miller et al. (1977) report a ^{14}C age of 45 200 years ±800 years B.P. for molluscs collected from the delta. They also correlated the Cape Smith strata with their Kogalu Member marine sediments and the overlying Eglinton Member Scott Inlet aeolian sands, these being the two uppermost members of Feyling-Hanssen's (1976) Clyde Foreland Formation. The strata at the five localities north of Scott Inlet are tentatively considered here to also represent the Clyde Foreland Formation.

REGIONAL GEOCHEMISTRY

Major and minor elements

Various chemical data are available for the bedrock map units in and adjacent to the map area, and the reader is referred to the "Introduction" and to sections on the individual map units. Spectrochemical analyses for individual samples are provided in Appendix 2. Statistical data for these samples are arranged by element in Appendix 3 and by map unit in Appendix 4. A summary of most of the data is present in Table 47 as means for six major rock lithologies. The results from Shaw et al. (1967) represent an eastern coastal strip that lies mainly south of the map area. Each of their four reported means probably includes analyses of both Archean and Aphebian rocks. Table 48 summarizes the data from about 500 spectrographic analyses for the map area, for which the individual analyses and statistical data are presented in the appendices. These chemical data are of a preliminary or reconnaissance nature. They are presented in this memoir to provide information for individual map units, to compare map units, and to make the data available to others. Some features of the data will be noted here while others have been noted in sections dealing with specific map units.

Although the crustal average presented by Shaw et al. (1967) for Baffin Island may prove to be reasonably accurate, only about one half of the Precambrian eastern coastal area and a small part of the island underlain by Precambrian rocks are represented. A crustal average for the map area is not presented here because most of the analyses are incomplete, more analyses are required for some map units, and the analyses should be weighted according to map unit distribution, not relative numbers of samples.

An indication of the variety of rock types and their ages that may be represented by the samples analyzed by Shaw et al. (1967) is obtained by comparing their sample locations with published maps, which were not available to them (Jackson and Taylor, 1972; Jackson and Morgan, 1978a, b; Jackson et al., 1978c, d; Jackson, 1984; Henderson, 1985a, b). The quartzofeldspathic group of samples (Table 47) in Shaw et al. (1967) undoubtedly represents a large variety of Archean and Aphebian rocks. Most of the samples came from 66°-69°N and only about twenty came from the map area.

The data available for quartzofeldspathic rocks (Table 30, 47; groups I, II, III, and V in Table 48) have been compared with analyses reported for similar rocks by others including Chappell (1978), Collins et al. (1982), Anderson (1983), Harvey (1983), White and Chappell (1983), Pearce et al. (1984), and Whalen et al. (1987). The analyses for Baffin rocks fall within the ranges reported by others for felsic to intermediate quartzofeldspathic rocks (e.g. Tables 31, 32). The patterns displayed by a few elements in the Baffin Island rocks, however, are somewhat different. The Ba and Sr values, for example, are commonly high compared with those in most other reports, while Zr and MgO values are a little low.

The average for foliated and nebulitic quartzofeldspathic rocks, considered to be Archean (Table 47, column B), is similar to those for massive Archean granitic and Aphebian charnockitic intrusions (column C) and late Aphebian granitic intrusions (column D). The greatest differences are in some minor trace elements; column B shows the least La and the most Ca and Cu, while column C shows the least Si and the most P, H (H_2O), C (CO_2), Ba, La, Ni, Sr, V, Zr, and Sc. Column D shows the least Ti, Fe, Mg, Sr, and V, and the most K, Li, Rb, and Cs. The migmatitic quartzofeldspathic rocks (column E) contain more Ti, Fe, Mn, Mg, Cu, and V than the other quartzofeldspathic rocks. This is probably due to greater contamination by paragneisses and cafemic rocks.

The average for Aphebian Piling Group metapelites in Table 47 (column H) probably represents insufficient samples to properly represent the metagreywacke turbidite sequence (Longstaff Bluff and Astarte River formations – Table of Formations). The average seems to be biased toward carbonate-bearing metasediments, and contains much less Al, Ti, Fe, Mn, Mg, Na, Ba, Cr, Cu, V, Zr, Ni, and (surprisingly) Sr, but much more La than the Archean Mary River (column G) metapelites. The latter reflect somewhat the more widespread occurrence of mafic and ultramafic igneous rocks compared with the Piling Group. Most of the values for the Neohelikian Arctic Bay Formation mean (column I) are either intermediate between those for the Mary River and Piling metapelites, or lower (e.g. Al, Ti, Mg, Ca, Na, Sr). The Baffin Island average for pelitic rocks (aluminous silicate rocks) presented by Shaw et al. (1967) probably comprises chiefly Piling and Hoare Bay groups samples (column F) but seems to resemble least the Piling Group mean for the map area (column H).

Although minor elements are less abundant in the Archean Mary River quartzite (column K) than in the Mary River metapelites, there is less difference than anticipated, and the Al content seems remarkably similar. The Neohelikian Adams Sound orthoquartzite samples (column L) have the least amount of minor elements present. Piling Group strata are the most likely source for the quartz-rich samples (column J) analyzed by Shaw et al. (1967).

Only a few Mary River Group (one-column M) and Piling Group (three-column N) calc-silicate samples were analyzed. Also, a few of the Mary River iron-formation analyses (column O) are for samples from the Eqe Bay-Grant Suttie Bay area (Tables 14, 17; Appendix 5; Crawford, 1973), just south of the map area (Fig. 1). The iron ore average (column P) is for Baffinland Iron Mines No. 1 deposit at Mary River (Baffinland Iron Mines Limited, 1964).

Table 47. Summary of chemical data for Clyde-Cockburn Land map area (weight per cent; *see* Table 48).

	Quartzofeldspathic					Pelitic sediments			
	A Shaw et al. (1967)	B Amn, Amn^h gr-Agr, Ma	C Agp, Ack Amn^i	D Ag Amg^i	E Amg, Amg^j Amp, bg	F Shaw et al. (1967)	G M, Ms M^l	H APs	I NAB
SiO_2	70.51*	74.3*	65.8*	74.8*		69.36*			
Al_2O_3	14.51*	13.0	13.4	12.7	13.0	14.50*	12.7	11.8	8.2
TiO_2	0.39*	0.38	0.45	0.14	0.47	0.58*	0.63	0.50	0.28
Fe_2O_3	0.71*					0.85*			
FeO	2.04*	2.6	2.6	1.3	3.5	4.10*	5.5	4.4	4.4
MnO	0.03*	0.040	0.037	0.031	0.056	0.06*	0.081	0.045	0.099
MgO	1.19*	1.1	1.1	0.80	1.5	1.83*	2.5	2.2	1.6
CaO	2.20*	+	3.36*	0.40*	+	2.92*	+	>1.1	0.46
Na_2O	3.19*	3.50*	3.8*	3.7*	±	2.00*	+	>0.8	0.54
K_2O	3.90*	4.49*	3.80*	5.67*		2.20*			
P_2O_5	0.10*	0.01*	0.20*	0.01*		0.10*			
H_2O	0.77*	0.2*	0.4*	0.3*		0.93*			
CO_2	0.03*	0.1*	0.2*	0.1*		0.04*			
S	0.04*					0.06*			
Total	99.61					99.53			
Ba	+	0.048	0.12	0.063	0.061	+	0.057	0.0044	0.015
Co	0.0053	-	-	-	-	0.0033	-	-	-
Cr	0.0024	-	-	-	-	0.0084	0.0072	0.0023	0.0028
Cu	0.0010	0.0024	0.0011	-	0.0041	0.0025	0.0031	-	0.0025
La		-	0.0089*	0.0068*	-		-	0.064	-
Ni	0.0010	-	0.001*	-	-	0.0023	0.003	-	-
Sr	0.020	0.027	0.034	0.019	0.030	0.023	0.019	0.0091	0.0040
V	0.0036	0.0047	0.0054	0.0024*	0.0069	0.0065	0.011	0.0026	0.0046
Zr	0.013	0.019	0.030	0.011	0.023	0.013	0.020	0.0093	0.027
Sc			0.0016*	0.00066*					
Li	0.0028		0.0015*	0.0035*		0.011			
Rb	0.011		0.0093*	0.036*					
Cs			0.00003*	0.0002*					
Samples, Total:	91	107	51	42	91	20	48	9	16
*:	69	1	9	1		17			

Note: Values are arithmetic means in weight per cent. Column O - analyses are from Baffinland Iron Mines Limited (1964). Column U - includes 18 chemical analyses provided by W.F. Fahrig (Geological Survey of Canada). Some elements within some samples in each sample grouping are determined as being present in amounts below the minimum level of determination. An element value of half this minimum level is assumed for a few of these samples. Similarly element values equal to the upper level of determination were assumed for a very few samples. * = number of samples used for indicated mean where less than total for a particular group; also, identifies the determinations for which this applies. All iron is shown as FeO except in columns A, F, J, O, and Q.

Table 47. (cont.).

	Quartz-rich sediments			Calc-silicates		Iron-formation		Cafemic rocks				
	J Shaw et al. (1967)	K Mq	L NAS	M Ms^n	N APM	O Mif, Mif^o Mif^s	P iron deposits	Q Shaw et al. (1967)	R Amn^f, gr^g Amg^g	S Mg Mb	T Mu	U Hg
SiO_2	87.85*					46.34*	0.47	43.84				49.40*
Al_2O_3	6.37*	13.0	2.6	4.0	2.5	1.5	0.49	9.55	11.7	10.2	3.6	13.8
TiO_2	0.2*	0.42	0.3	0.14	0.20	0.077	0.05	0.82	0.88	0.77	0.20	1.97
Fe_2O_3	0.00*					29.8*		3.58				
FeO	0.40*	4.0	0.18	2.6	0.66	16.9*	89.63	7.82	8.1	9.4	8.2	11.6
MnO	0.009*	0.045	-	0.56	0.034	0.12	0.18	0.21	0.17	0.18	0.17	0.19
MgO	0.23*	1.5	-	12.1	6.1	2.1		19.08	4.8	6.0	+	4.8
CaO	1.75*	0.70	0.036	+	+	0.59		7.50	+	+	-	10.2*
Na_2O	1.70*	+	0.031	0.051	0.26	0.071		0.92	+	+	0.18	2.63*
K_2O	0.30*					0.12*		0.33				0.53*
P_2O_5	0.04*					0.030*	0.087	0.29				0.16*
H_2O	0.51*					1.07*		2.42				
CO_2	0.17*					0.11*		2.75				
S	0.03*					0.08*		1.47				
Total	99.56							100.58				
Ba	0.011	0.052	0.04	0.0024	0.0050	0.00015		0.014*	0.057	0.022	0.0023	0.010
Co	0.021	-		-	-	0.0004		0.0026*	0.014	0.004	0.010	0.004
Cr	0.0013	-		0.0030	-	0.0069		0.0086*	0.019	0.046	0.27	0.006
Cu	0.0002	0.0029		-	-	0.0017		-	0.004	0.008	0.0020	0.020
La	-	-		0.079	0.06	-			0.01	0.01	-	-
Ni	0.0007	-		-	-	0.022		0.0012*	0.006	0.019	0.17	-
Sr	0.007	0.0082	0.0011	0.0078	0.0095	0.00054		0.0067*	0.035	0.014	0.0024	0.016
V		0.0063		-	0.0030	0.0027		-	0.020	0.017	0.0084	0.036*
Zr	0.0076	0.026	0.016	-	0.011	0.0070		0.015*	0.024	0.016	-	0.018
Sc												
Li	0.0047							0.0045*				
Rb								0.012				
Cs												
Samples, Total:	3	10	4	1	3	51	206	4	36	26	14	27
*:	2					16		2				18

+ = present in excess of upper determination limit. - = present in amount below lower determination limit. ± = some present in excess of upper determination limit, rest present in amount below lower determination limit. Blank = no data. Determination limits, legends, symbols, and original data including data not incorporated here are provided in Appendices 2 to 5, Table of Formations, and Tables 6, 14, 15, 17, and 48. See Appendix 4 for map symbols and superscripts. Means from Shaw et al. (1967) are for an eastern coastal strip that extends north into the map area.

The four samples Shaw et al. (1967) used for their cafemic mean (column Q) most likely came from Hoare Bay mafic metavolcanics and metaultramafics in the southern part of their sampled belt, from Hadrynian diabases, and/or Cape Dyer Cretaceous tholeiitic basalt. The high Mg content suggests the presence of an ultramafic component in the composite sample. The mafic remnants in the "Archean" quartzofeldspathic rocks and the Archean-Aphebian banded migmatites (column R) are similar chemically to the Archean Mary River metabasalt and metagabbro (column S) but the mean for the former (column R) contains more Al, Ti, Ba, Co, Sr, and Zr, and less Fe, Mg, Cr, Cu, and Ni than the mean for the latter (column S). The mean for Hadrynian Franklin diabases (column U) is least similar to the other three means for mafic rocks (R, S, T) in the map area, and the diabases may be the most differentiated. The diabases contain more Al, Ti, Fe, Cu, and V, and less Cr and Ni than the other three groups. Column T, the mean for Mary River ultramafic rocks, shows a relatively high Mg, Co, Ni, and Cr content and a low Al, Ti, Ca, Na, Ba, Cu, Sr, V, and Zr content.

Spectrographic analyses for individual map units and selected components in them are summarized in groupings in Table 48 in order to facilitate comparisons of compositions, assess possible origins and correlations, and better show some of the similarities and dissimilarities that governed the groupings made in Table 47. Means for Archean nebulitic (Table 48, column 1), foliated (columns 2, 3), and massive to weakly foliated porphyritic (column 4) granitic rocks are all similar. The porphyritic granites (column 4) contain slightly greater concentrations of most of the elements within detectable limits, but contain less Cu than the other three map units (Table 48).

Table 48. Summary of spectrographic analyses for Clyde-Cockburn Land map units (weight per cent).

	GROUP I							GROUP II		GROUP III			GROUP IV			
	1 Amn	2 Amn^b	3 $gr\text{-}Agr^{cde}$	4 Agp	5 Ack	6 Amn^i	7 Amg^j	8 Amg^i	9 $Ag^{k,c}$	10 Amg, Amg^a	11 Amp	12 bg	13 Mb	14 Mg	15 Amn^f	16 Amg^g
TiO_2	0.42	0.37	0.33	0.48	0.47	0.23	0.30	0.18	0.15	0.50	0.60	0.55	0.77	0.77	0.87	0.90
Al_2O_3	13.2	13.8	12.8	13.6	12.5	12.1	12.8	13.2	12.7	13.2	12.8	13.4	10.6	9.6	11.1	11.9
FeO	2.8	2.4	2.2	2.8	2.1	1.9	2.2	1.3	1.4	4.0	3.3	3.9	9.1	10.0	7.8	8.4
MnO	0.040	0.032	0.035	0.043	0.031	0.023	0.031	0.018	0.044	0.065	0.049	0.066	0.19	0.14	0.17	0.17
MgO	1.3	0.36	0.81	1.5	0.73	0.73	1.1	0.48	1.1	1.7	1.2	2.01	6.1	5.8	4.6	5.0
CaO	(+)	(+)	(+)	(+)	(+)	1.1	(+)	(+)	1.4	(+)	(+)	(+)	(+)	(+)	(+)	(+)
Na_2O	(+)	(+)	(+)	(+)	(+)	(+)	(+)	(+)	(+)	(+)	(+)	(+)	(+)	0.50	(+)	(+)
Ba	0.080	0.046	0.091	0.094	0.11	0.11	0.056	0.069	0.061	0.058	0.10	0.11	0.014	0.041	0.058	0.053
Co	(-)	(-)	(-)	(-)	(-)	(-)	(-)	(-)	(-)	(-)	(-)	(-)	0.0039	0.0033	(-)	(-)
Cr	0.004	(-)	(-)	(-)	(-)	(-)	0.0027	(-)	(-)	0.004	(-)	0.039	0.052	0.033	0.017	0.019
Cu	0.002	0.0028	0.0028	0.0012	0.0011	0.0011	0.0040	(-)	(-)	0.003	0.001	0.034	0.0085	0.0074	0.0042	0.0044
La	(-)	(-)	(-)	(-)	(-)	(-)	(-)	(-)	(-)	(-)	(-)	0.01	(-)	(-)	(-)	(-)
Ni	(-)	(-)	(-)	(-)	(-)	(-)	(-)	(-)	(-)	(-)	(-)	(-)	0.023	0.011	0.0077	0.0061
Sr	0.030	0.028	0.024	0.040	0.029	0.026	0.034	0.025	0.015	0.028	0.027	0.043	0.012	0.018	0.025	0.038
V	0.005	0.003	0.0037	0.0060	0.0049	0.0037	0.0041	(-)	(-)	0.008	0.006	0.009	0.021	0.022	0.018	0.021
Zr	0.020	0.012	0.020	0.035	0.034	0.014	0.016	0.015	(-)	0.024	0.030	0.024	0.014	0.024	0.028	0.023
Pb	(-)	(-)	(-)	(-)	(-)	(-)	(-)	(-)	(-)	(-)	(-)	(-)	(-)	(-)	(-)	(-)
Y																
Yb																
Samples:	52	7	36	18	14	10	21	18	23	58	9	3	18	8	11	24

	GROUP V									GROUP VI						
	17 Hg	18 $gr\text{-}Agr^g$	19 Mu	20 Mn	21 Amn^h	22 Ma	23 Mif^o	24 Mif^s	25 Mq	26 M,M^l,Ms	27 Amg^m	28 APs	29 Ms^n	30 APm	31 NAS	32 NAB
TiO_2	1.38	0.60	0.20	0.15	0.47	0.50	0.067	0.14	0.42	0.63	0.47	0.50	0.14	0.20	0.033	0.28
Al_2O_3	11.5	11.1	3.6	24.9	13.6	11.3	1.3	2.1	13.0	12.7	10.8	11.8	4.0	2.5	2.6	8.2
FeO	10.7	5.0	8.2	1.9	4.1	3.6	(+)	(+)	4.0	5.5	4.6	4.4	2.6	0.66	0.16	4.4
MnO	0.18	0.067	0.17	0.039	0.072	0.077	0.13	0.30	0.045	0.081	0.063	0.045	0.56	0.034	(-)	0.099
MgO	4.8	3.6	(+)	1.0	1.8	1.5	1.8	1.7	1.5	2.5	3.0	2.2	12.1	6.1	(-)	1.6
CaO	(+)	(+)	(-)	(+)	(+)	(+)	0.53	0.53	0.70	(+)	(+)	>1.1	(+)	(+)	0.036	0.46
Na_2O	(+)	(+)	0.18	(+)	(+)	(+)	0.031	0.032	(+)	(+)	(+)	>0.8	0.051	0.26	0.031	0.54
Ba	0.013	0.14	0.0023	0.019	0.041	0.034	0.0018	0.0052	0.052	0.057	0.055	0.052	0.0024	0.0050	0.04	0.015
Co	0.0034	(-)	0.010	(-)	(-)	(-)	0.0031	(-)	(-)	(-)	(-)	(-)	(-)	(-)	(-)	(-)
Cr	0.010	0.013	0.27	(-)	0.005	0.005	0.0054	0.0056	(-)	0.0072	0.017	0.035	0.0030	(-)	(-)	0.0028
Cu	0.019	0.0015	0.0020	(-)	0.003	0.002	0.0022	0.0015	0.0029	0.0031	0.0045	0.0030	(-)	(-)	(-)	0.0025
La	(-)	(-)	(-)	(-)	(+)	(-)	(-)	(-)	(-)	(-)	(-)	(-)	0.079	0.06	(-)	(-)
Ni	0.0047	(-)	0.17	(-)	0.003	(-)	0.0035	(-)	(-)	0.003	0.0035	(-)	(-)	(-)	(-)	(-)
Sr	0.016	0.058	0.0024	0.020	0.028	0.015	0.0010	(-)	0.0082	0.019	0.028	0.0094	0.0078	0.0095	(-)	0.0040
V	0.036	0.013	0.0084	(-)	0.0073	0.007	0.0068	0.0062	0.0063	0.011	0.010	0.016	(-)	0.0030	(-)	0.0046
Zr	0.027	0.013	(-)	(-)	0.014	0.016	(-)	(-)	0.026	0.020	0.018	0.020	(-)	0.010	(-)	0.027
Pb	(-)	(-)	0.10	(-)	(-)	(-)	0.088	0.066	(-)	(-)	(-)	(-)	(-)	(-)	(-)	(-)
Y							0.007									(-)
Yb							0.0009									(-)
Samples:	9	1	14	1	4	4	28	7	10	46	2	8	1	2	4	16

Note: Analyses are treated in the same manner as in Table 47. Values are arithmetic means in weight per cent. *See* appendices (especially Appendix 2 and Appendix 4) and Table of Formations for legends, determination limits, etc. (+) = present in excess of upper determination limit. (-) = present in amount below lower determination limit. Limits, in weight per cent, of reliable determination are: Ti = 0.02-5, Al = 0.1-15, Fe = 0.2-10, Mn = 0.01-1.25, Mg = 0.05-9, Ca = 0.02-1, Na = 0.01-0.5, Ba = 0.002-0.3, Co = 0.003-0.35, Cr = 0.003-0.5, Cu = 0.001-0.15, La = 0.07-2.5, Ni = 0.003-1, Sr = 0.001-0.4, V = 0.003-0.7, Zr = 0.01-2, Pb = 0.07-7, Y = 0.008-0.8, Yb = 0.001-0.125. All Fe shown as FeO. Oxide values calculated from element analyses. Map units are grouped (I-VI) according to chemical similarity (see text). Blanks mean no data.

The mean for Aphebian(?) charnockitic rocks (column 5) is more similar to Archean than Aphebian granitic rocks, and the major element means are most similar to foliated Archean granitic rocks (columns 2, 3). Titanium and minor element values are most similar to means for porphyritic Archean granitic rocks (column 4).

Late discordant massive granitic bodies in Archean nebulitic granitic rocks yield a mean (column 6) that most closely resembles the charnockitic mean (column 5) except for lower Ti, V, and Zr in the discordant bodies. Values for these three elements are more similar to those present in the mean for Archean foliated granitic rocks (columns 2, 3) or for the leucosome in banded migmatite (column 7). The leucosome mean resembles those for Archean nebulitic and foliated granitic rocks (columns 1, 2, 3).

Late Aphebian granites (column 9) are probably more quartz-rich than the Archean granitic rocks as they contain smaller amounts of most of the major and minor elements except for Mg and Mn. The discordant granitic bodies in banded migmatite (column 8) are very similar to the late Aphebian granites (column 9), but contain less Mn and Mg, and more Ca and Sr.

The means for banded migmatites (column 10) and porphyroblastic migmatites (column 11) are similar to one another, with the banded migmatites containing more Mn, Mg, Cr, and Cu, and less Ba than the porphyroblastic migmatites. The means for these migmatites also resembles those for nebulitic granitoid rocks (column 1).

The mean for quartz-biotite-feldspar gneiss (column 12) is similar to those for both nebulitic granitic gneiss (column 1) and banded migmatites (column 10). However this map unit contains more Cr, Cu, La, Sr, and V than any of the other Archean and Aphebian granitic rocks.

Means for Archean Mary River Group metabasalt (column 13) and metagabbro (column 14) are quite similar, with the metabasalt containing more Na, Co, Cr, Cu, and Ni, and less Ba and Zr. Means for mafic layers and inclusions in nebulitic granitoid gneiss (column 15) and banded migmatite (column 16) are remarkably similar to one another, and resemble the Mary River metagabbro (column 14) more than the metabasalt (column 13), although they do not resemble either closely. These mafic remnants contain more Ti, Al, Na, Ba, and Sr, and less Fe, Co, Cr, Cu, and Ni than the metagabbro. The similarity to one another suggests a similar source(s) for the mafic remnants in the nebulites and banded migmatites. In the field, Mary River Group remnants seem to occur in both map units (nebulitic granitoid gneiss, column 15; banded migmatite, column 16); but the variance between their means and the Mary River Group means suggests that there is either a large component from some other source that has modified the mean, or the mafic remnants represent a source other than the Mary River Group. Many of the values are intermediate between those for Mary River rocks (columns 13, 14) and Hadrynian diabases (column 17). Therefore an old mafic dyke swarm (e.g. map unit b – Table of Formations) may be a component. An analysis of a single sample from a mafic remnant in foliated granitic rocks (column 18) yielded results for many elements that are intermediate between the Mary River Group rocks and the mafic remnants (columns 15, 16).

Felsic metavolcanic rocks in Archean nebulitic granitoid gneiss (column 21) and in the Mary River Group (column 22) are remarkably similar. Those in the nebulites contain more Al, Ni, and Sr.

The differences between the Al means for oxide (column 23) and silicate (column 24) facies Mary River Group iron-formation are less than expected. The means for both facies include some analyses for aluminous facies rocks. Most of the aluminous facies analyses, however, which may contain as much as 50% of aluminous minerals, are included with the silicate facies samples. The oxide facies contains less Ti, Al, Mn, and Ba and more Co, Ni, Sr, Y, and Yb than the silicate facies.

Analyses of two metapelite remnants in banded migmatite yield a mean (column 27) that is very similar to the mean for Mary River Group metapelites (column 26) but does not resemble the Piling Group metapelite mean (column 28).

In summary, the spectrographic means for many of the map units may be placed in one of several groups (Group II not considered), the means in each group being more similar to one another than those outside the group. Also, some map units in some groups are more similar to one another than to other map units in the same group:

Group I:

(a) Archean nebulites (Amn), foliated granitoid gneisses (Amn^b, $gr\text{-}Agr^{cde}$), and Archean porphyritic granite (Agp) (*see* Mehnert (1968) for a definition of nebulite).

(b) Late Aphebian charnockitic rocks (Ack), late discordant granitic bodies in nebulites (Amn^i), and leucosome in banded migmatites (Amg^j).

Group III:

(a) Late discordant granitic bodies in banded migmatite (Amg^i), and porphyroblastic migmatite (Amp).

(b) Quartz-biotite-feldspar gneiss (bg).

Group IV:

(a) Mary River Group metabasalt (Mb), and Mary River Group metagabbro (Mg).

(b) Mafic remnants in nebulites (Amn^f), and mafic remnants in banded migmatite (Amg^g).

Group V:

Felsic metavolcanics in nebulites (Amn^h), and felsic metavolcanics in Mary River Group (Ma).

Group VI:

Metapelites in Mary River Group (M,M^1,Ms), and metapelites in banded migmatite (Amg^m).

Mean abundances (in weight per cent) and standard deviations for eleven elements, analyzed spectrographically, are shown in Figure 95. Eight of these elements (Al, Fe, Ti, Mg, Mn, Ba, Sr, Zr) occur within the limits of reliable detection in virtually every sample analyzed (Appendices 2-4, Table 48). Histograms of the spectrographic results for these eight elements were compared for twenty map units of which fifteen are shown in Table 49. This involved an examination of 120 histograms of which eight are shown in Figure 96 as examples of similar and dissimilar types.

The data in Table 49 show the conclusions drawn from the histograms and are constructed in a similar manner to distance charts for road maps. The value of one (1) is given to each pair of map units for which the histogram for each of the eight elements is similar. Thus the range of values (equivalency number) that each pair of map units may acquire is 0-8, and the more elements that are similar, the higher the number. The results are subjective, depend on the accuracy of the spectrographic analyses (*see* Appendices 1-3), and are probably affected by the mobilization of some elements during metamorphism. It was noted in compiling Table 49, for example, that histograms for elements Ba and Mn are similar for 12-13 of the 15 map units shown in the table.

Table 49 is an attempt to show whether or not the available spectrographic data for lithologically similar map units agree with field conclusions concerning their age relations and

a)

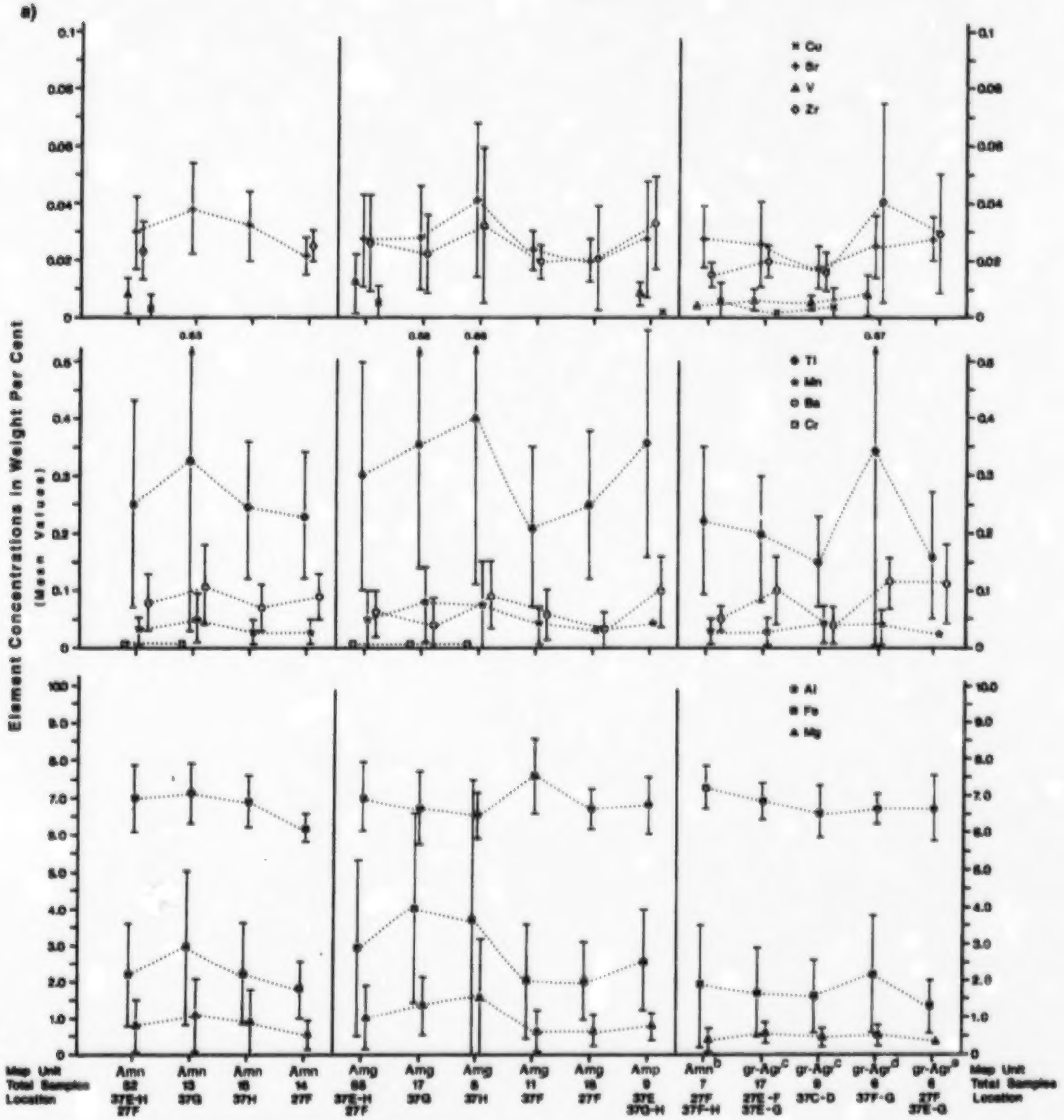

Notes: (1) Map unit symbols are those used on the published maps, indicated in Figure 1

(2) b: foliated granitoid component c: chiefly pink d: porphyritic e: migmatitic f: intermediate-mafic igneous component g: amphibolite and/or mafic igneous component i: late massive granitoid component j: leucosome l: anatectic o: oxide facies s: silicate facies

(3) vertical lines with bars show the standard deviations. (Not shown where identifying symbols are larger than s.d.)

(4) Basic data are shown in Appendix 1. Additional statistical data are provided in Table 4, and in Appendix 2.

Figure 95. *Line graphs for various map units showing mean abundances, in weight per cent, and the standard deviations for Al, Fe, Mg, Ti, Mn, Ba, Cr, Cu, Sr, V, and Zr.*

b)

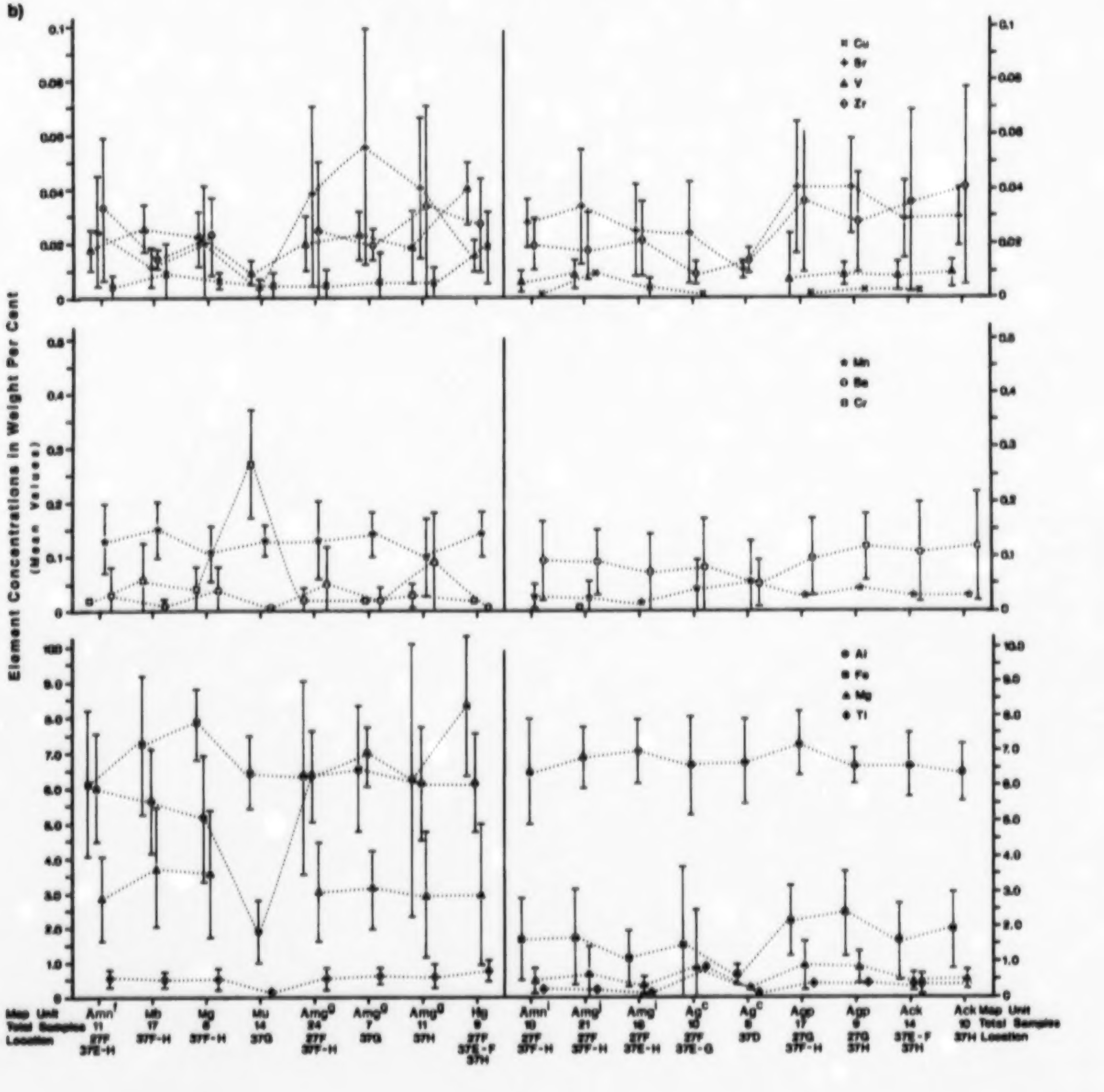

Figure 95. *(cont.).*

equivalencies. Units Amn and gr-Agr grade into each other in several places, and field relations suggest they may have a common origin and a similar age. Their equivalency number is 6.

Unit Ack is considered to include both younger Aphebian and older Archean intrusions that were metamorphosed by Aphebian granulite facies metamorphism. The unit shares an equivalency number of 5 with Amn, Amn^i, Amn^b, and Amg^i; and an equivalency number of 7 with gr-Agr and 8 with Amg^j. These are in agreement with field observations, but several bodies of Agp and Ag seem to be gradational with Ack in the field yet share equivalency numbers with one another and with Ack of only 2 or 3.

The highest equivalency numbers for Amg^j, the concordant leucosome in Amg, are 6 and 7, shared with Amn, Amn^b, and gr-Agr, rocks that may all be equivalent. The lowest values are 1 with Agp and 3 with Amp.

Small massive discordant bodies of late granitic rocks (Amn^i, Amg^i), are considered from field data to more likely represent small bodies of Aphebian Ag or Ack rather than the Archean granitic rocks (gr-Agr, Agp). Unit Amn^i shares an equivalency number of 4 with gr-Agr and Ag, 5 with Ack, but only 1 with Agp. Amg^i shares an equivalency number of 4 with gr-Agr, 5 with Ag and Ack, and 0 with Agp. The results are similar for both Amn^i and Amg^i, and may indicate that both Archean and Aphebian granitic rocks are represented, with Amg^i containing more Aphebian granitic rocks than Amn^i.

Archean Mary River Group amphibolite (Mb) is probably mostly metamorphosed pillowed basalt and shares an equivalency number of 4 with metagabbros (Mg) that are considered to be related to the Mary River igneous event (Table 7). Amphibolite remnants in units Amn (Amn^f) and Amg (Amg^g) share an equivalency number of 6 with each other and with Mb, but only 2 with Mg. This suggests that the amphibolite remnants in Amn and Amg more likely represent unit Mb than Mg.

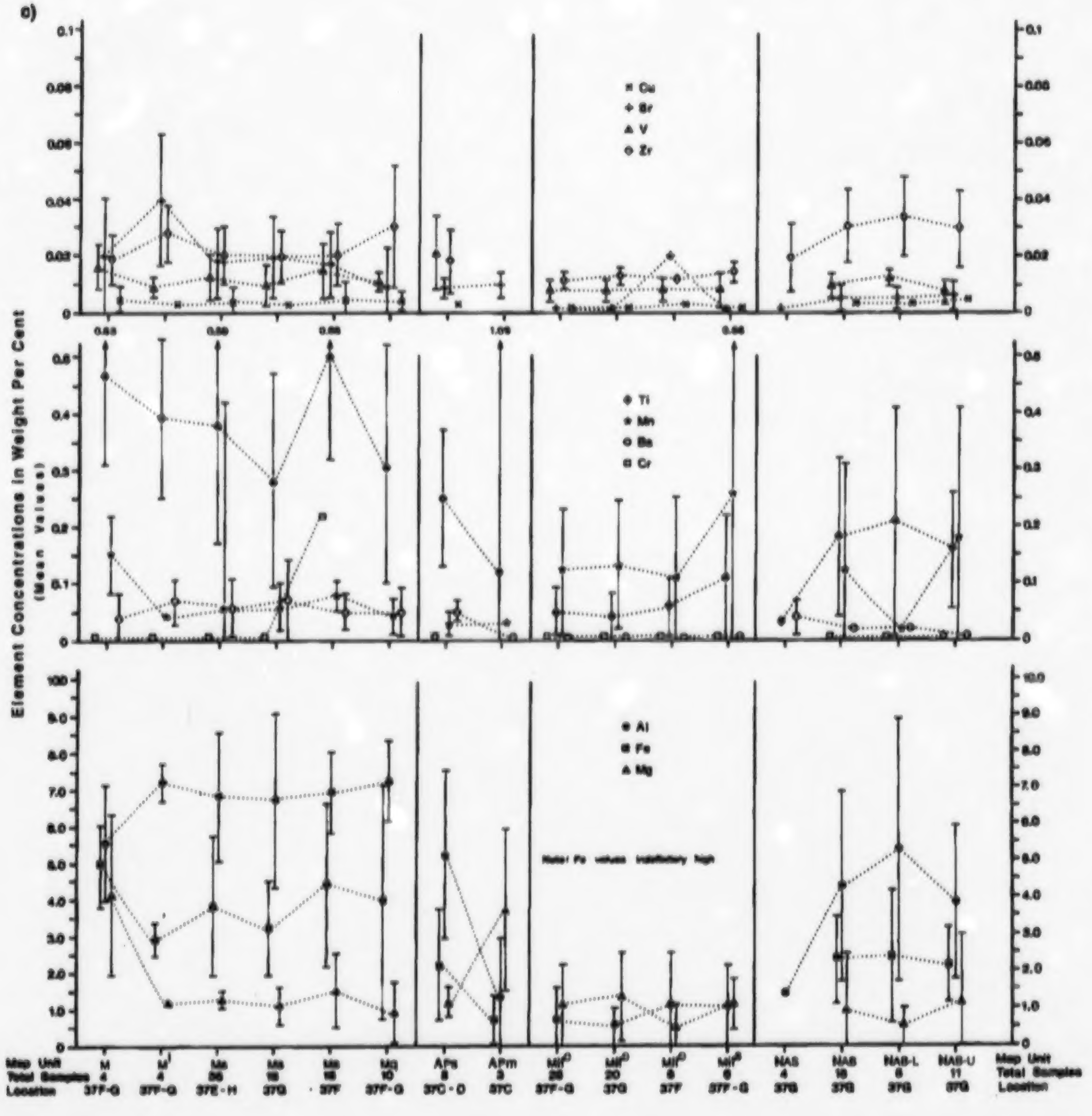

Figure 95 (cont.).

Table 49. Similarity of histograms for eight elements (Al, Fe, Ti, Mg, Mn, Ba, Sr, Zr) in the indicated map units.

Map unit	Amn^i	Amn^b	gr-Agr	Amp	Amg	Amg^j	Amg^i	Agp	Ack	Ag
Amn	2*	4	6	4	6	6	3	3	5	2
Amn^i		4	4	2	4	5	7	1	5	4
Amn^b			5	2	3	6	4	0	5	4
gr-Agr				3	4	7	4	1	7	3
Amp					2	3	1	4	3	1
Amg						4	4	3	4	1
Amg^j							5	1	8	4
Amg^i								0	5	5
Agp									2	2
Ack										3

Map unit	Mb	Mg	Amg^g
Amn^f	6	2	6
Mb		4	6
Mg			2

Notes:

*This "equivalency number" indicates the number of elements for which the histograms are similar (8 is the maximum possible). *See* Table of Formations for map unit symbols.
b - foliated granitoid component
f - intermediate-mafic igneous component
g - amphibolite and/or mafic igneous component
i - late massive granitoid component
j - concordant leucosome

Table 50. Baffin Island $\delta^{18}O$ determinations (Shieh and Schwarcz, 1978).

Rock type	Area	Samples	Range of $\delta^{18}O$	$\delta^{18}O$ mean
Quartzofeldspathic	66-72°N	69	Composite	8.1
Quartzofeldspathic	66-72°N	20	4.6-11.0	8.4
Quartzofeldspathic	South of 69°N	13	6.0-11.0	9.5
Quartzofeldspathic (High $\delta^{18}O$)	South of 69°N	11	9.0-11.0	10.2
Quartzofeldspathic (Low $\delta^{18}O$)	66-72°N	9	4.6-7.6	6.3
Quartzofeldspathic (Low $\delta^{18}O$)	North of 69°N	7	4.6-7.6	6.3
Pelitic	66-72°N	17	Composite	10.1
Pelitic	66-72°N	7	ca. 4.8-12	9.4
Cafemic	66-72°N	4	Composite	7.2
			Weighted average of composites	8.4

Oxygen isotopes

Shieh and Schwarcz (1978) determined $\delta^{18}O$ values for three of the Baffin Island composite samples analyzed by Shaw et al. (1967). They also analyzed 20 of the individual samples from the 69-sample composite for the quartzofeldspathic rocks and seven of the individual samples from the 17-sample composite for pelitic rocks. These 27 samples were selected at random. The results reported by Shieh and Schwarcz (1978) are summarized in Table 50. Shieh and Schwarcz

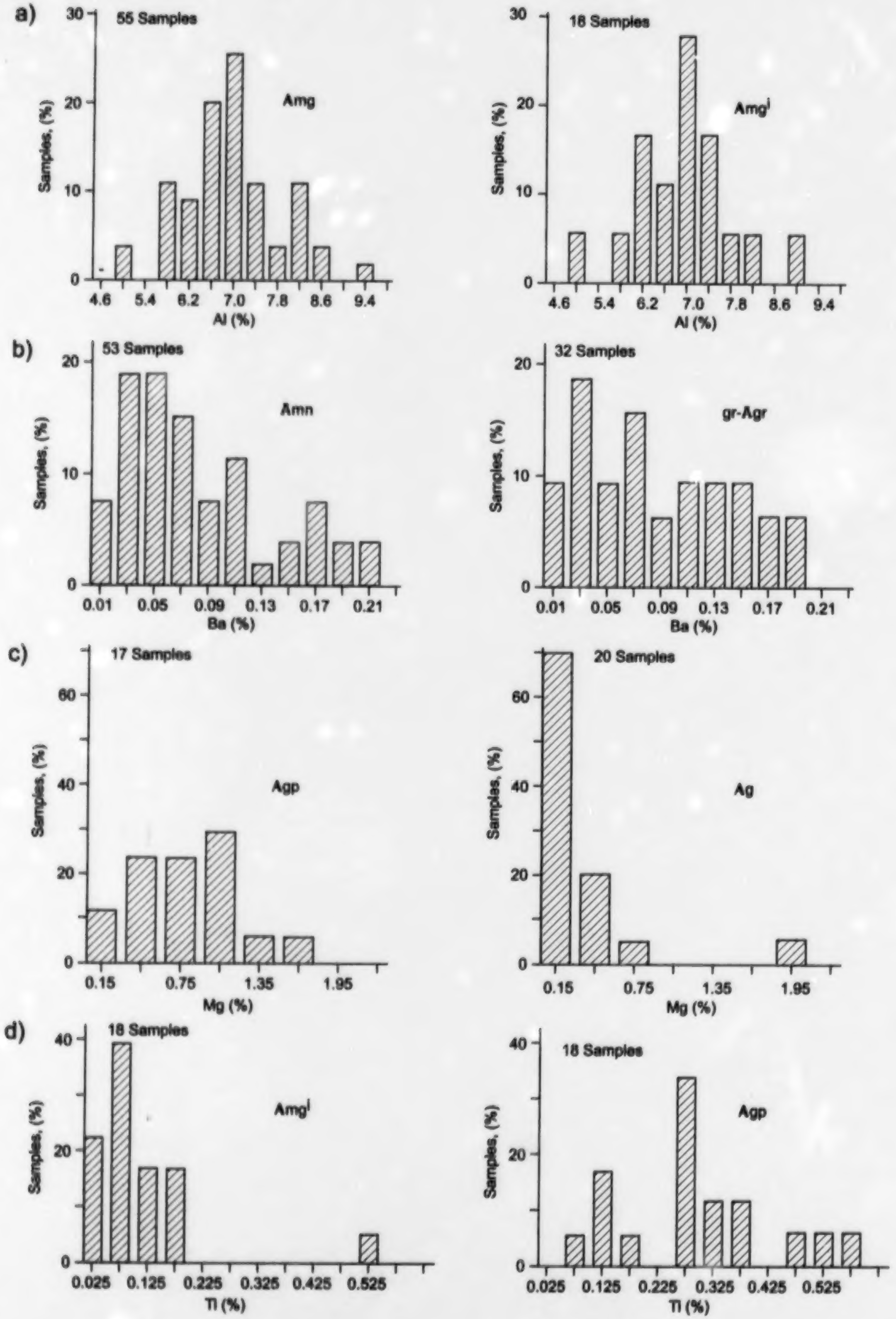

(1978) considered that the mean for quartzofeldspathic rocks is within the range shown for most granitic rocks of various ages, and saw no apparent correlation between SiO_2 content and $\delta^{18}O$. They did note a weak correlation in the metapelites, and that the ratios are similar to Archean metasediments elsewhere, but are considerably lower than those obtained for most late Proterozoic and Phanerozoic rocks of sedimentary origin. The cafemic mean is considered by Shieh and Schwarcz (1978) to be in the upper range of equivalent lithologies elsewhere.

Shieh and Schwarcz (1978) noted the bimodal distribution of their $\delta^{18}O$ values for quartzofeldspathic rocks, and that all of the 17 metapelite samples except one is from south of 69°N. After examining their sample distribution and comparing the locations with geological data the following observations may be made:

a) As noted by Shieh and Schwarcz (1978), all seven of the quartzofeldspathic samples from north of 69°N have low $\delta^{18}O$ values (4.6-7.6, mean = 6.3; Table 50). Five of these samples are from the map area and two are from just south of the map area. Four were taken from areas underlain by Archean nebulitic granitoid gneiss (Amn), one from an area of predominantly Archean foliated granitic rock (gr-Agr), one from an area of nebulites and banded migmatite, and one from an area of chiefly banded migmatite. Thus most of these seven samples probably represent Archean nebulites. All seven come from upper amphibolite facies terrane.

b) Small areas of nebulitic and banded granitoid basement gneisses occur on Cumberland Peninsula at the south end of the sampled belt (66-67°N). The two quartzofeldspathic samples that have yielded low $\delta^{18}O$ values from this region may have come from these (?)Archean basement gneisses.

c) Thirteen of the quartzofeldspathic samples analyzed individually were collected south of 69°N. All but the two noted in (b) above have $\delta^{18}O$ values (9.0-11.0, mean = 10.2, Table 50) similar to means for the metapelites (9.4, 10.1).

d) The quartzofeldspathic samples from south of 69°N probably represent mobilizate in Piling and Hoare Bay groups' migmatite, small and large granitic and charnockitic bodies that intrude the Piling and Hoare Bay supracrustal groups, and rocks that range in metamorphic grade from mid-amphibolite to granulite. A few samples might have come from Archean granitic rocks.

e) Six of the metapelite samples probably came from the Hoare Bay Group and ten from the Piling Group. The seventeenth sample came from a locality in the map area that is underlain by banded migmatite containing remnants of the Mary River Group.

Shieh and Schwarcz (1978) suggested that the quartzofeldspathic samples having low $\delta^{18}O$ values may represent rocks formed either by direct differentiation of basaltic-andesitic magma, or by partial melting of high grade gneisses in the lower crust that have values similar to basalts. In either case there seems to have been no major interaction with meteoric water since the emplacement of these rocks.

The metapelites and all but two of the quartzofeldspathic samples south of 69°N have similar high $\delta^{18}O$ values in spite of the presence of a large variety of rocks types, and a large variation in regional metamorphic grade. Shieh and Schwarcz (1978) suggested two possible explanations for this phenomenon:

1) the plutons and other quartzofeldspathic rocks were derived from the pelitic rocks through granitization and anatexis; and/or

2) the uniformity in $\delta^{18}O$ may be the result of isotopic exchange with the pelitic rocks through metamorphism.

A third possibility, that Aphebian granitic-charnockitic plutons reflect a mantle or deep crustal source with a peculiar isotopic composition, seems least likely. Also, Valley (1986) concluded that at present there are no convincing examples of large-scale, pervasive, lithostatically-pressured convection cells in metamorphic terranes. Hence large-scale isotopic homogenization is not likely. Therefore the larger plutons in this region would seem to represent remelted pelitic rocks. Valley (1986) cautions, however, that homogeneity can only be demonstrated by analysis of mineral separates, and that it is important to determine whether or not premetamorphic differences in isotopic ratios were present.

Samarium-neodymium and rubidium-strontium isotopic data for the Baffin Island quartzofeldspathic composite assembled by Shaw et al. (1967) and determined by McCulloch and Wasserburg (1978) are discussed in the "Regional geochronology" section.

REGIONAL GEOCHRONOLOGY

Four types of isotopic systems have been used to obtain ages for rocks and minerals on Baffin Island: Sm-Nd whole rock, Rb-Sr whole rock and mineral, U-Pb zircon and monazite, and K-Ar mineral and whole rock. Samarium-neodynium

Figure 96. *Examples of element histograms used to compare map units.* ***a)*** *Similar histograms for Al values in samples from banded migmatite* (Amg) *and late massive discordant granitic bodies in* Amg (Amg^{i}). ***b)*** *Similar histograms for Ba values in samples from nebulitic granitic migmatite* (Amn) *and foliated monzogranite-granodiorite* (gr-Agr). ***c)*** *Dissimilar histograms for Mg values in samples from porphyritic monzogranite-granodiorite* (Agp) *and massive monzogranite* (Ag). ***d)*** *Dissimilar histograms for Ti values in samples from late massive discordant granitic bodies in* Amg (Amg^{i}) *and massive porphyritic monzogranite-granodiorite* (Agp).

model ages for composite samples were determined by McCulloch and Wasserburg (1978). Most of the rest of the ages discussed here were determined at the Geochronology Laboratory of the Geological Survey of Canada, Ottawa. Where necessary, Rb-Sr ages have been recalculated using $M = 1.42 \times 10^{-11} a^{-1}$ (e.g. Wanless and Loveridge, 1978), and K-Ar ages have been corrected to reflect the new constants now in use.

The $\delta^{18}O$ data (Table 50) of Shieh and Schwarcz (1978) support Sm-Nd, U-Pb, and Rb-Sr data, and fieldwork, in identifying a major break in Baffin Island geology that coincides approximately with the Piling Fault Zone (*see* Fig. 111, 112) that separates subdomains 3a and 3b south of the north side of the Foxe Fold Belt (e.g. Jackson and Taylor, 1972; Jackson and Morgan, 1978a). The $\delta^{18}O$ data also indicate the presence of Archean crust in the southeastern part of Cumberland Peninsula.

Some age determinations noted here may be too imprecise to accurately date specific events, or to be accepted on their own. Many of these, however, coincide, or are in general agreement, with more precise determinations for rocks within the map and/or in adjacent regions. Used with caution they can help to indicate possible relationships that might be worth examining in more detail.

U-Pb zircon and monazite ages

Five U-Pb zircon concordia intercept ages were published several years ago for rocks within the map area, another for monzogranite northwest of the map area and three for granite-charnockite to the south (Jackson et al., 1990b). Eleven other published and four unpublished U-Pb zircon ages were produced earlier (Table 51, Fig. 98). A large number of additional U-Pb zircon and monazite igneous and metamorphic ages, not noted in Table 51, have been reported in several recent studies in north-central Baffin Island (Henderson and Parrish, 1992; Henderson and Henderson, 1994; Scammell and Bethune, 1995a, b), and in southernmost Baffin Island (e.g. Scott, 1996, 1997; Scott and Gauthier, 1996). Most of these ages occur in two age bracketts, ca. 2770-2709 Ma (north-central to north Baffin Island) and 1959-1806 Ma (central and south Baffin Island). A large number of laser-ablation Pb/Pb ages for single zircon grains from the Lake Harbour Group in southernmost Baffin Island range from 2471-1837 Ma (Scott and Gauthier, 1996). Three of the oldest U-Pb zircon ages are 2851 +20/-17 Ma (Fig. 27) for foliated tonalite that is basement to the Mary River Group in the map area and from the Eqe Bay area just south of the map area, ca. 2.84 Ga for a granite cobble in Piling Group conglomerate (Scammell and Bethune, 1995a, b), and 2888 ± 35 Ma for felsic metavolcanics (Mary River Group – discussed below) at Eqe Bay just south of the map area (Morgan, 1982) – are distinctly older than most other zircon ages (Fig. 98), and are considered here to represent continental crust that predates the Mary River Group. The 2850-2840 Ma detrital zircons in the Dewar Lakes quartzite of the Piling Group (Henderson and Parrish, 1992) probably came from this crust.

Table 51. Zircon U-Pb isotopic ages, Baffin Island.

Rock type	Map unit	Map area	Age (Ma)	Location	References
Porphyritic monzogranite	Agp	37G	2709 +4/-3	71°32′N; 77°26′W	This memoir; Jackson et al. (1990b)
Felsic metavolcanics	Ma	37G	2718 +5/-3	71°06′N; 77°23′W	"
Foliated tonalite	gr-Agr	37G	2851 +20/-17-U 1711-L	71°02′N; 77°31′W	"
Amphibolite[1]	Amg	37H	2734 +59/-45-U 1800-L	71°09′N; 75°23′W	"
Monzogranite[1]	Amg	37H	2522 +11/-10-U 1525-L	71°09′N; 75°23′W	"
Monzogranite	Ag	48D	2500-U 1522-L	73°20′N; 77°20′W	"
Banded granitic gneiss	Agn	37C	2713	69°51′N; 77°10′W	Morgan (1982)
Mary River Group, felsic metavolcanics	AMav	37C	2888 ± 35	69°43′N; 76°40′W	Morgan (1982)
Mary River Group, felsic metavolcanics	AMav	37C	2742 ± 28*	69°40′N; 76°48′W	Morgan (1982)
Pegmatite	AKgn	27D	1806 +15/-8	69°33′N; 76°53′W	Henderson (1985a); Henderson and Loveridge (1981)
Banded granitic gneiss	Agn	37D	2723 ± 44*	69°06′N; 75°14′W	Morgan (1983)
Granite-charnockite	AHg	27A	1895 +47/-21	68°04′N; 66°53′W	Henderson (1985b)
Charnockite[2]	AHg	27B	1853 +15/-11	68°09′N; 68°29′W	Henderson (1985b); Jackson et al. (1990b)
Charnockite[3]		26N	1870-1900	67°04′N; 68°34′W	This memoir; Jackson et al. (1990b)
Charnockite in migmatite		25N	1857 +21/-6	63°45′N; 68°32′W	This memoir; Jackson et al. (1990b)
Charnockite		26I	1870 ± 20	66°05′N; 65°45′W	Pidgeon and Howie, 1975

Note: The samples above the dashed line are from the map area. U-upper intercept, L-lower intercept.
1 - Samples are from the same outcrop. 2 - Monazite ^{207}Pb/^{206}Pb ages of 1833 ± 1.2 Ma and 1831 ± 1 Ma also obtained.
3 - Monazite ^{207}Pb/^{206}Pb age of 1854 ± 2 Ma also obtained. *Recalculated after Morgan (1982, 1983) were published.

Ages within the bracket 2752-2709 Ma are for the Mary River Group and for some associated granitic gneisses and plutons. Mary River Group felsic metavolcanics (Ma) within the map area have provided a precise zircon age of 2718 +5/-3 Ma (Fig. 54). Ages of ca. 2.72 Ga (Scammell and Bethune, 1995a, b) and 2752 ± 30 Ma and 2888 ± 35 Ma (Morgan, 1982) have been obtained for these rocks south of the map area. Morgan's ages are considered, for reasons given in discussing the age of the Mary River Group, to be less definitive than the newer ages presented here. Also, when considered together, the four points for the two ages reported by Morgan (1982) indicate an age of 2742 Ma, which is similar to the zircon age of 2734 +59/-45 Ma obtained for (possibly Mary River) amphibolite (Fig. 64) in migmatite near the head of Cambridge Fiord (NTS 37H). Data for the amphibolite gave a lower intercept age of 1800 Ma.

Banded granitic gneiss (Agn), basement to the Aphebian Piling Group south of the map area (Morgan, 1982, 1983), has yielded U-Pb zircon ages of ca. 2.77 (Scammell and Bethune, 1995a, b), and 2713 Ma and 2723 ± 40 Ma (Table 51). This unit probably includes gneisses that are both basement to the Archean Mary River Group and migmatites derived from the group. Similar zircon ages of 2709 +4/-3 Ma (Fig. 57; Table 51) and ca. 2.72 Ga (Scammell and Bethune, 1995a, b) have been obtained for a large plutonic body of porphyritic monzogranite (Agp) in map area NTS 37G, and a similar body in the Eqe Bay area respectively. Although it is not certain if the body in map area NTS 37G intrudes the Mary River Group, smaller, similar intrusions do. These ages imply that 43-9 Ma may have elapsed between Mary River Group deposition and intrusion of Agp granites.

The younger group of zircon ages (1959-1806 Ma) are for zircons and monazites from granite, charnockite, pegmatite, and the Piling Group and Lake Harbour Group supracrustals. The ages are for primary igneous and metamorphic crystals, and for detrital grains. Ages of 1806 Ma for two late- to post-tectonic pegmatites in the Foxe Fold Belt (Henderson, 1985a) and an age of ca. 1819 Ma for a post-tectonic granite in the Eqe Bay area (Scammell and Bethune, 1995a, b) are similar to the lower intercept age of 1800 Ma for 2734 Ma amphibolite at the head of Cambridge Fiord. These ages may be related to a relatively young thrusting event along the northeast side of Baffin Island discussed below (Northeast Baffin Thrust Belt) for which an age of ca. 1810 Ma is assumed.

Many of the ages in the 1959-1806 Ma range are for a huge anastomosing plutonic complex of charnockitic and associated granitic rocks, the Cumberland Batholith (Jackson et al., 1990a, b) and related satellite intrusions. The batholith extends from Home Bay westward to Foxe Basin and south to Cumberland Peninsula, Frobisher Bay, and south and west of Amadjuak Lake (Jackson and Morgan, 1978a). For the northern part of the batholith, two unpublished ages of 1836 Ma and 1959 Ma bracket the remainder of the group, which range from 1853 +15/-11 to 1895 +47/-21 Ma (Fig. 98; Table 51). Uranium-lead monazite ages of 1831 ± 1, 1833 ± 1.2, and 1854 ± 1.9 Ma have also been obtained from two samples (Jackson et al., 1990b). Zircons from two of the samples dated contain odd "vein-like" zones of zircon within zircon. Determinations for one of these samples are discordant, not collinear, and form a nonlinear array that indicates a possible lower intercept age of about 1900-1870 Ma. These results suggest that some older, possibly Archean zircons are present, have had a complex history, and were not completely remelted and/or recrystallized during an 1900-1830 Ma tectonothermal event.

Monzogranites at the head of Cambridge Fiord (NTS 37H) and northwest of the map area (NTS 48D) have provided U-Pb zircon upper intercept ages of 2522 +11/-10 Ma and 2500 Ma respectively (Table 51). Although the data points for both are collinear, they are very discordant and lie closer to the lower intercept ages of 1525 and 1522 Ma than the respective upper intercept ages of 2522 and 2500 Ma. The zircons dated are considered to be mixtures of late Archean zircons and of Aphebian igneous zircons grown in a melt formed from Archean parent rocks (Jackson et al., 1990b). The ages are not considered accurate because of the large discordances of the data points. It is noted that the upper intercept ages are similar to the peak of Nd T_{DM} model ages at 2.5-2.4 Ga obtained recently for the Baffin Orogen and discussed below. However, the monzogranite sample from northwest of the map area (NTS 48D) gave a Nd T_{DM} model age of 2.71 Ga which supports the conclusion given above that the protolith was Archean.

Sm-Nd ages

A regional setting was provided by the Sm-Nd and Rb-Sr model ages determined by McCulloch and Wasserburg (1978) on the Baffin Island quartzofeldspathic composite sample assembled by Shaw et al. (1967). McCulloch and Wasserburg (1978) detailed several assumptions and obtained a T Nd/CHUR model age of 2.74 ± 0.05 Ga and a T Sr/UR model age of 2.56 ± 0.03 Ga. They concluded that the continental crust of the Superior, Slave, and Churchill provinces (including Baffin Island) were all formed at about 2.7-2.5 Ga, and that this was a unique period in geological history. McCulloch and Wasserburg (1978) concluded that the Sm-Nd systematics are not substantially disturbed during sedimentation, diagenesis, or during remelting and metamorphism in a closed system. Jackson and Morgan (1978a) concluded that a large part of Baffin Island is underlain by Archean granitic rocks emplaced or metamorphosed about 2.8 Ga ago, and that at least two later major orogenic episodes are represented, one at about 2600-2550 Ma and the other 1964-1600 Ma ago. Data now available (*see* above section) suggest orogenic events at 2.85-2.84 Ga, 2.77-2.71 Ga, 1.90-1.81 Ga, and possibly at about 2.50 Ga.

The model age of 2.74 Ga is for a composite sample and may represent an average for samples both considerably younger and older than that age. This, however, does not appear to be the case on the basis of U-Pb and Rb-Sr age determinations, which to date have yielded relatively few indications of the presence of rocks significantly older than 2.74 Ga.

E. Hegner has analyzed about 160 samples from a large part of the northeastern Canadian Shield for Sm and Nd and used the analyses to calculate Nd T_{DM} model ages in joint projects with the author (117 samples) and T. Frisch (about 40 samples). The samples are from northeastern Quebec to northern Labrador, the Cape Smith region of northwestern Quebec, Baffin Island, Devon and Ellesmere islands, and Boothia Peninsula (Hegner and Jackson, 1990; Jackson et al., 1990a; Jackson and Hegner, 1991). As expected, the results for Baffin Island indicate that the T Nd/CHUR model age of 2.74 Ga by McCulloch and Wasserburg (1978) was an average age for rocks having a large range of ages (*see* Fig. 98). The two largest concentrations of Nd model ages for Baffin Island (3.0-2.7 Ga, 2.6-2.3 Ga) peak at 2.9-2.8 Ga and 2.5-2.4 Ga. Smaller peaks range from 3.7-3.6 Ga to 2.0-1.9 Ga. The oldest Nd T_{DM} model ages obtained (Hegner and Jackson, 1990) range from 3.7-3.3 Ga and occur in Baffin Island from Cumberland Peninsula northward. These older ages are obtained for map units Agn and Amn, or rocks similar to them that from field relations were considered to be relatively old. The range in ages obtained is similar to that obtained for rocks of the Nain Province in Labrador.

The major Nd T_{DM} model age concentration at 3.0-2.7 Ga and a small concentration at 3.1-3.0 Ga are present in both north and south Baffin Island (*see* Fig. 98), the former being represented throughout the island. As noted above, several U-Pb zircon ages for northern Baffin Island are concentrated in the 2.9-2.7 Ga range. Some of the latter ages were obtained for the same individual samples that also provided 3.0-2.7 Ga Nd T_{DM} model ages. Geological relations and the age determinations indicate that 2.9-2.7 Ga is a more accurate age for the late Archean episode of crustal separation from the mantle and formation of continental crust than the 2.7-2.5 Ga age suggested by McCulloch and Wasserburg (1978). Most of the Archean continental crust on Baffin Island was probably emplaced as juvenile crust about 2.9-2.7 Ga ago.

Archean and Aphebian granites and charnockites in northern Baffin Island all yield similar Nd model ages of 3.2-2.7 Ga which suggest they might all be about the same age (Jackson et al., 1990a). However, the Archean granites gave U-Pb zircon ages of 2.85-2.71 Ga whereas U-Pb data for the Aphebian granites indicate that Aphebian magmatic zircons grew in a melted Archean protolith where they were mixed with Archean zircons (Jackson et al., 1990b). The charnockites of northern Baffin Island may include Archean plutons that were metamorphosed in the late Aphebian, or Aphebian premetamorphic to synmetamorphic plutons, or both. Neodymium model ages of 2.90-2.85 Ga and U-Pb zircon ages of 2.75-2.71 Ga for Mary River Group volcanics and two late Archean granitic plutons suggest that these particular rocks may have been derived from somewhat older crust that was melted and recrystallized. Northern Baffin Island, including the map area, is part of a region (Committee Orogen) that is sandwiched between two late Aphebian orogenic regions, the 2.0-1.9 Ga Thelon Tectonic Zone on the north and the 1.90-1.84 Ga Baffin Orogen, part of the Trans-Hudson Orogen, on the south (*see* Fig. 110-112). The late Aphebian thermal and tectonic overprints identified by field and age determination studies (Tables 51-53; Jackson, 1978a, b; Jackson et al., 1990b) are probably related to formation of these orogenic belts which, however, is not reflected in the Nd model age for Baffin Island north of the Foxe Fold Belt (Jackson et al., 1990a).

Granitic plutons and gneisses within the Baffin Orogen of southern Baffin Island (Baffin Island south of latitude ca. 69°30′) (Jackson et al., 1990a, b) that are thought to be Archean yield Nd model ages of 3.4-2.6 Ga, concentrated at 3.0-2.7 Ga as on northern Baffin Island.

The second major concentration of Nd T_{DM} model ages for Baffin Island range from 2.6-2.3 Ga (peak at 2.5-2.4 Ga) and represent late Aphebian metasedimentary rocks of the Baffin Orogen and its granite-charnockite core, the Cumberland Batholith. To date, only two discordant U-Pb zircon ages for bedrock (discussed above) that are in this range, both from northern Baffin Island, have been determined (Jackson et al., 1990b). Numerous ages for detrital zircons from the Lake Harbour Group of southern Baffin Island also lie within the 2.6-2.3 Ga range, although most are younger (Scott and Gauthier, 1996). Uranium-lead zircon and monazite ages, including some for the same charnockite samples dated by Sm-Nd, range from 1.95-1.84 Ga. The U-Pb zircon ages of 2.18-2.16 Ga for detrital zircon in Piling Group (Henderson and Parrish, 1992) quartzite give a maximum age for the quartzite. The source of this zircon is not clear (*see* Fig. 98), but the source rock may have been ingested into the Cumberland Batholith (Henderson and Parrish, 1992). The Nd T_{DM} model ages of 2.2-1.9 Ga for the mafic and ultramafic rocks in the three supracrustal sequences surrounding the Cumberland Batholith (Hegner and Jackson, 1990; Jackson and Hegner, 1991) and a U-Pb zircon age of 1883 Ma for diorite in the lower Piling Group (Henderson and Parrish, 1992) suggest an age of about 1.9 Ga for the Piling Group. Jackson and Morgan (1978a) concluded that the Cumberland Batholith represents both young granitic intrusions, metamorphosed and deformed after emplacement, and Archean granitic rocks (also indicated by McCulloch and Wasserburg, 1978), remobilized and re-emplaced during a late Aphebian tectono-metamorphic event accompanied by granulite metamorphism. It is concluded from field relations, such as gradations between granite-charnockite on the one hand and paragneiss, migmatite, and nebulitic gneiss on the other (e.g. Jackson and Morgan, 1978a), and geochronology, that most of the Cumberland Batholith is a mixture containing considerable ca. 1.90 Ga juvenile crust, Aphebian supracrustals, and Archean crust. These components were melted, mixed so as to give intermediate Nd model ages, and emplaced at about 1.85 Ga. Probably not more than 50 Ma elapsed between the mafic volcanism and granite emplacement, and granulite metamorphism during the Baffin Orogeny (Jackson and Hegner, 1991).

Rb-Sr ages

Most Rb-Sr whole rock isochron and errorchron ages for rocks within the map area and elsewhere on Baffin Island are included in Table 52 (*see* Jackson, 1978a, b for several other errorchron ages). Three of these ages range from 2476 ± 72 Ma to 2642 ± 43 Ma and were obtained for various groupings of gneissic granitic samples from basement to the Mary River Group (Jackson, 1978b; Wanless and Loveridge, 1978). Two of the gneissic granite samples were collected from basement that has undergone potassium metasomatism adjacent to a younger Aphebian monzogranite body intruding the Mary River Group, and yielded a Rb-Sr age of 1930 Ma. A third sample (6 = JD40A-65; *see* Jackson, 1978b) is from the basal part of the Mary River Group (Jackson, 1978b). According to Wanless and Loveridge (1978), the data indicate that the samples do not represent a unique suite of rocks in which the systems have remained unaltered subsequent to final emplacement or metamorphism. They also suggest the indicated initial $^{87}Sr/^{86}Sr$ ratios are a little high for mantle rock suites of this age and would be compatible with the basement rocks having been emplaced originally about 2900 Ma ago. This conclusion is supported by the recently determined U-Pb zircon age of 2851 +20/-17 Ma for basement rocks to the Mary River Group (Table 51).

Gneisses that are basement to the Piling Group in the McBeth Gneiss Dome south of the map area (NTS 27C) have yielded Rb-Sr errorchron ages of 2697 and 2400 Ma and a younger errorchron age of 2033 Ma that is interpreted as an overprint (Table 52). An age in excess of 3930 Ma or 3310 Ma is indicated for one sample, which is either a remnant of

Table 52. Rb-Sr isochron age determinations, Baffin Island.

Rock type	Map unit	Map area	Age (Ma)	Intercept	MSWD	Location	References
Foliated and nebulitic granitic rocks	Agn	37G	I 2642 ± 43 I 2600 ± 68 I 2476 ± 72	0.7054 ± 0.0006 0.7057 ± 0.0012 0.7063 ± 0.0016	0.13 1.47 2.53	71°27'N; 79°47'W 71°27'N; 79°47'W 71°27'N; 79°47'W	Jackson (1978b); Wanless and Loveridge (1978)
Foliated and nebulitic granitic rocks	Amn, gr-Agr	27F	E 2159	0.7109		70°12'N; 69°50'W (ca.)	Jackson (1984); this memoir
Mary River Group, metasediments, mafic metavolcanics	Ms, Mb	37G	I 1971 ± 97	0.7102 ± 0.0016	1.49	37G/5	Jackson (1978b); Jackson and Morgan (1978a); Fryer (1971a, b)
Massive and nebulitic metacrystic granite-granodiorite	1	48B	I 2321 ± 76	0.7035 ± 0.0007	2.0	72°55'N; 85°40'W	Jackson et al. (1985, 1990b); Jackson and Sangster (1987)
Metamorphosed dykes: mafic, ultramafic	1	48B	E 1130 ± 79	0.7078 ± 0.0007		71°55'N; 85°40'W	Jackson et al. (1985, 1990b); Jackson and Sangster (1987)
Mary River Group mafic metavolcanics	Ammv	37C	E 2155 ± 122			69°38'N; 77°W	Morgan, 1982
Massive granite Massive granite	Ag Ag	27C 27C	E 1738 E 1756			69°31'N; 71°50'W 69°31'N; 71°50'W	Henderson (1985a) Henderson (1985a)
Nebulitic and foliated granitic rocks	Akgn	27C	E 2697 E 2400	0.6999	4.69	69°29'N; 70°30'W	Jackson (1978a); Wanless and Loveridge (1978); Henderson (1985a)
Nebulitic, foliated and massive granitic rocks, biotite paragneiss, amphibolite	Akgn, APs	27C	E 2033	0.7168	8.49	69°29'N; 70°30'W	Jackson (1978a); Wanless and Loveridge (1978); Henderson (1985a)
Banded granitic migmatite	Akgn	27B	E 1592 E 1633			68°37'N; 70°55'W 68°37'N; 70°55'W	Henderson (1985b) Henderson (1985b)
Massive charnockite	Ahg	27B	I 1730 ± 49	0.7149 ± 0.0034	0.33	68°9'N; 68°30'W	Henderson (1985b), Jackson and Morgan (1978a); Jackson et al. (1990b)
Migmatite (includes monzocharnockite)	3	25N	I 1877 ± 45	0.7047 ± 0.0028	0.38	63°45'N; 68°32'W (Frobisher Bay)	Blackadar (1967b); Jackson and Morgan (1978a); Jackson et al. (1990b)

Notes: I = isochron, E = errorchon. The samples above the dashed line are from the map area. Ages are based on the decay constant of $1.42 \times 10^{-11} a^{-1}$.

ancient material, or is from a rock that has undergone extensive radiogenic ^{87}Sr enrichment and/or rubidium depletion (Jackson, 1978a; Wanless and Loveridge, 1978). The same sample gave a Nd T_{DM} model age of 3.2 Ga (Jackson et al., 1990a).

Mary River metasediments, basic and felsic metavolcanics, and metagabbro from the Mary River area (NTS 27G) have been analyzed for Rb and Sr isotopes by Fryer (1971a, b). One suite of metasediments and basic volcanics yields an isochron of 1971 ± 97 Ma (Table 52, Fig. 97; Jackson, 1978b). Various groupings of samples and lithologies yield four isochrons (including 1971 Ma) that range from 1987 ± 124 to 1935 ± 45 Ma and three errorchrons that range from 2382 to 2018 Ma. All but one of the initial ratios are about 0.710. This is high for mantle derived rocks of this age, suggesting an older emplacement age for these rocks, which has now been indicated by the Archean Nd model ages and U-Pb zircon ages noted above. The isochron ages around 1971 Ma are taken to be metamorphic ages and to represent homogenization during the last regional intermediate- to high-grade metamorphism to affect northern Baffin Island. The errorchron ages probably are the result of the samples having been collected from two areas about 27 km apart. They may indicate an older emplacement age for these rocks.

A Rb-Sr errorchron age of 2159 Ma (Fig. 23) was obtained for four samples of nebulitic granitic rocks (Amn) and three samples of foliated granitic rocks (gr-Agr) in the Clyde River (NTS 27F) map area. The samples of Amn by themselves yield a slightly younger age and the gr-Agr samples an older age. The high initial ratio of 0.7109 suggests that 2159 Ma is a minimum, metamorphic age. The imperfect alignment of data points is probably related chiefly to the samples having been collected over a distance of 60 km (southwest-northeast). Similar Rb/Sr ages occur in the Mary River area (as discussed above) and adjacent to the map area (Table 52; Jackson, 1978a, b).

A Rb-Sr isochron age of 1730 ± 49 Ma has been obtained for potassium feldsparphyric massive charnockite that intrudes the Piling Group along the south side of the Foxe Fold Belt west of Nudlung Sound in southeastern map area NTS 27B (Table 52; Jackson and Morgan, 1978a; Jackson et al., 1990b). The isochron has a MSWD (mean square of the weighted deviates) of 0.33 with a high initial ratio of 0.7149. The same sample has recently yielded a U-Pb zircon age of 1853 +15/-11 Ma (Table 51), and monazite (cooling?) ages of 1831 ± 1 and 1833 Ma. Tabular charnockitic bodies in the region west of the site sampled for the Rb-Sr and zircon charnockite ages in southeast map area NTS 27B (*see* above; Jackson et al., 1990b) have been deformed and boudined on a large scale. Rocks in the Foxe Fold Belt north of the Cumberland Batholith have yielded Rb-Sr mineral and whole rock ages of 1756-1592 Ma and one U-Pb zircon age of 1806 Ma (Henderson and Loveridge, 1981; Henderson, 1985a, b; Tables 51, 52). These data and ages suggest that the region was affected by a slightly younger (resurgent?) event, less intense than the one that produced the granulite metamorphism. However, most K-Ar and Rb-Sr ages for rocks in the region about the dated charnockite, on the north side of the Cumberland Batholith west of Nudlung Sound, range from 1.7 to 1.6 Ga (Jackson et al., 1990b). It is also likely that the range in ages determined by the various methods indicates a period of prolonged cooling between 1.85 Ga and 1.6 Ga.

Samples from granulite migmatite at Iqaluit, near the south tip of the Cumberland Batholith have provided a Rb-Sr isochron age of 1877 ± 45 Ma (Table 52; Jackson et al., 1990b). One component of the migmatite is a tabular massive granite-charnockite intrusion 1-2 m thick. A sample of this intrusion was used for the Rb-Sr isochron and has yielded a zircon age of 1857 +12/-6 Ma (Tables 51, 52). Potassium-argon mineral ages from the Frobisher Bay area range between 1.84 Ga and 1.5 Ga. The pattern indicated by the above ages, and possibly the absence of monazite, suggest relatively rapid initial cooling following peak metamorphism, compared with the region west of Nudlung Fiord. Distribution of metamorphic facies and P-T determinations (e.g. Berman et al., 1993) suggest that rapid cooling would more likely have been caused by relatively rapid uplift than by relatively shallow emplacement of the southern end of the Cumberland Batholith.

A combined Rb-Sr whole rock isochron age of 2321 ± 76 Ma (Table 52) was obtained for the two youngest components (granite-granodiorite) of a four-component migmatite on northwestern Baffin Island (Jackson et al., 1985, 1990b). Metamorphosed mafic to ultramafic dykes that intrude the oldest, but not the two youngest, components gave an isochron age of 1130 ± 79 Ma. This is similar to a Rb-Sr whole rock errorchron age of 1129 Ma indicated by some of the points obtained for nearby Nauyat basalts (*see* Jackson et al., 1990b). Neither age is a primary emplacement age, and both may be related to subgreenschist facies metamorphism accompanying the closing of the Poseidon Ocean and/or movement along major northwest-trending faults in the region (Jackson and Iannelli, 1981).

All but one of the available Rb-Sr ages are for central and northern Baffin Island. Isochron ages, and errorchron ages with MSWD values less than 5.5, delineate five age groups (Table 51; Jackson, 1978a, b; McCulloch and Wasserburg, 1978; Wanless and Loveridge, 1978; Jackson and Iannelli, 1981; Jackson and Sangster, 1987; unpub. data by the Geochronology Section). These age groups are: 1) 2697-2476 Ma, 2) 2389-2255 Ma, 3) 1987-1935 Ma, 4) 1730 Ma, 1703 Ma, and 5) 1131 Ma, 1129 Ma.

Group 1 is probably related to the same events that provided the 2.9-2.7 Ga U-Pb zircon ages in northern Baffin Island (Fig. 98). Group 3 may be related to the 1.95-1.80 U-Pb zircon ages in similar fashion. Mineral and whole rock errorchron ages with MSWD values greater than 5.5 range from 2635-1592 Ma. Eight of these are concentrated between 2230 and 2018 Ma, bridging the gap between groups 2 and 3 listed above. Two (1756 Ma, 1738 Ma) approximate the 1730 Ma metamorphic age for charnockite in group 4.

K-Ar ages

K-Ar ages determined for the map area are listed in Table 53 and shown on Figure 97. Biotite and muscovite ages for Aphebian and Archean igneous and metamorphic rocks

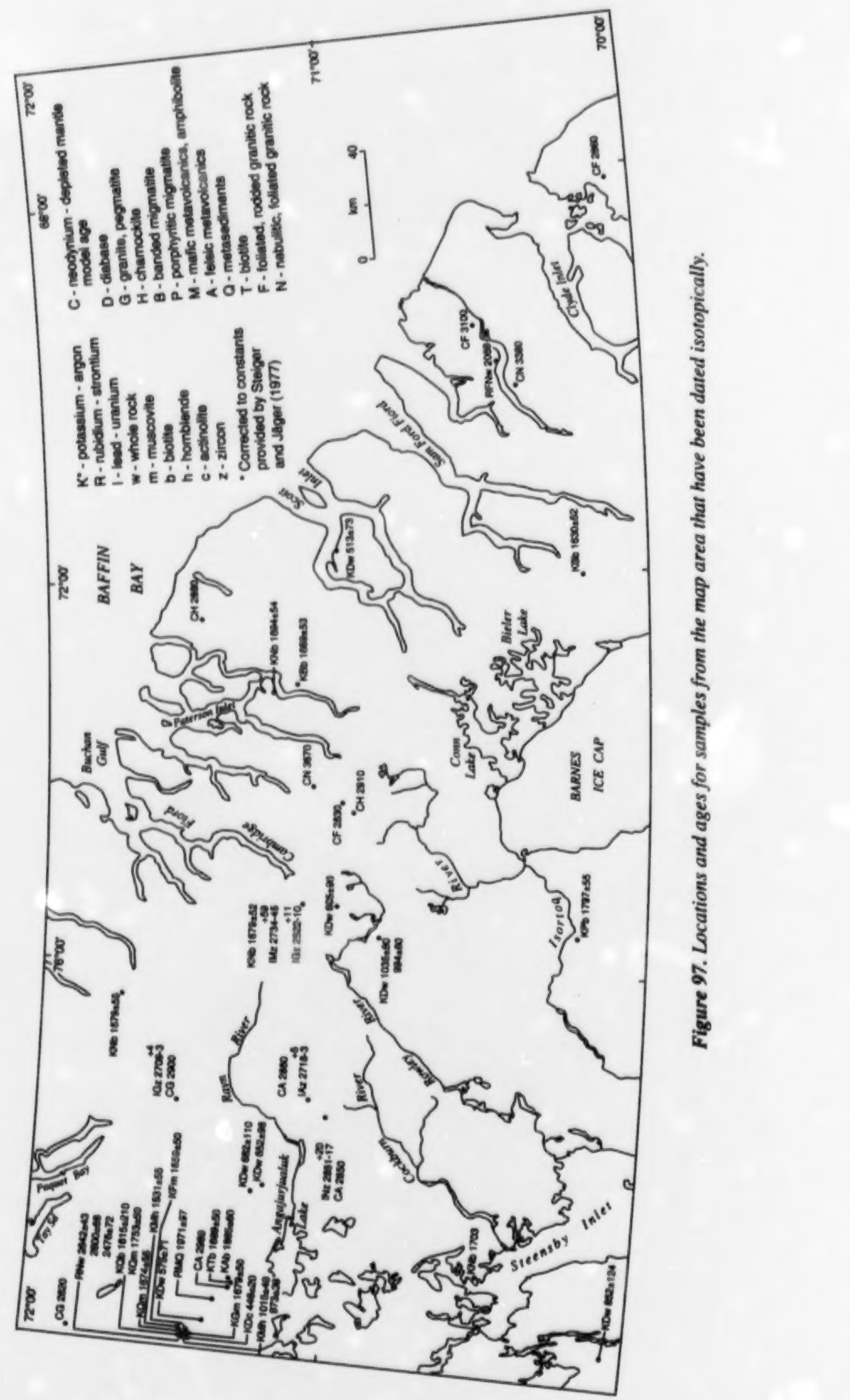

Figure 97. *Locations and ages for samples from the map area that have been dated isotopically.*

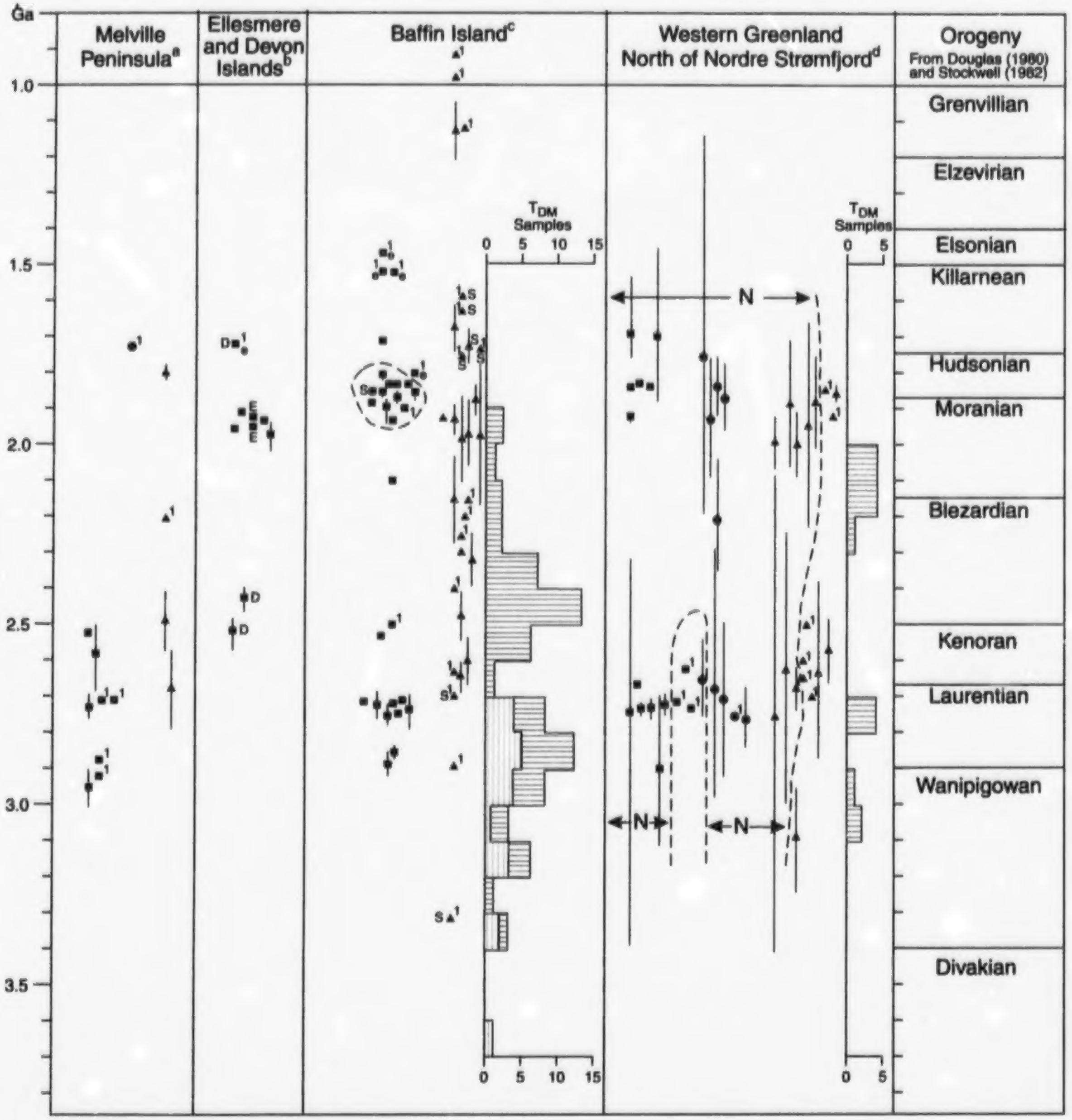

Figure 98. Comparison of U-Pb zircon, Pb-Pb, Rb-Sr, and Nd T_{DM} model ages. ***a)*** *Jackson and Taylor (1972); Frisch (1982), Henderson (1983),* ***b)*** *Frisch (1988), Frisch and Hunt (1988);* ***c)*** *Tables 51 and 52, Jackson (1978a, b), Wanless and Loveridge (1978); Jackson and Iannelli (1981), Morgan (1982, 1983), Henderson (1985a, b), Jackson et al. (1985, 1990a, b),* ***d)*** *Anderson and Pulvertaft (1985), Kalsbeek (1986), Kalsbeek et al. (1987). Squares = U-Pb zircon ages; circles = Pb-Pb ages; triangles = Rb-Sr ages; vertical lines = error limits; e = zircon lower intercept age; l = no error limit given. D = Devon Island, E = Ellesmere Island; N = Nagssugtoqidian Mobile Belt; S = southern Baffin Island (Baffin Orogen). Lined patterns show Nd T_{DM} model ages: horizontal = Baffin Orogen and Nagssugtoqidian mobile belt; vertical = northern Baffin Island.*

range from 1865 ± 60 to 1615 ± 210 Ma and have a mean of 1699 Ma. Most lie between 1750 and 1660 Ma. The 1865 Ma age is for biotite from a felsic metavolcanic boulder in metaconglomerate in basal Mary River Group strata below No. 1 iron deposit at Mary River. Muscovite from a late pegmatite near No. 4 iron deposit yielded an age of 1679 ± 50 Ma, which may approximate the age of pegmatite emplacement but is thought to be too young. Except for these two ages, the muscovite and biotite K-Ar ages seem to bear no relation to the relative ages of the host rocks. These ages (mean = 1699 Ma), except possibly for the age of the felsic metavolcanic boulder, are more likely to indicate times of postorogenic (?Hudsonian) cooling and uplift than orogeny.

Some K-Ar mineral ages for Aphebian and Archean rocks elsewhere on Baffin Island and on Melville Peninsula (corrected for new constants) are given for comparison below (Table 54).

Four K-Ar hornblende and actinolite ages for Mary River Group metabasalt range from 1531 to 446 Ma (Table 53). The dated samples all come from the vicinity of the Central Borden Fault Zone near No. 4 iron deposit in the Mary River area, with the sample location for the 1531 Ma age being farthest from the fault. These ages may be related to episodes of increased movement along the fault and/or emplacement of a large Hadrynian diabase along the fault in this area. The 1531 Ma age may indicate the time of fault inception and

Table 53. Whole rock and mineral K-Ar ages[1] for the Clyde-Cockburn Land map area.

Rock type	Map unit	Map sheet	Material dated	Age (Ma)	Location	Reference
Diabase	Hg	37G	Whole rock	575 ± 71	71°23′29″N; 79°41′27″W	Wanless et al. (1972)
Diabase	Hg	37G	Whole rock	682 ± 110	71°16′N; 78°20′W	Wanless et al. (1970)
Diabase	Hg	37G	Whole rock	652 ± 98	71°14′N; 78°15′W	Wanless et al. (1973)
Diabase	Hg	37H	Whole rock	605 ± 90	71°02′N; 75°20′W	Wanless et al. (1973)
Diabase	Hg	27G	Whole rock	513 ± 73	71°02′10″N; 71°43′45″W	Wanless et al. (1972)
Diabase	Hg	37F	Whole rock	852 ± 124	70°04′00″N; 79°36′15″W	Wanless et al. (1972)
Diabase	Hg	37E	Whole rock	1035 ± 80	70°53′N; 75°40′W*	Wanless et al. (1973)
Diabase	Hg	37E	Whole rock	994 ± 80	70°53′N; 75°40′W*	Wanless et al. (1973)
Pegmatite	Ag	37G	Muscovite	1679 ± 50	71°26′30″N; 79°51′00″W	Wanless et al. (1970)
Monzogranite	Amp	37E	Biotite	1797 ± 55	70°13′30″N; 75°37′15″W	Wanless et al. (1972)
Banded migmatite (granulite)	Amg	37H	Biotite	1669 ± 53	71°10′20″N; 73°06′15″W	Wanless et al. (1972)
Banded migmatite	Amg	37E	Biotite	1630 ± 52	70°13′00″N; 72°00′10″W	Wanless et al. (1972)
Amphibolite	Mb?	37G	Hornblende	1531 ± 55	71°27′59″N; 79°47′37″W	Wanless et al. (1970)
Metabasalt	Mb	37G	Hornblende	1015 ± 40	71°26′55″N; 79°53′49″W*	Wanless et al. (1970)
Metabasalt	Mb	37G	Hornblende	973 ± 39	71°26′55″N; 79°53′49″W*	Wanless et al. (1970)
Metabasalt	Mb	37G	Actinolite	446 ± 20	71°26′51″N; 79°53′38″W	Wanless et al. (1974)
Mica schist	Mq	37G	Biotite	1615 ± 210	71°29′N; 79°53′W*	Wanless et al. (1966)
Mica schist	Mq	37G	Muscovite	1753 ± 50	71°29′N; 79°53′W*	Wanless et al. (1966)
Quartzite	Mq	37G	Muscovite	1674 ± 55	71°27′48″N; 79°50′09″W	Wanless et al. (1970)
Felsic metavolcanic clast in Mq	Amn-Mq	37G	Biotite	1865 ± 60	71°19′N; 79°15′W	Wanless et al. (1970)
Biotitite rim on amphibolite	Mg?, b?	37G	Biotite	1689 ± 50	71°18′25″N; 79°15′11″W	Wanless et al. (1970)
Rodded monzogranite	gr-Agr	37G	Muscovite	1659 ± 50	71°27′N; 79°50′W	Wanless et al. (1970)
Nebulitic granitoid gneiss	Amn	37G	Biotite	1679 ± 55	71°44′20″N; 76°21′00″W	Wanless et al. (1972)
Nebulitic granitoid gneiss	Amn	37H	Biotite	1694 ± 54	71°15′N; 73°11′W	Wanless et al. (1972)
Nebulitic granitoid gneiss	Amn	37H	Biotite	1679 ± 52	71°08′50″N; 75°23′15″W	Wanless et al. (1972)
Nebulitic granitoid gneiss	Amn	37F	Biotite	1703	70°30′N; 79°00′W	Leech et al. (1963)

1 Corrected to the new constants now in use (Steiger and Jäger, 1977).

* Results from the same location are from the same sample.

Table 54. Comparison of K-Ar mineral ages for Aphebian and Archean rocks on Baffin Island and on Melville Peninsula (corrected for new constants).

Area	Samples*	Range (Ma)*	Mean (Ma)
Baffin Island north of map area and west of 80°W	12	2014-1595	1750
Map area	15	1865-1531	1697
Baffin Island south of map area to Cumberland Peninsula	29	1927-1579	1711
South Baffin Island	14	1840-1506	1639
Melville Peninsula (excludes age of 2657 Ma for colourless amphibole)	31	1920-1534	1666

*From Leech et al. (1963), Lowdon et al. (1963), Wanless et al. (1966, 1967, 1968, 1970, 1972, 1974, 1978, 1979), Stevens et al. (1982a, b).

446 Ma the latest significant movement, when early Paleozoic strata were downdropped on the south side of the fault. The 1015 Ma and 973 Ma ages (Table 53) are similar to the most common K-Ar ages obtained for Nauyat basalts to the northwest (Jackson and Iannelli, 1981). These ages and/or the 1131 Ma and 1129 Ma Rb-Sr ages noted above may be indicative of the time of subgreenschist facies metamorphism of the Neohelikian Bylot Supergroup and/or the closing of the Neohelikian Poseidon Ocean (Jackson and Iannelli, 1981, 1984).

Several K-Ar whole rock ages have been determined for late Proterozoic diabases. The ages range from 1035 to 513 Ma, and include an age of 575 Ma for the dyke that occurs in the vicinity of the locations of the hornblende and actinolite ages discussed above. Most dykes are probably Franklin dykes (723 Ma, *see* sections on "Ages and regional relations" under "Borden and Franklin diabase dykes (Hg)").

Two ages of 1035 Ma and 994 Ma (Table 53) for the same dyke suggest that it may be older than either the Borden or Franklin dykes. The dyke has yielded a paleomagnetic pole position of 191E,01S (169W,01S or 11E,01N), which plots close to that of the Mackenzie igneous event (site 10 *in* Fahrig et al., 1971; Berger and York, 1980). Therefore, this dyke and a few others in the map area and elsewhere in northern Baffin Island are probably Mackenzie dykes (e.g. sites 11 and 23 *in* Fahrig et al., 1971).

METAMORPHISM

Regional metamorphism

Data on metamorphism in the map area are included by Jackson and Morgan (1978a) in their paper on the metamorphism on Baffin and Bylot islands, and in the Metamorphic Map of the Canadian Shield (Fraser et al., 1978). Field relations (e.g. Archean rocks that have undergone at least three episodes of migmatization, and the presence of low- to medium-grade Archean Mary River strata directly above migmatites and granitic basement complex), and available age determinations, as discussed above, indicate that the Clyde-Cockburn Land map area is underlain chiefly by Archean rocks that were first deformed and metamorphosed twice in the Archean. As noted by Jackson and Morgan (1978a), however, no large areas probably remain that have totally escaped the effects of early- and late-Aphebian metamorphism and deformation. The results of the Aphebian activity are obvious in the Piling Group and in age determinations, which indicate Aphebian overprinting of Archean rocks and minerals.

Most mineral assemblages seem to be compatible and, when considered by themselves, to represent one main metamorphic event. Most also show minor effects of low grade retrogression, which probably occurred prior to emplacement of the Hadrynian diabase dykes. It is uncertain whether metamorphic mineral assemblages in Archean rocks are Archean, Aphebian, or mixtures of the two. Where Archean and Aphebian rocks occur together, their mineral assemblages seem internally compatible, on the regional scale of the fieldwork. However, parts of some large Archean granitic plutons, such as the one southeast of Paquet Bay (Fig. 99), are probably composed mostly of primary minerals and are little recrystallized except along shear zones. Also, the Bylot Island charnockite batholith has been dated at about 2.55 Ga (D.J. Scott, pers. comm., 1999), and some ultramafics in the Mary River area contain relict olivine and enstatite.

Hypersthene occurs enclosed in garnet in a metaultramafite, and staurolite rims serpentine in some garnet-biotite-chlorite-muscovite-rich rocks. Rims of blue-green hornblende occur on pyroxenes and brown-green hornblende, green biotite has superseded brown biotite, and sphene has crystallized out in lower grade biotite formed from higher grade biotite and has rimmed iron oxide. These and other petrographic relations may represent regression during cooling following a prograde metamorphism, or could represent a later event unrelated to the earlier one. The difficulty encountered in obtaining reasonably consistent pressures and temperatures from mineral assemblages of some samples, even though the minerals seem to be in equilibrium and unaltered, may be a consequence of incomplete re-equilibration during superposition of a later metamorphism on previously formed metamorphic assemblages.

The metamorphic facies are shown in Figure 99 without attempting to differentiate Archean and Aphebian assemblages or show overprinting of Archean by Proterozoic metamorphism. Estimates of metamorphic pressures and temperatures are summarized in Table 60 and on Figure 102. The author considers, however, that Archean and Aphebian rocks have been subjected to Aphebian, and, locally at least, late Proterozoic metamorphic conditions (Fraser et al., 1978; Jackson and Morgan, 1978a; *see* sections on "Origin" and "Age" of units Agp, Ag, and Ack).

Metamorphic grade ranges from greenschist to upper amphibolite and granulite facies over relatively short distances in the Mary River area and in the Eqe Bay-Grant-Suttie Bay area just south of the map area (Morgan et al., 1975, 1976; Jackson and Morgan, 1978a; Bethune and Scammell, 1993, 1997; Scammell and Bethune, 1995a). Both areas lie adjacent to faults and the metamorphic gradients seem to dip relatively steeply. Assemblages are listed in the descriptive section and in Jackson and Morgan (1978a) and for the most part are not repeated here.

A note is provided here concerning the assemblages noted in the following sections in order to avoid repetition. Unless stated specifically otherwise, about 120° grain boundaries are abundant and grain relations indicate contemporaneous growth in equilibrium assemblages. Specifically this holds for the aluminosilicate minerals, cordierite, staurolite, and other minerals especially helpful in unravelling P-T relations. The fibrous nature of late sillimanite is noted where it is pertinent. Where present cordierite, unless stated otherwise, is part of the stated assemblage and does not occur as late rims on other minerals. Some sphene and spinel do occur as late rims, but elsewhere they form discrete grains in equilibrium assemblages. Some rutile, sphene, and epidote occur as late phases disseminated in other minerals.

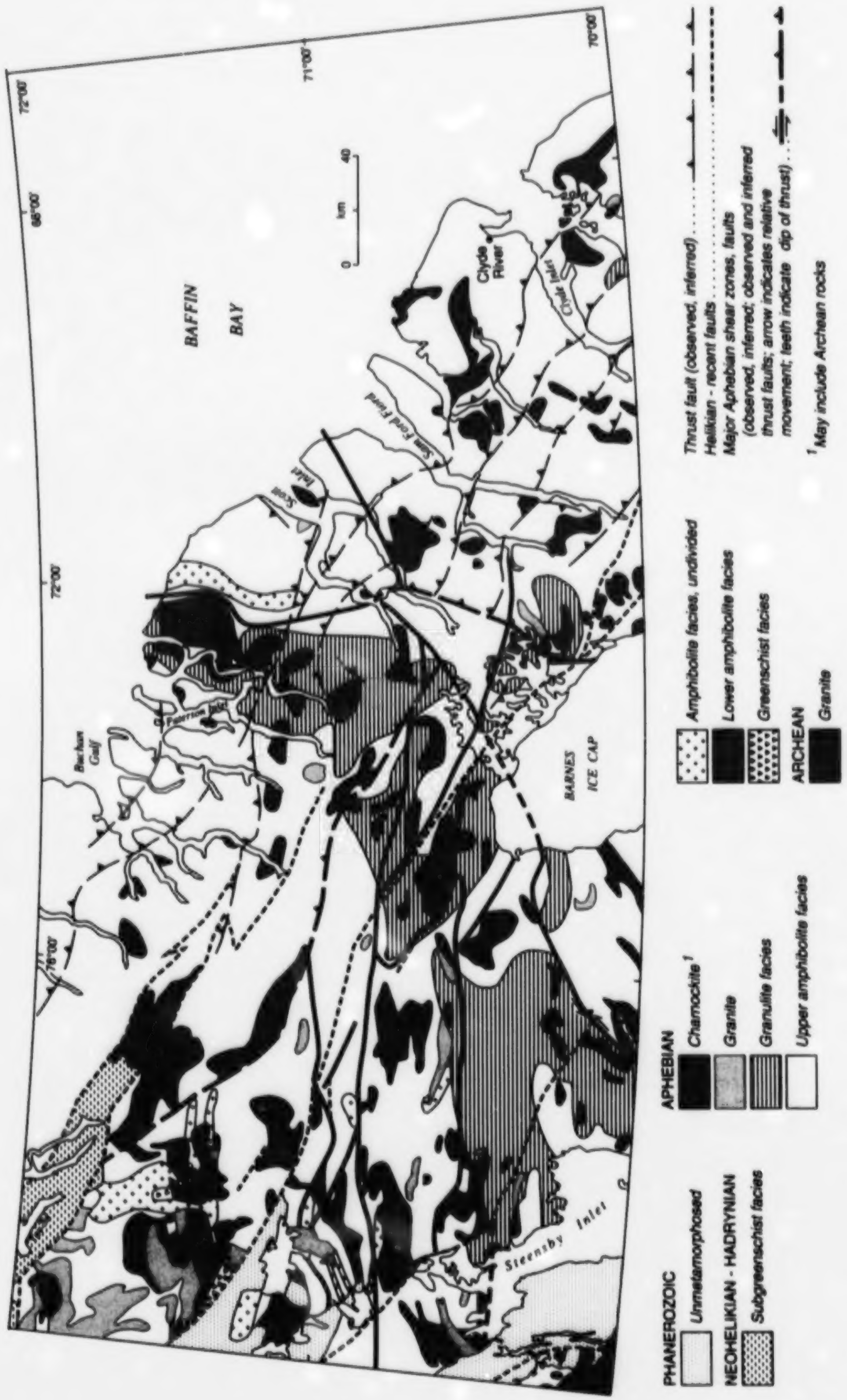

Figure 99. *Distribution of metamorphic facies and major granitic plutons in the map area. See Figures 101, 112 for more information.*

Where available, preliminary results from microprobe analyses are compared with conclusions based on petrographic relations in the following sections. Details of the analyses and thermobarometers are not provided.

Subgreenschist facies

Subgreenschist facies assemblages occur discontinuously within the greenschist facies zone within the Mary River Group in the Mary River area (Fig. 99). Typical mineral assemblages include:

quartz+oligoclase(?)+biotite+muscovite+chlorite+pumpellyite+prehnite+sphene, and

quartz+biotite+muscovite+chlorite+epidote+pumpellyite+prehnite.

The first assemblage is from a metasediment and the second is from a metamorphosed intermediate flow or sill. Mafic minerals and plagioclase in associated higher grade rocks are downgraded and partially recrystallized to upper subgreenschist facies minerals. The Mary River area is a lens of relatively low grade metamorphism in higher grade terrane, and the subgreenschist metamorphism may be a late retrograde event related to late Aphebian metamorphism. Rubidium-strontium data from the Mary River area preclude an Archean age for this low grade metamorphism. The spread of K-Ar mineral ages for the area (Table 53), and the proximity of the Mary River area to the Neohelikian-Phanerozoic Central Borden Fault Zone, suggest that low grade retrogression may be Neohelikian-early Hadrynian in age.

The Neohelikian Bylot Supergroup strata in the northwestern part of the map area are considered tentatively to be in the subgreenschist facies. This conclusion is based chiefly on the presence of prehnite and pumpellyite in the Nauyat volcanics in the basal part of the supergroup northwest of the map area (Jackson and Morgan, 1978a). Secondary albite, epidote, illite-muscovite, biotite, and stilpnomelane, and hornblende are also present. Uppermost strata in the sequence do not contain diagnostic minerals and may not have attained subgreenschist rank. Most Hadrynian (**Hg**) dykes throughout northwestern Baffin Island are less altered than the Bylot Supergroup and are not considered to have undergone the same metamorphism. Therefore the age of subgreenschist metamorphism is probably 1220-850 Ma, and may lie between 1130-950 Ma (Jackson and Iannelli, 1981).

The secondary alteration of the Hadrynian dykes may be deuteric although it is similar to the diaphthoresis present in all older rocks. Because of the paucity of secondary alteration in Phanerozoic rocks, the dyke alteration is considered to be Hadrynian.

Greenschist facies

Greenschist facies rocks occur chiefly in the Mary River Group in the Mary River area in a thin discontinuous zone along the north side of the Central Borden Fault Zone, and in a small area between this zone and the Milne Inlet Trough (Fig. 99). These low grade assemblages occur locally at several other places. Most of the greenschist facies rocks seem to be prograde, but their gradation locally into subgreenschist facies assemblages suggests that some of the greenschist facies rocks may also be retrograde.

The presence of chlorite, actinolite, clinozoisite, and albite rather than oligoclase, and the absence of staurolite, andalusite, and cordierite are considered indicative of greenschist facies. Prehnite seems to belong to some equilibrium assemblages in greenschist facies terrane.

Lower amphibolite facies

Although assemblages of this facies are more abundant than those of the greenschist, they are confined to the Mary River Group underlying a very small part of the map area. They occur as narrow lenses and have been differentiated from other facies in the west-central part of the map area and locally west of Buchan Gulf (Fig. 99). Lower amphibolite facies rocks are intermixed with upper amphibolite facies rocks in the western part of the map area and between Buchan Gulf and Scott Inlet.

A great variety of mineral assemblages is present. The presence of oligoclase (An ≥ 16) or more calcic plagioclase (with or without hornblende), staurolite, cordierite, andalusite, and muscovite with quartz and plagioclase, together with the absence of chlorite in contact with muscovite, and the absence of anatexis were used to identify lower amphibolite facies in the map area. Muscovite is apparently stable with hornblende in some assemblages. Tourmaline is rare in the Mary River Group, but is common in lower amphibolite and greenschist facies Piling Group south of the map area.

Lower amphibolite facies assemblages in metasediments are chiefly prograde and show little evidence of having been anatectized, retrograded, or both. However, mafic and ultramafic rocks in this facies are commonly extensively retrogressed.

Metamorphic grade, especially in several of the larger areas underlain by the Mary River Group increases outward toward the margins of these areas. This seems to be a common feature throughout the Committee Orogen, and might be related to steep thermal gradients during metamorphism, or to deformation after metamorphism.

Upper amphibolite facies

Most of the map area is underlain by upper amphibolite facies rocks (Fig. 99). The facies was identified by the absence of staurolite, the absence of muscovite in the presence of quartz and plagioclase (An>16), and by the occurrence of potassium feldspar, aluminosilicate minerals, cordierite, and garnet. Also, the assemblage quartz+cordierite+almandine+sillimanite is considered to be unstable in the presence of plagioclase (Winkler, 1979). Potassium feldspar is chiefly microcline; myrmekite, perthite, antiperthite, and accessory rutile are common. Signs of anatexis were accepted as indicative of upper amphibolite conditions in the absence of other diagnostic criteria. Cordierite is relatively rare in the northeastern part of the map area and epidote is uncommon throughout. Phlogopite occurs in some carbonate rocks. Mafic and ultramafic rocks contain cummingtonite, anthophyllite, and locally carbonate and phlogopite.

Metamorphic assemblages in most of the foliated and gneissic granitoid rocks are not diagnostic. Occurrence of deep red-brown biotite, brownish-green hornblende, rutile, myrmekite, perthite, antiperthite, and/or abundant anatexis in these rocks is taken as an indication that at least the upper amphibolite facies was attained.

Most upper amphibolite assemblages are considered to be prograde. Although some may have been retrogressed from granulites, this seems to be a local phenomenon and not a regional superposition. In a few places, migmatites, including some involving Mary River Group strata, have undergone a second episode of anatexis.

Granulite facies (chiefly Dexterity Granulite Belt)

A discontinuous belt of granulite facies rocks trends about 280 km southwest-northeast across Baffin Island past the north end of Barnes Ice Cap (Fig. 99). It is named here the Dexterity Granulite Belt because both the northeast part of the belt and the Dexterity Batholith (charnockite-enderbite) at its northeast end are well exposed along the 100 km long Dexterity Fiord. Narrow, lower grade zones, transverse to the granulite belt, are spatially related to Late Aphebian tectonic zones, Neohelikian–Phanerozoic faults, the southeast extension of the Borden Rift Basin, and Hadrynian Franklin dyke swarms. The zones separate the belt into three segments whose rocks yield different metamorphic temperatures and pressures (*see* Fig. 101, 112, 113). The hypersthene isograd, used as the boundary for the Dexterity Granulite Belt, cuts across rock types, regional and local trends, and the boundaries of several tectonic subdomains. Mary River Group strata, for example, occur throughout and on both sides of the belt; Piling Group strata outcrop in the southwest corner of the belt and south of it (*see* Fig. 101: 2a-2c, 3b, 7c; Fig. 114). Granulites in the southwest corner of the belt have been dated at 1827-1821 Ma (Scammell and Bethune, 1995a).

Two small areas of granulites to the south and east and west of the Barnes Ice Cap (Fig. 99) seem to be separated from the belt by lower grade rocks. Granulite and/or "subgranulite" facies rocks outcrop in numerous small areas in the upper amphibolite facies terrane, chiefly near the granulite belt, but also sporadically throughout the map area. These were either too small, or too uncertain to show as granulites on the maps of the area.

The appearance of metamorphic orthopyroxene, chiefly hypersthene (according to optics and several unpublished probe analyses), was taken to indicate the lower boundary of the granulite facies. Relics of primary orthopyroxene, present locally in metaigneous mafic and ultramafic rocks, may at some localities have been mistaken for their metamorphic counterparts. Myrmekite, perthite, antiperthite, and accessory rutile are more common than in the upper amphibolite facies, and orthoclase is at least as common as microcline. Garnet is common, and is probably chiefly pyrope-rich almandine (Jackson and Morgan, 1978a). Sillimanite and cordierite are common locally while cummingtonite, anthophyllite, spinel, and phlogopite are uncommon to rare. Aluminosilicate minerals occur in the same outcrop with hypersthene, but have not been found in the same thin section. Common assemblages in supracrustal strata and felsic gneisses include:

quartz+plagioclase+potassium feldspar+biotite+hypersthene,

quartz+plagioclase+hornblende+hypersthene± potassium feldsparb±iotite±clinopyroxene,

quartz+plagioclase+hornblende+clinopyroxene+hypersthene+(biotite or garnet),

quartz+plagioclase+biotite+clinopyroxene+hypersthene+garnet,

quartz+hypersthene+magnetite±garnet,

plagioclase+hornblende+hypersthene+(biotite or clinopyroxene),

Quartz+plagioclase+perthite+biotite+cordierite+(sillimanite or garnet),

quartz+plagioclase+biotite+garnet+sillimanite+(perthite or cordierite), and

quartz+biotite+garnet+sillimanite+spinel.

In the charnockites, assemblages containing quartz+plagioclase+potassium feldspar+biotite also commonly contain either hypersthene±hornblende or hornblende±clinopyroxene. Biotite is not always present. Some assemblages consist of quartz+plagioclase+garnet+hypersthene.

The hypersthene isograd bounding the granulites transgresses map units and regional and local trends, but is also parallel to local structures in many places, possibly because of deformation of isograd surfaces. A relatively straight, abrupt southern boundary northeast of Grant-Suttie Bay, and a curved, abrupt southern boundary at the northeast end of the belt coincide with fault zones (Isortoq Fault Zone, *see* Fig. 101, 112, 113, 114). Elsewhere the granulites are bordered by an irregular, diffuse, transitional zone of "subgranulites" that is in general prograde.

Minor retrograde minerals occur locally throughout most of the granulite terrane. These include, for example, hornblende rims on pyroxene and sphene rims on oxide minerals. Their formation probably occurred mostly during the waning stages of metamorphism. Their occurrence seems irregular and their degree of development does not seem to increase or decrease regionally. Low grade alteration products include chlorite, epidote, clay minerals, and hydrous iron oxides. Similarly, retrogression to amphibolite facies occurs only locally and does not seem to be related to a regional regression of granulite to amphibolite facies. Increase in metamorphic grade of the Mary River Group toward the granulites, with no indication that the lower grade rocks have been retrograded, indicate the presence of prograde metamorphism to granulite grade. This relationship has been obscured in several places by subsequent events such as late Proterozoic to Recent faulting, and emplacement of diabase dykes. The transition from lower grade to higher grade metamorphic rocks over short distances has been recognized chiefly on the north side of fault zones, as at Mary River and Eqe Bay, and along the south edge of the granulite belt east of Steensby Inlet and south of Buchan Gulf.

Some P-T considerations

Some reasonable estimates and comparisons of metamorphic pressures and temperatures may be made by comparing appropriate mineral assemblages for a specific lithology (relatively uniform composition) with a P-T petrogenetic grid. Metapelites of the Mary River Group (*see* section on "Upper member (0 to 122 m)" in "Metapelite-amphibolite unit", and Piling Group (*see* section on "Longstaff Bluff Formation (APs)") seem the most amenable, and the P-T grid (Fig. 100) by Carmichael (Carmichael et al., 1987) seems the best suited of several grids examined. Assemblages from metapelites and other rock types were utilized for the granulite facies. Subgreenschist and most greenschist facies assemblages were not considered. Because of the range of metamorphic grades in some areas (e.g. Mary River, Eqe Bay) the conclusions (Fig. 101, Table 55) also probably apply to only small areas.

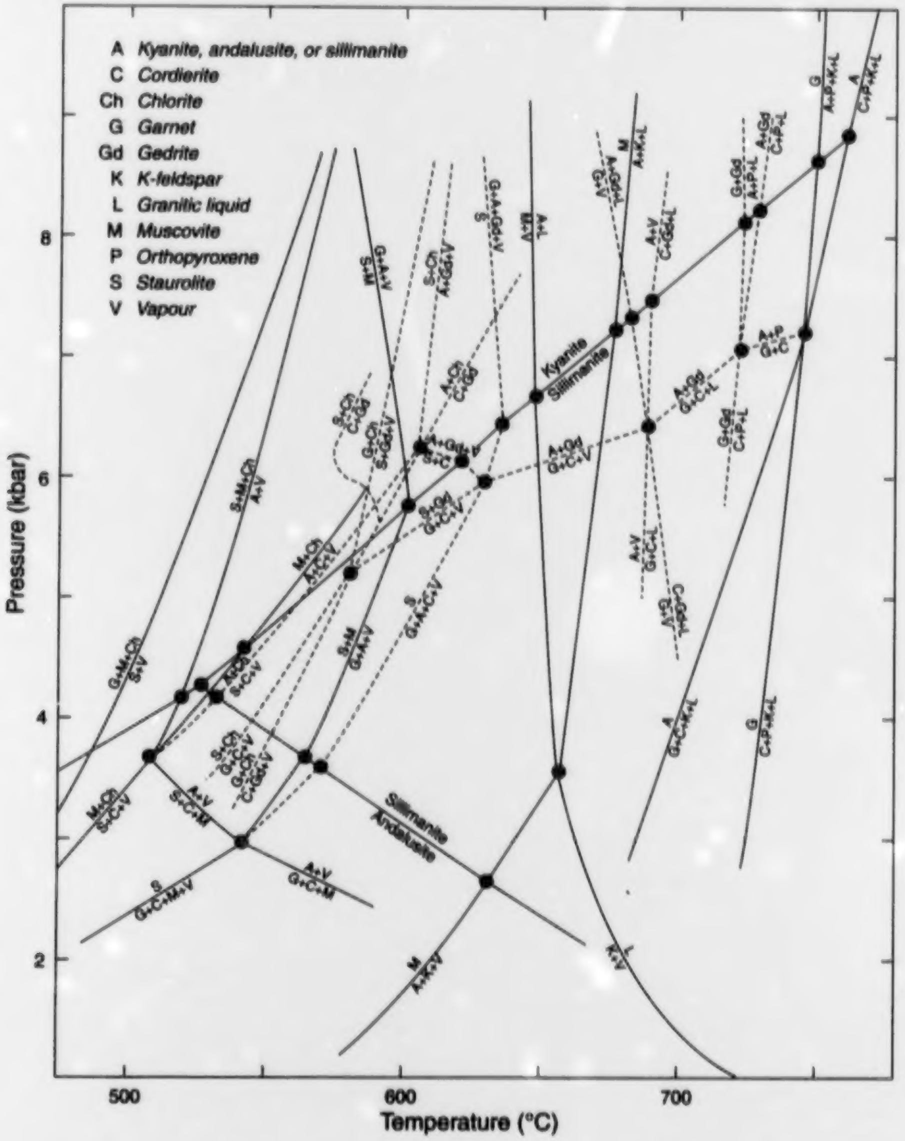

Figure 100. *Pressure-temperature (P-T) petrogenetic grid for part of the model system K_2O-Na_2O-FeO-MgO-Al_2O_3-SiO_2-H_2O (KNFMASH) relevant to the metamorphism of pelitic schists and gneisses that contain biotite, plagioclase, and quartz (from Carmichael et al., 1987).*

Preliminary determinations of metamorphic pressures and temperatures have been made using microprobe analyses of minerals from 29 samples (1-29) of various rock types in northern Baffin Island. The samples come from several different tectonic domains (1, 2, 3, 7, 8: Table 55 and Fig. 101). Most of the microprobe analyses were made by John Stirling (Geological Survey of Canada) assisted by the author. Five of the samples were analyzed by V. Kitsul (Yakutsk) and S. Bushmin (St. Petersburg), both of the Russian Academy of Sciences. Three of the five samples are duplicates repeated by ourselves for comparative purposes. Most of the pressure and temperature calculations were done by K. Venance and R. Berman using the latter's TWQ computer program (Berman, 1988, 1990, 1991). The analyses were also run through PTMETER (an unpublished computer calculation program by J. Percival and J. Maley) by the author because additional calculations were required for many of the samples to determine pressures or temperatures for use in thermobarometers. It also served as a check on TWQ results and some results determined earlier. The results used from PTMETER are chiefly for the two-pyroxene thermometers of Lindsley (1983) and Saxena et al. (1986), several garnet-biotite thermometers (chiefly Hodges and Spear, 1982), the feldspar thermometers of Haselton et al. (1983) and Whitney and Stormer (1977), the Newton and Haselton (1981) garnet-plagioclase-Al_4SiO_5-quartz barometer, and the CATS-anorthite-quartz barometer of Ellis (1980). The geobarometer of Martignole and Sisi (1981) was used for cordierite-garnet assemblages.

Eight areas (A-H, Fig. 101), in which useful supracrustal assemblages are relatively common and diverse, will be discussed first in relative detail. Different thermobarometers will be compared and their results will be compared with those obtained from a P-T grid. All reported microprobe analyses are for mineral cores, unless stated otherwise.

Area of Mary River No. 1-3A iron deposits

The samples used from this locality come from an area of about 30-40 km^2 (A-Fig. 101, Table 55) in tectonic subdomain 1a. Assemblages indicative of relatively small ranges of pressure and temperature are:

1) quartz+anthophyllite+biotite+muscovite+cordierite +sillimanite,

2) quartz+biotite+garnet+cordierite+andalusite+ (staurolite, or sillimanite+magnetite),

3) quartz+biotite+muscovite+cordierite+andalusite+ (kyanite, or sillimanite±plagioclase), and

4) quartz+biotite+cordierite+andalusite+kyanite+ sillimanite±staurolite±plagioclase.

These and other assemblages listed previously indicate that P-T conditions varied somewhat from one locality to another within this area (Fig. 102a), and with time. Assemblages 3 and 4 suggest metamorphic conditions at or very close to the triple point (0.43 GPa, 550°C: Carmichael et al., 1987; 0.38 GPa, 500°C: Holdaway, 1971). Assemblage 2 indicates conditions of 0.35 GPa and 570°C (Carmichael et al., 1987).

Mineral assemblages in two samples from one locality indicate that either P-T conditions changed during one main metamorphic event, or that the effects of one metamorphic event were superimposed on those of an earlier event:

5) quartz+biotite+cordierite+kyanite+andalusite+ staurolite+sillimanite+rutile, and

6) quartz+biotite+muscovite+andalusite+sillimanite.

Assemblage (5) consists mostly of biotite and cordierite that seem compatible with one another, and each of which is concentrated in alternate masses up to several centimetres across. Quartz is sparse. Most of the cordierite is poikiloblastic, containing sparse to abundant biotite crystals that are commonly relatively abundant in the core areas, and aligned with and slightly finer grained than the biotite in the biotite-rich areas. Some cordierite is altered to isotropic material. Kyanite occurs as disseminated porphyroblasts up to 1 cm long surrounded mostly by cordierite. The kyanite ranges from completely unaltered through slightly altered around the margins to completely altered to aggregates of fine grained muscovite. Staurolite occurs sparsely as small porphyroblasts and as small grains, adjacent to kyanite in the muscovite alteration zones rimming kyanite. Andalusite occurs mostly as anhedral porphyroblasts associated with cordierite and in simplectic intergrowths with cordierite that resemble graphic intergrowths. Sillimanite is a minor component that occurs late as thin laths that transect both cordierite and andalusite, and rarely, transect kyanite. Rounded rutile grains are rare. Minor chlorite is a late alteration mineral. The relationships seem most compatible with one major period of metamorphism in which pressure increased more rapidly than temperature at first. Temperature then increased during crystallization as pressure remained relatively constant at slightly less than the triple point pressure. The sillimanite in assemblage (6) is also late and is fibrolite formed at the expense of biotite.

Area of Mary River No. 4 iron deposit

Samples from this locality also come from an area of about 30-40 km^2 (B-Fig. 101; Table 55) in tectonic subdomain 1a. There are relatively few good metapelites in this area, hence a smaller variety of assemblages. The most pertinent ones are:

7) quartz+anthophyllite+biotite+cordierite+sillimanite± muscovite, and

8) quartz+biotite+garnet+magnetite+(cordierite, or staurolite±cordierite).

These and additional assemblages suggest that P-T conditions probably occurred somewhere within the area shown on Figure 102a, from roughly 0.36 GPa and 560°C to 0.6 GPa and 640°C. Preliminary feldspar geothermometry for one sample suggests temperatures of only 440-450°C for the same pressure range, which is low considering the presence of sillimanite and rarity or absence of andalusite and kyanite. That and the paucity of anthophyllite with staurolite and garnet suggest the P-T conditions may have attained 0.4-0.5 GPa and 560-580ºC. The feldspar thermometers of Haselton et al. (1983) and Whitney and Stormer (1977) indicate temperatures of 422°C and 490°C respectively at 0.6 GPa pressure. This is in agreement with the observation that these rocks seem to be at a somewhat higher grade than those at the No. 1-3A iron deposit area, and that the iron deposits are coarser grained in the No. 4 iron deposit area. Chlorite and prehnite are later retrograde minerals.

Turner River-Glacier Lake (NTS 37G)

The small variety of assemblages available for this about 20 km^2 area in tectonic subdomain 1a (C- Fig. 101; Table 55) may be interpreted as being compatible with a small range in P-T centred around 0.36 GPa and 570ºC (Fig. 100, 102a). This is based largely on three assemblages: one containing biotite, garnet, cordierite, andalusite, and sillimanite; a second containing muscovite, biotite, and sillimanite with quartz and plagioclase; and a third assemblage containing quartz, biotite, garnet, and anthophyllite.

Legend to Figure 101

NEOHELIKIAN (1.27 Ga)

░ *BORDEN RIFT BASIN (Tectonic Domain 8): sediments, volcanics*

ARCHEAN-LATE APHEBIAN

▧ *NORTHEAST BAFFIN THRUST BELT (Tectonic Domain 7, 1.8? Ga)*
- *7a - SE trends and SW-directed overthrusts in chiefly Archean rocks*
- *7b - varied trends in chiefly Archean rocks*
- *7c - SE trends in Aphebian and minor Archean rocks*

BAFFIN OROGEN (1.9-1.8 Ga): chiefly amphibolite to granulite grade

▨ *FOXE FOLD BELT (Tectonic Domain 3)*
ca. 1.9 Ga Piling Group and Archean-Aphebian gneiss complex
- *3b - E trends, greenschist in centre outward to amphibolite facies*
- *3a - NE trends, amphibolite- north to granulite-grade, but metamorphism alternates between higher and lower grade in crude subparallel belts*

COMMITTEE OROGEN (2.9-2.7 Ga?)

Chiefly Archean rocks (3.7-2.7 Ga?) and structure with varied Aphebian structural and metamorphic overprinting

■ *DEXTERITY GRANULITE BELT (1.82 Ga)*

■ *Granulite facies, considered to be Late Aphebian, but some may be Archean*

▤ *TECTONIC DOMAIN 2*
- *2c - E trends, aeromagnetic maps show high regional magnetic background*
- *2b - E trends, aeromagnetic maps show low regional magnetic background*
- *2a - Arcuate E trends truncate SE trends in 1b, aeromagnetic maps show high regional magnetic background*

▥ *TECTONIC DOMAIN 1*
- *1b - SE trends, may supersede 1a trends*
- *1a - Mixed trends (chiefly Archean?, oldest subdomain?), primary features relatively common, local subgreenschist-greenschist grade*

▩ *MARY RIVER GROUP (2.75-2.72 Ga) greenstone belts from Eqe Bay - (Fa,Fb), some greenschist grade, in subdomain 3a (NE to SE trends, chiefly Late Aphebian?)*

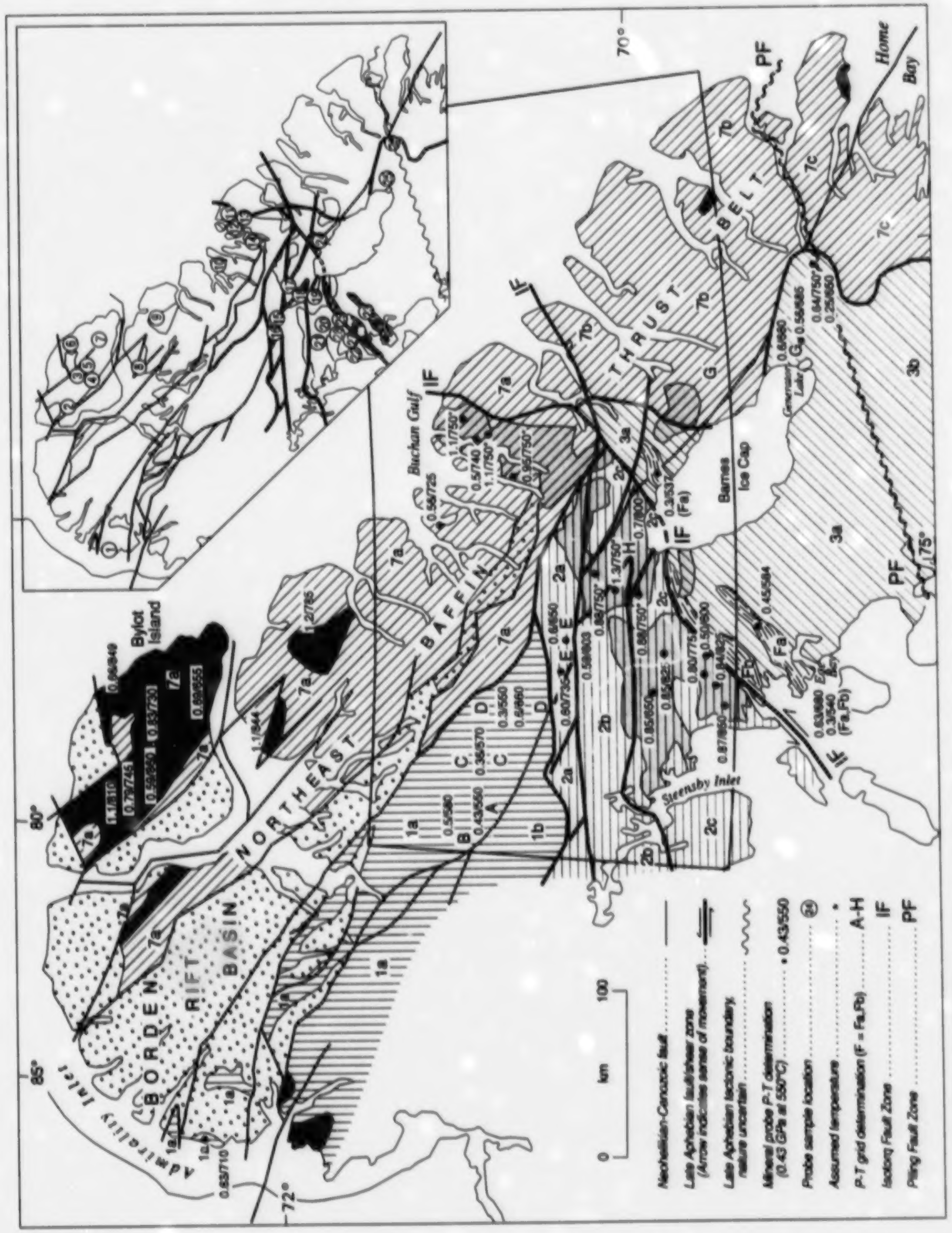

NORTHEAST BAFFIN THRUST BELT
BORDEN RIFT BASIN
Bylot Island
Admiralty Inlet
Buchan Gulf
Barnes Ice Cap
Steensby Inlet
Generator Lake
Home Bay
Eqe Bay
80°
85°
72°
70°
75°
1a
1b
2a
2b
2c
3a
3b
7a
7b
7c
A
B
C
D
E
F
G
H
Fa
IF
PF
0
km
100
Neohelikian-Cenozoic fault
Late Aphebian fault/shear zone (Arrow indicates sense of movement)
Late Aphebian tectonic boundary, nature uncertain
Mineral probe P-T determination (0.43 GPa at 550°C)
• 0.43/550
Probe sample location
Assumed temperature
P-T grid determination (F = Fa,Fb)
A-H
Isortoq Fault Zone
IF
Piling Fault Zone
PF

Figure 101. Preliminary metamorphic pressures and temperatures for tectonic domains of northern Baffin Island (Table 55; Fig. 112, 113). Estimates were made from a petrogenetic grid (Carmichael et al., 1987), combined with incomplete probe data where available (locations A-H), and from complete mineral probe analyses (locations 1-29). A: Mary River No. 1-3A iron deposits area; B: Mary River No. 4 iron deposit area, C: Turner River to Glacier Lake area; D: central, south-central NTS 37G; E: upper Rowley River area; Fa and Fb: Eqe Bay and Isortoq Fiord Mary River Group supracrustal belts (Fa and Fb extend northeasterly into outlined map area); G: Generator Lake area (45 km south of map area) to south end of Sam Ford Fiord; H: north end of Barnes Ice Cap. See Figures 112, 113 for additional legend.

Central, south-central map area NTS 37G

Most of the assemblages available are from an area in south-central map area NTS 37G that lies in southern tectonic subdomain 1a and extends slightly into subdomains 1b and 2a (D -Fig. 101; Table 55). Staurolite and anthophyllite have not been identified, and muscovite is abundant. The rocks have been partially melted (lit-par-lit gneiss), and intruded by pegmatites and small granite bodies. Two of the most pertinent assemblages are:

9) quartz+biotite+muscovite+andalusite+sillimanite± plagioclase±cordierite, and

10) quartz+microcline+plagioclase+biotite+muscovite+ sillimanite±cordierite±garnet.

The sillimanite in assemblage (9) is late and has crystallized around the margins of andalusite. The presillimanite assemblage may have crystallized at about 0.33 GPa and 550°C (Fig. 100, 102a). The absence of staurolite, presence of anatexis, and the coexistence of minerals in assemblage (10) allow P-T conditions up to about 0.6 GPa and 660°C (Fig. 100, 102a). Apparent absence of anthophyllite-grunerite, however, suggests pressures may have been somewhat lower.

Rowley River (northeast NTS 37F)

The Mary River Group in an area along the upper Rowley River area about 25 km^2 (E-Fig. 101; Table 55) within tectonic subdomain 2a has also been anatectized and intruded by pegmatites and small granitic bodies. The following are some of the more useful assemblages:

11) quartz+biotite+muscovite+cordierite+sillimanite+ magnetite±(plagioclase or staurolite),

12) quartz+plagioclase+garnet+sillimanite+cordierite+ biotite, and

13) quartz+plagioclase+orthoclase+grunerite+hornblende+ magnetite.

The presence of staurolite and relative paucity of potassium feldspar may indicate slightly lower temperatures than in southcentral map area NTS 37G. Some of the assemblages allow for P-T conditions up to about 0.6 GPa and 650°C (Fig. 100, 102a). Microprobe data for one sample from the same locality (17 – Fig. 101) indicate 0.59 GPa at 603°C. Another sample from several kilometres to the west (18 - Fig. 101) gave 0.6 GPa and 735°C for Mary River Group metabasalt.

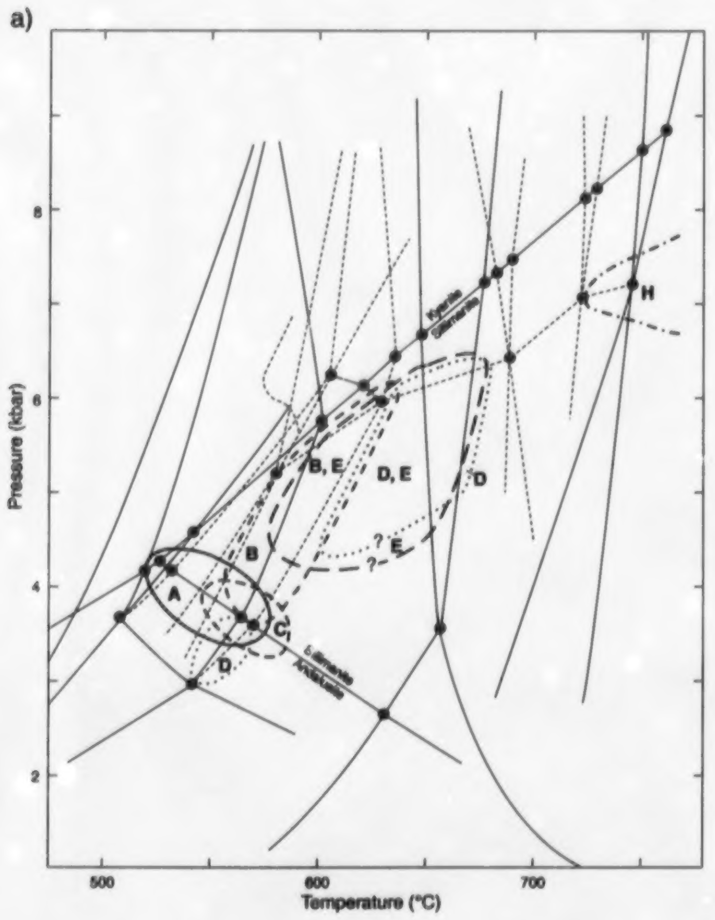

Figure 102a and b.

Pressure-temperature (P-T) estimates for the map area and Eqe Bay and Generator Lake areas just south of the map area. See Figure 101 for sample locations A-H. See also *Table 55.*

Eqe Bay (northeast NTS 37C) and east side of northern Barnes Ice Cap (NTS 37E)

These areas lie along the north side of tectonic subdomain 3a, where they are separated from the bordering Dexterity Granulite Belt to the north by the Isortoq Fault Zone (Fig. 101, 112-114). The Eqe Bay area (NTS 37C) in the west, just south of the map area, contains two supracrustal belts that are chiefly Mary River Group (Fa, Fb in Fig. 101; Table 55). They extend northeastward into the southern parts of map areas NTS 37E and 37F. Mineral assemblages, even over just a few kilometres, indicate a wide range of P-T conditions, as in the Mary River area (Jackson and Morgan, 1978a). Morgan et al. (1975) noted, and Bethune and Scammell (1993) corroborated, that the regional metamorphic grade increases both northwestward and southeastward from the southern (Fa – Fig. 101) supracrustal belt, and that the metamorphic grade in the northern belt (Fb) is distinctly higher than in the southern belt. Mary River Group strata have been variously anatectized and intruded by pegmatites and granite bodies. The more useful assemblages include:

14) quartz+cordierite+staurolite+sillimanite±garnet± (muscovite or biotite),

15) quartz+plagioclase+biotite+garnet+sillimanite+ orthoclase±muscovite±magnetite,

16) garnet+andalusite+cordierite+staurolite,

17) quartz+plagioclase+biotite+cordierite+staurolite+ (garnet+tourmaline, or anthophyllite)+chlorite(?), and

18) garnet±staurolite±kyanite.

Sillimanite occurs as late fibrolite in one thin section containing assemblage 17. Pressure-temperature conditions represented by these and other assemblages (*see* Bethune and Scammell, 1993; Morgan et al., 1975; Morgan, 1982; Scammell and Bethune, 1995a) may range from 0.3 GPa at 540°C to 0.6 GPa at 650°C and 0.63 GPa at 680°C. There are at least three main reasons why there is a large range of P-T conditions in the area. First, most of the assemblages are not very narrowly constrained; second, major northeast-trending fault zones in the area have produced abrupt changes in metamorphic grade, and third, deformation has probably produced

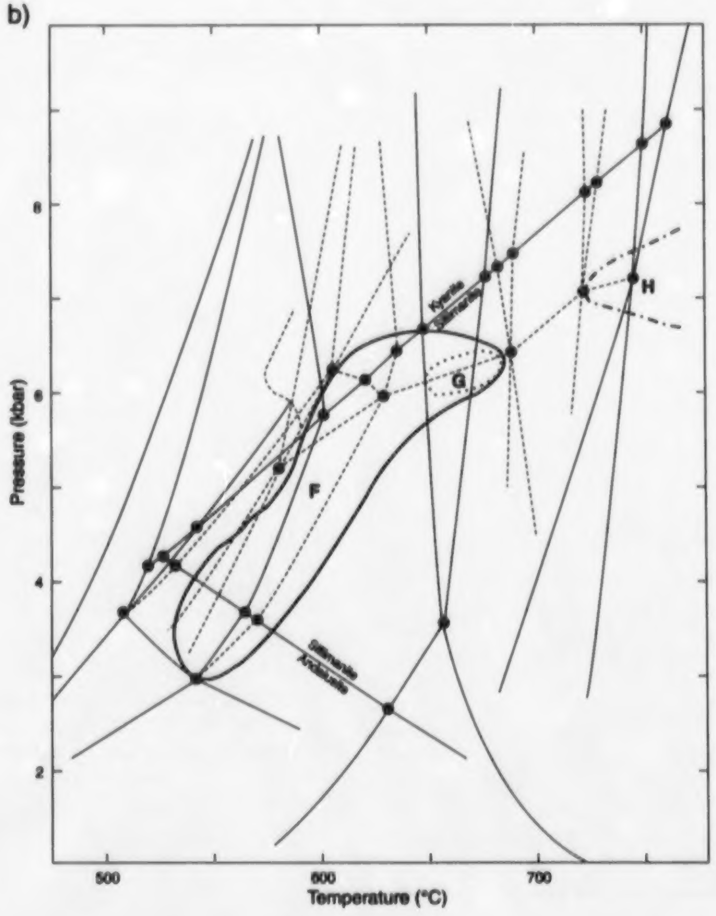

***Figure 102** (cont.)*

Table 55. Summary of P-T estimates, calculations.

Locality	Rock type	Method/ assemblage	Tectonic domain[1]	P (GPa)	T (°C)
A	MRGp pgn	P-T Grid	1a	0.43	550
	MRGp pgn	P-T Grid	1a	0.35	570
B	MRGp pgn	P-T Grid	1a	0.4-0.5	560-580
C	MRGp pgn	P-T Grid	1a	0.36	570
D	MRGp pgn	P-T Grid	1a	0.33	550
			1a, 2a	0.6	660
E	MRGp pgn	P-T Grid	2a	0.6	650
F	MRGp pgn	P-T Grid	3a	0.3-0.63	540-680
G	Piling Gp pgn	P-T Grid	3a-7a	0.61	660
H	MRGp pgn	P-T Grid	2c	0.7	800
(1)	paragneiss	1	1a	0.63	710
(2)	syenocharnockite	2	7a	1.10	810
(3)	pyribolite	3	7a	0.79	745
(4)	enderbite	1	7a	0.59	860 (0.52/755)
(5)	granoenderbite	3	7a	0.83	730
(6)	granoenderbite	6	7a	0.66	849
(7)	MRGp pyribolite	4	7a	0.69	655
(8)	MRGp metabasalt	3	7a	1.11	844
(9)	enderbite	6	7a	1.22	785
(10)	MRGp pgn	13	7a	0.56	725
(11)	monzocharnockite[3]	2	7a	1.12	750* (995)
(12)	MRGp pyribolite[2]	8	7a	0.5	740
(13)	syenocharnockite[3]	9	7a	1.12	750* (787)
(14)	felsic nebulite	6	7a	0.95	750* (1.09/833)
(15)	MRGp pgn	11	2a	0.59	603 (0.76/655)
(16)	MRGp pyribolite	5	2a	0.60	735
(17)	MRGp pyribolite	7	2c	0.88	750* (787, 856)
(18)	pyribolite	7	2b	1.28	750* (837, 914)
(19)	MRGp pgn	10	2c	0.88	750* (1.1/900)
(20)	pyribolite	4	2c	0.85	825
(21)	pyribolite	6	2c	0.85	650 (1.1/835; 920)
(22)	pyribolite	6	2c	0.87	850 (860, 920)
(23)	MRGp pgn	11	3a	0.45	584 (0.47/610)
(24)	MRGp pgn	12	3a	0.30	537 (0.34/665)
(25)	Piling Gp pgn	13	3a	0.56	685 (0.51/654)
(26)	Piling Gp pgn	13	3a	0.64	750* (0.25/650)
(27)	Piling Gp pgn	1	2c	0.84	825
(28)	Piling Gp pgn	1	2c	0.80	775
(29)	Piling Gp pgn	11	2c	0.50	600

MR – Mary River; Gp – Group; P–Piling; pgn – paragneiss

[1] *See* Figure 101 for localities and distribution of tectonic domains.

[2] Pyribolite is a metamorphic rock whose mafic minerals are chiefly pyroxenes.

[3] *See* Figure 15 regarding igneous classification.

[4] Cummingtonite is retrograde, hornblende includes prograde and retrograde varieties.

&*Indicates an assumed temperature. In most of these cases the temperature actually obtained seemed too high or too low because of the minerals present and the nature of the rock. The parentheses contain examples of values actually obtained for some of these samples, and/or values for a different calibration of the same thermobarometer.

Assemblages

1: gt-opx-bi-pl-qz
2: gt-opx-cpx-cg[4]-hb[4]-pl-qz-kf
3: gt-opx-cpx-bi-hb-pl-qz-kf
4: gt-opx-bi-hb-pl-qz
5: gt-bi-hb-pl-qz
6: opx-cpx-bi-hb-pl-qz-kf
7: opx-cpx-hb-pl-qz
8: opx-cpx-bi-pl-qz-kf
9: cpx-hb-bi-pl-qz-kf
10: gt-bi-sl-pl-qz
11: gt-bi-cd-sl-pl-qz
12: gt-bi-sl-pl-qz-kf
13: gt-bi-mv-sl-pl-qz-kf

bi-biotite, cpx-clinopyroxene, cd-cordierite, cg-cummingtonite, gt-garnet, hb-hornblende, kf-potassium feldspar, mv-muscovite, opx-orthopyroxene (hypersthene), pl-plagioclase, qz-quartz, sl-sillimanite

some of the steep gradients. The interpretation in Figure 102b suggests that about 0.6 GPa may have been a reasonable average maximum pressure. Wet chemical analyses of coexisting garnet and biotite in aluminous iron-formation (= ferruginous metapelite) at Eqe Bay (sample JDC 13-3, Appendix 5) yielded a temperature of 620°C at 0.6 GPa for the garnet-biotite thermometer of Hodges and Spear (1982). Probe analyses for a second sample from the southern supracrustal belt (Fa) in the Eqe Bay area (23 - Fig. 101) gave 591-635°C at 0.6 GPa for the garnet-biotite thermometer of Hodges and Spear (1982), 0.47 GPa at 560°C for the cordierite-garnet-sillimanite-quartz thermobarometer of Martignole and Sigi (1981), and 0.40-0.61 GPa at 557-603°C for the garnet-plagioclase-quartz-sillimanite barometer of Newton and Haselton (1981). A reasonable result for the equilibration of most of the minerals seems to be 0.45 GPa at 584°C (Table 55, Fig. 101).

Similar Mary River Group paragneisses on the east side of the northern end of Barnes Ice Cap were also analyzed by microprobe. A pressure of 0.4 GPa at 560°C was obtained (24, Fig. 101; Table 55).

Head, Sam Ford Fiord (southwest NTS 27F)-Generator Lake (northwest NTS 27C)

Several useful mineral assemblages in the Longstaff Bluff Formation of the Piling Group occur in an area that extends from Generator Lake at the southeast end of the Barnes Ice Cap (northwest NTS 27C), just south of the map area to the head of Sam Ford Fiord (southwest NTS 27F) (Fig. 1; G – Fig. 101, Table 55). This area extends from the southeast corner of tectonic subdomain 3a (Fig. 101), northeastward into the western part of the Northeast Baffin Thrust Belt (tectonic subdomain 7a). Although the metapelites have been anatectized and intruded by pegmatites, tourmaline occurs in some assemblages. Three of the more interesting assemblages are:

19) quartz+plagioclase+potassium feldspar+biotite+cordierite±sillimanite,

20) quartz+plagioclase+microcline+biotite+sillimanite±muscovite±garnet±magnetite, and

21) quartz+garnet+cordierite+sillimanite+anthophyllite-cummingtonite±hornblende.

The assemblages present suggest the P-T relations shown in Figure 102b (about 0.61 GPa at 660°C). Wet chemical analyses of coexisting garnet and biotite in aluminous facies iron-formation (= ferruginous metapelite) at Generator Lake (Appendix 5 – sample JDC 266-1) gave a temperature of 617°C at 0.6 GPa for the Hodges and Spear (1982) calibration of the garnet-biotite thermometer.

Microprobe analyses for a second sample (25 - Fig. 101, Table 55) indicate 720°C at 0.6 GPa for the garnet-biotite thermometer of Hodges and Spear (1982), 0.56 GPa at 685°C for TWQ, 0.48-0.62 GPa at 644°-662°C for the garnet-plagioclase-aluminosilicate-quartz barometer of Newton and Haselton (1981), and temperatures of 629° and 708°C for the feldspar thermometers of Haselton et al. (1983) and Whitney and Stormer (1977). The rocks contain abundant pegmatites 1-2 m thick, and a reasonable maximum for the metamorphic conditions in the Generator Lake area (subdomain 3a) is probably 0.56 GPa at 685°C.

Similar paragneisses to those east of Generator Lake occur to the north, in the Northeast Baffin Thrust Belt west of the head of Sam Ford Fiord (G - Fig. 101), but gave temperatures of 798° and 817°C at 0.6 GPa for the feldspar thermometers of Whitney and Stormer (1977) and of Haselton et al. (1983). However the rocks in both areas are probably of similar metamorphic grade.

Results for a sample of similar Piling paragneiss from about 50 km southeast of Generator Lake (26, Fig. 101; Table 55) indicate a pressure of 0.64 GPa at an assumed temperature of 750°C. However, the garnet-biotite thermometer of Hodges and Spear (1982) indicates about 650°C for that pressure. The Piling Group at the site contain only a few granitic and pegmatite dykes up to 2 m thick, and are not anatectized. Orthopyroxene is absent, the rocks are probably barely into the upper amphibolite facies, if that, and the metamorphic grade is probably somewhat lower than at Generator Lake. Therefore 650°C is considered to be a maximum temperature, for which TWQ gives a pressure of 0.25 GPa. These results are considered reasonable and are in agreement with the mineral assemblage present (e.g. Winkler, 1979).

Dexterity Granulite Belt

Two general types of assemblages have been distinguished in the granulite terrane (Fig. 99; Table 55): a) hypersthene-bearing with or without hornblende, clinopyroxene, and garnet; no sillimanite, cordierite, or spinel; b) sillimanite-bearing with or without cordierite, cummingtonite, garnet, and spinel; without hypersthene. Both types commonly contain biotite, quartz, plagioclase, and potassium feldspar. Most supracrustal assemblages come from the area around the northwest end of the Barnes Ice Cap (Fig. 99, H - Fig. 101, 114), and Mary River Group strata do not seem to be migmatized to any greater extent than in the upper amphibolite facies, which indicates that granulite metamorphism was relatively dry.

The various assemblages present seem to indicate that a range of P-T conditions is represented, which is probably related in part to the belt's overlapping of several tectonic subdomains (Fig. 101). The abundance of hypersthene throughout the belt indicates that, in general, temperatures of 700°C have been attained. The presence of cummingtonite-sillimanite assemblages without hypersthene in aluminous facies iron-formation (No. 12, Table 13) associated with hypersthene-bearing assemblages indicates an absence of high pressure granulites at those localities. Some assemblages contain abundant hornblende or biotite, or both, and many represent relatively low pressure conditions, compositional differences, or differences in P_{H_2O}. Several assemblages are of interest (*see* section on "Granulite facies", above), and include:

22) quartz+plagioclase+potassium feldspar+biotite+hypersthene,

23)quartz+plagioclase+biotite+clinopyroxene+hypersthene+garnet,

24)quartz+hypersthene+magnetite±garnet,

25)quartz+biotite+garnet+sillimanite+spinel+magnetite, and

26)quartz+plagioclase+potassium feldspar+garnet+biotite+(sillimanite or cordierite).

The abundance of sillimanite-cordierite-garnet assemblages, yet absence of sillimanite or cordierite or both with hypersthene, may be related in part to composition, but probably indicates that the metamorphic pressure was below that required for the association to form. Taking into account the P-T ranges derived for the lower grade rocks, a field approximating that shown in Figure 102b may be reasonable, and P-T conditions may have been about 0.7 GPa and 800°C for some assemblages.

The spinel-bearing assemblage (25), however, which occurs at the northwest end of the Barnes Ice Cap (locality H), suggests higher temperatures may have been present. In thin section, green spinel (hercynite?) occurs in part as rims around magnetite and contains a few inclusions of sillimanite. The spinel has formed at the expense of magnetite, garnet, and sillimanite. Most sillimanite and garnet seem compatible, but minor garnet also rims magnetite, and traces of sillimanite seem to have formed from garnet and, possibly, spinel. A few of the biotite grains transect the other minerals, and traces of late muscovite are also present. Cordierite occurs with sillimanite and magnetite in another assemblage from the same locality. The cordierite is considered to be a Mg variety because its refractive indices are clearly lower than those for quartz.

Pressure-temperature determinations for five samples of pyribolites and paragneisses in the southwest end of the Dexterity Granulite Belt indicate pressures of 0.80-0.87 GPa. Indicated temperatures in this region range from 650°C for the north-central part of the belt to 775°-850°C for the central and southern parts (20, 21, 22, 27, 28: Fig. 101, Table 55). Results for one sample of paragneiss from relatively close to the Isortoq Fault Zone (29), however, indicate 0.5 GPa at 600°C.

Three samples were taken across the central part of the Dexterity Granulite Belt north of the Barnes Ice Cap (17, 18, 19: Fig. 101, Table 55), the same region as locality H discussed above. Two samples, one of pyribolite and the other of paragneiss, gave pressures of 0.88 GPa for the north and south sides of the belt. The third sample, from the middle of the belt, gave 1.3 GPa for a pyribolite band in the margin of a charnockite pluton. A temperature of 750°C was assumed for all three samples because the actual temperatures obtained range from 787° to 914°C for the middle sample. Most of these temperatures seem high when the mineral assemblages and rock types are considered.

Similarly, temperatures ranging up to more than 995°C have been obtained for three samples from the northeast end of the Dexterity Granulite Belt (11-13: Fig. 101, Table 55). Two of the samples are charnockite from the Dexterity Batholith and one is from felsic nebulite (possibly older basement). Assuming a temperature of 750°C for the samples yields pressures of 0.95-1.12 GPa. A fourth sample (12), from pyribolite adjacent to the northwest margin of the Dexterity Batholith, gave 0.5 GPa at 740°C.

Northeast Baffin Thrust Belt

The northeast end of the Dexterity Granulite Belt is considered here to have been overridden by the younger (ca. 1.81-1.80 Ga) Northeast Baffin Thrust Belt (Fig. 101, 113; tectonic subdomain 7a). Therefore the pressure and temperature results for the east end of the granulite belt also apply to the thrust belt. In addition, a pressure of 0.56 GPa at 725°C was obtained for a paragneiss sample (10, Fig. 101) from the Buchan Gulf area to the north.

South of Bylot Island, 1.22 GPa at 785°C was obtained for an enderbite sample (9: Fig. 101, Table 55) from the east side of the thrust belt. A sample of metabasalt from the west side of the belt (8) gave 1.1 GPa at 844°C.

A sample of syenocharnockite from northwest Bylot Island yielded 1.1 GPa at 810°C (2: Fig. 101, Table 55). To the east, three samples of granoenderbite and enderbite, two (4, 5) from the sheared west side of the Bylot Batholith (Fig. 114) and one (6) from the relatively undeformed east side, gave 0.59-0.83 GPa at 730°-860°C. A sample of pyribolite (3) in the western Bylot Batholith gave 0.79 GPa at 745°C, whereas 0.69 GPa at 655°C was obtained for a pyribolite sample (7) from southeast of the batholith.

A pressure of 0.63 GPa at 710°C was obtained for a sample of paragneiss (1, Fig. 101) in mixed gneisses on the east side of Admiralty Inlet. This location is considered tentatively to lie in tectonic subdomain 1a rather than 7a; although the boundary between is probably found in the vicinity, its location is uncertain.

Contact metamorphism

The Dexterity Batholith, the largest charnockite body in the main granulite belt, lies east of Dexterity Fiord (NTS 37H), and the hypersthene isograd lies only a short distance away from the pluton around most of its perimeter. The regional distribution of the granulite belt, cutting across various rock types (*see* geological maps; Fig. 99), indicates that both the pluton and the hypersthene isograd are probably a product of the same metamorphic event. The charnockite pluton at the north end of the Barnes Ice Cap (NTS 37E) is also partially bordered by the hypersthene isograd, but equally large plutons in northwestern map area NTS 37G have affected adjacent rocks very little. While it seems very likely that both the granulite belt and the contained charnockite bodies owe their presence to the same regional event, it also seems likely that the aureoles are some sort of a contact metamorphic effect. Three possible explanations for these apparent thermal aureoles are:

a) They are related to emplacement of relatively hot magmatic bodies during metamorphism.

b) The thermal aureoles reflect the buildup of frictional heat around the margins during deformation.

c) Low grade metamorphism and dehydration of the marginal rocks during emplacement made it easier to superimpose a high grade assemblage during a later metamorphic event.

The first two possibilities seem the most likely.

Contact metamorphism adjacent to Helikian-Hadrynian diabase dykes is most obvious in Bylot Supergroup strata. A baked appearance and alteration of shale to slate or argillite extends as much as a metre away from the larger dykes. A slight colour change, in some places to a more greenish cast, is also common. Some gneisses also have a baked appearance adjacent to the dykes.

Summary and conclusions

Much of the map area has been affected by at least three episodes of regional metamorphism. The first (ca. 2.85-2.84 Ga) affected the granitic basement prior to deposition of the Mary River Group about 2.75-2.72 Ga ago. The second affected the Mary River Group and basement about 2.77-2.71 Ga ago, and the third, possibly the most intense and pervasive, is considered to be related to the 1.90-1.81 Ga events that forged Baffin Orogen and the huge Cumberland Batholith to the south and the 2.0-1.9 Ga Thelon Tectonic Zone to the northwest. Mineral associations and the absence of migmatites in much of the Mary River Group indicate that some of the group never underwent high grade regional metamorphism. Transition from very low- to high-grade regional metamorphism over short distances suggest either sporadic metamorphic highs or relatively steep thermal gradients and subsequent deformation. Separation of mineral assemblages related to the different metamorphic events is not yet feasible except locally. Available age determinations are compatible with the assumption that most assemblages originated with, or have been modified by the 2.0-1.80 Ga events.

Most of the map area is in the upper amphibolite facies of regional metamorphism, in the 0.55-0.65 GPa and 600°-680°C range. Subgreenschist to lower amphibolite facies terranes occur sporadically chiefly in a north-south belt in the western part of the map area (Fig. 99). Absence of anatexis in these low grade rocks indicates that they have probably not been metamorphosed to upper amphibolite or granulite grade and then retrograded.

Both field observations and pressure and temperature determinations indicate that metamorphic gradients are more abrupt south of the Dexterity Granulite Belt than north of it. Although gradual regional changes in metamorphic grade are common, the P-T and aeromagnetic data and structural trends (Fig. 111-114) indicate that step-like changes along fault zones and shear zones are more common than originally believed. For example, metamorphic discontinuities may coincide with the Central Borden Fault Zone, Milne Inlet Trough, and boundaries between tectonic subdomains. Pressures and temperatures may be about 0.05 GPa and 50°C higher in tectonic subdomain 2a than in 1a.

In general, the northern, western, and internal boundaries of the Dexterity Granulite Belt seem gradational and the hypersthene isograd crosses tectonic boundaries. Most of the granulite belt has probably attained 0.85 GPa or more at temperatures of 750°-850°C. These values are similar to but slightly higher than those obtained on and south of Bylot Island, and pressures are higher by 0.1-0.2 GPa than those obtained for the Cumberland Batholith in southern Baffin Island (Berman et al., 1993). Determined pressures and temperatures are relatively uniform for the southwest segment of the Dexterity Granulite Belt, and indicate a southeastward increase to about 0.85 GPa and 825°C along the southeast margin of the belt adjacent to the Isortoq Fault Zone. However, the central and northeast segments may contain a northeast-trending central zone of relatively high pressures and temperatures greater than 1.3 GPa and/or 970°C. These differences indicate that the three segments have been displaced relative to one another by faulting, of which Neohelikian-Cenozoic faulting was at least a component.

The Dexterity Granulite Belt is truncated along its southeast side by the Isortoq Fault Zone, south of which metamorphic pressures and temperatures are lower, although granulites occur locally. Paleopressures in the granulite belt are about 2.0-2.5 GPa higher than those south of the fault zone. Thus the south edge of the granulite belt has been uplifted about 8 km (7-9 km) relative to rocks on the south side of the fault. The lower temperatures obtained for the north side of the southwestern segment of the granulite belt suggest that it has also been tilted upward to the southeast. Relatively high pressures have been obtained for the two eastern segments (Fig. 101).

A zone of low- to medium-grade metamorphism occurs along the southern Eqe Bay supracrustal belt (Fa, Fig. 101) roughly 30 km southeast of, and parallel to, the Isortoq Fault Zone. This belt probably extends discontinuously to northeast of the Barnes Ice Cap. As observed by Morgan et al. (1975), the metamorphic grade increases both northwestward toward the fault zone and southeastward away from this low grade zone. Further south the regional metamorphic grade drops again along the south side of the Piling Fault Zone (Fig. 101, 113). The origin of the alternate higher and lower grade banding of the regional metamorphism is uncertain. It could be due to later warping or faulting unrelated to the metamorphic event. However, it seems more likely that it is related to compressive events during formation of the Dexterity Granulite Belt and the Isortoq Fault Zone late in the evolution of the Baffin Orogen (*see* "Isortoq Fault Zone" under "Structural geology").

Data presently available indicate that metamorphic pressures and temperatures are variable in the Northeast Baffin Thrust Belt. They are also higher than in the other tectonic domains of northern Baffin Island except within the Dexterity Granulite Belt (Fig. 101). Peak conditions in the thrust belt north of the granulite belt exceed 1 GPa and 800°C, and are compatible with the belt being a southwest-directed ductile thrust and nappe complex as discussed below. As noted by Jackson and Morgan (1978a), Baffin Island consists of three large fault blocks each of which has been tilted upward toward the northeast mainly in the Cenozoic. The largest block includes all of Baffin Island northward from Cumberland Peninsula (Fig. 113). It seems quite likely that, although

Table 56. Physical characteristics, Mary River high grade iron deposits (from Baffinland Iron Mines Limited, 1964, 1966).

Deposit No.	Length ft. (m)	Width ft. (m)	Surface exposure ft.^{2} (m^2)	Potential reserve long tons per vertical ft. (tonnes per vertical m)	Potential of open pit tonnage to depth million long tons (million tonnes)	Ore type
1	9800 (2987)	100 (31)	980 000 (91 045)	531 800 (1 772 664)	130.65 (132.74)	- pure magnetite or hematite or both
2	2000 (610)	20-230 (6-70)	160 000 (14 865)	20 000 (66 667)	7.00 (7.11)	- specularite
3	340 (104)	350 (107)	120 000 (11 148)	15 000 (49 999)	5.00 (5.08)	- hard blue hematite
3A	600 (183)	40-100 (12-30)	45 000 (4181)	5500 (18 333)	3.00 (3.05)	- magnetite and specular hematite
4	7800 (2377)	50-250 (15-76)	1 000 000 (92 903)	125 000 (1 416 666)	46.00 (46.74)	- magnetite lump

Note: Metric values are shown in parentheses and are calculated from original Imperial system values.

the uptilting probably does not account for all the difference in pressure, it likely accounts for differences of 0.1-0.2 GPa. The uptilting is also undoubtedly a factor in accounting for the greater number of small isolated granulite facies areas along the northeast side of the largest uptilted block.

The highest temperatures and/or pressures determined are for charnockite and pyribolite inclusions in charnockite (11, 18, Table 55). Also, charnockite-enderbite and pyribolite consistently give relatively high results. Although these temperatures seem high, they are probably indicative of relatively dry rocks that preserved indications of relatively high metamorphic grade. These results also suggest that the charnockitic plutons were hot when they were emplaced as deep seated, synmetamorphic, late-tectonic plutons whose dissipating heat contributed to the metamorphism of adjacent rocks. Granulite metamorphism, especially in the Dexterity Granulite Belt, has been considered to be Late Aphebian because of the granulite metamorphism of Piling Group strata, Rb-Sr and K-Ar ages that indicate that the region has been affected by Aphebian thermal events, and U-Pb zircon data for two widely separated granitic rocks (*see* section on "Ages of late massive granitic intrusions (Ag, Ack)") that indicate that some late plutons outside the granulite belt are late Aphebian mobilizate derived from Archean crust (Jackson and Morgan, 1978a; Jackson et al., 1990b). Uranium-lead zircon and monazite ages reported recently by Scammell and Bethune (1995a, b) dated the granulite metamorphism in the southwest corner of the Dexterity Granulite Belt at 1827-1821 Ma, and a nearby post-tectonic granite at ca. 1819 Ma.

The aeromagnetic data (Fig. 111) are typical for granulite terranes but the plutons are not obvious, which suggests they are not postmetamorphic. Also, the Dexterity Granulite Belt crosses Baffin Island through a broad ill-defined gravity low shown on the regional gravity map of Canada, similar to the one coinciding with the central part of the Cumberland Batholith in southern Baffin Island (Fig. 113). None of the charnockitic plutons are known to extend across the Isortoq Fault Zone, although a few small late granitic and charnockitic plutons occur south of the fault zone (e.g. in southern NTS 37E) and similar granitic plutons occur north of the granulite belt in map areas NTS 37E, 37F, and 37H. Also, the southwestward extension of the fault zone on Melville Peninsula (Fig. 113) seems to terminate in a group of granitic plutons, some of which are Late Aphebian (e.g. Ford Lake Pluton; Henderson et al., 1986; LeCheminant et al., 1987).

The distribution of Late Aphebian granitic plutons, including the charnockites (Fig. 112, 113, 114), does not show any obvious relation to the Isortoq Fault Zone. The Mary River Group extends across both the Dexterity Granulite Belt and the Isortoq Fault Zone, and the Piling Group across the fault zone north into the granulite belt. These features suggest that the Isortoq Fault Zone itself is not a suture, but rather a mid-continental tectonic zone as discussed below. In addition, these relationships together with the observation that the hypersthene isograd extends across some plutons suggest that at least some of the charnockitic plutons are older plutons that preserved the record of relatively high temperatures and pressures along the tectonic zone because they were relatively dry rocks to begin with. Most U-Pb zircon ages and all Nd model ages (Hegner and Jackson, 1990) for rocks older than the Piling Group in the metamorphic complex are Archean.

ECONOMIC GEOLOGY

A variety of mineral occurrences have been noted in the map area (Kranck, 1951; Eade, 1953; Gross, 1966; Jackson, 1966b, 1968, 1969, 1984; Jackson and Morgan, 1978b; Jackson et al., 1978b, c, d; Levy, 1978, 1979; Grant et al., 1986; Jackson and Sangster, 1987). However, the rugged terrain and difficulty of transport, poor weather, and remoteness of the region make exploration difficult and expensive. Only relatively large, high grade deposits in favourable topographic positions can be considered seriously as potential producers. Much of Baffin Island was prospected for diamonds on a reconnaissance scale in 1994.

Iron

To date, only iron deposits in the Mary River area (Fig. 106, 107) seem to contain potential for future production. The largest deposits were found at Mary River by Murray Watts in 1962 and five high grade deposits have since been outlined by Baffinland Iron Mines Limited (1964, 1966). The data in Tables 56 and 57 are taken from their reports. The No. 1 iron deposit alone contains over 130 million tonnes of high grade iron ore averaging more than 68 per cent soluble iron, with less than 1% silica and negligible amounts of other impurities such as P, S, Ti, and Mn (Table 57). No. 1 iron deposit (Fig. 40, 107) is very amenable to open pit mining. According to Baffinland Iron Mines Limited, the ore is hard, of lump quality, and blast furnace tests and direct reduction experiments show conclusively it is suitable for pig iron production. The total potential reserves of high grade ore in the Mary River area are estimated to be more than 300 million tonnes. Even larger tonnages of mineable low grade oxide facies iron-formation are present.

As noted in the section on oxide facies iron-formation and high grade iron oxide, at least one zone of nearly pure iron oxide is commonly present in oxide facies iron-formation. The thickest zone in the Mary River area may be 152 m thick; as much as 30 m are present east of Grant-Suttie Bay, and thinner zones occur at several other localities. Analyses of Davis Tube separations for selected samples of high grade iron from Mary River Group iron-formation, other than in the Mary River area, are provided in Table 58. More complete analyses for these samples are presented in Tables 14 and 15. Except for the one sample from the granulite terrane northwest of the Barnes Ice Cap (sample B275/1), there seems to be no correlation between per cent recovery and metamorphic grade.

Lead-zinc

Lead-zinc ore is currently being mined from the Society Cliffs Formation at Nanisivik in the west end of the Milne Inlet Trough about 125 km northwest of the Mary River area (northwest NTS 37G). Small amounts of silver and variable amounts of barite and fluorite are common. Similar galena-sphalerite mineralization occurs in Society Cliffs strata on the east side of the west fork of Paquet Bay near its mouth in northern map area NTS 37G. Several additional occurrences in the Uluksan Group extend northwest from this showing, along the White Bay Fault Zone (Jackson and Sangster, 1987). In addition, sparse small sphalerite crystals occur locally in Uluksan Group carbonates just north of the map area. The mine ore and most of the showings in Milne Inlet Trough are considered to be Mississippi Valley-type deposits.

Table 57. Average analyses in weight per cent for high grade iron deposits, Mary River area (NTS 37G) (from Baffinland Iron Mines Limited, 1964, 1966).

Deposit	1					2	3	3A	4
	South and north limb	North limb extension	South limb extension	Average[1]	Drillhole average				
Samples	**156**	**42**	**8**	**206**	**10**	**22**	**9**	**10**	**32**
Fe Total	69.76	70.62	62.91	69.67	66.24	68.03	68.13	68.70	66.84
Fe_2O_3 Total[2]	99.74	100.97	81.73	99.61	94.70	97.26	97.41	98.22	95.56
SiO_2	0.27	0.71	2.97	0.46	2.18	2.13	0.56	0.83	2.06
Al_2O_3	0.04	0.57	1.77	0.49	1.70	0.33	0.46	0.70	0.74
CaO					0.06				
MgO					0.54				
MnO	0.11	0.15	0.61	0.14	0.26[4]	0.02	0.07	0.03	0.11
TiO_2	0.05	0.05	0.05	0.05	0.06	0.05	0.05	0.05	0.05
P	0.016	0.104	0.109	0.038	0.030	0.010	0.035	0.047	0.081
S	0.015	0.010	0.018	0.014	0.116	0.006	0.004	0.007	0.016
LOI					0.63				
Total[3]	100.24	102.56	87.26	100.80	100.30	99.81	98.59	99.88	98.62

Notes: 1 - Average calculated for North and South Limb, North Limb Extension, and South Limb Extension.
2 - Fe_2O_3 Total calculated from Fe Total, which was obtained by analysis.
3 - Total calculated including Fe_2O_3 Total values and excluding Fe Total values.
4 - MnO calculated from Mn.
Blanks indicate no data.

Table 58. Analyses of Davis Tube separations (*see* Johnson and Maxwell, 1981) for selected samples of iron ore from Mary River Group iron-formation (Mif, Amif). *See* Tables 14 and 15.

Sample	Map area	Wt. Original sample	Wt. Head sample	Wt. conc.	Wt. tailings	Loss		% Fe_2O_3T Head sample	Wt. Fe_2O_3 Head sample	% Fe_2O_3T conc.	Wt. Fe_2O_3T conc.	Wt. Fe_2O_3T tailings	% Recovery conc.
						Wt.	%						
C19/1	37C[f]	3405	50	12.0	36.4	1.6	3.2	55.85	27.9	90.00	10.8	17.1	38.7
C21/2	37C[e]	1192	50	0.6	48.4	1.0	2.0	88.60	44.3	101.70	0.6	43.7	1.4
J112/1	37F[c]	1022	50	48.5	0.6	0.9	1.8	100.70	50.0	102.00	48.5	1.5	97
J248/5	37F[c]	2979	50	12.2	36.2	1.6	3.2	84.10	42.1	101.50	12.2	29.9	29.0
B293/2	37F[c]	936	50	0.2	49.0	0.8	1.6	51.41	25.7	100.00	0.2	25.5	0.8
B118/2	37G[b]	1078	50	20.2	28.4	1.4	2.8	48.95	24.5	92.00	18.6	5.9	75.9
B275/1	37E[d]	1589	50	47.6	1.2	1.2	2.4	101.30	50.0	100.70	47.6	2.4	95.2

Davis Tube separations by CANMET mineral sciences laboratories, analyses by GSC laboratories.

All weights (Wt.) in grams	% = weight per cent	c = Rowley River area	e = Isortoq Fiord
conc. = concentrate	b = Ravn River area	d = Northwest Barnes Ice Cap	f = Eqe Bay

Small blobby grains of galena occur locally with chalcopyrite, pyrite, pyrrhotite, and sphalerite in several minor shear zones and one quartz vein south of No. 1 iron deposit at Mary River adjacent to the Central Borden Fault Zone. Galena, sphalerite, and chalcopyrite mineralization has been noted at several localities in strata of both Mary River and Piling groups south of the western part of the map area by Morgan et al. (1975). A sample from micaceous schist from the Piling Group in map area NTS 27C (exact location uncertain) contains 13% zinc in sphalerite, 0.06% copper, 0.05% lead, 0.01% each of cobalt and nickel, and 1.37 g/t of silver (Table 60). The Piling Group is correlated with the Karrat Group, which contains the Black Angel lead-zinc deposit in northern West Greenland.

Copper, molybdenum

In addition to the chalcopyrite associated with galena at No. 1 iron deposit, chalcopyrite, with pyrite, occurs locally in the Mary River Group iron-formation and associated rocks at various places, chiefly in map area NTS 37G. Traces of chalcopyrite have also been reported from the Clyde region (NTS 27D-G, northeast NTS 37E) by Kranck (1951). Malachite staining is associated chiefly with mafic boudins at several localities in the Buchan Gulf area (NTS 37H) and atacamite occurs in migmatitic rocks at the south end of The Mitres (northwest NTS 37H). Chalcopyrite and malachite staining occur in several rock types in the Eqe Bay – Grant-Suttie Bay area, just south of the map area.

Semiquantitative analyses of gypsum and red gypsiferous shale from the Society Cliffs Formation just north of the map area have indicated as much as 0.15% Cu (Table 59). The sedimentary environment is considered favourable for the deposition of sedimentary copper (Jackson et al., 1975), although the particular facies involved are rare in the map area.

Molybdenite occurs in a shear zone, and in pegmatite, in the northern part of the Mary River area on the southwest side of the Murray River. A few blebs of molybdenite were also seen on the north side of Clyde River south of the map area.

Ultramafic rocks

It was the ultramafic rocks that first drew Murray Watts's attention in the Mary River area. These have since been examined by several companies but so far nothing of real economic interest has been found. Spectrographic analyses indicate an average of 0.17% (0.089-0.24) Ni, 0.27% (0.036-0.47) Cr, and 0.10% (0.073-0.13) Pb (Tables 23, 48; Appendices 2-4).

Cross-fibre veinlets of chrysotile asbestos, as much as 1 cm across, occur chiefly south and southeast of No. 1 iron deposit at Mary River. The asbestos in some places appears to be developed at the present rock surface and not to extend very far into the rock. The largest concentrations of veinlets were seen in two 15 cm thick contact zones that border a 60 cm thick amphibolite dyke. Traces of asbestos were seen elsewhere, chiefly in map area NTS 37G. Ultramafic rock on a small island at the mouth of Sam Ford Fiord in northwestern map area NTS 27F also contains asbestos.

Table 59. Semiquantitative analyses of gypsum and gypsiferous shale, Society Cliffs Formation (NSC).

Sample Map area Map unit	J218/2 38B NSC	J218/3 38B NSC	J219/1 38B NSC	J219/2 38B NSC
Al	0.3	0.3	5.0	0.3
Ti	0.010	0.007	0.15	0.007
Fe	0.15	0.10	1.5	0.2
Mn	0.02	0.015	0.07	0.010
Mg	1.0	1.0	5.0	0.3
Ca	5.0	5.0	5.0	5.0
Ba	0.015	0.02	0.03	0.010
Be	NF	NF	NF	NF
Ce	NF	NF	NF	NF
Co	NF	NF	NF	NF
Cr	NF	NF	0.015	NF
Cu	0.003	0.0010	0.15	0.0010
La	NF	NF	NF	NF
Ni	NF	NF	NF	NF
Pb	NF	NF	NF	NF
Sr	0.2	0.2	0.10	0.15
V	NF	NF	0.02	NF
Y	0.01	0.02	NF	NF
Yb	0.05	0.05	NF	NF
Zn	NF	NF	NF	NF
Zr	NF	NF	0.03	NF

Values determined in weight per cent by semiquantitative spectrochemical methods. Determinations expected to lie within one step of the figure reported in the series 1, 1.5, 2, 3, 5, and 7 only (eg. The true value of 0.2 is expected to lie between 0.15 and 0.3). NF - Not found.

Miscellaneous minerals

Seventeen grab samples were taken chiefly from rusty or sulphide-bearing zones in various rock types, mostly gneisses, and analyzed by semiquantitative spectrochemical methods (Table 60). The samples came from the map area and the area to the south. The results were disappointing, although 0.7% Cu was obtained for a sample from the same locality that contains atacamite (identified by X-ray) (C163/8, south end of The Mitres, northwest NTS 37H). It would seem that, as usual, most of the sulphide-bearing zones are barren. A lake sediment and water regional geochemical survey for the region adjoining the map area to the south and west of the Barnes Ice Cap, identified several localities that contain anomalously high values of arsenic, uranium, and/or various base metals (Cameron, 1986).

Three samples of quartz veins (1 in map area NTS 37G, 2 in map area NTS 27C) were assayed for gold by laboratories at the Canada Centre for Mineral and Energy Technology (CANMET). No gold was found, although traces of silver are present (Table 60).

Table 60. Analyses for base and precious metals.

Sample	J244	J130/6	C163/8	J259/3	J109/4	J110	B157	J412/2	J332/3	B458/7	J360/2	J378/2	C231/3	J339/4	M357*	J368/7	J370/5
Map unit	*Amg*	*Amg*	*Amg*	*Amg*	M	M	M	ADL	*APc*	*AAR*	*APs*	AKgn	*APs*	*APr*	*APs*	*APr*	*APr*
Map area	37H	37G	37H	37H	37G	37G	37G	37D	27C	37D	27C	27C	27C	27C	27C	27C	27C
Ni	NF	0.01	NF	NF	NF	NF	0.01	0.020	NF	0.020	0.01	0.020	0.030	0.01	0.01	0.01	0.01
Zn	NF	NF	NF	NF	NF	NF	NF	NF	NF	0.30	NF	NF	0.10	NF	13	NF	NF
Cu	0.010	0.020	0.70	0.0050	0.0015	0.0030	0.0010	0.020	0.0030	0.030	0.0050	0.0070	0.030	0.030	0.020	0.010	0.020
Co	NF	NF	NF	NF	NF	NF	NF	0.010	NF	0.010	NF	NF	NF	NF	0.01	NF	NF
Pb	NF	NF	NF	NF	NF	NF	NF	NF	NF	NF	NF	NF	NF	NF	0.05	0.10	0.070
Mo	NF	NF	NF	NF	NF	NF	NF	NF	0.01	NF	0.01	NF	NF	NF	NF	NF	NF
Ag							0.0005								0.0001	0.0005	0.0005
Au							NF									NF	NF

Values determined in weight per cent by semiquantitative spectrochemical methods. Values reported are expected to lie within one step of the figure reported in the series 1, 1.5, 2, 3, 5, and 7 (*see* Table 56).
See references noted for description of map units in specific map areas: 37G - Jackson et al., 1978a; 37H - Jackson et al., 1978b; 37D - Morgan, 1983; 27C - Henderson, 1985a.
NF = Not found; * Precise location not known. Blanks indicate no data.

Data from adjoining areas to the south suggest that pegmatites within the map area may contain minerals of possible economic interest. Kranck (1951) noted the abundance of tourmaline and fluorite in pegmatites of the Clyde region, and recorded the presence of columbite in pegmatite at Eskimo Hill, Generator Lake. Cerny (1988) has studied in detail the mineralogy of the Eskimo Hill pegmatites. High radioactivity has been reported in breccia, shear zones, and pegmatites by Morgan et al. (1975).

Uranium mineralization underlies two airborne radioactivity anomalies north of Fury and Hecla Strait, west of the map area (Chandler et al., 1980; Ciesielski and Maley, 1980; Maurice, 1982; Ciesielski, 1983; Maurice and Charbonneau, 1983; Chandler, 1988). The uranium occurs in late granite and associated pegmatites subjacent to the unconformity at the base of the Fury and Hecla Group. Mineralization underlying the eastern anomaly occurs adjacent to faults along the unconformity below Fury and Hecla Group redbeds. Similar geological and structural relations exist adjacent to the Bylot Supergroup in northern map area NTS 37G. Some radioactive anomalies have been located adjacent to the basal contact of the Bylot Supergroup northwest of the map area by investigating companies, but the anomalies are small and apparently of little interest.

Blue cordierite crystals, up to 15 cm long and possibly of gem quality, occur in small pegmatites (≈30 cm thick) on a small island in Dexterity Fiord (southeast NTS 37H). The pegmatites intrude garnetiferous pyribolite, and the island is just south of the connection between the fiord and Patterson Inlet.

Gold

Gold has been found by Strathcona Mineral Services Ltd. (R. Von Guttenberg, pers. comm., 1993) in the Mary River Group of the Eqe Bay area, just south of the western part of the map area. The gold occurs in thin millimetre- to centimetre-thick sulphide lenses in quartz+amphibole+garnet±biotite schist and gneiss that also contain chlorite, cordierite, and staurolite. The host rock is interfolded with oxide facies iron-formation and is itself probably lean silicate- or aluminous-facies iron-formation. These rocks occur in a turbidite sequence a few thousand metres thick, probably in its lower part near the base (Morgan et al., 1975; Morgan, 1982; Bethune and Scammell, 1993, 1997; Scammell and Bethune, 1995a). Minerals in the sulphide lenses include sphalerite, galena, chalcopyrite, pyrite, and considerable arsenopyrite. Analysis of one grab sample indicates 7180 ppb of gold (≈7.2 g per tonne, or 0.23 oz per short ton). Archean gold deposits have been classified as belonging to two broad categories: epigenetic vein deposits, which are the most abundant, and rare but important sulphidic schist deposits (e.g. Roberts, 1987; Card et al., 1989).

The Eqe Bay occurrence appears to belong to the latter category, although Scammell and Bethune (1995a) have reported 320 ppb of gold in oxide facies iron-formation in the same area. Rusty, sulphide-bearing lenses are associated locally with iron-formation (especially the sulphide facies) and stratigraphically adjacent metasediments, and with mafic and ultramafic rocks in both the Mary River and Piling groups. This newly identified occurrence, together with the arsenic anomaly reported in the Piling Group by Cameron (1986), should heighten interest in the economic potential of both groups of rocks for hosting economic sulphide and gold deposits.

Carving stone

Stone (serpentinite, argillite, marble, etc.) suitable for carving or making stone prints occurs at several places on Baffin Island (e.g. Gibbins, 1982, 1987) and undiscovered sites may be present within the map area. Bylot Supergroup strata that have been contact metamorphosed adjacent to Hadrynian diabase is used at Arctic Bay, and suitable occurrences may exist in northern map area NTS 37G. Some of the Neohelikian and Paleozoic carbonate rocks might also be of use.

Serpentinite from Mary River is being used extensively at Pond Inlet and its use doubled carving productivity there (W. Gibbins, pers. comm., 1984). Small ultramafic bodies occur sporadically throughout the map area, chiefly with other Mary River Group rocks. Most of these may be too highly metamorphosed to be of good grade. Most of the best serpentinite is probably in map area NTS 37G.

Oil, natural gas

Neohelikian and Phanerozoic strata within the map area are too thin or discontinuous or both to contain oil and gas in economic quantities. Work offshore has verified the presence of oil, probably in Cretaceous strata, off Scott Inlet (Loncarevic and Falconer, 1977; Levy, 1978, 1979; Levy and MacLean, 1981; Grant et al., 1986).

STRUCTURAL GEOLOGY

The structural data for undifferentiated foliations, fold structures for which the nature is uncertain, and lineaments shown on the published maps (*see* map legends) are derived chiefly from low level helicopter and fixed wing observations and airphoto observations controlled by a grid of ground observations and detailed ground work in a few areas. Dips and plunges of planar and linear features seen from the air or on airphotos were estimated wherever possible. Most of the map area is well exposed, but observations were hampered by extensive snow cover during the early part of the season. Beautiful cliff exposures in the mountainous fiord region are difficult to access, and offset to some extent by upper plateau surfaces that are commonly either covered by snow and ice, felsenmeer, and/or drift.

The structural history of the Archean-Aphebian terrane is, to say the least, complex. More than one period of regional Archean deformation is considered to be present and the map area has been overprinted by late Aphebian deformation. However, foliations, including gneissosity, are generally parallel to the contacts of map units and to compositional layering within map units, including primary sedimentary and volcanogenic layering where recognizable. Two generations of foliations or lineations or both were recognized in some places and two to four generations of folds are commonly recognizable in the Aphebian Piling Group (e.g. Jackson, 1969; Morgan et al., 1976).

Large-scale fold structures (large outcrop and greater) are ubiquitous. They range from convoluted "wild folds" (extremely complex flow folds called "wildfolding" by Kranck (1955) and others) and isoclinal recumbent and upright folds in the Archean and Aphebian gneisses to gentle inclined and upright warps in Neohelikian and early Paleozoic strata adjacent to faults.

Recumbent folds, thrust faults, and brittle and ductile thrust sheets (nappes) were recognized in the Clyde Inlet-Gibbs Fiord region by Eade (1953), Kranck (1953, 1955), Jackson (1968), Jackson and Taylor (1972), and subsequent workers. These structures are abundant throughout the fiord country and may be equally abundant in the rest of the map area, where, however, their presence is largely inferred. The overprinting of Neohelikian to Recent northwest-trending faults and the warping of bedrock by movement along these faults has further complicated the picture. This late deformation has to be considered when interpreting aeromagnetic data for the Archean-Aphebian terrane.

Faults in the map area include: low-angle ductile thrusts, some with many kilometres of movement; brittle thrusts (*see* Fig. 108b); late steep normal and listric faults with as much as several 100 m of vertical movement; and small-scale faults of various types. Boundary zones between Archean-Aphebian tectonic domains in the map area are interpreted to be mostly ductile shear zones and thrusts along which reactivation of movement has superimposed younger post-Aphebian steep brittle faults (*see* Fig. 111-114; Jackson and Morgan, 1978b; Jackson et al., 1978b, c, d; Jackson, 1984).

The likelihood of thrusts being present in southeastern map area NTS 37F-southwestern map area NTS 37E, along the northern edge of map area NTS 37F, and in the Mary River area has been noted above in discussing folds. A steep north-dipping shear zone includes a thrust dipping 20 degrees north along the north side of the No. 3-3A iron deposit area (Fig. 36). This thrust has brought basement gneisses up against the Mary River Group, but its extent is uncertain. The northeast-plunging mélange (Fig. 18) south of No. 1 iron deposit, and a thin (several centimetres), east-dipping mylonite zone along the west edge of the iron deposit, might also be related to a thrust zone.

Various small-scale structures such as breccia, agmatite, anatexis, boudinage, schlieren and inclusions, crossbeds, and unconformities have been noted for individual map units (*see* Fig. 21, 28, 42-45, 60, 61, 78-80). Some examples of small-scale folds are shown in Figure 103.

Archean-Aphebian recumbent folds, nappes

Large, near isoclinal to isoclinal, overturned to recumbent folds, and minor upright folds, are well displayed throughout most of the fiord region, especially in the Buchan Gulf area (Fig. 104, 105; *see* Fig. 108, 112). These folds and coeval thrusts are considered to be late Aphebian (*see* below). Similar folds are believed to occur throughout the map area, but away from the fiord terrain, are largely inferred from structural data. Most, but not all, of these folds trend southeast-northwest, and have subhorizontal axes and either northeast- or southwest-dipping limbs. Fold axes extend along strike for 30 km or more in the Buchan Gulf area (NTS 37H; Fig. 104). Some folds seem to be stacked on top of one another while others are jumbled (Fig. 104, 105). Some axial zones can be traced, perpendicular to their noses, for 6 km or more along cliff walls as relatively thin subhorizontal bands. Some of the latter folds maintain a fold structure in the axial zone for a considerable distance from the nose (Fig. 105d), whereas others develop a planar structure much nearer the nose (Fig. 105b). Both types show abundant evidence of ductile shear.

A spectacular fold structure in northeastern map area NTS 37G contains several smaller folds clustered in a domal area. The structure is capped by a planar zone that dips northward (to the right, Fig. 105a) under other fold structures. This planar feature, and other similar features to the north and elsewhere, are probably ductile thrust zones. Movement of the overlying rock here seems to be sinistral relative to the underlying structure, but this conclusion is tenuous.

Another spectacular structure on the west side of Clyde Inlet at the south edge of map area NTS 27F (Fig. 105e) may be overlain by nappes similar to the thrust-bounded nappes along Gibbs Fiord. The simple recumbent fold pattern outlined by the folded dykes probably belies the true complexity of Amn (*see* Kranck, 1953, 1955), a complexity that is hinted at by the presence of a loose network of older beaded dykes barely visible in the fiord wall.

A horizontal isocline on the west side of Gibbs Fiord becomes a ductile zone with a planar fabric within a short distance south of its nose (Fig. 105b), and becomes part of a subhorizontally layered sequence that is considered to be a sequence of alternating ductile, stretched, thrust zones and nappes (*see* section on "Faults").

The southeast-trending belt of thrusts and nappes in the fiord region, described above, is part of a larger belt, the late Aphebian Northeast Baffin Thrust Belt (*see* below), that extends from Bylot Island and Borden Peninsula southeast past Henry Kater Peninsula, to south of Maktak Fiord, a distance of about 970 km. Throughout at least the northern part of this belt (northwest from Henry Kater Peninsula), the recumbent folds undulate parallel to their axes so that in regions of low relief

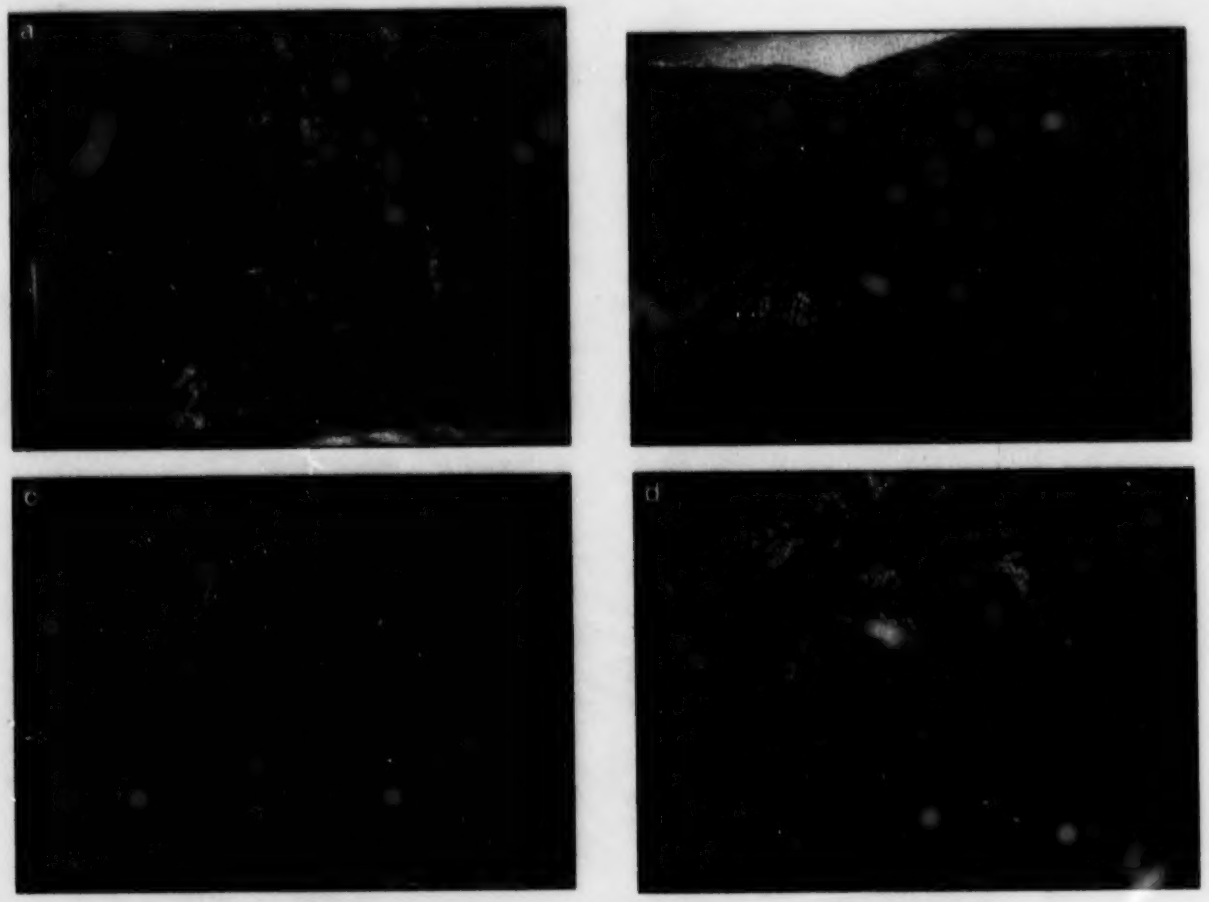

Figure 103. ***a)*** *Boudined and plastically deformed pegmatite in the core of a tight, upright antiform bordered by small-scale folds on both sides in unit* Amg, *east of Paquet Bay, on the north edge of NTS 37G. Photograph by A. Davidson. GSC 204343-P.* ***b)*** *Near-isoclinal fold with vertical axis outlined by remnants of thinly banded Mary River Group paragneiss* (Ms) *and amphibolite* (Mb - *dark coloured bands in middle distance) in banded migmatite* (Amg). *Note the plastic deformation and axial fault in the fold structure to the left behind the main fold. View north on the south side of Clyde Inlet, east of Cormack Arm (NTS 27F). Photograph by W.C. Morgan. GSC 186662.* ***c)*** *Recumbent fold in migmatite* (Amg) *at the head of Clark Fiord (NTS 37E, northeast), looking north. Photograph by S.L. Blusson. GSC 185597.* ***d)*** *Complex folding and anatexis in* Amg, *south-central map area NTS 37G. Photograph by S.L. Blusson. GSC 185504*

their surface expression resembles southeast-trending open folds. This is especially obvious on Bylot Island (NTS 38C; Jackson and Davidson, 1975), where recumbent fold noses occur in several of the nunataks, and in map area NTS 37H. Several crossfolds are also scattered throughout this belt.

Complex, hook-shaped fold structures are outlined by the Mary River Group in the Mary River area, northeast of the Neohelikian to Recent Central Borden Fault Zone. Lineations in the No. 4 iron deposit area (Fig. 106) show that both the Mary River Group and its basement were deformed together to form the lineations. Bedding and gneissosity attitudes indicate that a recumbent fold, possibly a nappe associated with a northwest-trending thrust, may have been refolded into an easterly plunging synform. Some of the stratigraphic relations present could be explained by thrust faults. A crudely similar more complicated structure in the No. 1 iron deposit area (Fig. 107) has been disjointed by later faulting. A northeast-plunging sheath fold about 40 m across and outlined by iron-formation, may indicate the presence of much larger similar structures. The ages of these structures probably lie between 2709 and ca. 1825 Ma.

The uniform northeast strikes of foliations and map units in southwestern map area NTS 37E-southeastern map area NTS 37F, and the east-west orientation of the Mary River Group along the north edge of map area NTS 37F together with the strong predominance of easterly-trending, north-dipping foliations and aligned Mary River Group segments throughout most of map area NTS 37F (domain 2, below) are suggestive of shearing, thrusting, and stacking of isoclinal, south- and southeast-verging folds (possibly nappes) by repeated thrusting. This strong overprinting is probably of middle- to late Aphebian age (*see* Domain 2).

Late open folds

Bylot Supergroup strata occupy a large open syncline in the fault-bounded Milne Inlet Trough of northern map area NTS 37G. The fold plunges gently northwest, and is inclined to the northeast, a feature that is demonstrated by the asymmetric aeromagnetic pattern obtained for Milne Inlet Trough (*see* Fig. 111; compare with Fig. 13, 112-114 for location). Dips are rarely as much as 20 degrees northeast on the southern limb and locally attain 65 degrees southwest along the northern edge. Smaller folds developed within the larger fold are reminiscent of wrench faulting, but the timing of such faulting is uncertain. Similar folds occur in early Paleozoic and Cretaceous-Eocene strata adjacent to faults elsewhere in the map area and in Borden Basin. Also, in and northwest of the map area, Neohelikian-Hadrynian dykes extend across the Bylot Supergroup-basement contact without obvious offset (Jackson and Sangster, 1987). The large Milne Inlet Trough fold was formed chiefly in response to downdropping along the listric White Bay Fault Zone on the northeastern margin of the trough.

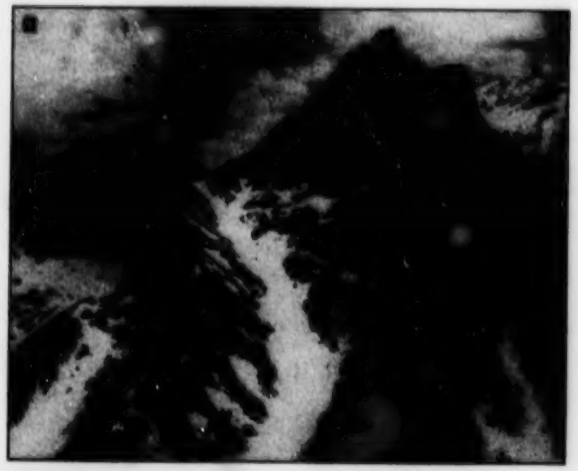

Figure 104. ***a)*** *View northwest at the nose of a fold in Mary River Group migmatite* (Amg), *east side of Coutts Inlet, northwest corner of map area NTS 37H. Local relief 900 m, peak about 1100 m. Photograph by W.J. Crawford. GSC 186343.* ***b)*** *View southeast at recumbent folds in* Amg *in a cliff on the east side of Cambridge Fiord, southeast of Livingston Island (NTS 37H, west). Relief about 900 m. Photograph by A. Davidson. GSC 204194-H.* ***c)*** *View west at cliffs on the west side of Royal Society Fiord from Pollock Head (NTS 37H). Structures are considered to be stacked nappes in* Amg, *and on strike with structures shown in b), 20 km to the northwest. Photograph by W.C. Morgan. GSC 186610*

Early Paleozoic strata are folded into gentle folds adjacent to the Central Borden Fault Zone north of Angajurjualuk Lake. Also, Paleozoic strata farther northwest along the fault zone dip as much as 40 degrees away from the fault.

Archean-Aphebian thrusts, shears

East-west shear zones

Three major east-west boundary zones are interpreted as shear zones separating tectonic domains 1b from 2a, 2a from 2b, and 2b from 2c (*see* Fig. 112, 113). Sparse lineation measurements indicate mostly low to moderate plunges subparallel to the boundaries which are marked by sharp, distinct breaks in the aeromagnetic patterns (*see* Fig. 111), and which approximate the locations of late brittle faults (Jackson and Morgan, 1978b; Jackson et al., 1978b, c, d; Jackson, 1984).

East-west straightening has occurred in domains 2a, 2b, and 2c, although foliations on opposite sides of a boundary commonly have somewhat different trends. Dominant trends are southeast in the western part of domain 1b but swing easterly as the boundary between domains 1b and 2a is approached to the south (*see* Fig. 112, 113; Jackson et al., 1978b, d). Therefore, sinistral movement is inferred along this boundary.

The subparallel orientation of the metamorphic isograds (considered to be late Aphebian) to the boundaries, the coincidence of much of the hypersthene isograd with one or another of these boundaries, the involvement of the Piling Group in the tectonic activity and granulite metamorphism suggest that the shear zones, and straightening, is mostly of late Aphebian age (Fig. 99, *see* Fig. 111-113; Jackson and Morgan, 1978a; Jackson et al., 1978b, d). As noted above, U-Pb zircon and monazite ages of 1829-1821 Ma (Scammell and Bethune, 1995a, b) affirm this conclusion.

The easterly trending, presumably steep Piling Fault Zone south of the map area (*see* Fig. 113) is parallel to the east-west shear zones noted above, to which its origin may be related. As discussed elsewhere, the Piling Fault is defined mostly by differences in trends and style of folding, $\delta^{18}O$ and Sm-Nd data, and the aeromagnetic pattern from one side of the fault to the other.

Isortoq Fault Zone

The Isortoq Fault Zone (Fig. 101, *see* Fig. 112-114) extends northeast from Isortoq Fiord, south of the map area, northeast under the north end of the Barnes Ice Cap to west of Sillem Island (*see* Fig. 111-114). There it may bifurcate, one branch trending northeasterly along Gibbs Fiord and the other northerly along the southeast side of a large charnockite body, the Dexterity Batholith, on the east coast (*see* Fig. 114; Jackson and Morgan, 1978b; Jackson et al., 1978c, d; Morgan, 1982; Jackson, 1984).

The Isortoq Fault Zone separates the charnockite-bearing, Dexterity Granulite Belt of subdomains 2a, 2b, 2c, and central 7a to the northwest from mostly upper amphibolites of subdomains 3a and southern 7a to the southeast (Fig. 99, 101; *see* Fig. 112, 113). From just east of the Barnes Ice Cap westward, the fault and foliations southeast of it trend uniformly northeast in an arc convex to the northwest. East of Steensby Inlet the Mary River Group, on the south side of the fault, outlines major folds overturned to the northwest (northwest vergence), possibly indicative of thrusting, in that direction (Jackson et al., 1978d; Morgan, 1982) Bethune and Scammell, 1997. Northwest of the fault, foliations are mostly easterly and more variable than to the southeast. They also bend southward adjacent to the Isortoq Fault Zone in a manner suggesting dextral movement.

Foliations in the vicinity of the northeastern part of the Isortoq Fault Zone are relatively heterogeneous, and relations are less clear, but most foliations adjacent to the Dexterity Fiord charnockite batholith, just west of the northern fault splay, dip northwesterly, suggesting shearing and southeastward overthrusting or tilting of the charnockite body.

The aeromagnetic patterns on either side of the Isortoq Fault Zone are distinctly different from one another (Fig. 111). The pattern to the northwest has higher nanotesla values and is more irregular. That to the southeast is much more subdued and even, except immediately adjacent to the fault where Mary River Group paragneiss with iron-formation trends parallel to the fault (Fig. 111). However a regional arcuate pattern, convex toward the northwest, is discernible in the aeromagnetics from the fault for about 150 km to the southeast, near the south end of the Barnes Ice Cap. The abruptness of the pattern change along the fault southwest of the Barnes Ice Cap indicates the presence of a steep boundary or contact (P. McGrath, pers. comm., 1990). The more subdued and gradual change northeast of the Barnes Ice Cap suggests a more moderate dip to the southeast. Numerous brittle faults occur in the vicinity of the Isortoq Fault Zone, and its northeastern part (map areas NTS 27G, 37H; Fig. 101; *see* Fig. 112, 114) approximates the southern side of an area for which a large number of earthquakes have been recorded (Basham et al., 1977; Jackson et al., 1977; Reid and Falconer, 1982; Shih et al., 1988).

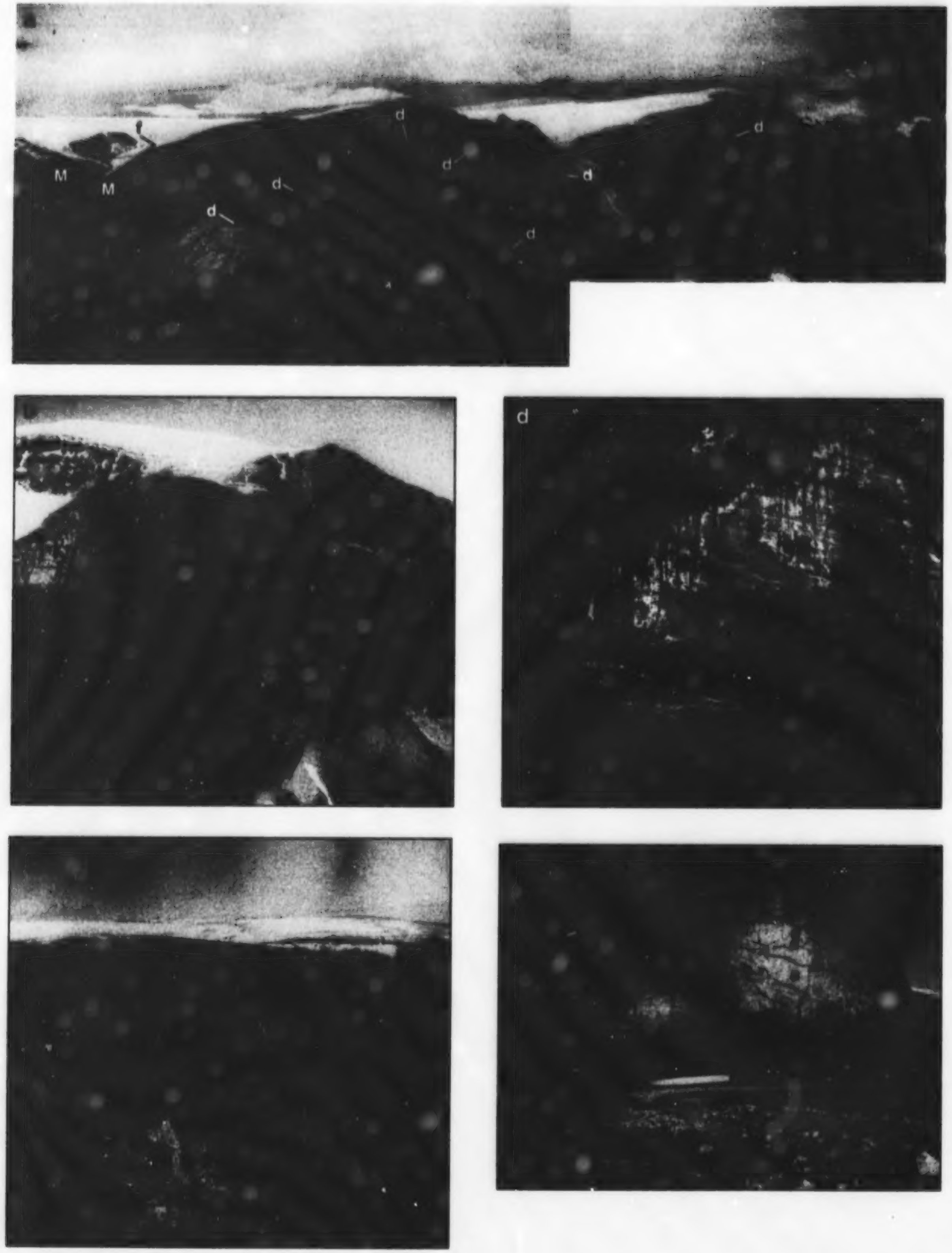

Figure 105. ***a)*** *View northwest and north at recumbent fold structures in* Amg*, possibly containing deformed mafic dykes, overlain by a zone with planar banding, west side of North Arm in the northeast corner of map area NTS 37G. The planar zone is interpreted as a ductile thrust zone that dips to the north under an antiformal fold overturned to the south. Fold structures are intruded by younger undeformed(?) mafic dykes (d), some of which are beaded. A fault zone (f) occurs on the left and Mary River Group (M) occurs on top of the folds on the left. Elevations to 1040 m on the left and to 1530 m on the right. Photographs by W.J. Crawford. GSC 186330, 186331.* ***b)*** *Isoclinal recumbent fold in* Amg *in the west wall of Gibbs Fiord, east coast of Sillem Island near the north edge of map area NTS 27F. Fold limbs greatly attenuated and extend southward (left) beyond the view for at least 6 km. Elevations to 760 m. The arrow points to the centre of view shown in d). Photograph by S.L. Blusson. GSC 185781.* ***c)*** *Sinistrally sheared isoclinal recumbent fold (nappe). Looking northwest at the southeastern cliff on Scott Island (NTS 37H, southeast). The fold is in* Amg *overlying* Amn*, and folding persists along most of the southeastern cliff (see Fig. 21a). Elevation is about 460 m. Photograph by S.L. Blusson. GSC 185677.* ***d)*** *Core of the fold nose in b). Note plastic deformation and conjugate shears, especially in the lower central part of the photo. Photograph by S.L. Blusson. GSC 185782.* ***e)*** *View northwest at a recumbent fold in* Amn *overlain by* Amg*, west side of Clyde Inlet at the south edge of map area NTS 27F. The structure is outlined by amphibolite dykes (b) that have been transposed subparallel to the gneissosity. Smaller beaded amphibolite (a) dykes criss-cross the granitic gneiss* (Amn)*. The planar zone capping the structure may contain a thrust near its base.* See also *Kranck (1953, 1955). Distance to cliff is about 3 km and highest point is about 1070 m. Photograph by W.C. Morgan. GSC 201934-A*

In 1992, R. Berman and the author identified mylonites along a 10 km stretch of the Isortoq Fault Zone that extends northeast from the south side of the Steensby Inlet map sheet (Jackson et al., 1978d). This mylonite zone dips about 50 degrees southeast and is about 50 m wide. It is mostly blastomylonite that contains rounded and rotated fragments of quartz, antiperthitic plagioclase, minor microcline, and rare myrmekite in a finely sheared and recrystallized matrix composed mostly of quartz, plagioclase, and green to brown biotite. Accessory epidote, pyrite, pyrrhotite, local prehnite, and traces of apatite and variably metamict zircon are also present. Sheared and fragmented garnet is associated with quartz, plagioclase, muscovite, and clinopyroxene in one rock, and is crushed in another. Coarse, rotated, poikiloblastic garnet grains also occur in slightly crushed quartz-plagioclase-biotite gneiss along the edge of the mylonite zone. Rocks bordering the mylonite zone are in the upper amphibolite facies to perhaps locally the granulite facies. Although some cataclasis occurred during fairly high grade metamorphism, most of the mylonite now preserved was at least reworked during later low- to medium-grade metamorphism.

Field observations at one site and the study of several oriented thin sections indicate that the axes of small folds (including sheath folds) and mineral lineations are subparallel, and that the recorded movement is sinistral, with the granulites on the northwest side having moved up obliquely to the west at about 40 degrees to the horizontal. Similar conclusions were reached by Bethune and Scammell (1993), who identified brittle faults and narrow mylonite zones along Isortoq Fiord. Considering that the Dexterity Granulite Belt may have risen about 8 km relative to the southeast side (see section on regional metamorphism), and assuming no other directions of movement, these data suggest that the resultant movement of the northwest side was only about 12 km obliquely up to the west, the horizontal component being 10 km.

Thrusts in Northeast Baffin Thrust Belt

Cliffs in the Northeast Baffin Thrust Belt (*see* Fig. 112) commonly display sequences of stacked planar layers or zones that vary slightly in mafic content, but which present an overall uniform appearance (Fig. 104, 105, 108). The layers have a maximum thickness of about 300 m but are commonly less than 200 m thick. This layering is exceptionally well displayed in a region extending from Ayr Lake (NTS 27F) northwest to Clark Fiord (southeast NTS 37H), particularly along Gibbs Fiord (Fig. 108a, b). The planar zones are composed of lenses and layers, the internal fabric of which is complicated and shows small thrusts and ductile shear (Fig. 105c, 108c, 109b, c). The planar zones are generally separated by thin, slightly undulating planes across which either small-scale structures commonly do not match or there is a slight but abrupt change in lithology.

The planar zones seem identical to the ductile thrust zone that occurs between fold structures on North Arm in northernmost map area NTS 37G (Fig. 105a), and to the ductile zone that extends south from a recumbent fold in a nappe on the east coast of Sillem Island (Fig. 105b, c). A few are similar to the ductile recumbent nappe capping Scott Island (Fig. 105d). It is concluded, therefore, that these stacks of planar zones probably represent alternating ductile thrust zones and ductile sheared nappes that developed contemporaneously (e.g. Fig. 108). The thin planes separating the zones may represent surfaces along which movement and brittle shear continued at the close of deformation after the rock had cooled.

A stack of similar but more discordant layers (Fig. 108d) outcrop on the west side of North Arm just south of the "domal" fold complex shown in Figure 105a. The layers in the stack dip southerly away from the domal complex and it may be that a series of thrust sheets moved off the domal area during deformation. A single thrust sheet at the entrance to Clark Fiord is at least 450 m thick (Fig. 108e).

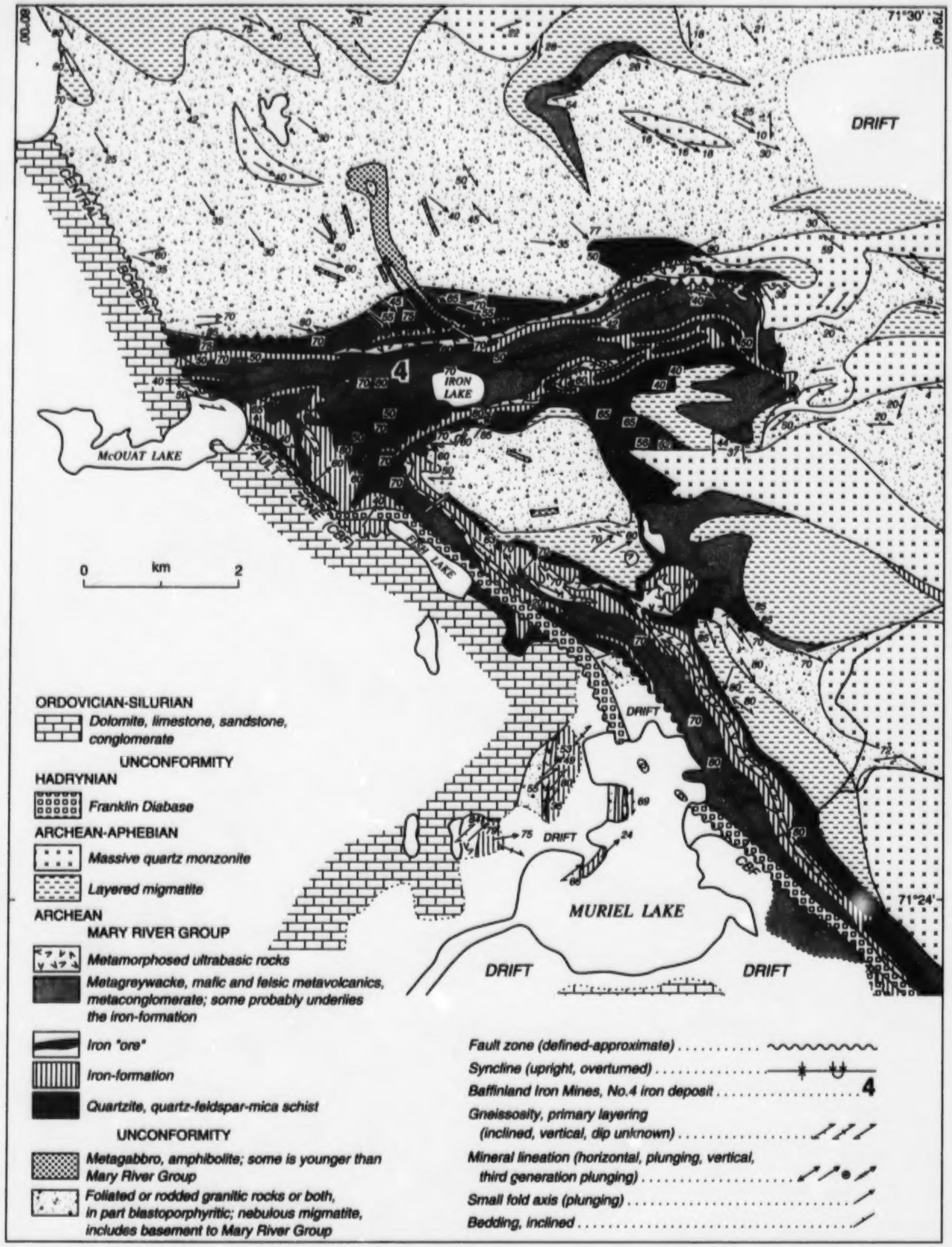
71°30'
79°40'
79°50'
DRIFT
4
IRON LAKE
McOUAT LAKE
CENTRAL BORDEN FAULT ZONE (CBF)
PINE LAKE
CBF
DRIFT
MURIEL LAKE
DRIFT
DRIFT
71°24'
0 km 2
ORDOVICIAN-SILURIAN
Dolomite, limestone, sandstone, conglomerate
UNCONFORMITY
HADRYNIAN
Franklin Diabase
ARCHEAN-APHEBIAN
Massive quartz monzonite
Layered migmatite
ARCHEAN
MARY RIVER GROUP
Metamorphosed ultrabasic rocks
Metagreywacke, mafic and felsic metavolcanics, metaconglomerate; some probably underlies the iron-formation
Iron "ore"
Iron-formation
Quartzite, quartz-feldspar-mica schist
UNCONFORMITY
Metagabbro, amphibolite; some is younger than Mary River Group
Foliated or rodded granitic rocks or both, in part blastoporphyritic; nebulous migmatite, includes basement to Mary River Group
Fault zone (defined-approximate)
Syncline (upright, overturned)
Baffinland Iron Mines, No.4 iron deposit 4
Gneissosity, primary layering (inclined, vertical, dip unknown)
Mineral lineation (horizontal, plunging, vertical, third generation plunging)
Small fold axis (plunging)
Bedding, inclined

Figure 106. Geology of the No. 4 iron deposit area, Mary River region (NTS 37G, west-central).

Piling Group strata occur in several thrusts and nappes south of the map area (Jackson, 1969; Morgan, 1983; Henderson, 1985a). Some of the thrust sheets and resultant basement-cover sandwiches are thin, and resemble those in the southern Rinkian belt of west Greenland (Pulvertaft, 1986). On the south edge of the map area the group has been overturned and overridden by basement gneisses (Amn) thrust southwestward at the head of Sam Ford Fiord (southwest NTS 27F - Jackson, 1984; *see* Kranck, 1953, 1955). This structure may mark the approximate southwestern extent of this thrusting-recumbent folding event in this area.

Several determinations of relative movement during ductile shear were made mostly on eastward- to southeastward-facing cliffs in the fiord region using photographs and with the help of S. Hanmer (e.g. Fig. 104, 105, 108c). All of them indicate sinistral movement. This, combined with the

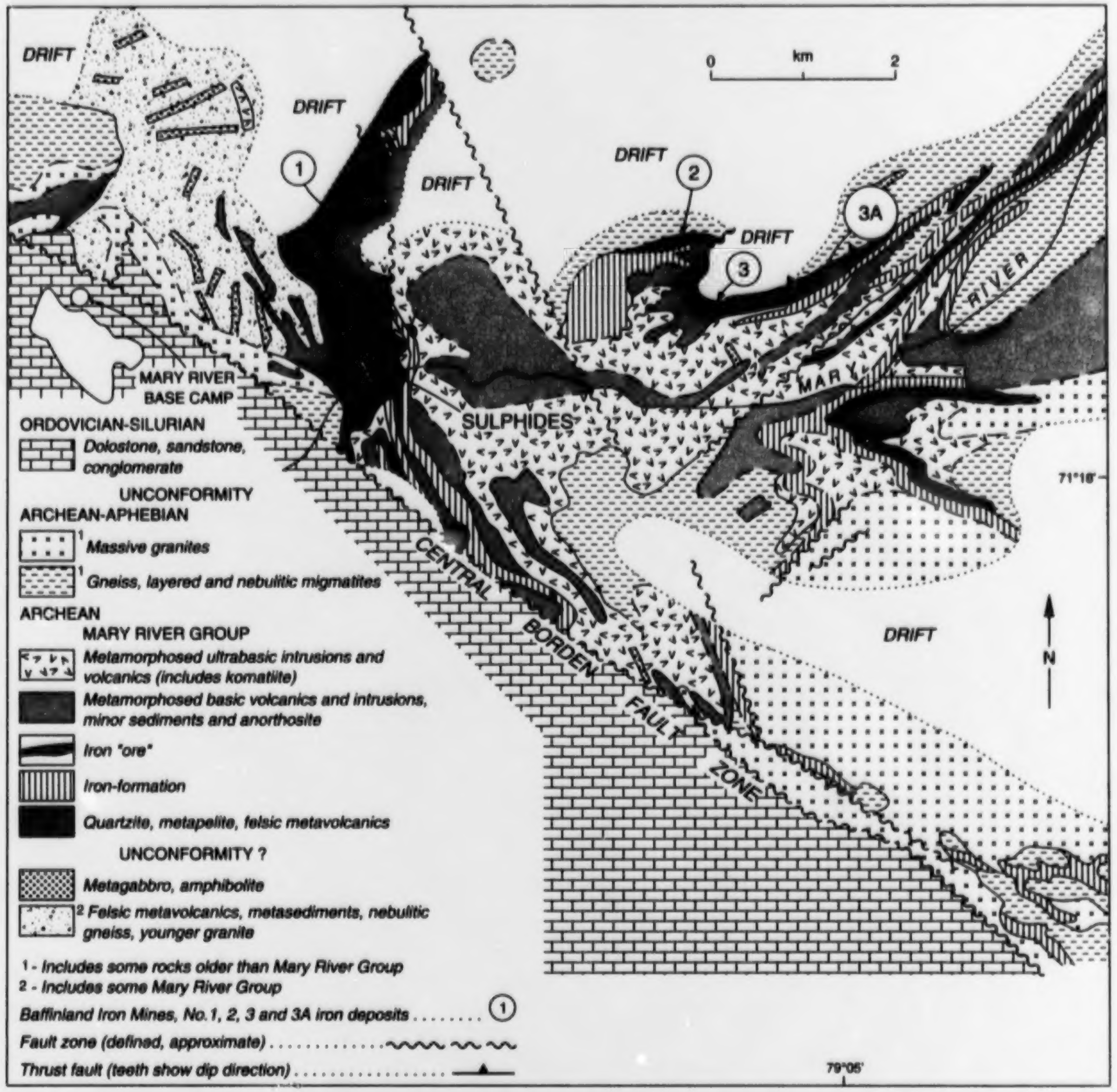
DRIFT
DRIFT
DRIFT
DRIFT
DRIFT
DRIFT
①
②
③
3A
0 km 2
MARY RIVER
MARY RIVER BASE CAMP
SULPHIDES
CENTRAL BORDEN FAULT ZONE
N
71°18'
79°05'
ORDOVICIAN-SILURIAN
Dolostone, sandstone, conglomerate
UNCONFORMITY
ARCHEAN-APHEBIAN
Massive granites ¹
Gneiss, layered and nebulitic migmatites ¹
ARCHEAN
MARY RIVER GROUP
Metamorphosed ultrabasic intrusions and volcanics (includes komatiite)
Metamorphosed basic volcanics and intrusions, minor sediments and anorthosite
Iron "ore"
Iron-formation
Quartzite, metapelite, felsic metavolcanics
UNCONFORMITY ?
Metagabbro, amphibolite
² Felsic metavolcanics, metasediments, nebulitic gneiss, younger granite
1 - Includes some rocks older than Mary River Group
2 - Includes some Mary River Group
Baffinland Iron Mines, No.1, 2, 3 and 3A iron deposits .... ①
Fault zone (defined, approximate)
Thrust fault (teeth show dip direction)

Figure 107. Geology of the No. 1-3A deposits area, Mary River region (NTS 37G, west-central). The Mary River base camp is at 79°19'45"W longitude and 71°18'56"N latitude.

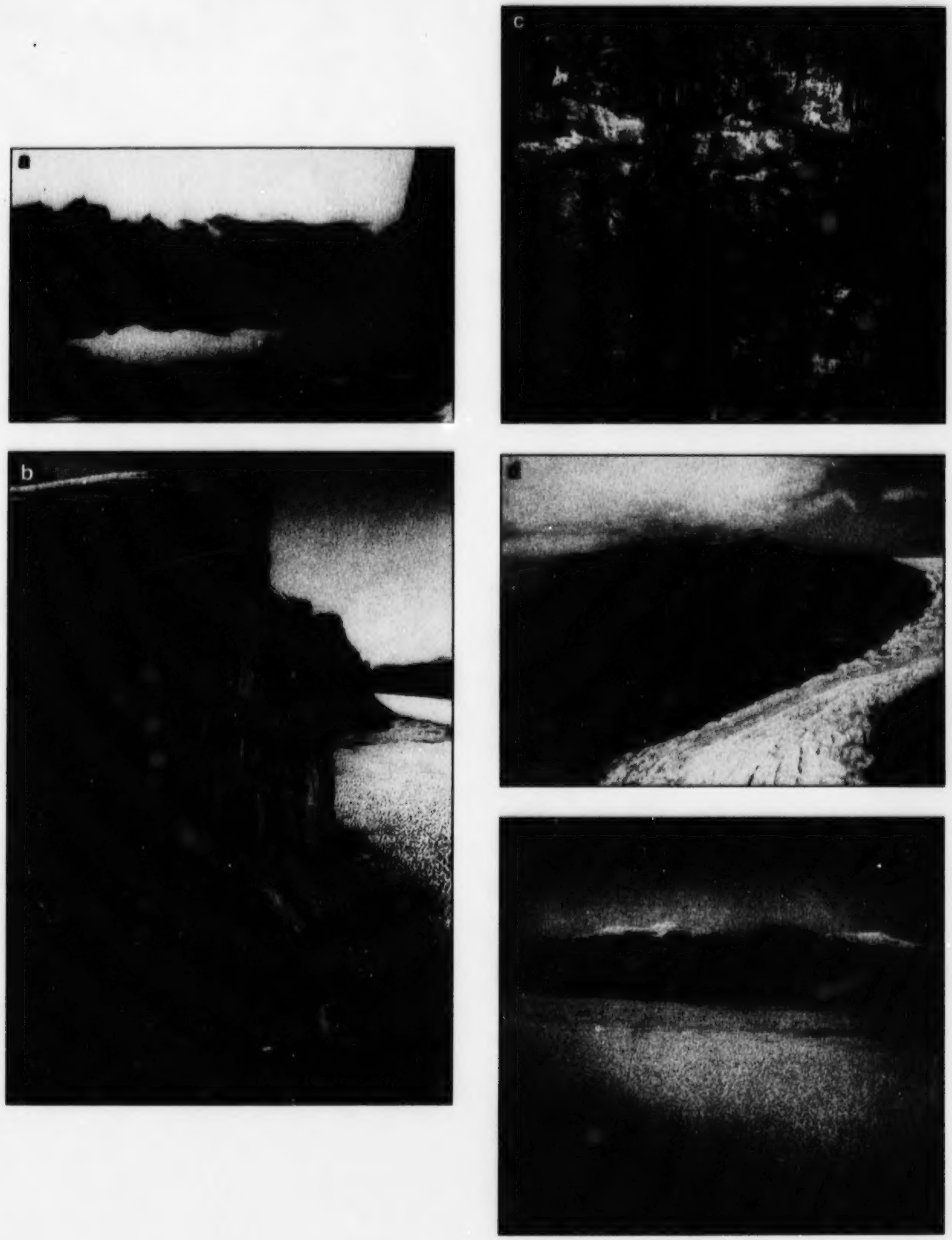

Figure 108.

a) View south across Gibbs Fiord at stacked nappes and ductile thrusts dipping 10°E, 4 km to the south in Amn, *west of Refuge Harbour (NTS 27F, northwest). Elevations to 1400 m. Photograph by S.L. Blusson. GSC 185775.*

b) Stacked layers (nappes and ductile thrusts) of nebulitic quartzofeldspathic gneiss (Amn) *on the north side of Gibbs Fiord (NTS 27F), about 20 km southwest of the location of Figure 105b and 14 km west-southwest of location of Figure 106a. Elevations to 1100 m. Photograph by S.L. Blusson. GSC 185756.*

c) Details of horizontal layers in Amg *in the west wall of Sam Ford Fiord south of the junction with Walker Arm (NTS 27F, northwest). The section is about 300 m high. Thrusts, small recumbent fold noses, and sinistral shear are visible. Photograph by S.L. Blusson. GSC 185846.*

d) View southwest at a stack of nappes and ductile thrust zones south of the domal fold complex shown in Figure 105a, west side of North Arm in the northeast corner of map area NTS 37G. Photograph by W.J. Crawford. GSC 186329.

e) View northwest across the mouth of Clark Fiord (NTS 27G) at a thick layer of Amn *possibly thrust southwest over a recumbent antiform of* mu *(in part* Amg*) on the right side of the photograph. The peak on the right side of the photo is about 920 m. Snow-capped peaks are 1220 m. Photograph by S.L. Blusson. GSC 185783.*

f) View southwest at recumbent folds and thrusts with sinistral movement in Amg, *south of Tay Sound (NTS 37G, northwest). The section is about 370 m high. Photograph by S.L. Blusson. GSC 185511*

attitudes of folds seen in cross-section and the predominance of northwest-trending fold axes, is taken to indicate northeast-southwest compression and overthrusting of ductile recumbent folds and nappes toward the southwest in the Northeast Baffin Thrust Belt. Kranck (1953, 1955) arrived at a similar conclusion. However, the Mary River Group in the Mary River area outcrops northeast of the Central Borden Fault Zone in hook-shaped fold patterns formed by at least two phases of folding (Fig. 106, 107). There is also a marked change in Archean-Aphebian regional trends across the Central Borden Fault Zone (*see* Fig. 111-113; Jackson et al., 1978b). It is possible therefore that the Central Borden Fault Zone developed along an older late Archean or late Aphebian northwest-trending thrust and nappe zone. If its age is late Aphebian, it may mark the southwestern limit of major overthrusting from the northeast, rather than the western limit presently suggested (*see* Fig. 112, 113, 114).

Post-Aphebian faults

A large number of brittle faults have been active in Baffin Island since Neohelikian time and steep to vertical, post-Aphebian, northwest-trending fault zones are common throughout Baffin Island. Two such zones separate Baffin Island into three northwest-trending major fault blocks: the large Cumberland Peninsula-Brodeur Peninsula block, the Hall Peninsula block, and the Incognita-Foxe Peninsula block. Each block has been tilted up to the northeast (Jackson and Morgan, 1978a). Neohelikian and Hadrynian dykes have been emplaced along and parallel to the faults.

Four major post-Aphebian fault zones extend into the map area: the White Bay, Tikerakdjuak, Central Borden, and Nina Bang fault zones (Jackson et al., 1975, 1978a; Jackson and Iannelli, 1981). Two others, the Hartz Mountain and the Aktineq fault zones, probably extend into the map area also, but have not been recognized. Most of these fault zones probably extend much farther to the southeast than indicated on the published maps (*see* Fig. 113). At least some of the faults are listric and the movement on them is considered to be chiefly dip-slip (Jackson and Sangster, 1987). As much as 1500 m of vertical movement has probably occurred along some of these faults.

The age of initial post-Aphebian faulting is uncertain, but a few of the faults coincide with old blastomylonite zones, and may have originated during cooling at the end of the last Aphebian metamorphism in this region, perhaps at about 1.8 Ga. The White Bay, Tikerakdjuak, and Central Borden fault zones may have developed along older structures as discussed above for the Central Borden Fault Zone. The Borden Rift Basin, of which the Milne Inlet Trough is a part, developed during Neohelikian syndepositional faulting along these faults, during what seems to have been the period of greatest fault activity.

Some of the faults were active only in the late Proterozoic while others have been active at various times up to the present. The Isortoq Fault Zone is presently active and the seismic activity along its northeast end, as noted above, is probably the strongest in eastern Canada. Also, glacial terraces (or beaches) have been offset on the southeast side of the fault zone to the southwest along the south edge of Steensby Inlet map area (Jackson et al., 1978d). Thus, many of the presently exposed relationships may have been considerably modified by Aphebian-Recent fault movements. (Jackson et al., 1978d; Jackson and Morgan, 1978a; Jackson and Iannelli, 1981, 1989; Jackson and Sangster, 1987). Available determinations from earthquake data indicate present-day northeast-southwest extension (e.g. Shih et al., 1988).

Lineations

Linear features that were commonly measured in the field include fold axes, mineral and mineral aggregate lineations, and mullion structure. Commonly, the Archean-Aphebian gneisses have been sheared and recrystallized into strongly lineated pencil gneisses and a planar fabric that ranges from well developed to virtually absent (Fig. 110). Most linear features lie in foliation planes and seem to be parallel to one another. In some areas, however, such as in western map area NTS 37G and various parts of map areas NTS 37H-27G, they tend to be at various angles to the foliation. Plunge of most lineations ranges from subhorizontal to 20-30°, but locally ranges up to 70° in map area NTS 37H. Plunges are relatively steep in map area NTS 37G and are as much as 80° locally in the western part of the map area, where aggregate rodding is relatively abundant. Also in map area NTS 37G, the azimuths of lineations are variable but northeast is most common. In map areas NTS 37H-27G most lineation azimuths are relatively uniform and plunge either west-northwest or east-southeast. Measurements are sparse for map areas NTS 37E and 37F where east-northeast to northeast plunges predominate and are relatively uniform in map area NTS 37F. Fold axis and mineral lineations in the Sam Ford Fiord and Clyde Inlet areas of map area NTS 27F tend to either be subperpendicular to or subparallel to the strike of the associated foliation. Azimuths are mostly northwest-southeast and southwest-northeast.

Lineation measurements are too sparse throughout most of the map area to be very useful. In general, however, they support the foliation trends and aeromagnetic data in outlining the areas into which the map area has been subdivided (*see* Fig. 112).

Measurements of linear features are relatively abundant in the No. 1-3A and No. 4 iron deposit areas (NTS 37G). Similar lineations in the basement rocks and in the overlying Mary River Group (Fig. 106) indicate that the lineations were formed when the rocks were deformed together by the same tectonic event and subsequently folded.

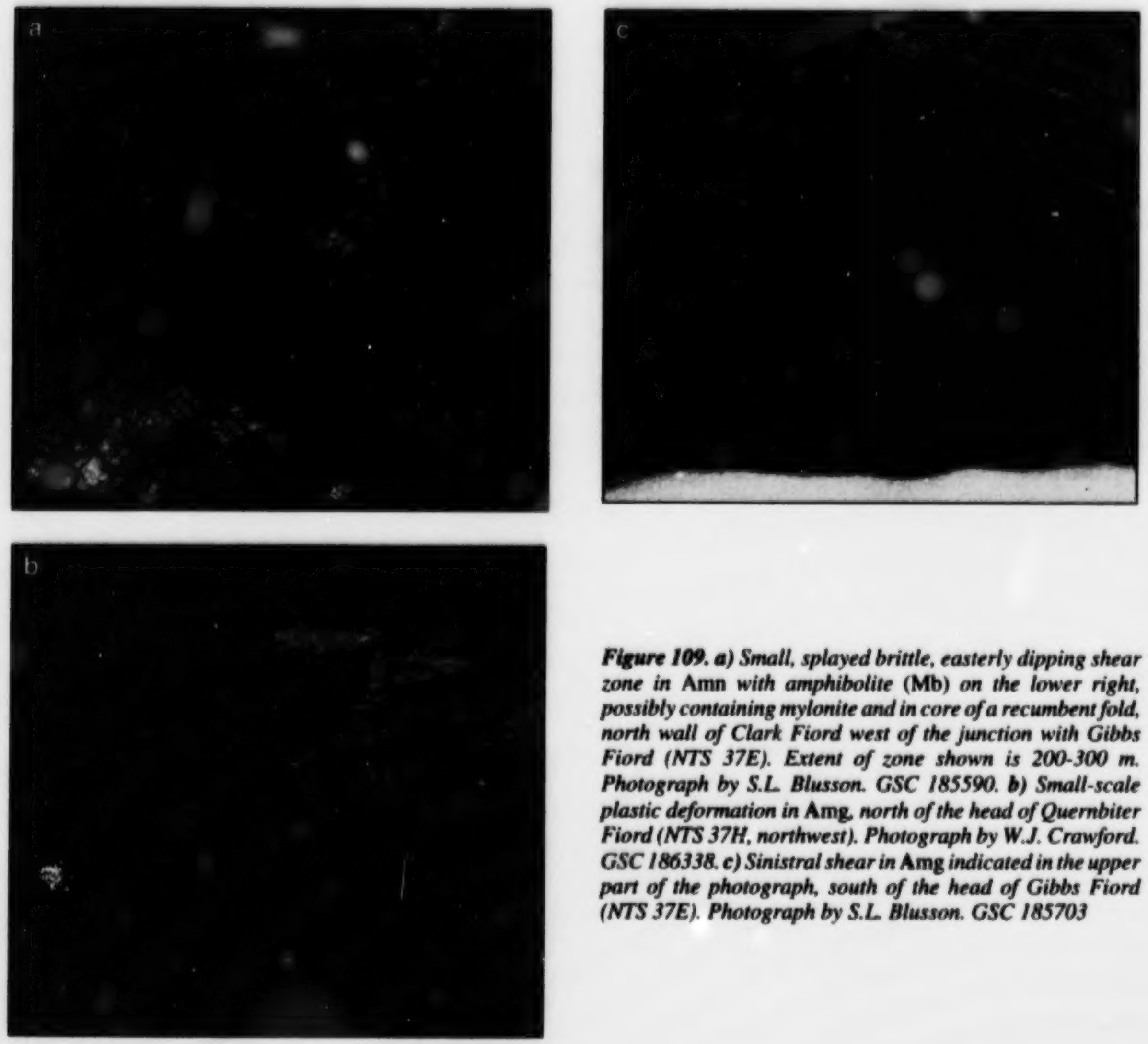

Figure 109. a) *Small, splayed brittle, easterly dipping shear zone in Amn with amphibolite* (Mb) *on the lower right, possibly containing mylonite and in core of a recumbent fold, north wall of Clark Fiord west of the junction with Gibbs Fiord (NTS 37E). Extent of zone shown is 200-300 m. Photograph by S.L. Blusson. GSC 185590.* ***b)*** *Small-scale plastic deformation in* Amg*, north of the head of Quernbiter Fiord (NTS 37H, northwest). Photograph by W.J. Crawford. GSC 186338.* ***c)*** *Sinistral shear in* Amg *indicated in the upper part of the photograph, south of the head of Gibbs Fiord (NTS 37E). Photograph by S.L. Blusson. GSC 185703*

Tectonic domains

The Precambrian of Baffin Island, including the map area, but excluding the region south of Brodeur and Borden peninsulas, has been divided into eight tectonic domains, some of which have been further subdivided (*see* Fig. 112-114). Five of the eight domains are represented in the map area (*see* Fig. 112, 113). The domains have been differentiated mostly on the basis of foliation trends, aeromagnetic patterns, predominant rock types, apparent truncation of trends in one domain by those in another, and where available, age determinations. Foliations tend to wrap around granitic plutons, although some foliations are truncated. All of the domains are considered to have a late Aphebian component that dominates in most domains because any pre-existing Archean structures were transposed, straightened, or otherwise deformed in the late Aphebian. Brief mention will be made of the domains outside the map area to provide a complete picture. Additional data are in the legend for Figure 113. Domains 1 and 2 lie within the Late Archean Committee Orogen, and domains 3 to 6 and most of 7 lie within the late Aphebian Baffin Orogen.

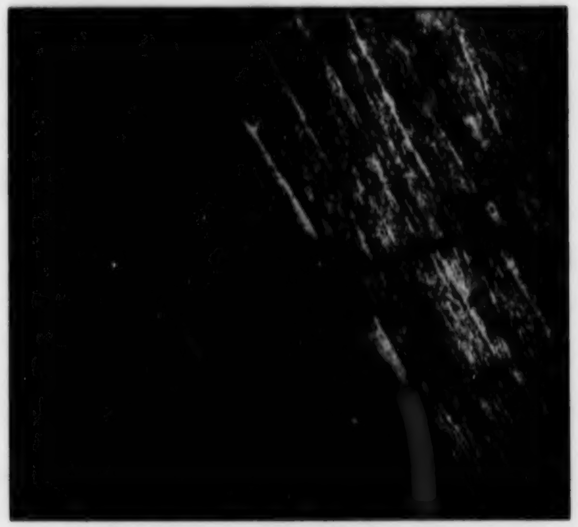

Figure 110. *Typical thinly banded gneiss with linear fabric in* Amg*, north edge of map area NTS 37G east of Paquet Bay and just west of the ice cap. Photograph by A. Davidson. GSC 204194-L*

Domain 1

Based on the above criteria, the area with the greatest likelihood of containing well preserved old Archean structures is domain 1 in the northwestern part of the map area (Fig. 111, in pocket; Fig. 112, 113; Fig. 114, in pocket). In it, foliations, lineations, and the aeromagnetic pattern are variable north of the Central Borden Fault Zone (subdomain 1a). Predominance of northeast-trending lineations in this part of domain 1, and the nature of the fold structures (e.g. Fig. 106) suggest that early northeast trends and recumbent fold structures were refolded about easterly trending axes, some of which plunge easterly. The aeromagnetic pattern is complicated by the extensive low negative anomaly that surrounds the relatively restricted but exceptionally high positive anomalies of the Mary River iron deposits. The prominent straight northwest-trending fabric in the aeromagnetic pattern (Fig. 111; *see* Fig. 112) may be related to Helikian-Recent faulting and/or to deformation related to the late Aphebian southwest overthrusting in subdomain 7a to the northeast. Trends in subdomain 1a are truncated and/or drawn into the southeast trends in the southwestern part of subdomain 7a. The tendency for Mary River Group strata to arc southward in the boundary zone (Jackson et al., 1978b) may be related to a dextral component of movement in this boundary zone.

In general, trends are much more heterogeneous in subdomain 1a than in 1b. Most of the boundary between the two subdomains coincides approximately with the HelikianPhanerozoic Central Borden Fault Zone, which probably developed along an older structure as noted above.

Foliations and lineations in subdomain 1b tend to become aligned southeastward and eastward as the south boundary with domain 2 is approached.

Domain 2

North-dipping, easterly trending foliations, interpreted to represent repeated south-directed thrusting, predominate throughout most of domain 2, and most of the relatively few measured lineations plunge northeast. Three major subdomains have been recognized: a narrow northern belt (2a) and a broad southern belt (2c), both with generally high magnetic expression, separated by a belt (2b) with low magnetic expression (Fig. 111-113). Trends and structures in the northeastern part of domain 2 are overprinted and truncated by northwest-trending structures in subdomain 7a.

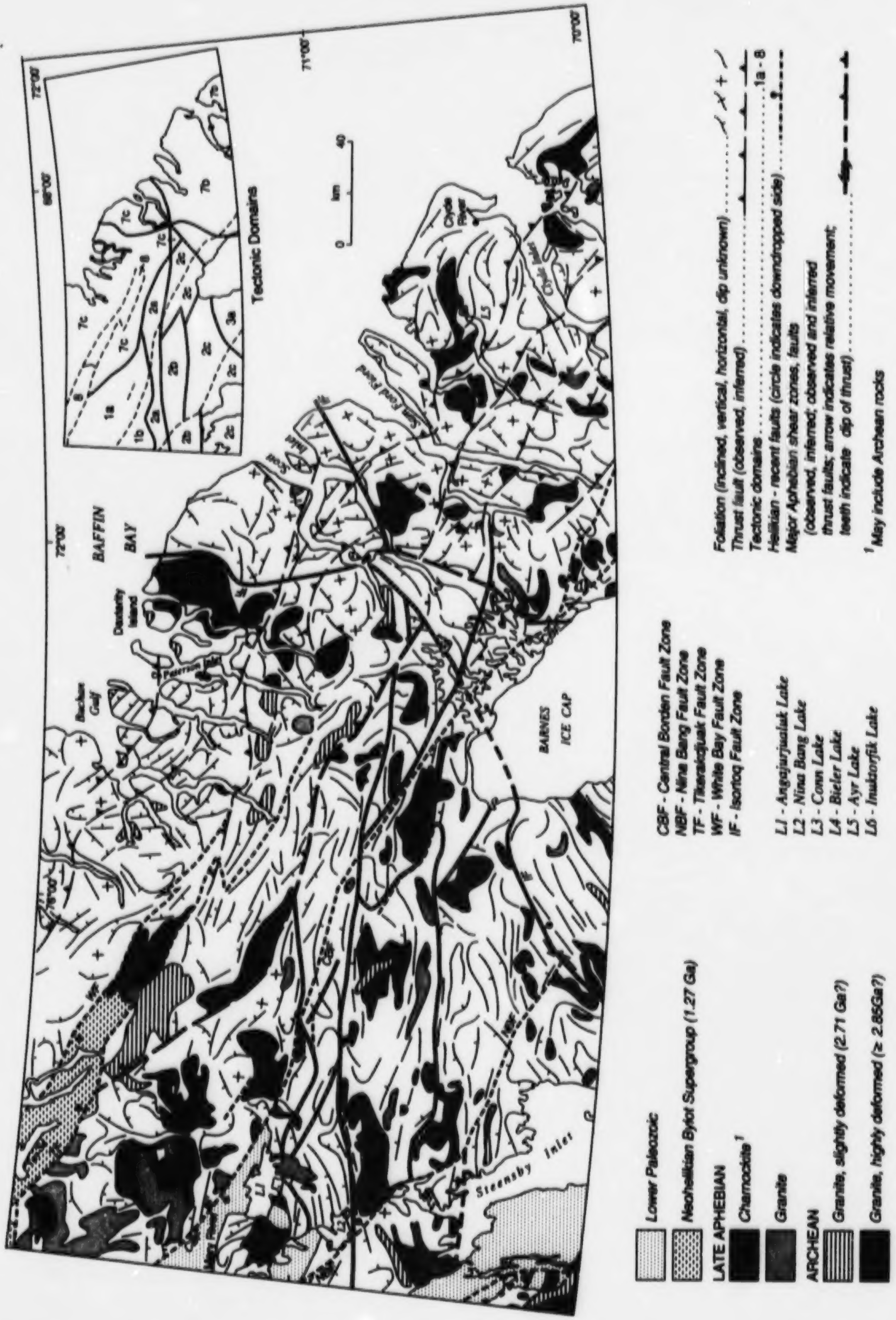
Tectonic Domains
0 km 40
72°00'
71°00'
70°00'
68°00'
BAFFIN BAY
BARNES ICE CAP
Dexterity Island
Buchan Gulf
Clyde River
Steensby Inlet
Lower Paleozoic
Neohelikian Bylot Supergroup (1.27 Ga)
LATE APHEBIAN
Charnockite¹
Granite
ARCHEAN
Granite, slightly deformed (2.71 Ga?)
Granite, highly deformed (≥ 2.85Ga?)
CBF - Central Borden Fault Zone
NBF - Nina Bang Fault Zone
TF - Tikerakdjuak Fault Zone
WF - White Bay Fault Zone
IF - Isortoq Fault Zone
L1 - Angajurjualuk Lake
L2 - Nina Bang Lake
L3 - Conn Lake
L4 - Bieler Lake
L5 - Ayr Lake
L6 - Inuktorfik Lake
Foliation (inclined, vertical, horizontal, dip unknown)
Thrust fault (observed, inferred)
Tectonic domains 1a - 8
Helikian - recent faults (circle indicates downdropped side)
Major Aphebian shear zones, faults (observed, inferred; observed and inferred thrust faults; arrow indicates relative movement; teeth indicate dip of thrust)
¹ May include Archean rocks

Figure 112. Tectonic domains, major structural features, and granitic plutons in the Clyde-Cockburn map area. Compare with Figures 113, 114.

Although trends in the southern part of subdomain 1b merge with those of northern subdomain 2a there is an abrupt change in the aeromagnetic pattern, as well as an abrupt increase in both abundance of Mary River Group strata and in magnetic expression along an east-west line that is taken as the boundary between subdomains 1b and 2a. The wavy nature of the boundary with arcuate trends convex southwestward, and increased straightening southward on the south side suggest both sinistral movement and possible thrusting. The high magnetic expression of subzone 2a is due to an abundance of Mary River Group strata with iron-formation and a lack of granitic plutons (Fig. 112). Both the bedrock and the aeromagnetic anomalies present a virgate structure on the north side but a straight planar boundary along the south side. The southern boundary of subdomain 2a is considered to be a fault or shear zone that follows the south side of the high magnetic zone, and along which sinistral movement is indicated. Low northwest-trending anomalies mark the positions of late faults and late Proterozoic dykes; some of the anomalies appear to show dextral displacement.

Subdomain 2b owes its low magnetic expression to a paucity of Mary River Group strata and an abundance of felsic plutons (Fig. 111-114). A slight east-trending discordance in foliations marks the boundary between subdomains 2b and 2c which is sharp and slightly sinuous. A sharp, low-angle discordance is also shown by the aeromagnetic data and the contact is probably a fault or shear zone.

The abundant Mary River and Piling group remnants in subdomain 2c (*see* "Mary River Group", "Aeromagnetic pattern", "Piling Group", "Occurrence in map area") and the magnetite in abundant granulite facies rocks, probably explain the high background magnetic expression of this subdomain (Fig. 99, 101, 111, 112). Deformation of Piling Group strata, in southern subdomain 2c by the late east-west stacked thrusts and nappes (*see also* "Archean-Aphebian recumbent folds, nappes") and overprinting of the structures and the Mary River and Piling groups by the younger Dexterity Granulite Belt indicate the late east-west structures are between 2.16 and 1.82 Ga in age (*see* "U-Pb zircon and monazite ages" and "Age" in "Piling Group").

Domain 3: Foxe Fold Belt

Domain 3 is the Foxe Fold Belt on Baffin Island, the most northerly of the three tectonic belts that rim the Cumberland Batholith in the Baffin Orogen (Fig. 113; Fig. 114, in pocket). More data on the Baffin Orogen are provided in Jackson and Taylor (1972), Jackson and Morgan (1978a), and Jackson et al. (1990b). Structures in the Foxe Fold Belt are outlined mostly by the late Aphebian Piling Group. Three major subdomains have been delineated, which from north to south are: 3b with northeasterly trends, 3a with relatively early easterly trends, and 3c with easterly to southeasterly trends (Fig. 113). Domain 3 structures are overprinted and truncated to the northeast by the northwest-trending structures in subdomains 7a, 7b, and 7c (Fig. 112). The dominant trends noted here, as for domain 2, were probably formed between 2.16 and 1.82 Ga.

Domain 3 is a large area of low magnetic expression (Fig. 111), in which subdomain 3b has the lowest. Scattered low diffuse or muted magnetic highs throughout domain 3 probably represent rock types below the surface. Basement gneisses outcrop in small domal areas within the Piling Group at the site of some of these muted anomalies, and show up as tiny, well defined highs within the muted anomalies. Some linear muted anomalies suggest the presence of northwest-trending faults or diabase dykes or both.

An anorthosite sill lies along a northeast-trending fault that parallels the Isortoq Fault Zone about 30 km southeast of it in subdomain 3b. The anorthosite extends toward a diffuse north-trending anomaly west of the Barnes Ice Cap that does not seem to be represented by the surface geology and may mark a buried pluton (Fig. 111).

Surface geology of subdomain 3b (Jackson and Morgan, 1978b; Jackson et al., 1978d; Morgan, 1982; Jackson, 1984; Henderson, 1985a) is compatible with the suggestion that the subdued pattern that is convex toward the northwest and discernible for 150 km southeast to the Piling Fault represents thrusts. Equally subdued but straight north-trending zones are otherwise similar. However, their banding is parallel to the north-south magnetometer flight lines which they probably reflect (Fig. 111). Metamorphic grade of supracrustals in subdomain 3b increases both northward from the Piling Fault Zone, and southward from the Eqe Bay Belt (*see* "Eqe Bay (northeast NTS 37C) and east side of northern Barnes Ice Cap (NTS 37E)"). Piling Group strata north of the fault zone occur in nappe structures and interleaved with basement gneisses by thrust faulting (G.D. Jackson, unpub. data, 1968; Morgan, 1983; Henderson, 1985a).

Central subdomain 3a consists mostly of east-trending, upright, near isoclinal folds in the low grade Piling Group, which commonly approximate parallel folds and are thought to be relatively early. The south boundary (M - Fig. 113) seems gradational although the rocks change rather abruptly southward into Piling Group anatectites of subdomain 3c, the fold patterns of which are much more irregular and which have been deformed with their basement. Field mapping (Morgan, 1983; Henderson, 1985a) shows that a fault or shear zone must occur at about the position of the Piling Fault (Fig. 113) between upright-folded, east-trending, upper Piling Group strata (Astarte River Formation) of subdomain 3a to the south, and subdomain 3b to the north in which more plastically deformed, mostly northeast-trending, lower Piling Group strata predominate over upper Piling Group strata. A subtle change in the aeromagnetic pattern also occurs along this boundary zone, on the north side of which domal areas of basement gneisses surrounded by Piling Group strata are common.

Foliations in subdomain 3b trend more uniformly northeast, toward the northwest and the arcuate boundary with domain 2, which is the Isortoq Fault Zone. As already described, this fault zone shows up strikingly on the aeromagnetic map (Fig. 111). Sinistral shearing has occurred along this zone which may also mark the northern extent of northwestern thrusting along the north side of the Foxe Fold Belt as already described above. The northeastern part of the

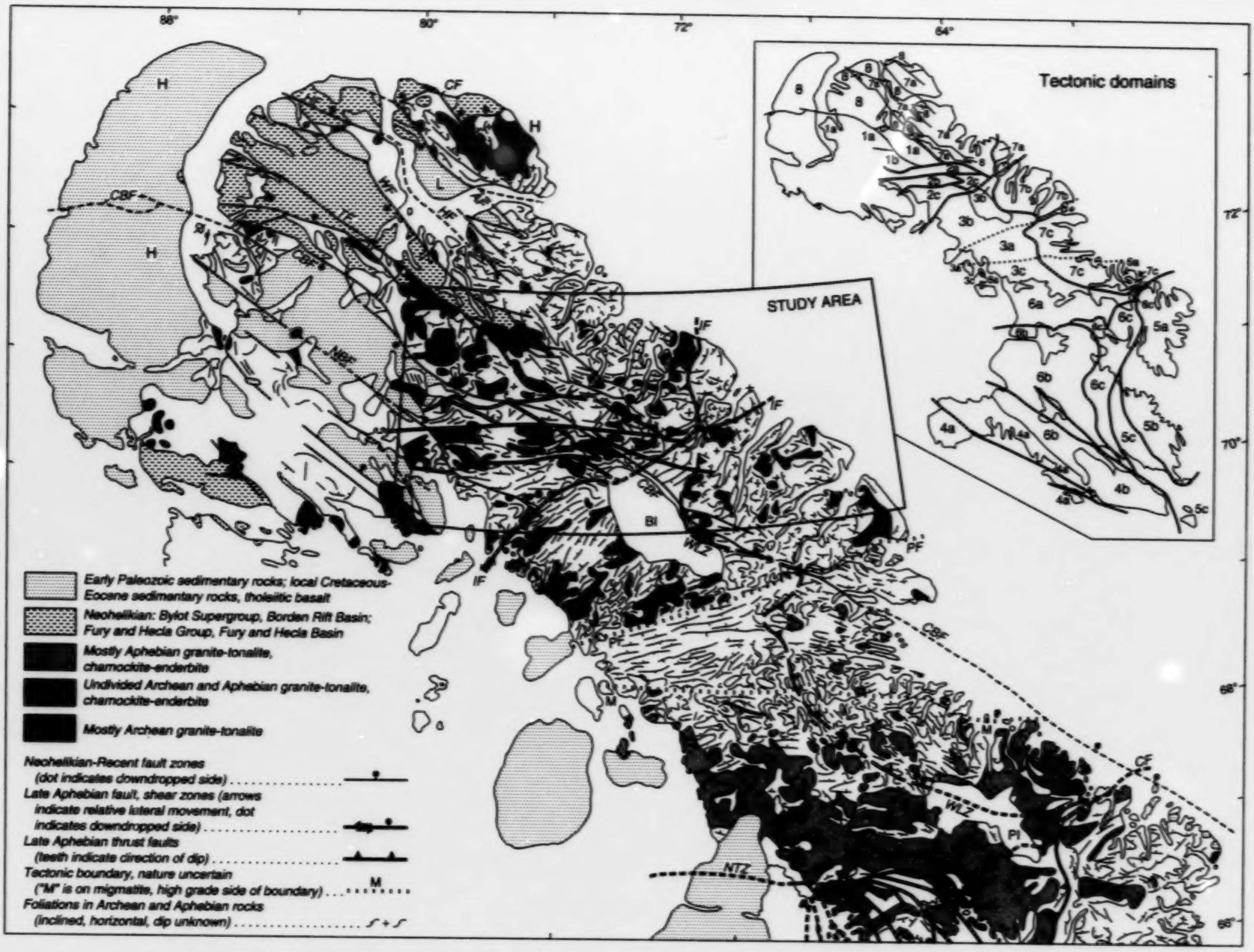
88°
80°
72°
64°
72°
70°
66°
68°
Tectonic domains
8
1a
1b
2a
2b
2c
3a
3b
3c
4a
4b
5a
5b
5c
6a
6b
6c
7a
7b
7c
STUDY AREA
H
L
CF
WF
HF
CBF
NBF
IF
BI
WLZ
PF
M
PI
NTZ
Early Paleozoic sedimentary rocks; local Cretaceous-Eocene sedimentary rocks, tholeiitic basalt
Neohelikian: Bylot Supergroup, Borden Rift Basin; Fury and Hecla Group, Fury and Hecla Basin
Mostly Aphebian granite-tonalite, charnockite-enderbite
Undivided Archean and Aphebian granite-tonalite, charnockite-enderbite
Mostly Archean granite-tonalite
Neohelikian-Recent fault zones (dot indicates downdropped side)
Late Aphebian fault, shear zones (arrows indicate relative lateral movement, dot indicates downdropped side)
Late Aphebian thrust faults (teeth indicate direction of dip)
Tectonic boundary, nature uncertain ("M" is on migmatite, high grade side of boundary)
Foliations in Archean and Aphebian rocks (inclined, horizontal, dip unknown)

Figure 113. Relationships of tectonic domains, major structural features, and granitic plutons in the map area to similar features in the rest of Baffin Island. See *Figures 112, 114 for additional names, abbreviations, references, and geology.*

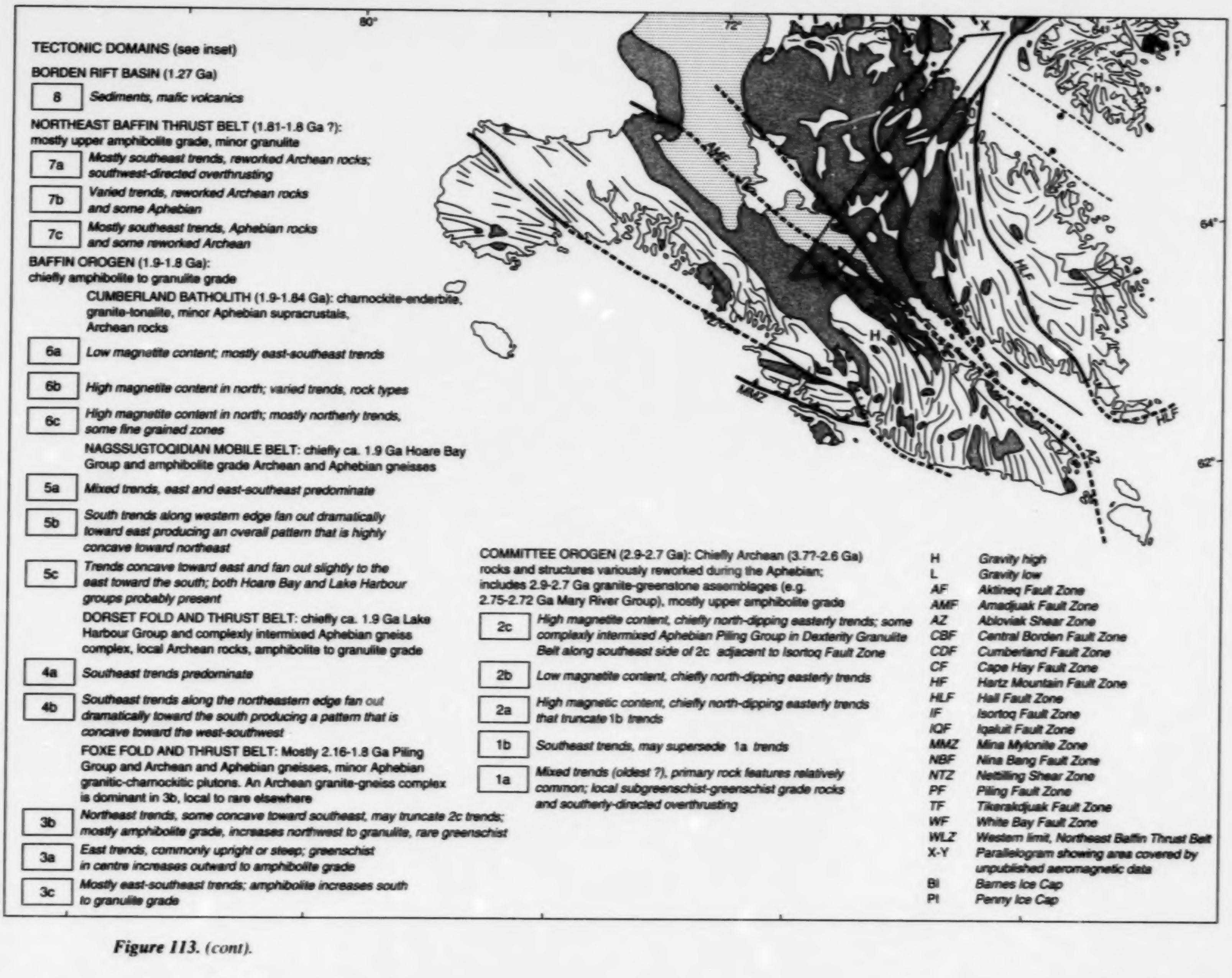
80°
72°
64°
62°
X
AMF
HLF
H
MMZ
AZ
TECTONIC DOMAINS (see inset)
BORDEN RIFT BASIN (1.27 Ga)
8 Sediments, mafic volcanics
NORTHEAST BAFFIN THRUST BELT (1.81-1.8 Ga ?): mostly upper amphibolite grade, minor granulite
7a Mostly southeast trends, reworked Archean rocks; southwest-directed overthrusting
7b Varied trends, reworked Archean rocks and some Aphebian
7c Mostly southeast trends, Aphebian rocks and some reworked Archean
BAFFIN OROGEN (1.9-1.8 Ga): chiefly amphibolite to granulite grade
CUMBERLAND BATHOLITH (1.9-1.84 Ga): charnockite-enderbite, granite-tonalite, minor Aphebian supracrustals, Archean rocks
6a Low magnetite content; mostly east-southeast trends
6b High magnetite content in north; varied trends, rock types
6c High magnetite content in north; mostly northerly trends, some fine grained zones
NAGSSUGTOQIDIAN MOBILE BELT: chiefly ca. 1.9 Ga Hoare Bay Group and amphibolite grade Archean and Aphebian gneisses
5a Mixed trends, east and east-southeast predominate
5b South trends along western edge fan out dramatically toward east producing an overall pattern that is highly concave toward northeast
5c Trends concave toward east and fan out slightly to the east toward the south; both Hoare Bay and Lake Harbour groups probably present
DORSET FOLD AND THRUST BELT: chiefly ca. 1.9 Ga Lake Harbour Group and complexly intermixed Aphebian gneiss complex, local Archean rocks, amphibolite to granulite grade
4a Southeast trends predominate
4b Southeast trends along the northeastern edge fan out dramatically toward the south producing a pattern that is concave toward the west-southwest
FOXE FOLD AND THRUST BELT: Mostly 2.16-1.8 Ga Piling Group and Archean and Aphebian gneisses, minor Aphebian granitic-charnockitic plutons. An Archean granite-gneiss complex is dominant in 3b, local to rare elsewhere
3b Northeast trends, some concave toward southeast, may truncate 2c trends; mostly amphibolite grade, increases northwest to granulite, rare greenschist
3a East trends, commonly upright or steep; greenschist in centre increases outward to amphibolite grade
3c Mostly east-southeast trends; amphibolite increases south to granulite grade
COMMITTEE OROGEN (2.9-2.7 Ga): Chiefly Archean (3.7?-2.6 Ga) rocks and structures variously reworked during the Aphebian; includes 2.9-2.7 Ga granite-greenstone assemblages (e.g. 2.75-2.72 Ga Mary River Group), mostly upper amphibolite grade
2c High magnetite content, chiefly north-dipping easterly trends; some complexly intermixed Aphebian Piling Group in Dexterity Granulite Belt along southeast side of 2c adjacent to Isortoq Fault Zone
2b Low magnetite content, chiefly north-dipping easterly trends
2a High magnetic content, chiefly north-dipping easterly trends that truncate 1b trends
1b Southeast trends, may supersede 1a trends
1a Mixed trends (oldest ?), primary rock features relatively common; local subgreenschist-greenschist grade rocks and southerly-directed overthrusting
H Gravity high
L Gravity low
AF Aktineq Fault Zone
AMF Amadjuak Fault Zone
AZ Abloviak Shear Zone
CBF Central Borden Fault Zone
CDF Cumberland Fault Zone
CF Cape Hay Fault Zone
HF Hartz Mountain Fault Zone
HLF Hall Fault Zone
IF Isortoq Fault Zone
IQF Iqaluit Fault Zone
MMZ Mina Mylonite Zone
NBF Nina Bang Fault Zone
NTZ Nettilling Shear Zone
PF Piling Fault Zone
TF Tikerakdjuak Fault Zone
WF White Bay Fault Zone
WLZ Western limit, Northeast Baffin Thrust Belt
X-Y Parallelogram showing area covered by unpublished aeromagnetic data
BI Barnes Ice Cap
PI Penny Ice Cap

Figure 113. (cont).

boundary is interpreted as having been deformed by the late deformation represented by subdomains 7a and 7b, but was probably protected from greater deformation by the Dexterity Fiord Batholith.

Domain 4: Dorset Fold Belt

Remnants of the late Aphebian Lake Harbour Group, and a variety of other map units, occur in the Dorset Fold Belt of the Baffin Orogen (Fig. 114; Blackadar, 1967b; St-Onge et al., 1996a). Some of the gneisses are considered here to be of Archean origin based on apparent field relations and Nd T_{DM} model ages (Hegner and Jackson, 1990; Jackson et al., 1990a). Recent U-Pb geochronology (Scott, 1996, 1997; Scott and Gauthier, 1996) date the Lake Harbour Group at 1934-1845 Ma, suggest the group contains negligible Archean detritus, and indicate that Archean rocks are uncommon or rare.

Trends are chiefly southeast in the larger subdomain 4a (Fig. 113). In subdomain 4b, to the southeast, the regional trends show a strong southwestward virgation and most dips are eastward. Subdomain 4b also contains more small granitic plutons than does subdomain 4a. The source of the gravity high on western Meta Incognita Peninsula is uncertain. The fold belt extends southeast to south of eastern Ungava Bay (Jackson and Taylor, 1972). Recent fieldwork by St-Onge and associates (Hanmer et al., 1996; St-Onge et al., 1996a, b) has identified late Aphebian rifting and extensive southwest-verging folds and thrust imbrications and possible mid-crustal-level detachments.

Domain 5: Nagssugtoqidian Mobile Belt

This domain lies within the Nagssugtoqidian Mobile Belt, underlies most of Hall and Cumberland peninsulas, and contains three subdomains (Fig. 113, 114; Jackson et al., 1990a; Jackson and Hegner, 1991). On Hall Peninsula, supracrustals in subdomain 5c resemble the Lake Harbour Group whereas those in subdomain 5b resemble the Hoare Bay Group of subdomain 5a on Cumberland Peninsula. Trends are most uniform in subdomain 5c and most heterogeneous in subdomain 5a (Fig. 113). Subdomains 5b and 5c are separated by a distinct boundary along which virgation and truncation suggest dextral movement along a shear zone. Granulites and charnockites to the northwest overlie northwest-dipping amphibolite facies rocks to the southeast along the boundary between subdomains 5a and 6c on Cumberland Peninsula. These relations are considered to be a result of southeastward overthrusting. Scott and Gauthier (1996) showed that the Lake Harbour Group of western Hall Peninsula was likely deposited before 1852 Ma. Scott (1996) correlated these supracrustals with the Tasiuyak gneiss of northern Labrador, which is considered here to be part of the Lake Harbour Group.

Domain 6: Cumberland Batholith

This domain consists of the Cumberland granite-charnockite batholith, core of the Baffin Orogen (Fig. 113, 114). Its northern boundary with the anatectites of subdomain 3c is chiefly intrusive and irregular but abrupt. Concentrations of earthquake epicentres along this boundary (Basham et al., 1977; Shih et al., 1988) suggest recent faulting along it. Three subdomains (6a, 6b, 6c) are differentiated from one other on the basis of structural trends, magnetite content (Fig. 113, 114; Blackadar, 1967b; Jackson et al., 1990a, b) and magnetic expression where available (*see* parallelogram X-Y, Fig. 113), proportion of granite to charnockite, and lithologies of associated rocks. They are also inferred from these data (which include striking virgate or fan-shaped bedrock and aeromagnetic patterns, flinty blastomylonites, and lineated paragneisses) to be in part separated from one another, and from domain 4 and subdomain 5c, by dextral and sinistral shear zones (Fig. 113, 114). The northern subdomain 6a is truncated on the east by overprinting of southeast-trending structures in subdomain 7c (Fig. 113). Late Aphebian overthursting outward from the (possibly mushroom-shaped) Cumberland Batholith has been observed and inferred along all sides of the batholith, but chiefly along its southwest margin (Henderson et al., 1989; Jackson et al., 1990b; Hanmer et al., 1996; St-Onge et al., 1996a, b).

Domain 7: Northeast Baffin Thrust Belt

Southeast foliation trends predominate along the northeast coast of Baffin Island for more than 970 km in the Northeast Baffin Thrust Belt and appear to truncate or supercede trends to the west in domains 1 to 4. The belt contains three aligned subdomains (Fig. 112, 113). Southeast trends predominate in the northwestern (7a) and southeastern (7c) subdomains that are separated by subdomain 7b, about 160 km long and containing mixed trends. It is bounded on the north by Gibbs Fiord and the Isortoq Fault Zone and on the south by Aulitivik Island and the Piling Fault Zone. The Neohelikian Central Borden Fault Zone probably represents reactivation along an earlier late Aphebian structure. Relationships between subdomain 7b and subdomains 7a and 7c are poorly understood. Southeast trends predominate in the last two and the trends in all three are considered to overprint and cut the trends of tectonic domains to the southwest (Fig. 112, 113). Southeast trends decrease in prominance toward the southwest, and the nature of the western boundary of the thrust belt is uncertain. The relatively abrupt change in trends across this boundary west of subdomain 7a suggests that here the boundary is a fault zone or shear zone. This boundary also coincides with the largest swarm of Hadrynian Franklin dykes in northern Baffin Island. In general southeast-directed trends are more prominent in subdomain 7a than in subdomain 7c, and in the northern and southern parts of subdomain 7a than in its middle part. Predominance of southeast-directed trends decreases southeastward in subdomain 7c.

Subdomain 7a extends from Bylot Island and Borden Peninsula southeast to Gibbs Fiord, a distance of 510 km. Stacks of ductile thrusts and nappes, well displayed in the northern part of subdomain 7a, were described above. The deformation has reoriented and smeared out remnants of Mary River Group in a northwest-southeast direction at a large angle to the regional trend of the Committee Orogen. The Isortoq Fault Zone has also been deformed in this domain (Fig. 112, 114). The southeast overprinting is less obvious at the southeastern end of subdomain 7a where some map units locally trend in other directions adjacent to the Isortoq Fault Zone. As discussed above, this deformation is considered to represent chiefly overthrusting toward the southwest. While it may be responsible for some of the upper amphibolite saddles in the Dexterity Granulite Belt within the map area (Fig. 99), late Proterozoic to Recent faulting and late Proterozoic dyke intrusion have also probably been factors in forming the saddles.

Subdomain 7c extends from Aulitivik Island and the Piling Fault Zone southeast to Maktak Fiord (about 300 km), where the west boundary merges with the major thrust along the northeastern part of the Cumberland Shear Zone separating charnockite to the northwest (subdomain 6a) from the Hoare Bay Group to the southeast (subdomain 5a). Relationships are less clear in subdomain 7c than in subdomain 7a (Fig. 113, 114). The overprint of southeast trends in subdomain 7c may becomes less clear to the southeast because the proportion of supracrustal rocks to relatively competent granite-charnockite is much less in the southeastern part of the area. This late deformation may also become weaker toward the southeast. Concentrations of earthquake epicentres in subdomain 7a northeast of the Penny Ice Cap (Basham et al., 1977; Shih et al., 1988) coincide with late northwest-trending crush zones in monzogranite and in monzocharnockite, and may be related to Hadrynian-Recent faulting.

Henderson and Tippett (1980) and Henderson and Loveridge (1981) considered upright, northwest-trending (F_4) folds to be the latest deformation in the northernmost part of subdomain 7c (e.g. Aulitivik Island). Whether or not this deformation is the distal southwest equivalent of the southwest-directed ductile deformation is not known. Henderson and Loveridge (1981) obtained a U-Pb zircon age of 1806 +15/-8 Ma for a little-deformed tonalite pegmatite filling an extension fracture in an amphibolite layer in basement granodiorite gneiss just north of Henry Kater Peninsula. The authors also concluded that this is the age of the most recent penetrative deformation in the region. Therefore, the 1806 Ma age may be either an approximate or a minimum age for the formation of the Northeast Baffin Thrust Belt.

Domain 8: Borden Basin

Borden Basin (Fig. 111-114) has been interpreted to be a Neohelikian aulacogen that developed in response to syndepositional rifting along listric faults at about 1.27 Ga (Jackson et al., 1975; Olsen, 1977; Jackson and Iannelli, 1981; Jackson and Sangster, 1987). The Milne Inlet Trough is the major graben in the basin, and Figures 112 and 113 show that it probably developed near the contact zone between subdomain 7a on the northeast and subdomain 1a on the west. The faulting that formed the graben and Borden Basin may have extended from Henry Kater Peninsula, northwest to Cornwallis Island, a distance of about 1600 km (Jackson and Iannelli, 1981). However, individual fault zones may have been extended along strike by later Phanerozoic movement. Bedrock and aeromagnetic data (Fig. 111) show that Milne Inlet Trough was tilted down toward the northeast, so that the Eqalulik and Uluksan groups were deformed into an open syncline inclined northeastward and plunging gently northwest. The negative gravity anomaly in Milne Inlet Trough at Milne Inlet corresponds to the locale where the thickest measured sections of the Arctic Bay Formation and the Uluksan Group were deposited (Jackson and Iannelli, 1981).

Borden Basin is bounded on the south by the Central Borden Fault Zone which, aeromagnetic data show, continues westward across Brodeur Peninsula under undisturbed early Paleozoic strata. The area to the south is also marked by a gravity high. This high and another gravity high on northwestern Brodeur Peninsula probably represent late Precambrian horsts.

REGIONAL SYNTHESIS

The results of this reconnaissance bedrock and chemical survey, when considered with age determinations, more detailed work in the Mary River and Eqe Bay areas, geophysical data, and studies in adjacent regions, permit some general comments on structural subdivisions, the nature of their boundaries, regional correlations, and the general history.

As relatively little has been published on Baffin Island geology, brief summaries of certain points (Fig. 111-114) are included here, to provide a framework for the map area (Fig. 112), and to demonstrate how the geological history of the map area is interrelated with that of the rest of Baffin Island (Fig. 113) and other adjacent regions of the northeastern Canadian Shield (Fig. 114).

Several correlations were either made or commented on earlier in the text and are shown in Figure 114, which shows Greenland and Canada in the predrift position depicted by Le Pichon et al. (1977). Several other reconstructions either move Greenland away from Ellesmere Island, or up against eastern Ellesmere Island, neither of which agrees with the known geology (e.g. Frisch and Dawes, 1982; Wynne et al., 1988; Okulitch et al., 1990). The fit of Le Pichon et al. (1977), however, has the same type of problem with Devon and Bylot islands. The position of Devon Island was modified slightly to overcome this. Taylor's (1982) solution of moving the rotation point of Greenland also seems reasonable. The correlations and fold belts shown in Figure 114 indicate that, since deposition of the 2759-2718 Ma Mary River Group, northern Greenland, as a separate entity, probably has not moved significantly farther from Canada than it is at present. The reader is referred to the text above and to Figure 114 for references concerning topics discussed for the region represented by Figure 114. Of the fold belts and supracrustals discussed in this section, the Committee Orogen and its contained supracrustals originated in the Archean; the rest are Aphebian. Archean granitic plutons (Fig. 112, 114), abundant within and north of the Foxe Fold Belt, probably represent at least three ages of plutonism (e.g. Table 51).

Baffin Island has been divided into two main blocks (Fig. 112, 114; Jackson et al., 1990a, b). The smaller northern block includes most of the map area, and is part of the 2000 km long Archean Committee Orogen (Fig. 114; Jackson and Taylor, 1972). The orogen in northern Baffin Island contains Archean felsic basement and supracrustal and plutonic sequences that were deformed and metamorphosed in the Archean and again in the late Aphebian when several granitic plutons were also emplaced. The larger southern part of the island, the late Aphebian Baffin Orogen, contains the huge late Aphebian (ca. 1.85 Ga) Cumberland Batholith. It is rimmed by three large penecontemporaneous fold belts containing ca. 1.9 Ga supracrustals.

Archean Nd T_{DM} model ages have been obtained for all of the Archean rocks, and for the late Aphebian granites in the northern block (Fig. 98). In southern Baffin Island, the late Aphebian metasediments and most of the Cumberland Batholith give chiefly similar Aphebian Nd T_{DM} model ages, but the basement gneisses and late Aphebian granites outside the batholith give Archean Nd model ages. Upper amphibolite metamorphic grade predominates over granulite grade in northern Baffin Island, but the two grades are about equally widespread in the southern block (Jackson and Morgan, 1978a; Jackson et al., 1990a, b). Compositions of most minerals in the assemblages probably reflect late Aphebian metamorphism, although the Archean is considered to contain Archean assemblages at least partially recrystallized to Aphebian. Available data favours a late Aphebian age for all the major granulite terranes. Mineral-based temperature-pressure calculations for Baffin Island indicate maximum values of about 900°C and 0.6 GPa for the Cumberland Batholith and Bylot Island batholith and some higher maximum values, of 1.1 GPa and 900°C for the map area and other high grade terranes on Baffin Island (G.D. Jackson, unpub. data, 1992; Berman et al., 1993). Therefore late Aphebian, relatively high temperature/low- to locally high-pressure metamorphic conditions persisted throughout most of Baffin Island. Presence of early kyanite in a few places such as Mary River and Eqe Bay indicate relatively high pressures occurred at least locally, and generally were followed by lower pressures or higher temperatures or both.

The oldest rocks throughout Baffin Island occur in a deformed granitic to quartzofeldspathic (possibly basement) complex that in the northern block (domains 1, 2, 7a, and 8 of Fig. 112 and 113), including the map area, is composed mostly of nebulitic granitic gneisses (Agn, Amn), and deformed and metamorphosed granitic plutons (gr-Agr). These ancient rocks have yielded ages by various methods (Fig. 98) of 3.7-2.8 Ga with a major concentration of ages at 2.85 Ga, which approximates the age of the Wanipogowan Orogeny of Douglas (1980) and Stockwell (1982). A few ages of about 2.9 Ga have been obtained for similar rocks on Melville Peninsula and West Greenland north of Nordre Strømfjord (Fig. 98). The 2.85 Ga concentration of ages is taken to approximate a time of major accretion of continental crust in the region of Figure 114. Small concentrations of Nd model ages at 3.15 Ga and 3.35 Ga may also represent times of continental crust accretion, but not necessarily at those times.

In the map area, these old rocks contain remnants of amphibolite that have a different chemical signature than similar rocks in the Mary River Group, and from field evidence are probably older. The old rocks underwent deformation, metamorphism, and anatexis followed by intrusion of mafic dyke swarms, uplift, and erosion prior to deposition of the late Archean Mary River Group on them.

Committee Orogen

Most of northern Baffin Island, including the map area, lies within the late Archean Committee Orogen, which extends 2000 km from west of Baker Lake to northern West Greenland (Fig. 114). The extent of the linear Committee Orogen and the possible coeval nature of the mafic and ultramafic rocks in it were first remarked on by Jackson (1966b). The belt is defined chiefly by deformed late Archean greenstone sequences such as the correlative Mary River (M, AM; Baffin Island) and Prince Albert (Melville Peninsula) groups. Uranium-lead zircon ages considered here to be most reliable (*see* section on "Age of the Mary River Group (M, AM)") indicate that these greenstone sequences are 2.76-2.72 Ga. Within the map area, the 2.76-2.72 Ga interval is considered to represent a rifting event with deposition of the Mary River Group in a volcanic arc environment. As already discussed above, the chemistry of both the older and later Archean granitic rocks most closely resembles that of continental island arc granites. In adjacent regions, late Archean U-Pb zircon ages for quartzofeldspathic rocks and a few mafic rocks (e.g. Prince Albert Group) in the Committee Orogen on Melville Peninsula, and northwest Greenland, also cluster in the 2.76-2.70 Ga range, although most Greenland ages in this range are from the Nagssugtoqidian Mobile Belt farther south. The Rb-Sr data cluster at slightly younger ages (Fig. 98, 114), but probably represent the same event. A few zircon ages of 2.709-2.706 Ga have been obtained for only slightly younger megacrystic monzogranite on Melville Peninsula and in the map area (Agp). Therefore forty to less than nine million years may have elapsed between the deposition of the Mary River and Prince Albert groups and subsequent deformation, metamorphism, and granite emplacement (e.g. Jackson et al., 1990b; Jackson and Hegner, 1991).

The 2.76-2.70 Ga interval corresponds in time to the Laurentian Orogeny of Douglas (1980) and Stockwell (1982), and is also considered to be a time of major accretion of continental crust. Older U-Pb zircon ages (2.95-2.87 Ga) for some rocks considered to also belong to the Prince Albert and Mary River groups (*see* section on "Age of the Mary River Group (M, AM)"), together with Nd T_{DM} model ages for the map area of 2.90-2.86 Ga for rocks giving late Archean and late

Aphebian U-Pb zircon ages (Fig. 98; "Regional geochronology" section) indicate this was also probably a time of major reworking of older crust.

Uranium-lead zircon ages of 2.6-2.4 Ga are uncommon for granitic gneisses and plutons on Melville Peninsula, Devon Island, and northern Baffin Island (Fig. 98) but are more common to the west in the Baker Lake-southwestern Boothia Peninsula region (LeCheminant and Roddick, 1991; Frisch and Parrish, 1992), and may represent a rejuvenation of activity at about the time of the Kenoran Orogeny of Douglas (1980) and Stockwell (1982). This activity seems to be absent on northwestern Greenland (Fig. 98).

Cavanaugh and Seyfert (1977; Seyfert and Cavanaugh, 1978) have suggested that deposition of the Mary River Group and the correlative Prince Albert Group was related to a late Aphebian suture between the Committee and Foxe Fold belts of Jackson and Taylor (1972). Although the Mary River and Prince Albert groups are Archean, the position of the northeastern part of the proposed suture approximates the position of the late Aphebian Isortoq Fault Zone and its suggested extension into Melville Peninsula (Fig. 114). The boundary between the southern Committee Fold Belt and the Queen Maud Uplift on the west corresponds with the northeast extension of a suture proposed by Gibb and Halliday (1974). Neodymium T_{DM} model ages of 3.6-3.1 Ga have been reported for the Queen Maude Uplift (Thériault et al., 1994) and of 2.9-2.4 Ga for the southwestern Committee Orogen (Dudás et al., 1991). A range of 3.7-2.8 Ga was obtained for the orogen on northern Baffin Island (Jackson et al., 1990a). The western boundary has been extended northeast through an area containing an abrupt change in structural trends in southern Boothia Peninsula (Fig. 112; Heywood, 1961; Blackadar, 1967a). The proximity and parallelism of this boundary to the Thelon Tectonic Zone to the west suggest that this boundary, whatever it is, may also be of Aphebian age. It is not yet known whether these boundary zones of the Committee Orogen developed along pre-existing major late Archean structures or whether they are entirely late Aphebian structures, possibly related to sutures, that truncate the sides of the Committee Orogen. Occurrence of the Mary River Group in the Foxe Fold Belt southeast of the Isortoq Fault Zone on Baffin Island, and of the Prince Albert Group in the Foxe Fold Belt on Melville Peninsula (Fig. 114) suggest a late Aphebian age.

Precise ages of late Aphebian granitic plutons in northern Baffin Island (Fig. 112, 114) are uncertain, although the following ages may have some relevance (Tables 51, 52; Fig. 98; section on "Regional geochronology"):

a) Rb-Sr errorchron age of 2159 Ma for map units Amn and gr-Agr in map area NTS 27F;
b) Rb-Sr isochron ages of 1987-1935 Ma for the Mary River Group in the Mary River area;
c) Rb-Sr ages of 1930 Ma for K-metasomatism in the Mary River area;
d) Rb-Sr errorchron age of 2033 Ma for possible Piling Group in the McBeth Gneiss Dome south of the map area (NTS 37C).

These ages suggest that some late Aphebian metamorphism and granitic plutons in north Baffin Island may be slightly older than others, and may be closer in age to those of the Thelon Tectonic Zone and southeast Ellesmere Island (Fig. 98; Henderson and van Breemen, 1992). A few ages of 1.8-1.7 Ga indicated for Melville Peninsula, Devon Island, and north Baffin Island may be unreliable but are similar to a U-Pb zircon age of 1.71 Ga for a small pluton on Somerset Island (Frisch and Hunt *in* Jackson et al., 1990a), and a few ages from the Nagssugtoqidian Mobile Belt in western Greenland (Fig. 98, 114).

Isortoq Fault Zone, Dexterity Granulite Belt

The Isortoq Fault Zone is interpreted as the approximate northern limit of major northwesterly directed late Aphebian overthrusting related to deformation of the Aphebian Piling Group, and the northern limit of the Foxe Fold Belt (*see* Fig. 114). The apparent deformation and truncation of the easterly trends in subdomain 2c indicate that the fault zone postdates those trends. It is clearly a major structure that could be related to north-directed subduction although its orientation, favours south-dipping subduction; but it is unlikely that it marks a suture zone, and whether the charnockite bodies in the adjacent Dexterity Granulite Belt to the north are all late Aphebian plutons or include metamorphosed Archean plutons reoriented parallel to the fault zone remains to be determined.

As noted above, however (*see* "Summary and conclusions" of section "Metamorphism"), the known geology of the region suggests that the Isortoq Fault Zone is a mid-continental tectonic zone. South-directed thrusts and south-verging folds may predominate north of the fault, whereas at least some major parallel structures immediately southeast of the southeast-dipping fault zone, are overturned to the northwest, and are associated with crudely parallel alternating higher- and lower-grade metamorphic belts. These features and the relatively high pressures obtained for the Dexterity Granulite Belt suggest that both the fault zone and the granulite belt originated in a compressive regime during overthrusting from the southeast that may have followed thrusting from the north. The region northwest of the fault zone would have been depressed at this time. The discordant relationships that the Dexterity Granulite Belt has with faults, rock types, and tectonic subdomains and the ca. 1825 Ma U-Pb zircon and monazite ages determined for the southwest end of the belt (Scammell and Bethune, 1995a, b) indicate that the belt formed late in the orogen, and that it represents chiefly a thermal event. Some heat may have been supplied to an already hot terrane by decompression related to rapid uplift along the Isortoq Fault Zone that followed the thrusting. Some of the charnockitic intrusions may also have been emplaced and supplied heat at this time. Most of the rebound north of the fault zone probably occurred later as compressive forces waned regionally. Initial extensional movements may have occurred during a reversal of movement along the old thrust planes, but the presence of late, steep, subparallel brittle faults (Fig. 109a), and the very steep aeromagnetic gradient along the fault zone indicate the latest movements were along near-vertical faults.

It is concluded from the above comments that the Isortoq Fault Zone and Dexterity Granulite Belt probably formed relatively late (ca. 1825 Ga) along the southeast margin of the Committee Origin during the evolution of the Baffin Orogen to the southeast. The formation of alternate higher grade and lower grade metamorphic belts to the southeast may also be related to compression followed by decompression (*see* "Summary and conclusions" under "Metamorphism"). The extent of the ca. 1825 Ma activity northwestward from the Dexterity Granulite Belt is not known. The belt's northern boundary ranges from discordant to subparallel to adjacent structural trends in Domain 2, and the boundary between domains 1 and 2 may approximate the northern extent of this relatively late Aphebian thermal activity. Although the 2770-2709 and 1959-1806 Ma age groups defined by U-Pb zircon and monazite ages for central and northern Baffin Island (*see* "Regional geochronology") cast doubt on the accuracy and meaning of the 2389-1935 Rb-Sr ages for northern Baffin Island, the 1987-1935 Rb-Sr isochron ages reported for the Mary River Group in the Mary River area might reflect thermal activity related to formation of the Thelon Tectonic Zone to the northwest. However, gneisses in northwestern Baffin Island, much closer to the Thelon Tectonic Zone appear to be unaffected by the latter's emplacement, and have yielded a metamorphic Rb-Sr isochron age of 2321 Ma (Jackson et al., 1990b).

Baffin Orogen

The late Aphebian Baffin Orogen (domains 3-6, south end of domain 7, Fig. 113) is a large, unique node in the northeastern part of the Trans-Hudson Orogen (Lewry and Collerson, 1990). It includes all of Baffin Island south of the Committee Fold Belt and extends westward into Melville Peninsula, eastward into western Greenland and southward into northern Quebec and Labrador (Fig. 113, 114; Jackson and Taylor, 1972; Bridgwater et al., 1973; Hoffman, 1990a; Jackson et al., 1990a, b). The immense Cumberland Batholith (ca. 1.85 Ga) forms the core of the orogen and is bordered by three late Aphebian fold and thrust belts. The Cumberland Batholith (domain 4 – Fig. 113) contains discordant and concordant anastomosing plutons, mostly monzogranite-monzocharnockite with rare related intermediate-mafic rocks including anorthosite, and interspersed with minor lenses and inclusions of basement gneisses and bordering supracrustals. Granulite facies rocks crudely outline and incompletely rim the batholith, and are most abundant southwest of the batholith (Fig. 113, 114; Jackson and Morgan, 1978a).

Chemically, the Cumberland Batholith shows more K and Na than the Archean rocks, and plots as calc-alkaline to alkaline, I- to S-type granites in a volcanic arc of an active continental margin (Tables 30-32; Fig. 69, 73; G.D. Jackson, unpub. data, 1982; Hegner and Jackson, 1990; Jackson et al., 1990a; Jackson and Hegner, 1991). The association of the batholith with Archean gneisses supports this conclusion. The similarity in early Aphebian Nd T_{DM} model ages obtained for both the late Aphebian metapelites and the batholith indicate that the batholith is a mixture of Archean crust, and late Aphebian juvenile crust and metasediments. Some individual plutons in the batholith are highly deformed (Jackson et al., 1990b) while others are not, indicating, as do the zircon ages, emplacement over a period of time during late deformation. The hypersthene isograd and other metamorphic facies boundaries cut across structures and stratigraphy in the adjacent Piling Group (Jackson and Morgan, 1978a), but the crude metamorphic aureoles around the batholith and some individual plutons indicate a close relationship between pluton emplacement and metamorphism. Similar relations have been noted for the Prøven charnockite which is also considered to be a magmatic arc (Grocott and Pulvertaft, 1990).

Uranium-lead zircon ages for the Cumberland Batholith of 1.90-1.84 Ga, but mostly 1.86-1.85 Ga, (e.g. Table 51, Fig. 98) approximate the age of emplacement. Slow cooling provided concordant monazite ages of 1.85-1.83 Ga that are twenty to thirty million years younger than zircon ages for the same samples; some zircons show evidence of inheritance (Jackson et al., 1990b; Henderson and Henderson, 1994; Scott, 1997). Neodymium T_{DM} model ages range from 3.27 to 2.10 Ga, and 24 of the 26 ages are 2.7-2.4 Ga, including some for the zircon samples. These data indicate that the batholith may be composed of 30-50% Archean crust mixed with juvenile late Aphebian crust (Hegner and Jackson, 1990; Jackson et al., 1990a; Jackson and Hegner, 1991).

Uranium-lead zircon and monazite ages have been obtained for penecontemporaneous plutons occurring in extensions of, or in regions adjacent to, the Baffin Orogen (Fig. 114). The Prøven charnockite in western Greenland has a Rb-Sr age of 1.86 Ga (Kalsbeek, 1986) and is considered to be the northeast extension of the Cumberland Batholith (Fig. 114; Bridgwater et al., 1973; Jackson et al., 1990a). It also is bordered by granulites (Grocott and Pulvertaft, 1990). Bertrand and others (Bertrand, 1991; Bertrand et al., 1993) have related the evolution of the Torngat Orogen to four distinct stages and the emplacement of several types of relatively small granite-enderbite intrusions. Principal ages include arc magmatism (chiefly hypersthene-tonalite) at 1880 Ma, peak metamorphism at 1858-1853 Ma, anatectic granites (including hypersthene-bearing mobilisates) at 1844 Ma, intrusive granite veins at 1837 Ma, regrowth of zircons in granite veins at 1825-1822 Ma, intrusive granite at 1806 Ma, and leucogranites and pegmatites at 1794-1773 Ma. A somewhat broader range of ages (1910-1719 Ma) has been recorded by Scott and Machado (1994), and Scott (1995).

Relatively small felsic plutons also occur in the Nagssugtoqidian Shear Zone (1.92-1.82 Ga, ca. 1.78 Ga; Kalsbeek et al., 1987; Kalsbeek and Nutman, 1996), in the Kuujjuaq Batholith southwest of Ungava Bay (1.84-1.83 Ga; Machado et al., 1988; Perreault and Hynes, 1990), and in the Cape Smith Belt (1.90-1.84 Ga; Parrish, 1989). More extensive felsic plutonic belts are associated with granulites and include some mafic bodies, as for instance the Narsajuaq Arc north of the Cape Smith Belt (1.86-1.82 Ga, ca. 1.75 Ga; Parrish, 1989; St-Onge and Lucas, 1992), and the slightly younger plutonic belts in the Wager Bay region southwest of Melville Peninsula (1.84-1.82 Ga; Heywood, 1967; Henderson et al., 1986; LeCheminant et al., 1987; Gordon, 1988), and in the De Pas Batholith south of Ungava Bay (1.84-1.81 Ga; Van Der Leeden et al., 1990).

The three fold belts bordering the Cumberland batholith contain late Aphebian supracrustal sequences that are partially migmatized, intruded by the batholith, and are associated with some Archean basement gneisses and small late Aphebian granitic plutons that are probably related to the batholith (i.e. satellite plutons)(Fig. 113, 114; Blackadar, 1967b; Jackson and Taylor, 1972; Jackson and Morgan, 1978a; Taylor, 1982; Henderson et al., 1988; Grocott and Pulvertaft, 1990; St-Onge et al., 1996a; Scott, 1996, 1997). On the north, the Foxe Fold Belt, which underlies about one third of the map area, is defined by the late Aphebian Penrhyn, Piling, Karrat, and Anâp Nuna groups.

On Baffin Island, the Piling Group presents a classic metamorphic gradation southward (subdomains 3b, 3c, Fig. 113) from subgreenschist(?) facies in the middle of the Foxe Fold Belt through lower and upper amphibolite facies (anatectites) into granulite facies adjacent to the Cumberland Batholith (domain 4). The picture is complicated by increased deformation and metamorphism of the Piling Group northward to granulite grade in the Dexterity Granulite Belt, which was uptilted along its southeast margin adjacent to the Isortoq Fault Zone (Fig. 113, 114).

The Dorset Fold Belt (domain 5, Fig. 113) is defined by the late Aphebian Lake Harbour Group in southern Baffin Island and northeastern Quebec-Labrador and possible correlatives on Southampton Island. The Nagssugtoqidian Mobile Belt (domain 6, Fig. 113) is defined on Baffin Island by the Hoare Bay Group, which may extend into northeastern Quebec-Labrador south of Cape Chidley, by minor Lake Harbour Group strata, and by unnamed strata between Disko Island (Fig. 114), and the Nagssugtoqidian Front (Fig. 114).

Supracrustal sequences in all three fold belts contain a lower, relatively thin quartzite-marble shelf sequence overlain by a thick basinal metagreywacke-pelite turbidite sequence. The latter contains mafic and ultramafic rocks and iron-formation in their basal parts (e.g. Jackson and Taylor, 1972).

That early rifting accompanied Piling Group shelf deposition is indicated by abrupt regional emplacement of mafic and ultramafic flows and intrusions at the base of a thick widespread turbiditic succession whose deposition also began abruptly; the sporadic occurrence elsewhere in lower Piling Group strata of minor mafic-ultramafic rocks; regions where the basal shelf quartzite is abruptly thicker than elsewhere; and scattered low broad aeromagnetic anomalies that probably indicate the presence of uplifted basement at relatively shallow depth. Early rifting has also been noted in the Dorset Fold Belt in south Baffin Island (St-Onge et al., 1996b), and the discontinuous nature and variations in thicknesses of mafic and ultramafic rocks, quartzite, marble, and iron-formation in the Hoare Bay Group is attributed at least partially to rifting. Whether or not the early rifting and mafic igneous activity is related to plume activity is a moot point. However, preliminary results from chemical studies of mafic and ultramafic rocks are compatible with plume activity (E. Anderson, pers. comm., 1997).

Neodymium T_{DM} model ages for the Piling, Lake Harbour, and Hoare Bay groups and U-Pb zircon ages (detrital and metamorphic) for the Piling and Lake Harbour groups (Henderson and Parrish, 1992; Henderson and Henderson, 1994; Scammell and Bethune, 1995b; Scott and Gauthier, 1996; *see* section on "Age" in section "Piling Group"), together with similarities in stratigraphy and alignment along strike (Fig. 113, 114), indicate that these three groups (and by inference the other related supracrustals noted above) are correlative at about 1.9 Ga. They are considered to have developed initially in the same shelf region or shallow basin on continental crust (Jackson and Taylor, 1972; Grocott and Pulvertaft, 1990). Known distribution of mafic rock types suggest either three marginal basins may then have evolved within the main basin, coinciding approximately with the three fold belts, or that one large basin developed, rimmed on the south by island arcs. For comparison, U-Pb zircon ages of 2.0-1.92 Ga have been obtained for gabbros and rhyolite in the Cape Smith Belt, and about 1.83 Ga for the Sugluk Group in the Narsajuaq Arc (Parrish, 1989; St-Onge and Lucas, 1992). Sedimentation of the northern Kaniapiskau Supergroup probably began between 2.15 and 2.14 Ga (Machado et al., 1989).

Several small massive satellite granitic plutons intrude the supracrustals in the three rimming fold belts of the Baffin Orogen and are considered to be late Aphebian. Some in the Foxe and Dorset fold belts have been dated and give U-Pb zircon ages that are mostly younger than the Cumberland Batholith (1.84-1.80 Ga, 1.78 and 1.76 Ga; Henderson and Henderson, 1994; Scammell and Bethune, 1995b; Scott and Gauthier, 1996). Some plutons give Archean Nd T_{DM} model ages and are considered to be derived in part from Archean crust, like Aphebian intrusions in the Committee Fold Belt (*see* section on origin of late Aphebian granites).

The upper part of the Piling Group is considered here to have been deposited following collision in a foredeep or back arc basin with northward thrusting in the back of the basin (domain 3) related to northward dipping subduction. Although present in the map area, amphibolites and ultramafic rocks are common at the base of in the Piling Group turbidites only from the middle of the Foxe Fold Belt southward into the Cumberland Batholith at least as far as Cumberland Sound. Grocott and Pulvertaft (1990) concluded that the correlative Karrat Group on western Greenland was deposited in a back-arc basin related to northward dipping subduction (Kalsbeek et al., 1987) in the Nagssugtoqidian Mobile Belt.

Available ages (Fig. 98) indicate that the basal Piling Group shelf strata are not older than 2.16 Ga, that the mafic volcanics and sills in the basal turbidites are about 1.90 Ga, and that much of the Cumberland Batholith is about 1.86-1.85 Ga. The ages suggest that about 10-30 Ma may have elapsed between the time of mafic volcanism and intrusion of associated mafic and ultramafic rocks on the one hand and the first intrusion of extensive felsic plutons. About 40-50 Ma may have elapsed between the mafic volcanism and deposition of the overlying turbidites, emplacement of some granitic plutons in the supracrustals, intense deformation including some tabular granite-charnockite bodies peripheral to the batholith, additional felsic intrusion, and granulite metamorphism (Jackson and Hegner, 1991). High grade metamorphism may have continued for another 20-30 Ma after the main intrusions.

The late Aphebian metamorphism throughout most of Baffin Island and west and northwest Greenland is high temperature and low to moderate pressure (Jackson and Morgan, 1978a; Cortemiglia et al., 1985; Grocott and Pulvertaft, 1990; Jackson and Hegner, 1991; Table 60). Recent published and unpublished geothermobarometric studies for Baffin Island indicate temperatures of up to 900°C, locally, and pressures of 0.49-0.76 GPa for the Cumberland Batholith, up to 850°C (1.1 GPa/810°C) for Bylot Island, and slightly higher temperatures in some of the other high grade regions (cf. Fig. 101, Table 60; Jackson and Morgan, 1978a; Cortemiglia et al., 1985). Relatively high pressure assemblages occur locally, some of which (e.g. kyanite at Mary River) may be Archean. Most late Aphebian ages correspond in time to the Moranian and Hudsonian orogenies of Douglas (1980) and Stockwell (1982), or Hoffman's (1988) formation of Laurentia.

Hoffman (1990a, b) has proposed that the Baffin Orogen was forged during the assembly of northeast Laurentia by the late Aphebian collision of three major crustal masses: the northeastern Superior, Nain, and northeastern Churchill (Rae) provinces. He also suggested that the crudely triangular shape of the orogen, especially the apparent westward taper of the Foxe Fold Belt on Melville Peninsula reflects the shape of the original basin, which opened to the southeast in response to collision, and that the opening of the basin resulted in a thinning of the lithosphere which provided the heat to generate the crustal melt for the Cumberland Batholith and the surrounding granulite metamorphism. Jackson et al. (1990a) and Jackson and Hegner (1991) also considered that three crustal masses were involved but suggested that a fourth relatively small block that included southern Baffin Island separated from the region to the north only to be pushed back together during the collision, and was not bent southward to be caught between the northeast Superior and Nain blocks as was proposed by Hoffman (1990b). The late syntectonic overthursting away from the margins of the Cumberland Batholith seems compatible with such a separation and closure. Numerous remnants of Piling Group strata extend northward from south-central Baffin Island to north of the Isortoq Fault Zone and, west of Foxe Basin, strata that could be Penhryn Group correlatives, occur both south and a considerable distance north of the assumed western end of the Foxe Fold Belt. As yet, we have little information on the actual limits of the depositional basin(s), or on the correlative nature of coeval sequences. It seems more likely that the apparent westerly pinching out of the Foxe Fold Belt and the Penhryn Group are secondary tectonic features that do not represent primary basin boundaries.

Hoffman (1990b) has also proposed that the Abloviak Shear Zone extends north from the Torngat Orogen into Frobisher Bay and across Hall Peninsula in the position of shear zone CZ2-CZ of the Cumberland Shear Zones (Fig. 113, 114) which he suggested may be a northwest-dipping suture. The known geology such as charnockites overlying northerly dipping amphibolite facies on Cumberland Peninsula is compatible with this suggestion. Field mapping by Blackadar (1967b), Jackson (1971; Jackson and Taylor, 1972), Hanmer et al. (1996), St-Onge et al. (1996a), and aeromagnetic data indicate the presence of several shear or thrust zones in the southern part of the Baffin Orogen (Fig. 113, 114), four of which pass through Frobisher Bay. The relative movements shown on either side of the Amadjuak (AMF) and Cumberland (CDF) shear zones (Fig. 113, 114) indicate movement westward away from the junction of the two shear zones, similar to a situation described by Hanmer (1987).

Two other boundary zones, in addition to the relatively obvious ones bounding the Cumberland Batholith on the south (Fig. 113, 114), seem more likely candidates for Hoffman's boundary zone although Piling Group strata of similar stratigraphic position occur on both sides of both features:

a) the Piling Fault Zone (Fig. 113) at the boundary between lower grade Piling Group strata to the south and higher grade Piling strata to the north.
b) the Nettilling Shear Zone (Fig. 113), which separates low-iron charnockite and granite to the north from high-iron equivalents to the south. The rocks to the south are also structurally more complexly interrelated with supracrustals and basement gneisses than the low-iron suite.

Van Kranendonk et al. (1993) concluded that the Superior Province indentation was the last major collisional event during the assembly of northeast Laurentia rather than the first as proposed by Hoffman (1990a, b). In both models the boundary between Hoffman's northern and southern Rae subprovinces was taken as the north edge of the Cumberland Batholith. However, there is no obvious indication of such a major boundary within or adjacent to this extremely irregular prograde belt within which metamorphic grade, plutonism, and deformation increase southward into the batholith proper. Also, the basal Piling quartzite of the Dewar Lakes Formation lies unconformably on the basement complex in windows and outliers from the Barnes Ice Cap southward across the Foxe Fold Belt to south of the Penny Ice Cap and the Hoare Bay Group. Relations there are uncertain, but the two groups seem conformable.

A crude Z-shaped regional trend is outlined by foliations and lithologies in the Cumberland Batholith and on Hall Peninsula. In addition, a strong easterly to southeasterly regional trend, superimposed on a northeast trend in the Hoare Bay Group on Cumberland Peninsula, is subparallel to the regional trend in the northern Cumberland Batholith to the northwest (Fig. 113). The batholith may, in part, owe its present equidimensional shape, and regional variations in level of magnetism (magnetite content) and deformation, to the stacking of segments of a once linear plutonic belt (e.g. Sierra Nevada Batholith, Andes) during strike-slip movement along some of its more prominent bounding and internal shear zones. The structures and rock types southeast of the batholith (Fig. 113, 114) are compatible with the terrane on Cumberland and Hall peninsulas being an extension of the Nagssugtoqidiana Mobile belt in West Greenland (Jackson et al., 1990a; Jackson and Hegner, 1991). They are not compatible with the emplacement of the Burwell terrane as depicted by Hoffman (1990a, b) or with the emplacement of the Disko terrane as depicted by Van Kranendonk et al. (1993).

Neodymium model ages and some Rb-Sr data suggest that some crust may be at least 3.7 Ga within the fault block that extends from Cumberland Peninsula to northwestern Baffin Island (Hegner and Jackson, 1990; Jackson et al., 1990a; Jackson and Hegner, 1991). This data raises the possibility that this immense fault block may be a deformed and metamorphosed extension of the Nain Province. Although local components in rocks of the Minto block in the northeast Superior Province are also probably as old as ca. 3.5 Ga (e.g. Skulski et al., 1996; Fig. 114), several other features crudely parallel the northerly to northwesterly trend of the Nain-northeast Baffin Island region belt noted above and make the idea of the Nain Province extending into northeastern Baffin Island at least more intriguing. These include the eastern, sinuous boundary for the occurrence of carbonate and calc-silicate strata of the Lake Harbour and Piling groups; the 1.90-1.85 Ga age of the granitic-charnockitic plutons in the Cumberland Batholith-northern Torngat belt (Burwell magmatic arc, Scott, 1997), whereas similar plutons to the west average about 30 Ma younger; and, although few localities have been sampled, an abundance of Archean detrital zircons in the Ramah and Piling groups, but a dearth of Archean detrital zircons in the Tasiuyak paragneiss and Lake Harbour Group (Henderson and Parrish, 1992; Scott and Gauthier, 1996).

The following features should also be considered in tectonic reconstructions: the apparent continuation of the late Archean Committee Orogen northeastward into North-West Greenland, tying it to North America by late Archean time; the likelihood of a minor short-lived separation of South Baffin Island from the rest of the northeast Churchill Province; the possible involvement of plume activity in the evolution of the Baffin Orogen; the overthrusting away from the (possibly mushroom-shaped) Cumberland Batholith at its margins; the possibility that the shape of the batholith represents a stacking of faulted segments of a once-linear plutonic belt; and the similarity in age, spatial relations, and evolution of the late Aphebian supracrustal depositional basins. The easterly trending Nettilling Shear Zone and the northerly trending Abloviak and Cumberland shear zones (Fig. 114) may represent older collisional events (ca. 1.9-1.85 Ga) that preceded the 1.82-1.80 collisional event (St-Onge et al., 1996b; Scott, 1997) between northern Quebec and southern Baffin Island.

Origin of late Aphebian granites

Regional Sm-Nd data and a few U-Pb zircon ages indicate that some smaller late Aphebian granitic plutons in the map area, and probably throughout Baffin Island, were formed chiefly by the melting of Archean sialic crust. A similar conclusion has recently been reached by Scott (1997) for a syenite intrusion in the Dorset Fold Belt of southern Baffin Island. Little or no Proterozoic juvenile crust was added. On the other hand the Cumberland Batholith, as described above, is a mixture of Archean and ca. 1.9 Ga juvenile crust. Archean felsic plutons are more potassic than the older Archean gneisses, and the late Aphebian felsic plutons are slightly more potassic than the late Archean plutons (Fig. 20; G.D. Jackson, unpub. data, 1982). Both groups of felsic plutons are in compositional ranges close to that of minimal granitic melts (roughly equivalent amounts of silica, plagioclase, and potassium feldspar). It has been suggested that magmas of such compositions are likely to solidify at depth rather than to erupt (Morgan and Burke, 1985). This may explain the apparent dearth of felsic volcanics associated with the late Aphebian felsic plutons.

As noted above, geothermobarometry for Baffin Island indicate a few high temperature areas for parts of the Cumberland Batholith, on Bylot Island, and elsewhere. A few high pressure assemblages are also present (e.g. Jackson and Morgan, 1978a). However, most of the late Aphebian plutons, at least in the Baffin Orogen, are low- to intermediate-level intrusions, the magma source of which was at even greater depths. Crustal thickening by continent-continent collision has been invoked in several studies to explain large regions that are underlain by thick continental crust, commonly with granulites and charnockites exposed at the surface. Such a model is proposed for the Baffin Orogen and the Dexterity Granulite Belt north of the Isortoq Fault Zone (Fig. 99, 113, 114). The model described by Dewey and Burke (1973) and Morgan and Burke (1985) seems to best fit the data for Baffin Island. Thickening is ascribed to subduction, imbricate thrusting, and ductile creep. The thickened crust effectively weakens the lithosphere and leads to partial melting in the lower crust. The large region of high temperature, low- to intermediate-pressure, high grade metamorphism cored by the huge Cumberland Batholith, and the composition of the batholith, suggest that more than just crustal thickening may have been required to generate the heat needed to produce such large amounts of anatexis and granitic magma. Initial crustal thinning is suggested by the presence of a widespread basal shelf sequence. Thickening of the continental crust followed, accompanied by thickening of the underlying lithospheric mantle. This could lead to delamination and a falling off of the lower thermal boundary layer of the lithospheric mantle which would be replaced by hot asthenosphere (e.g. Houseman et al., 1981; England and Houseman, 1989). If this mechanism operates, a rise in surface elevation follows thickening of the continental lithosphere and loss of the thermal boundary layer. The overthrusting outward from the margins of the Cumberland Batholith noted above (*see* "Domain 6: Cumberland Batholith") may be evidence of such activity, regardless of the original shape of the batholith.

Northeast Baffin Thrust Belt

One of the last late Aphebian events was probably the development of the southwest thrusting and compression in the Northeast Baffin Thrust Belt (ca. 1.81-1.80 Ga) along the northeast coast of Baffin Island. According to this interpretation, the Rinkian-Northeast Baffin Thrust Belt is a late tectono-metamorphic feature that crosscuts the Dexterity Granulite Belt, and cuts diagonally across the Foxe Fold Belt in eastern Baffin Island, and the Rinkian Belt should not be equated with the slightly older main Foxe Fold Belt. The

Rinkian-Northeast Baffin Thrust Belt may be related to collision of a fourth large sialic crust block east of the eastern Committee Orogen and Foxe Fold Belt in West and North-West Greenland. The relation of this event to the east-southeast trends in the Hoare Bay Group and northern Cumberland Batholith, or to the late northward indentation of the northeast Superior Province proposed by Van Kranendonk et al. (1993) is not clear. Similarities of foliation patterns and of fold and thrust styles in the westward direction of the ductile thrusting and vergence of nappe structures, and the apparent alignment of the southern boundary fault of the Rinkian Belt in West Greenland with the western boundary of the Northeast Baffin Thrust Belt indicate that the thrust belt is likely the western extension of the Rinkian Belt (Fig. 112-114; Escher, 1984, 1985a, b, c; Grocott and Pulvertaft, 1990).

According to Grocott and Pulvertaft (1990), the Aphebian Karrat Group, in the Rinkian Belt, following its deposition, was first subjected to high temperature-low pressure metamorphism during west-northwest-east-southeast extension and growth of diapiric mantled gneiss domes. As metamorphism continued, the deformation changed to west-northwest ductile overthrusting and interleaving of basement and cover. This was followed by high temperature ductile westward overthrusting during which westerly verging sheath-like nappes and asymmetric mantled gneiss domes, especially characteristic of the northern Rinkian Belt, were also probably formed. In addition, final Aphebian displacements occurred in the Rinkian Belt during brittle northerly thrusting, which may be represented on Baffin Island by the Isortoq Fault Zone. The abundance of lineations subparallel to the deduced direction of overthrusting in the central part of subdomains 7a (Jackson et al., 1975) and in 7b (Jackson, 1984) suggests that sheath- like folds may be present in these regions. Most lineations in subdomain 7a are at a high angle to the direction of overturning and thrusting (Jackson and Davidson, 1975; Jackson et al., 1975, 1978b, c).

Milne Inlet Trough

The Milne Inlet Trough of Borden Rift Basin has been interpreted as an aulacogen that developed during the opening of the Helikian Poseidon Ocean (Jackson and Iannelli, 1981). A more precise age of 1.27 Ga for this event has been provided recently by baddeleyite ages for Mackenzie dykes (LeCheminant and Heaman, 1991). The Milne Inlet Trough seems to have formed close to the boundary between domains 1 and 7 (Fig. 112).

Deposition of the Bylot Supergroup has been related to regional tectonic events by Jackson and Iannelli (1981, 1989) and Iannelli (1992). The Adams Sound Formation was probably deposited during regional extension and crustal thinning of a passive rift phase. Overlying Arctic Bay strata were deposited as a result of extensive block faulting during active rifting and development of the main horsts and grabens of Borden Rift Basin. Regional downwarp, subsidence, and cooling followed, with development of a passive divergent margin and deposition of the Society Cliffs Formation dolostones. Although not represented in the map area, subsequent sedimentation continued as a second rift phase developed in an active convergent margin and was followed by downwarp of a passive convergent margin.

Uplift episodes, crustal thickness

Recent Sm-Nd determinations for Baffin Island (Hegner and Jackson, 1990; Jackson et al., 1990a) suggest that some of the sialic crust on Baffin Island, including the map area, may have separated from the mantle at about 3.2 Ga, and much of it by 2.9 Ga (Fig. 98). At least one period of uplift and erosion had to have preceded or accompanied deposition of the Mary River Group. Therefore at least six episodes of denudation have occurred in the region culminating in, and/or interspersed with, episodes of sedimentation and/or volcanism represented by:

1) Mary River Group (2.75-2.72 Ga);
2) Piling Group (ca. 2.16-1.88 Ga);
3) Bylot Supergroup (1.27-1.19 Ga);
4) early Paleozoic strata (0.5-0.4 Ga);
5) Eclipse Group, Cape Dyer basalt (0.14-0.04 Ga).

It is difficult to estimate how much crust may have been denuded prior to deposition of the Mary River Group. Paucity of clasts of high grade or even low- to medium-grade gneisses indicates it probably was not a great thickness, perhaps 10 km or less. Involvement of the Mary River Group in the map area, in the formation of late Archean migmatite, and the pressure-temperature relations suggested by some Mary River mineral assemblages thought to be Archean, suggest that 15-20 km may have been denuded in some places at least prior to deposition of the Piling Group. Granulite facies Piling Group rocks are now exposed at the surface, and locally the Bylot Supergroup unconformably overlies granulites that were probably formed at the same time as those in the Piling Group. Therefore in some areas, 25-30 km of crust were probably eroded by the time Neohelikian sedimentation began. The presence of prehnite-pumpellyite assemblages indicates that less than 10 km has been eroded from above the exposed Bylot Supergroup and probably included both Paleozoic strata and the Eclipse Group. The above figures may be local maxima and are not necessarily complementary. They do suggest that a considerable thickness, possibly 40-50 km or more, has been denuded at least locally.

Sialic crust thicknesses have been calculated from earthquake data for the Buchan Gulf area, which includes granulites. Values range from 32-40 km, the latter figure being the most recent (Jackson et al., 1977; Reid and Falconer, 1982). Shih et al. (1988) consider the crust below Baffin Island to be at least 35 km thick. Therefore late Aphebian crustal thicknesses may have been greater than 75 km, at least locally. This again raises the question of how granulites are formed at 0.5-0.7 kPa (18-25 km) with 40 km of crust below. Certainly a crustal underplating episode subsequent to the granulite forming event would probably leave a discernible imprint on the area. Perhaps some of the determined ages that do not seem to be related to any major event (Fig. 98, Tables 51-53) may actually be a record of such activity.

Summary

Continuation on the late Archean (2.9-2.7 Ga) Committee Orogen northeastward into North-West Greenland would tie the latter to northern North America by late Archean time, and if Nain Province rocks do extend up the east coast of Baffin Island they would have to have been emplaced prior to deposition of the Piling Group and likely before the Committee Orogen was formed.

Southern Baffin Island may have been separated form the Churchill Province to the north for a short period of time and the two blocks pushed back together again during the amalgamation of Laurentia. The close similarity in age and stratigraphy of the mid-late Aphebian strata in the 1.9-1.8 Ga Baffin Orogen suggest the possibility that the deposition began in a single basin in a shelf environment that evolved into either three marginal basins or a single large basin bordered on the south by island arcs. The present shape of the Cumberland Batholith may have been formed by the stacking of faulted segments of a once-linear plutonic belt. Syn- to late-tectonic overthrusting away from the batholith on all sides does not necessarily indicate otherwise, but does suggest that some process of delamination and underplating may have contributed heat during formation of the Cumberland Batholith (*see* "Origin of late Aphebian granites"). The easterly trending Nettilling Shear Zone and the northerly trending Abloviak and Cumberland shear zones (Fig. 114) may represent older collisional events (ca. 1.9-1.85 Ga) that preceded the 1.82-1.80 collisional event (St-Onge et al., 1996b; Scott, 1997) between northern Quebec and southern Baffin Island.

The Northeast Baffin Thrust Zone (ca. 1.81-1.80 Ga), formed during southwest-northeast compression and the latest Aphebian regional tectonic feature imprinted on Baffin Island, may be the northwestward continuation of the Rinkian in western Greenland. The northwest-trending Neoheolikian Milne Inlet Trough of Borden Rift Basin developed along the northern extension of the western boundary of the Northeast Baffin Thrust Zone which is also paralleled by swarms of 723 Ma Franklin diabase dykes. Both the Milne Inlet Trough and Franklin dykes formed during southwest-northeast extension.

At least six episodes of denudation are interspersed with five episodes of sedimentation and/or volcanism at about 0.4-0.7 Ga intervals. Aphebian crustal thicknesses may have exceeded 75 km at least locally.

REFERENCES

Agar, F. and Farquharson, G.
1980: The world's most northerly metal mine; *in* Risk Taking in Canadian Mining, (ed.) J. Carrington; Pitt Publishing Company, Toronto, p. 133-141.

Anderson, J.L.
1983: Proterozoic anorogenic granite plutonism of North America; Geological Society of America, Memoir 161, p. 133-154.

Anderson, M.C. and Pulvertaft, T.C.R.
1985: Rb-Sr whole rock "ages" from reworked basement gneiss in the Umanak area, central West Greenland; Geological Society of Denmark, Bulletin 34, p. 205-212.

Andrews, J.T.
1963: The cross-valley moraines of north-central Baffin Island: a quantitative analysis; Canadian Geographical Branch, Geographical Bulletin, no. 20, p. 82-129.

Andrews, J.T.
1966: Pattern of coastal uplift and glaciation, west Baffin Island, N.W.T.; Canadian Geographical Branch, Geographical Bulletin, v. 8, p. 174-193.
1970: A geomorphological study of post-glacial uplift with particular reference to Arctic Canada; London Institute of British Geographers, 156 p.
1982: Holocene glacier variations in eastern Canadian Arctic: a review; Striae, v. 18, p. 9-13.

Andrews, J.T. and Barnett, M.
1979: Holocene (Neoglacial) moraine and proglacial lake chronology, Barnes Ice Cap, Canada; Boreas, v. 8, p. 341-358.

Andrews, J.T. and Miller, G.H.
1979: Glacial erosion and ice sheet divides, northeastern Laurentide ice sheet, on the basis of the distribution of limestone erratics; Geology, v. 7, p. 592-596.
1984: Quaternary glacial and nonglacial correlations for the eastern Canadian Arctic; *in* Quaternary Stratigraphy of Canada – A Canadian Contribution to IGCP Project 24, (ed.) R.J. Fulton; Geological Survey of Canada, Paper 84-10, p. 101-116.

Andrews, J.T., Guennel, G.K., Wray, J.L., and Ives, J.D.
1972: An early Tertiary outcrop in north-central Baffin Island, Northwest Territories, Canada: environment and significance; Canadian Journal of Earth Sciences, v. 9, p. 233-238.

Andrews, J.T., Miller, G.H., Vincent, J.-S., and Shilts, W.W.
1984: Quaternary correlations in Arctic Canada; *in* Quaternary Stratigraphy of Canada – A Canadian Contribution to IGCP Project 24, (ed.) R.J. Fulton; Geological Survey of Canada, Paper 84-10, p. 124-134.

Andrews, J.T., Szabo, B.J., and Isherwood, W.
1975: Multiple tills, radiometric ages, and assessment of the Wisconsin glaciation in eastern Baffin Island, N.W.T., Canada: a progress report; Arctic and Alpine Research, v. 7, p. 39-59.

Annesley, I.R.
1989: Petrochemistry of the Woodburn Lake Group komatiitic suite, Amer Lake, N.W.T., Canada; PhD. thesis, University of Ottawa, Ottawa, Ontario, 404 p.

Appel, P.W.U.
1987: Geochemistry of the Early Archean Isua iron-formation, West Greenland; *in* Precambrian Iron-Formations, (ed.) P.W.U. Appel and G.L. LaBerge; Theophrastus Publications, S.A., Athens, p. 31-67.

Appel, P.W.U. and LaBerge, G.L.
1987: Precambrian Iron-Formations; Theophrastus Publications, S.A., Athens, 674 p.

Arndt, N.T., Naldrett, A.J., and Pyke, D.R.
1977: Komatiitic and iron-rich tholeiitic lavas of Munro Township, northeast Ontario; Journal of Petrology, v. 18, pt. 2, p. 319-369.

Ashton, K.E.
1988: Precambrian geology of the southeastern Amer Lake area (66H/1), near Baker Lake, N.W.T.: a study of the Woodburn Lake group, an Archean, orthoquartzite-bearing sequence in the Churchill structural province; PhD. thesis, Queen's University, Kingston, Ontario, 267 p.

Baffinland Iron Mines Limited
1964: Engineering report no. 2 for Baffinland Iron Mines Limited on the Mary River Iron Deposits; company report, v. 1 (text) – 179 p., v. 2 (maps).
1966: The Mary River project of Baffinland Iron Mines Limited; company report, 19 p.

Baker, J.H. and Drucker, W.H.
1985: Proterozoic 1.8-1.9 Ga S-type granites from W. Bergslagen, Central Sweden; *in* The Petrology and Geochemistry of 1.8-1.9 Ga Granitic Magmatism and Related Seafloor Hydrothermal Alteration and Ore Forming Processes, W. Bergslagen, Sweden, (ed.) J.H. Baker; Goeteborgs Universitets Arsskrift, Papers of Geology, series 1, no. 21, p. 89-122.

Baragar, W.R.A.

1977: Volcanism of the stable crust; *in* Volcanic Regimes in Canada, (ed.) W.R.A. Baragar, L.C. Coleman, and J.M. Hall; Geological Association of Canada, Special Paper 16, p. 377-405.

Barker, F.

1979: Trondhjemite: definition, environment and hypothesis of origin; *in* Trondhjemites, Dacites, and Related Rocks, (ed.) F. Barker; Elsevier Publishing Co., New York, p. 1-11.

Barker, F., Arth, J.G., and Hudson, T.

1981: Tonalites in crustal evolution; Philosophical Transactions of the Royal Society of London, Series A, v. 301, p. 293-303.

Basham, P.W., Forsyth, D.A., and Wetmiller, R.J.

1977: The seismicity of northern Canada; Canadian Journal of Earth Sciences, v. 14, p. 1646-1667.

Beardmore, R.

1978: Regional analysis of natural region 37: the eastern Arctic lowlands; National Parks Branch, Indian and Northern Affairs Department, 125 p.

Berger, G.W. and York, D.

1980: Reinterpretation of the North American apparent polar wander curve for the interval 800-1500 Ma; Canadian Journal of Earth Sciences, v. 17, p. 1229-1235.

Berman, R.G.

1988: Internally-consistent thermodynamic data for stoichiometric minerals in the system Na_2O-K_2O-CaO-MgO-FeO-Fe_2O_3-Al_2O_3-SiO_2-TiO_2-H_2O-CO_2; Journal of Petrology, v. 29, p. 445-522.

1990: Mixing properties of Ca-Mg-Fe-Mn garnets; The American Mineralogist, v. 75, p. 328-344.

1991: Thermobarometry using multiequilibrium calculations: a new technique with petrologic applications; Canadian Mineralogist, v. 29, p. 833-855.

Berman, R.G., Venance, K.E., Arscott, P., Frisch, T., and Jackson, G.

1993: Metamorphic map of the Canadian Shield: recent progress; *in* Abstracts with Programs, Geological Society of America, 1993 annual meeting, Boston, Massachusetts, p. A286.

Bernier, J.E.

1910: Report on the Dominion of Canada Government Expedition to the Arctic Islands and Hudson Strait on board the D.G.S. Arctic (Cruise of the Arctic 1908-9); Ottawa, Government Printing Bureau, 529 p.

1911: Report on the Dominion Government Expedition to the Northern Waters and Arctic Archipelago, Ottawa, Department of Marine and Fisheries, 161 p.

Bertrand, J.-M.

1991: Evolution of a collision zone: U-Pb dating of the Torngat Orogen, North River-Nutak transect area, Labrador; *in* Toronto 1991, Program with Abstracts, Geological Association of Canada and Mineralogical Association of Canada joint annual meeting with Society of Economic Geologists, v. 16, p. A11.

Bertrand, J.-M., Roddick, J.C., Van Kranendonk, M.J., and Ermanovics, I.

1993: U-Pb geochronology of deformation and metamorphism across a central transect of the Early Proterozoic Torngat Orogen, North River map area, Labrador; Canadian Journal of Earth Sciences, v. 30, p. 1470-1489.

Bethune, K.M. and Scammell, R.J.

1993: Preliminary Precambrian geology in the vicinity of Eqe Bay, Baffin Island, Northwest Territories; *in* Current Research, Part C; Geological Survey of Canada, Paper 93-1C, p. 19-28.

1995: Relationship of a greenschist-granulite facies transition to regional structure in the vicinity of Eqe Bay, north-central Baffin Island, NWT (abstract); *in* Geological Association of Canada, Program with Abstracts, v. 20, Victoria, British Columbia, p. A-8.

1997: Precambrian geology, Koch Island area, District of Franklin, Northwest Territories (part of NTS 37C); Geological Survey of Canada, Open File 3391, three coloured map sheets, scale 1:50 000, one text and figure sheet.

Bethune, K.M., Scammell, R.J., and Jackson, G.D.

1996: The Isortoq Fault Zone: a major Paleoproterozoic structure related to the development of the Foxe Fold Belt, north-central Baffin Island, Northwest Territories (abstract); *in* Geological Association of Canada, Program with Abstracts, v. 21, Winnipeg, Manitoba, p. A-8.

Blackadar, R.G.

1956: Geological reconnaissance of Admiralty Inlet, Baffin Island, Arctic Archipelago, Northwest Territories; Geological Survey of Canada, Paper 55-6, 25 p.

1958a: Fury and Hecla Strait, District of Franklin, Northwest Territories; Geological Survey of Canada, Map 3-1958 at 1:506 880 (with marginal notes).

1958b: Foxe Basin North, District of Franklin, Northwest Territories; Geological Survey of Canada, Map 4-1958 at 1:506 880 (with marginal notes).

1963: Additional notes to accompany Map 3-1958 (Fury and Hecla Strait) and Map 4-1958 (Foxe Basin North); Geological Survey of Canada, Paper 62-35, 24 p.

1965: Geological reconnaissance of the Precambrian of northwestern Baffin Island, Northwest Territories; Geological Survey of Canada, Paper 64-42, 25 p.

1967a: Precambrian geology of Boothia Peninsula, Somerset Island, and Prince of Wales Island, District of Franklin; Geological Survey of Canada, Bulletin 151, 62 p., 2 maps at 1:506 880 scale.

1967b: Geological reconnaissance southern Baffin Island, District of Franklin; Geological Survey of Canada, Paper 66-47, 32 p.

1968a: Milne Inlet, District of Franklin; Geological Survey of Canada, Map 1235A, with marginal notes, scale 1:253 440.

1968b: Phillips Creek, District of Franklin; Geological Survey of Canada, Map 1239A, with marginal notes, scale 1:253 440.

1968c: Erichsen Lake, District of Franklin; Geological Survey of Canada, Map 1242A, with marginal notes, scale 1:253 440.

1970: Precambrian geology northwestern Baffin Island, District of Franklin; Geological Survey of Canada, Bulletin 191, 89 p.

Blomquist, S. and Elander, M.

1981: Sabine's gull (*Xema sabini*), Ross's gull (*Rhodostethia rorea*) and ivory gull (*Pagophila eburnea*). Gulls in the Arctic: a review; Arctic, v. 34, no. 2, p. 122-132.

Boas, F.

1885: Baffin-Land; Petermann's Geographische Mitteilungen, Ergaenzungsheft, no. 80, 100 p.

1887: The geography and geology of Baffin-Land; Royal Society of Canada, Transactions, section 4, p. 79-84.

Bolton, T.E. and Sinclair, G.W.

1967: Report on fossils collected from Mary River area, northern Baffin Island, 1965. Submitted by G.D. Jackson (NTS 37G 5&6); Geological Survey of Canada, internal report, no. 01-1967-GWS/TEB.

Bolton, T.E., Sanford, B.V., Copeland, M.J., Barnes, C.R., and Rigby, J.K.

1977: Geology of Ordovician rocks, Melville Peninsula and region, southeast District of Franklin; Geological Survey of Canada, Bulletin 269, 137 p.

Borchert, H.

1960: Genesis of marine sedimentary ores; Institute of Mining and Metallurgy Bulletin, v. 640, p. 261-279.

Bostock, H.S.

1970a: Physiographic regions of Canada; Geological Survey of Canada, Map 1254A, scale 1:5 000 000.

1970b: Physiographic subdivisions of Canada; *in* Geology and Economic Minerals of Canada, (ed.) R.J.W. Douglas; Geological Survey of Canada, Economic Geology Report 1, Chapter 2, p. 10-30.

Boyd, J.A.

1970: Report of geological and geophysical investigations of the Eqe Bay claim group on west coast of Baffin Island, Northwest Territories, Canada; Patino Mining Corporation, company report.

Braterman, P.S. and Cairns-Smith, A.G.

1987: Iron photoprecipitation and the genesis of the banded iron-formations; *in* Precambrian Iron-Formations, (ed.) P.W.U. Appel and G.L. LaBerge; Theophrastus Publications, S.A., Athens, p. 215-245.

Bridgwater, D. and Schiotte, L.

1991: The Archaean gneiss complex of northern Labrador, a review of current results, ideas and problems; Geological Society of Denmark, Bulletin, v. 39, p. 153-166.

Bridgwater, D., Escher, A., Jackson, G.D., Taylor, F.C., and Windley, B.F.

1973: Development of the Precambrian Shield in West Greenland, Labrador and Baffin Island; American Association of Petroleum Geologists, Arctic Geology, Memoir 19, p. 99-116.

Brisbin, D.I.

1979: Stratigraphy, structure and metamorphism of the Piling Group on Ilutalik Island and vicinity, Home Bay, Baffin Island, N.W.T.; BSc. thesis, Queen's University, Kingston, Ontario, 32 p.

Brown, G.C.

1981: Space and time in granite plutonism; Royal Society of London, Philosophical Transactions, series A, v. 301, p. 321-336.

Brown, I.C.

1952: A nomenclature of igneous rocks; Transactions, Canadian Institute of Mining and Metallurgy, v. 55, p. 53-56.

Buchan, K.L. and Halls, H.C.

1990: Paleomagnetism of Proterozoic mafic dyke swarms of the Canadian Shield; *in* Mafic Dykes and Emplacement Mechanisms, (ed.) A.J. Parker, P.C. Rickwood, and D.H. Tucker; Publication no. 23, International Geological Correlation Program, Project 257, p. 209-230.

Burden, E. and Holloway, D.

1985: Palynology and age of the Scott Inlet inliers of Baffin Island (Northwest Territories); Canadian Journal of Earth Sciences, v. 22, p. 1542-1545.

Cameron, E.M.

1986: Regional geochemical reconnaissance, an introduction to the interpretation of data from central Baffin Island, District of Franklin; Geological Survey of Canada, Paper 86-10, 22 p.

Cameron, E.M. and Garrels, R.M.

1980: Geochemical compositions of some Precambrian shales from the Canadian Shield; Chemical Geology, v. 28, p. 181-197.

Campbell, F.H.A.

1973: Sedimentary rocks of the Prince Albert Group, District of Keewatin; *in* Report of Activities, Part A, April to October, 1972; Geological Survey of Canada, Paper 73-1A, p. 141-142.

1974: Paragneisses of the Prince Albert Group; *in* Report of Activities, Part A, April to October, 1973; Geological Survey of Canada, Paper 74-1A, p. 159-160.

Card, K.D., Poulsen, K.H., and Robert, R.

1989: The Archean Superior Province of the Canadian Shield and its lode gold deposits; Eonomic Geology, Monograph 6, p. 19-36.

Carmichael, D.M., Helmstaedt, H.H., and Thomas, N.

1987: A field trip in the Frontenac Arch with emphasis on stratigraphy, structure and metamorphism; Department of Geological Sciences, Queen's University, Kingston, Ontario, 24 p.

Cavanaugh, M.D. and Seyfert, C.K.

1977: Apparent polar wander paths and the joining of the Superior and Slave provinces during Proterozoic time; Geology, v. 5, p. 207-211.

Cerny, P.

1988: The Plex (Eskimo Hill) Pegmatites, Generator Lake, Baffin Island, N.W.T.; Canada Department of Indian and Northern Affairs, N.W.T., Geology Division, Progress Report on the Evaluation of the Rare-Metal Pegmatites in N.W.T., 9 p. plus figures and tables.

Chandler, F.W.

1988: Geology of the late Precambrian Fury and Hecla Group, northwest Baffin Island, District of Franklin; Geological Survey of Canada, Bulletin 370, 30 p., map at scale 1:125 000.

Chandler, F.W. and Stevens, R.D.

1981: Potassium-argon age of the late Proterozoic Fury and Hecla Formation, northwest Baffin Island, District of Franklin; *in* Current Research, Part A; Geological Survey of Canada, Paper 81-1A, p. 37-40.

Chandler, F.W., Charbonneau, B.W., Ciesielski, A., Maurice, Y.T., and White, S.

1980: Geological studies of the late Precambrian supracrustal rocks and underlying granitic basement, Fury and Hecla Strait area, Baffin Island, District of Franklin; *in* Current Research, Part A; Geological Survey of Canada, Paper 80-1A, p. 125-132.

Chappell, B.W.

1978: Granitoids from the Moonbi district, New England Batholith, Eastern Australia; Journal of the Geological Society of Australia, v. 25, p. 267-283.

Chernis, P.J.

1976: Stratigraphy, structure and metamorphism of the Piling Group at Dewar Lakes, Baffin Island, N.W.T.; BSc. thesis, Carleton University, Ottawa, Ontario, 64 p.

Christie, K.W. and Fahrig, W.F.

1983: Paleomagnetism of the Borden dykes of Baffin Island and its bearing on the Grenville Loop; Canadian Journal of Earth Sciences, v. 20, p. 275-289.

Church, M.

1972: Baffin Island sandurs: a study of arctic fluvial processes; Geological Survey of Canada, Bulletin 216, 208 p.

Ciesielski, A.

1983: Description et notes sur la pétrologie des granites de la région du détroit de Fury et Hecla, nord-ouest de l'île Baffin; *in* Current Research, Part A; Geological Survey of Canada, Paper 83-1A, p. 89-101.

Ciesielski, A. and Maley, J.

1980: Basement of Agu Bay area and Gifford River area, Baffin Island, Northwest Territories; Geological Survey of Canada, Open File 687.

Clayton, R.H. and Thorpe, L.

1982: Geology of the Nanisivik zinc-lead deposits; *in* Precambrian Sulphide Deposits, (ed.) R.W. Hutchinson, C.D. Spence, and J.M. Franklin; Geological Association of Canada, Special Paper 25, p. 729-758.

Clemmey, H. and Badham, N.

1982: Oxygen in the Precambrian atmosphere: an evaluation of geological evidence; Geology, v. 10, p. 141-146.

Coleman, R.G. and Donato, M.M.

1979: Oceanic plagiogranite revisited; *in* Developments in Petrology, Elsevier Scientific Publishing Company, New York, no. 6, chapter 5, *in* Trondhjemites, Dacites, and Related Rocks, (ed.) F. Baker; p. 149-165.

Collins, W.J., Beams, S.D., White, A.J.R., and Chappell, B.W.

1982: Nature and origin of A-type granites with particular reference to southeastern Australia; Contributions to Mineralogy and Petrology, v. 80, p. 189-200.

Cominco Limited

1977: Baffin recce, Baffin Island, N.W.T. – 1976; assessment report by R.C. Armstrong, 45 p., maps at 1:50 000 scale.

1981: Baffin recce, Au/base metals; assessment report by R.N. Randall, 18 p., map at 1:250 000 scale.

Condie, K.C.

1985: Secular variation in the composition of basalts: an index to mantle evolution; Journal of Petrology, v. 26, p. 545-563.

Cortemiglia, G.C., Messiga, B., and Terranova, R.

1985: Caratteri geologici epetrografici dell area del Summit Lake nell'Isola Baffin (Arcipelago Artico Canadese); Bolletina Societa Geologica Italiana, v. 104, p. 123-142.

Crawford, W.J.P.

1973: Metamorphic iron formations of Eqe Bay and adjacent parts of northern Baffin Island; PhD. thesis, University of Washington, Seattle, Washington, 101 p.

Crocket, J.H. and Bowins, R.J.

1985: Grant 132, Rare earth element properties of Archean iron formations and their host rocks – some results from the Temagami and Boston iron formations; *in* Geoscience Research Grant Program, Summary of Research, 1984-1985, (ed.) V.G. Milne; Ontario Geological Survey, Miscellaneous Paper 127, p. 10-14.

Daniels, J.L.

1956: The metamorphic petrology of the Precambrian rocks of northern Baffin Island; PhD. thesis, Manchester University, Manchester, England, 143 p.

Dawes, P.R.

1976: Precambrian to Tertiary of northern Greenland; *in* Geology of Greenland, (ed.) A. Escher and W.S. Watt; Geological Survey of Greenland, p. 248-303.

Dawes, P.R. and Frisch, T.

1981: Geological reconnaissance of the Greenland Shield in Melville Bugt, northwest Greenland; Grønlands Geologiske Undersøgelse, Rapp. 105, p. 18-25.

Dawes, P.R., Larsen, O., and Kalsbeek, F.

1988: Archean and Proterozoic crust in North-West Greenland: evidence from Rb-Sr whole-rock age determinations; Canadian Journal of Earth Sciences, v. 25, p. 1365-1373.

de Kemp, E.A. and Scott, D.J.

1998: Geoscience compilation of northern Baffin Island and Northern Melville Peninsula, Northwest Territories; Geological Survey of Canada, Open File D3636, two CD-ROMs, vol. 1 and 2.

Derry, L.A. and Jacobsen, S.B.

1990: The chemical evolution of Precambrian seawater: evidence from REEs in banded iron formations; Geochimica et Cosmochimica Acta, v. 54, p. 2965-2977.

Dewey, J.F. and Burke, K.C.A.

1973: Tibetan, Varisian, and Precambrian basement reactivation: products of continental collision; Journal of Geology, v. 81, p. 683-692.

Dick, H.J.B. and Fisher, R.L.

1984: Mineralogic studies of the residues of mantle melting: abyssal and alpine-type peridotites; *in* Kimberlites II, The Mantle and Crust-Mantle Relationships, (ed.) J. Kornprobst; Elsevier Science Publications, New York, p. 295-308.

Dimroth, E.

1975: Paleo-environment of iron-rich sedimentary rocks; Geologische Rundschau, v. 64, p. 751-767.

1977: Facies Models 6: Diagenetic facies of iron formation; Geoscience Canada, v. 4, p. 83-88.

Dimroth, E. and Kimberley, M.M.

1976: Precambrian atmospheric oxygen: evidence in the sedimentary distributions of carbon, sulfur, uranium and iron; Canadian Journal of Earth Sciences, v. 13, p. 1161-1185.

Dimroth, E., Baragar, W.R.A., Bergeron, R., and Jackson, G.D.

1970: The filling of the Circum-Ungrava geosyncline; *in* Symposium on Basins and Geosynclines of the Canadian Shield, (ed.) A.J. Baer; Geological Survey of Canada, Paper 70-40, p. 45-142.

Douglas, R.J.W.

1980: Proposals for time classification and correlation of Precambrian rocks and events in Canada and adjacent areas of the Canadian Shield, part 2: a provisional standard for correlating Precambrian rocks; Geological Survey of Canada, Paper 80-24, 19 p.

Dredge, L.A., Dyke, A.S., Hodgson, D.A., Hooper, M.J.G., and Klassen, R.A.

1998: Surficial geology compilation, northern Baffin Island and northern Melville Peninsula, Northwest Territories; Geological Survey of Canada, Open File 3634, two coloured map sheets, scale 1:500 000.

Dudás, F.O., LeCheminant, A.N., and Sullivan, R.W.

1991: Reconnaissance Nd isotopic study of granitoid rocks from the Baker Lake region, District of Keewatin, N.W.T., and observations on analytical procedures; *in* Radiogenic Age and Isotopic Studies: Report 4, Geological Survey of Canada, Paper 90-2, p. 101-112.

Dyke, A.S.

1974: Deglacial chronology and uplift history: northeastern sector, Laurentide ice sheet; University of Colorado, Institute of Arctic and Alpine Research, Occasional Paper No. 12, 73 p.

Dyke, A.S., Dredge, L.A., and Vincent, J-S.

1982: Configuration and dynamics of the Laurentide ice sheet during the late Wisconsin maximum; Géographie physique et Quaternaire, v. 36, p. 5-14.

Eade, K.E.

1953: The petrology of the gneisses of the Clyde area, Baffin Island; PhD. thesis, McGill University, Montreal, Quebec, 175 p.

El Bouseily, A.M. and El Sokkary, A.A.

1975: The relations between Rb, Ba and Sr in granitic rocks; Chemical Geology, v. 16, p. 207-219.

Ellis, D.J.

1980: Osumilite-sapphirine-quartz granulites from Enderby Land Antartica. P-T conditions of metamorphism, implications for garnet-cordierite equilibria and the evolution of the deep crust; Contributions to Mineralogy and Petrology, v. 74, p. 201-210.

England, P. and Houseman, G.

1989: Extension during continental convergence, with application to the Tibetan Plateau; Journal of Geophysical Research, v. 94, no. B12, p. 17561-17579.

Ermanovics, I. and Van Kranendonk, M.

1998: Geology of the Archean Nain Province and Paleoproterozoic Torngat Orogen in a Transect of the North River-Nutak map areas, Newfoundland (Labrador) and Quebec; Geological Survey of Canada, Bulletin 497,156 p.

Ermanovics, I.F, Van Kranendonk, M., Corriveau, L., Mengel, F., Bridgwater, D., and Sherlock, R.

1989: The Boundary Zone of the Nain-Churchill provinces in the North River-Nutak map areas, Labrador; *in* Current Research, Part C; Geological Survey of Canada, Paper 89-1C, p. 385-394.

Escher, A.

1971: Geological map of Greenland, Sondre Strømfjord-Nûgssuaq; Grønlands Geologiske Undersøgelse, map at 1:500 000 scale.

Escher, J.C.

1984: Tasiussaq, 73 V.1 SYD, Geologisk Kort Over Grønland; Geological Survey of Greenland, map at 1:100 000 scale.

1985a: Ussing Isfjord, 73 V.1 Nord, Geologisk Kort Over Grønland; Geological Survey of Greenland, map at 1:100 000 scale.

1985b: Kuvdlorssuaq, 74 V.1 Nord/Syd, Geologisk Kort Over Grønland; Geological Survey of Greenland.

1985c: Upernavik Isfjord, Geological Map of Greenland, Sheet 4; Geological Survey of Greenland, map at 1:500 000 scale.

Ewers, G.R. and Scott, P.A.

1977: Geochemistry of the Cullen granite, Northern Territory; Bureau of Mineral Research, Journal of Australian Geology and Geophysics, v. 2, p. 165-176.

Fahrig, W.F.

1987: The tectonic setting of continental mafic dyke swarms: failed arm and early passive margin; *in* Mafic Dyke Swarms, (ed.) H.C. Halls and W.F. Fahrig; Geological Association of Canada, Special Paper 34, p. 331-348.

Fahrig, W.F. and Schwarz, E.J.

1973: Additional paleomagnetic data on the Baffin diabase dykes and a revised Franklin pole; Canadian Journal of Earth Sciences, v. 10, p. 576-581.

Fahrig, W.F. and West, T.D.

1986: Diabase dyke swarms of the Canadian Shield; Geological Survey of Canada, Map 1627A at approximately 1:4 873 900 scale.

Fahrig, W.F., Christie, K.W., and Jones, D.L.

1981: Paleomagnetism of the Bylot basins: evidence for Mackenzie continental tensional tectonics; *in* Proterozoic Basins of Canada, (ed.) F.H.A. Campbell; Geological Survey of Canada, Paper 81-10, p. 302-312.

Fahrig, W.F., Irving, E., and Jackson, G.D.

1971: Paleomagnetism of the Franklin diabases; Canadian Journal of Earth Sciences, v. 8, no. 4, p. 455-467.

1973: Test of nature and extent of continental drift as provided by study of Proterozoic dike swarms of Canadian Shield; American Association of Petroleum Geologists, Arctic Geology, Memoir 19, p. 583-586.

Falconer, G.

1962: Glaciers of northern Baffin and Bylot islands, N.W.T.; Canada Geographical Branch, Geographical Paper no. 33, 31 p., plus photos.

1966: Preservation of vegetation and patterned ground under a thin ice body in northern Baffin Island, N.W.T.; Canada Geographical Branch, Geographical Bulletin, v. 8, p. 194-200.

Falconer, G., Ives, J.D., Løken, O.H., and Andrews, J.T.

1965: Major end moraines in eastern and central Arctic Canada; Canada Geographical Branch, Geographical Bulletin, v. 7, p. 137-153.

Feyling-Hanssen, R.W.

1976: The stratigraphy of the Quaternary Clyde Foreland Formation, Baffin Island, illustrated by the distribution of benthic foraminifera; Boreas, v. 5, p. 57-94.

Floran, R.J. and Papike, J.J.

1978: Mineralogy and Petrology of the Gunflint Iron Formation, Minnesota-Ontario: correlation of compositional and assemblage variations at low to moderate grade; Journal of Petrology, v. 19, pt. 2, p. 215-288.

Forester, R.W. and Gray, N.

1967: Geological studies on Baffin Island, 1966; *in* Field Report, North-Central Baffin Island, 1966, (ed.) O.H. Løken; Canada Geographical Branch, p. 93-96.

Fraser, J.A., Heywood, W.W., and Mazurski, M.

1978: Metamorphic map of the Canadian Shield; Geological Survey of Canada, Map 1475A, scale 1:3 500 000.

Frisch, T.

1982: Precambrian geology of the Prince Albert Hills, western Melville Peninsula, Northwest Territories; Geological Survey of Canada, Bulletin 346, 70 p., coloured map at 1:250 000 scale.

1988: Reconnaissance geology of the Precambrian Shield of Ellesmere, Devon and Coburg islands, Canadian Arctic Archipelago; Geological Survey of Canada, Memoir 409, 102 p., 3 coloured maps at 1:250 000 scale.

Frisch, T. and Dawes, P.R.

1982: The Precambrian Shield of northernmost Baffin Bay; correlation across Nares Strait; *in* Nares Strait and the Drift of Greenland: A Conflict in Plate Tectonics, (ed.) P.R. Dawes and J.W. Kerr; Meddelelser om Grønland, v. 8, p. 79-88.

Frisch, T. and Hunt, P.A.

1988: U-Pb zircon and monazite ages from the Precambrian Shield of Ellesmere and Devon islands, Arctic Archipelago; *in* Radiogenic Age and Isotopic Studies: Report 2; Geological Survey of Canada, Paper 88-2, p. 117-125.

1993: Reconnaissance U-Pb geochronology of the crystalline core of the Boothia Uplift, District of Franklin, Northwest Territories; *in* Radiogenic Age and Isotopic Studies: Report 7; Geological Survey of Canada, Paper 93-2, p. 3-22.

Frisch, T. and Parrish, R.R.

1992: U-Pb zircon ages from the Chantrey Inlet area, northern District of Keewatin, Northwest Territories; *in* Radiogenic Age and Isotopic Studies: Report 5; Geological Survey of Canada, Paper 91-2, p. 35-41.

Frisch, T. and Sandeman, H.A.I.

1991: Reconnaissance geology of the Precambrian Shield of the Boothia Uplift, northwestern Somerset Island and eastern Prince of Wales Island, District of Franklin; *in* Current Research, Part C; Geological Survey of Canada, Paper 91-1C, p. 173-178.

Fryer, B.J.

1971a: Age and trace element compositions of Algoma-type iron-formations of the Canadian Shield; *in* Variations in Isotopic Abundances of Strontium, Calcium and Argon and Related Topics – Nineteenth Annual Progress Report for 1971; Department of Earth and Planetary Sciences, Massachusetts Institute of Technology, Cambridge, Massachusetts, p. 85-96.

1971b: Canadian Precambrian iron-formations; ages and trace element compositions; PhD. thesis, Massachusetts Institute of Technology, Cambridge, Massachusetts, 174 p.

Galley, A.G., Jackson, G.D., and Iannelli, T.R.

1983: Neohelikian subaerial basalts with ocean-floor type chemistry, northwestern Baffin Island; *in* Geological Association of Canada, Program with Abstracts, v. 8, p. A25.

Gauthier, M., Brown, A.C., and Morin, G.

1987: Small iron-formations as a guide to base- and precious-metal deposits in the Grenville Province of southern Quebec; *in* Precambrian Iron-formations, (ed.) P.W.U. Appel and G.L. LaBerge; Theophrastus Publications, S.A., Athens, p. 297-327.

Geldsetzer, H.

1973a: Syngenetic dolomitization and sulfide mineralization; *in* Ores in Sediments, (ed.) G.G. Amstutz and A.J. Bernard; Springer-Verlag, New York, p. 115-127.

Geldsetzer, H.

1973b: The tectono-sedimentary development of an algal-dominated Helikian succession on northern Baffin Island, N.W.T.; *in* Proceedings of the Symposium on the Geology of the Canadian Arctic, (ed.) J.D. Aitken and D.J. Glass; Canadian Society of Petroleum Geologists, Geological Association of Canada, p. 99-126.

Ghazban, F., Ford, D.C., and Schwarcz, H.P.

1986: Multistage dolomite formation at Nanisivik, NWT, Canada; Geological Society of America, Abstracts with Programs, 1986, p. 612.

Gibb, R.A. and Halliday, D.W.

1974: Gravity measurements in southern District of Keewatin and southeastern District of Mackenzie, N.W.T.; Earth Physics Branch, Ottawa, Gravity Map Series, no. 124-131.

Gibbins, W.A.

1982: DIAND-GNWT-COOP-Soapstone project Baffin Island 1981; Canada, Department of Indian Affairs and Northern Development, Geology Section, internal report, 7 p.

1987: Carving stone and Inuit carvings: unique northern Canadian resources; Canada, Department of Indian and Northern Affairs, Northwest Territories, Geology Division, internal report, 22 p.

Gilbert, R., Syvitski, J.P.M., and Taylor, R.B.

1985: Reconnaissance study of proglacial Stewart Lakes, Baffin Island, District of Franklin; *in* Current Research, Part A; Geological Survey of Canada, Paper 85-1A, p. 505-510.

Gole, M.J. and Klein, C.

1981: Banded iron-formations through much of Precambrian time; The Journal of Geology, v. 89, p. 169-183.

Goodwin, A.M.

1973: Archean iron-formations and tectonic basins of the Canadian Shield; Economic Geology, v. 68, p. 915-933.

Gordon, T.M.

1988: Precambrian geology of the Daly Bay area, District of Keewatin; Geological Survey of Canada, Memoir 422, 21 p., coloured map at 1:250 000 scale.

Grabau, A.W.

1904: On the classification of sedimentary rocks; American Geologist, v. 33, p. 228-247.

Graf, C.W.

1974: A trace metal analysis across the Arctic Bay-Society Cliffs formations contact, Borden Peninsula, Baffin Island, Northwest Territories; BSc. Thesis, University of British Columbia, Vancouver, British Columbia, 63 p.

Graf, J.L., Jr.

1978: Rare earth elements, iron formations and sea water; Geochimica et Cosmochimica Acta, v. 42, p. 1845-1850.

Grant, A.C., Levy, E.M., Lee, K., and Moffat, J.D.

1986: Pisces IV research submersible finds oil on Baffin Shelf; *in* Current Research, Part A; Geological Survey of Canada, Paper 86-1A, p. 65-69.

Gray, N.H.

1966: Geological studies in central Baffin Island – 1965; *in* Field Report, North-Central Baffin Island, (ed.) O.H. Løken; Canada Geographical Branch, p. 74-78.

Grocott, J.

1989: Structural constraints on Early Proterozoic assembly of NE Laurentia: evidence from Baffin Island and West Greenland; *in* Montréal 1989, Geological Association of Canada and Mineralogical Association of Canada, Program with Abstracts, v. 14, p. A10.

Grocott, J. and Pulvertaft, T.C.R.

1990: The early Proterozoic Rinkian belt of central West Greenland; *in* The Early Proterozoic Trans-Hudson Orogen of North America, (ed.) J.F. Lewry and M.R. Stauffer; Geological Association of Canada, Special Paper 37, p. 443-463.

Gross, G.A.

1965: Geology of iron-deposits in Canada; *in* Volume I, General Geology and Evaluation of Iron Deposits; Geological Survey of Canada, Economic Geology Report 22, 181 p.

1966: The origin of high grade iron deposits on Baffin Island, Northwest Territories; Canadian Mining Journal, v. 87, p. 111-114.

1973: The depositional environment of principal types of Precambrian iron-formations; *in* Genesis of Precambrian Iron and Manganese Deposits, Proceedings of the Kiev Symposium, 1970; UNESCO, Earth Sciences, v. 9, p. 15-21.

1980: A classification of iron formations based on depositional environments; Canadian Mineralogist, v. 18, p. 215-222.

1983: Tectonic systems and the deposition of iron-formation; Precambrian Research, v. 20, p. 171-187.

1986: The metallogenetic significance of iron-formation and related stratafer rocks; Journal Geological Society of India, v. 28, no. 2 and 3, p. 92-108.

1987: Mineral deposits on the deep seabed; Marine Mining, v. 6, p. 109-119.

1991: Genetic concepts for iron-formation and associated metalliferous sediments; *in* Mineral Deposits: Historical Perspectives of Genetic Concepts and Case Histories of Famous Discoveries, (ed.) R.W. Hutchinson and R.I. Grauch; Society of Economic Geologists, Mongraph 8, p. 51-81.

Gross, G.A. and McLeod, C.R.

1980: A preliminary assessment of the chemical composition of iron formations in Canada; Canadian Mineralogist, v. 18, p. 223-229.

1987: Metallic minerals on the deep seabed; Geological Survey of Canada, Paper 86-21 and Map 1659A, 65 p.

Gross, G.A. and Yeo, G.M.

1987: Iron formations: hydrolithic stratafer sediments; Geological Survey of Canada, internal report, 14 p., 1 diagram.

Grotzinger, J.P.

1986: Cyclicity and paleoenvironmental dynamics, Rocknest platform, northwest Canada; Geological Society of America Bulletin, v. 97, p. 1208-1231.

Guimond, R.

1963: Exciting iron ore discovery on Baffin Island; Precambrian, January, p. 6-8.

Hanmer, S., St-Onge, M.R., and Scott, D.J.

1996: Structural geology of the Meta Incognita thrust belt, south Baffin Island, Northwest Territories; *in* Current Research 1996-C; Geological Survey of Canada, p. 73-81.

Hanmer, S.K.

1987: Granulite facies mylonites: a brief structural reconnaissance north of Stony Rapids, northern Saskatchewan; *in* Current Research, Part A; Geological Survey of Canada, Paper 87-1A, p. 563-572.

Harvey, M.A.

1983: A geochemical and Rb-Sr study of the Proterozoic augen orthogneiss on the Molde Peninsula, west Norway; Lithos, v. 16, p. 325-338.

Haselton, H.T. Jr., Hovis, G.L., Hemingway, B.S., and Robie, R.A.

1983: Calorimetric investigation of the excess entropy of mixing in albite-sanidine solid solutions; lack of evidence for Na, K short range order and implications for two-feldspar thermometry; American Mineralogist, v. 68, p. 398-413.

Heaman, L.M., LeCheminant, A.N., and Rainbird, R.H.

1990: A U-Pb baddeleyite study of Franklin igneous events; Geological Association of Canada and Mineralogical Association of Canada, Program with Abstracts, v. 15, p. A55.

Hegner, E. and Jackson, G.D.

1990: Nd isotopic constraints on Late Archean and Early Proterozoic crust formation in Baffin and Ellesmere islands, northern Labrador and Ungava Peninsula, eastern Canada; *in* Abstracts for the American Geophysical Union fall meeting, December 3-7, 1990. EOS, Transactions American Geophysical Union, v. 71, p. 1689.

Henderson, G. and Pulvertaft, T.C.R.

1987: Geological Map of Greenland, 1:100 000, Marmorilik, 71 V. 2 Syd, Pangnertôq, 72 V. 2 Syd; Grønlands Geologiske Undersøgelse, 72 p.

Henderson, J.B. and van Breemen, O.

1992: U-Pb zircon ages from an Archean orthogneiss and a Proterozoic metasedimentary gneiss of the Thelon Tectonic Zone, District of Mackenzie, Northwest Territories; *in* Radiogenic Age and Isotopic Studies: Report 5; Geological Survey of Canada, Paper 91-2, p. 25-33.

Henderson, J.R.

1982: Geology of the Foxe Fold Belt in the Home Bay area (27SE and SW), Baffin Island, N.W.T.; Geological Survey of Canada, Open File 849, four 1:250 000 scale geological maps.

1983: Structure and metamorphism of the Aphebian Penrhyn Group and its Archean basement complex in the Lyon Inlet area, Melville Peninsula, District of Franklin; Geological Survey of Canada, Bulletin 324, 50 p., coloured map at 1:100 000 scale.

1985a: McBeth Fiord-Cape Henry Kater, District of Franklin, Northwest Territories; Geological Survey of Canada, Map 1605A, coloured, scale 1:250 000.

1985b: Ekalugad Fiord-Home Bay, District of Franklin, Northwest Territories; Geological Survey of Canada, Map 1606A, coloured, scale 1:250 000.

Henderson, J.R. and Henderson, M.N.

1994: Geology of the Dewar Lakes area, central Baffin Island, District of Franklin, N.W.T. (parts of 27B and 37A), Geological Survey of Canada, Open File 2924, scale 1:100 000.

Henderson, J.R. and Loveridge, W.D.

1981: Age and geological significance of a tonalite pegmatite from east-central Baffin Island; *in* Rb-Sr and U-Pb isotopic age studies, Report 4, *in* Current Research, Part C; Geological Survey of Canada, Paper 81-1C, p. 135-137.

Henderson, J.R. and Tippett, C.R.

1980: Foxe Fold Belt in western Baffin Island, District of Franklin; *in* Current Research, Part A; Geological Survey of Canada, Paper 80-1A, p. 147-152.

Henderson, J.R., Grocott, J., Henderson, M.N., Falardeau, F., and Heijke, P.

1988: Results of fieldwork in Foxe Fold belt near Dewar Lakes, Baffin Island, N.W.T.; *in* Current Research, Part C; Geological Survey of Canada, Paper 88-1C, p. 101-108.

Henderson, J.R., Grocott, J., Henderson, M.N., and Perrault, S.

1989: Tectonic history of the Lower Proterozoic Foxe-Rinkian Belt in central Baffin Island, N.W.T.; *in* Current Research, Part C; Geological Survey of Canada, Paper 89-1C, p. 185-197.

Henderson, J.R., LeCheminant, A.N., Jefferson, C.W., Coe, K., and Henderson, M.N.

1986: Preliminary account of the geology around Wager Bay, District of Keewatin; *in* Current Research, Part A; Geological Survey of Canada, Paper 86-1A, p. 159-176.

Henderson, J.R., Shaw, D., Mazurski, M., Henderson, M., Green, R., and Brisbin, D.

1979: Geology of part of Foxe Fold Belt, central Baffin Island, District of Franklin; *in* Current Research, Part A; Geological Survey of Canada, Paper 79-1A, p. 95-99.

Heywood, W.W.

1961: Geological notes, northern District of Keewatin, parts of 56, 57, 66 and 67; Geological Survey of Canada, Paper 61-18, 9 p., map at 1:506 880 scale.

1967: Geological notes, northeastern District of Keewatin and southern Melville Peninsula, District of Franklin, Northwest Territories (parts of 46, 47, 56, 57); Geological Survey of Canada, Paper 66-40, 20 p.

1974: Geological reconnaissance of northern Melville Peninsula; District of Franklin (parts of 47A,B,C,D); *in* Report of Activities, Part A, April to October 1973; Geological Survey of Canada, Paper 74-1, Pt. A, p. 134.

Heywood, W.W. and Sanford, B.V.

1976: Geology of Southampton, Coats and Mansel islands, District of Keewatin, Northwest Territories; Geological Survey of Canada, Memoir 382, 35 p.

Hodges, K.V. and Spear, F.S.

1982: Geothermometry, geobarometry, and the Al_2SiO_5 triple point at Mt. Moosilauke, New Hampshire; American Mineralogist, v. 67, p. 1118-1134.

Hodgson, D.A. and Haselton, G.M.

1974: Reconnaissance glacial geology, northeastern Baffin Island; Geological Survey of Canada, Paper 74-20, 10 p., with map 1395A at 1:500 000 scale.

Hoffman, P.F.

1987: Early Proterozoic foredeeps, foredeep magmatism, and Superior-type iron-formations of the Canadian Shield; *in* Proterozoic Lithospheric Evolution, (ed.) A. Kröner; Geodynamics Series of American Geophysical Union, v. 17, p. 85-98.

1988: United plates of America, the birth of a craton: Early Proterozoic assembly and growth of Laurentia; Annual Review of Earth and Planetary Science, v. 16, p. 543-603.

1989: Precambrian geology and tectonic history of North America; *in* The Geology of North America – An Overview, (ed.) A.W. Bally and A.R. Palmer; Geological Society of North America, Boulder, Colorado, v. A, p. 447-512.

1990a: Subdivision of the Churchill Province and extent of the Trans-Hudson Orogen; *in* The Early Proterozoic Trans-Hudson Orogen of North America, (ed.) J.F. Lewry and M.R. Stauffer; Geological Association of Canada, Special Paper 37, p. 15-39.

1990b: Dynamics of the tectonic assembly of northeast Laurentia in geon 18 (1.9-1.8 Ga); Geoscience Canada, v. 17, p. 222-226.

Hofmann, H.J. and Jackson, G.D.

1994: Shale-facies microfossils from the Proterozoic Bylot Supergroup, Baffin Island, Canada; Paleontological Society, Memoir 37 (Journal of Paleontology, v. 68, no. 4, supplement), 39 p.

Holdaway, M.J.

1971: Stability of andalusite and the aluminum silicate phase diagram; American Journal of Science, v. 271, p. 97-131.

Holland, H.D.

1973: The oceans: a possible source of iron in iron formations; Economic Geology, v. 68, p. 1169-1172.

Holm, N.G.

1987: Possible biological origin of banded iron-formations from hydrothermal solutions; *in* Origins of Life, (ed.) J.P. Ferris; v. 17, p. 229-250.

Hough, J.L.

1958: Fresh-water environment of deposition of Precambrian banded iron-formations; Economic Geology, v. 28, p. 414-430.

Houseman, G.A., McKenzie, D.P., and Molnar, P.

1981: Convective instability of a thickened boundary layer and its relevance for the thermal evolution of continental convergent belts; Journal of Geophysical Research, v. 86, no. B7, p. 6115-6132.

Hughes, C.J.

1972: Spilites, keratophyres, and the igneous spectrum; Geological Magazine, v. 109, p. 513-527.

Iannelli, T.R.

1979: Stratigraphy and depositional history of some upper Proterozoic sedimentary rocks in northwestern Baffin Island, District of Franklin; *in* Current Research, Part A; Geological Survey of Canada, Paper 79-1A, p. 45-56.

1992: Revised stratigraphy of the late Proterozoic Bylot Supergroup, northern Baffin Island, Arctic Canada: implications for the evolution of Borden Basin; PhD. thesis, University of Western Ontario, London, Ontario, 420 p.

Irvine, T.N. and Baragar, W.R.A.

1971: A guide to the chemical classification of the common volcanic rocks; Canadian Journal of Earth Sciences, v. 8, p. 523-548.

Ives, J.D.

1964: Deglaciation and land emergence in northeastern Foxe Basin, N.W.T.; Canada Geographical Branch, Geographical Bulletin, no. 21, p. 54-65.

Ives, J.D. and Andrews, J.T.

1963: Studies in the physical geography of north-central Baffin Island, N.W.T.; Canada Geographical Branch, Geographical Bulletin, no. 19, p. 5-48.

Ives, J.D. and Buckley, J.T.

1969: Glacial geomorphology of Remote Peninsula, Baffin Island, N.W.T., Canada; Arctic and Alpine Research, v. 1, p. 83-96.

Jackson, G.D.

1962: The geology of the Neal (Virot) Lake area, west of Wabush Lake, Labrador, with special reference to iron deposits; PhD. thesis, McGill University, Montreal, Quebec, 337 p.

1966a: North Baffin Island; *in* Report of Activities; Geological Survey of Canada, Paper 66-1, p. 14-15.

1966b: Geology and mineral possibilities of the Mary River region, northern Baffin Island; Canadian Mining Journal, v. 87, no. 6, p. 57-61.

1968: Operation Bylot, north-central Baffin Island (27, 37, 38, 48); *in* Report of Activities, Part A; Geological Survey of Canada, Paper 68-1, pt. A, p. 144-145.

1969: Reconnaissance of north-central Baffin Island; *in* Report of Activities, Part A; Geological Survey of Canada, Paper 69-1, pt. A, p. 171-176.

1971: Operation Penny Highlands, south-central Baffin Island; *in* Report of Activities, Part A; Geological Survey of Canada, Paper 71-1, pt. A, p. 138-140.

1978a: McBeth Gneiss Dome and associated Piling Group, central Baffin Island, District of Franklin; *in* Rubidium-Strontium Isotopic Age Studies, Report 2, (ed.) R.K. Wanless and W.D. Loveridge; Geological Survey of Canada, Paper 77-14, p. 14-17.

1978b: Basement gneisses and the Mary River Group, No. 4 Deposit area, northwest Baffin Island, District of Franklin; *in* Rubidium-Strontium Isotopic Age Studies, Report 2, (ed.) R.K. Wanless and W.D. Loveridge; Geological Survey of Canada, Paper 77-14, p. 18-24.

1984: Geology, Clyde River, District of Franklin, Northwest Territories; Geological Survey of Canada, Map 1582A, with expanded legend and brief marginal notes, scale 1:250 000.

1986: Notes on Proterozoic Thule Group, northern Baffin Bay; *in* Current Research, Part A; Geological Survey of Canada, Paper 86-1A, p. 541-552.

Jackson, G.D. and Cumming, L.M.

1981: Evaporites and folding in the Neohelikian Society Cliffs Formation, northeastern Bylot Island, Arctic Canada; *in* Current Research, Part C; Geological Survey of Canada, Paper 81-1C, p. 35-44.

Jackson, G.D. and Davidson, A.

1975: Geology of the Bylot Island map-area; Geological Survey of Canada, Paper 74-29, 12 p., and Map 1397A, coloured, with expanded legend, scale 1:250 000.

Jackson, G.D. and Hegner, E.
1991: Evolution of Late Archean to Early Proterozoic crust based on Nd isotopic data for Baffin Island and northern Quebec and Labrador; in Toronto 1991, Program with Abstracts; Geological Association of Canada, v. 16, p. A59.

Jackson, G.D. and Iannelli, T.R.
1981: Rift-related cyclic sedimentation in the Neohelikian Borden Basin, northern Baffin Island; *in* Proterozoic Basins of Canada, (ed.) F.H.A. Campbell; Geological Survey of Canada, Paper 81-10, p. 269-302.
1984: Borden Basin, N.W. Baffin Island: mid-Proterozoic rifting and possible ocean opening; *in* Geological Association of Canada, Program with Abstracts, v. 9, London, p. 76.
1989: Neohelikian reef complexes; *in* Reefs, Canada and Adjacent Areas; (ed.) H.H.J. Geldsetzer, N.P. James, and G.E. Tebbutt; Canadian Society of Petroleum Geologists, Memoir 13, p. 55-63.

Jackson, G.D. and Morgan, W.C.
1978a: Precambrian metamorphism on Baffin and Bylot islands; *in* Metamorphism in the Canadian Shield, (ed.) J.A. Fraser and W.W. Heywood; Geological Survey of Canada, Paper 78-10, p. 249-267.
1978b: Geology, Conn Lake, District of Franklin; Geological Survey of Canada, Map 1458A, coloured, with expanded legend, scale 1:250 000.

Jackson, G.D. and Sangster, D.F.
1987: Geology and resource potential of a proposed national park, Bylot Island and northwest Baffin Island, Northwest Territories; Geological Survey of Canada, Paper 87-17, 31 p., and map at 1:250 000 scale.

Jackson, G.D. and Taylor, F.C.
1972: Correlation of major Aphebian rock units in the northeastern Canadian Shield; Canadian Journal of Earth Sciences, v. 9, p. 1650-1669.

Jackson, G.D., Davidson, A., and Morgan, W.C.
1975: Geology of the Pond Inlet map-area, Baffin Island, District of Franklin; Geological Survey of Canada, Paper 74-25, 33 p., and Map 1396A, coloured, with expanded legend, scale 1:250 000.

Jackson, G.D., Frisch, T., Hegner, E., and Hunt, P.A.
1990a: U-Pb geochronology, Nd model ages and tectonics of the eastern Arctic Canadian Shield; *in* Forum 1990, Program with Abstracts; Geological Survey of Canada, p. 12.

Jackson, G.D., Hunt, P.A., Loveridge, W.D., and Parrish, R.R.
1990b: Reconnaissance geochronology of Baffin Island, N.W.T.; *in* Radiogenic Age and Isotopic Studies: Report 3; Geological Survey of Canada, Paper 89-2, p. 123-148.

Jackson, G.D., Iannelli, T.R., Knight, R.D., and Lebel, D.
1985: Neohelikian Bylot Supergroup of Borden Rift Basin, northwestern Baffin Island, District of Franklin; *in* Current Research, Part A; Geological Survey of Canada, Paper 85-1A, p. 639-649.

Jackson, G.D., Iannelli, T.R., Narbonne, G.M., and Wallace, P.J.
1978a: Upper Proterozoic sedimentary and volcanic rocks of northwestern Baffin Island; Geological Survey of Canada, Paper 78-14, 15 p.

Jackson, G.D., Iannelli, T.R., and Tilley, B.J.
1980: Rift-related late Proterozoic sedimentation and volcanism of northern Baffin and Bylot islands, District of Franklin; *in* Current Research, Part A; Geological Survey of Canada, Paper 80-1A, p. 319-328.

Jackson, G.D., Morgan, W.C., and Davidson, A.
1978b: Geology, Icebound Lake, District of Franklin; Geological Survey of Canada, Map 1451A, coloured, with expanded legend, scale 1:250 000.
1978c: Geology, Buchan Gulf-Scott Inlet, District of Franklin; Geological Survey of Canada, Map 1449A, coloured, with expanded legend, scale 1:250 000.
1978d: Geology, Steensby Inlet, District of Franklin; Geological Survey of Canada, Map 1450A, coloured, with expanded legend, scale 1:250 000.

Jackson, H.R., Keen, C.E., and Barrett, D.L.
1977: Geophysical studies on the eastern continental margin of Baffin Bay and in Lancaster Sound; Canadian Journal of Earth Sciences, v. 14, p. 1991-2001.

James, D.T., Connelly, J.N., Wasteneys, H.A., and Kilfoil, G.J.
1996: Paleoproterozoic lithotectonic divisions of the southeastern Churchill Province, western Labrador; Canadian Journal of Earth Sciences, v. 33, p. 216-230.

James, H.L.
1954: Sedimentary facies in iron-formation; Economic Geology, v. 49, p. 235-293.

James, H.L. and Sims, P.K. (ed.)
1973: Precambrian iron-formation of the world; Economic Geology, v. 68, p. 913-1173.

James, H.L. and Trendall, A.F.
1982: Banded iron formation: distribution in time and paleoenvironmental significance; *in* Mineral Deposits and the Evolution of the Biosphere, (ed.) H.D. Holland and M. Schidlowski; Springer-Verlag, Berlin, p. 199-218.

James, N.P.
1984: Shallowing-upward sequences in carbonates; *in* Facies Models, second edition, (ed.) R.G. Walker; Geoscience Canada, Reprint Series 1, Geological Association of Canada, p. 213-228.

Jaques, A.L., Chappell, B.W., and Taylor, S.R.
1983: Geochemistry of cumulus peridotites and gabbros from the Marum ophiolite complex, northern Papua, New Guinea; Contributions to Mineralogy and Petrology, v. 82, p. 154-164.

Jensen, I.S.
1985: Geochemistry of the central granitic stock in the Glitrevann cauldron within the Oslo rift, Norway; Norsk Geologisk Tidsskrift, v. 65, p. 201-216.

Jensen, L.S.
1976: A new craton plot for classifying subalkalic volcanic rocks; Ontario Division of Mines, Miscellaneous Paper 1976, 22 p.

Johnson, W.M. and Maxwell, J.A.
1981: Whole rock and mineral analysis; John Wiley and Sons, New York, second edition, 489 p.

Kalsbeek, F.
1986: The tectonic framework of the Precambrian shield of Greenland; a review of new isotopic evidence; *in* Developments in Greenland Geology, (ed.) F. Kalsbeek and W.S. Watt; Grønlands Geologiske Undersøgelse, Rapp. no. 128, p. 55-64.

Kalsbeek, F. and Nutman, A.P.
1996: Anatomy of the Early Proterozoic Nagssugtoqidian orogen, West Greenland, explored by reconnaissance SHRIMP U-Pb zircon dating; Geology, v. 24, no. 6, p. 515-518.

Kalsbeek, F., Pidgeon, R.T., and Taylor, P.N.
1987: Nagssugtoqidian mobile belt of West Greenland: a cryptic 1850 Ma suture between two Archaean continents – chemical and isotopic evidence; Earth and Planetary Science Letters, v. 85, p. 365-385.

Keen, C.E., Barrett, D.L., Manchester, K.S., and Ross, D.I.
1972: Geophysical studies in Baffin Bay and some tectonic implications; Canadian Journal of Earth Sciences, v. 9, p. 239-256.

Keen, C.E., Keen, M.J., Ross, D.I., and Lack, M.
1974: Baffin Bay: a small ocean basin formed by seafloor spreading; American Association of Petroleum Geologists Bulletin, v. 56, p. 1080-1108.

Kimberley, M.M.
1974: Origin of iron-formation by diagenetic replacement of calcareous oolite; Nature, v. 250, p. 319-320.
1989: Exhalative origins of iron formations; *in* Ore Geology Reviews, Elsevier, Amsterdam, v. 5, p. 13-145.

King, H.F.
1969: Geological significance of stratiform ore deposits; *in* Sedimentary Ores Ancient and Modern, (ed.) H.J. Clifford; Proceedings, 15th Inter-university Geological Congress, University of Leicester, Special Publication, Department of Geology of the University of Leicester, Leicester, England, p. 97-106.

Klein, C.
1983: Diagenesis and metamorphism in Precambrian banded iron formations; *in* Iron Formations: Facts and Problems, (ed.) A.F. Trendall and R.C. Morris; Elsevier, New York, p. 417-469.

Knight, R.D. and Jackson, G.D.
1994: Sedimentology and stratigraphy of the Mesoproterozoic Elwin Subgroup (Aqigilik and Sinasiuvik formations), uppermost Bylot Supergroup, Borden Rift Basin, northern Baffin Island; Geological Survey of Canada, Bulletin 455, 43 p.

Korstgaard, J., Ryan, B., and Wardle, R.
1987: The boundary between Proterozoic and Archean crustal blocks in central West Greenland and northern Labrador; *in* Evolution of the Lewisian and Comparable Precambrian High Grade Terrains, (ed.) R.G. Park and J. Tarney; Geological Society, Special Publication, no. 27, p. 247-259.

Korstgaard, J.A. (ed.)
1979: Nagssugtoqidian geology; Grønlands Geologiske Undersøgelse, Rapp. 89, 146 p.

Kovalenko, V.I.
1977: The geochemical trend in the evolution of alkali granite magmas; Geochemistry International, v. 14, no. 6, p. 1659-1672.

Kranck, E.H.
1951: Mineral possibilities of Baffin Island; Canadian Institute of Mining and Metallurgy, Transactions, v. 54, p. 438-439.
1953: Interpretation of gneiss structures with special reference to Baffin Island; Geological Association of Canada, Proceedings, v. 6, pt. 1, p. 54-68.
1955: The bedrock geology of Clyde area in northeastern Baffin Island; Acta Geographica, v. 14, p. 226-248.

Kranck, S.H.
1961: A study of phase equilibria in a metamorphic iron formation; Journal of Petrology, v. 2, pt. 2, p. 137-184.

Kukal, Z.
1990: The rate of geological processes; Earth Science Reviews, v. 28, no. 1, 2, and 3, 284 p.

Laajoki, D. and Lavikainen, S.
1977: Rare-earth elements in the Archean iron formation and associated schists in Ukkolanvaara, Ilomantsi, S.E. Finland; Bulletin of the Geological Society of Finland, v. 49, pt. 2, p. 105-123.

LaBerge, G.L.
1973: Possible biological origin of Precambrian iron formation; Economic Geology, v. 68, p. 1098-1109.

LaBerge, G.L., Robbins, E.L., and Han, T.-M.
1987: A model for the biological precipitation of Precambrian iron-formations – A: geological evidence; *in* Precambrian Iron Formations, (ed.) P.W.U. Appel and G.L. LaBerge; Theophrastus Publications, S.A., Athens, p. 69-96.

Leake, B.E.
1978: Nomenclature of amphiboles; Canadian Mineralogist, v. 16, p. 501-520.

LeCheminant, A.N. and Heaman, L.M.
1991: U-Pb ages for the 1.27 Ga Mackenzie igneous events, Canada: support for a plume initiation model; Geological Association of Canada, and Mineralogical Association of Canada, Program with Abstracts, v. 16, p. A73.

LeCheminant, A.N. and Roddick, J.C.
1991: U-Pb zircon evidence for widespread 2.6 Ga felsic magmatism in the central District of Keewatin, N.W.T.; *in* Radiogenic Age and Isotopic Studies: Report 4, Geological Survey of Canada, Paper 90-2, p. 91-99.

LeCheminant, A.N., Roddick, J.C., Tessier, A.C., and Bethune, K.M.
1987: Geology and U-Pb ages of early Proterozoic calc alkaline plutons northwest of Wager Bay, District of Keewatin; *in* Current Research, Part A; Geological Survey of Canada, Paper 87-1A, p. 773-782.

Leech, G.B., Lowdon, J.A., Stockwell, C.H., and Wanless, R.K.
1963: Age determinations and geological studies (including isotopic ages - Report 4); Geological Survey of Canada, Paper 63-17, p. 55, 56.

Lemon, R.R.H. and Blackadar, R.G.
1963: Admiralty Inlet area, Baffin Island, District of Franklin; Geological Survey of Canada, Memoir 328, 84 p.

Le Pichon, X., Sibnet, J.C., and Francheteau, J.
1977: The fit of the continents around the North Atlantic Ocean; Tectonophysics, v. 38, p. 169-209.

Lepp, H.
1987: Chemistry and origin of Precambrian iron-formations; *in* Precambrian Iron-Formations, (ed.) P.W.U. Appel and G.L. LaBerge; Theophrastus Publications, S.A., Athens, p. 3-30.

Levy, E.M.
1978: Visual and chemical evidence for a natural seep at Scott Inlet, Baffin Island, District of Franklin; *in* Current Research, Part B; Geological Survey of Canada, Paper 78-1B, p. 21-26.
1979: Further chemical evidence for natural seepage on the Baffin Island shelf; *in* Current Research, Part B; Geological Survey of Canada, Paper 79-1B, p. 379-383.

Levy, E.M. and MacLean, B.
1981: Natural hydrocarbon seepage at Scott Inlet and Buchan Gulf, Baffin Island shelf, 1980 update; *in* Current Research, Part A; Geological Survey of Canada, Paper 81-1A, p. 401-403.

Lewry, J.F. and Collerson, K.D.
1990: The Trans-Hudson Orogen: extent, subdivision, and problems; *in* The Early Proterozoic Trans-Hudson Orogen of North America, (ed.) J.F. Lewry and M.R. Stauffer; Geological Association of Canada, Special Paper 37, p. 1-14.

Lindsley, D.H.
1983: Pyroxene thermometry; American Mineralogist, v. 68, p. 477-493.

Løken, O.H.
1966: Baffin Island refugia older than 54 000 years; Science, v. 153, p. 1378-1380.
1967: Observations on the submarine geomorphology along part of the east coast of Baffin Island; *in* Field Report, North-central Baffin Island (for 1966); Canada Geographical Branch, p. 59-63.

Løken, O.H. and Hodgson, D.A.
1971: On the submarine geomorphology along the east coast of Baffin Island; Canadian Journal of Earth Sciences, v. 8, p. 185-195.

Loncarevic, B.D. and Falconer, R.K.H.
1977: An oil slick occurrence off Baffin Island; *in* Report of Activities, Part A; Geological Survey of Canada, Paper 77-1A, p. 523-524.

Loring, D.H.
1984: Trace-metal geochemistry of sediments from Baffin Bay; Canadian Journal of Earth Sciences, v. 21, p. 1368-1378.

Low, A.P.
1906: The Cruise of the Neptune, 1903-1904; Government Printing Bureau, Ottawa, 355 p.

Lowdon, J.A., Stockwell, C.H., Tipper, H.W., and Wanless, R.K.
1963: Age determinations and geological studies (including isotopic ages-report 3); Geological Survey of Canada, Paper 62-17, p. 31-32.

Lucas, S.B. and St-Onge, M.R.
1991: Evolution of Archean and early Proterozoic magmatic arcs in northeastern Ungava Peninsula, Quebec; *in* Current Research, Part C; Geological Survey of Canada, Paper 91-1C, p. 109-119.

Ludden, J.N. and Gélinas, L.
1982: Trace element characteristics of komatiites and komatiitic basalts from the Abitibi metavolcanic belt of Quebec; *in* Komatiites, (ed.) N.T. Arndt and E.G. Nisbet; George Allen and Unwin, London, p. 331-346.

MacGregor, A.M.
1927: Problem of Pre-Cambrian atmosphere; South Africa Journal of Science, v. 24, p. 155-172.

Machado, N., Goulet, N., and Gariépy, C.
1989: U-Pb geochronology of reactivated Archean basement and Hudsonian metamorphism in the northern Labrador Trough; Canadian Journal of Earth Sciences, v. 26, p. 1-15.

Machado, N., Perreault, S., and Hynes, A.
1988: Timing of continental collision in the northern Labrador Trough, Quebec: evidence from U-Pb geochronology; *in* Geological Association of Canada, Program with Abstracts, v. 13, p. 76.

MacLean, B.
1978: Marine geological-geophysical investigations in 1977 of the Scott Inlet and Cape Dyer-Frobisher Bay areas of the Baffin Island continental shelf; *in* Current Research, Part B; Geological Survey of Canada, Paper 78-1B, p. 13-20.

MacLean, B. (cont.)
1982: Investigations of Baffin Island shelf from surface ship and research submersible in 1981; *in* Current Research, Part A; Geological Survey of Canada, Paper 82-1A, p. 445-447.

MacLean, B. and Falconer, R.K.H.
1979: Geological/geophysical studies in Baffin Bay and Scott Inlet-Buchan Gulf and Cape Dyer-Cumberland Sound areas of the Baffin Island Shelf; *in* Current Research, Part B; Geological Survey of Canada, Paper 79-1B, p. 231-244.

MacLean, B. and Williams, G.L.
1983: Geological investigations of Baffin Island shelf in 1982; *in* Current Research, Part B; Geological Survey of Canada, Paper 83-1B, p. 309-315.

MacLean, B., Falconer, R.K., and Levey, E.M.
1981: Geological, geophysical and chemical evidence for natural seepage of petroleum off the northeast coast of Baffin Island; Canadian Petroleum Geology, v. 29, p. 75-79.

Markham, C.R.
1881: The voyages of William Baffin, 1612-1622; Hakluyt Society, London, 192 p.

Martignole, J. and Sisi, J.-C.
1981: Cordierite-garnet-H_2O equilibrium: a geological thermometer, barometer, and water fugacity indicator; Contributions to Mineralogy and Petrology, v. 77, p. 38-46.

Mathiassen, T.
1927: Archaeology of the Central Eskimos, I – Descriptive part, 327 p., II – The Thule culture and its position within the Eskimo culture; *in* Report of the Fifth Thule Expedition, 1921-1924; Gyldendalske Boghandel, Nordisk Forlag, Copenhagen, v. 4, no. 4, 208 p.
1933: Contributions to the geography of Baffin Land and Melville Peninsula; *in* Report of the Fifth Thule Expedition, 1921-1924; Gyldendalske Boghandel, Nordisk Forlag, Copenhagen, v. 1, no. 3, 102 p.

Maurice, Y.T.
1982: Uraniferous granites and associated mineralization in the Fury and Hecla Strait area, Baffin Island, N.W.T.; *in* Uranium in Granites, (ed.) Y.T. Maurice; Geological Survey of Canada, Paper 81-23, p. 101-113.

Maurice, Y.T. and Charbonneau, B.W.
1983: Recognition of uranium concentration processes in granites and related rocks using airborne radiometric measurements; *in* Current Research, Part A; Geological Survey of Canada, Paper 83-1A, p. 277-284.

Maxwell, J.B.
1981: Climatic regions of the Canadian Arctic Islands; Arctic, v. 34, p. 225-240.

McCulloch, M.T. and Wasserburg, G.J.
1978: Sm-Nd and Rb-Sr chronology of continental crust formation; Science, v. 200, p. 1003-1011.

McLaren, P.L. and McLaren, M.A.
1982: Waterfowl populations in eastern Lancaster Sound and western Baffin Bay; Arctic, v. 35, p. 149-157.

Mehnert, K.R.
1968: Migmatites and the Origin of Granitic Rocks; Elsevier Publishing Co., New York, 393 p.

Miall, A.D., Balkwill, H.R., and Hopkins, Jr., W.S.
1980: Cretaceous and Tertiary sediments of Eclipse Trough, Bylot Island area, Arctic Canada, and their regional setting; Geological Survey of Canada, Paper 79-23, 20 p.

Miller, G.H.
1976: Anomalous local glacier activity, Baffin Island, Canada: paleoclimatic implications; Geology, v. 4, p. 502-504.
1979: Radiocarbon date list IV, Baffin Island, N.W.T., Canada; INSTAAR Occasional Paper no. 29, University of Colorado, Boulder, Colorado, 61 p.

Miller, G.H., Andrews, J.T., and Short, S.K.
1977: The last interglacial-glacial cycle, Clyde Foreland, Baffin Island, N.W.T.: stratigraphy, biostratigraphy, and chronology; Canadian Journal of Earth Sciences, v. 14, p. 2824-2857.

Morgan, P. and Burke, K.
1985: General features, collisional plateaus; Tectonophysics, v. 119, p. 137-151.

Morgan, W.C.
1982: Geology, Koch Island, District of Franklin; Geological Survey of Canada, Map 1535A, coloured, scale 1:250 000, with expanded legend.

Morgan, W.C. (cont.)
1983: Geology, Lake Gillian, District of Franklin; Geological Survey of Canada, Map 1560A, coloured, scale 1:250 000, with expanded legend.

Morgan, W.C. and Taylor, F.C.
1972: Granulite facies metamorphosed basic dykes of the Torngat mountains, Labrador; Mineralogical Magazine, v. 38, p. 666-669.

Morgan, W.C., Bourne, J., Herd, R.K., Pickett, J.W., and Tippett, C.R.
1975: Geology of the Foxe Fold Belt, Baffin Island, District of Franklin; *in* Report of Activities, Part A; Geological Survey of Canada, Paper 75-1A, p. 343-347.

Morgan, W.C., Okulitch, A.V., and Thompson, P.H.
1976: Stratigraphy, structure, and metamorphism of the west half of the Foxe Fold Belt, Baffin Island; *in* Report of Activities, Part A; Geological Survey of Canada, Paper 76-1A, p. 387-391.

Mueller, R.F.
1960: Compositional characteristics and equilibrium relations in mineral assemblages of a metamorphosed iron formation; American Journal of Science, v. 258, no. 1, p. 449-497.

Myers, J.S.
1975a: Igneous stratigraphy of Archaean anorthosite at Majoraqap qâva, near Fiskenaesset, south-west Greenland; Grønlands Geologiske Undersøgelse, Rapp. 74, p. 3-27.
1975b: Pseudo-fractionation trend of the Fiskenaesset anorthosite complex, southern West Greenland; Grønlands Geologiske Undersøgelse, Rapp. 75, p. 77-80.

Naldrett, A.J. and Cabri, L.J.
1976: Ultramafic and related mafic rocks: their classification and genesis with special reference to the concentrations of nickel sulphides and platinum-group elements; Economic Geology, v. 71, p. 1131-1158.

Newton, R.C. and Haselton, H.T.
1981: Thermodynamics of the garnet-plagioclase-Al_2SiO_5-quartz geobarometer; *in* Thermodynamics of Minerals and Melts, (ed.) R.C. Newton; Springer Verlag, New York, p. 131-147.

Nutman, A.P.
1984: Precambrian gneisses and intrusive anorthosite of Smithson Bjerge, Thule district, North-West Greenland; Grønlands Geologiske Undersøgelse, Rapp. 119, 31 p., map at 1:50 000 scale.

Okulitch, A.V., Dawes, P.R., Higgins, A.K., Soper, N.J., and Christie, R.L.
1990: Towards a Nares Strait solution: structural studies on southeastern Ellesmere Island and Northwestern Greenland; Marine Geology, v. 93, p. 369-384.

Olson, R.A.
1970: King Resources Company exploration – 1970, White Bay area, Baffin Island, N.W.T.; company report by Trigg, Woollett and Associates Ltd., and Geowest Services Ltd., for King Resources Ltd.
1977: Geology and genesis of zinc-lead deposits within a late Precambrian dolomite, northern Baffin Island, N.W.T.; PhD. thesis, University of British Columbia, Vancouver, British Columbia, 371 p.
1984: Genesis of paleokarst and strata-bound zinc-lead sulphide deposits in a Proterozoic dolostone, northern Baffin Island, Canada; Economic Geology, v. 79, p. 1059-1103.

Palmer, H.C., Baragar, W.R.A., Fortier, M., and Foster, J.H.
1983: Paleomagnetism of Late Proterozoic rocks, Victoria Island, Northwest Territories, Canada; Canadian Journal of Earth Sciences, v. 20, p. 1456-1469.

Parrish, R.R.
1989: U-Pb geochronology of the Cape Smith Belt and Sugluk block, northern Quebec; Geoscience Canada, v. 16, p. 126-130.

Parry, W.E.
1821: Journal of a Voyage for the Discovery of a North-West Passage from the Atlantic to the Pacific, 1819-20; John Murray, London, 310 p.
1824: Journal of a second voyage for the discovery of a north-west passage from the Atlantic to the Pacific performed in the years 1821-22-23; *in* His Majesty's Ships Fury and Hecla, John Murray, London, 571 p.

Pearce, J.A.
1980: Geochemical evidence for the genesis and eruptive setting of lavas from Tethyan ophiolite; *in* Ophiolites, Proceedings of the International Ophiolite Symposium, Cyprus, 1979, (ed.) A. Panayiotou; Geological Survey Department, Cyprus, p. 261-272.

Pearce, J.A. and Cann, J.R.
1973: Tectonic setting of basic volcanic rocks determined using trace element analyses; Earth and Planetary Science Letters, v. 19, p. 290-300.

Pearce, J.A., Harris, N.B.W., and Tindle, A.G.
1984: Trace element discrimination diagrams for the tectonic interpretation of granitic rocks; Journal of Petrology, v. 25, p. 956-983.

Pehrsson, S.J. and Buchan, K.L.
1999: Borden dykes of Baffin Island, Northwest Territories: a Franklin U-Pb baddeleyite age and a paleomagnetic reinterpretation; Canadian Journal of Earth Sciences, v. 36, p. 65-73.

Perrault, S. and Hynes, A.
1990: Tectonic evolution of the Kuujjuaq terrane, New Quebec Orogen; Geoscience Canada, v. 17, p. 238-240.

Pettijohn, F.J.
1975: Sedimentary Rocks, third edition; Harper and Row, New York, 628 p.

Pidgeon, R.T. and Howie, R.A.
1975: U-Pb zircon age from a charnockitic granulite from Pangnirtung on the east coast of Baffin Island; Canadian Journal of Earth Sciences, v. 12, p. 1046-1047.

Pitcher, W.S.
1982: Granite type and tectonic environment; *in* Mountain Building Processes, (ed.) K.J. Hsü; Academic Press, London, chapter 1-3, p. 19-40.

Potter, P.E., Maynard, J.B., and Pryor, W.A.
1980: Sedimentology of Shale; Springer-Verlag, New York, 306 p.

Poulsen, C.
1946: Notes on Cambro-Ordovician fossils collected by the Oxford University Ellesmere Land expedition, 1934-35; Quarterly Journal of the Geological Society of London, v. 102, no. 407, p. 299-337.

Prest, V.K.
1970: Quaternary geology of Canada; *in* Geology and Economic Minerals of Canada, (ed.) R.J.W. Douglas; Geological Survey of Canada, Chapter 12, p. 676-764.

Prest, V.K., Grant, D.R., and Rampton, V.N.
1968: Glacial map of Canada; Geological Survey of Canada, Map 1253A, scale 1:5 000 000.

Pulvertaft, T.C.R.
1986: The development of thin thrust sheets and basement-cover sandwiches in the southern part of the Rinkian belt, Umanak district, west Greenland; *in* Developments in Greenland Geology, (ed.) F. Kalsbeek and W.S. Watt; Grønlands Geologiske Undersøgelse, Rapp. 128, p. 75-87.

Rainbird, R.H., Nesbitt, H.W., and Donaldson, J.A.
1990: Formation and diagenesis of a sub-Huronian saprolith: comparison with a modern weathering profile; The Journal of Geology, v. 98, p. 801-822.

Reeves, R., Michell, E., Mansfield, A., and McLaughlin, M.
1983: Distribution and migration of the bowhead whale, Balaena mysticetus, in the eastern North American Arctic; Arctic, v. 36, p. 5-64.

Reid, I. and Falconer, R.K.H.
1982: A seismicity study in northern Baffin Bay; Canadian Journal of Earth Sciences, v. 19, p. 1518-1531.

Reimer, T.O.
1987: Weathering as a source of iron in iron-formations: the significance of alumina-enriched paleosols from the Proterozoic of southern Africa; *in* Precambrian Iron-formations, (ed.) P.W.U. Appel and G.L. LaBerge; Theophrastus Publications, S.A., Athens, p. 601-619.

Reinhardt, E.W. and Jackson, G.D.
1973: Use of a geological field data collecting form on Operation Bylot, north-central Baffin Island, 1968; Geological Survey of Canada, Paper 73-35, 29 p.

Richardson, D.G. (ed.)
1999: North Baffin partnership project: summary of geoscience investigations; Geological Survey of Canada, Open File 3637.

Robbins, E.I., LaBerge, G.L., and Schmidt, R.G.
1987: A model for the biological precipitation of Precambrian iron formations – B: morphological evidence and modern analogues; *in* Precambrian Iron-formations, (ed.) P.W.U. Appel and G.L. LaBerge; Theophrastus Publications, S.A., Athens, p. 97-139.

Roberts, R.G.
1987: Ore deposit models no. 11. Archean lode gold deposits; Geoscience Canada, v. 14, p. 37-52.

Robertson, W.A. and Baragar, W.R.A.
1972: The petrology and paleomagnetism of the Coronation Sills; Canadian Journal of Earth Sciences, v. 9, p. 123-139.

Rock, N.M.S. and Leake, B.E.
1984: The International Mineralogical Association amphibole nomenclature scheme: computerization and its consequences; Mineralogical Magazine, v. 48, p. 211-227.

Roddick, J.C., Henderson, J.R., and Chapman, H.J.
1992: U-Pb ages from the Archean Whitehills-Tehek lakes supracrustal belt, Churchill Province, District of Keewatin, Northwest Territories; *in* Radiogenic Age and Isotopic Studies: Report 6; Geological Survey of Canada, Paper 92-2, p. 31-40.

Ronov, A.B. and Migdisov, A.A.
1971: Geochemical history of the crystalline basement and the sedimentary cover of the Russian and North American platforms; Sedimentology, v. 16, p. 137-185.

Ross, Sir J.
1819: A Voyage of Discovery Made Under the Orders of the Admiralty in His Majesty's Ships Isabella and Alexander for the Purpose of Exploring Baffin's Bay, and Inquiring into the Probability of a North-West Passage; John Murray, London, 252 p.

St-Onge, M.R. and Lucas, S.B.
1990: Evolution of the Cape Smith Belt: Early Proterozoic continental under-thrusting, ophiolite obduction, and thick-skinned folding; *in* The Early Proterozoic Trans-Hudson Orogen of North America, (ed.) J.F. Lewry and M.R. Stauffer; Geological Association of Canada, Special Paper 37, p. 313-351.
1992: New insights on the crustal structure and tectonic history of the Ungava Orogen (Québec), Kovik Bay and Cap Wolstenbolme map areas; *in* Current Research, Part C; Geological Survey of Canada, Paper 92-1C, p. 31-41.

St-Onge, M.R., Hanmer, S., and Scott, D.J.
1996a: Geology of the Meta Incognita Peninsula, south Baffin Island, Northwest Territories: tectonostratigraphic units and regional correlations; *in* Current Research 1996-C; Geological Survey of Canada, p. 63-72.

St-Onge, M.R., Lucas, S.B., and Scott, D.J.
1996b: Anatomy of an arc-continent collision zone: new views on the Ungava-Baffin segment of Trans-Hudson Orogen; *in* The Geological Society of America, Abstracts with Programs, 1996 Annual Meeting, p. A313-A314.

Sanford, B.V.
1977: Ordovician rocks of Melville Peninsula, southeastern District of Franklin; *in* Geology of Ordovician rocks, Melville Peninsula and region, southeastern District of Franklin, by T.E. Bolton, B.V. Sanford, M.J. Copeland, C.R. Barnes, and J.K. Rigby; Geological Survey of Canada, Bulletin 269, p. 7-21.

Sangster, D.F.

1998; Mineral deposits compilation and metallogenic domains, northern Baffin Island and northern Melville Peninsula; Geological Survey of Canada, Open File 3635, one coloured map sheet, scale 1:1 000 000.

Saxena, S.K., Sykes, J., and Eriksson, G.

1986: Phase equilibria in the pyroxene quadrilateral; Journal of Petrology, v. 27, pt. 4, p. 843-852.

Scammell, R.J. and Bethune, K.M.

1995a: Archean and Proterozoic lithology, structure, and metamorphism in the vicinity of Eqe Bay, Baffin Island, Northwest Territories; *in* Current Research 1995-C; Geological Survey of Canada, p. 53-66.

1995b: Geology and U-Pb geochronology in the Eqe Bay region, Baffin Island, Northwest Territories (abstract); *in* Program with Abstracts, Geological Association of Canada, Victoria, v. 20, p. A-94.

Schau, M.

1977: "Komatiites" and quartzites in the Archean Prince Albert Group; *in* Volcanic Regimes in Canada, (ed.) W.R.A. Baragar, L.S. Coleman, and J.M. Halls; Geological Association of Canada, Special Paper 16, p. 341-354.

1978: Metamorphism of the Prince Albert Group, District of Keewatin; *in* Metamorphism in the Canadian Shield, (ed.) J.A. Fraser and W.W. Heywood; Geological Survey of Canada, Paper 78-10, p. 203-213.

1982: Geology of the Prince Albert Group in parts of Walker Lake and Laughland Lake map areas, District of Keewatin; Geological Survey of Canada, Bulletin 337, 62 p.

Schau, M. and Beckett, M.

1986: High grade metamorphic rocks of northwestern Melville Peninsula, District of Franklin; *in* Current Research, Part A; Geological Survey of Canada, Paper 86-1A, p. 667-674.

Schau, M. and Digel, M.

1989: Gossans in high grade gneisses from the Blacks Inlet area, west coast of Melville Peninsula, District of Franklin, N.W.T.; *in* Current Research, Part C; Geological Survey of Canada, Paper 89-1C, p. 395-403.

Schau, M. and Henderson, J.B.

1983: Archean chemical weathering at three localities on the Canadian Shield; Precambrian Research, v. 20, p. 189-224.

Schau, M. and Heywood, W.W.

1984: Geology, northern Melville Peninsula, N.W.T. (47A,B,C, D); Geological Survey of Canada, Open File 1046, map at 1:500 000 scale.

Schau, M., Tremblay, F., and Christopher, A.

1982: · Geology of Baker Lake map area, District of Keewatin:a progress report; *in* Current Research, Part A; Geological Survey of Canada, Paper 82-1A, p. 143-150.

Schwab, F.L.

1976: Modern and ancient sedimentary basins: comparative accumulation rates; Geology, v. 4, p. 723-727.

Schweinsburg, R.E., Lee, L.J., and Latour, P.B.

1982: Distribution, movement and abundance of polar bears in Lancaster Sound, Northwest Territories; Arctic, v. 35, p. 159-169.

Schwellnus, J.E.G.

1957: Ore controls in deposits of the Knob Lake area, Labrador Trough; PhD. thesis, Queen's University, Kingston, Ontario, 96 p.

Scott, D.J.

1995: U-Pb geochronology of the northeastern Rae Povince, Part 1: a preliminary report on the Lac Lomier Complex, northern Labrador: *in* Eastern Canadian Shield Onshore-Offshore Transect (ECSOOT) Transect Meeting, 1994, (comp.) R.J. Wardle and J. Hall; University of British Columbia, Report 45, p. 122-128.

1996: Geology of the Hall Peninsula east of Iqaluit, southern Baffin Island, Northwest Territories; *in* Current Research 1996-C; Geological Survey of Canada, p. 83-91.

1997: Geology, U-Pb & Pb-Pb geochronology of the Lake Harbour area. southern Baffin Island: implications for the Paleoproterozoic tectonic evolution of NE Laurentia; Canadian Journal of Earth Sciences (Lithoprobe contribution 790, PCSP/ÉPCP Contribution 02396), v. 34, p. 140-155.

Scott, D.J. and de Kemp, E.A.

1998: Bedrock geology compilation, northern Baffin Island and northern Melville Peninsula, Northwest Territories; Geological Survey of Canada, Open File 3633, two coloured map sheets, scale 1:500 000, and one text and legend sheet.

Scott, D.J. and Gauthier, G.

1996: Comparison of TIMS (U-Pb) and laser ablation microprobe ICP-MS (Pb) techniques for age determination of detrital zircons from Paleoproterozoic metasedimentary rocks from northeastern Laurentia, Canada, with tectonic inplications; Chemical Geology, v. 131, p. 127-142.

Scott, D.J. and Godin, L.

1995: Preliminary geological investigation of the Lake Harbour Group and surrounding gneissic rocks near Lake Harbour and Markham Bay, southern Baffin Island, Northwest Territories; *in* Current Research 1995-C; Geological Survey of Canada, p. 67-76.

Scott D.J. and Machado, N.

1994: U-Pb geochronology of the northern Torngat Orogen: results from work in 1993; *in* Eastern Canadian Shield Onshore-Offshore Transect (ECSOOT) Meeting, 1993, (comp.) R.J. Wardle and J. Hall; Université du Québec à Montréal, Report 34, p. 141-155.

Seyfert, C.K. and Cavanaugh, M.D.

1978: Apparent polar wander paths and the joining of the Superior and Slave provinces during early Proterozoic time: reply; Geology, v. 6, p. 133-135.

Shaw, D.M., Reilly, G.A., Muysson, J.R., Pattenden, G.E., and Campbell, F.E.

1967: An estimate of the chemical composition of the Canadian Precambrian Shield; Canadian Journal of Earth Sciences, v. 4, p. 829-853.

Shegelski, R.J.

1987: The depositional environment of Archean iron formations, Sturgeon-Savant greenstone belt, Ontario, Canada; *in* Precambrian Iron-formations, (ed.) P.W.U. Appel and G.L. LaBerge; Theophrastus Publications, S.A., Athens, p. 329-344.

Shieh, Y.N. and Schwarcz, H.P.

1978: The oxygen isotope composition of the surface crystalline rocks of the Canadian Shield; Canadian Journal of Earth Sciences, v. 15, p. 1773-1782.

Shih, K.G., Kay, W., Woodside, J., Jackson, R., Adams, J., Drysdale, J., Bell, J.S., and Podrouzek, A.J.

1988: Crustal thickness, seismicity and stress orientations of the continental margin of Eastern Canada; Geological Survey of Canada, Map 1710A, scale 1:5 000 000.

Sim, V.W.

1964: Terrain analysis of west-central Baffin Island, N.W.T.; Canada, Geographical Branch, Geographical Bulletin, no. 21, p. 66-92.

Simonson, B.M.

1985: Sedimentological constraints on the origins of Precambrian iron-formations; Geological Society of America Bulletin, v. 96, p. 244-252.

Skulski, T., Percival, J.A., and Stern, R.A.

1996: Archean crustal evolution in the central Minto block, northern Quebec: *in* Radiogenic Age and Isotopic Studies: Report 9; Geological Survey of Canada, Current Research 1995-F, p. 17-31.

Smith, E.I.

1978: Precambrian rhyolites and granites in south-central Wisconsin: field relations and geochemistry; Geological Society of America Bulletin, v. 89, p. 875-890.

Smith, H.S. and Erlank, A.J.

1982: Geochemistry and petrogenesis of komatiites from the Barberton greenstone belt, South Africa; *in* Komatiites, (ed.) N.T. Arndt and E.G. Nisbet; George Allen and Unwin, London, p. 347-393.

Statistics Canada

1991: Canada Year Book; Government of Canada, Ottawa, Ontario, 577 p.

Steiger, R.H. and Jäger, E.

1977: Subcommission on geochronology: convention on the use of decay constants in geo- and cosmochronology; Earth and Planetary Science Letters, v. 36, p. 359-362.

Stevens, R.D., Delabio, R.N., and Lachance, G.R.

1982a: Age determinations and geological studies, K-Ar isotopic ages, Report 15; Geological Survey of Canada, Paper 81-2, p. 25-28.

1982b: Age determinations and geological studies, K-Ar isotopic ages, Report 16; Geological Survey of Canada, Paper 82-2, p. 30-33, 40, 41.

Stirling, I. and Calvert, W.

1983: Environmental threats to marine mammals in the Canadian Arctic; Polar Record, v. 21, p. 433-449.

Stockwell, C.H.

1982: Proposals for time classification and correlation of Precambrian rocks and events in Canada and adjacent areas of the Canadian Shield, part 1:a time classification of Precambrian rocks and events; Geological Survey of Canada, Paper 80-19, 135 p.

Streckeisen, A.

1974: How should charnockitic rocks be named?; *in* Géologie des domaines cristallins, Société Géologique de Belgique, Liège, p. 349-360.

1976: To each plutonic rock its proper name; Earth Science Reviews, v. 12, p. 1-33.

1979: Classification and nomenclature of volcanic rocks, lamprophyres, carbonatites, and melilitic rocks: recommendations and suggestions of the IUGS Subcommission on the Systematics of Igneous Rocks; Geology, v. 7, p. 331-335.

Sutherland, P.C.

1853: On the geological and glacial phaenomena of the coasts of Davis' Strait and Baffin's Bay; Geological Society of London, Quarterly Journal, v. 9, p. 296-312.

Taylor, F.C.

1982: Precambrian geology of the Canadian North Atlantic Borderlands; *in* Geology of the North Atlantic Borderlands, (ed.) J.W. Kerr, A.J. Fergusson, and L.C. Machan; Canadian Society of Petroleum Geologists, Memoir 7, p. 11-30.

1985: Precambrian geology of the Half Way Hills area, District of Keewatin; Geological Survey of Canada, Memoir 415, 19 p.

1986: Geology, Cape Dorchester-Cape Dorset, District of Franklin, Northwest Territories; Geological Survey of Canada, Map 1607A, scale 1:250 000.

Teichert, C.

1937: Late pre-Cambrian sedimentary formations of Cockburn Land; *in* Ordovician and Silurian Faunas from Arctic Canada, Report of the Fifth Thule Expedition, 1921-24, v. 1, no. 5; Gyldendalske Boghandel, Nordisk Forlag, Copenhagen, p. 27-32, map at 1:3 000 000 scale.

Tella, S., Heywood, W.W., and Loveridge, W.D.

1985: A U-Pb age on zircon from a dacite porphyry, Amer Lake map area, District of Keewatin, N.W.T.; *in* Current Research, Part B; Geological Survey of Canada, Paper 85-1B, p. 371-374.

Thériault, R.J., Henderson, J.B., and Roscoe, S.M.

1994: Nd isotopic evidence for early to mid-Archean crust from high grade gneisses in the Queen Maud Block and south of the McDonald Fault, western Churchill Province, Northwest Territories; *in* Radiogenic Age and Isotopic Studies: Report 8; Geological Survey of Canada, Current Research 1994-F, p. 37-42.

Tippett, C.R.

1978: A detailed cross-section through the southern margin of the Foxe Fold Belt in the vicinity of Dewar Lakes, Baffin Island, District of Franklin; *in* Current Research, Part A; Geological Survey of Canada, Paper 78-1A, p. 169-173.

1979: Basement-supracrustal rock relationships on the southern margin of the Foxe Fold Belt, central Baffin Island, District of Franklin; *in* Current Research, Part A; Geological Survey of Canada, Paper 79-1A, p. 101-105.

1980: A geological cross-section through the southern margin of the Foxe Fold Belt, Baffin Island, Arctic Canada, and its relevance to the tectonic evolution of the northeastern Churchill Province; PhD. thesis, Queen's University, Kingston, Ontario, 409 p.

Towe, K.M.

1983: Precambrian atmospheric oxygen and banded iron formations: a delayed ocean model; Precambrian Research, v. 20, p. 161-170.

Tremblay, A.

1921: Cruise of the Minnie Maud; Arctic Exchange and Publishing Ltd., Québec, 583 p.

Trendall, A.F.

1973: Iron-formations of the Hamersley Group of Western Australia: type examples of varied Precambrian evaporites; *in* Genesis of Precambrian Iron and Manganese Deposits, Proceedings of the Kiev Symposium, 1970; UNESCO Earth Sciences 9, Paris, p. 257-270.

Trendall, A.F. and Morris, R.C. (ed.)

1983: Iron-formation: Facts and Problems; Elsevier, New York, 558 p.

Trettin, H.P.

1969: Lower Paleozoic sediments of northwestern Baffin Island, District of Franklin; Geological Survey of Canada, Bulletin 157, 70 p.

1975: Investigations of lower Paleozoic geology, Foxe Basin, northeastern Melville Peninsula, and parts of northwestern and central Baffin Island; Geological Survey of Canada, Bulletin 251, 177 p.

Trigg, Woollett and Associates Ltd. and Geowest Services Ltd.

1970: King Resources Company exploration - 1970, Strathcona project, Baffin Island, N.W.T.; company report for King Resources Limited.

Valley, J.W.

1986: Stable isotope geochemistry of metamorphic rocks; *in* Stable Isotopes in High Temperature Geological Processes; Reviews in Mineralogy, (ed.) J.W. Valley, H.P. Taylor, Jr., and J.R. O'Neil; Mineralogical Society of America, Washington, District of Columbia, v. 16, chap. 13, p. 445-481.

Van der Leeden, J., Bélanger, M., Danis, D., Girard, R., and Martelain, J.

1990: Lithotectonic domains in the high-grade terrain east of the Labrador Trough (Quebec); *in* The Early Proterozoic Trans-Hudson Orogen of North America, (ed.) J.F. Lewry, and M.R. Stauffer; Geological Association of Canada, Special Paper 37, p. 371-386.

Van Hise, C.R. and Leith, C.K.

1911: The geology of the Lake Superior region; United States Geological Survey, Monograph 52, 641 p.

Van Kranendonk, M.J., St-Onge, M.R., and Henderson, J.R.

1993: Paleoproterozoic tectonic assembly of Northeast Laurentia through multiple indentations; Precambrian Research, v. 63, p. 325-347.

Van Kranendonk, M.J., Wardle, F.C., Mengel, F.C., Campbell, L.M., and Reid, L.

1994: New results and summary of the Archean and Paleoproterozoic geology of the Burwell domain, northern Torngat Orogen, Labrador, Quebec, and Northwest Territories; *in* Current Research 1994-C; Geological Survey of Canada, p. 321-332.

Wanless, R.K. and Loveridge, W.D.

1978: Rubidium-strontium isotopic age studies, Report 2 (Canadian Shield); Geological Survey of Canada, Paper 74-2, 70 p.

Wanless, R.K., Stevens, R.D., Lachance, G.R., and DeLabio, R.N.

1970: Age determinations and geological studies, K-Ar isotopic ages, Report 9; Geological Survey of Canada, Paper 69-2A, p. 32-36.

1972: Age determinations and geological studies, K-Ar isotopic ages, Report 10; Geological Survey of Canada, Paper 71-2, p. 34-40.

1973: Age determinations and geological studies, K-Ar isotopic ages, Report 11; Geological Survey of Canada, Paper 73-2, p. 28-30.

1974: Age determinations and geological studies, K-Ar isotopic ages, Report 12; Geological Survey of Canada, Paper 74-2, p. 22, 30, 31.

1978: Age determinations and geological studies, K-Ar isotopic ages, Report 13; Geological Survey of Canada, Paper 77-2, p. 35, 36, 41, 42.

1979: Age determinations and geological studies, K-Ar isotopic ages, Report 14; Geological Survey of Canada, Paper 79-2, p. 31-33, 46.

Wanless, R.K., Stevens, R.D., Lachance, G.R., and Edmonds, C.M.

1967: Age determinations and geological studies, K-Ar isotopic ages, Report 7; Geological Survey of Canada, Paper 66-17, p. 64-69.

1968: Age determinations and geological studies, K-Ar isotopic ages, Report 8; Geological Survey of Canada, Paper 67-2, Part A, p. 61-64.

Wanless, R.K., Stevens, R.D., Lachance, G.R., and Rimsaite, J.Y.H.

1966: Age determinations and geological studies, K-Ar isotopic ages, Report 6; Geological Survey of Canada, Paper 65-17, p. 26-30.

Wardle, R.J., Ryan, B., and Ermanovics, E.
1990: The eastern Churchill Province, Torngat and New Québec orogens: an overview; Geoscience Canada, v. 17, p. 217-222.
Weeks, L.J.
1927: The geology of parts of eastern Arctic Canada; Geological Survey of Canada, Summary Report 1925, part C, p. 136-141.
1928: Cumberland Sound area, Baffin Island; Geological Survey of Canada, Summary Report 1927, Part C, p. 83-95.
Whalen, J.B., Currie, K.L., and Chappell, B.W.
1987: A-type granites: geochemical characteristics, discrimination and petrogenesis; Contributions to Mineralogy and Petrology, v. 95, p. 407-419.
White, A.J.R. and Chappell, B.W.
1983: Granitoid types and their distribution in the Lachlan Fold Belt, southeastern Australia; Geological Society of America, Memoir 159, p. 21-34.
Whitney, J.A. and Stormer, J.C. Jr.
1977: The distribution of $NaAlSi_3O_8$ between coexisting microcline and plagioclase and its effect on geothermometric calculations; American Mineralogist, v. 62, p. 687-691.
Windley, B.F.
1971: The stratigraphy of the Fiskenaesset anorthosite complex; Grønlands Geologiske Undersøgelse, Rapp. 35, p. 19-21.
1984: The Evolving Continents, second edition; John Wiley & Sons, New York, 399 p.
Winkler, H.J.F.
1979: Petrogenesis of metamorphic rocks; Springer-Verlag, New York, fifth edition, 348 p.
Wynne, P.J., Irving, E., and Osadetz, K.G.
1988: Paleomagnetism of Cretaceous volcanic rocks of the Sverdrup Basin - magnetostratigraphy, paleolatitudes, and rotations; Canadian Journal of Earth Sciences, v. 25, p. 1220-1239.
Zhai, M.-G. and Windley, B.F.
1989: Banded iron formation in high-grade gneisses in northern China and implications for early crustal growth; Transactions of the Institute of Mining and Metallurgy, Section B: Applied Earth Sciences, p. B32-B34.

APPENDIX 1

Weather observations, north-central Baffin Island

Period	Location	No. of Days					Min. temp. °C	Max. temp. °C	Relative humidity (%)	Comments
		Rain	Snow	Fog	High winds	Calm				
June 9-15, 1968	HB, C1		4	2	1					
June 18-23, 1965	MR		1							
June 16-23, 1968	HB, C1	1	2	5						
June 24-30, 1965	MR		4			2	-1-+2			Temperature measured at 6:20 a.m.
June 24-30, 1968	C1	2	2	3	1		-1-+5	+7-+11	75-100	
July 1-6, 1965	MR		3		3	1	-1-+1			Temperature measured at 6:20 a.m. One maximum temperature of 5°C?, one relative humidity of 46%
July 1-6, 1968	C1	4			1		0-+3	+12-+13	71-94	
July 7-14, 1965	MR	2					+3-+8			Temperature measured at 6:20 a.m. Relative humidity for four days. July 11 – winds to 64 km/h
July 7-14, 1968	C2	5	1		4	1			86-100	
July 15-21, 1965	MR	4	1		1		+4-+5			Temperature measured at 6:20 a.m., July 15-17 Very high winds July 21. July 15 – winds to 80 km/h, barometer 97.5 kPa
July 15-21, 1968	C2	3	2	3	2	2	0-+3	+4-+12	78-100	
July 22-29, 1965	MR	3			1					Very high winds July 22
July 22-29, 1968	C3			2		5	-1-+1	+7-+14	70-100	
July 30-Aug 5, 1965	C4	4	1		4	1				
July 30-Aug 5, 1968	C4	2		3		1	-1-+1	+9-+17	57-96	
Aug. 6-11, 1965	MR	3	3		2					Very high winds August 11
Aug. 6-11, 1968	C4		1	4	2		-1-+2	+7-+10	53-98	
Aug. 12-19, 1965	MR	1	2		4	4				
Aug. 12-19, 1968	C5					1	-2-+3	+7-+15	30-70	
Aug. 20-24, 1965	MR	2	1							
Aug. 20-24, 1968	C6			1		1	-2-+1	+9-+13	78-100	
Sept. 1-8, 1965	MR	5	2	2	2					
Sept. 1-6, 1968	C6, HB	2		2						

HB = Hall Beach, 215 km southwest of Eqe Bay
MR = Mary River
C1 = Camp 1 (e.g. *see* Fig. 1) - 69°47'N latitude, 76°2'W longitude
C2 = Camp 2 - 71°8'N latitude, 78°12'W longitude
C3 = Camp 3 at Pond Inlet
C4 = Camp 4 - 71°9'N latitude, 75°23'W longitude
C5 = Camp 5 - 69°48'N latitude, 70°47'W longitude
C6 = Camp 6 at Longstaffe Bluff Airstrip, 90 km southeast of Eqe Bay

APPENDIX 2

Spectrographic analyses and locations for individual samples from map units.
2a. Spectrographic analyses for map units in weight per cent element.
2b. Sample locations in UTM co-ordinates.

All sample numbers are preceded by JD and followed by 68 (the year) in field notes and on samples. The first three digits indicate the station number, and the last two identify the sample taken at a specific location. Thus 23103 = JD231/3-68 and is sample no. 3 taken at station JD231. 13400 = JD134-68 and, nearly always, is the only sample taken at station JD134. All samples at a given station have the same UTM coordinates.

Appendix 2a. Spectrographic analyses for map units in weight per cent element.

Sample	Map sheet	Map unit	Al	Fe	Ca	Na	Mg	Ti	Mn	Ba	Co	Cr	Cu	La	Ni	Pb	Sr	V	Y	Yb	Zr
13201	37G	Amn	7.5	3.3	0.85	+	1.4	0.24	0.042	0.029	-	0.012	-	-	-	-	0.016	0.0061	-	-	0.030
13301	"	"	7.2	0.73	0.96	+	0.16	0.066	-	0.18	-	-	0.0010	-	-	-	0.033	-	-	-	0.012
13400	"	"	7.0	1.8	+	+	0.40	0.19	0.024	0.036	-	-	-	-	-	-	0.019	-	-	-	0.024
23101	"	"	5.2	6.7	+	+	2.9	1.1	0.090	0.087	-	0.0070	0.0020	-	0.0036	-	0.029	0.026	-	-	0.065
23103	"	"	6.4	7.5	+	+	3.4	0.80	0.15	0.11	0.0031	0.024	0.0082	0.028	0.0070	-	0.024	0.025	-	-	0.019
23202	"	"	8.6	0.88	+	+	0.28	0.14	-	0.20	-	-	-	-	-	-	0.072	-	-	-	0.033
23203	"	"	7.9	2.0	+	+	0.49	0.21	0.019	0.18	-	-	0.0017	-	-	-	0.061	0.0046	-	-	0.014
23301	"	"	7.6	1.3	+	+	0.41	0.19	0.017	0.012	-	-	-	-	-	-	0.035	-	-	-	0.030
23302	"	"	7.0	0.91	+	+	0.27	0.11	0.011	0.058	-	-	-	-	-	-	0.033	-	-	-	-
23401	"	"	6.4	3.6	+	+	1.8	0.29	0.088	0.058	-	0.021	-	-	0.0031	-	0.032	0.0091	-	-	0.026
23402	"	"	7.5	3.0	+	+	1.3	0.31	0.048	0.15	-	0.0042	0.0019	-	-	-	0.049	0.0076	-	-	0.019
23501	"	"	7.2	2.5	+	+	0.86	0.27	0.035	0.21	-	-	0.0020	-	-	-	0.046	0.0058	-	-	0.021
23600	"	"	7.0	3.1	+	+	0.98	0.34	0.038	0.14	-	0.0031	-	-	-	-	0.040	0.0098	-	-	0.013
22102	37H	"	7.8	2.4	+	+	0.56	0.25	0.030	0.041	-	-	-	-	-	-	0.026	0.0048	-	-	0.014
23800	"	"	8.0	1.6	+	+	0.55	0.19	0.019	0.065	-	-	0.0010	-	-	-	0.042	-	-	-	-
24400	"	"	7.1	2.0	+	+	0.66	0.24	0.031	0.015	-	-	0.0027	-	-	-	0.026	0.0045	-	-	0.031
24402	"	"	6.3	2.9	+	+	0.52	0.41	0.028	0.095	-	-	0.020	-	-	-	0.034	0.0057	-	-	0.029
25100	"	"	7.8	8.0	+	+	0.38	0.13	0.011	0.067	-	-	0.0015	-	-	-	0.036	-	-	-	0.010
25401	"	"	6.6	2.0	+	+	0.68	0.27	0.032	0.13	-	-	-	-	-	-	0.023	0.0047	-	-	0.015
25402	"	"	6.6	1.8	+	+	0.63	0.24	0.028	0.091	-	-	-	-	-	-	0.021	0.0038	-	-	0.013
25403	"	"	5.6	5.5	+	+	4.0	0.49	0.091	0.030	-	0.054	0.0018	-	0.011	-	0.018	0.020	-	-	0.014
25503	"	"	6.4	0.92	0.88	+	0.38	0.17	0.012	0.11	-	-	-	-	-	-	0.053	-	-	-	-
25504	"	"	6.6	1.1	+	+	0.41	0.14	0.015	0.12	-	-	-	-	-	-	0.051	-	-	-	-
27001	"	"	6.6	3.0	+	+	1.3	0.36	0.041	0.056	-	-	0.0017	-	-	-	0.038	0.0097	-	-	0.010
27003	"	"	7.1	4.7	+	+	1.3	0.24	0.062	0.032	-	0.0032	0.0024	-	-	-	0.035	0.012	-	-	0.021
27202	"	"	7.9	0.65	+	+	0.24	0.057	0.018	0.031	-	-	-	-	-	-	0.040	-	-	-	0.012
27302	"	"	6.2	1.2	+	+	0.31	0.13	0.015	0.041	-	-	-	-	-	-	0.012	-	-	-	0.016
27501	"	"	6.7	2.6	+	+	0.65	0.32	0.036	0.074	-	-	0.0013	-	-	-	0.022	0.0066	-	-	0.030
03500	37F	"	7.4	1.2	+	+	0.43	0.13	0.018	0.076	-	-	-	-	-	-	0.030	-	-	-	0.012
04000	"	"	6.9	0.69	+	+	0.24	0.10	0.014	0.019	-	-	-	-	-	-	0.024	-	-	-	-
04200	"	"	8.4	2.5	+	+	0.74	0.20	0.027	0.026	-	-	0.0068	0.029	-	-	0.022	0.0055	-	-	0.027
05700	"	"	7.6	0.68	+	+	0.31	0.10	0.011	0.027	-	-	-	-	-	-	0.033	-	-	-	-
12102	"	"	6.9	1.7	+	+	0.41	0.23	0.022	0.16	-	-	-	-	-	-	0.029	-	-	-	0.015
04200	"	"	9.9	2.6	2.8	+	0.86	0.21	0.029	0.027	-	0.0015	0.0073	-	-	-	0.024	0.0061	-	-	-
05300	37E	"	8.0	2.0	+	+	0.63	0.33	0.028	0.038	-	-	0.0012	-	-	-	0.029	0.0052	-	-	0.029
06301	"	"	7.7	0.80	+	+	0.13	0.072	-	0.055	-	-	-	-	-	-	0.036	-	-	-	-
06302	"	"	7.9	2.9	+	+	1.1	0.30	0.041	0.019	-	-	0.0039	-	-	-	0.033	0.0058	-	-	0.026
06401	"	"	8.9	2.1	+	+	0.50	0.27	0.024	0.040	-	-	0.0011	-	-	-	0.025	0.0038	-	-	0.019
27800	27F	"	6.1	0.97	0.29	+	0.76	0.10	0.015	0.11	-	-	-	-	-	-	0.012	-	-	-	0.028
28101	"	"	6.0	0.55	0.70	+	0.15	0.064	-	0.17	-	-	-	-	-	-	0.023	-	-	-	-
28102	"	"	6.1	2.9	+	+	0.78	0.31	0.050	0.079	-	-	0.0016	-	-	-	0.021	0.0085	-	-	0.028
28103	"	"	5.5	0.46	0.64	+	0.12	0.050	-	0.16	-	-	-	-	-	-	0.024	-	-	-	-
28202	"	"	5.6	1.6	0.80	+	0.28	0.15	0.015	0.090	-	-	-	-	-	-	0.024	-	-	-	0.022
28301	"	"	6.5	1.7	+	+	0.61	0.23	0.026	0.046	-	-	0.0023	-	-	-	0.020	0.0036	-	-	0.031
28302	"	"	6.8	1.7	0.84	+	0.89	0.23	0.033	0.068	-	-	-	-	-	-	0.021	-	-	-	0.015
28401	27F	"	6.3	2.0	+	+	0.59	0.24	0.024	0.046	-	-	0.0013	-	-	-	0.017	0.0050	-	-	0.026
28601	"	"	6.3	1.8	+	+	0.45	0.29	0.023	0.065	-	-	0.0014	-	-	-	0.023	0.0047	-	-	0.029
28802	"	"	6.4	1.9	+	+	0.54	0.23	0.019	0.12	-	-	0.0013	-	-	-	0.033	0.0047	-	-	0.027
29001	"	"	6.6	2.1	+	+	0.57	0.33	0.038	0.11	-	-	0.0010	-	-	-	0.026	0.0055	-	-	0.032
29002	"	"	6.5	2.0	+	+	0.48	0.23	0.027	0.058	-	-	-	-	-	-	0.023	0.0045	-	-	0.028
29403	"	"	6.2	3.5	+	+	1.4	0.49	0.064	0.037	-	-	0.0012	-	-	-	0.016	0.010	-	-	0.033
29900	"	"	6.6	1.8	0.70	+	0.67	0.23	0.025	0.070	-	-	-	-	-	-	0.0091	0.0037	-	-	0.014
00300	37C	"	5.7	0.89	0.43	+	0.33	0.086	0.013	0.17	-	-	-	-	-	-	0.021	-	-	-	-
08001	37G	Amg	8.1	4.1	+	+	1.1	0.47	0.051	0.022	-	0.0069	0.0031	0.034	0.0037	-	0.076	0.012	-	-	0.049
08301	"	"	7.6	2.9	+	+	1.9	0.79	0.039	0.043	-	-	0.0021	0.029	-	-	0.016	0.013	0.0087	-	0.064
09403	"	"	6.7	5.8	+	+	1.2	0.48	0.081	0.022	-	0.0049	0.0079	-	-	-	0.017	0.015	-	-	0.018
09600	"	"	6.2	8.2	+	+	3.4	0.50	0.24	0.011	0.0031	0.026	0.0013	-	0.0088	-	0.0093	0.031	-	-	0.014
09702	"	"	6.8	2.9	+	+	1.9	0.29	0.055	0.057	-	0.016	-	-	0.0046	-	0.035	0.0088	-	-	0.023
12902	"	"	6.6	2.4	+	+	1.2	0.18	0.044	0.081	-	0.0071	0.0025	-	-	-	0.035	0.0050	-	-	0.011
13002	"	"	6.3	2.8	+	+	1.3	0.21	0.051	0.025	-	0.0076	0.0078	-	-	-	0.016	0.0075	-	-	0.017
13006	"	"	5.8	9.2	+	0.49	2.2	0.75	0.16	0.011	0.0030	0.0066	0.042	-	-	-	0.012	0.042	-	-	0.016
15302	"	"	7.2	1.5	+	+	0.48	0.16	0.023	0.13	-	-	-	-	-	-	0.041	-	-	-	0.016
22703	"	"	8.0	2.6	+	+	1.4	0.36	0.039	0.021	-	0.0043	-	-	-	-	0.052	0.0070	-	-	0.013

Appendix 2a (cont.)

Sample	Map sheet	Map unit	Al	Fe	Ca	Na	Mg	Ti	Mn	Ba	Co	Cr	Cu	La	Ni	Pb	Sr	V	Y	Yb	Zr
22800	37G	Amg	8.3	1.0	+	+	0.38	0.14	0.018	0.011	-	-	-	-	-	-	0.025	-	-	-	0.011
22901	"	"	5.2	7.3	+	+	2.1	0.55	0.19	0.0074	-	0.011	0.0041	-	0.0033	-	0.014	0.026	-	-	0.015
22902	"	"	7.4	0.91	+	+	0.33	0.078	0.024	0.064	-	-	-	-	-	-	0.030	-	-	-	0.019
22500	"	"	6.6	3.3	+	+	1.4	0.44	0.060	0.051	-	0.0059	0.0018	-	-	-	0.049	0.010	-	-	0.027
22601	"	"	5.7	5.6	+	+	1.0	0.36	0.058	0.039	-	0.0034	0.0071	-	-	-	0.016	0.010	-	-	0.020
22602	"	"	5.1	6.1	+	+	1.3	0.36	0.10	0.026	-	0.0044	0.0066	-	-	-	0.013	0.012	-	-	0.022
13703	"	"	6.6	0.64	0.51	+	0.11	0.048	-	0.10	-	-	-	-	-	-	0.021	-	-	-	-
24201	37H	"	6.7	1.5	1.0	+	0.75	0.24	0.017	0.12	-	-	-	-	-	-	0.045	-	-	-	0.017
22300	"	"	7.2	2.5	+	+	1.0	0.34	0.042	+	-	0.0037	-	-	-	-	0.064	0.0084	-	-	0.019
22402	"	"	6.9	2.9	+	+	1.1	0.43	0.035	0.16	-	0.0047	0.0067	-	-	-	0.082	0.0098	-	-	0.025
24300	"	"	7.0	2.2	+	+	1.1	0.28	0.040	0.16	-	0.0058	-	-	-	-	0.064	0.0071	-	-	0.034
25502	"	"	7.0	2.9	+	+	1.6	0.39	0.060	0.018	-	-	0.0051	-	-	-	0.024	0.0095	-	-	0.011
25704	"	"	5.7	0.33	0.31	+	0.10	0.084	-	0.11	-	-	-	-	-	-	0.021	-	-	-	-
26003	"	"	6.0	13.0	8.6	1.2	5.3	1.1	0.24	0.0096	0.0060	0.019	0.0019	-	0.0099	-	0.0087	0.047	0.0077	-	0.091
26901	"	"	5.7	4.4	+	+	1.5	0.36	0.065	0.070	-	0.014	0.0038	-	-	-	0.019	0.013	-	-	0.030
03800	37F	"	6.9	5.2	+	+	1.8	0.37	0.071	0.083	-	0.0064	0.0025	-	-	-	0.032	0.014	-	-	0.019
04300	"	"	6.6	0.35	+	+	0.16	0.054	-	0.13	-	-	0.0011	-	-	-	0.024	-	-	-	-
04501	"	"	6.8	1.5	+	+	0.26	0.095	0.084	0.065	-	-	0.0011	-	-	-	0.011	-	0.0083	-	0.029
04700	"	"	9.6	3.5	+	+	1.3	0.31	0.068	0.026	-	-	0.0035	-	-	-	0.030	0.0076	-	-	0.012
05801	"	"	7.6	2.6	+	+	0.77	0.41	0.043	0.015	-	-	0.0033	-	-	-	0.020	0.010	-	-	0.022
05802	"	"	8.8	2.4	+	+	0.62	0.31	0.043	0.073	-	-	0.0016	-	-	-	0.020	0.0071	-	-	0.025
05902	"	"	7.3	0.38	+	+	0.13	0.11	0.014	0.11	-	-	-	-	-	-	0.019	-	-	-	-
06101	"	"	8.1	1.0	+	+	0.42	0.10	0.018	0.019	-	-	-	-	-	-	0.035	-	-	-	-
06103	"	"	8.2	0.89	+	+	0.24	0.11	0.012	0.087	-	-	-	-	-	-	0.024	-	-	-	-
11501	"	"	7.5	0.91	+	+	0.25	0.079	0.028	0.038	-	-	-	-	-	-	0.029	-	-	-	0.013
12301	"	"	6.7	3.5	+	+	1.0	0.39	0.047	0.033	-	-	0.0043	-	-	-	0.018	0.011	-	-	0.017
05200	37E	"	7.7	3.5	+	+	0.94	0.51	0.055	0.035	-	-	0.0031	-	-	-	0.024	0.0094	-	-	0.014
05601	"	"	8.4	1.8	+	+	0.65	0.24	0.016	0.036	-	-	-	-	-	-	0.041	0.0039	-	-	0.034
06500	"	"	7.1	2.4	+	+	1.0	0.23	0.046	0.018	-	-	-	-	-	-	0.016	0.0055	-	-	0.014
11701	"	"	8.3	0.79	+	+	0.22	0.068	0.014	0.027	-	-	-	-	-	-	0.027	-	-	-	0.021
29601	27F	"	6.7	1.2	0.86	+	0.61	0.17	0.021	0.042	-	-	0.0013	-	-	-	0.014	-	-	-	0.020
27901	27F	"	6.5	1.7	0.73	+	0.65	0.25	0.024	0.066	-	-	-	-	-	-	0.017	0.0034	-	-	0.021
28502	"	"	6.0	1.4	0.55	+	0.38	0.19	0.017	0.11	-	-	-	-	-	-	0.016	-	-	-	0.019
28701	"	"	7.1	2.6	+	+	0.79	0.36	0.039	0.082	-	-	0.0011	-	-	-	0.031	0.0085	-	-	0.042
28900	"	"	7.1	3.2	+	+	0.86	0.26	0.035	0.073	-	-	0.0016	-	-	-	0.038	0.0090	-	-	0.026
29100	"	"	6.2	1.1	0.96	+	0.37	0.14	0.015	0.069	-	-	-	-	-	-	0.020	-	-	-	0.024
29201	"	"	6.6	2.6	+	+	0.71	0.30	0.036	0.034	-	-	0.0011	-	-	-	0.015	0.0062	-	-	0.046
29202	"	"	6.8	4.1	+	+	0.65	0.34	0.046	0.012	-	-	-	-	-	-	0.017	0.011	-	-	0.077
29300	"	"	7.1	1.8	+	+	0.87	0.24	0.030	0.068	-	-	-	-	-	-	0.026	0.0051	-	-	0.037
29502	"	"	7.6	1.5	+	+	0.51	0.21	0.019	0.081	-	-	0.0010	-	-	-	0.023	0.0031	-	-	0.022
29503	"	"	6.8	3.3	+	+	1.4	0.55	0.050	0.021	-	-	0.0010	-	-	-	0.020	0.011	-	-	0.018
29602	"	"	6.9	2.6	+	+	1.3	0.42	0.037	0.024	-	0.0033	-	-	-	-	0.022	0.010	-	-	0.057
29701	"	"	5.8	0.22	0.68	+	0.076	0.047	-	0.027	-	-	-	-	-	-	0.011	-	-	-	0.012
29702	"	"	6.2	0.28	0.71	+	0.093	0.048	-	0.027	-	-	-	-	-	-	0.010	-	-	-	-
29802	"	"	7.6	2.7	+	+	0.70	0.27	0.031	0.045	-	-	-	-	-	-	0.017	0.0069	-	-	0.028
10101	37G	Amg^{a}	7.4	0.49	+	0.56	0.20	0.39	-	0.0046	-	-	-	0.037	-	-	0.070	0.0042	-	-	0.045
10103	"	"	6.8	0.28	+	0.59	0.11	0.40	-	0.0043	-	-	-	0.039	-	-	0.065	0.0040	-	-	0.055
10106	"	"	6.4	1.1	0.66	+	0.26	0.20	0.016	0.072	-	-	-	-	-	-	0.015	-	-	-	0.031
08200	"	Amp	6.3	3.8	+	+	0.67	0.73	0.052	0.087	-	-	0.0024	-	-	-	0.021	0.012	0.0083	-	0.052
13101	"	"	6.5	5.6	+	+	1.7	0.63	0.065	0.052	-	0.0066	0.0019	-	0.0039	-	0.019	0.013	-	-	0.034
24101	37H	"	7.5	3.1	+	+	0.87	0.42	0.031	0.17	-	-	0.0030	-	-	-	0.073	0.0098	-	-	0.019
26201	"	"	5.7	1.3	0.82	+	0.45	0.18	0.030	0.051	-	-	-	-	-	-	0.010	-	-	-	-
26203	"	"	5.9	1.4	0.83	+	0.48	0.23	0.026	0.054	-	-	-	-	-	-	0.013	-	-	-	0.018
26400	"	"	6.6	1.9	+	+	0.41	0.36	0.025	0.16	-	-	-	-	-	-	0.031	0.0050	-	-	0.038
27401	"	"	6.8	2.1	0.96	+	0.56	0.19	0.050	0.033	-	-	0.0010	-	-	-	0.0098	0.0030	-	-	0.012
05401	37E	"	7.5	2.1	+	+	0.77	0.21	0.032	0.15	-	-	0.0010	-	-	-	0.029	0.0046	-	-	0.036
05402	"	"	7.9	1.9	+	+	0.80	0.25	0.031	0.15	-	-	0.0010	-	-	-	0.032	0.0067	-	-	0.053
26502	27G	bg	8.1	3.5	+	+	1.3	0.42	0.058	0.14	-	0.0058	0.0040	-	-	-	0.050	0.011	-	-	0.025
26503	37H	"	6.5	3.3	+	+	1.4	0.35	0.063	0.091	-	0.0058	0.0060	0.028	-	-	0.039	0.011	-	-	0.032
26600	"	"	6.7	2.1	+	+	0.85	0.22	0.032	0.11	-	-	-	-	-	-	0.039	0.0050	-	-	0.016
13202	37G	Amn^{b}	7.1	0.68	0.88	+	0.21	0.087	0.011	0.068	-	-	-	-	-	-	0.022	-	-	-	0.013
23901	37H	"	7.9	2.1	+	+	1.1	0.30	0.036	0.067	-	-	0.014	-	-	-	0.043	0.0054	-	-	0.013
03901	37F	"	7.3	0.67	+	+	0.21	0.097	-	0.053	-	-	-	-	-	-	0.029	-	-	-	-

Appendix 2a (cont.)

Sample	Map sheet	Map unit	Al	Fe	Ca	Na	Mg	Ti	Mn	Ba	Co	Cr	Cu	La	Ni	Pb	Sr	V	Y	Yb	Zr
04101	37F	Amn[b]	7.6	1.2	+	+	0.35	0.16	0.015	0.024	-	-	-	-	-	-	0.040	-	-	-	-
11503	"	"	6.5	5.5	+	+	0.26	0.47	0.068	0.041	-	-	0.0019	-	-	-	0.014	0.0040	-	-	0.022
12101	"	"	7.7	1.7	+	+	0.43	0.21	0.018	0.016	-	-	-	-	-	-	0.028	0.0035	-	-	0.014
29402	27F	"	6.6	1.4	0.95	+	0.45	0.19	0.021	0.049	-	-	0.001	-	-	-	0.018	-	-	-	0.011
09000	37G	gr-Agr[c]	7.2	1.7	+	+	0.82	0.19	0.034	0.19	-	0.0040	0.0019	-	-	-	0.045	0.0034	-	-	0.024
09201	"	"	7.4	0.76	0.78	+	0.46	0.22	0.023	0.18	-	-	0.0012	-	-	-	0.025	-	0.013	-	-
12800	"	"	7.1	0.61	0.89	+	0.36	0.076	0.011	0.13	-	-	-	-	-	-	0.047	-	-	-	-
13501	"	"	7.3	0.71	0.81	+	0.34	0.13	0.013	0.11	-	-	0.0010	-	-	-	0.030	-	-	-	0.022
13502	"	"	5.7	2.3	+	+	1.1	0.18	0.055	0.14	-	0.0081	-	-	-	-	0.029	0.0037	-	-	0.011
14101	"	"	7.3	4.9	+	+	1.1	0.51	0.041	0.17	-	-	0.0017	-	-	-	0.057	0.013	-	-	0.028
14501	"	"	6.4	0.79	0.49	+	0.43	0.10	0.016	0.081	-	-	-	-	-	-	0.0089	-	-	-	0.012
14503	"	"	7.1	1.3	0.96	+	0.50	0.15	0.018	0.033	-	-	0.0014	-	-	-	0.0060	-	-	-	0.024
23001	"	"	6.9	0.58	+	+	0.13	0.051	-	0.16	-	-	-	-	-	-	0.039	-	-	-	-
23003	"	"	6.6	0.97	+	+	0.17	0.063	-	0.13	-	-	0.0010	-	-	-	0.035	-	-	-	0.016
03301	37F	"	6.5	3.0	+	+	0.67	0.29	0.051	0.038	-	-	0.0010	-	-	-	0.011	0.0051	-	-	0.020
03302	"	"	6.7	2.7	+	+	0.58	0.27	0.044	0.057	-	-	0.0015	-	-	-	0.014	0.0048	-	-	0.021
11103	"	"	6.4	1.3	0.74	+	0.47	0.17	0.025	0.038	-	-	0.0037	-	-	-	0.0085	-	-	-	0.015
12302	37F	gr,Agr[c]	7.2	2.9	+	+	0.77	0.30	0.049	0.031	-	-	-	-	-	-	0.021	0.0093	-	-	0.017
06200	37E	"	7.4	0.57	+	+	0.33	0.089	-	0.039	-	-	-	-	-	-	0.026	-	-	-	0.016
30000	27E,F	"	6.7	2.4	+	+	0.79	0.28	0.036	0.058	-	-	0.0013	-	-	-	0.020	0.0061	-	-	0.033
31800	"	"	6.9	1.8	+	+	0.45	0.23	0.036	0.12	-	-	0.0015	-	-	-	0.025	0.0048	-	-	0.027
00801	37C,D	"	5.9	1.3	0.90	+	0.37	0.13	0.021	0.063	-	-	0.0017	0.032	-	-	0.017	-	-	-	0.010
00802	"	"	6.6	2.8	+	+	0.80	0.24	0.075	0.0065	-	0.0072	-	-	-	-	0.018	0.0053	-	-	0.031
00901	"	"	6.8	3.3	+	+	0.72	0.30	0.040	0.014	-	-	0.0013	-	-	-	0.027	0.0069	-	-	0.014
00902	"	"	5.9	0.66	0.75	+	0.24	0.063	-	0.078	-	-	-	-	-	-	0.018	-	-	-	0.012
00903	"	"	6.2	1.1	+	+	0.24	0.11	0.021	0.050	-	-	-	-	-	-	0.021	-	-	-	0.014
01800	"	"	6.2	0.43	0.54	+	0.12	0.055	-	0.023	-	-	-	-	-	-	0.0054	-	-	-	-
02000	"	"	8.3	1.4	+	+	0.42	0.14	0.021	0.078	-	-	0.0072	-	-	-	0.023	-	-	-	0.017
02401	"	"	6.9	2.1	+	+	0.69	0.20	0.071	0.015	-	0.0042	-	-	-	-	0.018	0.0036	-	-	-
02800	"	"	6.4	0.96	0.30	+	0.62	0.11	0.013	0.061	-	-	-	-	-	-	0.0040	-	-	-	0.016
08701	37G	gr[d]	7.1	2.6	+	+	0.49	0.44	0.032	0.14	-	-	0.0015	-	-	-	0.024	0.0073	-	-	0.041
08702	"	"	6.6	5.2	+	+	1.0	0.96	0.074	0.16	-	0.0037	0.0041	0.035	-	-	0.024	0.018	0.013	0.0011	0.099
10301	"	"	6.7	1.7	+	+	0.33	0.20	0.019	0.16	-	-	-	-	-	-	0.042	0.0029	-	-	0.018
12901	"	"	7.0	2.0	+	+	0.62	0.21	0.022	0.076	-	-	-	-	-	-	0.029	0.0032	-	-	0.024
03201	37F	"	6.6	0.38	0.72	+	0.13	0.040	-	0.10	-	-	-	-	-	-	0.026	-	-	-	-
24509	"	"	6.0	1.5	0.57	+	0.38	0.18	0.028	0.094	-	-	-	-	-	-	0.0079	-	-	-	0.020
09202	37G	gr,Agr[e]	7.2	1.2	0.81	+	0.28	0.14	0.014	0.16	-	-	-	-	-	-	0.029	-	-	-	0.019
10302	"	"	6.1	0.31	0.50	+	0.11	0.031	-	0.18	-	-	-	-	-	-	0.033	-	-	-	-
03202	37F	"	8.1	1.1	+	+	0.23	0.11	0.018	0.022	-	-	-	-	-	-	0.034	-	-	-	-
06901	37E	"	6.8	1.0	+	+	0.30	0.087	0.013	0.040	-	-	0.0093	-	-	-	0.018	-	-	-	0.014
31900	27F	"	5.6	1.9	+	+	0.58	0.22	0.030	0.070	-	-	-	-	-	-	0.017	0.0039	-	-	0.022
32000	"	"	6.1	2.3	+	+	0.53	0.34	0.034	0.15	-	-	0.0019	-	-	-	0.030	0.0083	-	-	0.060
23201	37G	Amn[f]	6.7	7.6	+	+	3.6	0.94	0.13	+	0.0033	0.020	0.0048	0.044	0.0051	-	0.070	0.026	-	-	0.050
25501	37H	"	5.7	4.8	+	+	3.1	0.47	0.11	0.024	-	0.022	0.0069	-	0.010	-	0.019	0.011	-	-	-
27201	"	"	6.7	8.2	+	+	3.7	0.49	0.15	0.0036	0.0047	0.027	0.015	0.030	0.014	-	0.012	0.030	-	-	0.014
11603	37F	"	4.2	5.6	+	0.28	4.0	0.35	0.14	0.16	-	0.033	0.0025	-	0.024	-	0.037	0.013	-	-	0.029
11604	"	"	6.1	7.1	+	+	2.6	0.41	0.14	0.012	-	0.012	0.0013	-	0.0053	-	0.0085	0.020	-	-	0.015
03902	"	"	7.2	8.6	+	+	2.5	0.90	0.11	0.031	0.0030	0.0068	0.0043	-	0.0047	-	0.039	0.025	-	-	0.019
06402	37E	"	8.3	3.4	+	+	1.6	0.37	0.069	0.029	-	0.0052	0.0024	-	-	-	0.030	0.011	-	-	0.019
28201	27F	"	6.5	2.1	+	+	0.69	0.32	0.024	0.041	-	-	0.0012	-	-	-	0.015	0.0071	-	-	0.038
28203	"	"	6.5	4.9	+	+	1.8	0.44	0.11	0.012	-	-	0.0052	-	-	-	0.036	0.016	-	-	0.016
28402	"	"	4.3	8.4	+	+	2.8	0.61	0.22	0.018	-	0.0073	0.0017	-	0.0037	-	0.0070	0.022	0.016	0.0015	0.094
28801	"	"	2.6	6.2	+	0.50	4.8	0.36	0.20	0.0084	-	0.052	0.0012	-	0.013	-	0.0049	0.016	-	-	-
24901	37H	gr[g]	5.9	3.9	+	+	2.2	0.36	0.067	0.14	-	0.013	0.0015	-	-	-	0.058	0.013	-	-	0.013
07600	37G	Mb	6.1	7.4	+	0.52	3.4	0.59	0.18	0.0086	0.0031	0.0076	0.0081	-	0.0032	-	0.0077	0.028	-	-	0.015
00770	"	"	6.4	7.7	+	+	3.6	0.57	0.14	0.016	0.0024	0.025	0.0060	-	0.0049	-	0.0059	0.029	-	-	0.011
09303	"	"	8.8	7.6	+	+	2.7	0.61	0.20	0.017	0.0038	0.0052	0.0015	0.031	0.0056	-	0.022	0.025	-	-	0.020
09901	"	"	4.4	6.4	+	+	5.9	0.25	0.18	0.0038	0.0056	0.14	-	-	0.055	-	0.0061	0.018	-	-	-
10009	"	"	4.2	6.7	+	0.30	6.4	0.20	0.20	0.0033	0.011	0.25	0.0048	0.027	0.18	-	0.017	0.016	-	-	-
12503	"	"	5.5	5.1	+	+	3.2	0.39	0.092	0.052	-	0.019	0.0017	-	0.0061	-	0.029	0.019	-	-	0.017
12703	"	"	5.8	8.3	+	+	2.3	0.70	0.11	0.0070	0.0032	-	0.018	-	-	-	0.011	0.049	-	-	0.015
13001	"	"	5.8	7.8	+	+	3.6	0.45	0.15	0.0091	0.0034	0.020	0.0071	-	0.0091	-	0.013	0.027	-	-	0.014
13005	"	"	6.7	9.7	+	0.51	1.8	0.80	0.19	0.019	0.0038	-	0.048	-	-	-	0.015	0.035	-	-	0.017

Appendix 2a (cont.)

Sample	Map sheet	Map unit	Al	Fe	Ca	Na	Mg	Ti	Mn	Ba	Co	Cr	Cu	La	Ni	Pb	Sr	V	Y	Yb	Zr
23702	37H	Mb	2.9	7.2	+	0.54	7.0	0.36	0.16	0.0055	0.0059	0.11	0.0038	-	0.022	-	0.0027	0.014	-	-	0.011
26902	"	"	5.4	8.2	+	+	2.4	0.67	0.13	0.022	0.0047	0.0072	0.0083	-	0.0046	-	0.015	0.027	-	-	0.014
04600	37F	"	5.6	9.7	+	+	2.7	0.88	0.19	0.0066	0.0043	0.010	0.011	0.030	0.0034	-	0.0074	0.037	-	-	0.018
11207	"	"	6.9	7.3	+	+	4.1	0.44	0.15	0.0070	0.0036	0.027	0.0027	-	0.011	-	0.013	0.031	-	-	0.012
12202	"	"	6.5	0.96	0.77	+	0.12	0.090	0.010	0.044	-	-	-	-	-	-	0.011	-	-	-	0.020
12401	"	"	5.9	7.1	+	+	3.7	0.37	0.14	0.0075	0.0030	0.036	0.0019	-	0.014	-	0.0089	0.027	-	-	-
24505	"	"	2.7	8.3	+	0.35	5.6	0.18	0.23	0.0033	0.0057	0.23	-	-	0.070	0.072	0.0012	0.011	-	-	-
24602	"	"	5.3	6.4	+	+	3.5	0.41	0.15	0.0073	0.0025	0.013	0.0083	-	-	-	0.014	0.023	-	-	-
00703	37D	"	5.3	5.9	+	+	3.5	0.37	0.13	0.0065	-	0.033	0.0070	-	0.012	0.12	0.018	0.021	0.041	-	0.041
75B01	37G	Mg	6.5	+	0.13	0.030	1.2	0.092	0.052	0.032	-	-	0.0019	-	0.0034	-	-	0.0036	-	-	0.016
75B02	"	"	6.4	+	0.057	0.035	1.2	0.40	0.033	0.047	-	-	0.0047	-	-	0.10	0.0015	0.011	-	-	0.032
08400	"	"	6.8	7.8	+	+	4.5	0.59	0.17	0.017	0.0048	0.021	0.0072	0.067	0.017	0.074	0.022	0.027	-	-	0.029
10401	"	"	2.0	8.3	+	0.40	6.2	0.32	0.14	0.025	0.0052	0.099	0.0099	-	0.023	-	0.0053	0.024	-	-	0.011
10402	"	"	2.8	7.5	+	0.51	4.7	0.35	0.14	0.051	0.0032	0.039	0.0079	-	0.010	-	0.024	0.027	-	-	0.012
23903	37H	"	5.4	8.1	+	+	2.4	0.88	0.095	0.14	-	0.013	0.0092	-	0.0051	-	0.061	0.030	-	-	0.048
03400	37F	"	5.1	6.0	+	0.51	5.1	0.18	0.12	0.0047	0.0039	0.076	0.0079	-	0.019	-	0.0047	0.019	-	-	-
09503	"	"	5.6	9.2	+	0.27	3.1	0.86	0.16	0.013	0.0042	0.017	0.011	-	0.0069	-	0.020	0.033	-	-	0.014
09801	37G	Mu	3.6	6.9	+	0.44	8.9	0.21	0.13	0.0025	0.0081	0.21	0.0040	-	0.099	0.080	0.0028	0.016	-	-	-
09802	"	"	3.6	6.9	+	0.12	+	0.17	0.089	0.0023	0.0099	0.21	-	-	0.17	0.10	0.0096	0.012	-	-	-
09902	"	"	3.2	6.5	+	0.45	8.0	0.19	0.15	0.0023	0.0067	0.20	0.0017	-	0.089	0.073	0.0025	0.014	-	-	-
09903	"	"	2.5	5.9	+	0.28	+	0.15	0.10	0.0034	0.0088	0.20	-	-	0.16	0.11	0.0064	0.011	-	-	0.011
10702	"	"	1.0	7.0	0.44	-	+	0.058	0.11	0.0021	0.014	0.47	-	-	0.24	0.13	-	0.0059	-	-	-
10703	"	"	0.82	4.4	+	0.11	+	0.076	0.15	0.0020	0.0068	0.30	-	-	0.14	0.082	-	-	-	-	-
10704	"	"	0.34	6.5	0.29	-	+	0.10	0.12	0.0021	0.016	0.036	-	-	0.20	0.12	-	-	-	-	-
10705	"	"	1.6	5.8	+	0.028	+	0.075	0.13	0.0023	0.011	0.33	-	-	0.23	0.12	-	0.0067	-	-	-
10706	"	"	1.3	6.8	0.39	0.014	+	0.059	0.10	-	0.012	0.39	-	-	0.21	0.13	-	0.0054	-	-	-
10707	"	"	1.3	5.5	+	0.051	+	0.071	0.15	0.0024	0.0088	0.29	-	-	0.21	0.12	-	0.0052	-	-	-
10708	"	"	1.2	5.7	+	0.060	-	0.069	0.17	0.0024	0.0083	0.30	-	-	0.18	0.11	-	0.0047	-	-	-
12601	"	"	2.1	7.7	+	0.090	+	0.16	0.15	0.0022	0.010	0.28	0.013	-	0.15	0.10	0.0028	0.012	-	-	-
12701	"	"	2.1	7.0	+	0.059	+	0.13	0.11	-	0.0086	0.28	0.0039	-	0.13	0.085	0.0018	0.011	-	-	-
12702	"	"	2.3	7.8	+	0.080	+	0.15	0.11	0.0021	0.011	0.30	0.0016	-	0.14	0.099	0.0039	0.012	-	-	-
11203	37F	Mu[a]	8.6	3.0	0.044	0.036	1.5	0.27	0.034	0.025	-	-	0.0011	-	-	-	-	0.0044	-	-	0.022
06902	37E	Mn	13.0	1.5	+	+	0.61	0.090	0.030	0.019	-	-	-	-	-	-	0.020	-	-	-	-
08902	37G	Amg[g]	7.2	7.9	+	+	4.1	0.47	0.14	0.0050	0.0045	0.026	0.030	0.032	0.012	-	0.0094	0.027	-	-	0.012
09101	"	"	6.3	+	+	0.59	4.2	0.81	0.20	0.0065	0.0072	0.013	0.0018	0.034	0.0062	-	0.015	0.041	-	-	0.020
10802	"	"	6.5	5.1	+	+	3.5	0.43	0.11	0.013	-	0.034	0.0011	-	0.015	-	0.091	0.016	-	-	0.025
10803	"	"	5.3	8.9	+	+	4.2	0.45	0.15	0.0042	0.0040	0.014	0.0013	-	0.0078	-	0.11	0.025	-	-	0.012
13601	"	"	6.8	5.2	+	+	2.5	0.53	0.11	0.019	-	0.012	0.0010	-	-	-	0.024	0.018	-	-	0.019
13701	"	"	7.4	7.6	+	0.54	1.3	0.94	0.19	0.056	-	-	0.0057	-	-	-	0.10	0.018	-	-	0.026
15102	"	"	7.2	4.6	+	+	2.1	0.51	0.091	0.053	-	0.0074	0.0021	-	-	-	0.040	0.017	-	-	0.025
22201	37H	"	3.2	6.4	+	0.59	5.1	0.44	0.12	0.055	0.0041	0.045	0.022	-	0.015	-	0.014	0.025	-	-	0.013
22403	"	"	6.4	2.1	+	+	0.65	0.36	0.029	0.23	-	-	0.0018	-	-	-	0.079	0.0065	-	-	0.023
24202	"	"	4.8	3.3	+	+	2.5	0.35	0.057	0.067	-	0.017	0.0072	-	0.0034	-	0.023	0.010	-	-	0.013
25601	"	"	5.9	5.9	+	+	3.0	0.65	0.11	0.19	-	0.017	0.0013	0.029	0.0049	-	0.044	0.023	-	-	0.024
25602	"	"	7.3	3.0	+	+	1.3	0.34	0.053	0.030	-	-	0.0028	-	-	-	0.048	0.0098	-	-	0.016
25703	"	"	7.4	6.3	+	+	1.8	0.083	0.083	0.032	-	-	0.0045	-	-	-	0.090	0.022	-	-	0.030
25802	"	"	7.0	4.5	+	+	2.1	0.48	0.084	0.054	-	0.0092	-	-	-	-	0.048	0.012	-	-	0.022
25902	"	"	6.4	4.0	+	+	1.7	0.51	0.056	0.24	-	-	0.0048	-	-	-	0.041	0.013	-	-	0.028
26002	"	"	7.4	16.0	11.0	1.4	6.5	1.4	0.27	0.011	0.0083	0.022	0.0023	0.015	0.012	-	0.015	0.054	0.012	-	0.14
26004	"	"	8.1	6.6	4.6	+	2.4	0.63	0.095	0.10	0.0020	0.0081	0.0052	-	0.0040	-	0.041	0.020	-	-	0.035
26703	"	"	3.5	7.2	+	0.48	4.6	0.31	0.15	0.0073	0.0027	0.060	-	-	0.0095	-	0.0052	0.019	-	-	-
06102	37F	"	7.3	8.3	+	+	3.6	0.61	0.21	0.0090	0.0035	0.024	0.0013	0.028	0.0080	-	0.015	0.027	-	-	0.014
11404	"	"	6.0	8.0	+	+	3.8	0.51	0.21	0.023	0.0045	0.021	0.0016	-	0.0087	-	0.0084	0.030	-	-	0.012
27902	27F	"	7.5	5.7	+	+	2.1	0.51	0.12	0.024	-	0.0077	0.0015	-	-	-	0.024	0.020	-	-	0.013
28001	"	"	5.9	4.5	+	+	2.6	0.31	0.11	0.010	-	0.013	0.0035	-	0.0060	-	0.013	0.015	-	-	0.018
28002	"	"	5.7	4.5	+	+	2.5	0.24	0.14	0.012	-	0.016	0.0023	-	0.0051	-	0.012	0.013	-	-	-
29604	"	"	3.6	9.4	+	+	4.7	0.36	0.30	0.014	0.0031	0.083	0.0011	-	0.016	-	0.0024	0.018	0.016	0.0013	0.014
13302	37G	Hg	6.6	8.3	+	+	1.9	0.54	0.13	0.0065	-	-	0.019	-	-	-	0.015	0.035	-	-	0.015
14502	"	"	7.9	7.0	+	+	1.6	0.97	0.11	0.0079	0.0023	-	0.021	-	-	-	0.017	0.044	-	-	0.017
14300	"	"	7.5	7.5	+	+	2.3	0.86	0.13	0.0082	0.0039	0.0091	0.020	0.037	0.0053	-	0.021	0.038	-	-	0.019
14900	"	"	6.5	6.7	+	+	0.85	1.0	0.15	0.016	-	-	0.048	-	-	-	0.020	0.019	-	-	0.031
15101	"	"	5.7	9.8	+	+	3.0	0.75	0.17	0.0079	0.0051	0.0063	0.023	0.027	0.0050	-	0.014	0.045	-	-	0.018
25200	37H	"	5.2	12.0	9.0	1.4	6.9	0.77	0.23	0.022	0.0076	0.031	0.011	-	0.013	-	0.010	0.047	0.0086	-	0.067

Appendix 2a (cont.)

Sample	Map sheet	Map unit	Al	Fe	Ca	Na	Mg	Ti	Mn	Ba	Co	Cr	Cu	La	Ni	Pb	Sr	V	Y	Yb	Zr
25201	37H	Hg	3.5	9.2	+	0.58	5.0	0.72	0.19	0.017	0.0051	0.025	0.0092	0.029	0.0073	-	0.0077	0.035	-	-	0.034
04802	37F	"	7.0	5.8	+	+	3.4	0.51	0.082	0.020	0.0027	0.013	0.014	0.031	0.0058	-	0.018	0.026	-	-	0.015
06903	37E	"	5.3	8.1	+	0.50	1.2	1.3	0.12	0.015	-	-	0.0050	-	-	-	0.026	0.031	-	-	0.025
10502	37G	Amn^{h}	7.7	1.6	+	+	0.45	0.18	0.024	0.062	-	-	-	-	-	-	0.035	-	-	-	0.019
10503	"	"	7.2	4.3	+	+	2.4	0.36	0.068	0.034	-	0.016	0.0010	-	0.0066	-	0.044	0.013	-	-	0.014
22101	37H	"	7.4	5.4	+	+	1.2	0.43	0.11	0.014	-	-	0.010	-	-	-	0.023	0.014	-	-	0.019
27301	"	"	6.5	1.5	+	+	0.30	0.13	0.022	0.054	-	-	-	-	-	-	0.012	-	-	-	-
07800	37G	Ma	6.7	0.87	+	+	0.68	0.085	0.025	0.014	-	-	0.0028	-	-	-	0.0083	-	-	-	0.013
12501	"	"	6.7	3.2	+	+	1.8	0.28	0.054	0.050	-	0.013	0.0016	-	0.0030	-	0.035	0.010	-	-	0.015
14704	"	"	5.2	6.6	+	+	0.62	0.80	0.14	0.057	-	-	0.0038	-	-	-	0.013	0.017	-	-	0.031
23703	37H	"	5.4	0.46	0.19	+	0.52	0.034	0.018	0.015	-	-	-	-	-	-	0.0017	-	-	-	-
23102	37G	Amn^{i}	2.5	-	0.062	0.29	0.050	-	-	0.083	-	-	-	-	-	-	0.0088	-	-	-	-
23902	37H	"	6.8	1.4	0.56	+	0.30	0.12	-	+	-	-	0.0018	-	-	-	0.069	-	-	-	-
27002	"	"	7.4	3.9	+	+	1.6	0.44	0.056	0.042	-	-	0.0029	-	-	-	0.040	0.012	-	-	0.019
27004	"	"	7.5	2.8	+	+	0.79	0.19	0.032	0.22	-	-	0.0018	-	-	-	0.044	0.0071	-	-	0.019
04102	37F	"	5.5	0.36	0.81	+	0.14	0.052	-	0.20	-	-	-	-	-	-	0.031	-	-	-	-
11602	"	"	7.8	0.56	0.81	+	0.27	0.051	0.013	0.0098	-	-	-	-	-	-	0.013	-	-	-	0.011
11601	"	"	6.9	0.43	0.41	+	0.063	-	-	0.066	-	-	-	-	-	-	0.0068	-	-	-	-
28204	27F	"	6.2	0.81	0.35	+	0.13	0.061	-	0.12	-	-	-	-	-	-	0.022	-	-	-	0.012
28602	"	"	7.0	1.7	+	+	0.43	0.19	0.026	0.058	-	-	-	-	-	-	0.026	0.0034	-	-	0.023
29401	"	"	6.5	2.1	+	+	0.60	0.28	0.029	0.042	-	-	0.0011	-	-	-	0.018	0.0054	-	-	0.035
15100	37G	Amg^{j}	6.4	0.48	0.84	+	0.13	0.056	-	0.057	-	-	-	-	-	-	0.016	-	-	-	-
08100	"	"	5.7	0.73	0.32	+	0.14	0.069	0.011	0.042	-	-	-	-	-	-	0.012	-	-	-	0.011
08901	"	"	7.6	0.73	+	+	0.18	0.077	0.012	0.22	-	-	-	-	-	-	0.079	-	-	-	0.012
09402	"	"	8.4	1.3	+	+	0.38	0.12	0.019	0.040	-	-	-	-	-	-	0.047	-	-	-	0.013
13602	"	"	7.0	0.55	0.20	+	0.33	0.048	0.011	0.21	-	-	-	-	-	-	0.023	-	-	-	-
15301	"	"	7.2	2.1	+	+	0.49	0.17	0.021	0.14	-	-	0.0013	-	-	-	0.040	0.0037	-	-	0.022
22701	"	"	7.4	0.58	+	+	0.32	0.13	-	0.072	-	-	-	-	-	-	0.039	-	-	-	0.011
22702	"	"	7.3	4.5	+	+	2.8	0.45	0.092	0.012	-	0.0050	0.0012	-	-	-	0.052	0.015	-	-	0.021
22704	"	"	6.6	0.56	+	+	0.21	0.077	-	0.10	-	-	-	-	-	-	0.035	-	-	-	-
22401	37H	"	6.7	5.7	+	+	2.5	0.57	0.095	0.042	-	0.0086	0.064	0.028	-	-	0.094	0.018	-	-	0.043
24000	"	"	7.9	1.2	+	+	0.41	0.16	0.017	0.036	-	-	0.0016	-	-	-	0.041	-	-	-	0.012
25702	"	"	5.3	0.43	0.51	+	0.20	0.078	-	0.15	-	-	-	-	-	-	0.029	-	-	-	-
25903	"	"	6.3	2.0	0.75	+	0.76	0.31	0.020	0.12	-	-	0.0021	-	-	-	0.034	0.0061	-	-	0.028
27403	"	"	6.2	0.95	0.86	+	0.17	0.089	0.013	0.063	-	-	-	-	-	-	0.011	-	-	-	-
04801	37F	"	6.3	0.71	0.33	+	0.52	0.061	-	0.12	-	-	-	-	-	-	0.031	-	-	-	-
05901	"	"	7.6	1.4	+	+	0.28	0.15	0.018	0.047	-	-	0.0025	-	-	-	0.019	-	-	-	0.011
06001	"	"	8.4	1.2	+	+	0.47	0.15	0.020	0.073	-	-	-	-	-	-	0.036	-	-	-	0.017
07002	37E	"	5.7	3.1	+	+	1.6	0.30	0.047	0.065	-	0.015	0.0017	-	-	-	0.023	0.0080	-	-	-
11702	"	"	6.5	3.4	+	+	1.0	0.34	0.045	0.049	-	-	0.0031	-	-	-	0.022	0.0080	-	-	0.029
28501	27F	"	6.2	2.4	+	+	0.47	0.35	0.028	0.092	-	-	0.0015	-	-	-	0.020	0.0072	0.0087	-	0.062
29703	"	"	5.9	1.0	0.73	+	0.18	0.12	-	0.056	-	-	-	-	-	-	0.016	-	-	-	0.020
08002	37G	Amg^{l}	7.0	1.9	+	+	0.23	0.16	0.018	0.12	-	-	-	-	-	-	0.027	-	-	-	0.030
09102	"	"	6.8	1.5	+	+	0.60	0.17	0.020	0.055	-	-	0.0046	-	-	-	0.014	-	-	-	0.014
09401	"	"	7.8	1.5	+	+	0.14	0.075	0.014	0.057	-	-	-	-	-	-	0.021	-	-	-	0.022
09701	"	"	7.3	0.25	+	+	0.11	0.033	-	0.0051	-	-	-	-	-	-	0.012	-	-	-	-
10801	"	"	9.2	1.4	+	+	0.14	0.057	-	0.017	-	-	-	-	-	-	0.053	-	-	-	0.011
13003	"	"	6.8	1.0	+	+	0.32	0.14	0.013	0.015	-	-	0.0064	-	-	-	0.031	-	-	-	0.057
13004	"	"	7.4	0.95	0.73	+	0.24	0.064	-	0.13	-	-	-	-	-	-	0.035	-	-	-	0.013
13702	"	"	7.4	0.71	0.89	+	0.17	0.084	0.015	0.14	-	-	-	-	-	-	0.055	-	-	-	0.011
25701	37H	"	5.8	-	0.33	+	0.065	0.030	-	0.042	-	-	-	-	-	-	0.014	-	-	-	-
25603	"	"	8.3	0.32	0.58	+	0.11	0.039	-	0.29	-	-	-	-	-	-	0.063	-	-	-	-
26005	"	"	5.2	0.52	0.28	+	0.20	0.089	-	0.028	-	-	-	-	-	-	0.0076	-	-	-	-
26702	"	"	7.0	1.6	+	+	0.60	0.18	0.018	0.038	-	-	-	-	-	-	0.030	0.0033	-	-	0.017
09502	37F	"	6.7	1.3	0.74	+	0.46	0.14	0.033	0.10	-	-	-	-	-	-	0.0075	-	0.0098	-	0.020
06602	37E	"	6.3	0.87	+	+	0.22	0.11	0.011	0.059	-	-	-	-	-	-	0.018	-	-	-	-
28702	27F	"	6.6	-	0.25	+	-	0.028	-	0.017	-	-	-	-	-	-	0.0071	-	-	-	-
29501	"	"	7.1	3.3	+	+	1.4	0.52	0.051	0.021	-	-	0.0010	-	-	-	0.021	0.011	-	-	0.020
29603	"	"	6.3	0.42	0.70	+	0.18	0.061	-	0.052	-	-	-	-	-	-	0.015	-	-	-	0.039
29801	"	"	6.3	0.42	0.45	+	0.066	0.056	-	0.050	-	-	-	-	-	-	0.014	-	-	-	-
08602	37G	Ag^{k}	7.0	6.8	+	+	1.9	0.34	0.076	0.040	-	0.021	0.0076	-	0.011	-	0.021	0.012	-	-	0.014
10903	"	"	7.2	0.71	+	+	0.39	0.062	0.015	0.11	-	-	-	-	-	-	0.020	-	-	-	0.013
00102	37C,D	"	6.9	0.35	0.79	+	0.10	0.024	-	0.024	-	-	-	-	-	-	0.0057	-	-	-	-

Appendix 2a (cont.)

Sample	Map sheet	Map unit	Al	Fe	Ca	Na	Mg	Ti	Mn	Ba	Co	Cr	Cu	La	Ni	Pb	Sr	V	Y	Yb	Zr
00402	37C,D	Ag^{x}	6.2	0.43	0.23	+	3.2	-	0.12	0.0020	-	-	-	-	-	-	-	-	-	-	-
01701	"	"	6.8	0.50	0.33	+	0.22	0.057	-	0.051	-	-	0.0011	-	-	-	0.0090	-	-	-	-
08500	37G	Ag^{c}	6.6	0.23	0.39	+	0.11	0.033	-	0.019	-	-	-	-	-	-	0.0047	-	-	-	-
08800	"	"	6.1	0.28	0.46	+	0.073	0.026	-	0.0058	-	-	-	-	-	-	0.0023	-	0.011	-	0.011
10501	"	"	6.7	-	0.054	+	-	-	-	0.014	-	-	-	-	-	-	0.0048	-	-	-	-
14102	"	"	8.7	0.33	0.069	+	0.090	0.028	-	0.23	-	-	-	-	-	-	0.052	-	-	-	-
11402	37F	"	6.7	1.5	0.87	+	0.55	0.18	0.018	0.18	-	-	-	-	-	-	0.034	-	-	-	-
12201	"	"	4.0	6.3	+	+	5.3	0.36	0.11	0.013	0.0033	0.072	0.0014	-	0.031	-	0.040	0.017	-	-	0.017
05502	37E	"	5.8	-	0.17	+	0.079	-	-	0.059	-	-	-	-	-	-	0.0075	-	-	-	-
06700	"	"	6.8	-	0.85	+	0.081	0.033	-	0.050	-	-	-	-	-	-	-	-	-	-	-
32101	27F	"	6.1	0.83	0.80	+	0.27	0.12	0.011	0.19	-	-	-	-	-	-	0.029	-	-	-	-
32102	"	"	8.7	1.4	+	+	0.34	0.17	0.015	0.047	-	-	0.0010	-	-	-	0.038	-	-	-	0.014
00602	37D	"	7.3	0.43	0.26	+	0.061	-	0.080	0.0020	-	-	-	-	-	-	-	-	-	-	-
00704	"	"	9.0	0.97	0.18	+	0.77	0.18	0.068	0.13	-	0.021	-	-	-	-	0.013	-	-	-	-
01100	"	"	5.6	0.87	0.25	+	0.40	0.096	0.012	0.038	-	-	0.0014	-	-	-	0.0061	-	-	-	0.013
01901	"	"	6.0	0.83	0.87	+	0.15	0.097	-	0.050	-	-	-	-	-	-	0.011	-	-	-	0.020
01902	"	"	5.5	-	0.52	0.58	0.076	-	-	0.023	-	-	-	-	-	-	0.0077	-	-	-	-
02100	"	"	6.3	0.55	0.69	+	0.18	0.092	0.010	0.038	-	-	-	-	-	-	0.010	-	-	-	0.015
02200	"	"	7.5	0.48	0.53	+	0.20	0.13	0.011	0.084	-	-	-	-	-	-	0.015	-	-	-	0.010
02301	"	"	6.4	0.37	0.17	+	0.091	-	0.19	0.0022	-	-	-	-	-	-	-	-	-	-	-
13801	37G	Agp	8.7	2.5	+	+	1.1	0.35	0.035	+	-	-	0.0012	-	-	-	0.085	0.0078	-	-	0.049
13803	"	"	8.7	2.7	0.28	+	3.0	0.12	0.039	0.0094	-	-	-	-	-	-	0.0080	0.0030	-	-	-
13901	"	"	7.6	1.5	0.56	+	0.44	0.27	0.030	0.017	-	-	-	-	-	-	0.0080	0.0039	-	-	0.075
13902	"	"	8.7	1.7	0.60	+	0.42	0.25	0.026	0.018	-	-	-	-	-	-	0.0077	0.0048	-	-	0.095
14001	"	"	7.6	0.69	+	+	0.25	0.12	0.013	0.18	-	-	-	-	-	-	0.069	-	-	-	0.018
14002	"	"	7.3	2.0	+	+	0.84	0.27	0.030	0.17	-	-	0.0014	-	-	-	0.067	0.0052	-	-	0.019
24902	37H	"	6.7	2.1	+	+	0.66	0.36	0.026	0.18	-	-	0.0034	-	-	-	0.061	0.0055	-	-	0.014
25000	"	"	7.1	1.8	+	+	0.68	0.31	0.027	0.12	-	-	-	-	-	-	0.058	0.0052	-	-	0.018
25202	"	"	6.4	2.0	0.80	+	0.76	0.27	0.034	0.11	-	-	-	-	-	-	0.025	0.0054	-	-	0.029
25301	"	"	6.9	3.5	+	+	1.6	0.46	0.054	0.068	-	0.0040	0.0019	-	-	-	0.041	0.010	-	-	0.024
25302	"	"	7.5	2.8	+	+	1.3	0.37	0.043	0.081	-	0.0031	0.0012	-	-	-	0.055	0.0093	-	-	0.030
25801	"	"	6.0	0.52	0.33	+	0.077	0.070	-	0.013	-	-	-	-	-	-	0.0068	-	-	-	0.012
25901	"	"	6.6	4.3	+	+	0.94	0.58	0.047	0.22	-	-	0.0025	-	-	-	0.043	0.015	-	-	0.069
26100	"	"	6.4	3.5	+	+	1.1	0.53	0.045	0.18	-	-	0.0033	-	-	-	0.046	0.013	-	-	0.042
26501	"	"	5.9	1.3	0.96	+	0.58	0.16	0.029	0.12	-	-	-	-	-	-	0.032	-	-	-	0.015
11401	37F	"	7.7	3.1	+	+	1.0	0.30	0.050	0.076	-	-	-	-	-	-	0.042	0.0085	-	-	0.027
11300	"	"	6.9	1.3	+	+	0.54	0.14	0.019	0.058	-	-	-	-	-	-	0.035	-	-	-	-
02302	37D	"	6.8	2.2	+	+	0.91	0.27	0.044	0.084	-	-	0.0013	-	-	-	0.019	0.0058	-	-	0.013
26202	37H	"	5.6	1.1	0.69	+	0.38	0.16	0.023	0.037	-	-	-	-	-	-	0.011	-	-	-	0.020
26204	"	"	5.9	0.78	0.67	+	0.30	0.13	0.017	0.057	-	-	-	-	-	-	0.013	-	-	-	0.011
26301	"	"	6.0	2.3	0.84	+	0.38	0.53	0.030	0.26	-	-	0.0031	-	-	-	0.026	0.0085	-	-	0.088
26302	"	"	6.4	2.0	0.95	+	0.40	0.46	0.032	0.26	-	-	-	-	-	-	0.029	0.0079	-	-	0.092
26303	"	"	6.1	2.0	0.92	+	0.43	0.47	0.032	0.25	-	-	-	-	-	-	0.029	0.0074	-	-	0.091
26801	"	"	6.1	2.0	+	+	0.74	0.34	0.019	0.089	-	-	-	-	-	-	0.033	0.0052	-	-	0.014
26802	"	"	5.6	4.6	+	+	1.1	0.81	0.056	0.048	-	-	0.0047	-	-	-	0.028	0.019	-	-	0.049
26803	37H	Ack	6.4	1.9	+	+	0.73	0.27	0.023	0.12	-	0.0040	-	-	-	-	0.038	0.0038	-	-	0.017
27101	"	"	7.7	1.0	+	+	0.29	0.11	0.019	0.066	-	-	-	-	-	-	0.044	-	-	-	0.013
27103	"	"	7.8	0.93	+	+	0.26	0.098	0.016	0.057	-	-	-	-	-	-	0.044	-	-	-	0.011
04401	37F	"	7.3	0.63	0.49	+	0.14	0.091	0.015	0.18	-	-	0.0011	-	-	-	0.016	-	-	-	-
04502	"	"	5.3	0.44	0.42	+	0.074	0.066	-	0.011	-	-	-	-	-	-	0.0024	-	-	-	0.016
05602	37E	"	8.0	0.89	+	+	0.33	0.13	0.011	0.024	-	-	-	-	-	-	0.035	-	-	-	0.017
11900	"	"	7.8	2.3	+	+	0.62	0.26	0.028	0.041	-	-	0.0019	-	-	-	0.050	0.0062	-	-	0.025
10200	37G	M	6.5	6.2	+	+	2.2	0.69	0.10	0.082	-	0.0077	0.0057	-	-	-	0.048	0.028	-	-	0.030
24507	37F	"	6.8	5.0	+	+	2.8	0.48	0.091	0.023	-	0.013	0.0085	-	0.0081	-	0.024	0.016	-	-	0.018
24603	"	"	3.3	5.0	+	0.52	7.0	0.33	0.24	0.0028	-	0.0074	0.0013	-	-	-	0.0014	0.010	-	-	0.011
24605	"	"	5.3	3.6	+	+	4.5	0.38	0.16	0.069	-	0.014	-	-	0.0054	-	0.0064	0.011	-	-	0.017
15001	37G	M^{l}	7.4	2.5	+	+	1.0	0.31	0.042	0.065	-	0.0032	0.0012	-	-	-	0.043	0.0074	-	-	0.020
15002	"	"	7.5	2.9	+	+	1.3	0.36	0.050	0.031	-	0.0033	0.0029	-	-	-	0.041	0.0093	-	-	0.021
15003	"	"	7.2	3.5	+	+	1.2	0.59	0.038	0.13	-	-	0.0040	-	-	-	0.066	0.012	-	-	0.028
12405	37F	"	6.5	2.5	0.95	+	1.3	0.30	0.030	0.063	-	-	-	-	-	-	0.0086	0.0055	-	-	0.042
75D01	37G	Ms	7.5	2.1	0.071	0.16	0.92	0.14	0.015	0.24	-	-	-	-	-	-	0.0012	-	-	-	0.019
75D02	"	"	7.4	2.3	0.094	0.15	0.99	0.16	0.019	0.25	-	-	-	-	0.0097	-	0.0014	0.0029	-	-	0.019
09301	"	"	8.2	4.0	+	+	2.0	0.43	0.082	0.010	-	0.0068	0.0031	-	0.0049	-	0.025	0.016	-	-	0.016

Appendix 2a (cont.)

Sample	Map sheet	Map unit	Al	Fe	Ca	Na	Mg	Ti	Mn	Ba	Co	Cr	Cu	La	Ni	Pb	Sr	V	Y	Yb	Zr
09302	37G	Ms	9.0	2.4	+	+	1.2	0.33	0.041	0.046	-	-	0.0033	-	-	-	0.017	0.0089	-	-	0.017
09304	"	"	8.7	1.8	+	+	1.1	0.18	0.033	0.027	-	-	-	-	-	-	0.0190	-	-	-	0.020
10008	"	"	7.2	2.4	0.10	0.21	1.4	0.18	0.014	0.061	-	0.0082	-	-	-	-	0.0025	0.0068	-	-	0.010
10011	"	"	7.1	2.4	0.044	0.19	0.85	0.16	-	0.073	-	0.0086	0.0024	-	-	-	0.0023	0.0056	-	-	-
10609	"	"	6.4	3.4	+	+	0.28	0.30	0.084	0.069	-	-	-	-	-	-	0.017	-	-	-	0.046
10610	"	"	7.9	1.4	+	+	0.61	0.17	0.023	0.043	-	-	-	-	-	-	0.032	-	-	-	0.015
10901	"	"	8.1	5.2	+	0.58	0.86	0.57	0.17	0.0047	-	-	0.0016	0.026	-	-	0.023	0.028	-	-	0.016
10904	"	"	7.5	4.5	+	+	1.8	0.20	0.038	0.038	-	-	0.0049	-	-	-	0.014	-	-	-	0.018
11000	"	"	8.2	2.9	+	+	0.89	0.27	0.020	0.029	-	-	0.0073	-	-	-	0.027	0.0074	-	-	0.019
12502	"	"	6.1	4.0	+	+	2.5	0.35	0.062	0.058	-	0.020	0.0020	-	0.0070	-	0.031	0.012	-	-	0.016
14601	"	"	7.2	3.2	+	+	1.2	0.32	0.063	0.11	-	0.0073	0.0017	-	-	-	0.044	0.0098	-	-	0.025
14602	"	"	7.5	3.2	+	+	1.1	0.33	0.062	0.10	-	0.0078	0.0015	0.028	-	-	0.048	0.010	-	-	0.020
14701	"	"	0.34	+	+	0.033	0.55	0.024	0.054	0.0020	-	0.0050	0.0039	-	-	0.078	-	0.0045	-	-	0.015
14702	"	"	5.3	6.5	+	+	0.74	0.84	0.12	0.065	-	-	0.0020	-	-	-	0.017	0.018	-	-	0.033
14703	"	"	0.95	+	+	0.12	1.0	0.044	0.10	0.0050	-	0.0044	0.0025	-	-	0.082	-	0.0049	-	-	0.011
23701	37H	"	5.7	2.1	+	+	1.2	0.22	0.038	0.031	-	0.0045	0.0032	-	-	-	0.015	0.0062	-	-	0.031
09501	37F	"	6.9	9.9	0.70	0.22	4.7	0.72	0.14	0.061	0.0045	0.018	0.0026	-	0.0097	0.075	0.0057	0.033	-	-	0.015
11206	"	"	7.3	2.7	0.96	+	1.5	0.18	0.053	0.044	-	-	-	-	-	-	0.0077	-	-	-	0.012
11504	"	"	6.0	6.1	+	+	1.2	0.71	0.072	0.041	-	-	0.0022	-	-	-	0.014	0.034	-	-	0.017
12402	"	"	5.4	2.8	0.59	+	2.1	0.30	0.038	0.042	-	-	-	-	-	-	0.0041	0.0073	-	-	0.056
12403	"	"	6.2	3.1	+	+	0.56	0.39	0.060	0.090	-	-	0.0021	-	-	-	0.016	0.0068	-	-	0.036
24501	"	"	7.6	4.2	+	+	2.1	0.48	0.067	0.042	-	0.014	0.0012	-	0.0077	-	0.029	0.016	-	-	0.017
24502	"	"	7.3	4.1	0.93	+	1.9	0.56	0.12	0.044	-	0.013	0.0041	-	0.0061	-	0.024	0.016	-	-	0.020
24506	"	"	7.0	5.8	0.52	+	2.6	0.39	0.076	0.035	-	0.027	0.0050	-	0.0059	-	0.0058	0.015	-	-	0.013
24508	"	"	6.2	2.2	+	+	0.93	0.25	0.031	0.095	-	-	0.0018	-	-	-	0.035	0.0048	-	-	-
24601	"	"	6.4	4.1	+	+	1.8	0.47	0.086	0.019	-	-	0.0014	-	-	-	0.039	0.014	-	-	0.016
24701	"	"	6.8	1.9	0.61	+	0.77	0.55	0.026	0.12	-	-	0.0021	-	-	-	0.012	0.012	-	-	0.023
24702	"	"	6.8	2.1	0.98	+	0.99	0.46	0.043	0.063	-	-	0.0012	-	-	-	0.016	0.0099	-	-	0.020
24703	"	"	6.3	5.3	+	+	1.8	0.73	0.067	0.036	-	-	0.0062	-	-	-	0.019	0.023	-	-	0.020
24704	"	"	6.4	5.4	+	+	1.7	0.69	0.067	0.014	-	-	0.0059	-	-	-	0.026	0.023	-	-	0.018
24801	"	"	7.0	7.8	0.16	+	0.21	0.74	-	0.054	-	0.031	0.0015	-	-	-	0.0065	0.0097	-	-	0.016
24802	"	"	8.1	+	0.035	0.41	0.24	0.71	-	0.028	-	0.030	0.0015	-	-	-	0.0018	0.012	-	-	0.028
24804	"	"	6.9	4.2	+	+	1.4	0.37	0.068	0.042	-	0.018	0.030	-	0.0067	-	0.021	0.013	-	-	0.016
24809	"	"	10.0	2.3	0.035	0.096	0.58	0.30	-	0.027	-	-	-	-	-	-	-	0.0038	-	-	0.017
05501	37E	"	7.4	3.7	+	+	2.2	0.41	0.085	0.037	-	0.017	0.0010	-	0.0039	-	0.028	0.012	-	-	0.026
00101	37C	"	5.7	5.0	0.85	+	1.0	0.24	0.019	0.027	-	0.0085	0.0016	-	-	-	0.010	0.0078	-	-	0.012
00403	"	"	5.8	6.9	+	0.51	1.2	0.29	0.059	0.024	-	0.017	0.0058	-	0.0039	-	0.0098	0.013	-	-	0.012
75A01	37G	Mq	6.1	5.0	0.24	0.041	1.3	0.45	0.029	0.099	-	-	0.0016	-	-	-	0.0012	0.0083	-	-	0.025
75A02	"	"	6.9	5.2	0.24	0.043	1.3	0.41	0.030	0.077	-	-	0.0020	-	-	-	0.0013	0.0085	-	-	0.032
75C01	"	"	7.1	6.4	0.23	0.044	1.7	0.48	0.050	0.070	-	-	0.0058	-	-	-	-	0.012	-	-	0.071
75C02	"	"	9.2	9.7	0.28	0.075	2.5	0.59	0.062	0.12	-	0.0029	0.0077	-	0.0036	-	0.0017	0.016	-	-	0.059
76A01	"	"	6.6	0.52	0.27	+	0.30	0.020	0.013	0.021	-	-	0.0024	-	-	-	0.0028	-	-	-	0.011
76A02	"	"	6.4	-	0.23	+	0.14	-	-	0.020	-	-	-	-	-	-	0.0021	-	-	-	-
76A03	"	"	5.8	-	0.30	+	0.091	-	-	0.012	-	-	0.0064	-	-	-	0.0018	-	-	-	-
10902	"	"	8.3	1.4	+	+	0.54	0.18	0.030	0.028	-	-	0.0011	-	-	-	0.020	-	-	-	0.020
11205	37F	"	6.8	2.7	+	+	0.90	0.28	0.10	0.040	-	0.0056	-	-	-	-	0.0079	0.0099	-	-	0.020
11502	"	"	8.5	0.56	+	+	0.24	0.054	0.018	0.031	-	-	-	-	-	-	0.043	-	-	-	0.011
26702	37H	Amg^{m}	5.4	2.6	+	+	1.0	0.24	0.029	0.029	-	0.0098	0.0043	-	-	-	0.026	0.0066	-	-	0.015
07001	37E	"	6.0	4.5	+	+	2.5	0.33	0.069	0.081	-	0.024	0.0047	-	0.0054	-	0.030	0.014	-	-	0.021
03600	37F	Aps	8.7	+	+	0.54	2.4	0.39	0.12	0.042	-	0.22	0.0072	-	-	-	0.013	0.020	-	-	0.031
01004	37C,D	"	4.9	1.6	+	0.58	1.5	0.28	-	0.076	-	0.0064	0.0056	-	0.0070	-	0.0079	0.032	-	-	0.014
01005	"	"	5.3	0.97	+	+	1.5	0.29	-	0.074	-	0.0097	0.0071	-	-	-	0.0076	0.036	-	-	0.012
01201	"	"	6.0	2.9	0.68	+	0.94	0.31	0.029	0.047	-	0.0075	0.0017	-	-	-	0.015	0.0077	-	-	0.016
01202	"	"	0.02	0.06	-	-	-	0.011	0.0024	-	-	0.013	0.013	-	-	-	0.013	-	-	-	-
01300	37A	"	5.1	1.8	0.41	+	0.64	0.17	0.015	0.044	-	0.0041	0.0014	-	-	-	0.0085	-	-	-	0.016
01501	37A	Aps	5.4	1.7	0.60	+	0.60	0.21	0.015	0.041	-	0.0048	0.0016	-	-	-	0.0095	-	-	-	0.013
01503	"	"	8.2	4.6	0.80	+	1.6	0.37	0.042	0.079	-	0.013	0.0028	-	-	-	0.0087	0.015	-	-	0.014
01702	37C,D	"	6.5	4.0	0.61	+	1.3	0.37	0.050	0.016	-	0.011	0.0039	-	-	-	0.0051	0.013	-	-	0.042
24604	37F	Ms^{n}	2.1	2.0	+	0.038	7.3	0.084	0.43	0.0024	-	0.0030	-	0.078	-	-	0.0078	-	-	-	-
01001	37C	Apm	0.34	-	+	0.060	1.5	0.059	0.022	0.0020	-	-	-	0.079	-	-	0.013	-	-	-	-
01002	"	"	3.2	1.2	+	0.47	3.9	0.23	0.035	0.0058	-	0.0031	-	-	-	-	0.0055	0.0059	-	-	0.022
01003	"	"	0.38	0.25	+	0.032	5.8	0.059	0.021	0.0072	-	-	-	0.063	-	-	0.0098	-	-	-	-
07501	37G	Mif^{o}	0.44	+	-	-	0.12	0.030	0.036	0.0019	0.0050	0.0074	0.0035	-	0.0063	0.10	0.0015	0.011	0.0096	0.0015	0.011

Appendix 2a (cont.)

Sample	Map sheet	Map unit	Al	Fe	Ca	Na	Mg	Ti	Mn	Ba	Co	Cr	Cu	La	Ni	Pb	Sr	V	Y	Yb	Zr
07502	37G	Mif^{o}	0.55	+	0.028	0.015	0.12	0.036	0.045	0.0025	0.0060	0.0094	0.0039	-	0.0073	0.14	0.0017	0.014	0.012	0.0023	0.012
07504	"	"	0.42	+	0.024	0.012	0.11	0.035	0.047	0.0029	0.0060	0.0097	0.0033	-	0.0075	0.11	0.0020	0.012	0.013	0.0016	0.012
07505	"	"	0.31	+	-	-	0.093	0.029	0.045	0.0021	0.0045	0.010	0.0030	-	0.0058	0.086	0.0014	0.0089	0.0082	0.0010	-
07506	"	"	0.43	+	0.025	0.014	0.11	0.036	0.033	0.0024	0.0061	0.0093	0.0032	-	0.0084	0.10	0.0019	0.0012	0.0098	0.0018	0.012
07508	"	"	0.34	+	-	-	0.16	0.031	0.084	0.0025	0.0053	0.0093	0.0029	-	0.0074	0.095	0.0025	0.012	0.0087	0.0012	0.019
10002	"	"	0.56	+	0.39	-	0.64	0.023	0.014	0.0036	-	0.0037	0.0015	-	-	0.082	0.0023	0.0043	-	-	-
10004	"	"	0.80	+	0.40	0.011	0.31	0.028	0.057	0.0046	0.0022	0.0043	0.0020	-	-	0.070	0.0015	0.0052	-	-	-
10006	"	"	0.43	+	0.74	0.012	0.45	0.028	0.040	0.0028	0.0027	0.0047	0.0022	-	-	0.077	0.0030	0.0047	-	-	-
10007	"	"	0.35	+	0.39	0.030	2.0	0.024	0.21	0.0034	-	0.0033	0.0014	-	-	0.092	-	0.0037	-	-	-
10013	"	"	1.2	+	0.60	0.013	0.82	0.087	0.37	0.0025	0.0038	0.0085	0.0028	-	0.0040	0.10	0.0021	0.011	0.011	0.0013	0.013
10601	"	"	0.46	+	0.87	0.082	3.0	0.023	0.22	0.0039	-	-	0.0011	-	-	0.087	-	-	-	-	-
10602	"	"	0.55	+	+	0.080	3.2	0.037	0.15	-	-	-	0.0011	-	-	0.080	-	-	-	-	-
10603	"	"	-	+	0.66	0.021	2.9	-	0.30	0.0022	-	-	0.0014	-	-	0.087	-	-	-	-	-
10604	"	"	0.13	+	0.52	0.011	3.3	-	0.18	-	-	-	0.0012	-	-	0.088	-	-	-	-	-
10605	"	"	0.19	+	+	0.032	1.2	-	0.029	-	-	0.0041	0.0015	-	-	0.088	-	0.0034	-	-	-
10606	"	"	0.19	+	0.59	-	1.2	0.022	0.045	0.0020	-	0.0038	0.0015	-	-	0.089	-	0.0039	-	-	0.010
10607	"	"	2.6	+	+	0.17	3.1	0.17	0.24	0.0025	-	0.0047	0.0019	-	-	0.085	0.0019	0.0076	-	-	0.013
10608	"	"	0.11	-	0.54	-	1.9	-	0.055	-	-	0.0033	0.0015	-	-	0.093	-	0.0034	-	-	0.010
10612	"	"	0.58	+	0.59	0.011	1.1	-	0.32	-	-	0.0042	0.0018	-	-	0.089	-	0.0043	-	-	-
11101	37F	"	0.45	+	0.024	-	0.15	0.022	-	-	0.0036	0.0034	0.0021	-	-	-	-	0.0039	-	-	-
11102	"	"	0.65	+	0.023	-	0.062	-	-	-	-	0.0039	0.0017	-	-	-	-	0.0039	-	-	-
11202	"	"	0.83	+	0.023	-	0.099	0.031	-	-	0.0047	0.0075	0.0030	-	0.0049	0.11	0.0012	0.011	0.0094	0.0015	0.011
11204	"	"	0.42	+	0.14	-	0.31	0.035	0.057	-	0.0057	0.0085	0.0056	-	0.0088	0.13	0.0020	0.012	0.014	0.0022	0.013
24503	"	"	0.14	+	+	0.017	0.77	0.021	0.32	-	-	0.0038	0.0012	-	-	0.079	0.0033	0.0043	-	-	-
24805	"	"	0.53	+	0.024	-	0.29	0.048	-	0.0020	0.0053	0.0091	0.0026	-	0.0065	0.11	0.0014	0.014	0.011	0.0016	0.011
24806	"	"	1.9	+	0.032	0.021	0.37	0.12	0.024	0.0023	0.0030	0.0057	0.0016	-	0.0042	0.070	-	0.010	-	-	0.011
24808	37F	"	4.3	+	0.066	0.031	1.9	0.15	0.036	0.0038	0.0027	0.0033	0.0019	-	-	-	-	0.0060	-	-	0.013
10003	37G	Mif^{p}	3.0	+	0.42	0.017	1.8	0.26	1.1	0.017	-	0.011	0.0021	-	0.0030	0.079	-	0.017	-	-	0.016
10005	"	"	0.44	+	0.22	0.072	1.8	0.032	0.14	0.011	-	0.0031	0.0013	-	-	0.083	-	0.0037	-	-	-
10010	"	"	0.61	+	0.18	0.011	0.94	0.044	0.14	-	-	0.0048	0.0020	-	-	0.073	-	0.0042	-	-	-
10016	"	"	0.37	+	0.55	-	0.56	-	0.14	0.0033	-	-	0.0011	-	-	-	0.0012	-	-	-	-
24504	37F	"	0.23	+	0.55	-	0.96	0.022	0.073	-	-	0.0076	0.0012	-	-	0.081	0.0020	0.0047	-	-	-
24807	"	"	1.8	+	-	0.014	0.21	0.18	0.020	0.0024	0.0033	0.0087	0.0015	-	0.0037	-	-	0.011	-	-	0.012
00103	37C		0.85	-	0.74	0.045	0.71	0.036	0.024	-	-	0.0030	0.0018	-	-	0.076	-	-	-	-	-
14104	37G	NAS	1.1	-	0.029	0.013	-	-	-	0.012	-	-	-	-	-	-	-	-	-	-	0.010
14105	"	"	1.4	0.25	0.024	0.016	-	0.038	-	0.016	-	-	-	-	-	-	-	-	-	-	0.032
14201	"	"	1.5	-	0.025	0.029	-	-	-	0.048	-	-	-	-	-	-	0.0014	-	-	-	-
14202	"	"	1.6	-	0.024	0.035	-	0.021	-	0.084	-	-	-	-	-	-	0.0019	-	-	-	0.015
14100	"	NAB-L	11.0	4.0	0.19	0.24	1.2	0.47	0.017	0.034	-	0.0063	0.0049	-	-	-	0.0072	0.014	-	-	0.024
14106	"	"	1.8	0.37	0.027	0.10	0.10	0.090	-	0.0072	-	-	-	-	-	-	-	-	-	-	0.048
14107	37G	NAB-L	3.5	1.5	0.043	0.47	0.24	0.095	0.024	0.021	-	-	0.0023	-	-	-	0.0018	-	-	-	0.045
14108	"	"	7.0	3.8	0.079	0.44	0.86	0.36	0.014	0.023	-	0.0041	0.0023	-	-	-	0.0044	0.010	-	-	0.032
14109	"	"	3.4	-	0.92	0.39	0.090	0.025	0.015	0.0073	-	-	-	-	-	-	-	-	-	-	0.014
14110	"	NAB-U	1.1	3.7	+	0.36	6.5	0.082	0.33	0.0044	-	0.0030	-	0.064	-	-	0.0097	-	-	-	0.018
14111	"	"	4.4	2.0	0.062	+	0.34	0.10	-	0.012	-	-	0.0022	-	-	-	0.0024	-	-	-	0.031
14112	"	"	3.7	+	0.43	+	0.76	0.14	0.59	0.027	0.0024	0.0035	0.0057	-	0.0042	-	0.0040	0.0075	0.013	-	0.036
14113	"	"	7.1	2.8	0.079	+	0.66	0.35	-	0.021	-	0.0032	0.0028	-	-	-	0.0057	0.0090	-	-	0.040
14114	"	"	1.5	0.70	0.023	0.011	0.069	-	-	0.0040	-	-	-	-	-	-	-	-	-	-	-
14115	"	"	2.8	2.0	+	0.42	0.61	0.21	0.076	0.024	-	0.0054	0.0017	0.090	-	-	0.016	0.0037	-	-	0.014
14116	"	"	7.2	+	0.24	0.36	1.8	0.32	0.033	0.014	-	0.0055	0.0051	-	0.0065	-	0.0027	0.011	0.0087	-	0.019
14117	"	"	1.8	2.1	0.20	0.16	0.21	0.021	0.034	0.0042	-	-	0.0046	-	-	-	-	-	-	-	-
14118	"	"	2.8	0.89	0.040	0.43	0.20	0.097	-	0.013	-	-	0.0023	-	-	-	0.0015	-	-	-	0.042
14119	"	"	5.8	2.0	0.061	+	0.46	0.19	-	0.012	-	-	-	-	-	-	0.0029	0.0041	-	-	0.044
14120	"	"	4.4	3.6	+	+	1.1	0.13	0.036	0.011	-	-	0.0034	-	-	-	0.0044	-	-	-	0.013
Upper*	"	"	15.0	10.0	1.0	0.60	9.0	5.0	1.25	0.30	0.35	0.50	0.15	2.5	1.0	7.0	0.40	0.70	0.80	0.125	2.0
Lower*	"	"	0.10	0.20	0.02	0.01	0.05	0.02	0.01	0.002	0.003	0.003	0.001	0.07	0.003	0.07	0.001	0.003	0.008	0.001	0.01

*Limits of reliable determination

Note: Each of Be, Ce, Zn were identified in trace amounts in 5-8 samples, chiefly in map areas 37G, 37H, and in map units Amg, Hg, NAB-U. Legend as for Appendix 4 except:+ = present in amount above the limit of, reliable determination.
- = present in amount below the limit of detection or of reliable determination.

Appendix 2b. Sample locations in UTM co-ordinates.

Sample No.	Map Sheet	Zone	Easting	Northing
00101	37C	18	457000	7745800
00102	37C	18	457000	7745800
00103	37C	18	457000	7745800
00300	37C	18	455200	7738000
00402	37C	18	454700	7724800
00403	37C	18	454700	7724800
00602	37D	18	471200	7702700
00703	37D	18	475600	7695600
00704	37D	18	475600	7695600
00801	37D	18	478200	7693800
00802	37D	18	478200	7693800
00901	37D	18	480800	7688600
00902	37D	18	480800	7688600
00903	37D	18	480800	7688600
01001	37C	18	457000	7745800
01002	37C	18	457000	7745800
01003	37C	18	457000	7745800
01004	37D	18	457000	7745800
01005	37D	18	461900	7714300
01100	37D	18	491000	7677700
01201	37D	18	499600	7667800
01202	37D	18	499600	7667800
01300	37A	18	508400	7653000
01501	37A	18	498000	7658000
01503	37A	18	498000	7658000
01701	37D	18	487600	7663000
01702	37D	18	487600	7663000
01800	37D	18	483200	7658900
01901	37D	18	481500	7663700
01902	37D	18	481500	7663700
02000	37D	18	481600	7673000
02100	37D	18	477000	7683600
02200	37D	18	461300	7690400
02301	37D	18	463000	7696700
02302	37D	18	463000	7696700
02401	37C	18	457200	7704100
02800	37C	18	442300	7727400
03201	37F	18	447100	7766800
03202	37F	18	447100	7766800
03301	37F	18	439200	7770400
03302	37F	18	439200	7770400
03400	37F	18	439000	7771600
03500	37F	18	434800	7781100
03600	37F	18	431700	7784900
03800	37F	18	425600	7790400
03901	37F	18	418100	7798400
03902	37F	18	418100	7798400
04000	37F	18	412200	7801300
04101	37F	18	417100	7808600
04102	37F	18	417100	7808600
04200	37F	18	424600	7806800
04300	37F	18	429000	7801800
04401	37F	18	433800	7796800
04501	37F	18	438500	7788300
04502	37F	18	438500	7788300
04600	37F	18	447100	7773200
04700	37F	18	452600	7769000
04801	37F	18	452400	7768600
04802	37F	18	452400	7768600
05200	37E	18	488600	7768500
05300	37E	18	480800	7781700
05401	37E	18	476200	7790900
05402	37E	18	476200	7790900
05501	37E	18	470400	7797200
05502	37E	18	470400	7797200
05601	37E	18	464000	7806700
05602	37E	18	464000	7806700
05700	37F	18	458800	7809300
05801	37F	18	452900	7814400
05802	37F	18	452900	7814400
05901	37F	18	450600	7819800
05902	37F	18	450600	7819800
06001	37F	18	457200	7825300
06101	37F	18	460200	7831200
06102	37F	18	460200	7831200
06103	37F	18	460200	7831200
06200	37E	18	467400	7828000
06301	37E	18	469800	7818400
06302	37E	18	469800	7818400
06401	37E	18	476100	7807800
06402	37E	18	476100	7807800
06500	37E	18	480100	7800700
06602	37E	18	485800	7794400
06700	37E	18	489200	7796800
06901	37E	18	502000	7770400
06902	37E	18	502000	7770400
06903	37E	18	502000	7770400
07001	37E	18	502000	7766500
07002	37E	18	502000	7766500
07501	37G	17	563300	7913700
07502	37G	17	563300	7913700
07504	37G	17	563300	7913700
07505	37G	17	563300	7913700
07506	37G	17	563300	7913700
07508	37G	17	563300	7913700
07600	37G	17	562900	7912800
07700	37G	17	563000	7912700
07800	37G	17	563300	7912500
08001	37G	17	598000	7904400
08002	37G	17	598000	7904400
08100	37G	17	597000	7903900
08200	37G	17	595700	7901400
08301	37G	17	595400	7900800
08400	37G	17	595200	7900200
08500	37G	17	594000	7898400
08602	37G	17	594800	7899000
08701	37G	17	594400	7897400
08702	37G	17	594400	7897400
08800	37G	17	594000	7896700
08901	37G	17	606800	7892400
08902	37G	17	606800	7892400
09000	37G	18	397400	7891100
09101	37G	18	406300	7898600
09102	37G	18	406300	7898600
09201	37G	18	416400	7884600
09202	37G	18	416400	7884600
09301	37G	18	411900	7881600
09302	37G	18	411900	7881600
09303	37G	18	411900	7881600
09304	37G	18	411900	7881600
09401	37G	18	424400	7879600
09402	37G	18	424400	7879600
09403	37G	18	424400	7879600
09501	37F	18	427400	7873200
09502	37F	18	427400	7873200
09503	37F	18	427400	7873200
09600	37G	18	434000	7878400
09701	37G	18	428000	7888200
09702	37G	18	428000	7888200
09801	37G	18	415500	7892500
09802	37G	18	415500	7892500
09901	37G	18	414400	7891200
09902	37G	18	414400	7891200
09903	37G	18	414400	7891200
10002	37G	18	413600	7890400
10003	37G	18	413600	7890400
10004	37G	18	413600	7890400
10005	37G	18	413600	7890400
10006	37G	18	413600	7890400
10007	37G	18	413600	7890400
10008	37G	18	413600	7890400
10009	37G	18	413600	7890400
10010	37G	18	413600	7890400
10011	37G	18	413600	7890400
10013	37G	18	413600	7890400
10016	37G	18	413600	7890400
10101	37G	18	403000	7893000
10103	37G	18	403000	7893000
10106	37G	18	403000	7893000
10200	37G	18	394800	7896400
10301	37G	17	606500	7897600
10302	37G	17	606500	7897600
10401	37G	17	606200	7894500
10402	37G	17	606200	7894500
10501	37G	18	411200	7894400
10502	37G	18	411200	7894400
10503	37G	18	411200	7894400
10601	37G	18	420100	7905800
10602	37G	18	420100	7905800
10603	37G	18	420100	7905800
10604	37G	18	420100	7905800
10605	37G	18	420100	7905800
10606	37G	18	420100	7905800
10607	37G	18	420100	7905800
10608	37G	18	420100	7905800
10609	37G	18	420100	7905800
10610	37G	18	420100	7905800
10612	37G	18	420100	7905800
10702	37G	18	422300	7906000
10703	37G	18	422300	7906000
10704	37G	18	422300	7906000
10705	37G	18	422300	7906000
10706	37G	18	422300	7906000
10707	37G	18	422300	7906000
10708	37G	18	422300	7906000
10801	37G	18	392300	7890300
10802	37G	18	392300	7890300
10803	37G	18	392300	7890300
10901	37G	18	409600	7881700
10902	37G	18	409600	7881700
10903	37G	18	409600	7881700
10904	37G	18	409600	7881700
11000	37G	18	413800	7881400
11101	37F	18	426000	7872100
11102	37F	18	426000	7872100
11103	37F	18	426000	7872100
11202	37F	18	426000	7873400
11203	37F	18	426000	7873400
11204	37F	18	426000	7873400
11205	37F	18	426000	7873400
11206	37F	18	426000	7873400
11207	37F	18	426000	7873400
11300	37F	18	437600	7857700
11401	37F	18	441700	7854600
11402	37F	18	441700	7854600
11404	37F	18	441700	7854600
11501	37F	18	452800	7842100
11502	37F	18	452800	7842100
11503	37F	18	452800	7842100
11504	37F	18	452800	7842100
11601	37F	18	453800	7833400
11602	37F	18	453800	7833400
11603	37F	18	453800	7833400
11604	37F	18	453800	7833400
11701	37E	18	465000	7832800
11702	37E	18	465000	7832800
11900	37E	18	464000	7837600
12101	37F	18	455800	7849400
12102	37F	18	455800	7849400
12201	37F	18	445600	7864500
12202	37F	18	445600	7864500
12301	37F	18	439500	7874400
12302	37F	18	439500	7874400
12401	37F	18	435100	7875800
12402	37F	18	435100	7875800
12403	37F	18	435100	7875800
12405	37F	18	435100	7875800
12501	37G	18	428400	7884200
12502	37G	18	428400	7884200
12503	37G	18	428400	7884200
12601	37G	18	419900	7885200
12701	37G	18	408900	7886100
12702	37G	18	408900	7886100
12703	37G	18	408900	7886100
12800	37G	17	600900	7893500
12901	37G	17	596200	7894700
12902	37G	17	596200	7894700
13001	37G	17	603500	7901200
13002	37G	17	603500	7901200
13003	37G	17	603500	7901200
13004	37G	17	603500	7901200
13005	37G	17	603500	7901200
13006	37G	17	603500	7901200
13101	37G	18	401800	7907600
13201	37G	18	406600	7968000
13202	37G	18	406600	7908000
13301	37G	18	412200	7912800
13302	37G	18	412200	7912800
13400	37G	18	419100	7919600
13501	37G	18	428600	7921400
13502	37G	18	428600	7921400
13601	37G	18	422400	7925000
13602	37G	18	422400	7925000
13701	37G	18	419200	7933600
13702	37G	18	419200	7933600
13703	37G	18	419200	7933600
13801	37G	18	413900	7938600
13803	37G	18	413900	7938600

Appendix 2b (cont.)

Sample No.	Map Sheet	Zone	Easting	Northing
13901	37G	18	409600	7946400
13902	37G	18	409600	7946400
14001	37G	18	400400	7954200
14002	37G	18	400400	7954200
14100	37G	18	391200	7961100
14101	37G	18	391200	7961100
14102	37G	18	391200	7961100
14104	37G	18	391200	7961100
14105	37G	18	391200	7961100
14106	37G	18	391200	7961100
14107	37G	18	391200	7961100
14108	37G	18	391200	7961100
14109	37G	18	391200	7961100
14110	37G	18	391200	7961100
14111	37G	18	391200	7961100
14112	37G	18	391200	7961100
14113	37G	18	391200	7961100
14114	37G	18	391200	7961100
14115	37G	18	391200	7961100
14116	37G	18	391200	7961100
14117	37G	18	391200	7961100
14118	37G	18	391200	7961100
14119	37G	18	391200	7961100
14120	37G	18	391200	7961100
14201	37G	17	599300	7962400
14202	37G	17	599300	7962400
14300	37G	17	598000	7958000
14501	37G	18	392200	7944200
14502	37G	18	392200	7944200
14503	37G	18	392200	7944200
14601	37G	18	402000	7935000
14602	37G	18	402000	7935000
14701	37G	18	404600	7932100
14702	37G	18	404600	7932100
14703	37G	18	404600	7932100
14704	37G	18	404600	7932100
14900	37G	18	412200	7925600
15001	37G	18	411200	7922100
15002	37G	18	411200	7922100
15003	37G	18	411200	7922100
15100	37G	18	404000	7918400
15101	37G	18	404000	7918400
15102	37G	18	404000	7918400
15301	37G	17	600800	7904700
15302	37G	17	600800	7904700
22101	37H	18	486800	7899400
22102	37H	18	486800	7899400
22201	37H	18	479400	7906400
22300	37H	18	474400	7912600
22401	37H	18	471400	7915300
22402	37H	18	471400	7915300
22403	37H	18	471400	7915300
22500	37G	18	463900	7925400
22601	37G	18	464400	7932600
22602	37G	18	464400	7932600
22701	37G	18	461600	7928500
22702	37G	18	461600	7928500
22703	37G	18	461600	7928500
22704	37G	18	461600	7928500
22800	37G	18	457000	7937600
22901	37G	18	452500	7943900
22902	37G	18	452500	7943900
23001	37G	18	447400	7949600
23003	37G	18	447400	7949600
23101	37G	18	439400	7958000
23102	37G	18	439400	7958000
23103	37G	18	439400	7958000
23201	37G	18	437600	7963600
23202	37G	18	437600	7963600
23203	37G	18	437600	7963600
23301	37G	18	445500	7967500
23302	37G	18	445500	7967500
23401	37G	18	452600	7960000
23402	37G	18	452600	7960000
23501	37G	18	458000	7953400
23600	37G	18	461900	7946200
23701	37H	18	466500	7944200
23702	37H	18	466500	7944200
23703	37H	18	466500	7944200
23800	37H	18	467400	7934800
23901	37H	18	474400	7929200
23902	37H	18	474400	7929200
23903	37H	18	474400	7929200
24000	37H	18	479400	7920700
24101	37H	18	481300	7917300
24201	37H	18	486400	7907200
24202	37H	18	486400	7907200
24300	37H	18	486900	7902100
24400	37H	18	489000	7893600
24402	37H	18	489000	7893600
24501	37F	18	454800	7869450
24502	37F	18	454800	7869450
24503	37F	18	454800	7869450
24504	37F	18	454800	7869450
24505	37F	18	454800	7869450
24506	37F	18	454800	7869450
24507	37F	18	454800	7869450
24508	37F	18	454800	7869450
24509	37F	18	454800	7869450
24601	37F	18	451850	7869800
24602	37F	18	451850	7869800
24603	37F	18	451850	7869800
24604	37F	18	451850	7869800
24605	37F	18	451850	7869800
24701	37F	18	452000	7870000
24702	37F	18	452000	7870000
24703	37F	18	452000	7870000
24704	37F	18	452000	7870000
24801	37F	18	451400	7870000
24802	37F	18	451400	7870000
24804	37F	18	451400	7870000
24805	37F	18	451400	7870000
24806	37F	18	451400	7870000
24807	37F	18	451400	7870000
24808	37F	18	451400	7870000
24809	37F	18	451400	7870000
24901	37H	18	500000	7904000
24902	37H	18	500000	7904000
25000	37H	18	504300	7899600
25100	37H	18	516800	7901500
25200	37H	18	525600	7899800
25201	37H	18	525600	7899800
25202	37H	18	525600	7899800
25301	37H	18	540700	7901600
25302	37H	18	540700	7901600
25401	37H	18	551400	7902000
25402	37H	18	551400	7902000
25403	37H	18	551400	7902000
25501	37H	18	556500	7910600
25502	37H	18	556500	7910600
25503	37H	18	556500	7910600
25504	37H	18	556500	7910600
25601	37H	18	561500	7921400
25602	37H	18	561500	7921400
25603	37H	18	561500	7921400
25701	37H	18	558600	7931800
25702	37H	18	558600	7931800
25703	37H	18	558600	7931800
25704	37H	18	558600	7931800
25801	37H	18	563700	7940600
25802	37H	18	563700	7940600
25901	37H	18	560000	7948000
25902	37H	18	560000	7948000
25903	37H	18	560000	7948000
26002	37H	18	569700	7944500
26003	37H	18	569700	7944500
26004	37H	18	569700	7944500
26005	37H	18	569700	7944500
26100	37H	18	573500	7950600
26201	37H	18	590800	7949000
26202	37H	18	590800	7949000
26203	37H	18	590800	7949000
26204	37H	18	590800	7949000
26301	37H	18	592000	7948800
26302	37H	18	592000	7948800
26303	37H	18	592000	7948800
26400	37H	18	598600	7945600
26501	37H	19	394200	7937100
26502	27G	19	394200	7937100
26503	37H	19	394200	7937100
26600	37H	18	597500	7922300
26702	37H	18	790600	7919600
26703	37H	18	790600	7919600
26801	37H	18	580300	7917000
26802	37H	18	580300	7917000
26803	37H	18	580300	7917000
26901	37H	18	571900	7914100
26902	37H	18	571900	7914100
27001	37H	18	565300	7906600
27002	37H	18	565300	7906600
27003	37H	18	565300	7906600
27004	37H	18	565300	7906600
27101	37H	18	563200	7896200
27103	37H	18	563200	7896200
27201	37H	18	556400	7890800
27202	37H	18	556400	7890800
27301	37H	18	543600	7893700
27302	37H	18	543600	7893700
27401	37H	18	527800	7894900
27403	37H	18	527800	7894900
27501	37H	18	519000	7894400
27800	27F	19	451200	7770400
27901	27F	19	457600	7775600
27902	27F	19	457600	7775600
28001	27F	19	465100	7775800
28002	27F	19	465100	7775800
28101	27F	19	470000	7783800
28102	27F	19	470000	7783800
28103	27F	19	470000	7783800
28201	27F	19	480500	7791400
28202	27F	19	480500	7791400
28203	27F	19	480500	7791400
28204	27F	19	480500	7791400
28301	27F	19	491500	7796900
28302	27F	19	491500	7796900
28401	27F	19	501900	7800000
28402	27F	19	501900	7800000
28501	27F	19	511000	7802700
28502	27F	19	511000	7802700
28601	27F	19	512400	7809000
28602	27F	19	512400	7809000
28701	27F	19	520600	7808300
28702	27F	19	520600	7808300
28801	27F	19	529700	7822900
28802	27F	19	529700	7822900
28900	27F	19	510600	7834900
29001	27F	19	497400	7837400
29002	27F	19	497400	7837400
29100	27F	19	506200	7827800
29201	27F	19	505000	7820300
29202	27F	19	505000	7820300
29300	27F	19	500000	7811700
29401	27F	19	491200	7808600
29402	27F	19	491200	7808600
29403	27F	19	491200	7808600
29501	27F	19	483000	7803600
29502	27F	19	483000	7803600
29503	27F	19	483000	7803600
29601	27F	19	470800	7799600
29602	27F	19	470800	7799600
29603	27F	19	470800	7799600
29604	27F	19	470800	7799600
29701	27F	19	465200	7791800
29702	27F	19	465200	7791800
29703	27F	19	465200	7791800
29801	27F	19	457000	7783000
29802	27F	19	457000	7783000
29900	27F	19	448600	7778300
30000	27F	19	443700	7767000
31800	27E	19	543800	7773200
31900	27F	19	539800	7783200
32000	27F	19	531000	7774500
32101	27F	19	521400	7769000
32102	27F	19	521400	7769000
75A01	37G	17	563000	7913200
75A02	37G	17	563000	7913200
75B01	37G	17	563000	7913200
75B02	37G	17	563000	7913200
75C01	37G	17	562600	7913000
75C02	37G	17	562600	7913000
75D01	37G	17	563000	7913200
75D02	37G	17	563000	7913200
76A01	37G	17	563000	7913200
76A02	37G	17	563000	7913200
76A03	37G	17	563000	7913200

APPENDIX 3

Some statistical data for spectrochemical analyses in Appendix 2, arranged by element

Element	Map unit	Location	No. of samples	Mean	Median	Mode	Minimum	Maximum	Standard deviation
Al	Amn	37E-H, 27F	52	7.0	6.8	6.4	5.2	9.9	0.91
	Amn	37G	13	7.1	7.2	7.1	5.2	8.6	0.82
	Amn	37H	15	6.9	6.6	6.8	5.6	8.0	0.72
	Amn	27F	14	6.2	6.3	6.2	5.5	6.8	0.37
	Amg	37E-H, 27F	55	7.0	6.9	6.8	5.1	9.6	0.90
	Amg	37G	17	6.7	6.6	6.4	5.1	8.3	0.97
	Amg	37H	8	6.5	6.7	6.8	5.7	7.2	0.63
	Amg	37F	11	7.6	7.5	6.8	6.6	9.6	0.96
	Amg	27F	15	6.7	6.8	6.8	5.8	7.6	0.54
	Amp	37E, G-H	9	6.8	6.6	6.4?	5.7	7.9	0.75
	Amn^{b}	27F, 37F-H	7	7.3	7.3	–	6.5	7.9	0.54
	gr-Agr^{c}	27E-F, 37E-G	17	6.9	6.9	6.5?	5.7	7.4	0.46
	gr-Agr^{c}	37C, D	9	6.6	6.4	–	5.8	8.3	0.74
	gr^{d}	37F, G	6	6.7	6.7	6.7?	6.0	7.1	0.40
	gr-Agr^{e}	27F, 37E-G	6	6.7	6.1	6.1?	5.6	8.1	0.90
	Amn^{f}	27F, 37E-H	11	5.9	6.5	6.3	2.6	8.3	1.6
	Mb	37F-H	17	5.6	5.8	5.8	2.7	8.8	1.5
	Mg	37F-H	8	5.1	5.4	6.0?	2.0	6.8	1.8
	Mu	37G	14	1.9	1.6	1.2	0.34	3.6	0.93
	Amg^{g}	27F, 37F-H	24	6.3	6.4	7.4	3.2	8.1	1.3
	Amg^{g}	37G	7	6.7	6.8	–	5.3	7.4	0.70
	Amg^{g}	37H	11	6.1	6.4	7.3?	3.2	8.1	1.6
	Hg	27F, 37E-F, 37H	9	6.1	6.5	–	3.5	7.9	1.4
	Amn^{i}	27F, 37F-H	10	6.4	6.8	6.9?	2.5	7.8	1.5
	Amg^{j}	27F, 37F-H	21	6.8	6.6	6.2	5.3	8.4	0.89
	Amg^{i}	27F, 37E-H	18	7.0	6.9	6.8	5.2	9.2	0.91
	Ag^{c}	27F, 37E-G	10	6.6	6.6	6.7	4.0	8.7	1.4
	Ag^{c}	37D	8	6.7	6.4	6.0?	5.5	9.0	1.2
	Agp	37F-H, 27G	17	7.2	7.1	–	5.9	8.7	0.89
	Agp	37H, 27G	9	6.6	6.6	6.7	5.9	7.5	0.52
	Ack	37E-F, 37H	14	6.6	6.1	–	5.3	8.0	0.94
	Ack	37H	10	6.4	6.1	6.1	5.6	7.8	0.77
	M	37F-G	4	5.5	5.5	–	3.3	6.8	1.6
	M^{l}	37F-G	4	7.2	7.3	–	6.5	7.5	0.45
	Ms	37E-H	38	6.8	7.0	6.9	0.34	10.	1.8
	Ms	37G	18	6.7	7.4	7.4	0.34	8.9	2.4
	Ms	37F	18	6.9	6.8	6.9?	5.4	10.	1.1
	Mq	37F-G	10	7.2	6.9	6.9	5.8	9.2	1.1
	APs	37C-D	8	5.2	5.3	5.3?	0.029	8.2	2.3
	APm	37C	3	1.3	3.8	–	0.34	3.2	1.6
	Mif^{o}	37F-G	28 (1–)	0.73	0.44	0.44	(–)	4.3	0.89
	Mif^{o}	37G	20 (1–)	0.56	0.43	0.44	(–)	2.6	0.54
	Mif^{o}	37F	8	1.1	0.55	–	0.14	4.3	1.4
	Mif^{s}	37F-G	6	1.1	0.48	–	0.23	3.0	1.1
	NAS	37G	4	1.4	1.5	–	1.1	1.6	0.22
	NAB	37G	16	4.3	3.5	3.5?	1.1	11.	2.6
	NAB-L	37G	5	5.3	3.5	3.5?	1.8	10.8	3.6
	NAB-U	37G	11	3.9	3.7	–	1.1	7.2	2.1
Fe	Amn	37E-H, 27F	52	2.2	1.9	1.9	0.46	7.5	1.4
	Amn	37G	13	2.9	2.5	0.80	0.73	7.5	2.1
	Amn	37H	15	2.2	2.0	0.80	0.65	5.5	1.4
	Amn	27F	14	1.8	1.8	1.8	0.46	3.5	0.79
Fe	Amg	37E-H, 27F	55	2.9	2.6	2.7	0.22	12.5	2.4
	Amg	37G	17	4.0	2.9	2.8	0.64	9.2	2.6
	Amg	37H	8	3.7	2.5	2.5?	0.33	12.5	3.8
	Amg	37F	11	2.0	1.5	1.0?	0.35	5.2	1.6
	Amg	27F	15	2.0	1.8	2.8	0.22	4.1	1.1
	Amp	37E, G-H	9	2.6	2.1	2.0?	1.3	5.6	1.4
	Amn^{b}	27F, 37F-H	7	1.9	1.4	–	0.67	5.5	1.7
	gr-Agr^{c}	27E-F, 37E-G	17	1.7	1.3	0.77	0.57	4.9	1.2
	gr-Agr^{c}	37C, 37D	9	1.6	1.3	–	0.43	3.3	0.97
	gr^{d}	37F, 37G	6	2.2	1.8	1.7?	0.38	5.2	1.6
	gr-Agr^{e}	27F, 37E-G	6	1.3	1.1	1.1?	0.31	2.3	0.72
	Amn^{f}	27F, 37E-H	11	6.1	6.2	–	2.1	8.6	2.1
	Mb	37F-H	17	7.2	7.4	7.2	0.96	9.7	2.0
	Mg	37F-H	8(2+)	7.8	8.2	7.9?	6.0	(+)	1.0
	Mu	37G	14	6.4	6.5	6.6	0.34	7.8	0.93
	Amg^{g}	27F, 37F-H	24(1+)	6.3	6.0	4.5?	2.1	(+)	2.8
	Amg^{g}	37G	7(1+)	6.5	7.7	–	4.6	(+)	1.8
	Amg^{g}	37H	11	5.9	5.9	6.3	2.1	16.	3.6
	Hg	37E-H	9	8.3	8.1	–	5.8	12.	2.0
	Amn^{i}	27F, 37F-H	10(1–)	1.6	1.5	0.54?	(–)	3.9	1.2
	Amg^{j}	27F, 37F-H	21	1.7	1.2	0.64?	0.43	5.7	1.4
	Amg^{i}	27F, 37E-H	18(2–)	1.1	0.88	–	(–)	3.3	0.77
	Ag^{c}	27F, 37E-G	10(3–)	1.5	0.30	0.28?	(–)	6.3	2.2
	Ag^{c}	37D	8(1–)	0.64	0.50	0.46?	(–)	0.97	0.24
	Agp	37F-H, 27G	17	2.2	0.20	1.6?	0.52	4.3	1.0
	Agp	37H, 27G	9	2.4	2.1	2.0?	0.52	4.3	1.2
	Ack	37E-F, 37H	14	1.6	1.1	2.0	0.44	4.6	1.1
	Ack	37H	10	1.9	2.0	2.0	0.78	4.6	1.1
	M	37F-G	4	4.9	5.0	–	3.6	6.2	1.1
	M^{l}	37F-G	4	2.9	2.6	–	2.5	3.5	0.45
	Ms	37E-H	38(3+)	3.8	3.4	2.2	1.4	(+)	1.9
	Ms	37G	18(2+)	3.2	3.2	2.3	1.4	(+)	1.3
	Ms	37F	18(1+)	4.4	4.1	4.1	1.9	(+)	2.2
	Mq	37F-G	10(2–)	3.9	1.4	–	(–)	9.7	3.2
	APs	37C-D	8	2.2	1.7	1.7?	0.067	4.6	1.5
	APm	37C	3(1–)	0.71	0.25	–	(–)	1.2	0.65
	NAB	37G	16(2+,1–)	2.3	2.0	2.1	(–)	(+)	1.2
	NAB-L	37G	5(1–)	2.4	1.5	–	(–)	4.0	1.8
	NAB-U	37G	11(2+)	2.2	2.1	2.1	0.70	(+)	1.0
Ca	Amn^{i}	27F, 37F-H	10(4+)	0.50	0.81	–	0.062	(+)	0.29
	Amg^{j}	27F, 37E-H	21(13+)	0.57	–	–	0.20	(+)	0.26
	Amg^{i}	27F, 37E-H	18(9+)	0.55	–	–	0.25	(+)	0.24
	Ag^{c}	27F, 37E-G	10(2+)	0.46	0.47	0.84	0.054	(+)	0.35
	Ag^{c}	37D	8	0.43	0.26	–	0.17	0.87	0.26
	Agp	37F-H	17(11+)	0.59	–	–	0.28	(+)	0.26
	Agp	37H, 27G	9(6+)	0.70	–	–	0.33	(+)	0.33
	Ack	37E-F, 37H	14(7+)	0.71	–	–	0.42	(+)	0.21
	Ack	37H	10(5+)	0.81	–	–	0.67	(+)	0.13
	Ms	37E-H	38(24+)	0.42	–	–	0.035	(+)	0.38
	Ms	37G	18(14+)	0.0077	–	–	0.044	(+)	0.025
	Ms	37F	18(8+)	0.55	0.96	–	0.035	(+)	0.37
	Mq	37F-G	10(3+)	0.26	0.27	0.23	0.23	(+)	0.029
	APs	37C-D	8(2+, 1–)	0.62	0.62	–	(–)	(+)	0.14
	Mif^{o}	37F-G	28(4+, 3–)	0.32	0.39	0.024	(–)	(+)	0.29
	Mif^{o}	37G	20(3+, 3–)	0.45	0.52	0.039?	(–)	(+)	0.27
	Mif^{o}	37F	8(1+)	0.047	0.025	0.023?	0.023	(+)	0.043
	Mif^{s}	37F-G	6(1–)	0.38	0.22	0.55?	(–)	0.55	0.18

Note: (1–), (2+) indicates the number of samples within the population with values below or above the limit of determination, respectively. (–), (+) indicates minimum valua below determination limit and maximum value above determination limit. Map unit symbols conform to published maps (Fig. 1); superscripts are as indicated for Appendix 4. The question mark indicates some inaccuracy in determining the position of the mode.

Appendix 3 (cont.)

Element	Map unit	Location	No. of samples	Mean	Median	Mode	Minimum	Maximum	Standard deviation
Ca	NAS	37G	4	0.026	0.025	0.024?	0.024	0.029	0.0023
	NAB	37G	16(3+)	0.18	0.079	0.079?	0.023	(+)	0.25
	NAB-L	37G	5	0.25	0.079	–	0.027	0.92	0.38
	NAB-U	37G	11(3+)	0.14	0.20	0.061?	0.023	(+)	0.14
Na	Mg	37F-H	8(2+)	0.29	0.40	–	0.030	(+)	0.22
	Mu	37G	14(2–)	0.15	0.059	0.056?	(–)	0.45	0.15
	Amg^{g}	37H	11(8–)	7.8	–	–	(–)	11.	4.5
	Hg	37E-H	9(6+)	0.83	–	–	0.50	(+)	0.51
	Ms	37E-H	38(28+)	0.22	–	–	0.033	(+)	0.16
	Ms	37G	18(11+)	0.21	–	–	0.033	(+)	0.18
	Ms	37F	18(15+)	0.24	–	–	0.096	(+)	0.16
	Mq	37F-G	10(6+)	0.051	–	–	0.041	(+)	0.016
	APs	37C-D	8(6+, 1–)	0.59	–	–	(–)	(+)	–
	APm	37C	3	0.19	0.060	–	0.032	0.47	0.24
	Mif^{o}	37F-G	28(11–)	0.034	0.011	0.011	(–)	0.17	0.042
	Mif^{o}	37G	20(6–)	0.037	0.012	0.011	(–)	0.17	0.046
	Mif^{o}	37F	8(5–)	0.023	–	–	(–)	0.031	0.0074
	Mif^{s}	37F-G	6(2–)	0.028	0.012	–	(–)	0.072	0.029
	NAS	37G	4	0.023	0.018	–	0.013	0.035	0.010
	NAB	37G	16(5+)	0.31	0.42	0.43?	0.011	(+)	0.15
	NAB-L	37G	5	0.33	0.39	–	0.10	0.47	0.15
	NAB-U	37G	11(5+)	0.29	0.43	0.43?	0.011	(+)	0.17
Mg	Amn	37E-H, 27F	52	0.78	0.56	0.50	0.12	4.0	0.76
	Amn	37G	13	1.1	0.86	0.30	0.16	3.4	1.0
	Amn	37H	15	0.83	0.56	0.65	0.24	4.0	0.92
	Amn	27F	14	0.59	0.58	0.55	0.12	1.4	0.32
	Amg	37E-H, 27F	55	1.0	0.86	0.75	0.076	5.3	0.87
	Amg	37G	17	1.3	1.3	1.3	0.11	3.4	0.81
	Amg	37H	8	1.6	1.1	1.1	0.10	5.3	1.6
	Amg	37F	11	0.64	0.42	0.30	0.13	0.18	0.55
	Amg	27F	15	0.67	0.65	0.70	0.076	1.4	0.38
	Amp	37E, 37G-H	9	0.74	0.67	0.45?	0.41	1.7	0.39
	Amn^{b}	27F, 37F-H	7	0.42	0.35	–	0.21	1.1	0.30
	gr-Agr^{c}	27E-F, 37E-G	17	0.56	0.47	0.45	0.13	1.1	0.28
	gr-Agr^{c}	37C, 37D	9	0.47	0.42	–	0.12	0.80	0.25
	gr^{d}	37F, 37G	6	0.49	0.40	–	0.13	1.0	0.30
	gr-Agr^{e}	27F, 37E-G	6	0.34	0.29	0.27?	0.11	0.58	0.18
	Amn^{f}	27F, 37E-H	11	2.8	2.8	3.6?	0.69	4.8	1.2
	Mb	37F-H	17	3.7	3.5	3.6	0.12	7.0	1.7
	Mg	37F-H	8	3.5	3.1	–	1.2	6.2	1.8
	Amg^{g}	27F, 37F-H	24	3.0	2.5	2.3	0.65	6.5	1.4
	Amg^{g}	37G	7	3.1	3.5	4.2	1.3	4.2	1.2
	Amg^{g}	37H	11	2.9	2.4	2.0?	0.65	6.5	1.8
	Hg	37E-H	9	2.9	2.3	1.6?	0.85	6.9	2.0
	Amn^{i}	27F, 37F-H	10	0.44	0.27	–	0.062	0.81	0.29
	Amg^{i}	27F, 37E-H	21	0.64	0.38	0.18?	0.13	2.8	0.75
	Amg^{i}	27F, 37E-H	18(1–)	0.31	0.18	–	(–)	1.4	0.32
	Ag^{c}	27F, 37E-G	10(1–)	0.77	0.091	0.081?	(–)	5.3	1.7
	Ag^{c}	37D	8	0.24	0.16	0.076?	0.061	0.77	0.24
	Agp	37F-H, 27G	17	0.91	0.76	0.61?	0.077	3.0	0.67
	Agp	37H, 27G	9	0.85	0.76	0.72	0.077	1.6	0.44
	Ack	37E-F, 37H	14	0.44	0.38	0.40	0.074	1.1	0.27
	Ack	37H	10	0.50	0.39	0.40	0.26	1.1	0.27
	M	37F-G	4	4.1	3.1	–	2.2	7.0	2.2
	M^{i}	37F-G	4	1.2	1.2	–	1.0	1.3	0.13
	Ms	37E-H	38	1.3	1.1	0.89	0.21	4.7	0.21
	Ms	37G	18	1.1	1.0	0.88	0.28	2.5	0.53
	Ms	37F	18	1.5	1.4	–	0.21	4.7	1.0
	Mq	37F-G	10	0.91	0.57	–	0.091	2.5	0.80

Element	Map unit	Location	No. of samples	Mean	Median	Mode	Minimum	Maximum	Standard deviation
Mg	APs	37C-D	8(1–)	1.2	0.96	–	(–)	1.6	0.42
	APm	37C	3	3.7	3.9	–	1.5	5.8	2.2
	Mif^{o}	37F-G	28	1.1	0.45	0.11	0.062	3.3	1.1
	Mif^{o}	37G	20	1.3	0.82	0.11	0.093	3.3	1.2
	Mif^{o}	37F	8	0.49	0.30	0.32?	0.062	1.9	0.59
	Mif^{s}	37F-G	6	1.1	0.95	0.95?	0.21	1.8	0.66
	NAB	37G	16	0.95	0.46	0.22?	0.069	6.5	1.5
	NAB-L	37G	5	0.49	0.24	–	0.090	1.2	0.49
	NAB-U	37G	11	1.2	0.61	–	0.069	6.5	1.8
Ti	Amn	37E-H, 27F	52	0.25	0.23	0.23	0.050	1.1	0.18
	Amn	37G	13	0.33	0.24	–	0.066	1.1	0.30
	Amn	37H	15	0.24	0.24	0.22	0.057	0.49	0.12
	Amn	27F	14	0.23	0.23	0.23	0.050	0.49	0.11
	Amg	37E-H, 27F	55	0.30	0.28	0.37, 0.22	0.047	1.1	0.20
	Amg	37G	17	0.36	0.36	0.37, 0.47	0.048	0.79	0.22
	Amg	37H	8	0.40	0.35	–	0.084	1.1	0.29
	Amg	37F	11	0.21	0.11	0.080	0.054	0.41	0.14
	Amg	27F	15	0.25	0.25	0.25	0.047	0.55	0.13
	Amp	37E, 37G-H	9	0.36	0.25	0.25?	0.18	0.73	0.20
	Amn^{b}	27F, 37F-H	7	0.22	0.19	–	0.087	0.47	0.13
	gr-Agr^{c}	27E-F, 37E-G	17	0.19	0.18	–	0.051	0.51	0.11
	gr-Agr^{c}	37C, 37D	9	0.15	0.13	0.12	0.055	0.30	0.082
	gr^{d}	37F, 37G	6	0.34	0.21	0.20?	0.040	0.96	0.33
	gr-Agr^{e}	27F, 37E-G	6	0.16	0.12	–	0.031	0.34	0.11
	Amn^{f}	27F, 37E-H	11	0.52	0.44	0.36?	0.32	0.94	0.22
	Mb	37F-H	17	0.47	0.44	0.37	0.090	0.88	0.22
	Mg	37F-H	8	0.46	0.36	–	0.092	0.88	0.29
	Mu	37G	14	0.12	0.10	–	0.058	0.21	0.053
	Amg^{g}	27F, 37F-H	24	0.54	0.48	0.51?	0.24	1.4	0.25
	Amg^{g}	37G	7	0.59	0.51	0.48?	0.43	0.94	0.20
	Amg^{g}	37H	11	0.57	0.48	0.36?	0.31	1.4	0.32
	Hg	37E-H	9	0.83	0.77	0.75?	0.51	1.3	0.25
	Amn^{i}	27F, 37F-H	10(2–)	0.17	0.093	–	(–)	0.44	0.13
	Amg^{i}	27F, 37E-H	21	0.18	0.13	0.073?	0.048	0.57	0.15
	Amg^{i}	27F, 37E-H	18	0.11	0.075	0.032?	0.028	0.52	0.11
	Ag^{c}	27F, 37E-G	10(2–)	0.77	0.091	0.030?	(–)	0.36	0.12
	Ag^{c}	37D	8(3–)	0.12	0.094	0.095?	(–)	0.18	0.037
	Agp	37F-H, 27G	17	0.29	0.27	0.26	0.070	0.58	0.14
	Agp	37H, 27G	9(1–)	0.35	0.36	0.32	(–)	0.58	0.17
	Ack	37E-F, 37H	14	0.28	0.16	0.11?	0.066	0.81	0.22
	Ack	37H	10	0.34	0.27	0.12?	0.098	0.81	0.23
	M	37F-G	4	0.47	0.41	–	0.33	0.69	0.16
	M^{i}	37F-G	4	0.39	0.32	–	0.30	0.59	0.14
	Ms	37E-H	38	0.38	0.33	0.17	0.24	0.84	0.21
	Ms	37G	18	0.28	0.20	0.17	0.024	0.84	0.19
	Ms	37F	18	0.50	0.47	0.71	0.18	0.74	0.18
	Mq	37F-G	10(2–)	0.31	0.23	0.45?	(–)	0.59	0.21
	APs	37C-D	8	0.25	0.28	0.29?	0.011	0.37	0.12
	APm	37C	3	0.12	0.10	–	0.059	0.23	0.97
	Mif^{o}	37F-G	28(6–)	0.048	0.028	0.029?	(–)	0.17	0.042
	Mif^{o}	37G	20(5–)	0.043	0.028	0.029	(–)	0.17	0.039
	Mif^{o}	37F	8(1–)	0.060	0.031	–	(–)	0.15	0.050
	Mif^{s}	37F-G	6(1–)	0.11	0.038	0.0033?	(–)	0.26	0.11
	NAS	37G	4(2–)	0.030	–	–	(–)	0.038	0.012
	NAB	37G	16(1–)	0.18	0.10	0.0094?	(–)	0.47	0.14
	NAB-L	37G	5	0.21	0.095	–	0.025	0.47	0.20
	NAB-U	37G	11(1–)	0.16	0.13	–	(–)	0.35	0.10

Appendix 3 (cont.)

Element	Map unit	Location	No. of samples	Mean	Median	Mode	Minimum	Maximum	Standard deviation
Mn	Amn	37E-H, 27F	52(5–)	0.034	0.025	0.023?	(–)	0.15	0.027
	Amn	37G	13(2–)	0.051	0.035	0.017?	(–)	0.15	0.044
	Amn	37H	15	0.031	0.028	0.017?	0.011	0.091	0.021
	Amn	27F	14(1–)	0.030	0.024	0.027?	(–)	0.064	0.021
	Amg	37E-H, 27F	55(5–)	0.054	0.039	–	(–)	0.24	0.051
	Amg	37G	17(1–)	0.077	0.051	0.055	(–)	0.24	0.065
	Amg	37H	8(1–)	0.071	0.041	–	(–)	0.24	0.076
	Amg	37F	11(1–)	0.043	0.043	–	(–)	0.084	0.025
	Amg	27F	15(2–)	0.031	0.030	0.025	(–)	0.050	0.011
	Amp	37E, 37G-H	9	0.038	0.031	0.031?	0.025	0.065	0.014
	Amn^{b}	27F, 37F-H	7(1–)	0.028	0.018	–	(–)	0.068	0.021
	gr-Agr^{c}	27E-F, 37E-G	17(3–)	0.032	0.025	–	(–)	0.055	0.015
	gr-Agr^{c}	37C, 37D	9(2–)	0.037	0.021	0.021?	(–)	0.075	0.026
	gr^{d}	37F, 37G	6(1–)	0.035	0.023	0.019?	(–)	0.074	0.023
	gr-Agr^{e}	27F, 37E-G	6(1–)	0.022	0.014	0.014?	(–)	0.034	0.0094
	Amn^{f}	27F, 37E-H	11	0.13	0.13	0.14?	0.024	0.22	0.055
	Mb	37F-H	17	0.15	0.15	0.15	0.010	0.23	0.051
	Mg	37F-H	8	0.11	0.12	0.17?	0.033	0.17	0.050
	Mu	37G	14	0.13	0.12	0.11	0.089	0.17	0.025
	Amg^{g}	27F, 37F-H	24	0.13	0.12	0.11	0.029	0.30	0.068
	Amg^{g}	37G	7	0.14	0.14	–	0.091	0.20	0.042
	Amg^{g}	37H	11	0.10	0.084	–	0.029	0.27	0.066
	Hg	37E-H	9	0.14	0.13	0.12	0.082	0.23	0.043
	Amn^{i}	27F, 37F-H	10(5–)	0.031	–	–	(–)	0.056	0.016
	Amg^{j}	27F, 37F-H	21(5–)	0.031	0.017	0.015?	(–)	0.095	0.028
	Amg^{i}	27F, 37E-H	18(9–)	0.022	–	–	(–)	0.051	0.013
	Ag^{c}	27F, 37E-G	10(6–)	0.038	–	–	(–)	0.11	0.047
	Ag^{c}	37D	8(2–)	0.061	0.011	0.011?	(–)	0.18	0.069
	Agp	37F-H, 27G	17(1–)	0.034	0.030	0.031	(–)	0.054	0.011
	Agp	37H, 27G	9(1–)	0.038	0.034	0.027	(–)	0.054	0.010
	Ack	37E-F, 37H	14(1–)	0.025	0.020	0.017?	(–)	0.056	0.012
	Ack	37H	10	0.027	0.023	0.018	0.016	0.056	0.012
	M	37F-G	4	0.15	0.10	–	0.091	0.24	0.068
	M^{l}	37F-G	4	0.040	0.040	–	0.030	0.050	0.0084
	Ms	37E-H	38(4–)	0.063	0.054	0.67	(–)	0.17	0.36
	Ms	37G	18(1–)	0.059	0.041	–	(–)	0.17	0.043
	Ms	37F	18(3–)	0.067	0.060	0.67	(–)	0.14	0.030
	Mq	37F-G	10(2–)	0.042	0.029	0.030?	(–)	0.10	0.029
	APs	37C-D	8(2–)	0.026	0.015	0.015?	(–)	0.050	0.018
	APm	37C	3	0.026	0.022	–	0.021	0.035	0.0080
	Mif^{o}	37F-G	28(4–)	0.12	0.045	0.045	(–)	0.37	0.11
	Mif^{o}	37G	20	0.13	0.056	0.045	0.014	0.37	0.11
	Mif^{o}	37F	8(4–)	0.11	–	–	(–)	0.15	0.14
	Mif^{s}	37F-G	6	0.26	0.14	0.14?	0.020	1.1	0.40
	NAB	37G	16(6–)	0.12	0.016	0.15?	(–)	0.59	0.19
	NAB-L	37G	5(1–)	0.017	0.015	0.15	(–)	0.024	0.0046
	NAB-U	37G	11(5–)	0.18	0.033	0.35?	(–)	0.59	0.23
Ba	Amn	37E-H, 27F	52	0.080	0.065	0.035	0.012	0.21	0.053
	Amn	37G	13	0.11	0.11	0.055?	0.012	0.21	0.070
	Amn	37H	15	0.067	0.065	0.035	0.015	0.13	0.037
	Amn	27F	14	0.089	0.070	0.065	0.037	0.17	0.042
	Amg	37E-H, 27F	55(1+)	0.055	0.039	0.025	0.0074	(+)	0.040
	Amg	37G	17	0.042	0.026	0.025	0.0074	0.13	0.035
	Amg	37H	8(1+)	0.094	0.11	–	0.0095	(+)	0.063
	Amg	37F	11	0.062	0.065	0.035	0.015	0.13	0.039
	Amg	27F	15	0.029	0.028	0.025	0.012	0.11	0.028
	Amp	37E, 37G-H	9	0.10	0.087	0.052?	0.033	0.17	0.056
Ba	Amn^{b}	27F, 37F-H	7	0.046	0.049	–	0.016	0.068	0.020
	gr-Agr^{c}	27E-F, 37E-G	17	0.10	0.11	0.036	0.031	0.19	0.056
	gr-Agr^{c}	37C, 37D	9	0.043	0.050	–	0.0065	0.078	0.029
	gr^{d}	37F, 37G	6	0.12	0.10	–	0.076	0.16	0.037
	gr-Agr^{e}	27F, 37E-G	6	0.11	0.074	–	0.022	0.18	0.069
	Amn^{f}	27F, 37E-H	11(1+)	0.034	0.024	0.012?	0.0036	(+)	0.047
	Mb	37F-H	17	0.014	0.0075	0.0070	0.0033	0.052	0.014
	Mg	37F-H	8	0.041	0.027	0.049?	0.0047	0.14	0.041
	Mu	37G	14(2–)	0.0023	0.0023	0.0022?	(–)	0.0034	0.0004
	Amg^{g}	27F, 37F-H	24	0.053	0.023	0.011	0.0042	0.24	0.070
	Amg^{g}	37G	7	0.022	0.013	0.0051?	0.0042	0.056	0.023
	Amg^{g}	37H	11	0.093	0.055	0.054?	0.0073	0.24	0.087
	Hg	37E-H	9	0.013	0.015	0.0076?	0.0065	0.022	0.0058
	Amn^{i}	27F, 37F-H	10(1+)	0.093	0.067	–	0.36	(+)	0.073
	Amg^{j}	27F, 37F-H	21	0.086	0.065	0.045	0.012	0.22	0.056
	Amg^{i}	27F, 37E-H	18	0.069	0.050	0.054	0.0051	0.29	0.069
	Ag^{c}	27F, 37E-G	10	0.081	0.047	0.015?	0.0058	0.23	0.085
	Ag^{c}	37D	8	0.045	0.038	0.042?	0.0020	0.13	0.042
	Agp	37F-H, 27G	17(1+)	0.10	0.11	0.11?	0.0094	(+)	0.069
	Agp	37H, 27G	9	0.12	0.12	0.11	0.013	0.22	0.064
	Ack	37E-F, 37H	14	0.11	0.057	0.048?	0.011	0.26	0.092
	Ack	37H	10	0.12	0.066	0.057	0.037	0.26	0.095
	M	37F-G	4	0.044	0.029	–	0.0028	0.082	0.037
	M^{l}	37F-G	4	0.073	0.064	–	0.031	0.13	0.044
	Ms	37E-H	38	0.058	0.042	0.043	0.0020	0.025	0.053
	Ms	37G	18	0.069	0.046	0.063	0.0020	0.25	0.071
	Ms	37F	18	0.050	0.042	0.043	0.014	0.12	0.028
	Mq	37F-G	10	0.052	0.032	–	0.012	0.12	0.037
	APs	37C-D	8(1–)	0.054	0.045	–	(–)	0.079	0.023
	APm	37C	3	0.0050	0.0058	–	0.0020	0.0072	0.0027
	Mif^{o}	37F-G	28(10–)	0.0028	0.0021	0.0025?	(–)	0.0046	0.0080
	Mif^{o}	37G	20(5–)	0.0028	0.0024	0.0025?	(–)	0.0046	0.0080
	Mif^{o}	37F	8(5–)	0.0027	–	–	(–)	0.0038	0.0010
	Mif^{s}	37F-G	6(2–)	0.0084	0.0028	–	(–)	0.017	0.0070
	NAS	37G	4	0.040	0.018	–	0.012	0.084	0.034
	NAB	37G	16	0.015	0.013	0.013?	0.0040	0.034	0.0090
	NAB-L	37G	5	0.018	0.021	–	0.0072	0.034	0.011
	NAB-U	37G	11	0.014	0.012	0.0042?	0.0040	0.027	0.0079
Co	Amn^{f}	27F, 37E-H	11(8–)	0.0037	–	–	(–)	0.0047	0.0009
	Mb	37F-H	17(2–)	0.0044	0.0036	0.0033	(–)	0.011	0.0021
	Mg	37F-H	8(3–)	0.0043	0.0033	–	(–)	0.0052	0.0008
	Mu	37G	14	0.010	0.0088	0.0085	0.0067	0.016	0.0026
	Amg^{g}	27F, 37F-H	24(14–)	0.0044	–	–	(–)	0.0083	0.0020
	Amg^{g}	37G	7(4–)	0.0052	–	–	(–)	0.0072	0.0017
	Amg^{g}	37H	11(7–)	0.0043	–	–	(–)	0.0083	0.0028
	Hg	37E-H	9(3–)	0.0044	0.0027	–	(–)	0.0076	0.0019
	Mif^{o}	37F-G	28(13–)	0.0044	0.0022	0.0054	(–)	0.0061	0.0013
	Mif^{o}	37G	20(11–)	0.0046	–	0.0055?	(–)	0.0061	0.0015
	Mif^{o}	37F	8(2–)	0.0042	0.0032	–	(–)	0.0057	0.0012
Cr	Amn	37E-H, 27F	52(43–)	0.014	–	–	(–)	0.054	0.017
	Amn	37G	13(7–)	0.012	–	–	(–)	0.024	0.0088
	Amg	37E-H, 27F	55(36–)	0.0084	–	–	(–)	0.026	0.0061
	Amg	37G	17(5–)	0.0086	0.0049	–	(–)	0.026	0.0064
	Amg	37H	8(3–)	0.0095	0.0042	–	(–)	0.019	0.0069

Appendix 3 (cont.)

Element	Map unit	Location	No. of samples	Mean	Median	Mode	Minimum	Maximum	Standard deviation
Cr	Amn^{f}	27F, 37E-H	11(2–)	0.020	0.012	0.064?	(–)	0.052	0.015
	Mb	37F-H	17(3–)	0.064	0.019	–	(–)	0.25	0.085
	Mg	37F-H	8(2–)	0.044	0.019	–	(–)	0.099	0.036
	Mu	37G	14	0.27	0.28	0.30	0.036	0.47	0.10
	Amg^{g}	27F, 37F-H	24(5–)	0.024	0.013	0.013	(–)	0.083	0.020
	Amg^{g}	37G	7(1–)	0.018	0.013	0.013	(–)	0.034	0.010
	Amg^{g}	37H	11(4–)	0.026	0.0092	–	(–)	0.060	0.019
	Hg	37E-H	9(4–)	0.017	0.0063	–	(–)	0.031	0.011
	Amg^{j}	27F, 37E-H	21(18–)	0.0096	–	–	(–)	0.064	0.0052
	M	37F-G	4	0.010	0.0079	–	0.0074	0.014	0.0032
	M^{l}	37F-G	4(2–)	0.0032	–	–	(–)	0.0033	0.0001
	Ms	37E-H	38(21–)	0.014	–	–	(–)	0.031	0.0088
	Ms	37G	18(10–)	0.0086	–	0.0069?	(–)	0.020	0.0050
	Ms	37F	18(11–)	0.22	–	–	(–)	0.031	0.0075
	APs	37C-D	8	0.0086	0.0076	–	0.0041	0.013	0.0035
	Mif^{o}	37F-G	28(4–)	0.0060	0.0042	0.0037	(–)	0.010	0.0026
	Mif^{o}	37G	20(4–)	0.0062	0.0042	0.0040	(–)	0.010	0.0027
	Mif^{o}	37F	8	0.0057	0.0039	0.0036	0.0033	0.0091	0.0024
	Mif^{s}	37F-G	6(1–)	0.0070	0.0053	–	(–)	0.011	0.0031
	NAB	37G	16(9–)	0.0044	–	–	(–)	0.0063	0.0013
	NAB-L	37G	5(3–)	0.0052	–	–	(–)	0.0063	0.0016
	NAB-U	37G	11(6–)	0.0041	–	–	(–)	0.0055	0.0012
Cu	Amn	37E-H, 27F	52(26–)	0.003	–	–	(–)	0.020	0.0039
	Amg	37E-H, 27F	55(26–)	0.0045	0.0010	–	(–)	0.042	0.0075
	Amp	37E, G-H	9(3–)	0.0017	0.0010	0.0012	(–)	0.0030	0.0009
	Amn^{b}	27F, 37F-H	7(4–)	0.0058	–	–	(–)	0.014	0.0075
	gr-Agr^{c}	27E-F, 37E-G	17(6–)	0.0016	0.0010	–	(–)	0.0037	0.0008
	gr-Agr^{c}	37C, 37D	9(6–)	0.0034	–	–	(–)	0.031	0.0070
	gr^{d}	37F, 37G	6(4–)	0.0028	–	–	(–)	0.0041	–
	gr-Agr^{e}	27F, 37E-G	6(4–)	0.0056	–	–	(–)	0.0093	–
	Amn^{f}	27F, 37E-H	11	0.0042	0.0025	0.0012?	0.0012	0.015	0.0039
	Mb	37F-H	17(3–)	0.0094	0.0048	–	(–)	0.048	0.012
	Mg	37F-H	8	0.0074	0.0079	0.077	0.0019	0.011	0.0029
	Mu	37G	14(9–)	0.0048	–	–	(–)	0.013	0.0047
	Amg^{g}	27F, 37F-H	24(2–)	0.0048	0.0018	0.0012	(–)	0.030	0.0071
	Amg^{g}	37G	7	0.0061	0.0018	0.0013	0.0010	0.030	0.011
	Amg^{g}	37H	11(2–)	0.0057	0.0028	–	(–)	0.022	0.0062
	Hg	37E-H	9	0.019	0.019	0.020?	0.0050	0.048	0.013
	Amn^{i}	27F, 37F-H	10(6–)	0.0019	–	–	(–)	0.0029	0.0007
	Amg^{j}	27F, 37E-H	21(12–)	0.0087	–	–	(–)	0.064	0.021
	Amg^{i}	27F, 37E-H	18(15–)	0.0040	–	–	(–)	0.0064	0.0027
	Ag^{c}	27F, 37E-G	10(8–)	0.0012	–	–	(–)	0.0014	0.0003
	Agp	37F-H, 27G	17(10–)	0.0021	–	–	(–)	0.0034	0.0010
	Agp	37H, 27G	9(4–)	0.0025	0.0012	–	(–)	0.0034	0.0009
	Ack	37E-F, 37H	14(10–)	0.0027	–	–	(–)	0.0047	0.0016
	M	37F-G	4(3–)	0.0052	0.0019	–	(–)	0.0085	0.0036
	M^{l}	37F-G	4(1–)	0.0027	0.0017	–	(–)	0.0040	0.0014
	Ms	37E-H	38(9–)	0.0038	0.0018	0.0018	(–)	0.030	0.0053
	Ms	37G	18(6–)	0.0030	0.0017	0.0018	(–)	0.0073	0.0017
	Ms	37F	18(3–)	0.0046	0.0018	0.0014?	(–)	0.030	0.0072
	Mq	37F-G	10(3–)	0.0039	0.0018	0.0018?	(–)	0.0077	0.0027
	APs	37C-D	8(1–)	0.0034	0.0018	0.0016?	(–)	0.0071	0.0022
	Mif^{o}	37F-G	28	0.0022	0.0019	0.0015	0.0011	0.0056	0.0010
	Mif^{o}	37G	20	0.0021	0.0019	0.0015	0.0011	0.0039	0.00090
	Mif^{o}	37F	8	0.0025	0.0020	0.0018?	0.0012	0.0056	0.0014
	Mif^{s}	37F-G	6	0.0015	0.0014	0.0012?	0.0011	0.0021	0.00040
	NAB	37G	16(5–)	0.0034	0.0023	0.0023	(–)	0.0057	0.0014
	NAB-L	37G	5(2–)	0.0032	0.0023	–	(–)	0.0049	0.0015
	NAB-U	37G	11(3–)	0.0035	0.0023	0.0023	(–)	0.0057	0.0015

Element	Map unit	Location	No. of samples	Mean	Median	Mode	Minimum	Maximum	Standard deviation
La	APm	37C	3(1–)	0.071	0.063	–	(–)	0.079	0.0012
Ni	Amn^{f}	27F, 37E-H	11(3–)	0.010	0.0051	0.0050?	(–)	0.024	0.0070
	Mb	37F-G	17(4–)	0.030	0.0056	0.0043	(–)	0.18	0.049
	Mg	37F-H	8(1–)	0.012	0.0078	–	(–)	0.023	0.0075
	Mu	37G	14	0.17	0.16	0.20	0.089	0.24	0.045
	Amg^{g}	27F, 37F-H	24(9–)	0.0089	0.0049	–	(–)	0.016	0.0041
	Amg^{g}	37G	7(3–)	0.010	0.0062	–	(–)	0.015	0.0039
	Amg^{g}	37H	11(5–)	0.0081	0.0034	–	(–)	0.015	0.0048
	Hg	37E-H	9(4–)	0.0073	0.0050	–	(–)	0.013	0.0034
	M	37F-G	4(2–)	0.0067	–	–	(–)	0.0081	0.0036
	Ms	37E-H	38(29–)	0.0068	–	–	(–)	0.0097	0.0020
	Ms	37G	18(15–)	0.0072	–	–	(–)	0.0097	0.0024
	Ms	37F	18(13–)	0.0072	–	–	(–)	0.0097	0.0016
	Mif^{o}	37F-G	28(17–)	0.0065	–	–	(–)	0.0088	0.0016
	Mif^{o}	37G	20(13–)	0.0067	–	–	(–)	0.0084	0.0015
	Mif^{o}	37F	8(4–)	0.0061	–	–	(–)	0.0088	0.0020
	Mif^{s}	37F-G	6(4–)	0.0033	–	–	(–)	0.0037	0.00050
Pb	Mu	37G	14	0.10	0.10	0.11	0.073	0.13	0.018
	Mif^{o}	37F-G	28(3–)	0.094	0.088	0.088	(–)	0.14	0.018
	Mif^{o}	37G	20	0.093	0.088	0.088	0.070	0.14	0.016
	Mif^{o}	37F	8(3–)	0.10	0.070	0.11?	(–)	0.13	0.026
	Mif^{s}	37F-G	6(2–)	0.079	0.074	–	(–)	0.083	0.0045
Sr	Amn	37E-H, 27F	52	0.030	0.027	0.025	0.0091	0.072	0.012
	Amn	37G	13	0.038	0.033	0.035	0.016	0.072	0.016
	Amn	37H	15	0.032	0.034	0.025	0.012	0.053	0.012
	Amn	27F	14	0.021	0.021	0.022	0.0091	0.033	0.0061
	Amg	37E-H, 27F	55	0.027	0.021	0.018	0.0087	0.082	0.016
	Amg	37G	17	0.028	0.021	0.018	0.0093	0.076	0.018
	Amg	37H	8	0.041	0.024	–	0.0087	0.082	0.027
	Amg	37F	11	0.024	0.024	0.020	0.011	0.035	0.0072
	Amg	27F	15	0.020	0.017	0.017	0.010	0.038	0.0074
	Amp	37E, 37G-H	9	0.027	0.021	0.015?	0.0098	0.073	0.020
	Amn^{b}	27F, 37F-H	7	0.028	0.028	–	0.014	0.043	0.011
	gr-Agr^{c}	27E-F, 37E-G	17	0.026	0.025	–	0.0060	0.057	0.015
	gr-Agr^{c}	37C, 37D	9	0.017	0.018	0.018	0.0040	0.027	0.0075
	gr^{d}	37F, 37G	6	0.025	0.025	0.025?	0.0079	0.042	0.011
	gr-Agr^{e}	27F, 37E-G	6	0.027	0.029	0.032?	0.017	0.034	0.0076
	Amn^{f}	27F, 37E-H	11	0.025	0.019	–	0.0049	0.070	0.020
	Mb	37F-H	17	0.012	0.011	0.013	0.0012	0.029	0.0069
	Mg	37F-H	8(1–)	0.020	0.0056	0.0050?	(–)	0.061	0.021
	Mu	37G	14(7–)	0.0043	–	–	(–)	0.0096	0.0028
	Amg^{g}	27F, 37F-H	24	0.038	0.024	0.0095	0.0024	0.11	0.033
	Amg^{g}	37G	7	0.056	0.040	–	0.0094	0.11	0.043
	Amg^{g}	37H	11	0.041	0.041	0.042?	0.0034	0.090	0.026
	Hg	37E-H	9	0.016	0.017	0.020?	0.0077	0.026	0.0055
	Amn^{i}	27F, 37F-H	10	0.028	0.023	–	0.011	0.035	0.0086
	Amg^{j}	27F, 37F-H	21	0.034	0.031	–	0.011	0.094	0.021
	Amg^{i}	27F-37E-H	18	0.025	0.018	0.014?	0.0071	0.063	0.017
	Ag^{c}	27F, 37E-G	10(1–)	0.024	0.0076	0.0048?	(–)	0.052	0.019
	Ag^{c}	37D	8(2–)	0.011	0.0082	–	(–)	0.016	0.0034
	Agp	37F-H, 27G	17	0.041	0.042	0.0076?	0.0068	0.085	0.024
	Agp	37H, 27G	9	0.041	0.043	0.042	0.0068	0.061	0.017
	Ack	37E-F, 37H	14	0.029	0.029	0.028	0.0024	0.050	0.014
	Ack	37H	10	0.030	0.029	0.029	0.011	0.044	0.011
	M	37F-G	4	0.020	0.0089	–	0.0014	0.048	0.021
	M^{l}	37F-G	4	0.040	0.042	–	0.0086	0.066	0.023
	Ms	37E-H	38(3–)	0.018	0.016	–	(–)	0.048	0.012
	Ms	37G	18(2–)	0.020	0.017	0.0019?	(–)	0.048	0.014
	Ms	37F	18(1–)	0.017	0.014	0.0060	(–)	0.039	0.011
	Mq	37F-G	10(1–)	0.0091	0.0019	0.0018?	(–)	0.043	0.014

Appendix 3 (cont.)

Element	Map unit	Location	No. of samples	Mean	Median	Mode	Minimum	Maximum	Standard deviation
Sr	APs	37C-D	8(1–)	0.0088	0.0080	0.0084?	(–)	0.015	0.0029
	APm	37C	3	0.0095	0.0098	–	0.0055	0.013	0.0038
	Mif^{o}	37F-G	28(13–)	0.0020	0.0013	0.0017?	(–)	0.0033	0.00060
	Mif^{o}	37G	20(9–)	0.0020	0.0015	0.0018?	(–)	0.0030	0.00050
	Mif^{o}	37F	8(4–)	0.020	–	–	(–)	0.0033	0.00090
	Mif^{s}	37F-G	6(4–)	0.0016	–	–	(–)	0.0020	0.00060
	NAS	37G	4(2–)	0.0016	–	–	(–)	0.0019	0.00040
	NAB	37G	16(4–)	0.0052	0.0028	0.0023?	(–)	0.016	0.0041
	NAB-L	37G	5(2–)	0.0045	0.0018	–	(–)	0.0072	0.0027
	NAB-U	37G	11(2–)	0.0055	0.0029	0.0027?	(–)	0.016	0.0046
V	Amn	37E-H, 27F	52(21–)	0.0078	0.0045	0.0050	(–)	0.026	0.0057
	Amg	37E-H, 27F	55(18–)	0.012	0.0071	0.010	(–)	0.047	0.0096
	Amp	37E, 37G-H	9(2–)	0.0077	0.0050	–	(–)	0.013	0.0039
	Amn[b]	27F, 37F-H	7(4–)	0.0043	–	–	(–)	0.0054	0.0010
	gr-Agr[c]	27E-F, 37E-G	17(9–)	0.0063	–	–	(–)	0.013	0.0033
	gr-Agr[c]	37C, 37D	9(6–)	0.0053	–	–	(–)	0.0069	0.0017
	gr[d]	37F, 37G	6(2–)	0.0079	0.0030	–	(–)	0.018	0.0073
	gr-Agr[e]	27F, 37E-G	6(4–)	0.0061	–	–	(–)	0.0083	–
	Amn[f]	27F, 37E-G	11	0.018	0.016	0.011?	0.0071	0.030	0.0073
	Mb	37F-H	17(–)	0.026	0.027	0.027	(–)	0.049	0.0094
	Mg	37F-H	8	0.022	0.024	0.027	0.0036	0.033	0.010
	Mu	37G	14(2–)	0.0095	0.0068	0.0055?	(–)	0.016	0.0038
	Amg[g]	27F, 37F-H	24	0.021	0.018	0.015	0.0065	0.054	0.010
	Amg[g]	37G	7	0.023	0.018	0.017	0.016	0.041	0.0089
	Amg[g]	37H	11	0.019	0.019	–	0.0065	0.054	0.013
	Hg	37E-H	9	0.036	0.035	0.046?	0.019	0.047	0.0092
	Amn[i]	27F, 37F-H	10(6–)	0.0071	–	–	(–)	0.012	0.0038
	Amg[j]	27F, 37F-H	21(14–)	0.0094	–	–	(–)	0.018	0.0051
	Agp	37F-H, 27G	17(4–)	0.0074	0.0052	0.0052	(–)	0.085	0.024
	Agp	37H, 27G	9(2–)	0.0091	0.0055	0.0053	(–)	0.015	0.0039
	Ack	37E-F, 37H	14(7–)	0.0083	–	–	(–)	0.019	0.0049
	Ack	37H	10(4–)	0.0086	0.0041	–	(–)	0.019	0.0053
	M	37F-G	4	0.016	0.011	–	0.010	0.028	0.0081
	M[l]	37F-G	4	0.0085	0.0083	–	0.0055	0.012	0.0028
	Ms	37E-H	38(6–)	0.013	0.0098	–	(–)	0.034	0.0081
	Ms	37G	18(5–)	0.010	0.0058	0.0058?	(–)	0.028	0.0069
	Ms	37F	18(1–)	0.015	0.012	0.015?	(–)	0.034	0.0088
	Mq	37F-G	10(5–)	0.011	–	–	(–)	0.016	0.0030
	APs	37C-D	8(3–)	0.021	0.0087	–	(–)	0.036	0.013
	Mif^{o}	37F-G	28(4–)	0.0078	0.0048	0.0041	(–)	0.014	0.0038
	Mif^{o}	37G	20(4–)	0.0076	0.0044	0.0041	(–)	0.014	0.0038
	Mif^{o}	37F	8	0.0081	0.0062	0.0040?	0.0039	0.014	0.0040
	Mif^{s}	37F-G	6(1–)	0.0081	0.0045	0.0042?	(–)	0.017	0.0058
	NAB	37G	16(9–)	0.0086	–	–	(–)	0.014	0.0038
	NAB-L	37G	5(3–)	0.012	–	–	(–)	0.014	0.0027
	NAB-U	37G	11(6–)	0.0071	–	–	(–)	0.011	0.0033
Y	Mif^{o}	37F-G	28(18–)	0.011	–	–	(–)	0.014	0.0019
	Mif^{o}	37G	20(13–)	0.010	–	–	(–)	0.013	0.0018
	Mif^{o}	37F	8(5–)	0.011	–	–	(–)	0.014	0.0025
Yb	Mif^{o}	37F-G	28(18–)	0.0016	–	–	(–)	0.0023	0.0040
	Mif^{o}	37G	20(13–)	0.0015	–	–	(–)	0.0023	0.0040
	Mif^{o}	37F	8(5–)	0.0018	–	–	(–)	0.0022	0.0040
Zr	Amn	37E-H, 27F	52(10–)	0.023	0.019	0.029, 0.014	(–)	0.065	0.0099
	Amn	27F	14(2–)	0.026	0.027	0.027	(–)	0.033	0.0061
Zr	Amg	37E-H, 27F	55(7–)	0.026	0.019	0.017	(–)	0.091	0.017
	Amg	37G	17(1–)	0.022	0.017	0.015	(–)	0.064	0.014
	Amg	37H	8(1–)	0.032	0.020	–	(–)	0.091	0.027
	Amg	37F	11(4–)	0.020	0.013	–	(–)	0.029	0.0063
	Amg	27F	15(1–)	0.021	0.017	0.020	(–)	0.077	0.018
	Amp	37E, G-H	9(1–)	0.033	0.034	–	(–)	0.053	0.016
	Amn[b]	27F, 37F-H	7(2–)	0.015	0.013	–	(–)	0.022	0.0043
	gr-Agr[c]	27E-F, 37E-G	17(3–)	0.020	0.017	–	(–)	0.033	0.0063
	gr-Agr[c]	37C, 37D	9(2–)	0.016	0.014	0.015?	(–)	0.031	0.0070
	gr[d]	37F, 37G	6(1–)	0.040	0.021	0.019?	(–)	0.099	0.034
	gr-Agr[e]	27F, 37E-G	6(2–)	0.029	0.016	0.020?	(–)	0.060	0.021
	Amn[f]	27F, 37E-H	11(2–)	0.033	0.019	0.015?	(–)	0.094	0.026
	Mb	37F-H	17(5–)	0.015	0.014	0.017?	(–)	0.020	0.0031
	Mg	37F-H	8(1–)	0.023	0.015	0.013?	(–)	0.048	0.014
	Amg[g]	27F, 37F-H	24(2–)	0.025	0.018	0.012	(–)	0.14	0.026
	Amg[g]	37G	7	0.020	0.020	0.025	0.012	0.026	0.0059
	Amg[g]	37H	11(1–)	0.034	0.023	0.023	(–)	0.14	0.037
	Hg	37E-H	9	0.027	0.019	0.017?	0.015	0.067	0.017
	Amn[i]	27F, 37F-H	10(4–)	0.020	0.011	–	(–)	0.035	0.0086
	Amg[j]	27F, 37E-H	21(7–)	0.022	0.011	–	(–)	0.062	0.015
	Amg[i]	27F, 37E-H	18(7–)	0.022	0.011	–	(–)	0.057	0.014
	Ag[c]	27F, 37E-G	10(7–)	0.014	–	–	(–)	0.017	0.0028
	Ag[c]	37D	8(4–)	0.014	–	–	(–)	0.020	0.0041
	Agp	37F-H, 27G	17(2–)	0.036	0.027	0.017?	(–)	0.095	0.026
	Agp	37H, 27G	9	0.028	0.024	0.014	0.012	0.069	0.018
	Ack	37E-F, 37H	14(1–)	0.036	0.017	0.015?	(–)	0.092	0.033
	Ack	37H	10	0.041	0.017	0.012	0.011	0.092	0.036
	M	37F-G	4	0.019	0.017	–	0.011	0.030	0.0082
	M[l]	37F-G	4	0.028	0.022	–	0.020	0.042	0.010
	Ms	37E-H	38(2–)	0.021	0.017	0.017	(–)	0.056	0.0095
	Ms	37G	18(1–)	0.020	0.017	0.018	(–)	0.046	0.0085
	Ms	37F	18(1–)	0.021	0.017	0.017	(–)	0.056	0.011
	Mq	37F-G	10(2–)	0.031	0.020	–	(–)	0.071	0.022
	APs	37C-D	8(1–)	0.018	0.014	0.015?	(–)	0.042	0.011
	Mif^{o}	37F-G	28(14–)	0.012	–	0.011?	(–)	0.019	0.0021
	Mif^{o}	37G	20(11–)	0.013	–	0.011?	(–)	0.019	0.0026
	Mif^{o}	37F	8(3–)	0.012	0.011	0.011?	(–)	0.013	0.0011
	Mif^{s}	37F-G	6(4–)	0.014	–	–	(–)	0.016	0.0030
	NAS	37G	4(1–)	0.019	0.012	–	(–)	0.032	0.012
	NAB	37G	16(2–)	0.030	0.025	–	(–)	0.048	0.013
	NAB-L	37G	5	0.033	0.032	–	0.014	0.048	0.014
	NAB-U	37G	11(2–)	0.029	0.019	–	(–)	0.044	0.013

APPENDIX 4

Mean and median values of spectrographic analyses for map units. Additional data occur in Appendices 2 and 3.

	Location	Element: Mean/Median in weight per cent; (2–) (1+) = number of samples within population with values below (–) or above (+) respectively, the limit of detection of the analytical method							
Map unit	(Number of samples)	Al	Fe	Mg	Ti	Mn	Ba	Sr	Zr
Amn	37E-H, 27F	7.0	2.2	0.78	0.25	0.034 (5–)	0.080	0.030	0.023 (10–)
	(52)	6.8	1.9	0.56	0.23	0.025	0.065	0.027	0.019
	37G	7.1	2.9	1.1	0.33	0.051 (2–)	0.11	0.038	0.025 (1–)
	(13)	7.2	2.5	0.86	0.24	0.035	0.11	0.033	0.021
	37H	6.9	2.2	0.83	0.24	0.031	0.067	0.032	0.018 (3–)
	(15)	6.6	2.0	0.56	0.24	0.028	0.065	0.034	0.014
	37F	7.9	1.6	0.50	0.16	0.020	0.056	0.027	0.018 (3–)
	(6)	7.4	1.2	0.42	0.14	0.019	0.027	0.025	–
	37E	8.1	2.0	0.58	0.24	0.031 (1–)	0.038	0.031	0.025 (1–)
	(4)	8.0	2.1	0.56	0.29	0.026	0.039	0.030	0.022
	27F	6.2	1.8	0.59	0.23	0.030 (2–)	0.089	0.021	0.026 (2–)
	(14)	6.3	1.8	0.58	0.23	0.024	0.070	0.021	0.027
	37C	5.7	0.89	0.33	0.086	0.013	0.17	0.021	(1–)
	(1)								
Amg	37E-H, 27F	7.0	2.9	1.0	0.30	0.054 (5–)	0.055 (1+)	0.027	0.026 (7–)
	(55)	6.9	2.6	0.86	0.28	0.039	0.042	0.021	0.019
	37G	6.7	4.0	1.3	0.36	0.077 (1–)	0.042	0.028	0.022 (1–)
	(17)	6.6	2.9	1.3	0.36	0.051	0.026	0.021	0.017
	37H	6.5	3.7	1.6	0.40	0.071 (1–)	0.094 (1+)	0.041	0.032 (1–)
	(8)	6.7	2.5	1.1	0.35	0.041	0.11	0.024	0.020
	37F	7.6	2.0	0.64	0.21	0.043 (1–)	0.062	0.024	0.020 (4–)
	(11)	7.5	1.5	0.42	0.11	0.043	0.065	0.024	0.013
	37E	7.9	2.1	0.70	0.26	0.033	0.029	0.027	0.021
	(4)	7.8	2.1	0.68	0.23	0.017	0.028	0.026	0.017
	27F	6.7	2.0	0.67	0.26	0.031 (2–)	0.052	0.020	0.032 (1–)
	(15)	6.8	1.8	0.65	0.25	0.030	0.045	0.017	0.024
Amg^{a}	37G	6.9	6.3	1.9	0.33	0.016 (2–)	0.027	0.050	0.044
	(3)	6.8	4.9	2.0	0.39	–	0.0046	0.065	0.045
Amp	37E, 37G-H	6.8	2.6	0.74	0.36	0.038	0.10	0.027	0.033 (1–)
	(9)	6.6	2.1	0.67	0.25	0.031	0.087	0.021	0.034
bg	27G, 37H	7.1	3.0	1.2	0.33	0.051	0.11	0.043	0.024
	(3)	6.7	3.3	1.3	0.35	0.058	0.11	0.039	0.025
Amn^{b}	27F, 37F-H	7.3	1.9	0.42	0.22	0.028 (1–)	0.046	0.028	0.015 (2–)
	(7)	7.3	1.4	0.35	0.19	0.018	0.049	0.028	0.013
gr-Agr^{c}	27E-F, 37E-G	6.9	1.7	0.56	0.19	0.032 (3–)	0.10	0.026	0.020 (3–)
	(17)	6.9	1.3	0.47	0.18	0.025	0.11	0.025	0.017
	37C, D	6.6	1.6	0.47	0.15	0.037 (2–)	0.043	0.017	0.016 (2–)
	(9)	6.4	1.3	0.42	0.13	0.021	0.050	0.018	0.014
gr^{d}	37F, G	6.7	2.2	0.49	0.34	0.035 (1–)	0.12	0.025	0.040 (1–)
	(6)	6.7	1.8	0.40	0.21	0.023	0.10	0.025	0.021
gr-Agr^{e}	27F, 37E-G	6.7	1.3	0.34	0.16	0.022 (1–)	0.11	0.027	0.029 (2–)
	(6)	6.1	1.1	0.29	0.12	0.014	0.074	0.029	0.016

Legend

Note: Map unit symbols are those used on map sheets covering areas indicated in Figure 1, and are referred to in the text.

a: mylonite
b: foliated granitoid component
c: chiefly pink
d: porphyritic
e: migmatitic
f: intermediate-mafic igneous component
g: amphibolite and/or mafic igneous component
h: acid-intermediate volcanic component
i: late massive granitoid component
j: leucosome
k: white
l: anatectic
m: sedimentary component
n: calc-silicate
o: oxide facies
s: silicate facies
–: not determined, because too many or all of the values are outside the detection limits

V	Cu	Cr	Ni	Ca	Na	La	Co	Pb	Y	Yb
0.0078 (21–) 0.0045	0.0031 (26–) –	0.014 (43–) –	0.0061 (48–) –	0.95 (42+) –	(52+) –	0.028 (50–) –	0.0031 (51–) –	(52–) –		
0.012 (5–) 0.0058	0.0028 (7–) –	0.012 (7–) –	0.0046 (10–) –	0.91 (11+) –	(13+) –	0.028 (12–) –	0.0031 (12–) –	(13–) –		
0.0080 (6–) 0.0045	0.0040 (7–) 0.0010	0.029 (13–) –	0.011 (14–) –	0.88 (14+) –	(15+) –	(15–) –	(15–) –	(15–) –		
0.0058 (4–) –	0.0071 (4–) –	0.0015 (5–) –	(6–) –	2.8 (5+) –	(6+) –	0.029 (5–) –	(6–) –	(6–) –		
0.0049 (1–) 0.0041	0.0021 (1–) 0.0012	(4–) –	(4–) –	(4+) –	(4+) –	(4–) –	(4–) –	(4–) –		
0.0056 (5–) 0.0037	0.0014 (7–) –	(14–) –	(14–) –	0.66 (8–) –	(14+) –	(14–) –	(14–) –	(14–) –		
(1–)	(1–)	(1–)	(1–)	0.43	(1+)	(1–)	(1–)	(1–)		
0.012 (18–) 0.0071	0.0045 (26–) 0.0010	0.0084 (36–) –	0.0061 (50–) –	1.5 (45+) –	0.83 (53+)	0.031 (53–) –	0.0040 (52–) –	(55–) –		
0.015 (4–) 0.010	0.0078 (6–) 0.0021	0.0086 (5–) 0.0049	0.0051 (13–) –	0.51 (16+) –	0.49 (16+) –	0.031 (15–) –	0.0031 (15–) –	(17–) –		
0.016 (2–) 0.0088	0.0044 (4–) –	0.0095 (3–) 0.0042	0.0099 (7–) –	3.3 (5+) –	1.2 (7+) –	(8–) –	0.0060 (7–) –	(8–) –		
0.0098 (6–) –	0.0025 (4–) 0.0011	0.0084 (10–) –	(11–) –	(11+) –	(11+) –	(11–) –	(11–) –	(11–) –		
0.0063 (1–) 0.0047	0.0031 (3–) –	(4–) –	(4–) –	(4+) –	(4+) –	(4–) –	(4–) –	(4–) –		
0.0075 (5–) 0.0051	0.0012 (9–) –	0.0033 (14–) –	(15) –	0.75 (9+) –	(15+) –	(15–) –	(15–) –	(15–) –		
0.0041 (1–) 0.0040	(3–) –	(3–) –	(3–) –	0.68 (2+) –	0.57 (1+) 0.56	0.038 (1–) 0.037	(3–) –	(3–) –		
0.0077 (2–) 0.0050	0.0017 (3–) 0.0010	0.0066 (8–) –	0.0039 (8–) –	0.87 (6+) –	(9+) –	(9–) –	(9–) –	(9–) –		
0.0089 0.011	0.050 (1–) 0.040	0.058 (1–) 0.058	(3–) –	(3+) –	(3+)	0.028 (2–) –	(3–) –	(3–) –		
0.0043 (4–) –	0.0058 (4–) –	(7–) –	(7–) –	0.91 (5+) –	(7+) –	(7–) –	(7–) –	(7–) –		
0.0063 (9–) –	0.0016 (6–) 0.0010	0.0061 (15–) –	(17–) –	0.78 (11+) –	(17+) –	(17–) –	(17–) –	(17–) –		
0.0053 (6–) –	0.0034 (6–) –	0.0057 (7–) –	(9–) –	0.62 (5+) –	(9+) –	0.032 (8–) –	(9–) –	(9–) –		
0.0079 (2–) 0.0030	0.028 (4–) –	0.0037 (5–) –	(6–) –	0.64 (4+) –	(6+) –	0.035 (5–) –	(6–) –	(6–) –		
0.0061 (4–) –	0.0058 (4–) –	(6–) –	(6–) –	0.65 (4+) –	(6+) –	(6–) –	(6–) –	(6–) –		

Appendix 4 (cont.)

Map unit	Location (Number of samples)	Element: Mean/Median in weight per cent; (2–) (1+) = number of samples within population with values below (–) or above (+) respectively, the limit of detection of the analytical method																		
		Al	Fe	Mg	Ti	Mn	Ba	Sr	Zr	V	Cu	Cr	Ni	Ca	Na	La	Co	Pb	Y	Yb
Amn[f]	27F, 37E-H (11)	5.9 6.5	6.1 6.2	2.8 2.8	0.52 0.44	0.13 0.13	0.034 (1+) 0.024	0.025 0.019	0.033 (–) 0.019	0.018 0.016	0.0042 0.0025	0.020 (2–) 0.012	0.010 (3–) 0.0051	(11+) –	0.39 (9+) –	0.37 (9–) –	0.0037 (8–) –	(11–) –		
gr[g]	37H (1)	5.9	3.9	2.2	0.36	0.067	0.14	0.058	0.013	0.013	0.0015	0.013	(1–)	(1+)	(1+)	(1–)	(1–)	(1–)		
Mb	37F-H (17)	5.6 5.8	7.2 7.4	3.7 3.5	0.47 0.44	0.15 0.15	0.014 0.0075	0.012 0.011	0.015 (5–) 0.014	0.026 (1–) 0.027	0.0094 (3–) 0.0048	0.064 (3–) 0.019	0.030 (4–) 0.0056	0.77 (16+) –	0.45 (12+) –	0.0[illegible]9 (14–) –	0.0044 (2–) 0.0036	0.072 (16–) –		
	37D (1)	5.3	5.9	3.5	0.37	0.13	0.0065	0.018	0.041	0.021	0.0070	0.033	0.012	(1+)	(1+)	(1–)	(1–)	0.12		
Mg	37F-H (8)	5.1 5.4	7.8 7.8	3.5 3.1	0.46 0.36	0.11 0.12	0.041 0.027	0.020 (1–) 0.0056	0.023 0.015	0.022 0.024	0.0074 0.0079	0.044 (2–) 0.019	0.012 (1–) 0.0078	0.094 (6+) –	0.29 (2+) 0.40	0.067 (7–) –	0.0043 (3–) 0.0033	0.088 (6–) –		
Mu	37G (14)	1.9 1.6	6.4 6.5	8.4 (12+) –	0.12 0.10	0.13 0.12	0.0023 0.0023	0.0043 (7–) –	0.011 (13–) –	0.0095 (2–) 0.0068	0.0048 (9–) –	0.27 0.28	0.17 0.16	0.37 (11–) –	0.15 (2–) 0.061	(14–) –	0.010 0.0088	0.10 0.11		
Mu[a]	37F (1)	8.6	3.0	1.5	0.27	0.034	0.025	–	0.022	0.0044	0.0011	(1–)	(1–)	0.044	0.036	(1–)	(1–)	(1–)		
Mn	37E (1)	13.2	1.5	0.61	0.090	0.030	0.019	0.020	(1–)	(1–)	(1–)	(1–)	(1–)	(1+)	(1+)	(1–)	(1–)	(1–)		
Amg[g]	27F, 37F-H (24)	6.3 6.4	6.3 (1+) 6.0	3.0 2.5	0.54 0.48	0.13 0.11	0.053 0.023	0.038 0.024	0.025 (2–) 0.018	0.021 0.018	0.0048 (2–) 0.0018	0.024 (5–) 0.013	0.0089 (9–) 0.0049	7.8 (22+) –	0.71 (19+) –	0.028 (19–) –	0.0044 (14–) –	(24–) –		
	37G (7)	6.7 6.8	6.5 (1+) 7.7	3.1 3.5	0.59 0.51	0.14 0.14	0.022 0.013	0.056 0.040	0.020 0.020	0.023 0.018	0.0061 0.0018	0.018 (1–) 0.013	0.010 (3–) 0.0062	(7+) –	0.56 (5+) –	0.033 (5–) –	0.0052 (4–) –	(7–) –		
	37H (11)	6.1 6.4	5.9 5.9	2.9 2.4	0.57 0.48	0.10 0.084	0.093 0.055	0.041 0.041	0.034 (1–) 0.023	0.019 0.019	0.0057 (2–) 0.0028	0.026 (4–) 0.0092	0.0081 (5–) 0.0034	7.8 (9+) –	0.81 (8+) –	0.022 (9–) –	0.0043 (7–) –	(11–) –		
Hg	37E-H (9)	6.1 6.5	8.3 8.1	2.9 2.3	0.83 0.77	0.14 0.13	0.013 0.015	0.016 0.017	0.027 0.019	0.036 0.035	0.019 0.019	0.017 (4–) 0.0063	0.0073 (4–) 0.0050	9.0 (8+) –	0.83 (6+) –	0.031 (5–) –	0.0044 (3–) 0.0027	(9–) –		
Amn[h]	37G-H (4)	7.2 7.3	3.2 1.7	1.1 0.53	0.28 0.21	0.056 0.025	0.041 0.038	0.028 0.027	0.017 (1–) 0.016	0.013 (2–) –	0.0056 (2–) –	0.016 (3–) –	0.0066 (3–) –	(4+) –	(4+) –	(4+) –	(4–) –	(4–) –		
Ma	37G-H (4)	6.0 5.4	2.8 1.1	0.90 0.65	0.30 0.11	0.060 0.029	0.034 0.015	0.015 0.011	0.020 (1–) 0.014	0.014 (2–) –	0.0027 (1–) 0.0022	0.013 (3–) –	0.0030 (3–) –	0.19 (3+) –	(4+) –	(4–) –	(4–) –	(4–) –		
Amn[i]	27F, 37F-H (10)	6.4 6.8	1.6 (1–) 1.5	0.44 0.27	0.17 (2–) 0.093	0.031 (5–) –	0.093 (1+) 0.067	0.028 0.023	0.020 (4–) 0.011	0.0071 (6–) –	0.0019 (6–) –	(10–) –	(10–) –	0.50 (4+) 0.81	0.29 (9+) –	(10–) –	(10–) –	(10–) –		
Amg[j]	27F, 37E-H (21)	6.8 6.6	1.7 1.2	0.64 0.38	0.18 0.13	0.031 (6–) 0.017	0.086 0.065	0.034 0.031	0.022 (7–) 0.012	0.0094 (14–) –	0.0087 (12–) –	0.0096 (18–) –	(21–) –	0.57 (13+) –	(21–) –	0.028 (20–) –	(21–) –	(21–) –		
Amg[i]	27F, 37E-H (18)	7.0 6.9	1.1 (2–) 0.88	0.31 (1–) 0.18	0.11 0.075	0.022 (9–) –	0.069 0.050	0.025 0.018	0.022 (7–) 0.011	0.0071 (16–) –	0.0040 (15–) –	(18–) –	(18–) –	0.55 (9+) –	(18+) –	(18–) –	(18–) –	(18–) –		
Ag[k]	37G (2)	7.1 7.1	3.8 3.8	1.1 1.1	0.20 0.20	0.045 0.045	0.073 0.073	0.020 0.020	0.014 0.014	0.012 (1–) –	0.0076 (1–) –	0.021 (1–) –	0.011 (1–) –	(2+) –	(2+) –	(2–) –	(2–) –	(2–) –		
	37C, D (3)	6.6 6.8	0.43 0.43	1.2 0.22	0.040 (1–) 0.024	0.12 (2–) –	0.026 0.024	0.0074 (1–) 0.0057	(3–) –	(3–) –	0.0011 (2–) –	(3–) –	(3–) –	0.45 0.33	(3+) –	(3–) –	(3–) –	(3–) –		
Ag[c]	27F, 37E-G (10)	6.6 6.6	1.5 (3–) 0.30	0.77 (1–) 0.091	0.12 (2–) 0.033	0.038 (6–) –	0.081 0.047	0.024 (1–) 0.0076	0.014 (7–) –	0.017 (9–) –	0.0012 (8–) –	0.072 (9–) –	0.031 (9–) –	0.46 (2+) 0.47	(10+) –	(10–) –	0.0033 (9–) –	(10–) –		
	37D (8)	6.7 6.4	0.64 (1–) 0.50	0.24 0.16	0.12 (3–) 0.094	0.061 (2–) 0.011	0.045 0.038	0.011 (2–) 0.0082	0.014 (4–) –	(8–) –	0.0014 (7–) –	0.021 (7–) –	(8–) –	0.43 0.26	0.58 (7+) –	(8–) –	(8–) –	(8–) –		
Agp	37F-H, 27G (17)	7.2 7.1	2.2 2.0	0.91 0.76	0.29 0.27	0.034 (1–) 0.030	0.10 (1+) 0.11	0.041 0.042	0.036 0.027	0.0074 (4–) 0.0052	0.0021 (10–) –	0.0036 (15–) –	(17–) –	0.59 (11+) –	(17+) –	(17–) –	(17–) –	(17–) –		
	37H, 27G (9)	6.6 6.6	2.4 2.1	0.85 0.76	0.35 0.36	0.038 (1–) 0.034	0.12 0.12	0.041 0.043	0.028 0.024	0.0091 (2–) 0.0055	0.0025 (4) 0.0012	0.0036 (7–) –	(9–) –	0.70 (6+) –	(9+) –	(9–) –	(9–) –	(9–) –		
	37D (1)	6.8	2.2	0.91	0.27	0.044	0.084	0.019	0.013	0.0058	0.0013	(1–)	(1–)	(1+)	(1+)	(1–)	(1–)	(1–)		
Ack	37E-F, 37H (14)	6.6 6.1	1.6 1.1	0.44 0.38	0.28 0.16	0.025 (1–) 0.020	0.11 0.057	0.029 0.029	0.036 (1–) 0.017	0.0083 (7–) –	0.0027 (10–) –	0.0040 (13–) –	(14–) –	0.71 (7+) –	(14+) –	(14–) –	(14–) –	(14–) –		
	37H (10)	6.4 6.1	1.9 2.0	0.50 0.39	0.34 0.27	0.027 0.023	0.12 0.066	0.030 0.029	0.041 0.017	0.0086 (4–) 0.0041	0.0039 (8–)	0.0040 (9–)	(10–) –	0.81 (5+) –	(10+) –	(10–) –	(10–) –	(10–) –		

Appendix 4 (cont.)

Map unit	Location (Number of samples)	Element: Mean/Median in weight per cent; (2–) (1+) = number of samples within population with values below (–) or above (+) respectively, the limit of detection of the analytical method																		
		Al	Fe	Mg	Ti	Mn	Ba	Sr	Zr	V	Cu	Cr	Ni	Ca	Na	La	Co	Pb	Y	Yb
M	37F-G (4)	5.5 5.5	4.9 5.0	4.1 3.1	0.47 0.41	0.15 0.10	0.044 0.029	0.020 0.0089	0.019 0.017	0.016 0.011	0.0052 (1–) 0.0019	0.010 0.0079	0.0067 (2–) –	(4+) –	0.52 (3+) –	(4–) –	(4–) –	(4–) –		
M^{l}	37F-G (4)	7.2 7.3	2.9 2.6	1.2 1.2	0.39 0.32	0.040 0.040	0.073 0.064	0.040 0.042	0.028 0.022	0.0085 0.0083	0.0027 (1–) 0.0017	0.0032 (2–) –	(4–) –	0.95 (3+) –	(4+) –	(4–) –	(4–) –	(4–) –		
Ms	37E-H (38)	6.8 7.0	3.8 (3+) 3.4	1.3 1.1	0.38 0.33	0.063 (4–) 0.054	0.058 0.042	0.018 (3–) 0.016	0.021 (2–) 0.017	0.013 (6–) 0.0098	0.0038 (9–) 0.0018	0.014 (21–) –	0.0068 (29–) –	0.42 (24+) –	0.22 (28+) –	0.028 (36–) –	0.0045 (37–) –	0.078 (35–) –		
	37G (16)	6.7 7.4	3.2 (2+) 3.2	1.1 1.0	0.28 0.20	0.059 (1–) 0.041	0.069 0.046	0.020 (2–) 0.017	0.020 (1–) 0.017	0.010 (5–) 0.0058	0.0030 (6–) 0.0017	0.0086 (10–) –	0.0072 (15–) –	0.077 (14+) –	0.21 (11+) –	0.028 (16–) –	(16–) –	0.080 (16–) –		
	37F (18)	6.9 6.8	4.4 (1+) 4.1	1.5 1.4	0.50 0.47	0.067 (3–) 0.060	0.050 0.042	0.017 (1–) 0.014	0.021 (1–) 0.017	0.015 (1–) 0.012	0.0046 (3–) 0.0018	0.022 (11–) 0.022	0.0072 (13–) –	0.55 (8+) 0.96	0.24 (15+) –	(18–) –	0.0045 (17–) –	0.075 (17–) –		
	37C (2)	5.8 5.8	6.0 6.0	1.1 1.1	0.26 0.26	0.039 0.039	0.026 0.026	0.010 0.010	0.012 0.012	0.010 0.010	0.0037 0.0037	0.013 0.013	0.0039 (1–) –	0.85 (1+)	0.51 (1+) –	(2–) –	(2–) –	(2–) –		
Mq	37F-G (10)	7.2 6.9	3.9 (2–) 1.4	0.91 0.57	0.31 (2–) 0.23	0.042 (2–) 0.029	0.052 0.032	0.0091 (1–) 0.0019	0.031 (2–) 0.020	0.011 (5–) –	0.0039 (3–) 0.0018	0.0042 (8–) –	0.0036 (9–) –	0.26 (3+) 0.27	0.051 (6+) –	(10–) –	(10–) –	(10–) –		
Amg^{m}	37E, 37H (2)	5.7 5.7	3.6 3.6	1.6 1.6	0.28 0.28	0.049 0.049	0.055 0.055	0.028 0.028	0.018 0.018	0.010 0.010	0.0045 0.0045	0.017 0.017	0.0054 (1–) –	(2+) –	(2+) –	(2–) –	(2–) –	(2–) –		
APs	37F (1)	8.7	(1+)	2.4	0.39	0.12	0.042	0.013	0.031	0.020	0.0072	0.22	(1–)	(1+)	0.54	(1–)	(1–)	(1–)		
	37C, 37D (8)	5.2 5.3	2.2 1.7	1.2 (1–) 0.96	0.25 0.28	0.026 (2–) 0.015	0.054 (1–) 0.045	0.0088 (1–) 0.0080	0.018 (1–) 0.014	0.021 (3–) 0.0087	0.0034 (1–) 0.0018	0.0086 0.0076	0.0070 (7–) –	0.62 (2+, 1–) 0.62	0.59 (6+, 1–) –	(8–) –	0.013 (7–) –	0.013 (7–) –		
Ms^{n}	37F (1)	2.1	2.0	7.3	0.084	0.43	0.0024	0.0078	(1–)	(1–)	(1–)	0.0030	(1–)	(1+)	0.038	0.079	(1–)	(1–)		
APm	37C (3)	1.3 0.38	0.71 (1–) 0.25	3.7 3.9	0.12 0.10	0.026 0.022	0.0050 0.0058	0.0095 0.0098	0.022 (2–) –	0.0059 (2–) –	(3–) –	0.0031 (2–) –	(3–) –	(3+) –	0.19 0.060	0.071 (1–) 0.063	(3–) –	(3–) –		
Mif^{o}	37F, 37G (28)	0.73 (1–) 0.44	(28+) –	1.1 0.45	0.048 (6–) 0.028	0.12 (4–) 0.045	0.0028 (10–) 0.0021	0.0020 (13–) 0.0013	0.012 (14–) –	0.0078 (4–) 0.0048	0.0022 0.0019	0.0060 (4–) 0.0042	0.0065 (17–) –	0.32 (4+, 3–) 0.39	0.034 (11–) 0.011	(28–) –	0.0044 (13–) 0.0022	0.094 (3–) 0.088	0.011 (18–) –	0.0016 (18–) –
	37G (20)	0.56 (1–) 0.43	(20+) –	1.3 0.82	0.043 (5–) 0.028	0.13 0.056	0.0028 (5–) 0.0024	0.0020 (9–) 0.0015	0.013 (11–) –	0.0076 (4–) 0.0044	0.0021 0.0019	0.0062 (4–) 0.0042	0.0067 (13–) –	0.45 (3+, 3–) 0.52	0.037 (6–) 0.012	(20–) –	0.0046 (11–) –	0.093 0.088	0.010 (13–) –	0.0015 (13–) –
	37F (8)	1.1 0.55	(8+) –	0.49 0.30	0.060 (1–) 0.031	0.11 (4–) –	0.0027 (5–) –	0.0020 (4–) –	0.012 (3–) 0.011	0.0081 0.0062	0.0025 0.0020	0.0057 0.0039	0.0061 (4–) –	0.047 (1+) 0.025	0.023 (5–) –	(8–) –	0.0042 (2–) 0.0032	0.10 (3–) 0.070	0.011 (5–) –	0.0018 (5–) –
Mif^{s}	37F, 37G (6)	1.1 0.46	(6+) –	1.1 0.95	0.11 (1–) 0.038	0.26 0.14	0.0084 (2–) 0.0028 (1–)	0.0016 (4–) –	0.014 (4–) –	0.0081 (1–) 0.0045	0.0015 0.0014	0.0070 (1–) 0.0053	0.0033 (4–) –	0.38 (1–) 0.22	0.028 (2–) 0.012	(6–) –	0.0033 (5–) –	0.079 (2–) 0.074		
	37C (1)	0.85	(1–)	0.71	0.036	0.024		(1–)	(1–)	(1–)	0.0018	0.0030	(1–)	0.74	0.045	(1–)	(1–)	0.076		
NAS	37G (4)	1.4 1.5	0.25 (3–) –	(4–) –	0.030 (2–) –	(4–) –	0.040 0.018	0.0016 (2–) –	0.019 (1–) 0.012	(4–) –	(4–) –	(4–) –	(4–) –	0.026 0.025	0.023 0.018	(4–) –	(4–) –	(4–) –		
NAB	37G (16)	4.3 3.5	2.3 (2+, 1–) 2.0	0.95 0.46	0.18 (1–) 0.10	0.12 (6–) 0.016	0.015 0.013	0.0052 (4–) 0.0028	0.030 (2–) 0.025	0.0086 (9–) –	0.0034 (5–) 0.0023	0.0044 (9–) –	0.0054 (14–) –	0.18 (3+) 0.079	0.31 (5+) 0.42	0.77 (14–) –	0.0024 (15–) –	(16–) –	0.011 (14–) –	(16–) –
NAB-L	37G (5)	5.3 3.5	2.4 (1–) 1.5	0.49 0.24	0.21 0.095	0.017 (1–) 0.015	0.018 0.021	0.0045 (2–) 0.0018	0.033 0.032	0.012 (3–) –	0.0032 (2–) 0.0023	0.0052 (3–) –	(5–) –	0.25 0.079	0.33 0.39	(5–) –	(5–) –	(5–) –	(5–) –	(5–) –
NAB-U	37G (11)	3.9 3.7	2.2 (2+) 2.1	1.2 0.61	0.16 (1–) 0.13	0.18 (5–) 0.033	0.014 0.012	0.0055 (2–) 0.0029	0.029 (2–) 0.019	0.0071 (6–) –	0.0035 (3–) 0.0023	0.0041 (6–) –	0.0054 (9–) –	0.14 (3+) 0.20	0.29 (5+) 0.43	0.077 (9–) –	0.0024 (10–) –	(11–) –	0.011 (9–) –	(11–) –

APPENDIX 5

Additional chemistry for Mary River Group and Piling Group iron-formations

AREA	EQE BAY (37C)														
GROUP	MARY RIVER														
Lithology	Silicate-oxide facies														
	Rock	Magnetite	Magnetite[3]	Grunerite	Rock	Magnetite	Magnetite[3]	Grunerite	Rock[5]	Magnetite	Magnetite[3]	Rock[5]	Magnetite	Magnetite[3]
Sample No.	JDC 48E 30S				JDC 52W 46S				JDC 160W 02N			JDC 176E 02S		
Fe_2O_3T	48.3	100.59	102.59	40.42	38.2	94.58	101.81	43.50	53.3	98.95	102.41	71.5	99.62	102.65
SiO_2	46.8	4.41	0.00	50.76	56.9	4.59	0.00	50.39	36.5	2.82	0.00	26.3	1.91	0.00
Al_2O_3	0.98	0.32	0.33	0.64	0.53	0.19	0.20	0.34	0.58	0.30	0.31	0.18	0.09	0.09
TiO_2	0.03	0.08	0.08	0.01	0.00	0.09	0.10	0.01	0.03	0.04	0.04	0.01	0.01	0.01
Fe_2O_3	18.5	65.16	66.46	3.49	2.49	61.83	66.56	1.74	34.3	66.98	69.32	42.2	67.85	69.92
FeO	26.8	31.88	32.51	33.23	32.1	29.47	31.72	37.57	21.6	28.77	29.78	26.3	28.59	29.46
MnO	–	0.07	0.07	0.93	–	0.07	0.08	0.07	–	0.05	0.05	–	0.02	0.02
MgO	3.74	0.41	0.42	7.58	4.60	0.59	0.64	6.96	4.26	0.32	0.33	3.23	0.45	0.46
CaO	0.30	0.09	0.09	0.41	0.25	0.05	0.05	0.39	1.58	0.15	0.16	0.09	0.03	0.03
Na_2O	0.10	–	–	0.00	0.00	0.00	–	0.07	0.08	–	–	0.00	–	–
K_2O	0.00	–	–	0.00	0.00	0.00	–	0.01	0.00	–	–	0.00	–	–
P_2O_5	0.00	–	–	–	0.01	–	–	–	0.00	–	–	0.00	–	–
S	0.07	0.07	0.07	0.03	0.35	0.94	1.01	0.24	0.00	0.02	0.02	0.00	0.02	0.02
=O	0.02	0.03	0.03	0.01	0.13	0.35	0.36	0.09	0.00	0.01	0.01	0.00	0.01	0.01
$CO_2(T)$	0.00	–	–	–	0.13	–	–	–	0.00	–	–	0.00	–	–
$H_2O(T)$	1.94	–	–	1.90	2.05	–	–	2.22	0.74	–	–	0.88	–	–
Total	99.24	102.46	100.00	98.87	99.28	97.47	100.00	99.92	99.67	99.44	100.00	99.19	98.96	100.00
Ba	–	<0.001		0.0015	–	<0.001		<0.001	–	<0.001		–	<0.001	
Co	0.00	<0.002		<0.002	0.00	<0.002		<0.002	0.00	<0.002		0.00	<0.002	
Cr	0.0016	0.0058		<0.002	0.0012	0.0065		<0.002	<0.002	<0.002		<0.002	<0.002	
Cu	<0.00050	<0.0010		<0.001	0.0013	0.0025		0.0024	<0.001	<0.001		<0.001	<0.001	
Mn	0.34	0.044		0.72	0.39	0.044		0.051	0.15	0.040		0.094	0.015	
Ni	0.0011	<0.002		<0.002	0.0011	0.0046		<0.002	<0.002	<0.002		0.0045	<0.002	
Sr	–	0.00		0.00	–	0.00		0.00	–	0.00		–	0.00	
Ti	0.017	0.047		0.0085	0.0058	0.056		0.005	0.012	0.021		0.0039	0.006	
V	0.0026	0.0031		<0.001	<0.002	0.0091		<0.001	0.0012	<0.001		0.001	0.00	
Y	–	0.0013		0.001	–	0.00		<0.001	–	0.00		–	0.00	
Yb	–	<0.0005		<0.0005	–	<0.0005		<0.0005	–	<0.0005		–	<0.0005	
Zn	0.00	0.00		0.00	0.00	0.00		0.00	0.00	0.00		0.00	0.00	
Zr	0.0081	<0.01		<0.01	0.0075	<0.010		<0.010	<0.007	<0.01		0.10	<0.01	

0.00 = Looked for but not found; – = Not determined

Major oxides determined by conventional chemical, spectrochemical, atomic absorption, and other methods. Minor elements determined by quantitative optical emission spectroscopy methods, expected to be accurate to 15% of reported values. Nb, Sb, Ta, and W were either not found or not determined. Ag, As, B, Be, Ga, Mo, Pb, Sc, and Sn were not found in or not determined for most samples, but are probably present below the limit of quantitative determination in some.

[1] These rocks are almost entirely iron oxide and quartz.
[2] This concentrate is a mixture of magnetite and hematite.
[3] The silica content is reduced to 0, and the analysis recalculated to 100 per cent.
[4] This concentrate contains a very small amount of silicate minerals.
[5] The amphibole analysis is not shown because it indicated that the concentrate was impure.

AREA	EQE BAY (37C)													
GROUP	MARY RIVER													
Lithology	Silicate-oxide facies					High grade iron [1]			Oxide facies [1]					
	Rock[5]	Magnetite	Magnetite[3]	Rock[5]	Grunerite	Rock	Magnetite[2]	Hematite	Rock	Hematite	Hematite[3]	Rock	Magnetite	Magnetite[3]
Sample No.	JDC 56W 47S			JDC 115W 03N		JDC 21-1			JDC 122E 03S			JDC 48E 29S		
Fe_2O_3T	29.7	77.88	102.12	52.0	43.74	92.6	100.84	99.80	51.1	96.22	99.75	61.0	77.98	101.96
SiO_2	65.8	21.83	0.00	44.8	50.00	6.8	0.13	0.64	47.9	3.29	0.00	38.6	22.17	0.00
Al_2O_3	0.33	0.17	0.22	1.24	0.49	0.67	0.26	0.25	0.53	0.13	0.13	0.78	0.42	0.55
TiO_2	0.01	0.01	0.01	0.06	0.01	0.02	0.01	0.01	0.01	0.01	0.01	0.02	0.02	0.03
Fe_2O_3	15.0	51.55	67.60	31.3	0.00	92.0	82.40	99.03	50.3	96.05	99.58	41.5	52.61	68.78
FeO	13.2	23.69	31.06	18.6	39.63	0.56	16.59	0.69	0.77	0.15	0.16	17.5	22.83	29.84
MnO	–	0.05	0.07	–	0.63	–	0.03	0.00	–	0.07	0.07	–	0.05	0.07
MgO	3.48	0.70	0.92	1.80	6.80	0.02	0.01	0.00	0.03	0.01	0.01	0.63	0.45	0.59
CaO	0.07	0.07	0.09	0.99	0.20	0.04	0.00	0.00	0.02	0.03	0.03	0.20	0.09	0.12
Na_2O	0.00	–	–	0.05	0.15	0.00	–	–	0.09	–	–	0.00	–	–
K_2O	0.00	–	–	0.03	0.02	0.00	–	–	0.00	–	–	0.00	–	–
P_2O_5	0.05	–	–	0.00	–	0.00	–	–	0.00	–	–	0.00	–	–
S	0.02	0.03	0.04	0.00	0.18	0.00	0.02	0.02	0.01	<0.02	<0.02	0.00	0.02	0.03
=O	0.01	0.01	0.01	0.00	0.07	0.00	0.01	0.01	0.00	0.00	0.00	0.00	0.01	0.01
$CO_2(T)$	0.00	–	–	0.00	–	0.00	–	–	0.00	–	–	0.00	–	–
$H_2O(T)$	1.48	–	–	0.60	2.40	0.02	–	–	0.22	–	–	0.60	–	–
Total	99.43	98.09	100.00	99.47	100.44	100.13	99.44	100.63	99.88	99.75	100.00	99.83	98.65	100.00
Ba	–	<0.001		–	<0.001	–	<0.001	<0.001	–	<0.001		–	0.0018	
Co	0.00	<0.002		0.00	<0.002	0.00	0.015	0.00	0.00	<0.002		0.00	<0.002	
Cr	0.0012	<0.002		0.0023	<0.002	0.0067	0.020	0.00922	<0.002	<0.002		<0.002	<0.002	
Cu	<0.0005	<0.001		<0.001	<0.001	<0.001	0.0011	0.00	<0.001	<0.001		<0.001	<0.001	
Mn	0.12	0.036		0.14	0.49	0.002	0.022	0.00	0.031	0.052		0.037	0.037	
Ni	0.0013	<0.002		<0.002	<0.002	0.0029	0.21	0.0021	<0.002	<0.002		<0.002	<0.002	
Sr	–	0.00		–	0.00	–	0.00	0.00	–	0.00		–	0.00	
Ti	0.0019	0.0057		0.034	0.0050	0.0047	0.0032	0.00	0.0036	0.0046		0.012	0.010	
V	0.00	<0.001		0.0015	0.00	0.0018	0.00	0.0058	0.0013	<0.001		0.0022	<0.001	
Y	–	0.00		–	0.00	–	0.00	0.00	–	0.00		–	<0.001	
Yb	–	<0.0005		–	<0.0005	–	0.00055	<0.00050	–	<0.0005		–	<0.0005	
Zn	0.00	0.00		0.00	0.00	0.00	0.00	0.00	0.00	0.00		0.00	0.00	
Zr	<0.007	<0.01		<0.007	<0.01	0.00	<0.010	<0.010	0.00	<0.010		0.00	<0.010	

Appendix 5. (cont.)

AREA	EQE BAY (37C)									
GROUP	MARY RIVER									
Lithology	Oxide facies[1]			Aluminous facies						
	Rock	Magnetite	Magnetite[3]	Rock	Magnetite[4]	Chlorite	Rock	Garnet	Biotite	Staurolite
Sample No.	JDC 48W 19S			JDC 180W 36N			JDC 13-3			
Fe_2O_3T	54.4	94.55	101.02	35.1	96.93	28.58	15.5	41.11	24.86	13.81
SiO_2	45.6	6.58	0.00	43.1	2.72	28.34	55.7	36.78	34.68	30.82
Al_2O_3	0.67	0.53	0.57	10.51	1.08	20.23	17.21	19.73	18.82	47.8
TiO_2	0.03	0.04	0.04	0.65	1.12	0.62	0.63	0.22	1.55	0.62
Fe_2O_3	35.8	62.51	67.53	11.3	64.59	2.51	0.6	0.00	1.13	4.02
FeO	16.7	28.83	31.14	21.4	29.1	23.46	13.4	37.31	21.35	8.81
MnO	–	0.02	0.02	0.21	0.19	0.48	–	1.15	0.02	0.03
MgO	0.34	0.35	0.38	4.37	0.40	11.13	4.12	2.50	7.82	1.66
CaO	0.32	0.29	0.31	1.38	0.22	0.84	0.62	0.95	0.09	0.18
Na_2O	0.00	–	–	1.10	–	0.38	1.13	0.07	0.38	0.14
K_2O	0.00	–	–	0.50	–	0.23	2.90	0.04	8.40	0.36
P_2O_5	0.00	–	–	0.01	–	–	0.08	–	–	–
S	0.02	0.02	0.02	0.48	0.08	0.08	0.06	0.03	0.03	0.11
=O	0.01	0.01	0.01	0.18	0.03	0.03	0.02	0.01	0.01	0.04
$CO_2(T)$	0.01	–	–	0.00	–	–	0.00	–	–	–
$H_2O(T)$	0.46	–	–	3.79	–	9.72	2.52	<0.01	4.10	1.33
Total	99.94	99.16	100.00	98.62	99.47	97.99	98.99	98.77	98.36	95.84
Ba	–	0.0032		–	0.0024	0.0068	–	–	0.21	0.0023
Co	0.00	<0.002		0.004	<0.002	<0.002	0.0028	0.0023	0.0067	0.0067
Cr	<0.002	0.0024		0.031	0.11	0.014	0.025	0.023	0.045	0.039
Cu	<0.001	<0.001		0.0071	0.0023	0.0046	0.0047	0.00075	0.0017	0.0047
Mn	0.0094	0.015		0.17	0.092	0.37	0.081	0.89	0.016	0.021
Ni	<0.002	<0.002		0.10	0.0075	0.015	0.012	0.0012	0.026	0.011
Sr	–	0.00		–	0.0037	0.014	–	–	0.00	0.00
Ti	0.015	0.021		0.43	0.67	0.37	0.51	0.13	0.93	0.37
V	0.0017	<0.001		0.024	0.073	0.0071	0.024	0.015	0.062	0.027
Y	–	0.0013		–	0.00	0.00	–	–	0.00	0.003
Yb	–	0.0005		–	0.00063	<0.0005	–	–	<0.0005	<0.0005
Zn	0.00	0.00		0.00	0.00	0.00	0.00	–	0.00	0.11
Zr	0.00	<0.010		0.0083	<0.01	<0.01	0.019	0.020	<0.01	<0.01

AREA	GENERATOR LAKE (27C)								
GROUP	PILING								
Lithology	Aluminous facies								
	Rock	Anthophyllite	Garnet	Biotite	Rock	Cummingtonite	Rock	Edenitic hornblende	Cummingtonite
Sample No.	JDC 286-1				JDC 286-2		JDC 286-5		
Fe_2O_3T	21.3	27.62	36.13	19.11	10.6	20.33	16.10	19.27	28.10
SiO_2	52.1	49.14	39.54	36.84	57.9	54.88	49.20	43.10	52.30
Al_2O_3	15.99	7.72	19.10	17.6	11.68	0.77	13.60	12.39	1.40
TiO_2	0.93	0.80	0.40	1.28	0.64	0.06	1.56	0.78	0.48
Fe_2O_3	1.7	2.16	12.38	1.31	0.5	12.39	0.6	7.28	7.37
FeO	17.8	22.91	21.37	16.02	9.2	7.05	13.9	10.79	18.65
MnO	0.17	0.10	0.52	0.01	0.20	0.52	0.26	0.37	0.84
MgO	5.65	12.03	4.25	12.13	10.59	21.76	8.48	10.51	15.97
CaO	2.17	1.09	1.94	0.29	6.21	0.53	5.63	8.14	1.30
Na_2O	0.34	4.35	0.07	0.39	0.69	0.25	3.31	1.90	0.33
K_2O	0.72	0.33	0.04	7.65	0.07	0.03	0.65	0.23	0.02
P_2O_5	0.09	–	–	–	0.03	–	0.07	–	–
S	0.02	0.03	<0.02	0.04	0.00	<0.02	0.00	0.03	0.03
=O	0.01	0.01	0.00	0.02	0.00	0.00	0.00	0.01	0.01
$CO_2(T)$	0.00	–	–	–	0.00	0.00	0.00	–	–
$H_2O(T)$	1.66	1.60	–	3.92	1.32	2.03	1.96	1.82	1.98
Total	99.35	98.05	99.63	97.46	99.03	100.29	99.22	97.33	100.66
Ba	–	0.0052	–	0.14	–	<0.001	–	0.002	<0.001
Co	0.0044	0.0082	0.0047	0.019	0.0054	0.011	0.0049	0.0069	0.0081
Cr	0.052	0.057	0.063	0.27	0.22	0.19	0.018	0.036	0.0081
Cu	0.0019	0.0018	0.001	0.0011	0.0015	0.00	0.083	0.0014	0.0014
Mn	0.13	0.081	0.40	0.0077	0.19	0.40	0.22	0.29	0.65
Ni	0.023	0.048	0.0069	0.17	0.028	0.041	0.012	0.013	0.015
Sr	–	0.0034	–	0.00	–	0.00	–	0.00	0.00
Ti	0.54	0.36	0.30	0.77	0.42	0.037	0.82	0.47	0.29
V	0.025	0.036	0.025	0.11	0.020	0.020	0.035	0.091	0.011
Y	–	0.00	–	0.00	–	0.00	–	0.01	0.00
Yb	–	<0.0005	–	<0.0005	–	<0.0005	–	0.00075	<0.0005
Zn	0.00	0.00	0.00	0.00	0.00	0.00	0.00	0.00	0.00
Zr	0.018	<0.01	0.016	<0.01	<0.007	<0.01	0.011	<0.01	<0.01

APPENDIX 6

Additional chemistry for Mary River metapelites

AREA	EQE BAY (37C)						
GROUP	MARY RIVER						
Lithology	Rock	"Magnetite"	Magnesio-hornblende	Chlorite	Rock	Biotite	Chlorite
Sample number	JDC 160+50W 01N				JDC 13-1		
Fe_2O_3T	11.3	98.86	19.11	23.93	10.2	25.66	29.06
SiO_2	65.10	5.23	44.20	28.42	65.2	34.36	25.20
Al_2O_3	9.72	0.81	11.68	18.74	14.50	18.60	20.94
TiO_2	0.15	0.05	0.22	0.30	0.52	1.67	0.75
Fe_2O_3	3.4	63.83	5.92	3.36	1.2	1.32	0.00
FeO	7.1	27.02	11.87	18.51	8.1	21.90	26.37
MnO	0.16	0.07	0.46	0.40	–	0.08	0.15
MgO	5.69	0.36	10.20	16.53	3.15	7.83	10.45
CaO	2.34	0.53	8.49	0.32	0.68	0.05	0.06
Na_2O	0.94	–	1.08	0.25	1.61	0.37	0.52
K_2O	1.28	–	0.61	1.74	2.09	8.32	1.28
P_2O_5	0.12	–	–	–	0.07	–	–
S	0.00	0.05	0.03	<0.02	0.19	0.04	0.14
=O	0.00	0.02	0.01	0.00	0.07	0.02	0.05
CO_2T	0.00	–	–	–	0.00	–	–
H_2OT	3.16	–	2.40	9.64	1.72	4.00	–
Total	99.16	97.93	97.5	98.21	98.96	98.52	85.81
Ba	–	0.004	0.015	0.067	–	0.15	0.03
Co	0.00	0.00	0.00	0.00	0.0019	0.0036	0.0037
Cr	0.0071	0.009	0.018	0.016	0.02	0.055	0.045
Cu	<0.0005	<0.001	<0.001	<0.001	0.0099	0.0016	0.0015
Mn	0.022	0.057	0.36	0.31	0.047	0.059	0.12
Ni	0.002	0.00	0.0029	0.0062	0.0078	0.013	0.013
Sr	–	0.0036	0.0059	0.0023	–	0.00	0.00
Ti	0.089	0.032	0.13	0.18	0.41	1.0	0.45
U	0.0029	0.0058	0.0036	0.0018	0.015	0.044	0.025
Y	–	0.00	0.00	0.00	–	0.00	0.0016
Yb	–	0.00059	<0.0005	0.00	–	<0.0005	<0.0005
Zn	0.00	0.00	0.00	0.00	0.00	0.00	0.00
Zr	0.025	0.044	<0.01	<0.01	0.017	<0.01	<0.01

Note: 0.00 = Looked for but not found;
– = Not determined

Analyses carried out as indicated for Appendix 5

APPENDIX 7

Structural formulae and ratios for selected minerals in iron-formations and metapelites (amphibole nomenclature after Leake (1978) and Rock and Leake (1984))

	A. MARY RIVER GROUP IRON-FORMATION															
AREA	**MAP AREA**				**EQE BAY**											
Sample No.	**C 70/1-65[4]**		**B 278/6[4]**		**C 115W 03N[4]**		**C 180W 36N[4]**		**C 48E 30S[5]**		**C 52W 46S[5]**		**C 13/3 [5]**			
Mineral	**Cummingtonite**		**Ferrohypersthene**		**Grunerite**		**Chlorite**		**Grunerite**		**Grunerite**		**Almandine**		**Biotite**	
Ions **O**	**23**		**6**		**23**		**14**		**23**		**23**		**12**		**11**	
Si	8.268	8.268	2.028	2.028	7.928	8.000	2.436	3.000	8.061	8.061	8.012	8.012	3.024	3.024	2.776	3.000
Al(4)	0.000		0.000		0.072		0.564		0.000		0.000		0.000		0.224	
Al(6)	0.016		0.004		0.020		1.485		0.120		0.064		1.911		1.551	
Ti	0.000		0.000		0.001		0.040		0.001		0.001		0.014		0.093	
Cr	0.000		0.000		0.000		0.000		0.000		0.000		0.002		0.000	
Fe^{3+}	1.140	5.767	0.791	1.887	0.000	6.967	0.162	4.834	0.417	6.869	0.208	6.921	0.000	4.878	0.068	4.075
Fe^{2+}	1.713		0.399		5.254		1.686		4.412		4.990		2.565		1.429	
Mn	0.103		0.106		0.085		0.035		0.125		0.009		0.080		0.001	
Mg	2.795		0.587		1.607		1.426		1.794		1.649		0.306		0.933	
Ca	0.965		0.045		0.034		0.077		0.070		0.066		0.084		0.008	
Na	0.048	1.017	0.039	0.085	0.046	0.084	0.063	0.165	0.000	0.070	0.022	0.090	0.011	0.099	0.059	0.925
K	0.004		0.001		0.004		0.025		0.000		0.002		0.004		0.858	
Cations (total)	15.052		4.000		15.051		7.999		15.000		15.023		8.001		8.000	
Fe	42.48		61.73		75.28		54.59		70.83		75.08		84.51		61.38	
Mn	1.53		5.50		1.21		1.03		1.84		0.14		2.64		0.06	
Mg	41.62		30.46		23.02		42.10		26.31		23.82		10.09		38.24	
Ca	14.37		2.31		0.49		2.28		1.02		0.96		2.76		0.32	
$Mg/(Mg+Fe^{2+})$	0.62		0.60		0.23		0.46		0.29		0.25		0.11		0.40	
$Mg/(Mg+Fe+Mn)$	0.49		0.31		0.23		0.43		0.27		0.24		0.10		0.38	
$Fe^{2+}+Fe^{3+}$	2.85		1.19		5.25		1.85		4.83		5.20		2.565		1.497	

	Staurolite[1]	
Ions **O**	**48**	
Si	8.000	8.000
Al(4)	–	
Al(6)	16.221	
Si	0.874	
Ti	0.134	
Cr	0.013	18.113[2]
Fe^{3+}	0.871	
Mg	–	
Mg	0.713	
Fe^{2+}	2.121	
Mn	0.007	
Na	0.078	3.107[3]
K	0.132	
Ca	0.056	
OH	2.549	2.549
Cat. total	31.769	
Fe	79.40	
Mn	0.19	
Mg	18.92	
Ca	1.49	
$Mg/(Mg+Fe^{2+})$	0.25	
$Mg/(Mg+Fe+Mn)$	0.19	
$Fe^{2+}+Fe^{3+}$	2.99	

	B. PILING GROUP IRON-FORMATION								C. MARY RIVER GROUP METAPELITES								D. PILING GROUP METAPELITES			
AREA	**GENERATOR LAKE**								**EQE BAY**								**GENERATOR LAKE**			
Sample No.	**C 298/1[5]**						**C 298-2[5]**		**C 160+50W 01N[6]**				**C 13/1[6]**				**C 298/5[5]**			
Mineral	**Anthophyllite**		**Almandine**		**Biotite**		**Cummingtonite**		**Chlorite**		**Magnesio-hornblende**		**Biotite**		**Chlorite**		**Edenitic hornblende**		**Cummingtonite**	
Ions **O**	**23**		**12**		**11**		**23**		**14**		**23**		**11**		**14**		**23**		**23**	
Si	7.472	8.000	3.207	3.207	2.894	3.000	7.879	8.000	2.350	3.000	6.822	8.000	2.750	3.000	2.218	3.000	6.632	8.000	7.741	7.985
Al(4)	0.528		0.000		0.106		0.121		0.650		1.178		0.250		0.782		1.368		0.244	
Al(6)	0.856		1.825		1.524		0.009		1.176		0.946		1.504		1.390		0.879		0.000	
Ti	0.069		0.024		0.076		0.006		0.019		0.026		0.101		0.050		0.090		0.053	
Cr	0.000		0.006		0.000		0.000		0.000		0.000		0.000		0.000		0.000		0.000	
Fe^{3+}	0.247	6.823	0.755	4.609	0.077	4.151	0.024	6.917	0.209	4.748	0.687	5.597	0.079	4.089	0.000	4.763	0.843	5.658	0.821	6.808
Fe^{2+}	2.912		1.449		1.053		2.160		1.279		1.532		1.466		1.941		1.388		2.307	
Mn	0.013		0.036		0.001		0.063		0.028		0.060		0.005		0.011		0.048		0.105	
Mg	2.726		0.514		1.420		4.655		2.037		2.346		0.934		1.371		2.410		3.522	
Ca	0.178		0.169		0.024		0.062		0.028		1.404		0.004		0.006		1.342		0.206	
Na	0.103	0.345	0.011	0.184	0.059	0.850	0.070	0.157	0.040	0.252	0.323	1.847	0.057	0.911	0.089	0.239	0.567	1.954	0.095	0.305
K	0.064		0.004		0.767		0.005		0.184		0.120		0.849		0.144		0.045		0.004	
Cations (total)	15.168		8.000		8.001		15.074		8.000		15.444		8.000		8.002		15.612		15.098	
Fe	52.00		75.43		43.87		31.28		41.56		36.81		62.08		58.30		36.99		44.93	
Mn	0.21		1.22		0.03		0.90		0.78		1.00		0.22		0.34		0.80		1.51	
Mg	44.87		17.58		55.15		66.65		56.87		36.91		37.53		41.19		39.96		50.60	
Ca	2.92		5.77		0.95		1.17		0.79		23.28		0.17		0.17		22.25		2.96	
$Mg/(Mg+Fe^{2+})$	0.28		0.27		0.57		0.68		0.61		0.60		0.39		0.41		0.63		0.60	
$Mg/(Mg+Fe+Mn)$	0.46		0.19		0.56		0.67		0.57		0.51		0.38		0.41		0.51		0.52	
$Fe^{2+}+Fe^{3+}$	3.159		2.204		1.13		2.18		1.49		2.22		1.55		1.94		2.23		3.13	

Notes: 1. $\Sigma Fe = 80.8 = 100(Fe^{2+}+Fe^{3+}+Mn)/(Mg+Fe^{2+}+Fe^{3+}+Mn)$; 2. Includes V – .009; 3. Includes Zn – .029, Co – .002, Ni .008; 4, 5, 6: Chemical analyses provided in Table 15 and Appendices 5 and 6 respectively.

MAPS NOT FILMED

CARTES NON REPRODUITES

micromedia
a division of IHS Canada

20 Victoria Street
Toronto, Ontario M5C 2N8
Tel.: (416) 362-5211
Toll Free: 1-800-387-2689
Fax: (416) 362-6161
Email: info@micromedia.on.ca